REPORT NO.
UCB/EERC-87/20
DECEMBER 1987

EARTHQUAKE ENGINEERING RESEARCH CENTER

EARTHQUAKE RESPONSE OF TORSIONALLY-COUPLED BUILDINGS

by

REEM HEJAL

ANIL K. CHOPRA

A Report on Research Conducted Under
Grant CEE-8402271 from the
National Science Foundation

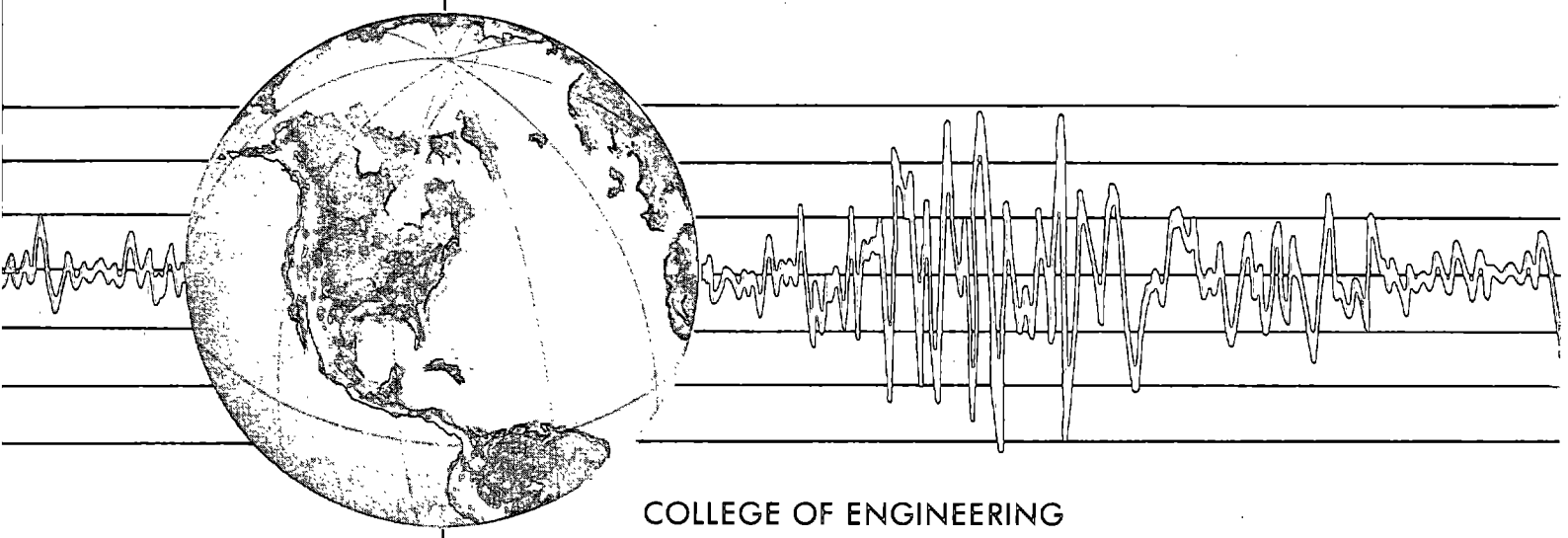

COLLEGE OF ENGINEERING

UNIVERSITY OF CALIFORNIA AT BERKELEY

-i-b

For sale by the National Technical Information Service, U.S. Department of Commerce, Springfield, Virginia 22161

See back of report for up to date listing of EERC reports.

REPORT DOCUMENTATION PAGE	1. REPORT NO. NSF/ENG-87043	2.	3. Recipient's Accession No. PB 90 208638/AS

4. Title and Subtitle

Earthquake Response of Torsionally-Coupled Buildings

5. Report Date December 1987

6.

7. Author(s) Reem Hejal and Anil K. Chopra

8. Performing Organization Rept. No. UCB/EERC -87/20

9. Performing Organization Name and Address

Earthquake Engineering Research Center
University of California
1301 South 46th Street
Richmond, California 94804

10. Project/Task/Work Unit No.

11. Contract(C) or Grant(G) No.

(C)

(G) CEE-8402271

12. Sponsoring Organization Name and Address

National Science Foundation
1800 G. Street, N.W.
Washington, D.C. 20550

13. Type of Report & Period Covered

14.

15. Supplementary Notes

16. Abstract (Limit: 200 words)

In Part I, the elastic response of torsionally-coupled, one-story framed buildings to earthquake ground motion is presented for a wide range of values of the various system parameters, including the beam-to-column stiffness ratio parameter which characterizes the degree of frame action.

In Part II, an effective procedure is developed for estimating the maximum response of a class of torsionally-coupled, multi-story buildings due to earthquake ground motion characterized by smooth response spectra.

In Part III, centers of rigidity, centers of twist, shear centers and static eccentricities are defined and procedures developed to determine their locations for one-story and multi-story buildings of general plan layouts. It is found that the various centers at each floor of a multi-story building generally do not coincide, and their locations not only depend on the geometric and stiffness characteristics of the building but also on the height-wise distribution of lateral forces. Thus, static eccentricities cannot be uniquely determined for multi-story buildings. A special class of buildings is identified. Since torsional provisions in most building codes are based on the evaluation of static eccentricities, the provisions should strictly be applied to the special class of buildings, and further work is necessary to develop code provisions for buildings not belonging to this special class.

17. Document Analysis a. Descriptors

earthquake engineering
one-story framed building
multi-story building
elastic response
beam-to-column stiffness ratio
response spectra
center of rigidity
center of twist
shear center
static eccentricity

b. Identifiers/Open-Ended Terms

c. COSATI Field/Group

18. Availability Statement: Release unlimited

19. Security Class (This Report) Unclassified

21. No. of Pages 336

20. Security Class (This Page) Unclassified

22. Price

-1-a

EARTHQUAKE RESPONSE OF TORSIONALLY-COUPLED BUILDINGS

by

Reem Hejal

Anil K. Chopra

A Report on Research Conducted under
Grant CEE-8402271 from the
National Science Foundation

Report No. UCB/EERC-87/20
Earthquake Engineering Research Center
University of California
Berkeley, California

December 1987

ABSTRACT

This investigation of the coupled lateral-torsional response of buildings with unsymmetric plan to earthquakes is organized in three parts.

In Part I, the elastic response of torsionally-coupled, one-story framed buildings to earthquake ground motion, characterized by response spectra of three different shapes, is studied. The earthquake response is presented for a wide range of values of the various system parameters, including the beam-to-column stiffness ratio parameter which characterizes the degree of frame action. The base shear and torque in a torsionally-coupled system is compared with the base shear in the corresponding torsionally-uncoupled system, and the effects of torsional coupling on earthquake forces are identified. Also investigated is the effect of frame action on the forces in frame members.

In Part II, an effective procedure is developed for estimating the maximum response of a class of torsionally-coupled, multi-story buildings due to earthquake ground motion characterized by smooth response spectra. Several properties characterize this class of buildings, the most important of which is: all frames (spanning along either of two orthogonal directions) have proportional lateral stiffness matrices. It is demonstrated that the maximum response of such a torsionally-coupled, N-story building in its nj^{th} mode of vibration can be determined exactly by analyzing (1) the response in the j^{th} vibration mode (j=1, 2, ..., N) of the corresponding torsionally-uncoupled, N-story system; and (2) the response in the n^{th} vibration mode (n=1, 2 for a one-way symmetric plan) of an associated torsionally-coupled, one-story system. The total response is then determined by an appropriate modal combination rule.

Utilizing the aforementioned analysis procedure, the earthquake response of torsionally-coupled buildings is presented for a wide range of system parameters. Based on these results, it is demonstrated that the building response depends significantly on the static eccentricity ratio e/r, the uncoupled torsional to lateral frequency ratio Ω, the beam-to-column stiffness ratio ρ, and the uncoupled, fundamental, lateral vibration period T_{y1}. It is concluded that the response contributions of the higher vibration modal-pairs increase with increasing T_{y1} and decreasing ρ. However, if T_{y1}

is in the acceleration- or velocity-controlled regions of the earthquake design spectrum, the first two vibration modal-pairs are sufficient to estimate the response to a useful degree of accuracy; the fundamental vibration modal-pair suffices if T_{y1} is in the acceleration-controlled region of the spectrum. By comparing the responses of torsionally-coupled buildings with those of corresponding torsionally-uncoupled systems, the effects of lateral-torsional coupling on building motions and forces, arising from lack of symmetry in building plan, are identified.

In Part III, centers of rigidity, centers of twist, shear centers and static eccentricities are defined and procedures developed to determine their locations for one-story and multi-story buildings of general plan layouts. It is found that, unlike one-story systems, the various centers at each floor of a multi-story building generally do not coincide, and their locations not only depend on the geometric and stiffness characteristics of the building but also on the height-wise distribution of lateral forces. Thus, static eccentricities can not be uniquely determined for multi-story buildings. A special class of buildings is identified, where the centers of rigidity, the centers of twist and the shear centers are coincident, load-independent and lie on a vertical line. Since torsional provisions in most building codes are based on the evaluation of static eccentricities, the provisions should strictly be applied to the special class of buildings, and further work is necessary to develop code provisions for buildings not belonging to this special class.

ACKNOWLEDGEMENTS

This research investigation was supported by the National Science Foundation under Grant CEE-8402271. The authors are grateful for this support.

This report is the same, except for some editorial changes, as Reem Hejal's doctoral dissertation which has been submitted to the University of California, Berkeley. The dissertation committee consisted of Professors A.K. Chopra (Chairman), E. L. Wilson and B. N. Parlett. The authors are grateful to Professors Wilson and Parlett for reviewing the manuscript and suggesting improvements.

PREFACE

This work on the earthquake response of torsionally-coupled buildings is organized in three parts:

- Part I: Earthquake Response of Torsionally-Coupled, One-story Buildings
- Part II: Earthquake Analysis and Response of a Special Class of Torsionally-Coupled, Multi-Story Buildings
- Part III: The Static Eccentricity Concept in Building Code Analyses

Table of Contents

PART III: THE STATIC ECCENTRICITY CONCEPT IN BUILDING CODE ANALYSES

PART I

EARTHQUAKE RESPONSE OF TORSIONALLY-COUPLED, ONE-STORY BUILDINGS

1. INTRODUCTION

Buildings subjected to ground shaking simultaneously undergo lateral as well as torsional motions if their structural plans do not have two axes of mass and stiffness symmetry. Coupled lateral-torsional motions can also occur in nominally symmetric buildings-- buildings with structural plans that have two axes of mass and stiffness symmetry-- if ground shaking includes a torsional component or due to unforseen conditions such as unbalanced load distributions or differences between actual and assumed mass and stiffness distributions. As a result of coupled lateral-torsional motions, the lateral forces experienced by various resisting elements (frames, shear walls, etc.) would differ from those experienced by the same elements if the building had symmetric plan and hence responded only in planar vibrations.

The dynamic response of a special class of torsionally-coupled multi-story buildings with resisting elements idealized as shear beams have been shown in previous studies to be related to the response of an associated one-story system with properties derived from those of the multi-story building [1,2]. Furthermore, torsional provisions of most building codes are based largely on results obtained by analyzing torsionally-coupled one-story systems. Since many multi-story buildings consist of moment-resisting frames for which a shear beam idealization may be inappropriate, it is necessary to reexamine the relations between such multi-story buildings and the associated one-story systems, and to study the effect of frame action on coupled lateral-torsional response of buildings. This study of the dynamic response of torsionally-coupled one-story buildings is a first step in this direction.

The earthquake response of torsionally-coupled one-story systems has been investigated extensively in the past few years. Parametric studies have been performed [3,4,5,6,7,8]; the effectiveness of the torsional provisions in building codes in capturing the important response features has been evaluated [4,5,9,10,11]; and different proposals to improve code provisions have been suggested [5,9,10,12,13,14].

The objectives of this investigation are: (1) to investigate how the elastic response of torsionally-coupled buildings is influenced by the various system parameters, including the effect of

frame action, characterized by the beam-to-column stiffness ratio; (2) to evaluate the effects of lateral-torsional coupling in building response; and (3) to investigate the effect of frame action on the member forces of resisting elements. The ground motion is assumed to be uniform over the base of the building so that torsional response arises only from asymmetry of building plan. The results of this investigation provide a basis for the analysis and understanding of the response of multi-story buildings, presented in Part II.

2. SYSTEMS AND DESIGN SPECTRA

The linear systems studied are idealized single-story buildings, each consisting of a rigid deck (or floor), where the mass of the structure is lumped, supported by massless, axially inextensible resisting elements. The resisting elements are frames, shear walls, columns or shear-wall cores, with their principal axes oriented along the principal axes, X and Y, of the system (Figure 1). The resisting elements are symmetrically located about the X-axis, which is an axis of symmetry for the building plan. The dynamic response of such systems to the horizontal component of ground motion along the Y-axis, the direction perpendicular to the axis of symmetry, is investigated. Since the building is not symmetric about the Y-axis, it will undergo coupled lateral-torsional motions. The responses are presented for a wide range of the system parameters which will be identified in Section 3.

The earthquake ground motion is characterized by its pseudo-acceleration response spectrum. Conservative values of system response can be obtained by idealizing the spectrum of an actual earthquake by a flat branch in the short-period range and by a hyperbolic branch in the long-period range (Figure 2), and taking the larger of the responses for the two branches [8]. Thus, two idealized response spectra are considered in this study: flat or period independent pseudo-acceleration spectrum, and hyperbolic pseudo-acceleration spectrum (or flat velocity spectrum). The two idealized spectra are especially useful since normalized response quantities of the system do not depend on the system vibrational periods but only on their ratios [1,3].

The system is also analyzed for the earthquake input characterized by the smooth design spectrum of Figure 3, which is developed by well known procedures [15] for excitations with maximum ground acceleration $\bar{a}_g$, velocity $\bar{v}_g$ and displacement $\bar{u}_g$ of 1g, 48 in/sec and 36 in, respectively. For a damping ratio of 5 % and 84.1 percentile response, amplification factors of 2.67, 2.32 and 2.04 are obtained from [15] for the maximum ground acceleration, velocity and displacement, respectively, leading to the design spectrum (Figure 3). Comparing the shape of the design spectrum to the $\bar{a}_g$-$\bar{v}_g$-$\bar{u}_g$ plot, it is apparent from Figure 3 that the response of short-period structures is controlled by ground acceleration, that of medium-period structures by the ground velocity and that

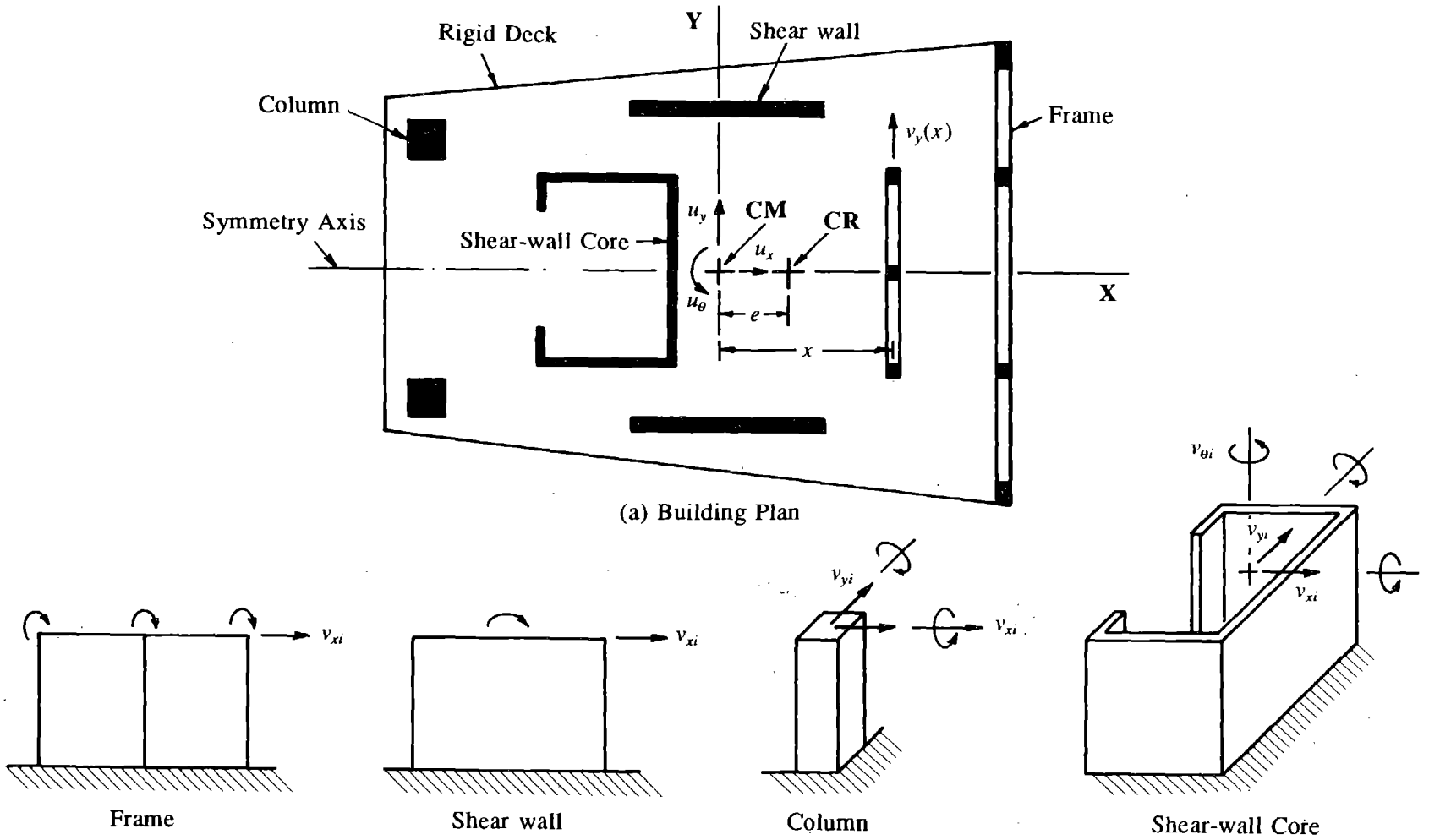

(a) Building Plan

(b) Element Elevation and Their Degrees of Freedom

FIGURE 1 One-story Building

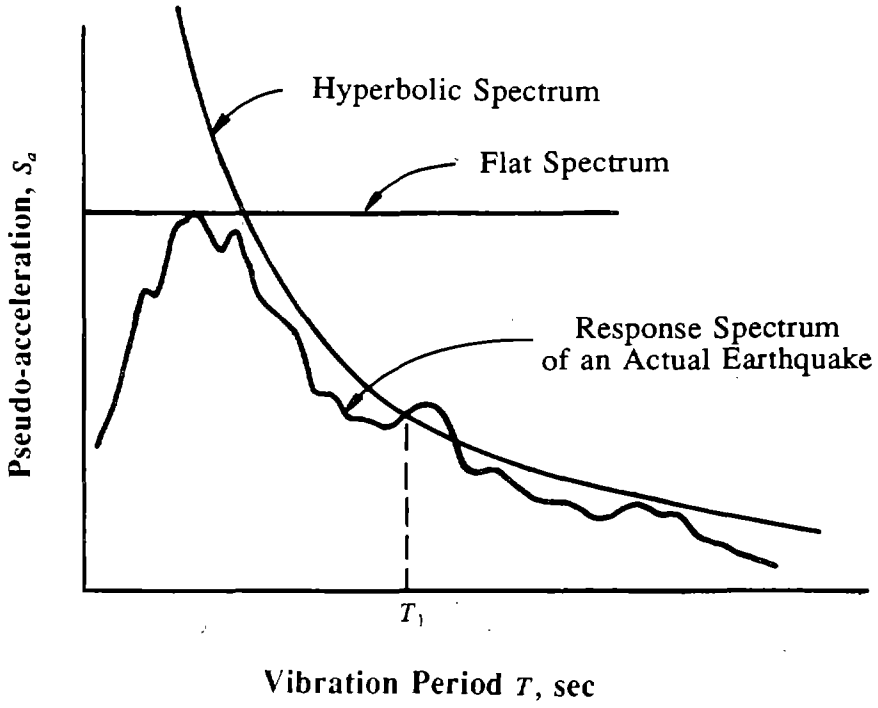

FIGURE 2 Flat and Hyperbolic Response Spectra

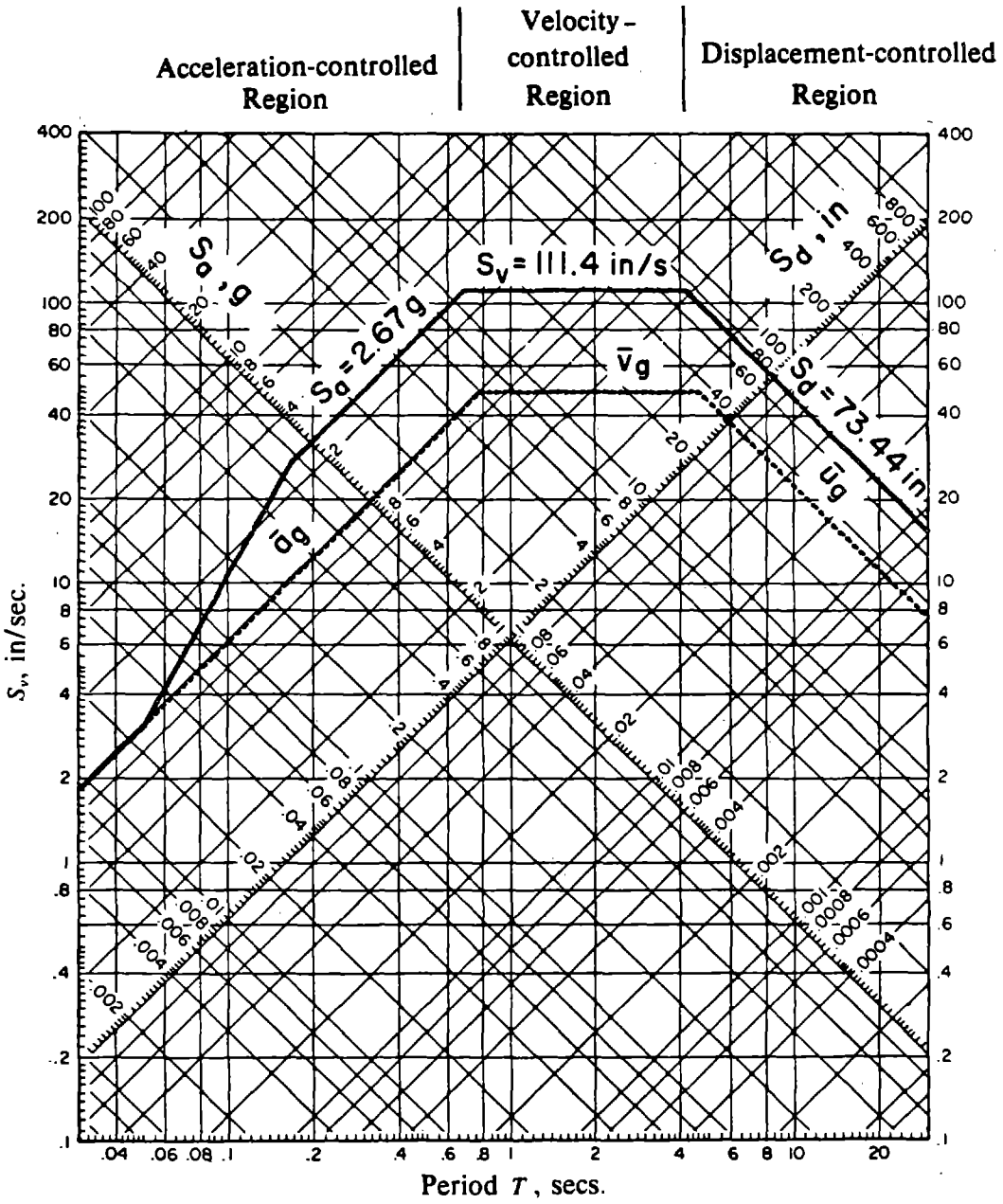

FIGURE 3 Design Spectrum for Ground Motions with Maximum Ground Acceleration $\bar{a}_g = 1g$, Velocity $\bar{v}_g$ = 48 in/sec and Displacement $\bar{u}_g$ = 36 in; Damping = 5 %

of long-period structures by ground displacement. The obtained spectrum can thus be subdivided into three regions: the acceleration-controlled region, the velocity-controlled region and the displacement-controlled region.

The design spectrum of Figure 3 is replotted in Figure 4 as a normalized pseudo-acceleration spectrum to emphasize that the spectral acceleration is constant (flat spectrum) in part of the acceleration-controlled region, and varies as $1/T$ (hyperbolic spectrum) in the velocity-controlled region.

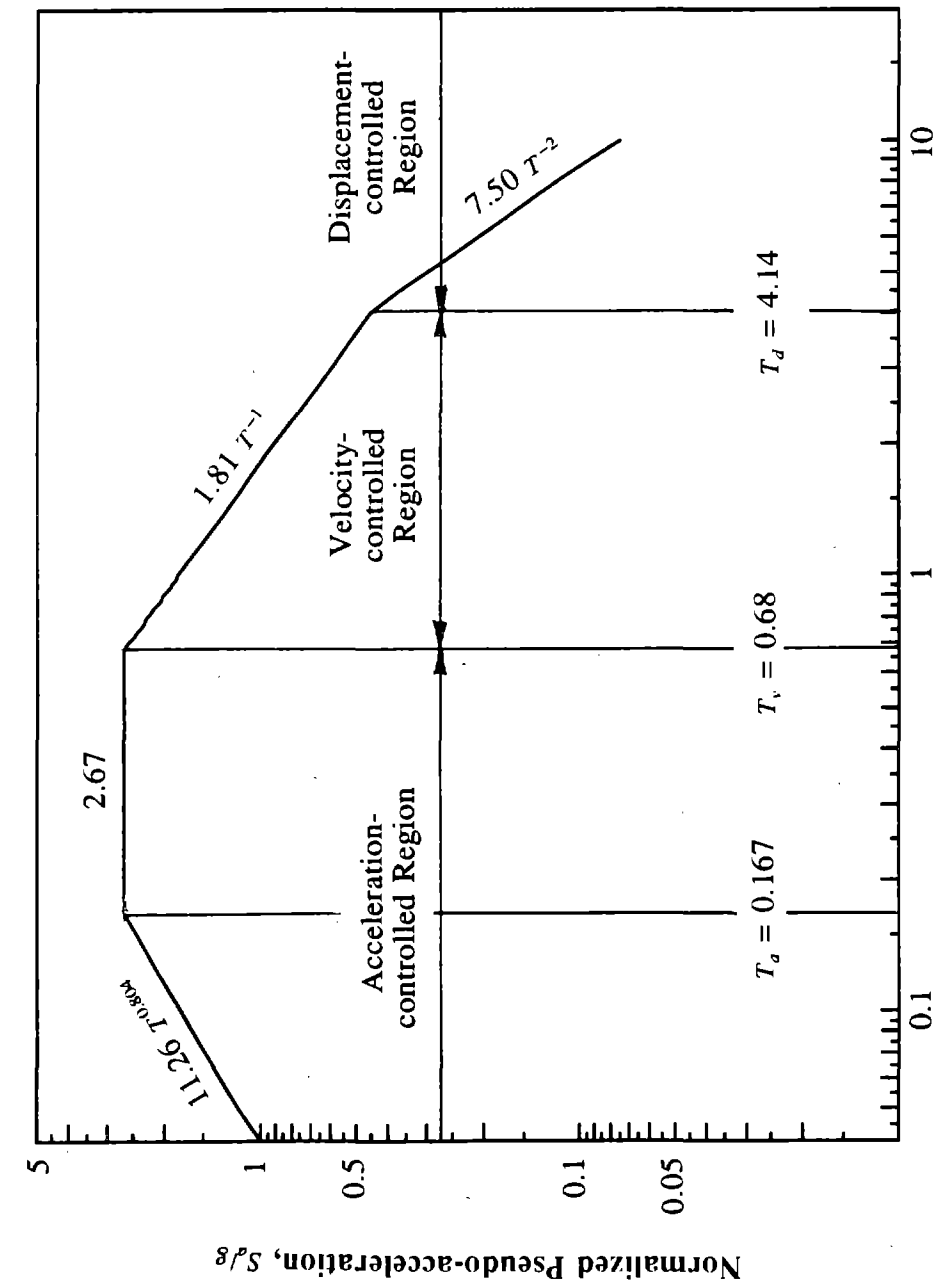

FIGURE 4 Normalized Pseudo-acceleration Design Spectrum

3. EQUATIONS OF MOTION

Due to the rigidity of the deck and symmetry of the mass and stiffness distributions about the X-axis, the single-story system has only two dynamic degrees of freedom: translational displacement u_y of the center of mass (CM) of the deck along the Y- axis, relative to the ground, and the rotation u_θ of the deck about a vertical axis. The equations of motion governing $\mathbf{u}$, the vector of system degrees of freedom defined by $\mathbf{u}^T = < u_y \; r u_\theta >$, where r is the radius of gyration of the floor about a vertical axis passing through its CM, will be developed in this section.

The building stiffness matrix, $\mathbf{K}$, is the sum of the resisting element stiffness matrices, $\mathbf{K}_i$, both developed for degrees of freedom $\mathbf{u}$:

$$\mathbf{K} = \sum_i \mathbf{K}_i \tag{3.1}$$

Frames and shear walls are assumed to contribute to system lateral stiffness only along the directions of their own planes. Shear deformations are negligible for frame members so that only flexural deformations are considered for frames. Columns contribute to system lateral stiffnesses along both the X- and Y- axes. Because the individual torsional stiffnesses of frames, shear walls and columns are negligible, the contributions of these resisting elements to the torsional stiffness of the building are primarily due to the lateral stiffnesses of these resisting elements. On the other hand, the torsional stiffness of a core element is significant, and its contribution to the torsional stiffness of the building is due to its torsional stiffness as well as to its lateral stiffnesses along the X and Y axes.

The stiffness matrix $\mathbf{K}_i$ of the i^{th} resisting element is determined by the following procedure:

1. Define the local degrees of freedom for each resisting element (Figure 1b) as follows:

   (a) For a shear wall define one translational degree of freedom at the floor level, along the plane of the shear wall, (X- or Y- axis), and a rotational degree of freedom about the horizontal axis perpendicular to its plane, (Y- or X- axis).

(b) For a frame define one translational degree of freedom at the floor level, along the plane of the frame, (X- or Y- axis), and a rotational degree of freedom per joint about horizontal axes perpendicular to the plane of the frame, (Y- or X- axis).

(c) For a column define two translational degrees of freedom at the floor level along the X- and Y- axes and two rotational degrees of freedom about the X- and Y- axes.

(d) For a core define five degrees of freedom: two translations along the principal axes of the core, two rotations about these axes, and one torsional rotation about a vertical axis passing through the shear center of the core.

2. Obtain a complete stiffness matrix for the resisting element for the degrees of freedom defined, taking into account flexural and shear deformations for shear walls and cores, and only flexural deformations for frames and columns.

3. Eliminate the joint rotational degrees of freedom of the resisting elements by the static condensation process. The resulting condensed matrix, $\mathbf{k}_i$, of a core element 'i' is diagonal and of dimension equal to three, satisfying the following equation:

$$\mathbf{Q}_i = \begin{Bmatrix} Q_{xi} \\ Q_{yi} \\ Q_{\theta i} \end{Bmatrix} = \begin{bmatrix} k_{xi} & 0 & 0 \\ 0 & k_{yi} & 0 \\ 0 & 0 & k_{\theta i} \end{bmatrix} \begin{Bmatrix} v_{xi} \\ v_{yi} \\ v_{\theta i} \end{Bmatrix} = \mathbf{k}_i \, \mathbf{v}_i \tag{3.2}$$

where k_{xi} and k_{yi} are the lateral stiffnesses of the element along the two principal directions, X and Y, and $k_{\theta i}$ is the torsional stiffness of the core about a vertical axis passing through its shear center. The applied static forces Q_{xi}, Q_{yi} and $Q_{\theta i}$ and resulting displacements v_{xi}, v_{yi} and $v_{\theta i}$ in these three directions are related through k_{xi}, k_{yi} and $k_{\theta i}$, respectively. Since $k_{\theta i}$ is negligible for columns, shear walls and frames, and k_{xi} is negligible for frames and shear walls oriented in the Y- direction, (k_{yi} is negligible for elements along the X- direction), equations (3.2) are simplified for these resisting elements. For columns, we obtain:

$$\mathbf{Q}_i = \begin{Bmatrix} Q_{xi} \\ Q_{yi} \end{Bmatrix} = \begin{bmatrix} k_{xi} & 0 \\ 0 & k_{yi} \end{bmatrix} \begin{Bmatrix} v_{xi} \\ v_{yi} \end{Bmatrix} = \mathbf{k}_i \, \mathbf{v}_i \tag{3.3}$$

For shear walls and frames oriented in the X- direction:

$$Q_{xi} = k_{xi}\, v_{xi} \tag{3.4a}$$

and for resisting elements oriented in the Y- direction:

$$Q_{yi} = k_{yi}\, v_{yi} \tag{3.4b}$$

4. Determine the transformation matrix, $\mathbf{a}_i$, relating the resisting element displacement vector, $\mathbf{v}_i$, to the system degrees of freedom, $\mathbf{u}$. For a core, $\mathbf{a}_i$ is given by:

$$\mathbf{v}_i = \begin{Bmatrix} v_{xi} \\ v_{yi} \\ v_{\theta i} \end{Bmatrix} = \begin{bmatrix} 0 & -y_i/r \\ 1 & x_i/r \\ 0 & 1/r \end{bmatrix} \begin{Bmatrix} u_y \\ ru_\theta \end{Bmatrix} = \mathbf{a}_i\, \mathbf{u} \tag{3.5}$$

where x_i and y_i are the X- and Y- coordinates of the shear center of a horizontal section of core 'i' relative to the CM of the system. Transformation matrix $\mathbf{a}_i$ of a column is given by:

$$\mathbf{v}_i = \begin{Bmatrix} v_{xi} \\ v_{yi} \end{Bmatrix} = \begin{bmatrix} 0 & -y_i/r \\ 1 & x_i/r \end{bmatrix} \begin{Bmatrix} u_y \\ ru_\theta \end{Bmatrix} = \mathbf{a}_i\, \mathbf{u} \tag{3.6}$$

where x_i and y_i are the X- and Y- distances of the column principal axes from the CM of the system. For frames and shear walls, with their planes parallel to the X- axis, $\mathbf{a}_i$ is obtained from:

$$v_{xi} = <\, 0 \quad -y_i/r\, > \begin{Bmatrix} u_y \\ ru_\theta \end{Bmatrix} = \mathbf{a}_i\, \mathbf{u} \tag{3.7}$$

where y_i is the distance of the frame or shear wall from the X- axis. Similarly, if the plane of the frame or shear wall is parallel to the Y- axis, $\mathbf{a}_i$ is given by:

$$v_{yi} = <\, 1 \quad x_i/r\, > \begin{Bmatrix} u_y \\ ru_\theta \end{Bmatrix} = \mathbf{a}_i\, \mathbf{u} \tag{3.8}$$

where x_i is the distance of the frame or shear wall from the Y- axis.

5. The contribution of resisting element 'i' to building stiffness matrix is $\mathbf{K}_i$, and is determined by:

$$\mathbf{K}_i = \mathbf{a}_i^T \mathbf{k}_i \mathbf{a}_i = \begin{bmatrix} K_{yi} & \frac{1}{r} K_{y\theta i} \\ \frac{1}{r} K_{\theta yi} & \frac{1}{r^2} K_{\theta i} \end{bmatrix} \tag{3.9}$$

where,

$$K_{yi} = k_{yi}$$

$$K_{y\theta i} = K_{\theta yi} = x_i \, k_{yi} \quad \text{and} , \tag{3.10}$$

$$K_{\theta i} = k_{\theta i} + x_i^2 \, k_{yi} + y_i^2 \, k_{xi}$$

As mentioned earlier, $k_{\theta i}$ is negligibly small for all types of resisting elements except cores, and that either k_{xi} or k_{yi} is negligible for frames and shear walls, depending on their orientations.

Using equation (3.1), the building stiffness matrix, **K**, for degrees of freedom **u**, is given by:

$$\mathbf{K} = \begin{bmatrix} K_y & \frac{1}{r} K_{y\theta} \\ \frac{1}{r} K_{\theta y} & \frac{1}{r^2} K_{\theta} \end{bmatrix} \tag{3.11}$$

with,

$$K_y = \sum_i K_{yi} = \sum_i k_{yi}$$

$$K_{y\theta} = K_{\theta y} = \sum_i K_{y\theta i} = \sum_i x_i \, k_{yi} \quad \text{and} , \tag{3.12}$$

$$K_{\theta} = \sum_i K_{\theta i} = \sum_i (\, k_{\theta i} + x_i^2 \, k_{yi} + y_i^2 \, k_{xi} \,)$$

The center of rigidity (CR) of a single-story system is the point on the rigid deck through which the application of a horizontal static force causes pure translation of the deck without any twist. Also, a static torsional moment about a vertical axis causes pure twist of the floor about the vertical axis passing through the CR. These two properties of the CR legitimize the use of different terminology for the same point, e.g. center of resistance, center of stiffness, center of twist, center

of rotation, center of torsion, shear center, ...etc.. Utilizing either one of these two properties, the distance between the CR and the CM of the floor of the single-story building, usually referred to as static eccentricity, can be shown to be:

$$e = \frac{K_{y\theta}}{K_y} = \frac{\sum_i x_i \, k_{yi}}{\sum_i k_{yi}} \tag{3.13}$$

The building mass matrix for degrees of freedom **u** is:

$$\mathbf{M} = \begin{bmatrix} m & 0 \\ 0 & m \end{bmatrix} \tag{3.14}$$

where m is the mass of the floor.

The undamped equations of motion for the single-story system, assuming linear behaviour, subjected to earthquake ground motion acceleration, $a_{gy}(t)$, along the Y- axis, are:

$$\begin{bmatrix} m & 0 \\ 0 & m \end{bmatrix} \begin{Bmatrix} \ddot{u}_y(t) \\ r\ddot{u}_\theta(t) \end{Bmatrix} + \begin{bmatrix} K_y & \frac{e}{r} K_y \\ \frac{e}{r} K_y & \frac{1}{r^2} K_\theta \end{bmatrix} \begin{Bmatrix} u_y(t) \\ r u_\theta(t) \end{Bmatrix} = -m \begin{Bmatrix} 1 \\ 0 \end{Bmatrix} a_{gy}(t) \tag{3.15}$$

It is apparent from these equations of motion that translational ground motion along the Y- axis will simultaneously cause both Y- lateral displacement of the CM as well as torsional rotation of the floor about a vertical axis.

Alternatively, the equations of motion can be written for degrees of freedom $\mathbf{v}^T = < v_y \; r u_\theta >$, where v_y is the lateral displacement at the CR, along the Y- axis, relative to the ground. Simple transformation of equations (3.15), yields:

$$\begin{bmatrix} m & -m\frac{e}{r} \\ -m\frac{e}{r} & m[1 + (e/r)^2] \end{bmatrix} \begin{Bmatrix} \ddot{v}_y(t) \\ r\ddot{u}_\theta(t) \end{Bmatrix} + \begin{bmatrix} K_y & 0 \\ 0 & \frac{1}{r^2} K_{\theta R} \end{bmatrix} \begin{Bmatrix} v_y(t) \\ r u_\theta(t) \end{Bmatrix} = -m \begin{Bmatrix} 1 \\ -e/r \end{Bmatrix} a_{gy}(t) \tag{3.16}$$

where,

$$K_{\theta R} = K_\theta - e^2 K_y \tag{3.17}$$

Clearly, if the static eccentricity, e, is zero, equations (3.15) and (3.16) become identical and also become uncoupled. In this case, the earthquake ground motion only causes lateral displacement governed by the first uncoupled equation:

$$m\,\ddot{v}_{yo}(t) + K_y v_{yo}(t) = -m\,a_{gy}(t) \quad \text{or} \quad \ddot{v}_{yo}(t) + \omega_y^2\, v_{yo}(t) = -\,a_{gy}(t) \tag{3.18}$$

in which,

$$\omega_y = \sqrt{\frac{K_y}{m}} \tag{3.19}$$

is the lateral vibration frequency of the corresponding uncoupled system. The second uncoupled equation leads to the torsional vibrational frequency of the corresponding torsionally-uncoupled system:

$$\omega_\theta = \sqrt{\frac{K_{\theta R}}{mr^2}} = \sqrt{\frac{K_\theta}{mr^2} - \left(\frac{e}{r}\right)^2 \omega_y^2} \tag{3.20}$$

The uncoupled system is obtained from the actual system by shifting its mass so that the CM coincides with the CR, without modifying the locations of the resisting elements (Figure 5).

Two other definitions of the uncoupled torsional vibration frequency were given in earlier investigations: $\sqrt{K_\theta / mr^2}$ in reference [3], and $\sqrt{K_{\theta R} / m\,(e^2 + r^2)}$ in references [7] and [9], for example. These are derived from equations (3.15) and (3.16), respectively, by neglecting the off-diagonal terms of these equations. The frequency $\sqrt{K_\theta / mr^2}$ can physically be interpreted as the uncoupled torsional vibration frequency of a system with coincident centers of mass and rigidity but with torsional stiffness at its center of rigidity equal to K_θ rather than $K_{\theta R}$, which implies a modified configuration of resisting elements compared to the actual coupled system. On the other hand $\sqrt{K_{\theta R} / m\,(e^2 + r^2)}$ is the uncoupled torsional vibration frequency of a system with coincident centers of mass and rigidity but with radius of gyration defined at its center of mass equal to $\sqrt{e^2 + r^2}$ rather than r, which implies modified mass properties. Therefore, both of these definitions

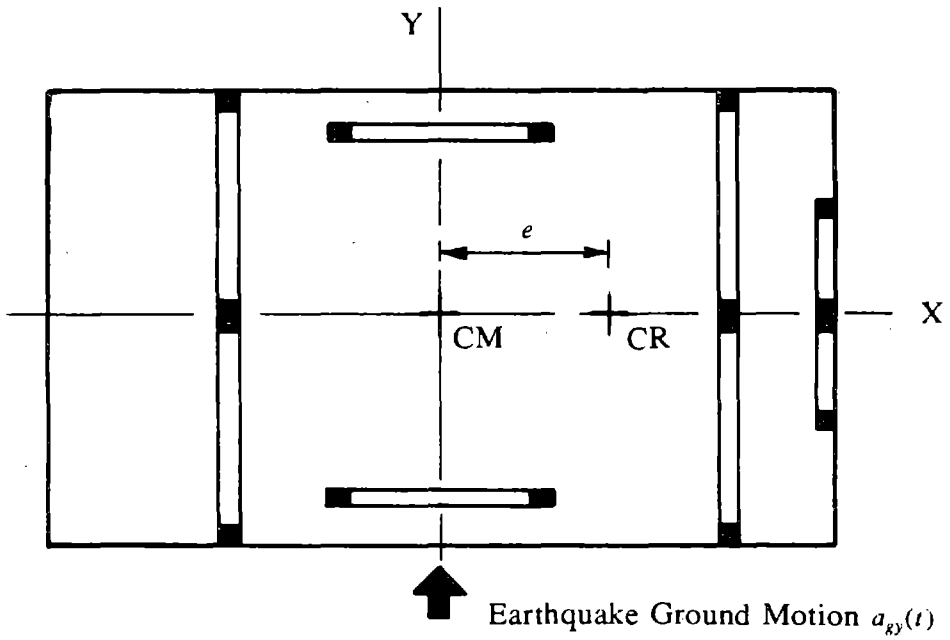

(a) Coupled Building

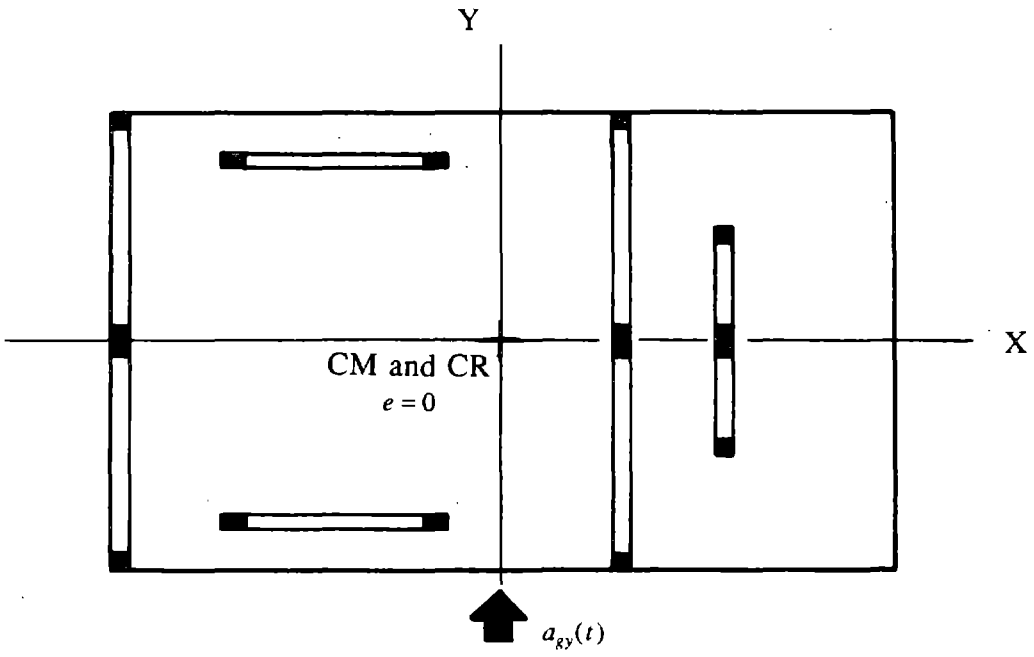

(b) Corresponding Uncoupled System

FIGURE 5 Torsionally-coupled Building and its Corresponding Uncoupled System

for the uncoupled torsional vibration frequency imply modification in either the stiffness or mass properties of the actual coupled system. Hence, the definition of equation (3.20) is preferred since it is the torsional frequency of an uncoupled system that has the same resisting elements configuration and mass distribution as the coupled system (Figure 5).

The undamped equations of motion of equations (3.15) are simplified to become:

$$\begin{Bmatrix} \ddot{u}_y(t) \\ r\ddot{u}_\theta(t) \end{Bmatrix} + \omega_y^2 \begin{bmatrix} 1 & e/r \\ e/r & \Omega^2 + (e/r)^2 \end{bmatrix} \begin{Bmatrix} u_y(t) \\ ru_\theta(t) \end{Bmatrix} = - \begin{Bmatrix} 1 \\ 0 \end{Bmatrix} a_{gy}(t) \tag{3.21}$$

where,

$$\Omega = \frac{\omega_\theta}{\omega_y} \tag{3.22}$$

is the uncoupled torsional to lateral frequency ratio. Clearly, the coupled lateral-torsional response of the system to ground motion, $a_{gy}(t)$, will depend on the three system parameters: e/r , Ω and ω_y.

Damping is defined in each of the two natural modes of vibration of the system. The damping ratio, ξ, is assumed to be the same in each mode of vibration.

4. ANALYSIS PROCEDURE

The systems described in Section 2, with their equations of motion presented in Section 3, are analyzed using the standard Response Spectrum Analysis (RSA) method, by which the maximum earthquake response of the system can be estimated by the following procedure:

1. Define the smooth pseudo-acceleration design spectrum for the structure at the particular site.
2. Define the structural properties of the system

   (a) Compute the mass, m, of the deck

   (b) Compute the stiffnesses, K_y , $K_{y\theta}$ and K_θ, of the building using equations (3.12)

   (c) Determine the radius of gyration, r, of the deck about a vertical axis passing through its CM

   (d) Compute the static eccentricity, e, from equation (3.13), and the eccentricity ratio, e/r

   (e) Compute the uncoupled lateral and torsional frequencies, ω_y and ω_θ, using equations (3.19) and (3.20), and the uncoupled torsional to lateral frequency ratio, $\Omega = \omega_\theta/\omega_y$.

   (f) Estimate damping ratio, ξ. In this study ξ is chosen to be 5 % in each mode of vibration.
3. Solve the eigen problem

$$\begin{bmatrix} 1-(\frac{\omega}{\omega_y})^2 & e/r \\ e/r & \Omega^2+(e/r)^2-(\frac{\omega}{\omega_y})^2 \end{bmatrix} \begin{Bmatrix} \alpha_y \\ \alpha_\theta \end{Bmatrix} = \begin{Bmatrix} 0 \\ 0 \end{Bmatrix} \tag{4.1}$$

for the natural vibration frequencies and mode shapes of the system. We obtain:

$$\bar{\omega}_n \equiv \frac{\omega_n}{\omega_y} = \left[\frac{1+(e/r)^2+\Omega^2}{2} \pm \sqrt{[\frac{1+(e/r)^2-\Omega^2}{2}]^2+(e/r)^2\Omega^2} \right]^{1/2} \quad (n=1,2) \tag{4.2}$$

and,

$$\boldsymbol{\alpha}_n = \begin{Bmatrix} \alpha_{yn} \\ \alpha_{\theta n} \end{Bmatrix} = \frac{1}{\sqrt{(e/r)^2 + (1 - \bar{\omega}_n^2)^2}} \begin{Bmatrix} -e/r \\ 1 - \bar{\omega}_n^2 \end{Bmatrix} \quad (n=1,2) \tag{4.3}$$

where the mode shapes have been normalized so that:

$$\boldsymbol{\alpha}_n^T \boldsymbol{\alpha}_n = \alpha_{yn}^2 + \alpha_{\theta n}^2 = 1 \tag{4.4}$$

4. Compute the maximum response in individual modes of vibration repeating the following steps for each mode:

(a) Corresponding to period T_n ($= 2\pi/\omega_n$) and damping ratio, ξ, read the pseudo-acceleration ordinate, S_{an}, of the earthquake design spectrum

(b) Compute the displacement vector at the CM from:

$$\mathbf{u}_n = \begin{Bmatrix} u_{yn} \\ ru_{\theta n} \end{Bmatrix} = \frac{\alpha_{yn}}{\omega_n^2} \begin{Bmatrix} \alpha_{yn} \\ \alpha_{\theta n} \end{Bmatrix} S_{an} = \frac{\alpha_{yn}}{\omega_n^2} S_{an} \boldsymbol{\alpha}_n \tag{4.5}$$

The lateral displacement at the CR, v_{yn}, is given by:

$$v_{yn} = u_{yn} + \frac{e}{r}(ru_{\theta n}) = \frac{\alpha_{yn}^2}{\omega_y^2} S_{an} \tag{4.6}$$

(c) Compute the equivalent force vector, $\mathbf{f}_n$, which applied statically at the CM causes displacements u_{yn} and $ru_{\theta n}$, from:

$$\mathbf{f}_n = \begin{Bmatrix} f_{yn} \\ f_{\theta n} \end{Bmatrix} = m\ \alpha_{yn} \begin{Bmatrix} \alpha_{yn} \\ \alpha_{\theta n} \end{Bmatrix} S_{an} = m\ \alpha_{yn}\ S_{an}\ \boldsymbol{\alpha}_n \tag{4.7}$$

The equivalent static torsional moment actually is equal to $rf_{\theta n}$.

(d) Compute, by statics, the base shear, V_n, base overturning moment, M_n, and the base torque at the CM, T_{Mn}, from the external forces f_{yn} and $rf_{\theta n}$:

$$V_n = f_{yn} = W\ \alpha_{yn}^2 \frac{S_{an}}{g} = W_n^* \frac{S_{an}}{g} \tag{4.8}$$

$$M_n = h\, f_{yn} = h\, V_n \tag{4.9}$$

$$T_{Mn} = r\, f_{\theta n} = W\, r\, \alpha_{yn}\, \alpha_{\theta n}\, \frac{S_{an}}{g} \tag{4.10}$$

where W is the weight of the one-story building, h its story height, and W_n^* its effective weight in the nth mode of vibration, such that:

$$\frac{W_n^*}{W} = \alpha_{yn}^2 \quad \text{with} \quad \sum_{1}^{2} W_n^* = W \tag{4.11}$$

The base torque at the center of rigidity, T_{Rn}, is obtained from:

$$T_{Rn} = T_{Mn} - e\, V_n = W\, r\, \alpha_{yn} (\alpha_{\theta n} - \frac{e}{r}\, \alpha_{yn})\, \frac{S_{an}}{g} = e_n^*\, V_n \tag{4.12}$$

where e_n^* can be referred to as the effective eccentricity in the nth mode of vibration, satisfying:

$$\frac{e_n^*}{r} = \frac{\alpha_{\theta n}}{\alpha_{yn}} - \frac{e}{r} \tag{4.13}$$

It is seen later (Section 6) that it is meaningful to express T_{Rn} in terms of W_n^*. Substituting equations (4.8) into (4.12), we obtain:

$$T_{Rn} = e_n^*\, W_n^*\, \frac{S_{an}}{g} = (e_n^*\, \frac{W_n^*}{W})\, (W\, \frac{S_{an}}{g}) \tag{4.14}$$

(e) Compute the internal forces in structural members of a resisting element 'i' associated with the vector of lateral and rotational displacements, determined from $\mathbf{u}_n$ obtained in step 4 (b), by:

$$\mathbf{v}_{in} = \mathbf{a}_i\, \mathbf{u}_n \tag{4.15}$$

where the transformation $\mathbf{a}_i$ depends on the type of resisting element (equations (3.5) to (3.8)). The joint rotations of the resisting element, which were statically condensed out earlier, are computed from $\mathbf{v}_{in}$ using its complete stiffness matrix, defined earlier in Section 3. Internal

forces in each member of the resisting element are then computed using the stiffness of the member and its joint rotations and displacements.

5. Determine an estimate of the maximum, r, of a response quantity by combining its modal maxima, r_n, according to an appropriate combination rule. Since the vibrational frequencies of such systems may be closely spaced, the cross-corelation between modal responses can be significant. Thus, the combination rule used, should take this effect into account. A heuristically motivated combination rule that considers this effect [6,8], was utilized in earlier investigations of the dynamics of torsionally coupled systems [ex. 1,2,3]. The more recent Complete Quadratic Combination (CQC) rule [17], which leads to essentially identical results as the earlier rule, is utilized in this work. According to the CQC rule, an estimate of the maximum r of the response quantity can be obtained from:

$$r = \left[\sum_{n=1}^{2} \sum_{m=1}^{2} \gamma_{nm} \, r_n \, r_m \right]^{1/2} \tag{4.16}$$

where γ_{nm} is the cross-correlation factor between modes 'n' and 'm', and r_n and r_m are the modal maxima of the response quantity in modes 'n' and 'm', respectively. The cross-correlation factors, γ_{nm}, are, in general, functions of the duration and frequency content of the ground motion, as well as the natural frequencies and modal damping ratios of the system. For smooth earthquake response spectra, representative of broad-frequence-band excitations, for long earthquake durations compared to the natural periods of the system, and for equal modal damping ratios, ξ, γ_{nm} is approximated by [17]:

$$\gamma_{nm} = \frac{8\xi^2 (1 + q_{nm}) \, q_{nm}^{1.5}}{(1 - q_{nm}^2)^2 + 4\xi^2 \, q_{nm} (1 + q_{nm})^2} \tag{4.17}$$

in which,

$$q_{nm} = \frac{\omega_n}{\omega_m} \tag{4.18}$$

Equation (4.16) can be written as:

$$r = \left[r_1^2 + r_2^2 + 2\gamma_{12} r_1 r_2 \right]^{1/2} \tag{4.19}$$

in which the first two terms represent the well-known combination rule: the Square-Root of the Sum of Squares (SRSS) of the modal maxima. The last term accounts for the cross-correlation between modes '1' and '2', and is especially important when the natural frequencies ω_1 and ω_2 are close to each other. In computing the modal maxima r_n from step 4, using equations (4.5) to (4.12), ..etc., r_n, the algebraic sign obtained for r_n should be retained. The last term in equation (4.19) assumes positive or negative values depending on whether r_1 and r_2 have the same or opposite algebraic signs.

In order to facilitate the subsequent interpretation of the effects of lateral-torsional coupling, the lateral displacement at the CR, v_y, the base shear, V, the base overturning moment, M, and the base torque at the CR, T_R, are expressed in normalized form:

$$\bar{v} = \frac{v_y}{v_{yo}} \quad , \quad \bar{V} = \frac{V}{V_o} \quad , \quad \bar{M} = \frac{M}{M_o} \quad \text{and} \quad \frac{e_d}{r} \equiv \bar{T}_R = \frac{T_R}{r\,V_o} \tag{4.20}$$

where v_{yo} , V_o and M_o are the maximum lateral displacement, base shear, and base overturning moment, of the corresponding torsionally-uncoupled system, defined earlier, with coincident centers of mass and rigidity, but all other properties identical to the actual system. The maximum uncoupled quantities are determined from:

$$v_{yo} = \frac{S_{ay}}{\omega_y^2} \, , \; V_o = m\, S_{ay} \quad \text{and} \quad M_o = m\, h\, S_{ay} \tag{4.21}$$

where S_{ay} is the pseudo-acceleration response spectrum ordinate corresponding to lateral vibration period ($T_y = 2\pi/\omega_y$) and damping ratio ξ of the uncoupled system.

The normalized quantity, $\bar{T}_R$, can be interpreted as the dynamic eccentricity, e_d, the distance from the CR of the system where the uncoupled base shear should be applied statically to cause a base torque equal to T_R at the CR of the system [3,7]. The ratio e_d/e then represents the dynamic amplification of the static torque eV_o. This definition of e_d is preferred over others [7] as it is akin

to the concept underlying building code provisions for torsional forces.

The parameters controlling the normalized response quantities of equations (4.20) are identified by considering the contributions of the n^{th} vibration mode to these normalized response quantities, which can be determined from equations (4.6) to (4.10) and (4.21), leading to:

$$\bar{v}_n = \bar{V}_n = \bar{M}_n = \alpha_{yn}^2 \frac{S_{an}}{S_{ay}} = \frac{W_n^*}{W} \frac{S_{an}}{S_{ay}} \tag{4.22}$$

and,

$$\frac{e_{dn}}{r} = \bar{T}_{Rn} = \alpha_{yn} (\alpha_{\theta n} - \frac{e}{r} \alpha_{yn}) \frac{S_{an}}{S_{ay}} = \frac{e_n^*}{r} \frac{W_n^*}{W} \frac{S_{an}}{S_{ay}} \tag{4.23}$$

The ratio of spectral ordinates S_{an} and S_{ay} is dependent, generally, on the values of T_n and T_y and on the shape of the spectrum. However, S_{an}/S_{ay} depends at most on the ratio T_n/T_y for the flat or hyperbolic idealized spectra, described in Section 2; it is equal to one or to $\bar{\omega}_n \equiv \omega_n/\omega_y = T_y/T_n$ for the two spectra, respectively. Thus, it can be observed from equations (4.2),(4.3),(4.19),(4.22) and (4.23) that the normalized responses depend only on e/r , Ω and ξ in the case of the idealized flat and hyperbolic pseudo-acceleration spectra, and on e/r , Ω , ω_y (or T_y) and ξ in the case of arbitrary-shaped spectra.

5. VIBRATION FREQUENCIES AND MODE SHAPES

The natural frequencies, ω_n (n=1,2), of the coupled system, normalized by ω_y, the uncoupled lateral frequency, are given by equation (4.2) and plotted in Figure 6 against $\Omega = \omega_\theta/\omega_y$, the uncoupled torsional to lateral frequency ratio, for three values of the eccentricity ratio, e/r: 0.05, 0.4 and 1.0. Also included for comparison are the uncoupled frequencies ω_y and ω_θ, normalized by ω_y, in order to identify the effects of lateral-torsional coupling on the natural vibration frequencies.

It is apparent from Figure 6 that the uncoupled frequencies, ω_y and ω_θ, are upper and lower bounds of the coupled frequencies, so that as e/r increases the fundamental frequency decreases below ω_θ and ω_y, while the second frequency increases above ω_y and ω_θ. Naturally, the coupled frequencies are closest to the uncoupled ones for systems with smallest e/r values. For torsionally-flexible systems, (i.e. Ω below unity), ω_θ is the upper bound for ω_1, while ω_y is the lower bound for ω_2. On the other hand, for torsionally-stiff systems, (i.e. Ω above unity), ω_y is the upper bound for ω_1, while ω_θ is the lower bound for ω_2. For systems with closely spaced uncoupled frequencies, (i.e. Ω around unity), the coupled frequencies are closest to one another, with the closeness most pronounced for systems with smaller values of e/r. The system is unstable for Ω equal to zero, since, in this case, the fundamental frequency, ω_1, is zero.

The displaced position of the deck of the structure vibrating in the n^{th} mode of vibration is shown in Figure 7. The lateral displacement at the CM equals α_{yn} while that at the CR equals $\alpha_{yn}\,\bar{\omega}_n^2$. The X-axis of symmetry rotates through an angle equal to $\alpha_{\theta n}/r$ about a point P at a distance $-r\alpha_{yn}/\alpha_{\theta n}$ from the CM. The lateral displacement at any point on the X-axis, located a distance x from the CM, is given by $\alpha_{yn} + (x/r)\,\alpha_{\theta n}$.

The lateral and torsional components, α_{yn} and $\alpha_{\theta n}$, of the n^{th} vibration mode shape, are plotted in Figure 8 against Ω for the three values of e/r: 0.05, 0.4 and 1.0. As a result of the orthogonality property of the vibration modes, $\boldsymbol{\alpha}_1^T\,\boldsymbol{\alpha}_2 = 0$, it can be shown that $\alpha_{y1} = \alpha_{\theta 2}$ and $\alpha_{y2} = -\alpha_{\theta 1}$. Thus, the lateral component of one mode equals the torsional component of the other. As Ω increases, the lateral component, α_{y1}, of the fundamental mode increases and its torsional component, $\alpha_{\theta 1}$,

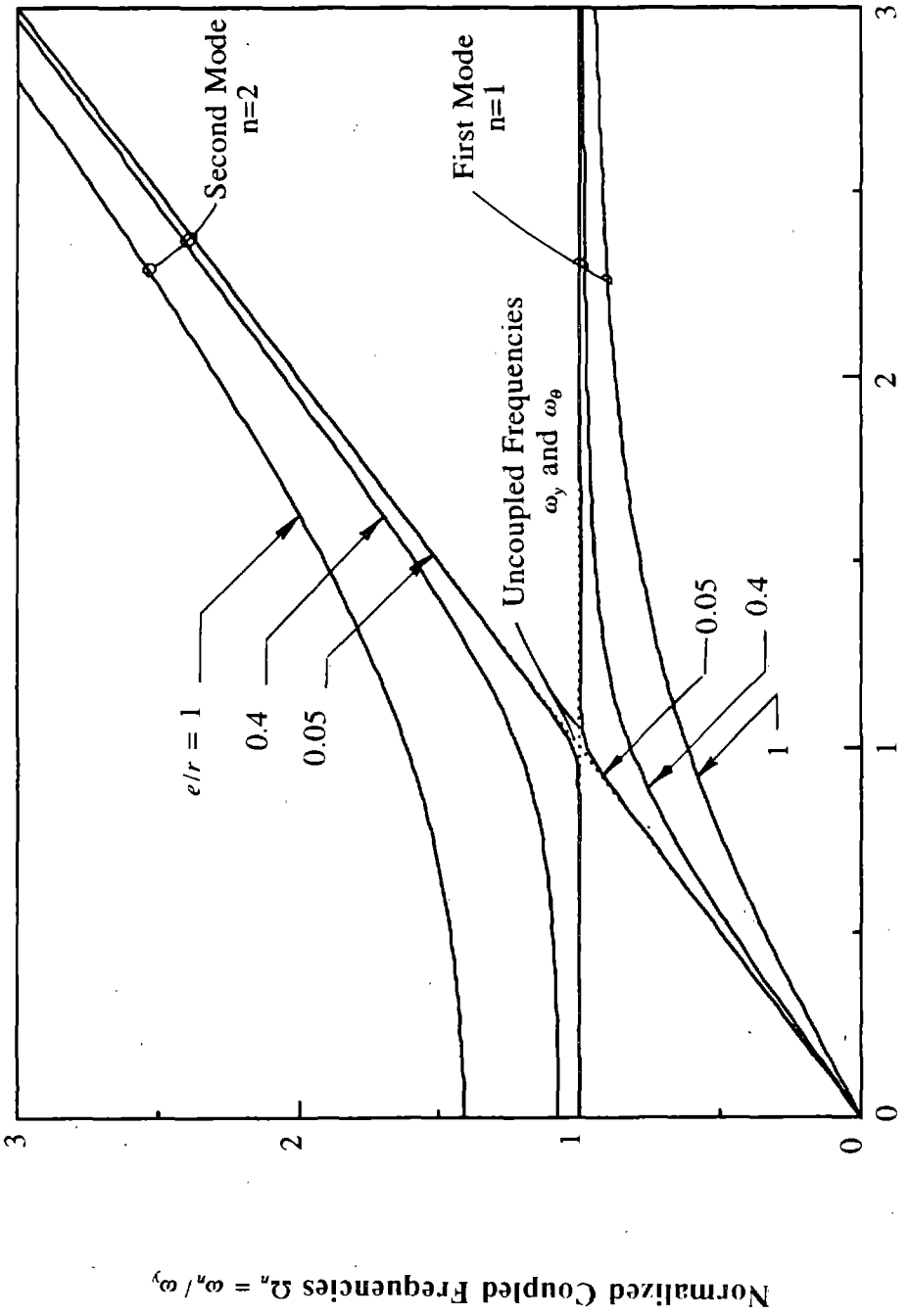

FIGURE 6 Natural Vibration Frequencies of Torsionally-coupled Building

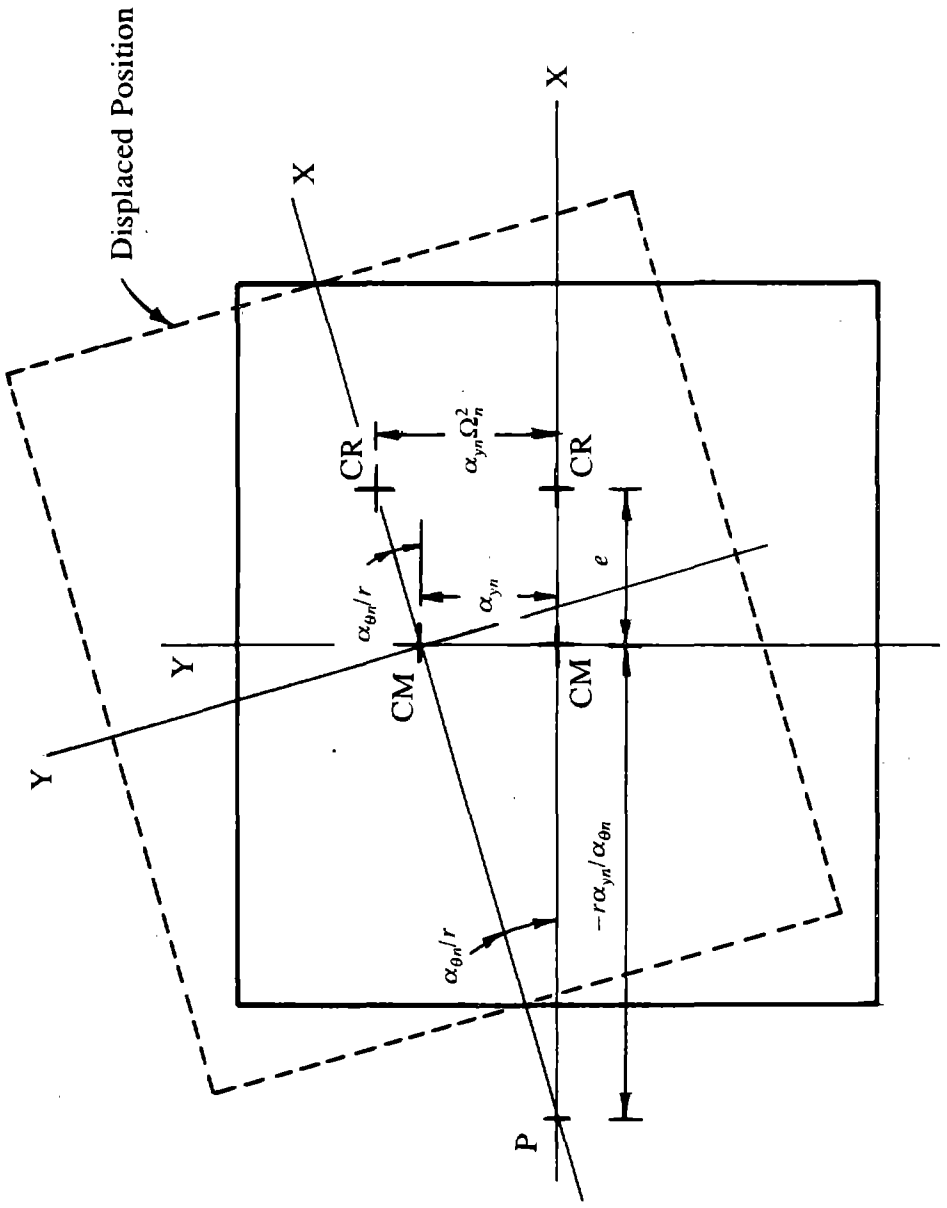

FIGURE 7 Displaced Position of Deck in the n^{th} Mode of Vibration

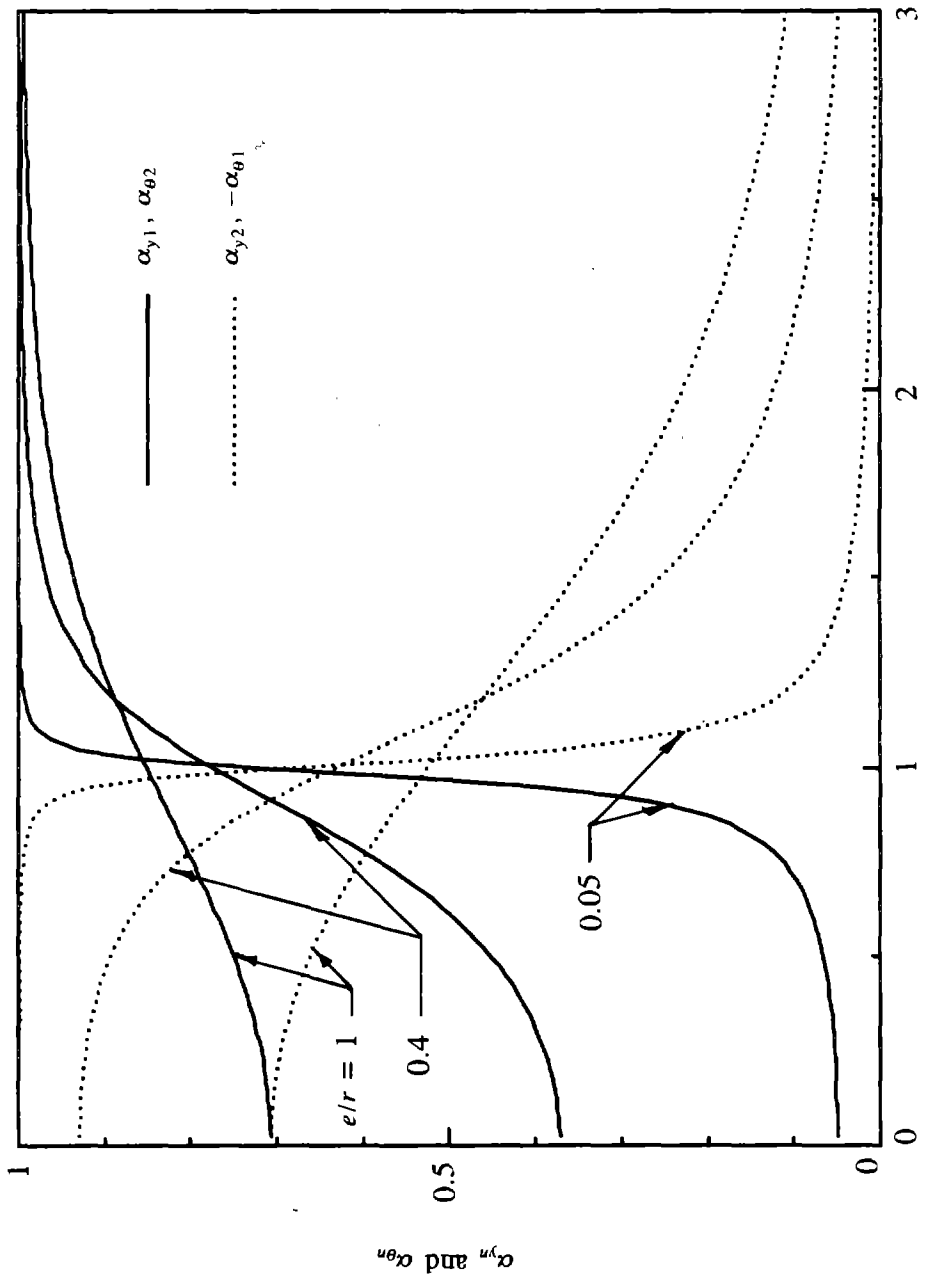

FIGURE 8 Lateral and Torsional Components α_{yn} and $\alpha_{\theta n}$, of Vibration Mode Shapes (n=1,2)

decreases. For torsionally-stiff ($\Omega > 1$) systems α_{y1} approaches unity and $\alpha_{\theta 1}$ approaches zero as Ω becomes large. Thus, in this case, the fundamental mode contains predominantly lateral motions and the second mode predominantly torsional motions. Torsionally-flexible ($\Omega < 1$) systems with smaller e/r ratios have smaller α_{y1} values than $\alpha_{\theta 1}$, but the modes are not predominantly lateral or torsional, unless e/r is very small. For systems with closely spaced uncoupled frequencies ($\Omega = 1$), the lateral and torsional motions are of comparable magnitude, especially for systems with small e/r.

The cross-correlation factor, γ_{12}, given in equation (4.17), is plotted in Figure 9 against Ω for various e/r values and for 5 % damping. The variation of γ_{12} is closely related to the spacing of ω_1 and ω_2. Since the two coupled frequencies are closest for systems with $\Omega = 1$ and small e/r values, γ_{12} is largest at $\Omega = 1$. For larger e/r values, the frequencies ω_1 and ω_2 are widely spaced for any value of Ω resulting in small γ_{12}. The cross-correlation term of equation (4.19) is, therefore, significant for systems with small e/r ratios and $\Omega = 1$, i.e. closely spaced uncoupled frequencies.

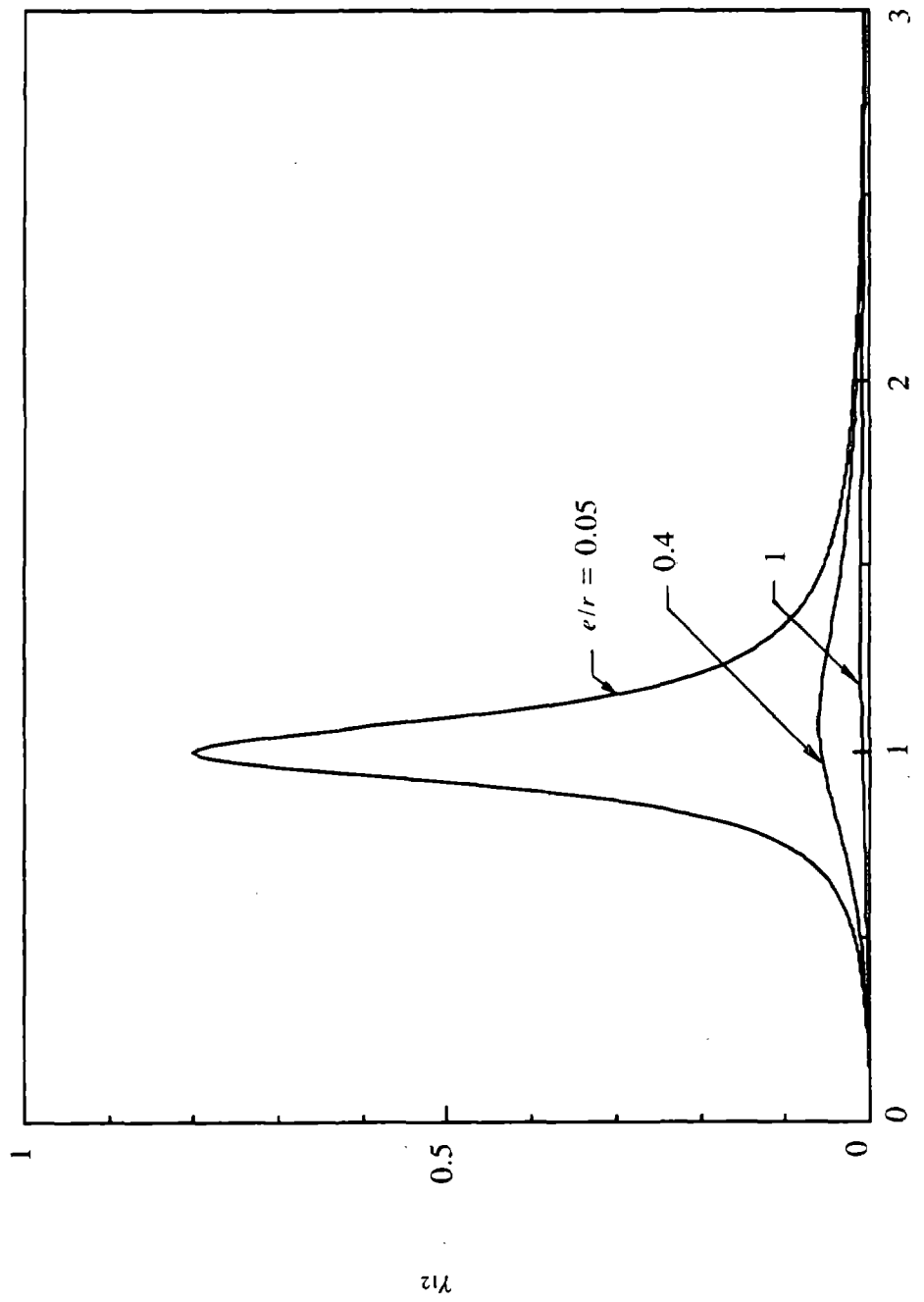

FIGURE 9 Cross-correlation Factor γ_{12} for 5 % Damping Ratio

6. EFFECT OF LATERAL-TORSIONAL COUPLING

The effect of lateral-torsional coupling on the response of one-story buildings to earthquake ground motion is investigated in this section. This is achieved by comparing the response of the torsionally-coupled building to the lateral response of the corresponding torsionally-uncoupled system for both the idealized (flat and hyperbolic) acceleration spectra and the general design spectrum of Figure 4.

Figure 10 shows the variations of the normalized base shear $\bar{V}$, (which also equals $\bar{v}$ and $\bar{M}$), and the dynamic eccentricity ratio e_d/r, (equations (4.20)), against the uncoupled frequency ratio Ω, for different e/r values, for flat and hyperbolic response spectra. For the corresponding torsionally-uncoupled system, $\bar{V} = 1$ and $e_d/r = 0$. The effect of lateral-torsional coupling is, therefore, measured by the deviation of $\bar{V}$ from unity and e_d/r from zero. The dynamic amplification of eccentricity is measured by the deviation of e_d/r from e/r; the latter is shown in Figure 10 by dashed lines.

The results of Figure 10 indicate that lateral-torsional coupling has the effect of reducing $\bar{V}$ and increasing e_d/r. These effects increase as e/r increases and are also dependent on Ω. For systems with smaller e/r values, $\bar{V}$ reaches its minimum value and e_d/r its maximum value, for values of Ω around unity, i.e. when the uncoupled lateral and torsional frequencies are close to each other. As e/r increases, $\bar{V}$ reaches its minimum values at values of Ω below unity, while e_d/r reaches its maxima for values of Ω above unity. For torsionally-stiff systems ($\Omega > 1$), $\bar{V}$ approaches unity as Ω becomes large, indicating that there is essentially no reduction in the base shear, while e_d/r approaches e/r, implying no dynamic amplification of eccentricity. For torsionally-flexible systems ($\Omega < 1$) with smaller e/r, there is little reduction in base shear. The dynamic eccentricity ratio, e_d/r, for torsionally-flexible systems ($\Omega < 1$) is less than e/r in the case of hyperbolic spectrum and approaches zero as Ω tends to zero, but e_d/r is almost equal to e/r in the case of flat spectrum, indicating no dynamic amplification.

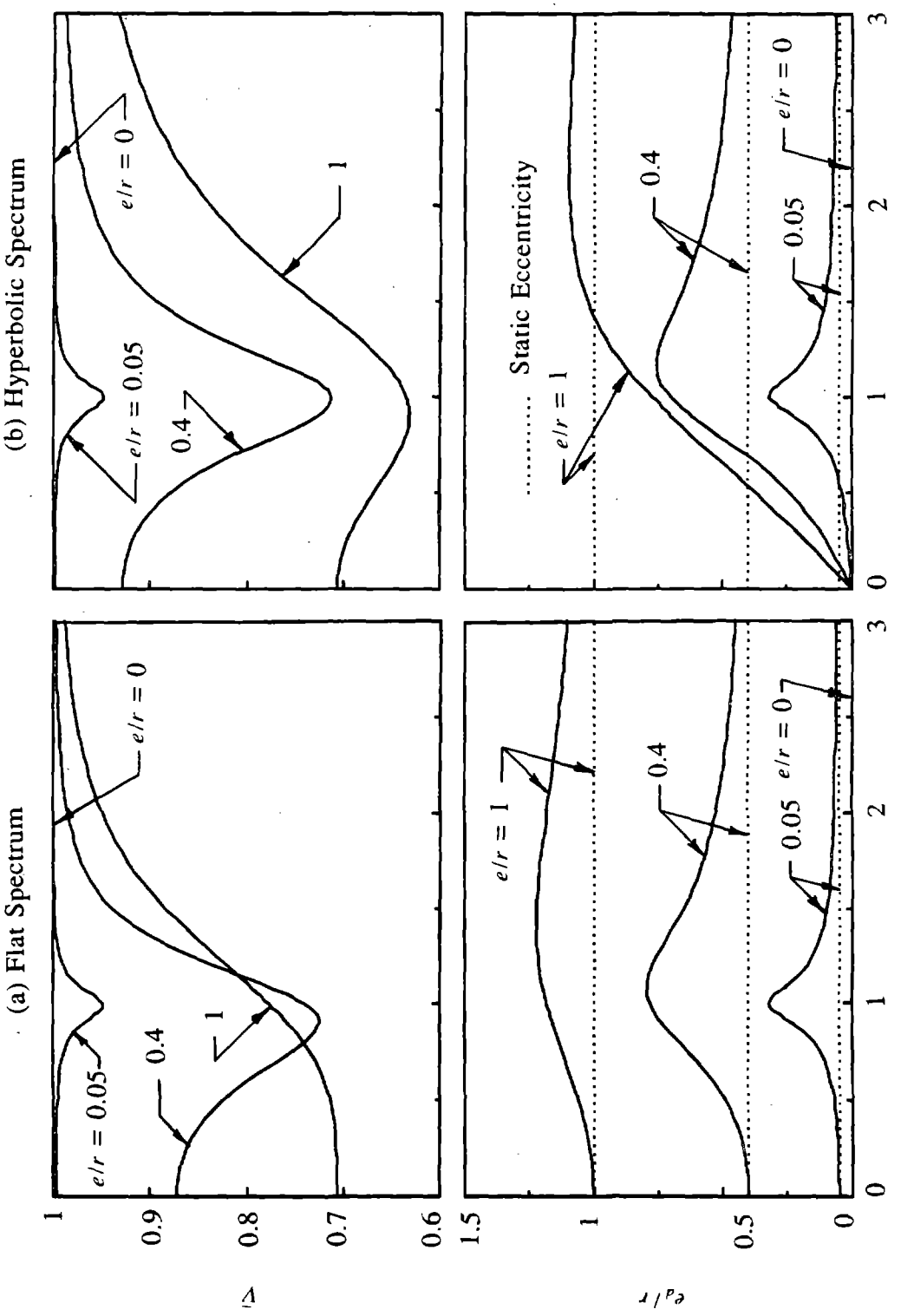

FIGURE 10 Normalized Base Shear $\bar{V}$ and Dynamic Eccentricity Ratio e_d/r for (a) Flat Spectrum and (b) Hyperbolic Spectrum; $\xi = 5\%$

Dynamic amplification of static eccentricity increases with decrease in e/r. For systems with smaller e/r ratios, dynamic amplification is most pronounced when the uncoupled frequencies are closely spaced, but for systems with larger e/r dynamic amplification is significant over a wider range of Ω below and above unity in the case of flat spectrum, and in the range of Ω above unity in the case of hyperbolic spectrum. However, the maximum dynamic amplification of static eccentricity is about the same for flat and hyperbolic spectra.

For arbitrary-shaped earthquake response spectra, the coupled lateral-torsional response of the structure depends on the uncoupled lateral vibration period T_y in addition to the system parameters e/r and Ω, which influenced the response of the structure in case of flat or hyperbolic spectra. In order to understand the role that T_y plays in structural response, $\bar{V}$ and e_d/e due to earthquake ground motion characterized by the design spectrum of Figure 4, are presented in Figures 11 and 12. Responses are presented as a function of Ω for different values of e/r ratios and two values of T_y equal to 0.25 and 2.5 sec. Also shown in these figures are $\bar{V}$ and e_d/e computed for the flat and hyperbolic spectra, to provide a basis for interpreting the response trends. The T_y values chosen, 0.25 and 2.5 sec, fall on the flat and hyperbolic branches of the spectrum of Figure 4, respectively.

Referring to Figure 11, the normalized base shear $\bar{V}$ for systems with small e/r is insensitive to the shape of the spectrum or to T_y. As e/r increases, $\bar{V}$ computed for the general spectrum follows either that determined for the flat or that for the hyperbolic spectrum depending on T_y. If T_y is in the acceleration-controlled region, (or the flat portion of the spectrum), $\bar{V}$ for the spectrum of Figure 4 is essentially the same as that for the flat spectrum, while if T_y is in the velocity-controlled region, (or the hyperbolic portion of the spectrum), $\bar{V}$ is essentially the same for the arbitrary and hyperbolic spectra. The deviations from the idealized curves increase with increase in e/r, and are relatively large for torsionally-flexible systems. The deviations are basically due to the coupled vibration periods of the system falling on different branches of the spectrum of Figure 4. As expected, based on Section 2, $\bar{V}$ due to flat and hyperbolic spectra are upper bounds of $\bar{V}$ for the general spectrum.

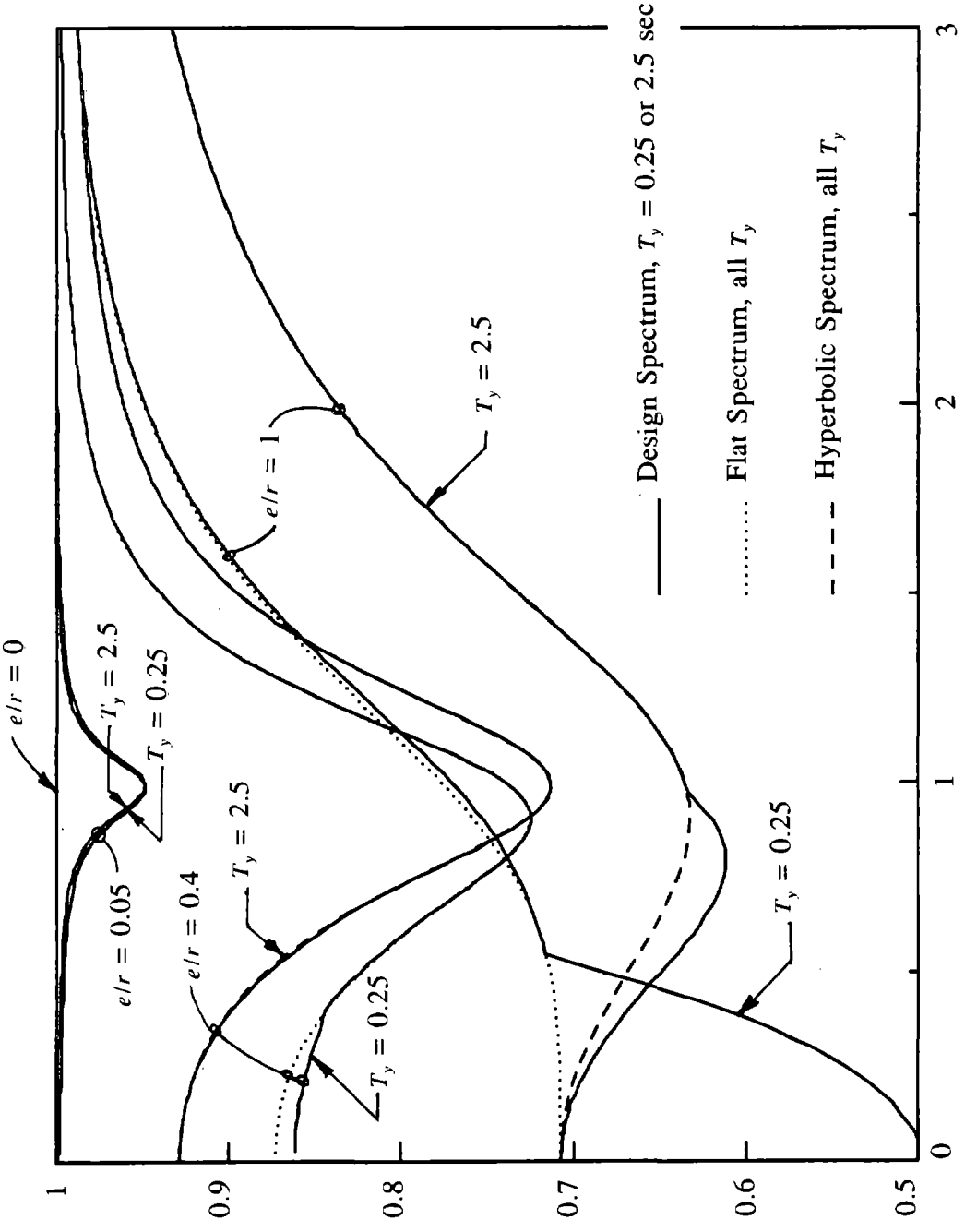

FIGURE 11 Normalized Base Shear $\bar{V}$ for Three Response Spectra; ξ = 5%

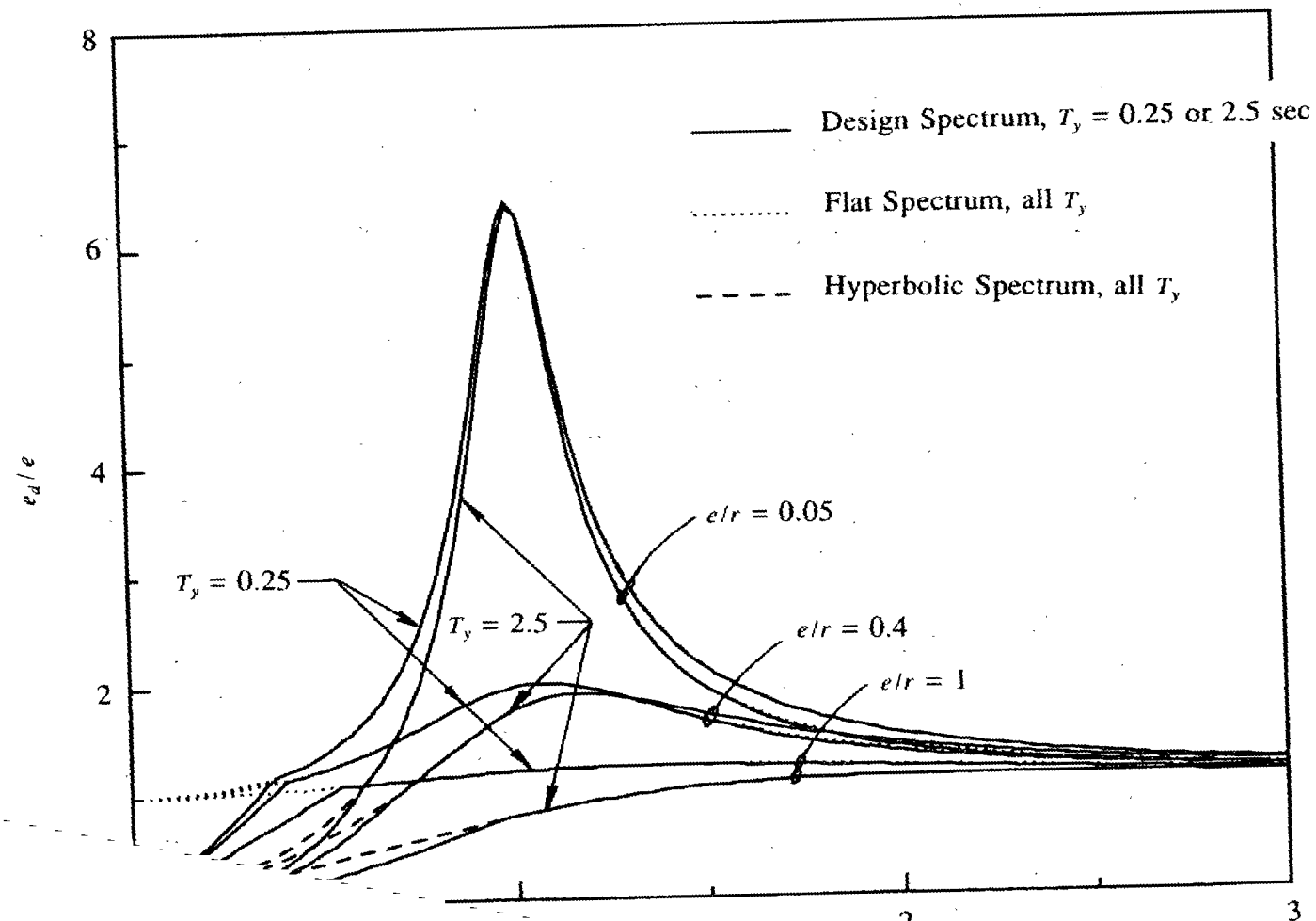
8
6
4
2
e_d / e
Design Spectrum, T_y = 0.25 or 2.5 sec
Flat Spectrum, all T_y
Hyperbolic Spectrum, all T_y
e/r = 0.05
e/r = 0.4
e/r = 1
T_y = 0.25
T_y = 2.5
2
3

Referring to Figure 12, the dynamic amplification of eccentricity, defined by $e_d/e = T_R/eV_o$, in systems subjected to ground motion characterized by the design spectrum of Figure 4 is essentially the same as that for the flat or the hyperbolic spectrum depending on T_y. The discrepancies occur for torsionally-flexible systems and are more pronounced for T_y equals 0.25 than 2.5 sec. This is because the base torque at the CR is dominated by the fundamental mode (see Appendix A), and for torsionally-flexible systems the fundamental vibration period is very long and falls on a different branch of the spectrum than T_y. As expected, based on Section 2, e_d/e due to flat and hyperbolic spectra are upper bounds of e_d/e for the general spectrum.

The maximum lateral displacements $v_y(x)$ of the symmetry axis of the building, normalized with respect to the lateral displacement v_{yo} of the corresponding torsionally-uncoupled system, are shown in Figure 13 for values of Ω equal to 0.5, 1.0 and 1.5, and values of e/r equal to 0.05, 0.4 and 1.0. The curves are computed using both idealized spectra, flat and hyperbolic, and the general design spectrum of Figure 4 for values of T_y equal to 0.25 and 2.5 sec. For systems with small e/r, the maximum lateral displacements of the symmetry axis are insensitive to the shape of the spectrum and are relatively close to the maximum lateral displacement v_{yo} for the corresponding uncoupled system. The base-shear plots of Figures 10 and 11 imply that for systems with larger e/r the maximum lateral displacement of the torsionally-coupled system at its CR ($x = e$) is smaller than v_{yo}, and this is confirmed by Figure 13. In contrast, the maximum lateral displacements at some other points on the symmetry axis may be larger than v_{yo}. The maximum lateral displacements at points on the symmetry axis on the flexible side of the building, (the side of the building opposite to where the CR lies relative to the CM, i.e. $x < e$), are generally larger than v_{yo}, increasing as x decreases below e and as e/r increases, being larger for torsionally-flexible systems compared to systems with closely spaced uncoupled frequencies or torsionally-stiff systems. The maximum lateral displacements at points of the symmetry axis on the stiff side of the building, (the side of the building where the CR lies relative to the CM, i.e. $x > e$), generally increase as x increases above e for torsionally-flexible systems and systems with closely spaced uncoupled frequencies, more so for the former, so that, in some cases, they become larger than v_{yo} as x increases over e. For

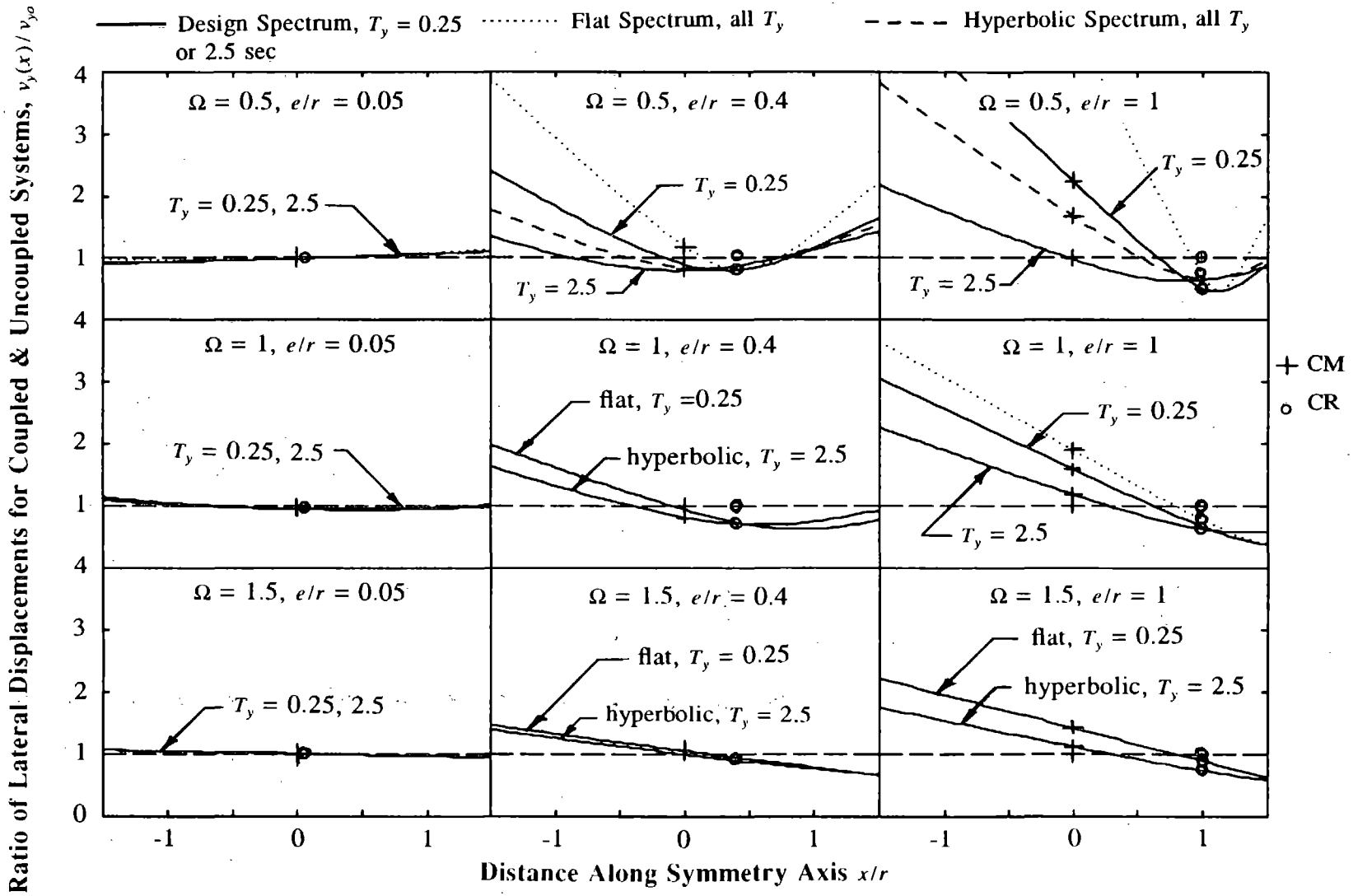

FIGURE 13 Maximum Lateral Displacements of Symmetry Axis of Building. Results are Presented for Combinations of Ω (0.5, 1 and 1.5) and e/r (0.05, 0.4 and 1) and for Three Response Spectra; ξ = 5%

torsionally-stiff systems, however, the maximum lateral displacements $v_y(x)$ vary linearly with x, decreasing as x increases, and are below v_{yo} for points on the stiff side of the building ($x > e$).

The maximum base shear, V, due to earthquake ground motion characterized by the design spectrum of Figure 4, is plotted against the uncoupled, lateral vibration period T_y in the form of response spectra (Figure 14). The value chosen to non-dimesionalize V is the maximum base shear for a rigid single-degree-of-freedom system with lumped weight W. Results are presented for Ω values equal to 0.5, 1.0 and 1.5 and e/r values of 0.05, 0.4 and 1.0. Also included in this figure for comparison is the normalized base shear V_o for the corresponding torsionally-uncoupled system, which is identical to the pseudo-acceleration spectrum. It is apparent that torsional coupling generally has the effect of reducing the base shear, with the amount of reduction depending on e/r and Ω, except for very short period systems with large e/r.

Figure 15 shows the base torque at the CR, T_R, normalized by $e_1^* W_1^* \bar{a}_g/g$, plotted against T_y in the form of a response spectrum for values of e/r equal to 0.05, 0.4 and 1, and for values of Ω equal 0.5, 1 and 1.5, due to ground motion characterized by the design spectrum of Figure 4. Referring to equation (4.14), the normalization factor chosen is the torque obtained if the maximum base shear $W\bar{a}_g/g$ of a rigid single-degree-of-freedom system of lumped weight W is applied at a distance $e_1^* W_1^*/W$, measured from the CR of the system. Also included in Figure 15 for comparison is the quantity $V_o(e_1^* W_1^*/W)$, the torque obtained if the base shear of the corresponding uncoupled system is applied at an eccentricity $e_1^* W_1^*/W$, also normalized by $e_1^* W_1^* \bar{a}_g/g$, i.e. $V_o g/W\bar{a}_g$, which is equivalent to the normalized pseudo-acceleration spectrum S_a/g. It is apparent from Figure 15 that, for torsionally-stiff systems, the normalized base torque spectrum is similar to the $V_o(e_1^* W_1^*/W)$ spectrum, although it is slightly underestimated by the latter for systems with smaller e/r, and overestimated for systems with larger e/r. For torsionally-flexible systems ($\Omega < 1$), the normalized base torque is considereably smaller than the pseudo-acceleration spectrum over a wide range of T_y in the acceleration-, velocity- and displacement-controlled regions of the spectrum, since the

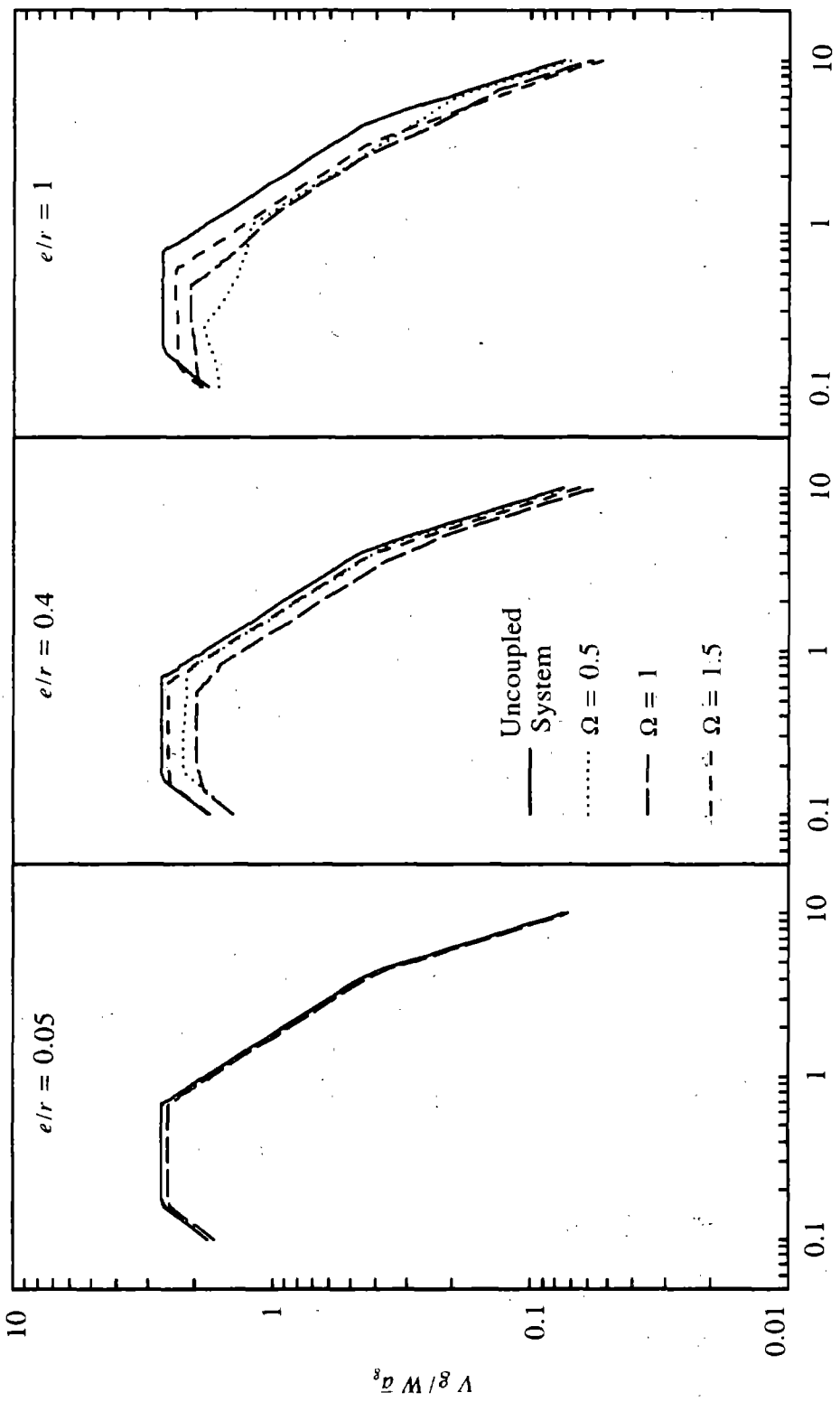

FIGURE 14 Normalized Base Shear Computed for Three Values of e/r and Ω; $\xi = 5\%$

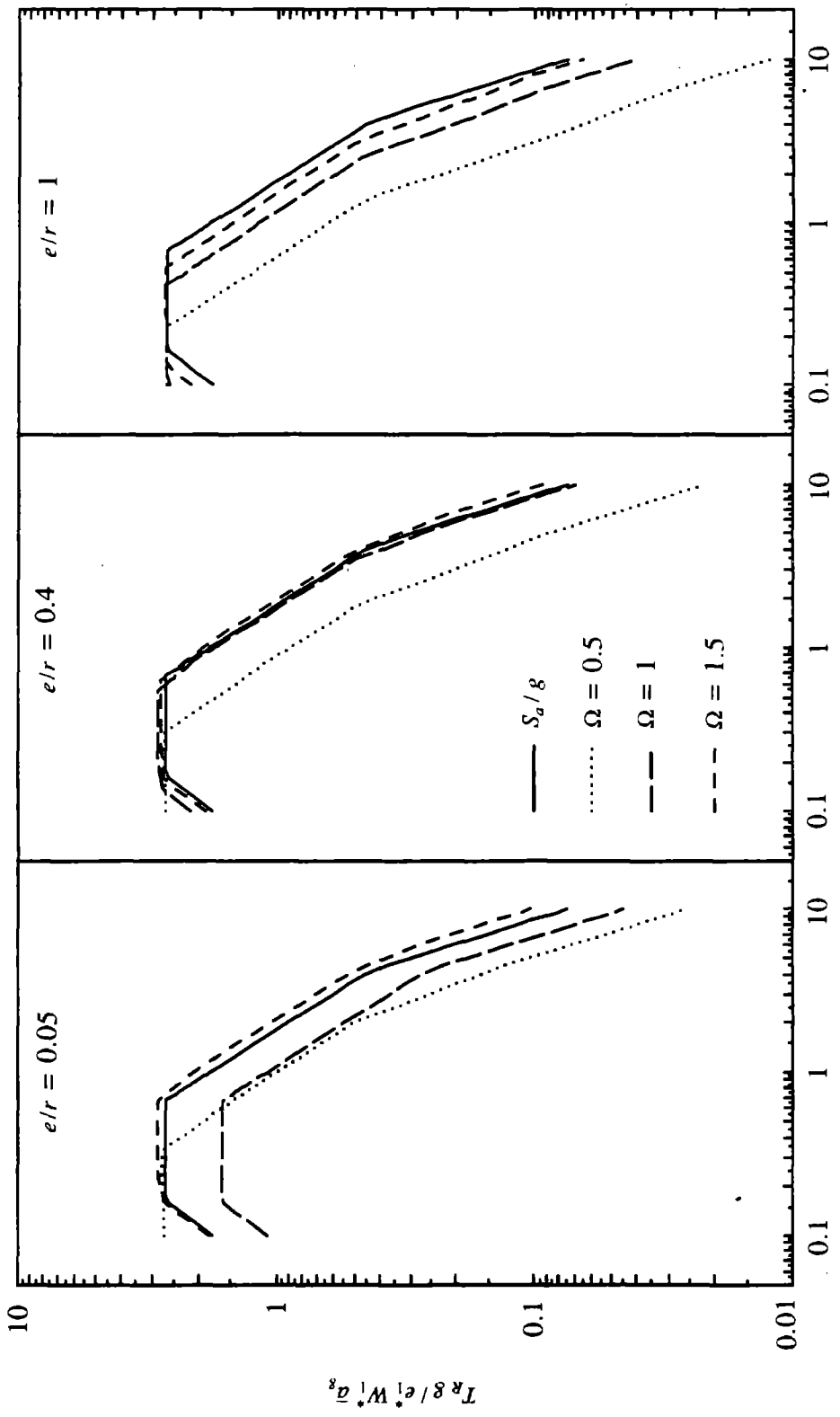

FIGURE 15 Normalized Base Torque at the CR Computed for Three Values of e/r and Ω; ξ = 5%

fundamental vibration period is much longer than T_y, causing its contribution to base torque to be small. On the other hand, the second mode contribution to base torque is significant for systems with small e/r and closely-spaced uncoupled frequencies (Appendix A), and the cross-correlation term for the base torque between the two modes is negative (Figure A.1), causing a reduction in the base torque, in this case, relative to $V_o e_1^* W_1^* / W$ in all regions of the spectrum.

Figure 16 shows v_y, the maximum lateral displacement at the CR, due to earthquake ground motion characterized by the design spectrum of Figure 4, normalized by the maximum ground displacement, $\bar{u}_g$, as a function of T_y for various values of e/r and Ω. Also shown in Figure 16 is v_{yo}, the maximum lateral displacement of the corresponding torsionally-uncoupled system, also normalized by $\bar{u}_g$. The variation of v_y with T_y follows that of v_{yo} with minimum discrepancies occuring for low e/r values. The variation with Ω is most pronounced for long-period systems with larger e/r values.

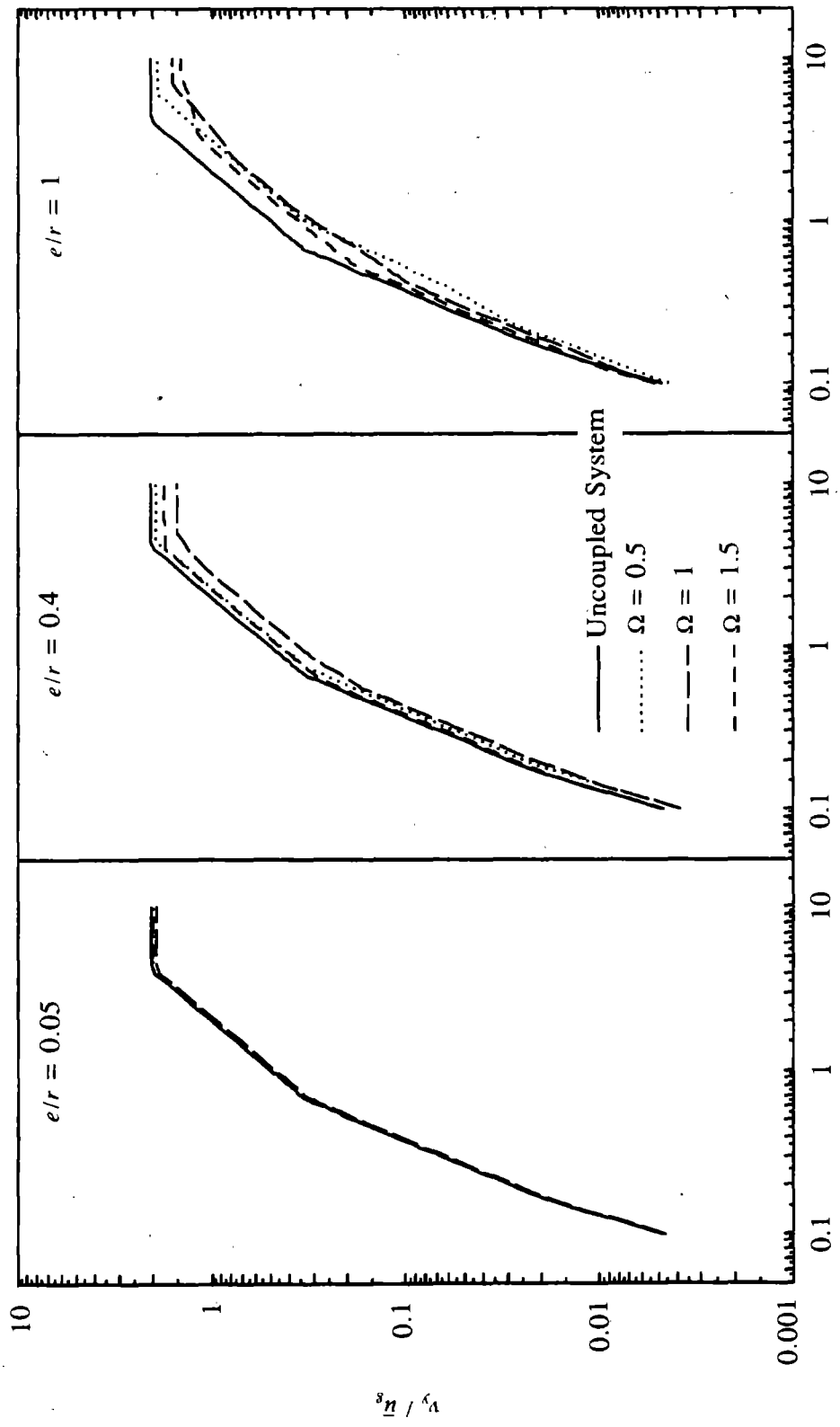

FIGURE 16 Normalized Lateral Displacement at the CR Computed for Three Values of e/r and Ω;

$\xi = 5\%$

7. EFFECT OF FRAME ACTION

The overall earthquake response of the system was shown in the previous sections to be influenced by the overall system parameters e/r , Ω and T_y (as well as by ξ and m, h or r). Therefore, the overall responses of two buildings with different floor plans and different types of resisting elements are identical provided these system parameters are the same for the two buildings. On the other hand, the local responses of the system, e.g. member forces in individual resisting elements, depend on the location of the element, whether it is a frame, shear wall, or shear-wall core, in addition to the overall parameters of the system. In particular, the forces in frame members depend, in part, on the degree of frame action.

The joint rotation index, ρ, of a frame, is defined as the ratio of the sum of the stiffnesses of all beams at the mid-height story of the frame to the summation of the stiffnesses of all the columns at the same story [18]. It is expressed by:

$$\rho = \frac{\sum_{beams} EI_b / L_b}{\sum_{columns} EI_c / L_c} \tag{7.1}$$

For a one-story, single-bay frame with column moment of inertia, I, bay width L and story height h, ρ becomes:

$$\rho = \frac{h}{2L} \frac{I_b}{I} \tag{7.2}$$

The parameter ρ is a measure of frame action. The limiting case $\rho = 0$ represents a flexural column with beams imposing no constraint to joint rotations, and the other limiting case $\rho = \infty$ represents a shear frame in which joint rotations are completely restrained and the deformations occur only through double curvature bending of the columns. Intermediate values of ρ represent frames with both beams and columns undergoing bending deformations with joint rotations.

To study the effect of frame action on local member forces, consider a frame spanning in the Y direction at a distance x from the CM of the building (Figure 1). The maximum lateral displacement of the frame $v_y(x)$, which is the combination of the contributions of the two vibration modes

of the building, depends on the system parameters e/r , Ω , T_y and ξ, as well as on x, but is independent of ρ. Member forces in the one-story frame are proportional to $v_y(x)$. For a single-bay frame with joint rotation index ρ, the frame base shear

$$V(x) = \frac{EI}{h^3} \frac{6(1+12\rho)}{1+3\rho} v_y(x) \tag{7.3}$$

The column base moment is given by:

$$M_c(x) = \frac{EI}{h^2} \frac{3(1+6\rho)}{1+3\rho} v_y(x) \tag{7.4}$$

and the beam moment, $M_b(x)$, and column axial force, $P_c(x)$, by:

$$M_b(x) = P_c(x) \frac{L}{2} = \frac{EI}{h^2} \frac{18\rho}{1+3\rho} v_y(x) \tag{7.5}$$

Figure 17 shows the variations of the proportionality constants of equations (7.3) to (7.5) as a function of ρ. As ρ decreases to zero, i.e. the beams become increasingly flexible, the beam moment and column axial force tend to zero while the base shear and column base moment tend to the corresponding values for cantilever columns, i.e. to $6EIv_y(x)/h^3$ and $3EIv_y(x)/h^2$, respectively. As ρ increases to infinity, $V(x)$, $M_c(x)$ and $M_b(x)$, and $P_c(x)$ tend to $24EIv_y(x)/h^3$, $6EIv_y(x)/h^2$ and $12EIv_y(x)/Lh^2$, respectively, the values for a shear building. Also it is apparent from Figure 17 that all member forces increase with increase in ρ, provided other parameters are kept constant.

As the member forces in a frame are proportional to the lateral displacement $v_y(x)$, their variation with positions x of the frame along the symmetry axis, can also be interpreted from Figure 13 presented earlier. It was shown that the lateral displacements of frames on the flexible and stiff sides of torsionally-flexible systems may be significantly larger than the lateral displacement of the corresponding torsionally-uncoupled system, and these displacements increase as e/r increases. The lateral displacements of frames on the flexible side of torsionally-stiff systems with large e/r, or systems with closely-spaced uncoupled frequencies may also be larger than in the uncoupled system. Therefore, the frames on either the flexible or the stiff side of the building may experience

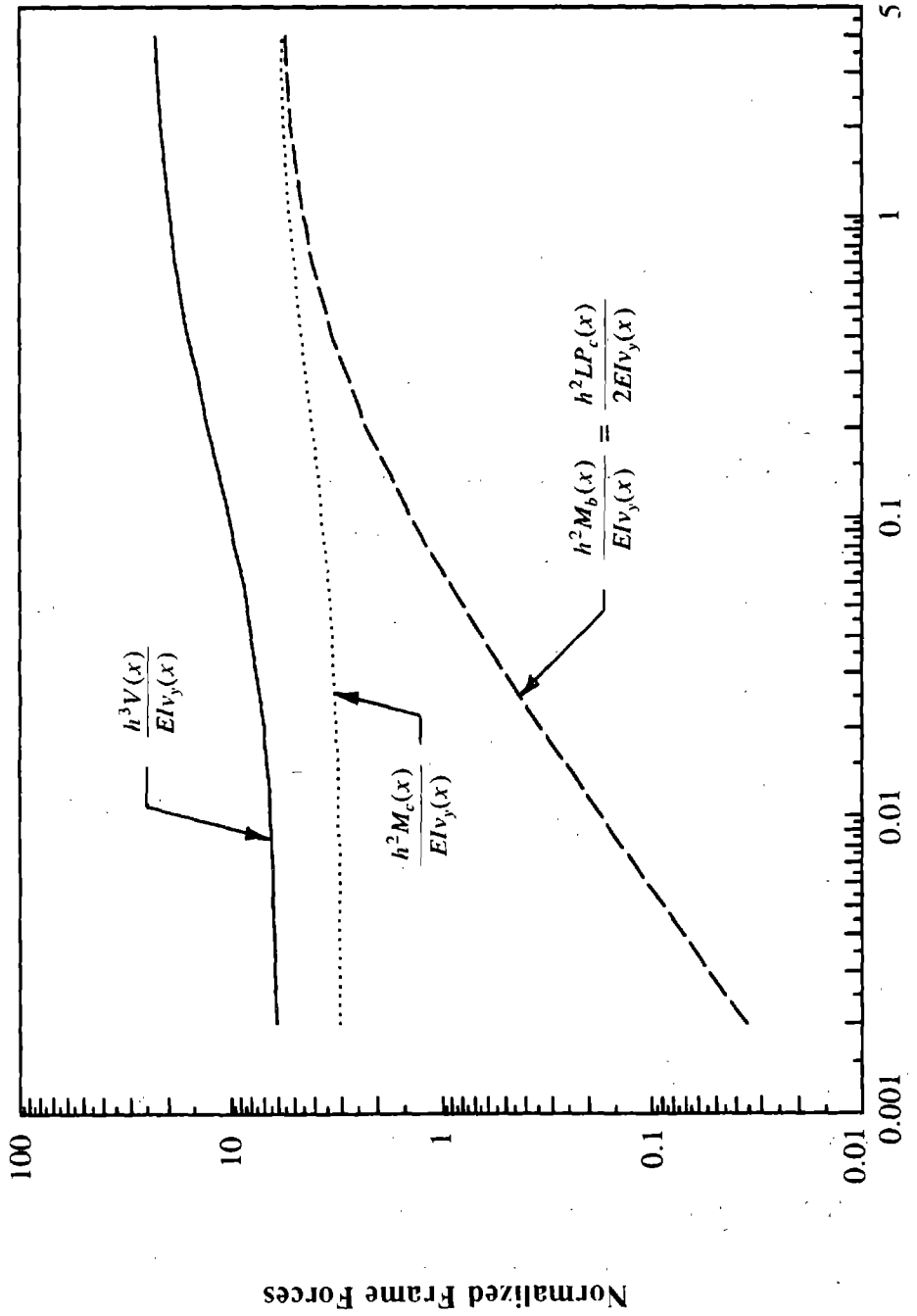

FIGURE 17 Effect of ρ on Normalized Forces in Frames: Base Shear $V(x)$, Column Moment $M_c(x)$, Beam Moment $M_b(x)$ and Column Axial Force $P_c(x)$

larger member forces due to lateral-torsional coupling, depending on the location of the frame, as well as on the overall system parameters.

8. CONCLUSIONS

This study of one-way symmetric buildings subjected to the horizontal component of ground motion, perpendicular to the axis of symmetry, leads to the following conclusions:

(1) The coupled lateral-torsional response of buildings to an earthquake depends on: the static eccentricity ratio e/r, the uncoupled torsional to lateral frequency ratio Ω, the uncoupled lateral vibration period T_y, and the damping ratio ξ of the structure. In addition to these parameters, ρ, the joint rotation index or the beam-to-column stiffness ratio of the resisting elements influences the member forces in individual elements of the building.

(2) Lateral-torsional coupling modifies the natural vibration frequencies of the system, with the effect decreasing with decreasing e/r and being smallest at $\Omega = 1$.

(3) The coupling between the lateral and torsional components of mode shapes is weak for torsionally-stiff systems ($\Omega > 1$), and for systems with small e/r and widely spaced uncoupled frequencies; for such systems each mode shape is predominantly lateral or torsional.

(4) Lateral-torsional coupling has the effect of reducing the base shear, base overturning moment and lateral displacement at the center of rigidity, but increasing the torque. These effects increase as e/r increases and are most pronounced for systems with Ω close to 1. For torsionally-stiff systems with Ω considerably greater than 1, there is essentially no reduction in base shear and the torque is essentially equal to the base shear times the static eccentricity, i.e. there is no dynamic amplification of static eccentricity. Systems with closely spaced uncoupled frequencies exhibit maximum dynamic amplification of static eccentricity, especially for smaller e/r ratios.

(5) The response spectra for base shear, base overturning moment and the lateral displacement at the center of rigidity of torsionally-coupled systems are similar in shape to the corresponding spectra for the uncoupled system, but with smaller ordinates with the amount of reduction depending strongly on e/r and Ω, but to a lesser degree on T_y, except for torsionally-flexible systems with large e/r ratios where the dependence on T_y is more pronounced.

(6) The normalized base torque spectrum for torsionally-stiff systems is similar to the $V_o(e_1^* W_1^*/W)$ spectrum, the product of the base shear for the uncoupled system and the dynamic eccentricity in the fundamental mode of vibration, although it is slightly underestimated by the latter for systems with smaller e/r and overestimated for larger e/r. However, for torsionally-flexible systems the base torque is grossly overestimated by $V_o(e_1^* W_1^*/W)$.

(7) The maximum lateral displacements of the symmetry axis at points on the flexible side of the building are generally larger than the lateral displacement v_{yo} for the uncoupled system, increasing as e/r increases and are larger for torsionally-flexible systems compared to torsionally-stiff systems or systems with closely spaced uncoupled frequencies. The maximum lateral displacements of the symmetry axis at points on the stiff side of the building are also generally larger than v_{yo} for torsionally-flexible systems and systems with closely spaced uncoupled frequencies, more so for the former than the latter. For torsionally-stiff systems, however, the maximum lateral displacements vary almost linearly with distance and are generally smaller than v_{yo} on the stiff side of the building.

(8) Any member force of a resisting element is proportional to the lateral floor displacement of the resisting element. As a result, maximum member forces of resisting elements of the coupled system may increase or decrease due to lateral-torsional coupling, depending on the position of the element and on the controlling parameters of the system. Thus, elements on the flexible or stiff side of the building may experience larger member forces than the corresponding uncoupled system.

REFERENCES

1. Kan, C.L. and Chopra, A.K., "Elastic Earthquake Analysis of a Class of Torsionally Coupled Buildings," ASCE, 103, ST4, pp. 821-838, 1977.

2. Kan, C.L. and Chopra, A.K., "Elastic Earthquake Analysis of Torsionally Coupled Multistorey Buildings," Earthquake Engineering and Structural Dynamics, 5, pp. 395-412, 1977.

3. Kan, C.L. and Chopra, A.K., "Effects of Torsional Coupling on Earthquake Forces in Buildings," ASCE, 103, ST4, pp. 805-820, 1977.

4. Rutenberg, A. and Pekau, O.A., "Earthquake Response of Asymmetric Buildings: A parametric Study," Proceedings, 4th Canadian Conference on Earthquake Engineering, Vancouver, June 1983.

5. Pekau, O.A. and Rutenberg, A., "Evaluation of the Torsional Provisions in the 1985 NBCC," 5th Canadian Conference on Earthquake Engineering, Ottawa, 1987.

6. Rosenblueth, E. and Elorduy, J., "Response of Linear Systems to Certain Transient Disturbance," Proceedings of the Fourth World Conference on Earthquake Engineering, Vol. 1, Santiago, Chile, pp. A1-185 to A1-196, 1969.

7. Erdik, M.O., "Torsional Effects in Dynamically Excited Structures," Ph.D. Thesis, Rice University, Houston, Texas, May 1975.

8. Newmark, N.M. and Rosenblueth, E., Fundamentals of Earthquake Engineering, Prentice-Hall, Englewood Cliffs, N.J., 1971.

9. Humar, J.L. and Awad, A.M., "Design For Seismic Torsional Forces," Proceedings, 4th Canadian Conference On Earthquake Engineering, Vol. 1, No. 1., 1982.

10. Dempsey, K.M. and Tso, W.K., "An Alternative Path to Seismic Provisions," Soil Dynamics and Earthquake Engineering, Vol. 1, No. 1., 1982.

11. Tso, W.K. and Meng, V., "Torsional Provisions in Building Codes," Canadian Journal of Civil Engineering, Vol. 9, pp. 38-46, 1982.

12. Tso, W.K., "A proposal to Improve the Static Torsional Provisions for the National Building Code of Canada," Canadian Journal of Civil Engineering, Vol. 10, pp. 561-565, 1983.

13. Heidebrecht, A.C. and Tso, W.K., "Proposed Seismic Loading Provisions for National Building Code of Canada 1985," Proceedings, 4th Canadian Conference on Earthquake Engineering, Vancouver, June 1983.

14. Rosenblueth, E., "Seismic Design Requirements in a Mexican 1976 Code," Earthquake Engineering and Structural Dynamics, Vol. 7, pp. 49-61, 1979.

15. Newmark, N.M. and Hall, W.J., "Vibrations of Structures Induced by Ground Motion," Chapter 29, Part I, in Shock and Vibration Handbook, eds. C.M. Harris and C.E. Crede, 2nd Ed., McGraw-Hill Inc., New York, 1976.

16. Hejal, R. and Chopra, A.K., "Earthquake Response of Torsionally-Coupled Buildings," Report No. UCB/EERC 87-**, Earthquake Engineering Research Center, University of California at Berkeley, Dec.? 1987.

17. Wilson, E.L., Der Kiureghian, A. and Bayo, E., "A Replacement for the SRSS Method in Seismic Analysis," Earthquake Engineering and Structural Dynamics, Vol. 9, pp. 187-192, 1981.

18. Blume, J.A., "Dynamic Characteristics of Multi-Story Buildings," Journal of the Structural Division, ASCE, Vol. 94, NO ST2, pp. 337-402, 1968.

APPENDIX A: MODAL CONTRIBUTIONS

In the interpretation of the effect of lateral-torsional coupling on the response of the building, it is necessary to study the contributions of the two modes to various response quantities.

First, the concept of unit modal response is introduced. It is the response of the structure in an individual mode of vibration with unit value for the pseudo-acceleration response ordinate, S_{an}. The unit response in the n^{th} vibration mode is given by equations (4.6), (4.8), (4.9) and (4.14) with $S_{an} = 1$ for the lateral displacement of the center of rigidity, base shear, base overturning moment, and base torque at the center of rigidity, respectively. The maximum value of any response quantity due to an individual vibration mode is the product of the unit response in that mode and the ordinate S_{an} of the pseudo-acceleration response spectrum corresponding to that mode.

In discussing the contributions of the two coupled modes to the response, it is useful to normalize the unit response in the n^{th} mode by the unit response of the uncoupled system. The unit modal base shear, base overturning moment and lateral displacement at the CR, normalized respectively by the unit base shear, base overturning moment and floor lateral displacement of the corresponding uncoupled system, are all represented by W_n^*/W, as is obvious from equation (4.22). From equation (4.23), the unit modal base torque at the CR normalized by the product of r and the unit base shear of the uncoupled system is given by $e_n^* W_n^*/rW$. The normalized unit modal lateral and torsional quantities W_n^*/W and $e_n^* W_n^*/rW$ are presented in Figure A.1 against Ω for various e/r values.

Referring to Figure A.1, the contribution of the second mode to the unit translational response of the system is negligible compared to that of the fundamental mode for torsionally-stiff systems. For torsionally-flexible systems, the fundamental mode contribution to unit translational response of the system is significantly lower than that of the second mode for smaller e/r values but is quite large for large e/r ratios. For systems with closely-spaced uncoupled frequencies, the two modes contribute almost equally to the unit translational response of the system for low to medium e/r values, but the second modal contribution is significantly smaller than that of the fundamental mode

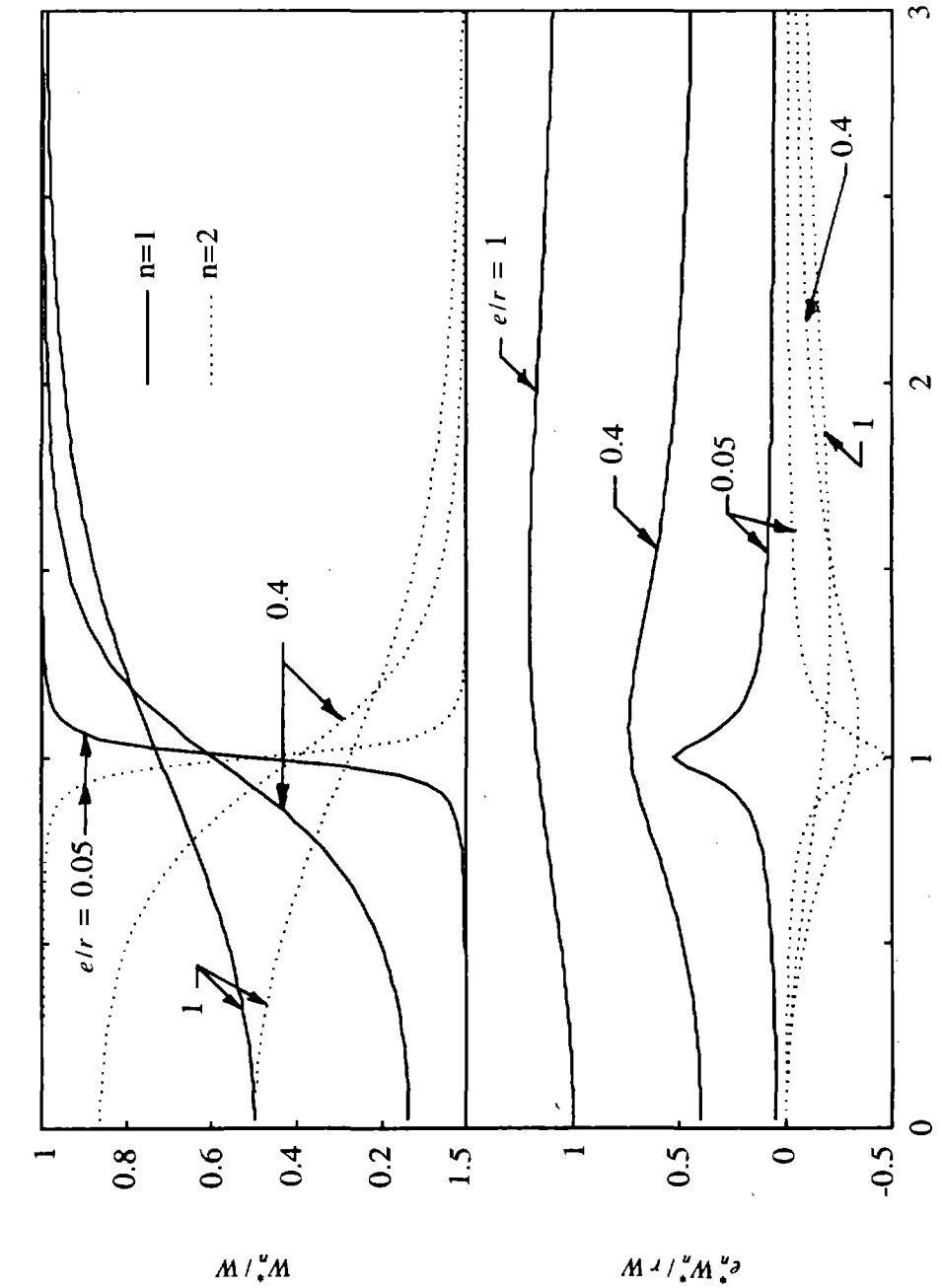

FIGURE A.1 Normalized Unit Modal Lateral and Torsional Quantites W_n^* / W and $e_n^* W_n^* / r W$

when e/r is large.

The second modal contribution to the unit base torque at the CR of the building is significantly smaller than that of the fundamental mode for medium to large values of e/r. The contribution of the fundamental mode to the unit base torque increases with increase in e/r, while that of the second mode decreases with the increase in e/r. The maximum modal contribution to unit base torque of the building occurs at values of Ω very close to one for small to medium e/r and larger than one for large e/r. When e/r is very small, the contributions of the two modes are almost equal when the uncoupled frequencies are closely-spaced.

The conclusions drawn from Figure A.1 combined with the observations of Section 5, lead us to the following conclusions:

(1) The unit translational response of coupled systems with predominantly lateral and predominantly torsional modes, is dominated by the predominantly lateral mode.

(2) The unit torsional response of coupled systems is dominated by the fundamental mode, except for systems with small e/r and closely-spaced uncoupled frequencies. In this latter case, the contributions of both modes are almost equal.

The actual contribution of a vibration mode to the response is the product of the unit modal contribution and the pseudo-acceleration ordinate. The actual modal contribution may be higher or lower than the unit modal contribution depending on the ordinate of the spectrum, which in turn depends on the vibrational period value and the shape of the spectrum.

APPENDIX B: NOTATION

$\mathbf{a}_i$ transformation matrix of element 'i', defined by either of equations (3.5), (3.6), (3.7) or (3.8)

$\bar{a}_g$ maximum ground acceleration

$a_{gy}(t)$ ground acceleration as a function of time

e static eccentricity defined as the distance between the centers of mass and rigidity

e_d dynamic eccentricity defined as the distance from the CR where the uncoupled base shear should be applied to cause base torque at the CR equal to T_R

e_n^* effective eccentricity in the n^{th} mode of vibration, defined by equation (4.12)

e_{dn} dynamic eccentricity in the n^{th} mode of vibration, defined by equation (4.23)

f_{yn} equivalent static lateral force in the n^{th} mode of vibration, defined by equation (4.7)

$f_{\theta n}$ equivalent static torsional force in the n^{th} mode of vibration, defined by equation (4.7)

$\mathbf{f}_n$ $\mathbf{f}_n^T = < f_{yn} \;\; f_{\theta n} >$

h height of single-story system

I_b moment of inertia of beams

I_c , I moments of inertia of columns

k_{xi} , k_{yi} lateral stiffnesses of element 'i' along the X and Y directions

$k_{\theta i}$ torsional stiffness of core 'i' about a vertical axis passing through its shear center

$\mathbf{k}_i$ stiffness matrix of element 'i' with respect to degrees of freedom $\mathbf{v}_i$

K_y , $K_{\theta y}$, $K_{y\theta}$ and K_θ

elements of $\mathbf{K}$, defined by equations (3.12)

$K_{\theta R}$ building torsional stiffness about a vertical axis passing through its CR, determined by equation (3.17)

K_{yi} , $K_{\theta yi}$, $K_{y\theta i}$ and $K_{\theta i}$

elements of $\mathbf{K}_i$, defined by equations (3.10)

$\mathbf{K}$ building stiffness matrix defined with respect to degrees of freedom $\mathbf{u}$

$\mathbf{K}_i$ stiffness matrix of element 'i' computed for degrees of freedom $\mathbf{u}$

L_b , L lengths of beams

L_c length of columns

m mass of deck

$\mathbf{M}$ building mass matrix defined with respect to $\mathbf{u}$

M , M_o base overturning moments of coupled and uncoupled systems, respectively

M_n base overturning moment of coupled system due to the n^{th} mode of vibration

$\overline{M}$ normalized coupled base overturning moment, defined by equation (4.20)

$\overline{M}_n$ normalized coupled base overturning moment in the n^{th} mode of vibration, defined by equation (4.22)

$M_b(x)$, $M_c(x)$ and $P_c(x)$

maximum beam moment, base column moment, and column axial force, respectively, of a frame spanning along the Y-axis at a distance x from the CM

q_{nm} coupled frequency ratio, ω_n/ω_m

Q_{xi} and Q_{yi} applied lateral forces at element 'i', along the X and Y directions, respectively

$Q_{\theta i}$ applied torsional moment at element 'i' about a vertical axis

$\mathbf{Q}_i$ vector of applied forces to element 'i', defined by either of equations (3.2) or (3.3)

r radius of gyration of deck about a vertical axis passing through its CM

r maximum of a response quantity of the coupled system

r_n maximum of r in the n^{th} mode of vibration

S_{ay} pseudo-acceleration response spectrum ordinate corresponding to T_y and ξ

S_{an} pseudo-acceleration response spectrum ordinate corresponding to T_n, (n=1,2), and ξ

T_n n^{th} natural vibration period of coupled system

T_y natural lateral vibration period of uncoupled system

T_R base torque of coupled system at its CR

T_{Mn} and T_{Rn} base torques of coupled system at its centers of mass and rigidity, respectively, due the n^{th} mode of vibration

$\bar{T}_R$ normalized coupled base torque at the CR, defined by equation (4.20)

$\bar{T}_{Rn}$ normalized coupled base torque at the CR, in the n^{th} mode of vibration, defined by equation (4.23)

$\bar{u}_g$ maximum ground displacement

$u_y(t)$ lateral displacement of CM along the Y-axis

$u_\theta(t)$ deck rotation about a vertical axis

$\mathbf{u}$ $\mathbf{u}^T = < u_y \; r u_\theta >$

$\mathbf{u}_n$ $\mathbf{u}_n^T = < u_{yn} \; r u_{\theta n} >$

u_{yn} and $u_{\theta n}$ lateral and torsional displacements in the n^{th} mode of vibration

$v_y(t)$ lateral displacements at the CR of the coupled system

$v_{yo}(t)$ lateral displacement of uncoupled system

v_{yn} lateral displacement at the CR in the n^{th} mode of vibration

$\bar{v}$ normalized coupled lateral displecment of CR, defined by equation (4.20)

$\bar{v}_n$ normalized coupled lateral displacement, in the n^{th} mode of vibration, defined by equation (4.22)

$\bar{v}_g$ maximum ground velocity

$\mathbf{v}$ $\mathbf{v}^T = < v_y \; ru_\theta >$

$\mathbf{v}_i$ vector of displacements of element 'i', defined by either of equations (3.2) or (3.3)

v_{xi} and v_{yi} lateral displacements of element 'i', along the X and Y principal directions of the element

$v_{\theta i}$ rotation of core 'i' about a vertical axis passing through its shear center

$v_y(x)$ lateral dispacment of a frame spanning along the Y-axis at a distance x from the CM

$\mathbf{v}_{in}$ lateral displacement of element 'i' in the n^{th} mode of vibration

V , V_o base shears of coupled and uncoupled systems, respectively

V_n base shear of coupled system due to the n^{th} mode of vibration

$\bar{V}$ normalized coupled base shear, defined by equation (4.20)

$\bar{V}_n$ normalized coupled base shear in the n^{th} mode of vibration, defined by equation (4.22)

$V(x)$ maximum base shear of a frame spanning along the Y-axis at a distance x from the CM

W total weight of the building

W_n^* effective weight in the n^{th} mode of vibration, defined by equation (4.8)

x_i and y_i X and Y coordinates of element 'i'

α_n $\boldsymbol{\alpha}_n^T = < \alpha_{yn} \;\; \alpha_{\theta n} >$, (n=1,2)

α_y and α_θ lateral and torsional components of natural coupled mode

α_{yn} and $\alpha_{\theta n}$ lateral and torsional components of the n^{th} natural coupled mode shape

ρ frame joint rotation index or beam-to-column stiffness ratio

ω	natural vibration frequency of coupled system
ω_n	n^{th} coupled natural vibration frequency, (n=1,2)
ω_y	lateral natural vibration frequency of uncoupled system, defined by equation (3.19)
ω_θ	torsional natural vibration frequency of uncoupled system, defined by equation (3.20)
Ω	uncoupled torsional to lateral frequency ratio, ω_θ/ω_y
$\bar{\omega}_n$	ω_n/ω_y
γ_{nm}	cross-correlation factor between coupled modes 'n' and 'm'
ξ	damping ratio, chosen to be 5 %
CM	center of mass
CR	center of rigidity

PART II

EARTHQUAKE ANALYSIS AND RESPONSE OF A SPECIAL CLASS OF TORSIONALLY-COUPLED, MULTI-STORY BUILDINGS

1. INTRODUCTION

Buildings subjected to ground shaking simultaneously undergo lateral as well as torsional motions if their structural plans do not have two axes of mass and stiffness symmetry. Coupled lateral-torsional motions can also occur in nominally symmetric buildings-- buildings with structural plans that have two axes of mass and stiffness symmetry-- due to unforseen conditions such as unbalanced load distributions or differences between actual and assumed mass and stiffness distributions, or if ground shaking includes a torsional component. As a result of coupled lateral-torsional motions, the lateral forces experienced by various resisting elements (frames, shear walls, etc.) would differ from those experienced by the same elements if the building had symmetric plan and hence responded only in planar vibrations.

The dynamic response of torsionally-coupled buildings can be determined with the aid of general-purpose computer codes [e.g. 1,2] based on standard modal analysis procedures. However, for a special class of buildings, it has been demonstrated [3] that the total response (including all vibration modes) of a torsionally-coupled, N-story, shear building with rigid floor-diaphragms-- a system with 3N degrees of freedom (DOF)-- to ground motion characterized by smooth response spectra may be determined by analyzing the total responses of two smaller systems: (1) a corresponding torsionally-uncoupled, N-story system-- a system with N DOF; and (2) an associated torsionally-coupled, one-story system-- a system with 3 DOF. This analysis procedure was shown to lead to "exact" results if the variation of earthquake spectral acceleration with vibration period is flat or hyperbolic. For arbitrary-shaped smooth spectra, the procedure was shown to lead to results that are not "exact" but are accurate to a useful degree.

One of the major objectives of this investigation is to extend the aforementioned analysis procedure to buildings consisting of moment-resisting frames, shear walls and other resisting elements for which the shear-beam idealization is inappropriate. For such a building, the procedure is demonstrated to be equally applicable provided it belongs to a special class of buildings identified later. It is also shown that, contrary to earlier conclusions [3], the procedure is not "exact" for shear buildings (or other types of buildings) even for flat or hyperbolic spectra. However, it is

demonstrated that, even for an arbitrary-shaped earthquake response spectrum, the response in a vibration mode of the building can be "exactly" determined from appropriate modal responses of the aforementioned smaller systems. The total response of the building can then be determined "exactly" using an appropriate modal combination rule.

Most previous studies of the response of torsionally-coupled buildings have also been concerned with multi-story buildings idealized as shear-beam models [4,5]. Response results obtained by the response-spectrum method for a ten-story shear-beam building with medium eccentricity ratio and uncoupled torsional to lateral frequency ratio slightly larger than unity, were compared to time history analysis and to static approaches that are inherent in building codes [4]. This study has shown that the response spectrum approach is quite accurate if correctly applied, while the static approaches give inconsistent results. The square root of the sum of squares (SRSS) of modal maxima as an estimate of maximum response was compared [5] to a more refined combination rule that takes into account the cross-correlation between modes [6] for twelve-story shear-beam buildings with fundamental uncoupled lateral vibration period of one sec, and uncoupled torsional to lateral frequency ratios ranging between 0.7 and 1.4. It was shown that the SRSS combination rule overestimates the base torque especially for systems with small eccentricity ratios and for uncoupled torsional to lateral frequency ratios between 0.75 and 1.25.

Recent work [7,8] has demonstrated that the earthquake responses of buildings undergoing only lateral vibration (i.e. no torsional motions) are significantly influenced by various parameters including the beam-to-column stiffness ratio (or the joint rotation index). The second objective of this study is to bring this parameter into the study of torsionally-coupled buildings. Thus, the earthquake response of torsionally-coupled buildings is investigated for a wide range of values of the beam-to-column stiffness ratio, the fundamental uncoupled lateral vibration period, the ratio of uncoupled torsional and lateral vibration frequencies, and the eccentricity between the centers of mass and centers of rigidity of the building. The effects of lateral-torsional coupling on building response are identified, the influence of the beam-to-column stiffness ratio is investigated, and the significance of the higher mode contributions in building response is established in order to provide

a basis for simplified analysis procedures [7].

2. SYSTEMS AND DESIGN SPECTRA

2.1 A Special Class of Buildings

The center of rigidity of a one-story system with a rigid deck is the point in the plan of the deck through which a horizontal static force must be applied for the deck to translate without torsion. If the force is along either of the principal axes, which are orthogonal and pass through the center of rigidity of the system, the deck translates in the same direction as the force. If a pure torsional moment is applied at the deck, torsion of the deck takes place around the center of rigidity.

Unlike one-story buildings, it is generally not possible to uniquely define the centers of rigidity of the various stories of a multi-story building. However, the centers of rigidity can be uniquely identified for buildings having the following properties:

1. The centers of mass of all floors lie on a vertical line
2. The resisting elements (frames, columns, shear walls or shear-wall cores) are arranged such that their principal axes form an orthogonal grid in plan and are connected at each floor level by a rigid diaphragm.
3. The lateral stiffness matrices of all resisting elements along one direction are proportional to each other; i.e. the lateral stiffness matrix of the i^{th} resisting element in the X direction $\mathbf{K}_{xi} = C_{xi}\,\mathbf{K}_x$, where C_{xi} is a proportionality constant and $\mathbf{K}_x$ is a characteristic stiffness matrix for the resisting elements. Similarly, the stiffness matrix of the i^{th} resisting element in the Y direction $\mathbf{K}_{yi} = C_{yi}\,\mathbf{K}_y$. The two reference matrices $\mathbf{K}_x$ and $\mathbf{K}_y$ may not be identical.

For buildings having the last two properties listed above, it is shown in Appendix A that the centers of rigidity of all stories lie on one vertical line. Thus, for this special class of buildings, the static eccentricity for each floor, which is defined as the distance between the center of mass of the floor and its center of rigidity, is the same.

Multi-story buildings with mixed types of resisting elements, such as frames and columns or frames and shear walls, spanning along the same direction, do not belong to this special class of buildings, since lateral stiffness matrices of such elements along the same direction are not

proportional.

2.2 Systems Considered

2.2.1 One-Way Symmetric Plans

The analysis procedure developed in Section 4 is for the special class of buildings defined in Section 2.1 with the additional restriction that all resisting elements spanning in any of the two orthogonal directions have proportional lateral stiffness matrices, i.e. $\mathbf{K}_x = \mathbf{K}_y$. Buildings considered are assumed to have floor plans symmetrical about one axis (e.g. Figure 1), although most of the analytical development is readily extendable to the more general case with no axes of symmetry. The buildings considered consist of several massless moment-resisting frames arranged in an orthogonal grid (e.g. Figure 1), connected at each story level by a rigid diaphragm. The mass of the building is lumped at the centers of mass of the various floors. The centers of mass and the centers of rigidity of such buildings lie on two vertical lines, a distance e apart. All floors have the same radius of gyration r about a vertical axis passing through their centers of mass.

2.2.2 Simple Plan

Utilizing the analysis procedure of Section 4, the response of buildings described in Section 2.2.1 with a simple plan is investigated in Sections 5 to 8. It is shown in Section 3.1 that this simple plan building is useful in studying the dynamics of the buildings described in Section 2.2.1.

The systems analyzed are idealized five-story buildings with all floors having an identical rectangular plan, symmetrical about the X-axis and consisting of three moment-resisting planar frames (Figure 2a), connected at each story level by a rigid diaghragm. The mass of the structure is lumped equally at the centers of mass of the five floors, which are assumed to coincide with the geometric centers of the floors, which lie on a vertical line. The mass at each floor is denoted by m, and r is the radius of gyration of each floor about the vertical axis passing through its center of mass.

The two identical frames oriented along the X- direction are located symmetrically at a distance y_2 on each side of the X-axis; each is identified as frame (2). The third frame, identified as

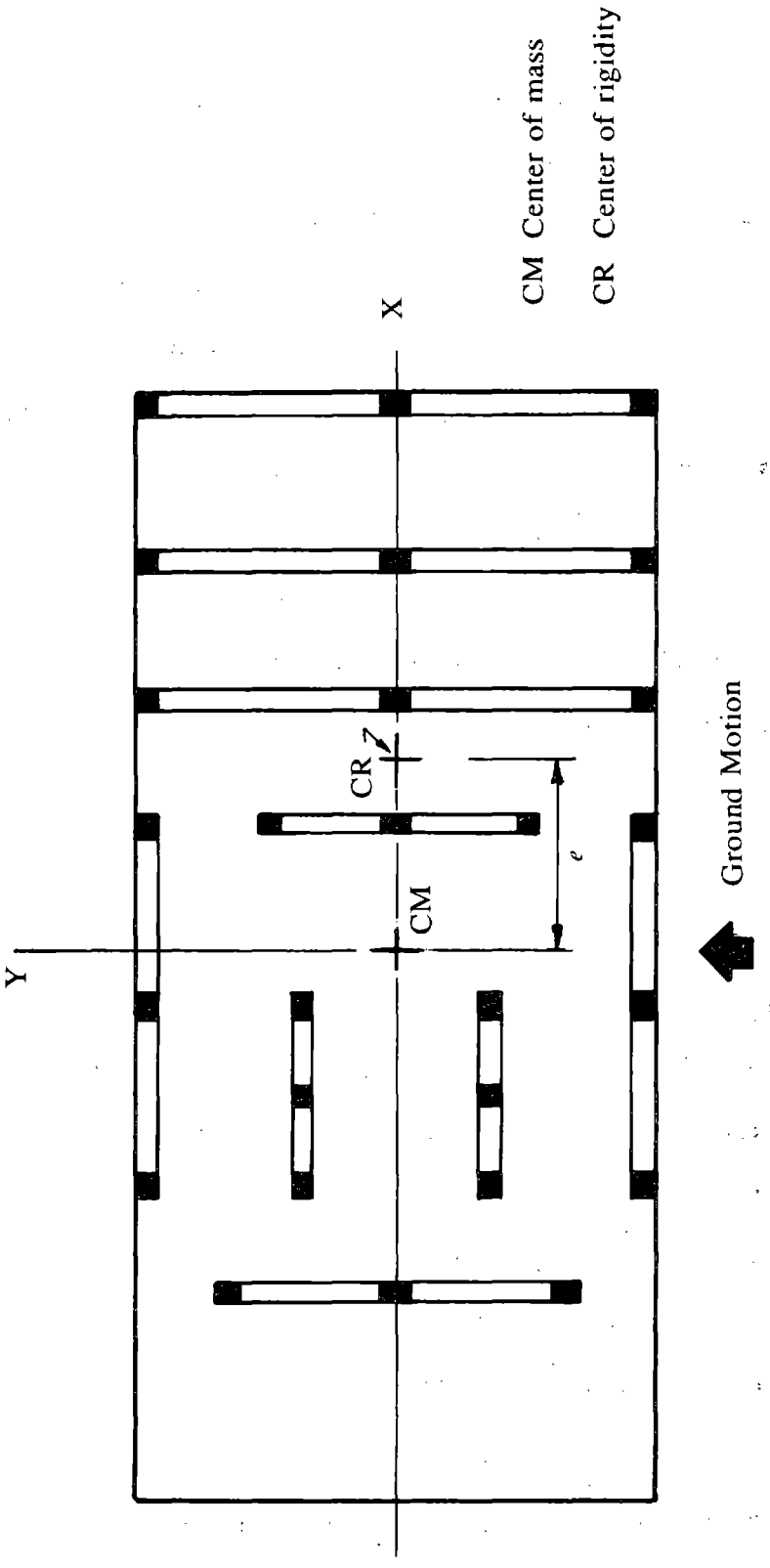

FIGURE 1 One-way Symmetric Floor Plan

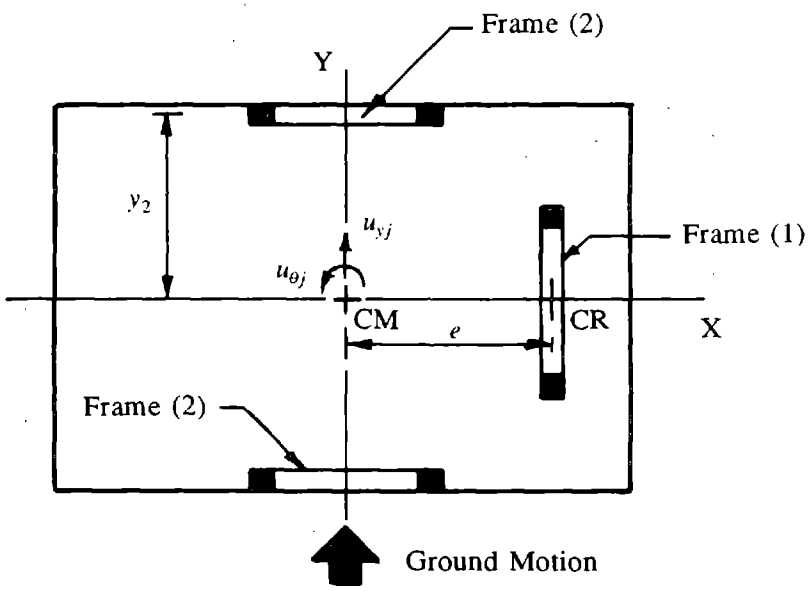

(a) Typical Floor Plan

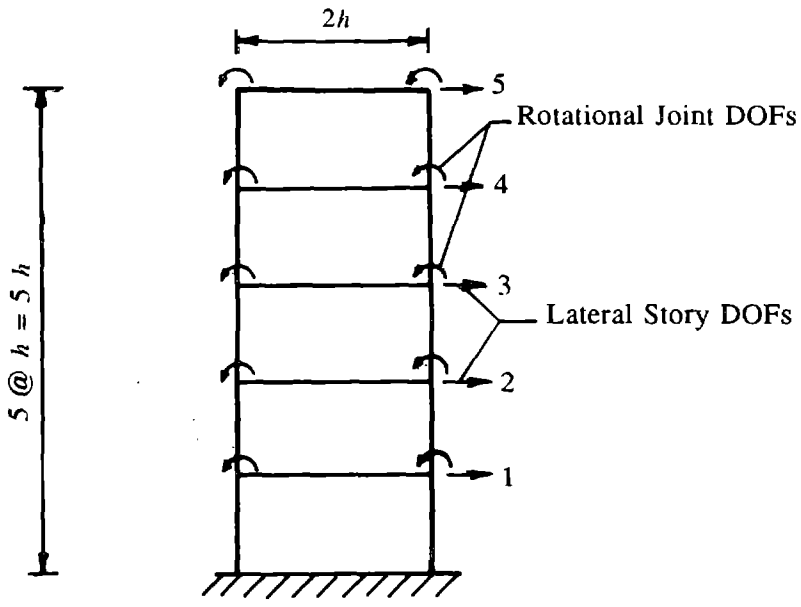

(b) Typical Frame Elevation

FIGURE 2 Five-story Building with a Simple Floor Plan

frame (1), is oriented in the orthogonal direction and is located eccentrically at a distance e away from the Y-axis. Since this is the only frame oriented along the Y-axis, and the X-axis is the axis of symmetry, the center of rigidity of each floor lies on its X-axis at a distance e from the center of mass of the floor. It follows that the static eccentricities of all floors are the same, equal to e, and the centers of rigidity of the floors all lie on a vertical line. The idealized building, therefore, belongs to the special class of multi-story buildings, described in Section 2.1.

The properties of each frame are uniform over height: constant story height, h, and one bay of width $2h$ (Figure 2b); all beams of a frame have the same flexural stiffness, EI_b, and the column stiffness, EI_c, does not vary with height. It is assumed that each frame contributes to the stiffness of the building only in the direction of its own plane, and that the torsional stiffness of each frame about any vertical axis in its own plane is negligible. All frame members are prismatic with constant cross-sections. Axial and shear deformations of members are neglected so that only flexural deformations are considered.

Damping is defined directly in each mode of vibration of the system. The damping ratio, ξ, expressed as a fraction of critical damping, is assumed to be the same in each mode of vibration.

Frame action is measured by the joint rotation index, ρ, which, as first introduced by Blume [9], is defined as the ratio of the sum of beam stiffnesses to the sum of column stiffnesses at the mid-height story of the frame:

$$\rho = \frac{\sum_{beams} EI_b / L_b}{\sum_{columns} EI_c / L_c} \tag{2.1}$$

in which L_b is the beam width and L_c the column height. For the uniform frames considered, equation (2.1) becomes:

$$\rho = \frac{1}{4} \frac{I_b}{I_c} = \frac{1}{4} \frac{I_b}{I} \tag{2.2}$$

By varying the stiffness ratio ρ, the entire range of behavior of a frame can be covered. For $\rho = 0$, the frame behaves as a flexural column with beams imposing no constraint to joint rotations. For

$\rho = \infty$, joint rotations are restrained so that the frame behaves as a shear beam. Intermediate values of ρ, therefore, present frames with both beam and column deformations and joint rotations. The joint rotation index of frame (1) is denoted by ρ_1, and that of frames (2) by ρ_2. In this study, it is assumed that $\rho_1 = \rho_2 = \rho$, a condition which, as will be seen later, implies that frames (1) and (2) have proportional lateral stiffness matrices.

The dynamic response of the systems described to the horizontal component of ground motion, assumed to be uniform over the base, along the Y-axis is investigated. Since the building is not symmetric about the Y-axis, it will undergo coupled lateral-torsional motions.

2.3 Ground Motion and Response Spectra

For earthquake response spectra of arbitrary shape the design forces need not be greater than those for either a hyperbolic or a flat spectrum that constitute upper bounds to the design spectrum in the range of periods less than the fundamental period of the structure (Figure 3). These two idealized spectra are useful since normalized response of the system does not depend on the system vibrational periods but only on their ratios [10], and because they are representative of the acceleration- and velocity-controlled regions of smooth design spectra.

The smooth design spectrum selected is shown in Figure 4. This spectrum is developed by well known procedures [11] for excitations with maximum ground acceleration, $\bar{a}_g$, velocity, $\bar{v}_g$, and displacement, $\bar{u}_g$ of 1g, 48 in/sec and 36 in respectively. Using a damping ratio of 5 % and 84.1 percentile response, amplification factors of 2.67, 2.32 and 2.04 are obtained from [11] for the acceleration-controlled, velocity-controlled and displacement-controlled regions of the spectrum, respectively. It is apparent from the shape of the design spectrum that the response of short period structures is controlled by ground acceleration, that of long period structures by the ground displacement and that of intermediate period structures by the ground velocity.

The design spectrum of Figure 4 is replotted in Figure 5 as a normalized pseudo-acceleration spectrum to emphasize that the spectral acceleration is constant (flat spectrum) in part of the acceleration-controlled region, and varies as $1/T$ (hyperbolic spectrum) in the velocity-controlled

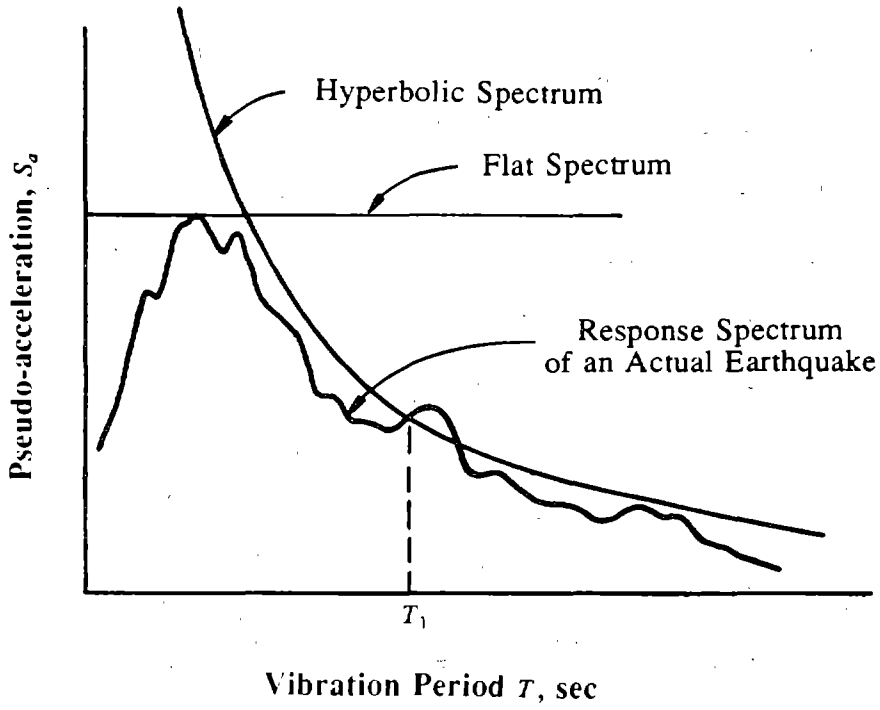

FIGURE 3 Flat and Hyperbolic Response Spectra

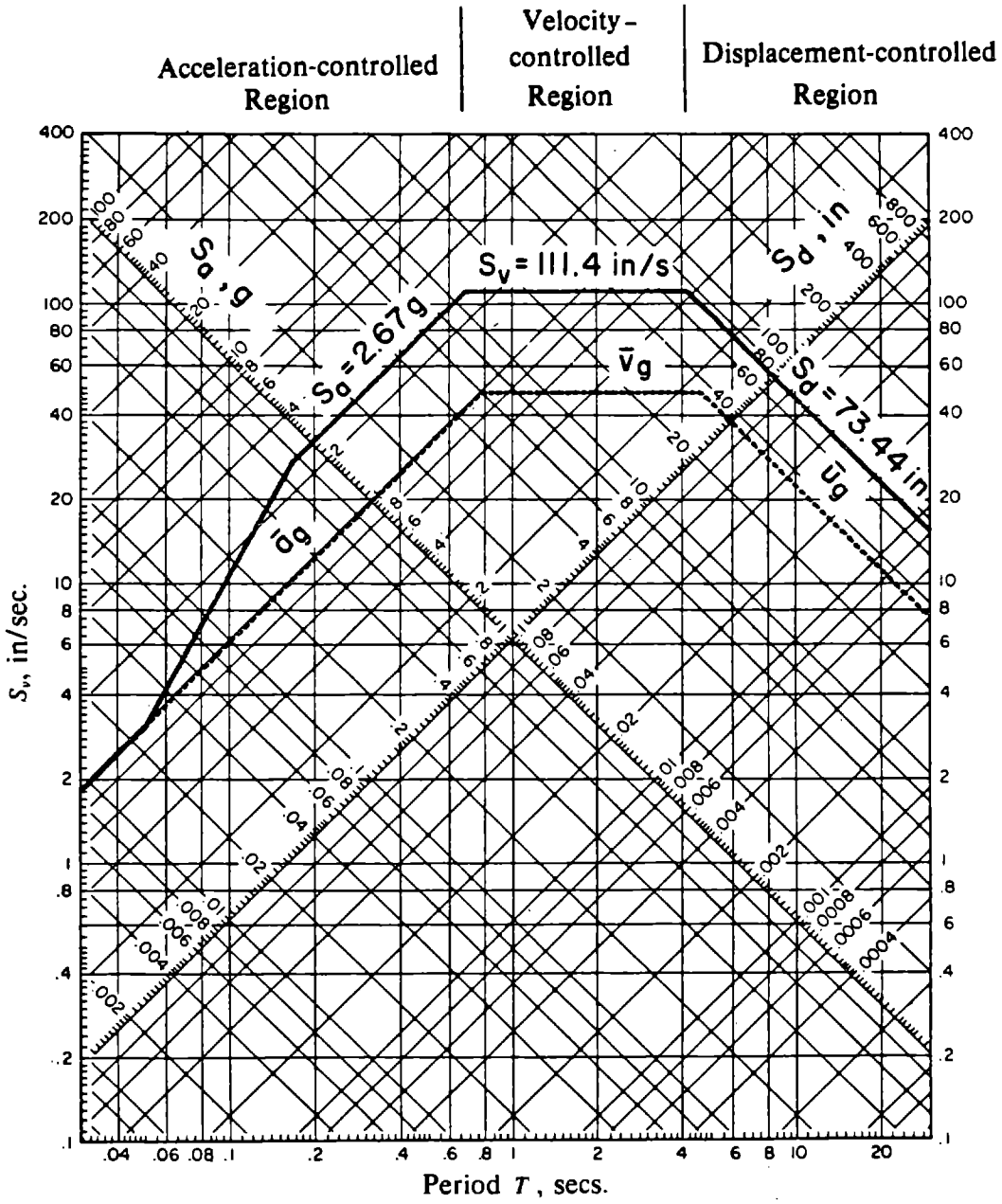

FIGURE 4 Design Spectrum for Ground Motions with Maximum Ground Acceleration $\bar{a}_g$ = 1g, Velocity $\bar{v}_g$ = 48 in/sec and Displacement $\bar{u}_g$ = 36 in; Damping = 5 %

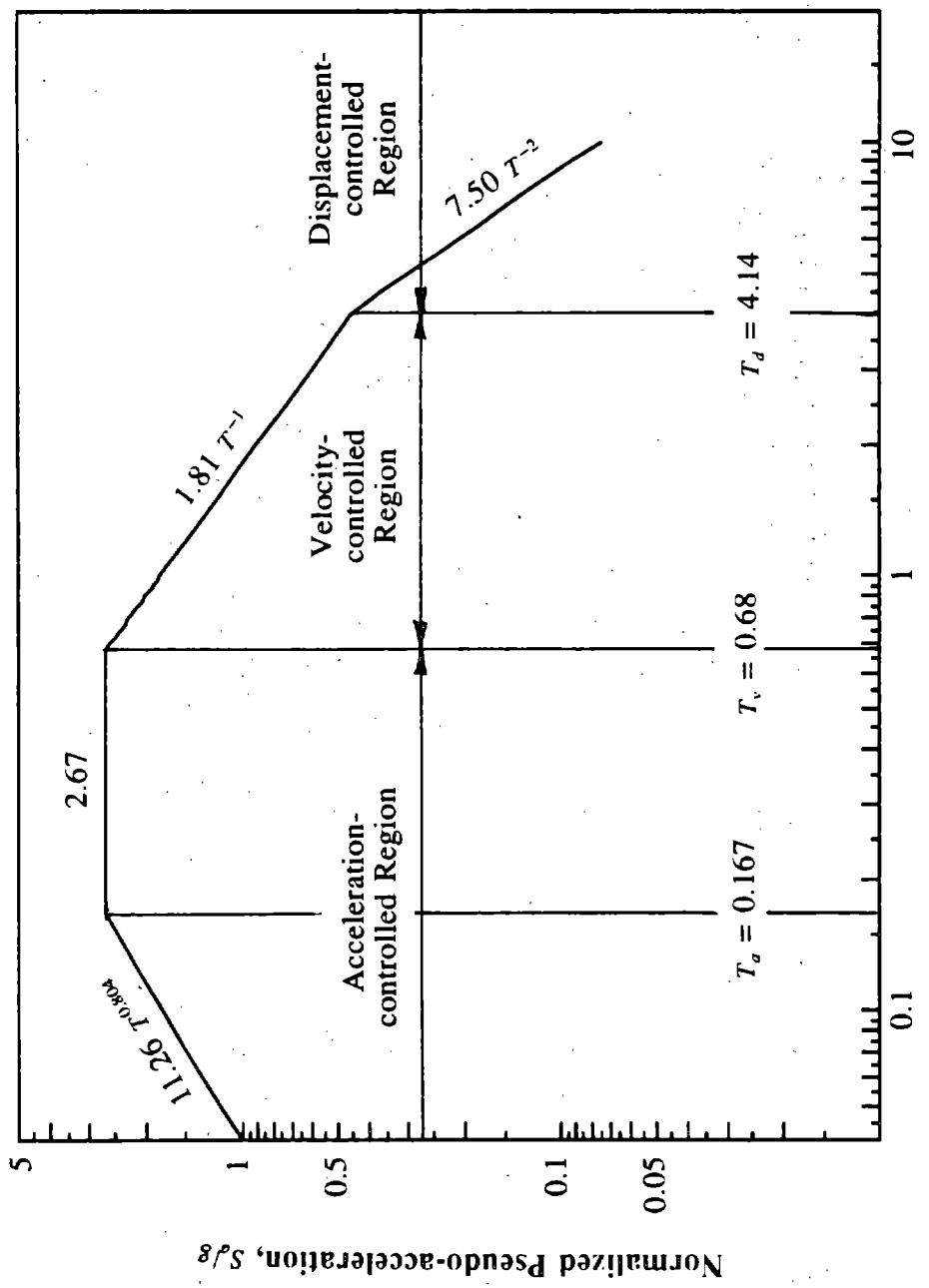

FIGURE 5 Normalized Pseudo-acceleration Design Spectrum

region.

3. EQUATIONS OF MOTION

3.1 Torsionally-Coupled, Multi-Story Buildings

3.1.1 One-Way Symmetric Plans

Each floor of a one-way symmetric building (e.g. Figure 1) has two degrees of freedom when subjected to ground motion along the Y-axis: translation along the Y-axis and rotation about a vertical axis. The displacement vector $\mathbf{u}$ for the system is defined by $\mathbf{u}^T = < \mathbf{u}_v^T \;\; r\mathbf{u}_\theta^T >$, where $\mathbf{u}_v$ is the vector of Y-lateral displacements of the centers of mass of the floors, relative to the ground; and $\mathbf{u}_\theta$ is the vector of deck rotations about a vertical axis; and r is the radius of gyration of each floor about a vertical axis passing through its center of mass.

The stiffness matrix of the idealized building, defined with respect to degrees of freedom $\mathbf{u}$, is given by:

$$\mathbf{K} = \sum_i \mathbf{K}_i \tag{3.1}$$

where $\mathbf{K}_i$ is the contribution of the i^{th} frame to the building stiffness matrix. $\mathbf{K}_i$ is related to the lateral stiffness matrix of the i^{th} frame which is determined by the following steps (see Appendix B for additional information):

(1) Define one lateral displacement degree of freedom per floor and one rotational degree of freedom per joint as shown in Figure 2b.

(2) Obtain a complete frame stiffness matrix with reference to the degrees of freedom defined.

(3) Statically condense out all the rotational degrees of freedom, since there are no external moments applied at the joints, to obtain the lateral stiffness matrix of the i^{th} frame, which is denoted by $\mathbf{k}_{xi}$ if the frame spans along the X-axis, and by $\mathbf{k}_{yi}$ if it spans along the Y-axis.

The contribution of the i^{th} frame to building stiffness matrix $\mathbf{K}_i$ is given by:

$$\mathbf{K}_i = \mathbf{a}_{xi}^T \mathbf{k}_{xi} \mathbf{a}_{xi} \quad \text{or} \quad \mathbf{K}_i = \mathbf{a}_{yi}^T \mathbf{k}_{yi} \mathbf{a}_{yi} \tag{3.2}$$

depending on the orientation of the frame plane. The transformation matrices $\mathbf{a}_{xi}$ and $\mathbf{a}_{yi}$ relating the

lateral degrees of freedom of the i[th] frame to the system degrees of freedom, **u**, are given by:

$$\mathbf{a}_{xi} = \begin{bmatrix} \mathbf{0} & -(y_i/r)\mathbf{I} \end{bmatrix} \quad \text{and} \quad \mathbf{a}_{yi} = \begin{bmatrix} \mathbf{I} & (x_i/r)\mathbf{I} \end{bmatrix} \tag{3.3}$$

where x_i is the distance of the i[th] frame oriented in the Y- direction from the centers of mass and y_i is the distance of the i[th] frame oriented in the X- direction from the centers of mass; and **I** and **0** are unit and zero matrices, respectively, of dimension N, the number of stories.

Substituting equation (3.3) in (3.2) and the latter in (3.1) leads to the building stiffness matrix:

$$\mathbf{K} = \begin{bmatrix} \mathbf{K}_y & \frac{1}{r}\mathbf{K}_{y\theta} \\ \frac{1}{r}\mathbf{K}_{\theta y} & \frac{1}{r^2}\mathbf{K}_{\theta} \end{bmatrix} \tag{3.4}$$

where,

$$\mathbf{K}_y = \sum_i \mathbf{k}_{yi}$$

$$\mathbf{K}_{y\theta} = \mathbf{K}_{\theta y} = \sum_i x_i \mathbf{k}_{yi} \quad \text{and,} \tag{3.5}$$

$$\mathbf{K}_{\theta} = \sum_i (x_i^2 \mathbf{k}_{yi} + y_i^2 \mathbf{k}_{xi})$$

The building stiffness matrix, **K**, given by equations (3.4) and (3.5) is applicable to any building with orthogonal-system of frames symmetrical about the X-axis. If the resisting frames oriented in the Y- direction have proportional lateral stiffness matrices, the building belongs to the special class of buildings identified in Section 2.1 and $\mathbf{K}_{y\theta}$ is proportional to $\mathbf{K}_y$. In other words, if:

$$\mathbf{k}_{yi} = C_{yi}\,\mathbf{k} \tag{3.6}$$

where **k** is the characteristic stiffness matrix for the frames, and C_{yi} is a proportionality constant for the i[th] frame, then:

$$\mathbf{K}_y = \left(\sum_i C_{yi}\right)\mathbf{k} = C_y\,\mathbf{k} \tag{3.7}$$

$$\mathbf{K}_{y\theta} = \mathbf{K}_{\theta y} = \left(\sum_i C_{yi}\, x_i \right) \mathbf{k} = C_{y\theta}\, \mathbf{k} = \frac{C_{y\theta}}{C_y}\, \mathbf{K}_y \tag{3.8}$$

The proportionality constant relating $\mathbf{K}_{y\theta}$ to $\mathbf{K}_y$ can be shown to be the static eccentricity, defined in Section 2.1, of the building (Appendix A), i.e.

$$e = \frac{C_{y\theta}}{C_y} = \frac{\sum_i C_{yi}\, x_i}{\sum_i C_{yi}} \tag{3.9}$$

The building stiffness matrix, $\mathbf{K}$, for buildings with constant static eccentricity is therefore given by:

$$\mathbf{K} = \begin{bmatrix} \mathbf{K}_y & \frac{e}{r}\mathbf{K}_y \\ \frac{e}{r}\mathbf{K}_y & \frac{1}{r^2}\mathbf{K}_\theta \end{bmatrix} \tag{3.10}$$

In the rest of this study, all resisting frames, spanning along either the X- or the Y-axis, are assumed to have proportional lateral stiffness matrices (see Section 2.2.1), i.e. $\mathbf{k}_{yi}$ is given by equation (3.6) and

$$\mathbf{k}_{xi} = C_{xi}\, \mathbf{k} \tag{3.11}$$

then, in addition to equations (3.7) to (3.10):

$$\mathbf{K}_\theta = \left(\sum_i C_{yi} x_i^2 + C_{xi} y_i^2 \right) \mathbf{k} = C_\theta\, \mathbf{k} = \frac{C_\theta}{C_y}\, \mathbf{K}_y = \left(e^2 + \frac{C_{\theta R}}{C_y}\right) \mathbf{K}_y \tag{3.12}$$

where,

$$\frac{C_{\theta R}}{C_y} = \frac{C_\theta}{C_y} - e^2 \tag{3.13}$$

will be shown in Section 4 to be directly related to the ratio of the j^{th} uncoupled torsional frequency to the j^{th} uncoupled lateral frequency of the building, and, for the class of buildings considered here, this ratio is independent of 'j'. The stiffness matrix of equation (3.10) can now be expressed as:

$$\mathbf{K} = \begin{bmatrix} \mathbf{K}_y & \frac{e}{r}\mathbf{K}_y \\ \frac{e}{r}\mathbf{K}_y & [\,(\frac{e}{r})^2 + \frac{C_{\theta R}}{r^2 C_y}\,]\,\mathbf{K}_y \end{bmatrix} \tag{3.14}$$

The undamped equations of motion of the building subjected to ground acceleration $a_{gy}(t)$ along the Y-axis are:

$$\begin{bmatrix} \mathbf{m} & \mathbf{0} \\ \mathbf{0} & \mathbf{m} \end{bmatrix} \begin{Bmatrix} \ddot{\mathbf{u}}_y(t) \\ r\ddot{\mathbf{u}}_\theta(t) \end{Bmatrix} + \begin{bmatrix} \mathbf{K}_y & \frac{e}{r}\mathbf{K}_y \\ \frac{e}{r}\mathbf{K}_y & [\,(\frac{e}{r})^2 + \frac{C_{\theta R}}{r^2 C_y}\,]\,\mathbf{K}_y \end{bmatrix} \begin{Bmatrix} \mathbf{u}_y(t) \\ r\mathbf{u}_\theta(t) \end{Bmatrix} = -\begin{Bmatrix} \mathbf{m}\,\mathbf{1} \\ \mathbf{0} \end{Bmatrix} a_{gy}(t) \tag{3.15}$$

where **m** is a diagonal mass matrix of dimension N, the number of stories, with diagonal entries equal to m_j, the mass at the j^{th} floor, j=1, ..., N; **1** and **0** are vectors of dimension N with all elements equal to one and zero, respectively.

3.1.2 Simple Plan

For the system of Figure 2a, equations (3.5) specialize to:

$$\begin{aligned} \mathbf{K}_y &= \mathbf{k}_{y1} \\ \mathbf{K}_{y\theta} &= \mathbf{K}_{\theta y} = e\,\mathbf{K}_y \\ \mathbf{K}_\theta &= e^2\mathbf{k}_{y1} + 2\,y_2^2\,\mathbf{k}_{x2} \end{aligned} \tag{3.16}$$

The stiffness matrix for the system of Figure 2a is, therefore, obtained by substituting equations (3.16) into (3.10):

$$\mathbf{K} = \begin{bmatrix} \mathbf{k}_{y1} & \frac{e}{r}\mathbf{k}_{y1} \\ \frac{e}{r}\mathbf{k}_{y1} & (\frac{e}{r})^2\mathbf{k}_{y1} + 2(\frac{y_2}{r})^2\mathbf{k}_{x2} \end{bmatrix} \tag{3.17}$$

If the joint rotation indices of frames (1) and (2) of the simple system of Figure 2a are equal, i.e. if $\rho_1 = \rho_2 = \rho$, (a condition which is assumed throughout this study), then the lateral stiffness matrices of the two frames are proportional (Appendix B):

$$\mathbf{k}_{x2} = \frac{I_2}{I_1}\,\mathbf{k}_{y1} \tag{3.18}$$

where I_1 and I_2 are the moments of inertia of the columns of frames (1) and (2), respectively. Substituting equation (3.18) into (3.16c) leads to:

$$\mathbf{K}_\theta = (\,e^2 + 2\,y_2^2\,\frac{I_2}{I_1}\,)\,\mathbf{k}_{y1} \tag{3.19}$$

Substituting equations (3.18) and (3.19) into (3.17), the stiffness matrix of the system of Figure 2a with $\rho_1 = \rho_2 = \rho$ is therefore given by:

$$\mathbf{K} = \begin{bmatrix} \mathbf{k}_{y1} & \frac{e}{r}\mathbf{k}_{y1} \\ \frac{e}{r}\mathbf{k}_{y1} & [\,(\frac{e}{r})^2 + 2(\frac{y_2}{r})^2\frac{I_2}{I_1}\,]\,\mathbf{k}_{y1} \end{bmatrix} \tag{3.20}$$

The undamped equations of motion of the system of Figure 2 subjected to ground acceleration $a_{gy}(t)$ along the Y-axis are:

$$\begin{bmatrix} \mathbf{m} & \mathbf{0} \\ \mathbf{0} & \mathbf{m} \end{bmatrix} \begin{Bmatrix} \ddot{\mathbf{u}}_y(t) \\ r\ddot{\mathbf{u}}_\theta(t) \end{Bmatrix} + \begin{bmatrix} \mathbf{k}_{y1} & \frac{e}{r}\mathbf{k}_{y1} \\ \frac{e}{r}\mathbf{k}_{y1} & [\,(\frac{e}{r})^2 + 2(\frac{y_2}{r})^2\frac{I_2}{I_1}\,]\,\mathbf{k}_{y1} \end{bmatrix} \begin{Bmatrix} \mathbf{u}_y(t) \\ r\mathbf{u}_\theta(t) \end{Bmatrix} = -\begin{Bmatrix} \mathbf{m}\,\mathbf{1} \\ \mathbf{0} \end{Bmatrix} a_{gy}(t) \tag{3.21}$$

Damping of the system is directly defined in each of the 2N natural modes of vibration of the system. The viscous damping factor ξ, expressed as a fraction of critical damping, is assumed to be the same in each mode of vibration.

The stiffness matrices for a building with general plan (e.g. Figure 1) (equation (3.14)) and for a building with the simple plan of Figure 2a (equation (3.20)) are identical provided the static eccentricity ratio e/r is the same for the two buildings, the lateral stiffness matrices are identical, i.e. $\mathbf{k}_{y1} = \mathbf{K}_y$, and $2\,(y_2/r)^2\,I_2/I_1 = C_{\theta R}/r^2 C_y$. The last of these conditions will be shown later to imply that the uncoupled torsional to lateral frequency ratios of the two buildings are equal. If in addition to these three conditions, m, the mass of each floor, and the damping ratio ξ are the same for the two buildings, it is apparent from equations (3.15) and (3.21) that the equations of motion of the

two buildings are identical, and hence their displacement responses to the same ground shaking are also identical. Thus, the conclusions from studying the dynamic response of the building of Figure 2a in Sections 5, 6, 7 and 8, are also applicable to buildings, described in Section 2.2.1, with more general plans, e.g. Figure 1.

3.2 Corresponding Torsionally-Uncoupled, Multi-Story Systems

Equations (3.15) and (3.21) govern the coupled lateral ($\mathbf{u}_y$)-torsional ($\mathbf{u}_\theta$) motions of the buildings described in Sections 2.2.1 and 2.2.2, respectively. If the centers of mass of these buildings coincide with the centers of rigidity, i.e. $e = 0$ (Figure 6), the building would not experience any torsional motions, i.e. $\mathbf{u}_\theta = \mathbf{0}$, when it is subjected to translational ground motion only. The undamped equations governing the motions of the corresponding torsionally-uncoupled, multi-story system with all properties identical to the torsionally-coupled, multi-story building except that $e = 0$ are:

$$\mathbf{m}\,\ddot{\mathbf{v}}_o(t) + \mathbf{K}_y\,\mathbf{v}_o(t) = -\mathbf{m}\,\mathbf{1}\,a_{gy}(t) \tag{3.22}$$

where $\mathbf{v}_o(t)$ is the vector of lateral floor displacements. These are also the equations of motion for the planar vibration of frame (1) of Figure 2a subjected to translational ground motion in its own plane.

3.3 Associated Torsionally-Coupled, One-Story System

It will be shown in Section 4 that the response of a torsionally-coupled, multi-story building with properties described in Section 2.2.1 can be related to the responses of two systems: the corresponding torsionally-uncoupled, multi-story system introduced in Section 3.2, and an associated torsionally-coupled, one-story system with the following properties: (1) the static eccentricity ratio e/r for the associated torsionally-coupled, one-story system is the same as for all the floors of the torsionally-coupled, multi-story building; and (2) the ratio $K_{\theta R}/r^2K_y$ of the associated torsionally-coupled, one-story system-- where $K_{\theta R}$ is the torsional stiffness defined at its center of rigidity, K_y its lateral stiffness along the Y-axis, and r its radius of gyration about a vertical axis passing through its center of mass-- equals the ratio $C_{\theta R}/r^2C_y$ of the torsionally-coupled, multi-story building, an equality which implies that the uncoupled torsional to lateral frequency ratio is

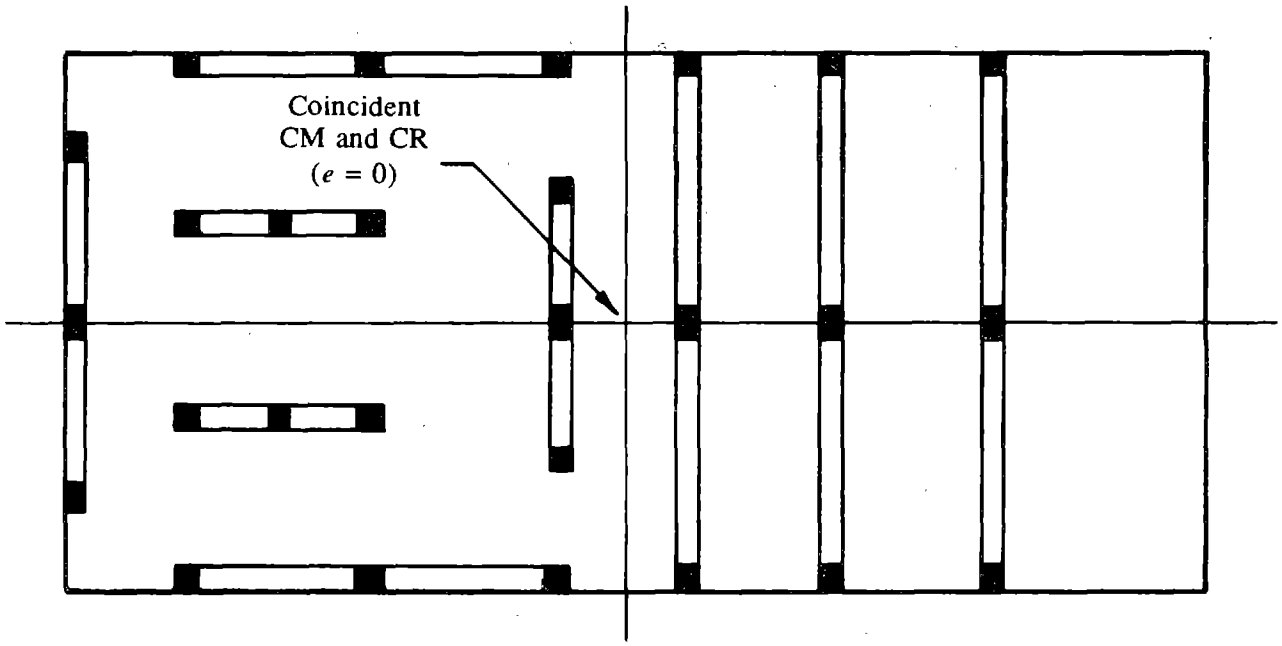

(a) Plan of Torsionally-uncoupled System Corresonding to One-way Symmetric Building of Figure 1

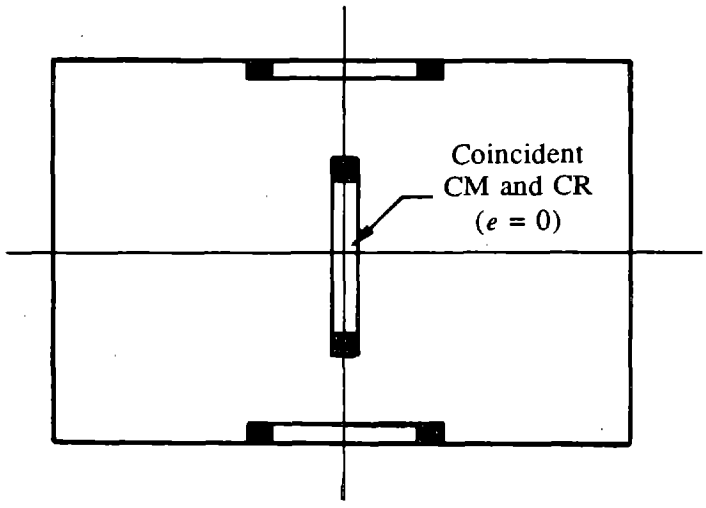

(b) Plan of Torsionally-uncoupled System Corresponding to Simple Plan of Figure 2a

FIGURE 6 Floor Plans of Corresponding Torsionally-uncoupled Systems

identical for the two systems (Section 4).

The equations of motion of the associated torsionally-coupled, one-story system subjected to ground acceleration $a_{gy}(t)$ along the Y-axis, are:

$$\begin{Bmatrix} \ddot{u}_y \\ r\,\ddot{u}_\theta \end{Bmatrix} + \omega_y^2 \begin{bmatrix} 1 & \frac{e}{r} \\ \frac{e}{r} & \frac{K_\theta}{r^2 K_y} \end{bmatrix} \begin{Bmatrix} u_y \\ r\,u_\theta \end{Bmatrix} = - \begin{Bmatrix} 1 \\ 0 \end{Bmatrix} a_{gy}(t) \tag{3.23}$$

where, the two degrees of freedom of the rigid deck are: u_y, the lateral displacement of the center of mass, along the Y-axis, relative to the ground, and u_θ, the deck rotation about a vertical axis; ω_y is the lateral vibration frequency of the corresponding torsionally-uncoupled, one-story system-- a system with coincident centers of mass and rigidity ($e = 0$) but all other properties identical to the associated torsionally-coupled, one-story system; and K_θ is the torsional stiffness defined at the center of mass. It can be shown that the torsional stiffness of the associated torsionally-coupled, one-story system defined at its center of rigidity is given by:

$$K_{\theta R} = K_\theta - e^2 K_y \tag{3.24}$$

4. ANALYSIS PROCEDURE

The maximum value (over time) of any response of a torsionally-coupled, N-story building, with one-axis of symmetry in plan, to earthquake ground motion in the horizontal direction perpendicular to the symmetry axis can be estimated by the Response Spectrum Analysis (RSA) procedure applied to the 2N-DOF system. In this section it is shown that, for buildings belonging to the special class (Section 2.1) with the additional restriction that all frames having proportional lateral stiffness matrices (Section 2.2.1), the earthquake response can be determined by analyzing two simpler systems: (1) the corresponding torsionally-uncoupled, N-story system described in Section 3.2; and (2) the associated torsionally-coupled, one-story system described in Section 3.3. Although this analysis procedure is developed for one-way symmetric buildings (e.g. Figure 1), it is extendable to the more general case of no axes of symmetry, as demonstrated earlier [3] for shear buildings.

4.1 Frequencies and Mode Shapes

The natural vibration frequencies and mode shapes of the N-story building are solutions of the eigen-problem of order 2N associated with equation (3.15):

$$\begin{bmatrix} \mathbf{K}_y - \omega^2 \mathbf{m} & \frac{e}{r}\mathbf{K}_y \\ \frac{e}{r}\mathbf{K}_y & [\,(\frac{e}{r})^2 + \frac{C_{\theta R}}{r^2 C_y}\,]\mathbf{K}_y - \omega^2 \mathbf{m} \end{bmatrix} \begin{Bmatrix} \boldsymbol{\phi}_y \\ \boldsymbol{\phi}_\theta \end{Bmatrix} = \begin{Bmatrix} \mathbf{0} \\ \mathbf{0} \end{Bmatrix} \tag{4.1}$$

It will be shown that these solutions of these equations can be expressed in terms of the frequencies and mode shapes of two systems: the corresponding torsionally-uncoupled, multi-story system, defined in Section 3.2; and the associated torsionally-coupled, one-story system introduced in Section 3.3.

For the corresponding torsionally-uncoupled, multi-story system $e = 0$ and the lateral and torsional components of motion are uncoupled; equation (4.1) then reduces to:

$$(\,\mathbf{K}_y - \omega_y^2\,\mathbf{m}\,)\,\boldsymbol{\psi} = \mathbf{0} \tag{4.2a}$$

and,

$$[\ \frac{C_{\theta R}}{r^2 C_y}\ \mathbf{K}_y - \omega_\theta^2\ \mathbf{m}\ ]\ \boldsymbol{\psi} = \mathbf{0} \tag{4.2b}$$

The lateral vibration frequencies ω_{yj} and mode shapes $\boldsymbol{\psi}_j$ of the uncoupled system are solutions of equations (4.2a). It is apparent that $\boldsymbol{\psi}_j$ are also the torsional mode shapes of the uncoupled system and the torsional frequencies $\omega_{\theta j}$ and lateral frequencies ω_{yj} are related by:

$$\frac{\omega_{\theta j}}{\omega_{yj}} = \sqrt{\frac{C_{\theta R}}{r^2 C_y}} \tag{4.3}$$

Equation (4.3) indicates that the ratio of the jth uncoupled torsional frequency $\omega_{\theta j}$ to the jth lateral frequency ω_{yj} does not depend on 'j'. The ratio of the jth uncoupled torsional frequency to the jth lateral frequency of the building is, from this point on, denoted by Ω, where:

$$\Omega = \frac{\omega_{\theta j}}{\omega_{yj}} = \sqrt{\frac{C_{\theta R}}{r^2 C_y}} \tag{4.4}$$

Next it is shown that the natural vibration mode shapes $\boldsymbol{\phi}$ of the torsionally-coupled building are of the following form:

$$\boldsymbol{\phi} = \begin{Bmatrix} \boldsymbol{\phi}_y \\ \boldsymbol{\phi}_\theta \end{Bmatrix} = \begin{Bmatrix} \alpha_y\, \boldsymbol{\psi}_j \\ \alpha_\theta\, \boldsymbol{\psi}_j \end{Bmatrix} \tag{4.5}$$

For $\boldsymbol{\phi}$ as given by equation (4.5) to be a mode shape, it must satisfy equation (4.1); thus:

$$\begin{bmatrix} \mathbf{K}_y - \omega^2 \mathbf{m} & \frac{e}{r}\mathbf{K}_y \\ \frac{e}{r}\mathbf{K}_y & [(\frac{e}{r})^2 + \Omega^2]\mathbf{K}_y - \omega^2 \mathbf{m} \end{bmatrix} \begin{Bmatrix} \alpha_y\, \boldsymbol{\psi}_j \\ \alpha_\theta\, \boldsymbol{\psi}_j \end{Bmatrix} = \begin{Bmatrix} \mathbf{0} \\ \mathbf{0} \end{Bmatrix} \tag{4.6}$$

wherein equations (4.3) and (4.4) have been utilized. Substituting equations (4.2) into equations (4.6), and premultiplying each of the two sub-matrix equations by $(1/\omega_{yj}^2)\,\boldsymbol{\psi}_j^T$ results in:

$$\begin{bmatrix} 1 - \bar{\omega}^2 & \frac{e}{r} \\ \frac{e}{r} & (\frac{e}{r})^2 + \Omega^2 - \bar{\omega}^2 \end{bmatrix} \begin{Bmatrix} \alpha_y \\ \alpha_\theta \end{Bmatrix} = \begin{Bmatrix} 0 \\ 0 \end{Bmatrix} \tag{4.7}$$

where $\bar{\omega} = \omega/\omega_{yj}$. Thus, $\boldsymbol{\phi}$ as given by equation (4.5) is a mode shape of the torsionally-coupled,

multi-story building provided $\boldsymbol{\alpha}$, where $\boldsymbol{\alpha}^T = < \alpha_y \quad \alpha_\theta >$ is an eigenvector of equation (4.7); the natural frequency of this coupled mode of vibration, $\omega = \bar{\omega}\, \omega_{yj}$, where $\bar{\omega}$ is the eigenvalue of equation (4:7).

It is possible to physically interpret equations (4.7) as the eigen-equations of the associated one-story system introduced in Section 3.3. Starting from equations (3.23), it can be shown that a natural vibration frequency ω and mode shape $\boldsymbol{\alpha}$ of the associated one-story system would satisfy the eigen-equation:

$$\begin{bmatrix} 1 - (\frac{\omega}{\omega_y})^2 & \frac{e}{r} \\ \frac{e}{r} & (\frac{e}{r})^2 + \Omega^2 - (\frac{\omega}{\omega_y})^2 \end{bmatrix} \begin{Bmatrix} \alpha_y \\ \alpha_\theta \end{Bmatrix} = \begin{Bmatrix} 0 \\ 0 \end{Bmatrix} \tag{4.8}$$

where:

$$\Omega = \frac{\omega_\theta}{\omega_y} = \sqrt{\frac{K_{\theta R}}{r^2 K_y}} \tag{4.9}$$

The frequencies ω_θ and ω_y are the torsional and lateral vibration frequencies of the corresponding torsionally-uncoupled, one-story system-- a system with coincident centers of mass and rigidity ($e = 0$) but all other properties identical to the associated torsionally-coupled, one-story system. Because equation (4.8) with $\omega_y = \omega_{yj}$ is identical to equation (4.7), it is apparent that the latter is the eigen-equation of the associated torsionally-coupled, one-story system, defined in Section 3.3, with eccentricity ratio equal to e/r, uncoupled torsional to lateral frequency ratio equal to Ω, and with the uncoupled lateral frequency ω_y equal to ω_{yj}, the j^{th} lateral frequency of the corresponding torsionally-uncoupled, multi-story system.

Hence, the natural frequencies, ω_{nj}, and mode shapes $\boldsymbol{\phi}_{nj}$ of a torsionally-coupled, multi-story building belonging to the special class of buildings, defined in Section 2.1, with the additional restriction of proportional lateral stiffness matrices of all resisting frames, introduced in Section 2.2.1, are given by:

$$\omega_{nj} = \bar{\omega}_n \, \omega_{yj} \tag{4.10}$$

and,

$$\phi_{nj} = \begin{Bmatrix} \phi_{ynj} \\ \phi_{\theta nj} \end{Bmatrix} = \begin{Bmatrix} \alpha_{yn} \psi_j \\ \alpha_{\theta n} \psi_j \end{Bmatrix} \tag{4.11}$$

for n = 1, 2 and j = 1, ..., N, where ω_{yj} and ψ_j are the natural frequencies and mode shapes in lateral vibration of the corresponding torsionally-uncoupled, N-story system; $\bar{\omega}_n$ and α_n are the normalized frequencies and mode shapes of the associated torsionally-coupled, one-story system. Solving these two eigen-problems is simpler than the standard method of solving equation (4.1), an eigenvalue problem of order 2N.

Clearly, equations (4.10) and (4.11) are satisfied due to the special form of the building stiffness matrix, given by equation (3.14), when the lateral stiffness matrices of all frames are mutually proportional. If this is not the case, the building stiffness matrix is given by equation (3.10), and it is not possible to achieve the simplification displayed by equations (4.10) and (4.11).

The coupled lateral-torsional responses of buildings, for which equations (4.10) and (4.11) are valid, to earthquake ground motion can be determined by analyzing the earthquake responses of the corresponding torsionally-uncoupled, N-story system, described in Section 3.2, and the associated torsionally-coupled, one-story system, introduced in Section 3.3, for the same ground excitation. The Response Spectrum Analysis (RSA) procedures for earthquake analysis of the two simpler systems are described in the next two sections. The results of these two analyses are utilized in Section 4.4 to simplify the RSA procedure for the torsionally-coupled buildings of Section 2.2.1, and the resulting analysis procedure is summarized in Section 4.5.

4.2 RSA of Corresponding Torsionally-Uncoupled, Multi-Story System

The planar vibration of the corresponding torsionally-uncoupled, N-story system due to ground motion along the Y-axis is governed by equation (3.22). The maximum response of this system can be estimated from the earthquake design spectrum by the following procedure:

1. Determine structural properties:

   (a) Compute the mass matrix, **m**, defined in Section 3.

   (b) Compute the lateral stiffness matrix $\mathbf{K}_y$, by the procedure outlined in Section 3.

   (c) Estimate modal damping ratios, ξ.

2. Solve the eigen-problem:

$$(\mathbf{K}_y - \omega_y^2 \mathbf{m}) \boldsymbol{\psi} = \mathbf{0} \tag{4.2a}$$

   to determine the natural vibration frequencies ω_{yj} (natural periods $T_{yj} = 2\pi/\omega_{yj}$) and mode shapes $\boldsymbol{\psi}_j$ for j=1, ..., N.

3. Compute the maximum response in individual modes of vibration by repeating the following steps for each vibration mode contributing significantly to the response:

   (a) Corresponding to period T_{yj} and damping ratio ξ of the jth mode, read the ordinate S_{aj} of the pseudo-acceleration response spectrum of the ground motion.

   (b) Compute the floor displacements vector, $\mathbf{v}_j$, from:

$$\mathbf{v}_j = \frac{L_j}{M_j \omega_{yj}^2} S_{aj} \boldsymbol{\psi}_j \tag{4.12}$$

   where,

$$L_j = \boldsymbol{\psi}_j^T \mathbf{m}\, \mathbf{1} \quad \text{and} \quad M_j = \boldsymbol{\psi}_j^T \mathbf{m} \boldsymbol{\psi}_j \tag{4.13}$$

   (c) Compute the equivalent, static lateral forces, $\mathbf{f}_j$, required to cause lateral displacements $\mathbf{v}_j$, from:

$$\mathbf{f}_j = \omega_{yj}^2 \mathbf{m} \mathbf{v}_j = \frac{L_j}{M_j} S_{aj} \mathbf{m} \boldsymbol{\psi}_j \tag{4.14}$$

   (d) Compute the vector of story shears, $\mathbf{V}_j$, and the vector of story overturning moments, $\mathbf{M}_j$, from:

$$\mathbf{V}_j = \mathbf{S}\,\mathbf{f}_j \tag{4.15}$$

$$\mathbf{M}_j = \mathbf{H}\,\mathbf{f}_j \tag{4.16}$$

in which, for a five-story building for example, **S** and **H** are summation matrices of the form:

$$\mathbf{S} = \begin{bmatrix} 1 & 1 & 1 & 1 & 1 \\ 0 & 1 & 1 & 1 & 1 \\ 0 & 0 & 1 & 1 & 1 \\ 0 & 0 & 0 & 1 & 1 \\ 0 & 0 & 0 & 0 & 1 \end{bmatrix} \quad \text{and} \quad \mathbf{H} = h \begin{bmatrix} 1 & 2 & 3 & 4 & 5 \\ 0 & 1 & 2 & 3 & 4 \\ 0 & 0 & 1 & 2 & 3 \\ 0 & 0 & 0 & 1 & 2 \\ 0 & 0 & 0 & 0 & 1 \end{bmatrix} \tag{4.17}$$

In particular, the base shear, V_{Bj}, and base overturning moment, M_{Bj}, are given by:

$$V_{Bj} = \mathbf{1}^T\,\mathbf{f}_j = \frac{L_j^2}{M_j}\,S_{aj} = W_j^*\,\frac{S_{aj}}{g} \quad \text{and,} \tag{4.18}$$

$$M_{Bj} = h < 1\ 2\ 3\ 4\ 5 > \mathbf{f}_j = h_j^*\,V_{Bj} \tag{4.19}$$

where,

$$W_j^* = \frac{L_j^2}{M_j}\,g \quad \text{and} \quad h_j^* = \frac{h < 1\ 2\ 3\ 4\ 5 > \mathbf{m}\,\boldsymbol{\psi}_j}{L_j} \tag{4.20}$$

are known as the effective weight and effective height for mode 'j'. The effective weight can be interpreted as the portion of the total weight of the building which is effective in producing the base shear due to the jth mode of vibration [12]. Since the base shear is equal to the resultant of the equivalent lateral forces $\mathbf{f}_j$, h_j^* may be interpreted as the height of the resultant force above the base [12].

(e) Compute forces F_j in structural members of a frame 'i' spanning along the Y-axis at a distance x_i from the centers of mass, by a static analysis of the frame subjected to the equivalent lateral forces, $[\,C_{yi} / (\sum_l C_{yl})\,]\,\mathbf{f}_j$, where C_{yi} was defined in equation (3.6). This is implemented by first recovering the condensed joint rotations corresponding to the floor lateral displacements $\mathbf{v}_j$, using the complete stiffness matrix of the frame. Beam moments, column moments and column axial forces are then computed using the relevant joint rotations and lateral

displacements, and the element stiffness matrices. (See Appendix C for additional details).

4. Determine an estimate of the maximum value r_o of any response quantity $r_o(t)$, by combining its modal maxima, r_j, according to:

$$r_o = \left[\sum_{j=1}^{N} r_j^2 \right]^{1/2} \tag{4.21}$$

The Square-Root of the Sum of Squares (SRSS) combination rule is satisfactory because the planar vibration frequencies ω_{yj} of the corresponding torsionally-uncoupled, N-story system are invariably well separated. As demonstrated in [7], the earthquake response of building frames may be satisfactorily estimated by including only the first two terms, i.e. the contributions of only the first two vibration modes, in equation (4.21); only the first mode contribution usually suffices if the fundamental vibration period is in the acceleration-controlled region of the earthquake design spectrum.

4.3 RSA of Associated Torsionally-Coupled, One-Story System

The response of the associated torsionally-coupled, one-story system defined in Section 3.3 to ground motion along the Y-axis is governed by equation (3.23). The maximum response of the system can be estimated from the earthquake response spectrum by the following procedure (see Part I for additional details):

1. Solve the eigen problem of equation (4.8) to obtain the natural vibration frequencies and mode shapes of the system, given by:

$$\bar{\omega}_n \equiv \frac{\omega_n}{\omega_y} = \left[\frac{1 + (e/r)^2 + \Omega^2}{2} \pm \sqrt{\left[\frac{1 + (e/r)^2 - \Omega^2}{2} \right]^2 + (e/r)^2 \Omega^2} \right]^{1/2}, \quad n=1,2 \tag{4.22}$$

and,

$$\boldsymbol{\alpha}_n = \begin{Bmatrix} \alpha_{yn} \\ \alpha_{\theta n} \end{Bmatrix} = \frac{1}{\sqrt{(e/r)^2 + (1 - \bar{\omega}_n^2)^2}} \begin{Bmatrix} -e/r \\ 1 - \bar{\omega}_n^2 \end{Bmatrix}, \quad n=1,2 \tag{4.23}$$

where the mode shapes have been normalized so that:

$$\boldsymbol{\alpha}_n^T \boldsymbol{\alpha}_n = \alpha_{yn}^2 + \alpha_{\theta n}^2 = 1 \tag{4.24}$$

2. Compute the maximum response in individual modes of vibration by repeating the following steps for each mode:

(a) Corresponding to period T_n ($= 2\pi/\omega_n$) of the n^{th} vibration mode and damping ratio, ξ, read the pseudo-acceleration ordinate, S_{an}, of the earthquake design spectrum

(b) Compute the displacement vector at the center of mass from:

$$\mathbf{u}_n = \begin{Bmatrix} u_{yn} \\ r u_{\theta n} \end{Bmatrix} = \frac{\alpha_{yn}}{\omega_n^2} \begin{Bmatrix} \alpha_{yn} \\ \alpha_{\theta n} \end{Bmatrix} S_{an} = \frac{\alpha_{yn}}{\omega_n^2} S_{an} \boldsymbol{\alpha}_n \tag{4.25}$$

The lateral displacement along the Y-axis at a distance x_i from the center of mass of the associated torsionally-coupled, one-story system is given by:

$$u_{yn}(x_i) = u_{yn} + \frac{x_i}{r} (r u_{\theta n}) \tag{4.26}$$

In particular, the lateral displacement at the center of rigidity, v_n, is determined by:

$$v_n = u_{yn} + \frac{e}{r} (r u_{\theta n}) = \frac{\alpha_{yn}^2}{\omega_y^2} S_{an} \tag{4.27}$$

(c) Compute the equivalent external forces which applied statically at the center of mass cause displacements u_{yn} and $r u_{\theta n}$, from:

$$\mathbf{f}_n = \begin{Bmatrix} f_{yn} \\ f_{\theta n} \end{Bmatrix} = m \, \alpha_{yn} \begin{Bmatrix} \alpha_{yn} \\ \alpha_{\theta n} \end{Bmatrix} S_{an} = m \, \alpha_{yn} \, S_{an} \, \boldsymbol{\alpha}_n \tag{4.28}$$

where m denotes the mass of the system. The equivalent static lateral force is f_{yn} and the torsional moment is $r f_{\theta n}$.

(d) Compute, by statics, the base shear, V_n, base overturning moment, M_n, and the base torque at the center of mass, T_{Mn}, from the external forces f_{yn} and $r f_{\theta n}$:

$$V_n = f_{yn} = W\ \alpha_{yn}^2\ \frac{S_{an}}{g} = W_n^*\ \frac{S_{an}}{g} \tag{4.29}$$

$$M_n = h\ f_{yn} = h\ V_n \tag{4.30}$$

$$T_{Mn} = r\ f_{\theta n} = W\ r\ \alpha_{yn}\ \alpha_{\theta n}\ \frac{S_{an}}{g} \tag{4.31}$$

where W is the total weight of the building, h its story height, and W_n^* its effective weight in the n^{th} mode of vibration, such that:

$$\frac{W_n^*}{W} = \alpha_{yn}^2 \quad \text{with} \quad \sum_1^2 W_n^* = W \tag{4.32}$$

The base torque at the center of rigidity, T_{Rn}, is obtained from:

$$T_{Rn} = T_{Mn} - e\ V_n = W\ r\ \alpha_{yn}\left(\alpha_{\theta n} - \frac{e}{r}\ \alpha_{yn}\right)\frac{S_{an}}{g} = e_n^*\ V_n \tag{4.33}$$

where e_n^* can be referred to as the effective eccentricity in the n^{th} mode of vibration, satisfying:

$$\frac{e_n^*}{r} = \frac{\alpha_{\theta n}}{\alpha_{yn}} - \frac{e}{r} \tag{4.34}$$

3. Determine an estimate of the maximum, r, of a response quantity by combining its modal maxima, r_n, according to an appropriate combination rule. Since the vibrational frequencies of torsionally-coupled systems may be closely spaced, the cross-corelation between modal responses can be significant, and should be considered in the combination rule used. A heuristically motivated combination rule that considers this effect [6,13] was utilized in earlier investigations of the dynamics of torsionally-coupled systems [3,10,14]. The more recent Complete Quadratic Combination (CQC) rule [15], which leads to essentially identical results as the earlier rule, is utilized in this work. According to the CQC rule, an estimate of the maximum r of the response quantity can be obtained from:

$$r = \left[\sum_{n=1}^{2} \sum_{m=1}^{2} \gamma_{nm} r_n r_m \right]^{1/2} \tag{4.35}$$

where γ_{nm} is the cross-correlation factor between modes 'n' and 'm', and r_n and r_m are the modal maxima of the response quantity in modes 'n' and 'm', respectively. The cross-correlation factors, γ_{nm}, are, in general, functions of the duration and frequency content of the ground motion, as well as the natural frequencies and modal damping ratios of the system. For smooth earthquake response spectra, representative of broad-frequency-band excitations, long earthquake durations compared to the natural periods of the system, and equal modal damping ratios, ξ, γ_{nm} is approximated by [16]:

$$\gamma_{nm} = \frac{8\xi^2 (1 + q_{nm}) q_{nm}^{1.5}}{(1 - q_{nm}^2)^2 + 4\xi^2 q_{nm} (1 + q_{nm})^2} \tag{4.36}$$

in which,

$$q_{nm} = \frac{\omega_n}{\omega_m} \tag{4.37}$$

Equation (4.35) can be written as:

$$r = \left[r_1^2 + r_2^2 + 2\gamma_{12} r_1 r_2 \right]^{1/2} \tag{4.38}$$

in which the first two terms represent the well-known combination rule: the Square-Root of the Sum of Squares (SRSS) of the modal maxima. The last term accounts for the cross-correlation between the two modes of the one-story systems and is especially important when the natural frequencies ω_1 and ω_2 are close to each other. In computing the modal maxima r_n from step 4, using equations (4.25) to (4.34), the algebraic sign obtained for r_n should be retained. The last term in equation (4.38) assumes positive or negative values depending on whether r_1 and r_2 have the same or opposite algebraic signs.

It will be seen later that it is useful to express the lateral displacements u_y at the center of mass, $u_y(x_i)$ at a distance x_i from the center of mass and v at the center of rigidity; the deck rotation

around a vertical axis u_θ, the base shear V, the base overturning moment M, and the base torques T_M and T_R at the centers of mass and rigidity, respectively, in normalized form:

$$\bar{u}_y = \frac{u_y}{v_o} \; , \; \bar{u}_\theta = \frac{r\,u_\theta}{v_o} \; , \; \bar{u}_y(x_i) = \frac{u_y(x_i)}{v_o} \; , \; \bar{v} = \frac{v}{v_o} \tag{4.39}$$

$$\bar{V} = \frac{V}{V_o} \; , \; \bar{M} = \frac{M}{M_o} \; , \; \bar{T}_M = \frac{T_M}{r\,V_o} \; , \; \frac{e_d}{r} = \bar{T}_R = \frac{T_R}{r\,V_o} \tag{4.40}$$

where v_o, V_o and M_o are the maximum lateral displacement, base shear and base overturning moment of the corresponding torsionally-uncoupled, one-story system, a system with coincident centers of mass and rigidity, but all other properties identical to the associated torsionally-coupled, one-story system. The uncoupled system responses are determined from the standard formulas for single-degree-of-freedom systems [12]:

$$v_o = \frac{S_{ay}}{\omega_y^2} \; , \; V_o = m\,S_{ay} \quad \text{and} \quad M_o = m\,h\,S_{ay} \tag{4.41}$$

where S_{ay} is the pseudo-acceleration response spectrum ordinate corresponding to lateral vibration period ($T_y = 2\pi/\omega_y$) and damping ratio ξ of the uncoupled system.

The normalized quantity, $\bar{T}_R$, can be interpreted as the dynamic eccentricity, e_d, the distance from the center of rigidity of the system where the uncoupled base shear should be applied statically to cause a base torque equal to T_R at the center of rigidity of the system [10]. The ratio e_d/e then represents the dynamic amplification of the static torque eV_o.

The contribution of the nth vibration mode to the normalized response quantities can be determined from equations (4.25) to (4.34), leading to:

$$\bar{\mathbf{u}}_n = \begin{Bmatrix} \bar{u}_{yn} \\ \bar{u}_{\theta n} \end{Bmatrix} = \frac{\alpha_{yn}}{\bar{\omega}_n^2} \begin{Bmatrix} \alpha_{yn} \\ \alpha_{\theta n} \end{Bmatrix} \frac{S_{an}}{S_{ay}} \tag{4.42}$$

$$\bar{u}_{yn}(x_i) = \bar{u}_{yn} + \frac{x_i}{r}\,\bar{u}_{\theta n} \tag{4.43}$$

$$\bar{v}_n = \bar{V}_n = \bar{M}_n = \alpha_{yn}^2 \frac{S_{an}}{S_{ay}} = \bar{W}_n^* \frac{S_{an}}{S_{ay}} \tag{4.44}$$

$$\bar{T}_{Mn} = \alpha_{yn}\, \alpha_{\theta n} \frac{S_{an}}{S_{ay}} \tag{4.45}$$

and,

$$\frac{e_{dn}}{r} = \bar{T}_{Rn} = \bar{T}_{Mn} - \frac{e}{r} \bar{V}_n = \frac{e_n^*}{r} \bar{W}_n^* \frac{S_{an}}{S_{ay}} \tag{4.46}$$

where $\bar{W}_n^*$ is the effective weight of the associated torsionally-coupled, one-story system expressed as a fraction of its total weight.

An estimate of the maximum normalized response $\bar{r}$, can be determined by CQC of its modal maxima $\bar{r}_n$, i.e.

$$\bar{r} = \left[\sum_{n=1}^{2} \sum_{m=1}^{2} \gamma_{nm}\, \bar{r}_n\, \bar{r}_m \right]^{1/2} \tag{4.47}$$

4.4 RSA of Torsionally-Coupled, Multi-Story Buildings

It was shown in Section 4.1 that the natural frequencies ω_{nj} and mode shapes ϕ_{nj} of a torsionally-coupled, N-story building belonging to the special class of buildings (defined in Section 2.1), with the additional restriction of proportional lateral stiffness matrices of all its frames (Section 2.2.1), can be determined from the j^{th} frequency and mode shape of the corresponding torsionally-uncoupled, N-story system and the n^{th} normalized frequency and mode shape of the associated torsionally-coupled, one-story system. It will be demonstrated next that the response in a natural vibration mode of the building can also be determined by analyzing the two smaller systems.

4.4.1 Modal Displacements

Transforming the equations of motion [equation (3.15)] of the torsionally-coupled, multi-story building to modal coordinates, it can be shown that the peak value of the displacement response in

the njth vibration mode is:

$$\mathbf{u}_{nj} = \begin{Bmatrix} \mathbf{u}_{ynj} \\ r\,\mathbf{u}_{\theta nj} \end{Bmatrix} = \frac{L_{nj}}{\omega_{nj}^2 M_{nj}} S_{anj}\, \boldsymbol{\phi}_{nj} \tag{4.48}$$

where S_{anj} is the pseudo-acceleration response spectrum ordinate corresponding to ω_{nj} (or period $T_{nj} = 2\pi/\omega_{nj}$) and damping ratio ξ for the njth vibration mode; and

$$L_{nj} = \boldsymbol{\phi}_{ynj}^T \mathbf{m}\, \mathbf{1} = \alpha_{yn}\, \boldsymbol{\psi}_j^T \mathbf{m}\, \mathbf{1} = \alpha_{yn} L_j \tag{4.49a}$$

in which equations (4.11) and (4.13a) have been introduced; and the generalized mass:

$$M_{nj} = \boldsymbol{\phi}_{ynj}^T \mathbf{m}\, \boldsymbol{\phi}_{ynj} + \boldsymbol{\phi}_{\theta nj}^T \mathbf{m}\, \boldsymbol{\phi}_{\theta nj} = (\alpha_{yn}^2 + \alpha_{\theta n}^2)\, \boldsymbol{\psi}_j^T \mathbf{m}\, \boldsymbol{\psi}_j = M_j \tag{4.49b}$$

in which equations (4.11), (4.24) and (4.13b) have been utilized. Substituting equations (4.10), (4.11) and (4.49) into (4.48) leads to the first parts of equations (4.50a) and (4.50b), and using equations (4.12) and (4.42), leads to the second parts:

$$\mathbf{u}_{ynj} = \frac{\alpha_{yn}^2}{\bar{\omega}_n^2} \frac{L_j}{\omega_{yj}^2 M_j} S_{anj}\, \boldsymbol{\psi}_j = \left(\frac{\alpha_{yn}^2}{\bar{\omega}_n^2} \frac{S_{anj}}{S_{aj}}\right) \mathbf{v}_j = \bar{u}_{ynj}\, \mathbf{v}_j \tag{4.50a}$$

and,

$$r\mathbf{u}_{\theta nj} = \frac{\alpha_{yn}\, \alpha_{\theta n}}{\bar{\omega}_n^2} \frac{L_j}{\omega_{yj}^2 M_j} S_{anj}\, \boldsymbol{\psi}_j = \left(\frac{\alpha_{yn}\, \alpha_{\theta n}}{\bar{\omega}_n^2} \frac{S_{anj}}{S_{aj}}\right) \mathbf{v}_j = \bar{u}_{\theta nj}\, \mathbf{v}_j \tag{4.50b}$$

where $\mathbf{v}_j$ is the vector of maximum lateral displacements of the corresponding torsionally-uncoupled, N-story system in the jth mode of vibration [equation (4.12)]; $\bar{u}_{ynj}$ and $\bar{u}_{\theta nj}$ are the normalized maximum values of the lateral displacement at the center of mass and the deck rotation, respectively, in the nth vibration mode of the associated torsionally-coupled, one-story system [equations (4.42)] with uncoupled lateral vibration frequency ω_y equal to ω_{yj}.

The vector of lateral displacements of a frame 'i' spanning along the Y-axis at a distance x_i from the centers of mass of the system, due to the njth mode of vibration is given by:

$$\mathbf{u}_{ynj}(x_i) = \mathbf{u}_{ynj} + \frac{x_i}{r}(r\mathbf{u}_{\theta nj}) = (\bar{u}_{ynj} + \frac{x_i}{r}\bar{u}_{\theta nj})\,\mathbf{v}_j = \bar{u}_{ynj}(x_i)\,\mathbf{v}_j \tag{4.51}$$

in which equations (4.50) and (4.43) are utilized to obtain the second and the third parts of the result; $\bar{u}_{ynj}(x_i)$ is the normalized lateral displacement at a distance x_i from the center of mass in the n^{th} vibration mode of the associated torsionally-coupled, one-story system [equation (4.43)] with uncoupled lateral vibration frequency ω_y equal to ω_{yj}. In particular, the vector of lateral displacements at the centers of rigidity of the building in the nj^{th} vibration mode is determined from:

$$\mathbf{v}_{nj} = \mathbf{u}_{ynj} + \frac{e}{r}(r\mathbf{u}_{\theta nj}) = (\bar{u}_{ynj} + \frac{e}{r}\bar{u}_{\theta nj})\,\mathbf{v}_j = \bar{v}_{nj}\,\mathbf{v}_j \tag{4.52}$$

wherein equations (4.23), (4.44) and (4.50) have been introduced to obtain the second and third parts of the result; $\bar{v}_{nj}$ is the normalized maximum lateral displacement at the center of rigidity in the n^{th} mode of vibration of the associated torsinally-coupled, one-story system [equation (4.44)] with uncoupled lateral vibration frequency ω_y equal to ω_{yj}.

4.4.2 Modal Story Shears and Overturning Moments

The equivalent static, lateral forces $\mathbf{f}_{ynj}$ and torsional moments $r\mathbf{f}_{\theta nj}$ required to cause lateral displacements $\mathbf{u}_{ynj}$ and deck rotations $\mathbf{u}_{\theta nj}$ are given by:

$$\mathbf{f}_{nj} = \begin{Bmatrix} \mathbf{f}_{ynj} \\ \mathbf{f}_{\theta nj} \end{Bmatrix} = \omega_{nj}^2 \begin{bmatrix} \mathbf{m}\,\mathbf{u}_{ynj} \\ \mathbf{m}\,(r\,\mathbf{u}_{\theta nj}) \end{bmatrix} \tag{4.53}$$

The vector of maximum story shears $\mathbf{V}_{nj}$ and the vector of maximum story overturning moments $\mathbf{M}_{nj}$ in the nj^{th} vibration mode are obtained by statics from the equivalent static lateral forces $\mathbf{f}_{ynj}$:

$$\mathbf{V}_{nj} = \mathbf{S}\,\mathbf{f}_{ynj} \quad \text{and} \quad \mathbf{M}_{nj} = \mathbf{H}\,\mathbf{f}_{ynj} \tag{4.54}$$

where **S** and **H** are summation matrices given earlier by equations (4.17). Substituting equation (4.50a) in equation (4.53) and the latter in equation (4.54), and utilizing equations (4.10), (4.14) to (4.16), (4.42) and (4.44), results in:

$$\mathbf{V}_{nj} = \bar{\omega}_n^2 \, \bar{u}_{ynj} \, \omega_{yj}^2 \, \mathbf{S}\mathbf{m}\mathbf{v}_j = (\alpha_{yn}^2 \frac{S_{anj}}{S_{aj}}) (\mathbf{S}\mathbf{f}_j) = \bar{V}_{nj} \mathbf{V}_j \tag{4.55a}$$

and,

$$\mathbf{M}_{nj} = \bar{\omega}_n^2 \, \bar{u}_{ynj} \, \omega_{yj}^2 \, \mathbf{H}\mathbf{m}\mathbf{v}_j = (\alpha_{yn}^2 \frac{S_{anj}}{S_{aj}}) (\mathbf{H}\mathbf{f}_j) = \bar{M}_{nj} \mathbf{M}_j \tag{4.55b}$$

where $\mathbf{V}_j$ and $\mathbf{M}_j$ are the vectors of maximum story shears and story overturning moments in the corresponding torsionally-uncoupled, multi-story system in its j^{th} vibration mode [equations (4.15) and (4.16)]; $\bar{V}_{nj}$ and $\bar{M}_{nj}$ are the normalized maximum base shear and base overturning moment in the n^{th} vibration mode of the associated torsionally-coupled, one-story system [equations (4.44)] with uncoupled lateral vibration frequency ω_y equal to ω_{yj}.

In particular, the maximum base shear V_{Bnj} is given by a special case of equation (4.55a):

$$V_{Bnj} = \bar{V}_{nj} \, V_{Bj} = (\bar{W}_n^* \frac{S_{anj}}{S_{aj}}) (W_j^* \frac{S_{aj}}{g}) = W_{nj}^* \frac{S_{anj}}{g} \tag{4.56}$$

wherein equations (4.18) and (4.44) have been utilized; and

$$W_{nj}^* = W_j^* \bar{W}_n^* \tag{4.57}$$

is the effective weight in the nj^{th} vibration mode of the torsionally-coupled, multi-story building. It equals the product of the effective weight W_j^* in the j^{th} vibration mode of the corresponding torsionally-uncoupled, multi-story system [equation (4.20a)], and the effective weight $\bar{W}_n^*$ in the n^{th} mode of the associated torsionally-coupled, one-story system expressed as a fraction of total weight [equation (4.44)].

Similarly, the maximum base overturning moment is obtained from equation (4.55b), which after utilizing equations (4.44), (4.19) and (4.56) leads to:

$$M_{Bnj} = \bar{M}_{nj} \, M_{Bj} = \bar{V}_{nj} \, h_j^* \, V_{Bj} = h_j^* \, V_{Bnj} = h_{nj}^* \, V_{Bnj} \tag{4.58a}$$

where,

$$h_{nj}^{*} = h_{j}^{*} \tag{4.58b}$$

i.e. the effective height h_{nj}^{*} of the torsionally-coupled, multi-story building in the njth mode of vibration is equal to the effective height h_{j}^{*} of the corresponding torsionally-uncoupled, multi-story system in the jth mode [equation (4.20b)].

4.4.3 Modal Torques

The vector of maximum story torques at the centers of mass of the building in the njth vibration mode is determined from $\mathbf{f}_{\theta nj}$ by statics:

$$\mathbf{T}_{Mnj} = r\,\mathbf{S}\,\mathbf{f}_{\theta nj} \tag{4.59}$$

Substituting equations (4.50b) in equation (4.53) and the latter in equation (4.59), and utilizing equations (4.10), (4.14), (4.15), (4.42) and (4.45), results in:

$$\mathbf{T}_{Mnj} = r\,\bar{\omega}_{n}^{2}\,\bar{u}_{\theta nj}\,\omega_{yj}^{2}\,\mathbf{S}\,\mathbf{m}\,\mathbf{v}_{j} = (\,\alpha_{yn}\,\alpha_{\theta n}\,\frac{S_{anj}}{S_{aj}}\,)\;r\mathbf{S}\,\mathbf{f}_{j} = \bar{T}_{Mnj}(\,r\mathbf{V}_{j}\,) \tag{4.60}$$

where $\bar{T}_{Mnj}$ is the normalized maximum base torque at the center of mass in the nth vibration mode of the associated torsionally-coupled, one-story system [equation (4.45)] with uncoupled lateral vibration frequency ω_{y} equal to ω_{yj}. The vector of maximum story torques at the centers of rigidity in the njth vibration mode is given by:

$$\mathbf{T}_{Rnj} = \mathbf{T}_{Mnj} - e\,\mathbf{V}_{nj} \tag{4.61a}$$

Utilizing equations (4.46), (4.55a) and (4.60), equation (4.61a) can be rewritten as:

$$\mathbf{T}_{Rnj} = (\,\bar{T}_{Mnj} - \frac{e}{r}\,\bar{V}_{nj}\,)\,(\,r\mathbf{V}_{j}\,) = \bar{T}_{Rnj}\,(\,r\mathbf{V}_{j}\,) \tag{4.61b}$$

in which $\bar{T}_{Rnj}$ is the normalized maximum base torque at the center of rigidity in the nth vibration mode of the associated torsionally-coupled, one-story system [equation (4.46)] with uncoupled lateral vibration frequency ω_{y} equal to ω_{yj}. In particular, the base torques at centers of mass and rigidity, T_{BMnj} and T_{BRnj}, are special cases of equations (4.60) and (4.61b):

$$T_{BMnj} = \bar{T}_{Mnj}(r\,V_{Bj}) \tag{4.62}$$

and,

$$T_{BRnj} = \bar{T}_{Rnj}(r\,V_{Bj}) = e_n^*\,\bar{V}_{nj}\,V_{Bj} = e_n^*\,V_{Bnj} = e_{nj}^*\,V_{Bnj} \tag{4.63}$$

in which equations (4.44), (4.46) and (4.56) have been substituted, and e_{nj}^* is the effective eccentricity of the torsionally-coupled, multi-story building in the njth coupled mode of vibration, equals the effective eccentricity e_n^* of the associated one-story system in the nth mode, from which we conclude that e_{nj}^* is independent of 'j'. It will be shown later that a more meaningful expression for T_{BRnj} is obtained by substituting equations (4.18) and (4.44) into (4.63), to get:

$$T_{BRnj} = e_n^*\,\bar{V}_{nj}\,V_{Bj} = e_n^*(\bar{W}_n^*\,\frac{S_{anj}}{S_{aj}})(W_j^*\,\frac{S_{aj}}{g}) = (e_n^*\bar{W}_n^*)(W_j^*\frac{S_{anj}}{g}) \tag{4.64}$$

4.4.4 Modal Member Forces

The maximum force F_{nj} in a structural member of frame 'i', spanning along the Y-axis at a distance x_i from the centers of mass of the system, may be determined by a static analysis of the frame associated with the vector of lateral floor displacements $\mathbf{u}_{ynj}(x_i)$, at the location of the frame [equation (4.51)]. Since, according to equation (4.51), $\mathbf{u}_{ynj}(x_i)$ is the product of the normalized lateral displacement $\bar{u}_{ynj}(x_i)$ in the nth vibration mode of the associated torsionally-coupled, one-story system with ω_y equal to ω_{yj} and the vector $\mathbf{v}_j$ of lateral displacements in the jth mode of the corresponding torsionally-uncoupled, N-story system, the member force F_{nj} in the frame can be expressed as:

$$F_{nj} = \bar{u}_{ynj}(x_i)\,F_j \tag{4.65}$$

where F_j is the force in the same member due to the jth vibration mode of the corresponding torsionally-uncoupled, multi-story system, determined by the analysis procedure described in Section 4.2.

4.4.5 Summary

It is demonstrated by equations (4.50) to (4.52), (4.55) to (4.56), (4.58a), (4.60), and (4.61b) to (4.65) that the maximum value of any response quantity, r_{nj}, of the torsionally-coupled, multi-story building due to its njth mode of vibration is given by:

$$r_{nj} = \overline{r}_{nj}\, r_j \qquad n=1,2;\ j=1,...,N \tag{4.66}$$

where r_j is the maximum value of the same (or related) response quantity in the corresponding torsionally-uncoupled, multi-story system in its jth mode of vibration (see Table 1); and $\overline{r}_{nj}$ is the normalized response quantity corresponding to r_{nj} (see Table 1) in the nth vibration mode of the associated torsionally-coupled, one-story system with uncoupled lateral vibration frequency ω_y equal to ω_{yj}.

4.4.6 Modal Combination

An estimate of the maximum, r, of a response quantity is determined by combining its modal maxima, r_{nj}, according to the CQC rule:

$$r = \left[\sum_{j=1}^{N} \sum_{k=1}^{N} \sum_{n=1}^{2} \sum_{m=1}^{2} \gamma_{nj,mk}\, \overline{r}_{nj}\, \overline{r}_{mk}\, r_j\, r_k \right]^{1/2} \tag{4.67}$$

where $\gamma_{nj,mk}$ is computed by equation (4.36) for frequency ratios $q_{nj,mk}$ given by:

$$q_{nj,mk} = \frac{\omega_{nj}}{\omega_{mk}} = \frac{\overline{\omega}_n\, \omega_{yj}}{\overline{\omega}_m\, \omega_{yk}} \tag{4.68}$$

Cross-correlation factor $\gamma_{nj,mk}$ depends on $q_{nj,mk}$ or the relative spacing of ω_{nj} and ω_{mk}; if $q_{nj,mk}$ is below 0.8 or above 1.25, $\gamma_{nj,mk}$ is negligibly small [15]. Because the lateral earthquake response of torsionally-uncoupled systems can usually be satisfactorily estimated by considering the contributions of only the first two modes of vibration, N may be replaced by 2 in the first two summations of equation (4.67), thus reducing the computational effort.

Table 1 Definitions of r_j and $\overline{r}_{nj}$ in equation (4.66) for various r_{nj}

r_{nj}	r_j	$\overline{r}_{nj}$
l^{th} story shear	l^{th} story shear	normalized base shear
l^{th} story torque	l^{th} story shear $\times r$	normalized base torque
l^{th} story overturning moment	l^{th} story overturning moment	normalized base overturning moment
lateral displ. of l^{th} floor at location x_i	lateral displ. of l^{th} floor	normalized lateral displ. at location x_i
member force in a frame at location x_i	member force in same frame	normalized lateral displ. at location x_i

Equation (4.67) is rewritten as:

$$r^2 = \sum_{j=1}^{N}\sum_{n=1}^{2} r_{nj}^2 + 2\sum_{j=1}^{N} \gamma_{1j,2j}\, r_{1j}\, r_{2j} + 2\sum_{j=1}^{N-1}\sum_{k=j+1}^{N} \gamma_{2j,1k}\, r_{2j}\, r_{1k}$$

$$+ 2\sum_{j=1}^{N-1}\sum_{k=j+1}^{N} \gamma_{1j,2k}\, r_{1j}\, r_{2k} + 2\sum_{j=1}^{N-1}\sum_{k=j+1}^{N} \gamma_{1j,1k}\, r_{1j}\, r_{1k} + 2\sum_{j=1}^{N-1}\sum_{k=j+1}^{N} \gamma_{2j,2k}\, r_{2j}\, r_{2k} \qquad (4.69)$$

in which the first double summation represents the SRSS combination rule, and the next five summations represent the cross-correlation terms between various groups of vibration modes. The first of these summations represents cross-correlation between vibration modes '1j' and '2j' of the same pair 'j' and the second represents cross-correlation between vibration modes '2j' and '1k', (j=1 to N-1 and k=j+1 to N), such as modes '21' and '12', or '21' and '13'. The last three summations represent cross-correlation terms between modes with vibration frequencies ω_{1j} and ω_{2k}, ω_{1j} and ω_{1k}, and ω_{2j} and ω_{2k}, (j=1 to N-1 and k=j+1 to N); in Section 5 these frequencies will be shown to be widely spaced, implying that $\gamma_{1j,2k}$, $\gamma_{1j,1k}$ and $\gamma_{2j,2k}$ (j=1 to N-1 and k=j+1 to N) are negligibly small, and the last three double summations of equation (4.69) may be dropped (more details are available in Appendix D). Equation (4.69) can, therefore, be reduced to:

$$r^2 \approx \sum_{j=1}^{N}\sum_{n=1}^{2} r_{nj}^2 + 2\sum_{j=1}^{N} \gamma_{1j,2j}\, r_{1j}\, r_{2j} + 2\sum_{j=1}^{N-1}\sum_{k=j+1}^{N} \gamma_{2j,1k}\, r_{2j}\, r_{1k} \qquad (4.70)$$

The last double summation of equation (4.70) was neglected in [3]. However, this summation can have significant contribution to the total response when frequencies ω_{2j} and ω_{1k} (e.g. ω_{21} and ω_{12}) are close, as will be shown in Section 8. In cases where this term is insignificant, equation (4.70) is approximated further to:

$$r^2 \approx \sum_{j=1}^{N}\sum_{n=1}^{2} r_{nj}^2 + 2\sum_{j=1}^{N} \gamma_{1j,2j}\, r_{1j}\, r_{2j} = \sum_{j=1}^{N}\sum_{n=1}^{2} r_{nj}^2 + 2\,\gamma_{12}\sum_{j=1}^{N} r_{1j}\, r_{2j} \qquad (4.71)$$

in which the fact that $\gamma_{1j,2j}$ is independent of 'j' is utilized [equations (4.36) and (4.68)].

4.4.7 Flat or Hyperbolic Earthquake Response Spectra

Equation (4.71) can be simplified greatly if the pseudo-acceleration spectrum varies hyperbolically, or is constant, with vibration period. For these two spectra, the ratios of the pseudo-acceleration ordinates S_{anj}/S_{aj} are $\bar{\omega}_n$ or 1, respectively, which are independent of 'j'. Therefore, the normalized response quantities $\bar{r}_{nj}$ of the associated torsionally-coupled, one-story system with uncoupled lateral vibration frequency ω_y equal to ω_{yj}, given by equations (4.42) to (4.46), become independent of 'j'; i.e. $\bar{r}_{nj} = \bar{r}_n$. Thus, equation (4.71) simplifies to:

$$r = \left[\left(\sum_{j=1}^{N} r_j^2 \right) \left(\bar{r}_1^2 + \bar{r}_2^2 + 2\gamma_{12} \bar{r}_1 \bar{r}_2 \right) \right]^{1/2} = r_o \, \bar{r} \tag{4.72}$$

in which equations (4.21) and (4.47) have been utilized to obtain the second part of the equation. Thus, the total (considering all natural vibration modes) response r of the torsionally-coupled, multi-story building is the product of (1) the total value r_o of the same (or related) response quantity in the corresponding torsionally-uncoupled, multi-story system (Table 1) computed by equation (4.21); and (2) $\bar{r}$, the total value of the normalized response quantity corresponding to r (Table 1) in the associated torsionally-coupled, one-story system, computed using equation (4.47). The result given by equation (4.72) was obtained for shear buildings in [3] since the third summation of equation (4.70) had been neglected on an intuitive basis. It is apparent from the preceding discussion that equation (4.72) is applicable only in the case of the idealized pseudo-acceleration spectra and only if the contribution of the third summation of equation (4.70) is negligible. The latter restriction was not recognized in [3].

4.5 Step-By-Step Summary of RSA of Torsionally-Coupled Buildings

Based on the preceding sections, the earthquake response of a torsionally-coupled, N-story building belonging to the special class of buildings defined earlier, with the additional restriction that the lateral stiffness matrices of all its frames are proportional to each other, can be determined by analyzing two smaller systems: (1) the corresponding torsionally-uncoupled, N-story system and

(2) a set of N associated torsionally-coupled, one-story systems with uncoupled lateral vibration frequency ω_y equal to ω_{yj}, j=1, ..., N, where ω_{yj} is the vibration frequency of the corresponding torsionally-uncoupled, multi-story system. The analysis procedure can be implemented by the following steps:

1. Define the corresponding torsionally-uncoupled, N-story system: a system with coincident centers of mass and rigidity but all other properties identical to the actual torsionally-coupled, multi-story building.

2. Compute the lower few vibration frequencies ω_{yj} and mode shapes $\boldsymbol{\psi}_j$ of this system defined in Step 1 by solving the eigen-problem of equation (4.2a).

3. Compute for each mode of vibration 'j' the maximum value of any desired response quantity r_j in the system defined in Step 1 due to the selected earthquake response spectrum; the procedure outlined in Section 4.2 is used in these computations. This step needs to be implemented only for the lower vibration modes contributing significantly to the response of the system. Based on Reference [7], it will usually be sufficient to implement this step for j=1,2.

4. Determine the static eccentricity, e, of the torsionally-coupled, N-story building using equation (3.9); the radius of gyration of each floor, r, about the vertical axis passing through the centers of mass; and the static eccentricity ratio, e/r.

5. Compute the uncoupled torsional to lateral frequency ratio Ω of the torsionally-coupled, N-story building by equation (4.4).

6. Define an associated torsionally-coupled, one-story system as having the same eccentricity ratio e/r (Step 4) and uncoupled torsional to lateral frequency ratio Ω (Step 5) as the N-story building.

7. Determine the normalized natural vibration frequencies $\bar{\omega}_n$ and mode shapes $\boldsymbol{\alpha}_n$ (n=1,2) of the system defined in Step 6 from equations (4.22) and (4.23).

8. Compute the natural vibration frequencies ω_{nj} and mode shapes $\boldsymbol{\phi}_{nj}$ of the torsionally-coupled, N-story building by substituting the frequencies ω_{yj} and mode shapes $\boldsymbol{\psi}_j$, computed in Step 2, and normalized frequencies $\bar{\omega}_n$ and mode shapes $\boldsymbol{\alpha}_n$, computed in Step 7, in equations (4.10) and (4.11). Computation of $\boldsymbol{\phi}_{nj}$ is not necessary unless the mode shapes of the building are desired.

9. Define an associated torsionally-coupled, one-story system as the system defined in Step 6 with uncoupled lateral vibration frequency ω_y equal to ω_{yj}.

10. Compute for the n^{th} mode of vibration (n=1,2) of the system defined in Step 9 the normalized response quantity $\overline{r}_{nj}$, corresponding to the desired response quantity r_{nj} (Table 1), by equations (4.42) to (4.46). This can be done efficiently by recognizing that each $\overline{r}_{nj}$ is the product of (1) a quantity that needs to be computed only once because it is independent of 'j', but depends on e/r and Ω; and (2) the ratio of the pseudo-acceleration response spectrum ordinates S_{anj} and S_{aj}, corresponding to ω_{nj} and ω_{yj}, respectively.

11. Compute for the nj^{th} mode of vibration of the torsionally-coupled, N-story building the maximum value of the desired response quantity r_{nj} from equation (4.66) as the product of r_j and $\overline{r}_{nj}$ (Table 1), determined in Steps 3 and 10, respectively.

12. Combine the modal maxima r_{nj} according to the CQC rule [equation (4.67)] to obtain an estimate of the response, r.

4.6 Computer Programs Implementation

Special purpose computer programs were developed to implement the analysis procedures outlined in the preceding sections. The programs take advantage of the special properties of buildings belonging to the special class with proportional lateral stiffness matrices of all resisting frames. The details of the implementations of the analysis procedures, flow charts of the programs and the necessary input data are presented in Appendix C. The programs compute normalized response quantities, defined in Sections 6 and 8, for buildings with the simplified plan of Figure 2a,

characterizing ground motion by idealized flat or hyperbolic pseudo-acceleration response spectrum or the general design spectrum described in Section 2.3.

The simplified plan (Figure 2a) described in Section 2.2.2 is a special case of the buildings described in Section 2.2.1 with more general plans, such as Figure 1, than Figure 2a; the analysis procedure developed for buildings with general plans is, therefore, applicable to the system (Figure 2a) of Section 2.2.2; the overall dynamic responses of the buildings of Sections 2.2.1 and 2.2.2 are identical provided they have the same structural properties identified in Section 3.1; thus, the results in subsequent sections 5, 6, 7 and 8 are obtained for the simplified model of Section 2.2.2 in terms of meaningful parameters, so that the results are applicable to buildings with more general plans than Figure 2a.

The response qautities r_j of the corresponding torsionally-uncoupled, multi-story system of the simplifed model of Figure 2a depend on ρ, T_{y1}, and ξ. On the other hand, The normalized quantities $\bar{r}_{nj}$ [equations (4.42) to (4.46)] of the associated one-story system with uncoupled lateral vibration frequency ω_y equal to ω_{yj} are products of quantities that depend solely upon e/r and Ω and the ratio of the pseudo-acceleration response spectrum ordinates S_{anj}/S_{aj}, which depends on the shape of the spectrum and on the relative positions of ω_{nj} and ω_{yj}, which in turn depend on the basic parameters e/r, Ω, ρ and T_{y1}. Thus, the response of the torsionally-coupled, multi-story building of Figure 2a depends on parameters e/r, Ω, ρ, T_{y1} and ξ. Obviously when the idealized flat and hyperbolic pseudo-acceleration spectra are assumed to characterize ground motion, the ratios S_{anj}/S_{aj} equal to 1 or $\bar{\omega}_n$, respectively, and hence $\bar{r}_{nj}$, in these two cases do not depend on ρ or T_{y1}. Thus, the input to the programs for the case of the idealized spectra is the static eccentricity ratio, e/r, the uncoupled torsional to lateral frequency ratio, Ω, the joint rotation index, ρ, and the damping ratio, ξ. In addition to these, the fundamental uncoupled lateral period, T_{y1}, is also input for the case of the general design spectrum.

4.7 Numerical Examples

4.7.1 Example 1

Consider the five-story building described in Section 2.2.2 with the ratio of its overall dimensions $B/A = 0.6$. Frames (1) and (2) are identical with column moment of inertia = I; each beam is of width = $2h$, where h denotes the story height, and moment of inertia = $2I$. The ratio $EI/mh^3 = 564.4$. Frames (2) are located at a distance y_2 from the X-axis, with $y_2/B = 0.476$. Frame (1) is located at a distance e from the Y-axis, with $e/A = 0.135$. The damping ratio in each mode of vibration $\xi = 5$ %. The building belongs to the special class of buildings considered in this study (Section 2.1). The response of the building to ground motion, characterized by the response spectrum of Figure 5, along the Y-axis is to be determined.

The analysis follows the step-by-step summary of the procedure presented in Section 4.5:

1. The corresponding torsionally-uncoupled, five-story system is shown in Figure 6b.

2. Solution of the eigen-problem of equation (4.2a) leads to natural vibration frequencies ω_{yj} and mode shapes $\boldsymbol{\psi}_j$ of the system defined in Step 1:

$$\omega_{y1} = 0.882\sqrt{\frac{EI}{mh^3}} = 20.944 \text{ rad/sec, and} \quad T_{y1} = 0.3 \text{ sec.}$$

$$\omega_{y_2} = 65.645 \text{ rad/sec, and} \quad T_{y_2} = 0.096 \text{ sec.}$$

$$\boldsymbol{\psi}_1^T = < 0.121 \;\; 0.294 \;\; 0.447 \;\; 0.559 \;\; 0.621 >$$

and

$$\boldsymbol{\psi}_2^T = < -0.357 \;\; -0.612 \;\; -0.413 \;\; 0.106 \;\; 0.562 >$$

The mode shapes have been normalized so that $\boldsymbol{\psi}_j^T \mathbf{m} \boldsymbol{\psi}_j = m$.

3. Utilizing equations (4.12) to (4.20) leads to the maximum responses in the first two vibration modes of the system of Figure 6b.

Table 2 shows the following results: story shears normalized by $W_1^* \bar{a}_g/g$, where W_1^* is the

Table 2 Modal Responses of Corresponding Torsionally-Uncoupled,

five-story System of Example 1

Story	Story Shears ÷ $W_1^* \bar{a}_g/g$		Story Overturning Moments ÷ $W_1^* h_1^* \bar{a}_g/g$		Column Moments ÷ $(EI/h^2)\bar{u}_g$		Beam Moments ÷ $(EI/h^2)\bar{u}_g$		Column Axial Forces ÷ $EI/h^3)ubg$	
	Mode 1	Mode 2	Mode 1	Mode 2	Mode 1	Mode 2	Mode 1	Mode 2	Mode 1	Mode 2
1	2.670	0.209	2.670	0.034	0.068	0.005	0.088	0.005	0.316	0.010
2	2.512	0.105	1.932	0.091	0.050	0.001	0.089	0.000	0.228	0.014
3	2.127	0.075	1.238	0.120	0.039	0.002	0.072	0.005	0.138	0.015
4	1.543	0.195	0.650	0.099	0.026	0.004	0.046	0.006	0.067	0.010
5	0.812	0.164	0.224	0.045	0.012	0.003	0.020	0.004	0.020	0.004

effective weight of the system in its fundamental mode of vibration, and $\bar{a}_g$ is the maximum ground acceleration (Section 2.3); story overturning moments normalized by $W_1^* h_1^* \bar{a}_g / g$, where h_1^* is the effective height of the system in its fundamental mode of vibration, and frame (1) column moments, beam moments and column axial forces normalized by $(EI/h^2)\,\bar{u}_g$, $(EI/h^2)\,\bar{u}_g$ and $(EI/h^3)\,\bar{u}_g$, respectively, where $\bar{u}_g$ is the maximum ground displacement (Section 2.3). For this example, $W_1^*/5\,m\,g = 0.835$ and $h_1^*/5\,h = 0.724$.

4. Since frame (1) is the only frame spanning along the Y-axis, equation (3.9) leads to the obvious conclusion that the static eccentricity e equals the distance of the frame from the Y-axis. For rectangular plans, the radius of gyration is given by:

$$r = \sqrt{\frac{A^2 + B^2}{12}}$$

Thus,

$$\frac{e}{r} = \frac{e}{A}\,\frac{A}{r} = 0.135\,\sqrt{\frac{12}{1 + \overline{0.6}^2}} = (0.135)\,(2.970) = 0.4$$

5. The uncoupled torsional to lateral frequency ratio is given by equation (4.4) with $C_{\theta R}/C_y = 2\,y_2^2$ in this example leading to:

$$\Omega = \sqrt{\frac{C_{\theta R}}{r^2\,C_y}} = \frac{y_2}{r}\sqrt{2} = \frac{y_2}{B}\,\frac{B}{A}\,\frac{A}{r}\,\sqrt{2} = (0.476)\,(0.6)\,(2.970)\,\sqrt{2} = 1.2$$

6. For the associated torsionally-coupled, one-story system, eccentricity ratio $e/r = 0.4$ from Step 4, and the uncoupled torsional to lateral frequency ratio $\Omega = 1.2$ from Step 5 .

7. The normalized natural vibration frequencies $\bar{\omega}_n$ and mode shapes $\boldsymbol{\alpha}_n$ (n=1,2) of the system defined in Step 6 are computed from equations (4.22) and (4.23), leading to:

$$\bar{\omega}_1 = 0.894, \text{ and } \quad \bar{\omega}_2 = 1.342,$$

$$\boldsymbol{\alpha}_1 = \begin{Bmatrix} \alpha_{y1} \\ \alpha_{\theta 1} \end{Bmatrix} = \begin{Bmatrix} -0.894 \\ 0.447 \end{Bmatrix}; \boldsymbol{\alpha}_2 = \begin{Bmatrix} \alpha_{y2} \\ \alpha_{\theta 2} \end{Bmatrix} = \begin{Bmatrix} -0.447 \\ -0.894 \end{Bmatrix}$$

8. From equation (4.10):

$$\omega_{11} = \bar{\omega}_1 \, \omega_{y1} = (0.894)(20.944) = 18.729 \text{ rad/sec}; \quad T_{11} = 0.335 \text{ sec}$$

$$\omega_{21} = \bar{\omega}_2 \, \omega_{y1} = (1.342)(20.944) = 28.094 \text{ rad/sec}; \quad T_{21} = 0.224 \text{ sec}$$

$$\omega_{12} = \bar{\omega}_1 \, \omega_{y2} = (0.894)(65.645) = 58.703 \text{ rad/sec}; \quad T_{12} = 0.107 \text{ sec}$$

$$\omega_{22} = \bar{\omega}_2 \, \omega_{y2} = (1.342)(65.645) = 88.055 \text{ rad/sec}; \quad T_{22} = 0.071 \text{ sec}$$

9. Define an associated torsionally-coupled, one-story system as the system defined in Step 6 with uncoupled lateral vibration frequency ω_y equal to ω_{yj}; for j=1, ω_y = 20.944 rad/sec, and for j=2, ω_y = 65.645 rad/sec.

10. From equations (4.44) and (4.46):

$$\bar{v}_{nj} = \bar{V}_{nj} = \bar{M}_{nj} = \alpha_{yn}^2 \frac{S_{anj}}{S_{aj}} = \bar{W}_n^* \frac{S_{anj}}{S_{aj}}$$

and,

$$\bar{T}_{Rnj} = \alpha_{yn} (\alpha_{\theta n} - \frac{e}{r} \alpha_{yn}) \frac{S_{anj}}{S_{aj}}$$

Substituting for α_{yn} and $\alpha_{\theta n}$ from step 7, and reading of S_{anj} and S_{aj} from the response spectrum of Figure 5 corresponding to periods T_{nj} and T_{yj} leads to the results of Table 3.

11. For each njth mode of vibration of the torsionally-coupled, N-story building the maximum value of the desired response quantity r_{nj} is given by the product of r_j (Table 2) and $\bar{r}_{nj}$ (Table 3) determined in Steps 3 and 10, respectively. The results are shown in Table 4 for base shear and torque.

12. Substituting the modal maxima into equation (4.67) leads to the total values of base shear and torque (Table 4).

Table 3 Normalized Modal Responses of Associated Torsionally-Coupled, One-story System of Example 1

Mode nj	α_{yn}	$\alpha_{\theta n}$	$\bar{V}_n$	$\bar{T}_{Rn}$	S_{anj}	S_{aj}	$\bar{V}_{nj}$	$\bar{T}_{Rnj}$
11	-0.894	0.447	0.8	-0.72	2.67	2.67	0.8	-0.72
21	-0.447	-0.894	0.2	0.32	2.67	2.67	0.2	0.32
12	-0.894	0.447	0.8	-0.72	1.87	1.71	0.875	-0.787
22	-0.447	-0.894	0.2	0.32	1.35	1.71	0.158	0.253

Table 4 Modal Responses of Torsionally-Coupled,

Five-story Building of Example 1

Mode nj	Base Shear ÷ $W_1^* \bar{a}_g/g$			Base Torque ÷ $rW_1^* \bar{a}_g/g$		
	V_{Bj}	$\bar{V}_{nj}$	V_{Bnj}	V_{Bj}	$\bar{T}_{Rnj}$	T_{BRnj}
11	2.670	0.8	2.136	2.670	-0.72	-1.922
21	2.670	0.2	0.534	2.670	0.32	0.854
12	0.209	0.8	0.167	0.209	-0.72	-0.150
22	0.209	0.2	0.042	0.209	0.32	0.067
Total	-	-	2.240	-	-	2.870

Table 5 Maximum Response of Torsionally-Coupled,

five-Story Building of Example 1

	Story Shears ÷ $(W_1^* \bar{a}_g / g)$		Story Torques at CR ÷ $(r W_1^* \bar{a}_g / g)$		Story OTM ÷ $(W_1^* h_1^* \bar{a}_g / g)$		Column Moments ÷ $[(EI/h^2)\bar{u}_g]$		Beam Moments ÷ $[(EI/h^2)\bar{u}_g]$		Column Axial Forces ÷ $[(EI/h^3)\bar{u}_g]$	
	No. Of Modes Considered											
Story	4	10	4	10	4	10	4	10	4	10	4	10
1	2.240	2.241	2.870	2.871	2.230	2.230	0.057	0.057	0.074	0.074	0.264	0.264
2	2.101	2.101	2.694	2.694	1.615	1.615	0.042	0.042	0.074	0.074	0.190	0.190
3	1.777	1.778	2.281	2.282	1.039	1.039	0.033	0.033	0.060	0.060	0.116	0.116
4	1.299	1.299	1.668	1.668	0.550	0.550	0.022	0.022	0.039	0.039	0.057	0.057
5	0.692	0.693	0.890	0.893	0.191	0.192	0.010	0.010	0.017	0.017	0.017	0.017

Computations similar to Table 4 for other response quantities leads to Table 5, wherein results are presented considering the contributions of four vibration modes (j=1, 2; and n=1, 2), as in the computations of Table 4. Also presented are the responses considering all ten vibration modes (j=1, 2, 3, 4, 5; and n=1, 2). It is apparent that for this example, it is sufficient to consider only the first two pairs of vibration modes associated with the first two vibration modes of the torsionally-uncoupled system. Because the fundamental vibration period T_{y1} is in the acceleration-controlled region of the spectrum (Figure 5), according to [7] even the fundamental modal-pair alone would suffice.

4.7.2 Example 2

In order to compare results obtained from equations (4.67) or (4.69), (4.70), and (4.71) or (4.72), consider the building analyzed in Section 4.7.1 with the following modifications: the plan of the building is square, i.e. $B/A = 1$; each frame is assumed to behave as two columns, i.e. the moments of inertia of the beams are taken as zero; each column of frames (2) have a moment of inertia I_2 equal $0.5I$; and the static eccentricity e is chosen such that $e/A = 0.163$. Using the step-by-step procedure of Section 4.5, the response of the building to earthquake ground motion, along the Y-axis, characterized by idealized flat and hyperbolic response spectra, is computed for two cases: (a) $y_2/B = 0.408$, and (b) $y_2/B = 0.490$.

The static eccentricity ratio of the building considered is given by:

$$\frac{e}{r} = \frac{e}{A}\frac{A}{r} = (0.163)\sqrt{\frac{12}{1+(B/A)^2}} = (0.163)\sqrt{6} = 0.4$$

and the uncoupled torsional to lateral frequency ratio Ω is determined from:

$$\Omega = \sqrt{\frac{C_{\theta R}}{r^2 C_y}} = \frac{y_2}{r}\sqrt{2\frac{I_2}{I}} = \frac{y_2}{r} = \frac{y_2}{B}\frac{B}{A}\frac{A}{r} = \frac{y_2}{B}\sqrt{6}$$

Thus, in case (a):

$$\Omega = \frac{y_2}{B}\sqrt{6} = 0.408\sqrt{6} = 1$$

and in case (b):

$$\Omega = \frac{y_2}{B}\sqrt{6} = 0.490\sqrt{6} = 1.2$$

For each of the five vibration modes of the corresponding torsionally-uncoupled, five-story system, the maximum base shear V_{Bj} and the base overturning moment M_{Bj} [or the base column moment in frame (1)], computed by Steps 1 to 3 of Section 4.5, are presented in Table 6, for flat and hyperbolic spectra. The response in each vibration mode has been normalized with respect to the contribution of the fundamental mode.

The normalized frequencies $\bar{\omega}_n$ and mode shapes $\boldsymbol{\alpha}_n$ of the associated torsionally-coupled, one-story system are given by:

for case (a),

$$\bar{\omega}_1 = 0.8198 \quad \text{and} \quad \bar{\omega}_2 = 1.2198$$

$$\boldsymbol{\alpha}_1 = \begin{Bmatrix} \alpha_{y1} \\ \alpha_{\theta 1} \end{Bmatrix} = \begin{Bmatrix} -0.7733 \\ 0.6340 \end{Bmatrix}; \quad \boldsymbol{\alpha}_2 = \begin{Bmatrix} \alpha_{y_2} \\ \alpha_{\theta 2} \end{Bmatrix} = \begin{Bmatrix} -0.6340 \\ -0.7733 \end{Bmatrix}$$

and for case (b),

$$\bar{\omega}_1 = 0.8944 \quad \text{and} \quad \bar{\omega}_2 = 1.3416$$

$$\boldsymbol{\alpha}_1 = \begin{Bmatrix} \alpha_{y1} \\ \alpha_{\theta 1} \end{Bmatrix} = \begin{Bmatrix} -0.8944 \\ 0.4472 \end{Bmatrix}; \quad \boldsymbol{\alpha}_2 = \begin{Bmatrix} \alpha_{y_2} \\ \alpha_{\theta 2} \end{Bmatrix} = \begin{Bmatrix} -0.4472 \\ -0.8940 \end{Bmatrix}$$

The normalized modal quantities $\bar{r}_{nj}$ of the associated torsionally-coupled, one-story systems for j=1, 2, ..., 5 are determined by implementing computational Steps 6 through 10 of Section 8 leading to the results presented in Table 7.

The modal responses of the torsionally-coupled, five-story building are given in Table 8a and 8b, for the flat and hyperbolic spectra, respectively, normalized with respect to the corresponding forces due to the fundamental mode of the corresponding torsionally-uncoupled system. Combination of the normalized modal responses according to equations (4.67) or (4.69), (4.70), and (4.71)

Table 6 Normalized Modal Responses of Corresponding Torsionally-Uncoupled, Five-Story System of Example 2 for flat and hyperbolic spectra

Mode j	Flat Spectrum		Hyperbolic Spectrum	
	V_{Bj}/V_{B1}	M_{Bj}/M_{B1}	V_{Bj}/V_{B1}	M_{Bj}/M_{B1}
1	1.0	1.0	1.0	1.0
2	0.3040	0.0873	1.9411	0.5576
3	0.1033	0.0182	1.8685	0.3298
4	0.0485	0.0064	1.6969	0.2240
5	0.0176	0.0020	0.9151	0.1041

Table 7 Normalized Modal Responses of Associated Torsionally-Coupled, One-Story System of Example 2 for Cases (a) $\Omega = 1.0$, and (b) $\Omega = 1.2$

Case (a): $\Omega = 1.0$				
Spectrum	$\bar{V}_1$	$\bar{V}_2$	$\bar{T}_{R1}$	$\bar{T}_{R2}$
Flat	0.5981	0.4019	-0.7295	0.3295
Hyperbolic	0.4903	0.4903	-0.5981	0.4019
Case (b): $\Omega = 1.2$				
Spectrum	$\bar{V}_1$	$\bar{V}_2$	$\bar{T}_{R1}$	$\bar{T}_{R2}$
Flat	0.8000	0.2000	-0.7200	0.3200
Hyperbolic	0.7155	0.2683	-0.6440	0.4293

Table 8a Modal Responses of Torsionally-Coupled, Five-Story Building of Example 2 for Flat Spectrum in Cases (a) $\Omega = 1.0$ and (b) $\Omega = 1.2$

Case (a): $\Omega = 1.0$

V_{Bnj}/V_{B1}					
n	j				
	1	2	3	4	5
1	0.5981	0.1818	0.0618	0.0290	0.0105
2	0.4019	0.1222	0.0415	0.0195	0.0071
$T_{BRnj}/r\,V_{B1}$					
1	-0.7295	-0.2218	-0.0753	-0.0354	-0.0128
2	0.3295	0.1002	0.0340	0.0160	0.0058
M_{Bnj}/M_{B1}					
1	0.5981	0.0522	0.0109	0.0038	0.0012
2	0.4019	0.0351	0.0073	0.0026	0.0008

Case (b): $\Omega = 1.2$

V_{Bnj}/V_{B1}					
n	j				
	1	2	3	4	5
1	0.8000	0.2432	0.0826	0.0388	0.0141
2	0.2000	0.0608	0.0206	0.0097	0.0035
$T_{BRnj}/r\,V_{B1}$					
1	-0.7200	-0.2189	-0.0744	-0.0349	-0.0126
2	0.3200	0.0973	0.0330	0.0155	0.0056
M_{Bnj}/M_{B1}					
1	0.8000	0.0699	0.0146	0.0051	0.0016
2	0.2000	0.0175	0.0036	0.0013	0.0004

Table 8b Modal Responses of Torsionally-Coupled, Five-Story Building of Example 2 for Hyperbolic Spectrum in Cases (a) $\Omega = 1.0$, and (b) $\Omega = 1.2$

Case (a): $\Omega = 1.0$

V_{Bnj}/V_{B1}					
n	j				
	1	2	3	4	5
1	0.4903	0.9517	0.9161	0.8320	0.4486
2	0.4903	0.9517	0.9161	0.8320	0.4486
$T_{BRnj}/r\,V_{B1}$					
1	-0.5981	-1.1609	-1.1174	-1.0148	-0.5473
2	0.4019	0.7802	0.7510	0.6821	0.3678
M_{Bnj}/M_{B1}					
1	0.4903	0.2734	0.1617	0.1098	0.0510
2	0.4903	0.2734	0.1617	0.1098	0.0510

Case (b): $\Omega = 1.2$

V_{Bnj}/V_{B1}					
n	j				
	1	2	3	4	5
1	0.7155	1.3890	1.3370	1.2142	0.6548
2	0.2683	0.5209	0.5014	0.4553	0.2455
$T_{BRnj}/r\,V_{B1}$					
1	-0.6440	-1.2501	-1.2033	-1.0928	-0.5893
2	0.4293	0.8334	0.8022	0.7285	0.3929
M_{Bnj}/M_{B1}					
1	0.7155	0.3990	0.2360	0.1603	0.0745
2	0.2683	0.1496	0.0885	0.0601	0.0279

Table 9a Responses of Torsionally-Coupled, Five-Story Building of Example 2 for Flat Spectrum computed by equations (7.19), (7.22) and (7.24)

Modal Combination by	Case (a): Ω = 1.0			Case (b): Ω = 1.2		
	V_B/V_{Bo}	T_{BR}/rV_{Bo}	M_B/M_{Bo}	V_B/V_{Bo}	T_{BR}/rV_{Bo}	M_B/M_{Bo}
Eq. (7.19)	0.7412	0.7826	0.7398	0.8366	0.7712	0.8355
Eq. (7.22)	0.7405	0.7821	0.7397	0.8359	0.7706	0.8354
Eq. (7.24)	0.7396	0.7830	0.7396	0.8353	0.7715	0.8353

Table 9b Responses of Torsionally-Coupled, Five-Story Building of Example 2 for Hyperbolic Spectrum computed by equations (7.19), (7.22) and (7.24)

Modal Combination by	Case (a): Ω = 1.0			Case (b): Ω = 1.2		
	V_B/V_{Bo}	T_{BR}/rV_{Bo}	M_B/M_{Bo}	V_B/V_{Bo}	T_{BR}/rV_{Bo}	M_B/M_{Bo}
Eq. (7.19)	0.7820	0.6502	0.7252	0.8337	0.6989	0.7879
Eq. (7.22)	0.7697	0.6384	0.7221	0.8203	0.6863	0.7847
Eq. (7.24)	0.7131	0.7011	0.7131	0.7780	0.7539	0.7780

or (4.72) are included in Tables 9a and 9b.

It is clear from Table 9a that for this example equation (4.72) leads to accurate results in the case of flat spectrum. For the hyperbolic spectrum, equations (4.67) and (4.72) differ by about 6 to 8%, being larger for $\Omega = 1.0$ than for $\Omega = 1.2$.

5. VIBRATION FREQUENCIES AND MODE SHAPES

It is apparent from equations (4.10) and (4.11) that the natural vibration frequencies ω_{nj} of the torsionally-coupled, multi-story building are closely related to the frequencies ω_{yj} and mode shapes $\boldsymbol{\psi}_j$ of the corresponding torsionally-uncoupled, multi-story system (Section 4.2) and to the normalized frequencies $\bar{\omega}_n$ and mode shapes $\boldsymbol{\alpha}_n$ of the associated torsionally-coupled, one-story system (Section 4.3).

The coupled natural frequencies ω_{nj} normalized by ω_{yj} are independent of 'j' (equation (4.10)) with the ratios ω_{nj}/ω_{yj} equal to $\bar{\omega}_n$, which depend only on the eccentricity ratio e/r and the uncoupled torsional to lateral frequency ratio Ω. Thus, the normalized frequencies ω_{1j}/ω_{yj} and ω_{2j}/ω_{yj} of the j^{th} modal pair vary with Ω and e/r in the same manner as $\bar{\omega}_1$ and $\bar{\omega}_2$, respectively, The ratios ω_{nj}/ω_{yj} $(=\bar{\omega}_n)$ are plotted in Figure 7 against Ω for three values of e/r: 0.05, 0.4 and 1. Also included for comparison are the uncoupled frequencies ω_{yj} and $\omega_{\theta j}$, both normalized by ω_{yj}, in order to identify the effects of lateral-torsional coupling on the natural vibration frequencies. It is apparent from Figure 7 that the uncoupled frequencies ω_{yj} and $\omega_{\theta j}$ are upper and lower bounds of the coupled frequencies; as e/r increases, ω_{1j} decreases below $\omega_{\theta j}$ and ω_{yj}, while ω_{2j} increases above ω_{yj} and $\omega_{\theta j}$. Naturally, the coupled frequencies are closest to the uncoupled ones for systems with smallest e/r values. For torsionally-flexible systems (i.e. $\Omega<1$), $\omega_{\theta j}$ is the upper bound of ω_{1j}, while ω_{yj} is the lower bound for ω_{2j}. On the other hand, for torsionally-stiff systems (i.e. $\Omega>1$), ω_{yj} is the upper bound for ω_{1j}, while $\omega_{\theta j}$ is the lower bound for ω_{2j}. For systems with closely spaced uncoupled frequencies (i.e. Ω around unity), the coupled frequencies are closest to one another, with the closeness most pronounced for systems with smaller values of e/r. The building is unstable for Ω equal to zero, since, in this case the fundamental frequency ω_{11} is zero.

The coupled natural frequencies ω_{nj} normalized by the fundamental uncoupled lateral frequency ω_{y1} equals the product of $\bar{\omega}_n$ and the ratio of the vibration frequencies of the corresponding torsionally-uncoupled, multi-story system ω_{yj}/ω_{y1} (equation (4.10)). The frequency ratio ω_{yj}/ω_{y1} is presented in Figure 8, which indicates that the corresponding torsionally-uncoupled, multi-story

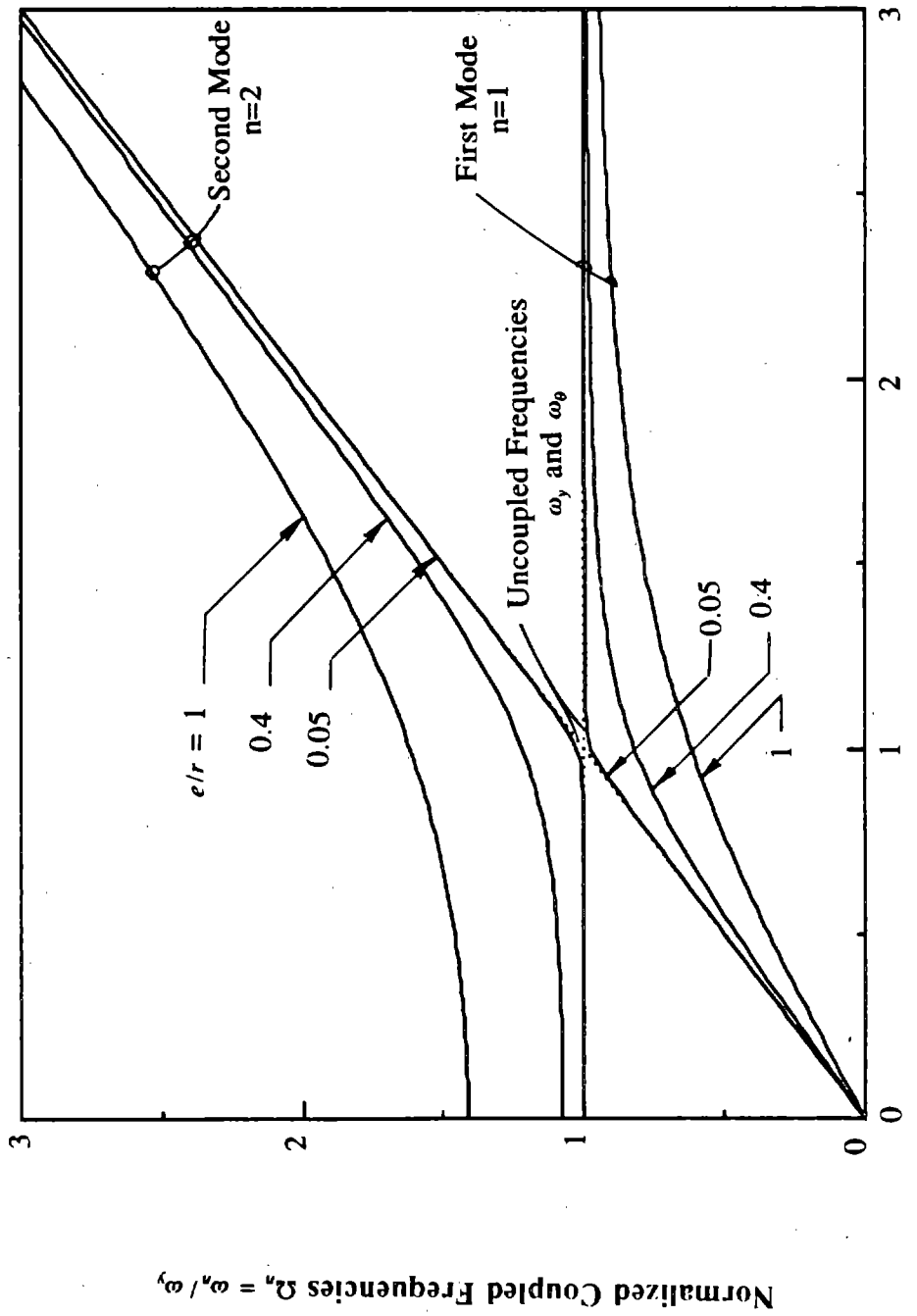

FIGURE 7 Natural Vibration Frequencies of Associated Torsionally-coupled One-story System

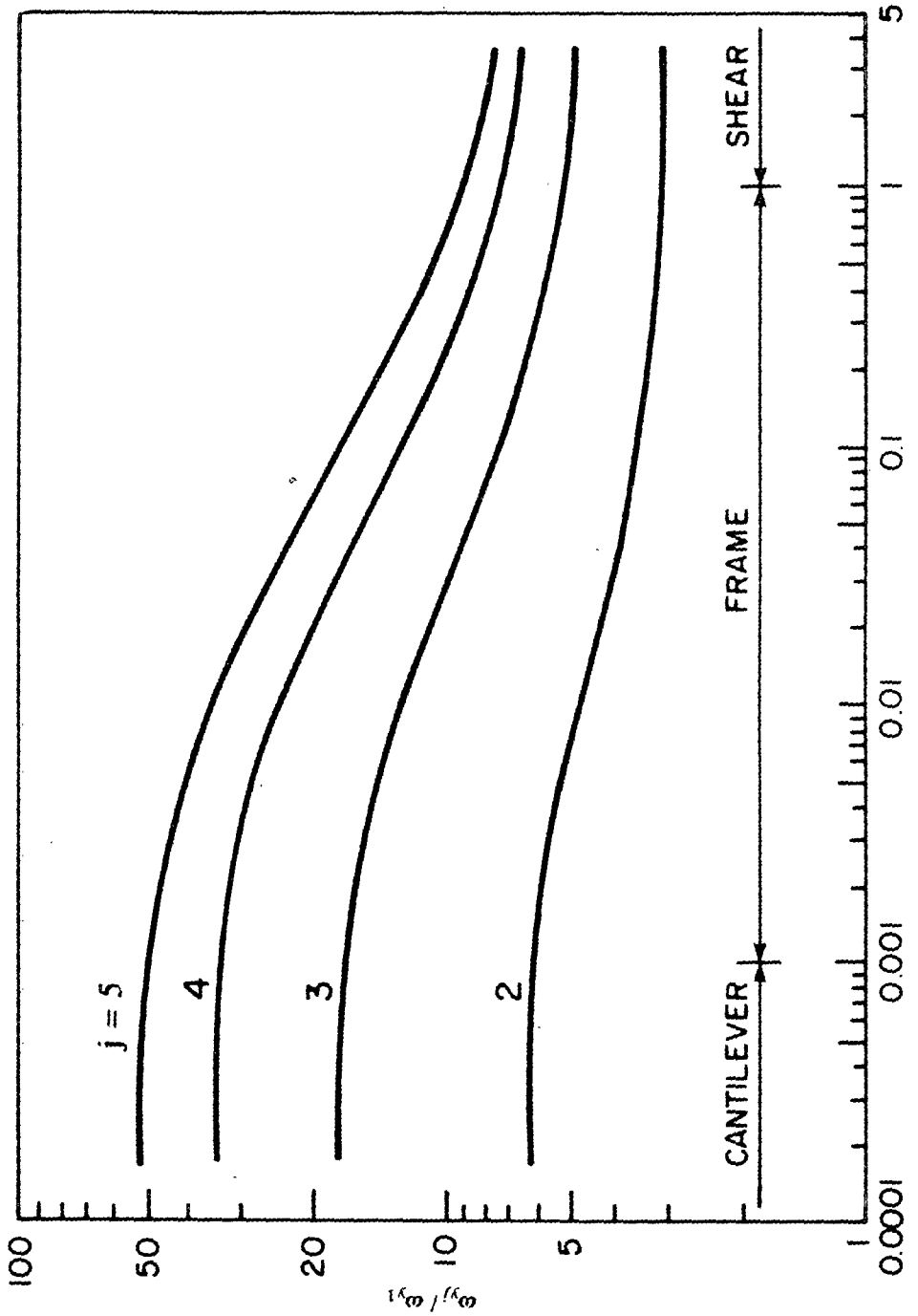

FIGURE 8 Natural Frequency Ratios for Corresponding Torsionally-uncoupled Multi-story System. (Adapted from [12]).

system behaves as a cantilever beam for small values of ρ and as a shear beam for large ρ. For intermediate values of ρ the corresponding torsionally-uncoupled, multi-stor behaves as a frame. The ratios ω_{nj}/ω_{y1} are shown in Figure 9 against Ω for e/r equal 0. three values of ρ equal to 0, 0.125 and ∞, representing the three different ranges of ρ. the preceding observations the fundamental normalized frequency pair, consisting of ω_1 ω_{21}/ω_{y1}, which are equal to $\bar{\omega}_1$ and $\bar{\omega}_2$, respectively, are independent of ρ. However, higl tion frequency pairs vary with ρ due to the dependence of ω_{yj}/ω_{y1} on ρ (Figure 8).

The coupled mode shapes are directly related by equation (4.11) to the mode shap corresponding torsionally-uncoupled, multi-story system, shown in Figure 10. Both latera sional components, ϕ_{ynj} and $\phi_{\theta nj}$, of the coupled mode shape ϕ_{nj} are proportional to the shape of the corresponding torsionally-uncoupled system (Section 4.2) ψ_j, with proportion stants α_{yn} and $\alpha_{\theta n}$, shown in Figure 11, equal to the lateral and torsional components of the of vibration of the associated torsionally-coupled, one-story system (Section 4.3). As a res orthogonality property of the one-story mode shapes, $\boldsymbol{\alpha}_1^T \boldsymbol{\alpha}_2 = 0$, it can be sh $\alpha_{y1}=\alpha_{\theta 2}$ and $\alpha_{y2}=-\alpha_{\theta 1}$. Thus, the lateral component of a coupled mode of pair 'j' equal sional component of the second mode of pair 'j', i.e. $\phi_{y1j}=\phi_{\theta 2j}$ and $\phi_{y2j}=-\phi_{\theta 1j}$.

It is apparent from Figure 11 that as Ω increases α_{y1} (or $\alpha_{\theta 2}$) increases while α_{y} decreases. For torsionally-stiff (Ω>1) systems α_{y1} approaches unity and α_{y2} approaches increases. Thus, in this case, the coupled modes ϕ_{1j} contain predominantly lateral motion predominantly torsional motions, as demonstrated by Figure 12a. Torsionally-flexible (tems with smaller e/r ratios have smaller α_{y1} values than α_{y2}, but the modes are not pred lateral or torsional, as is clear from Figure 12b. For systems with closely spaced uncou quencies (Ω close to 1), α_{y1} and $\alpha_{\theta 1}$ are of comparable magnitudes especially for syst small e/r. Therefore, the lateral and torsional components of a coupled mode shape are of order of magnitude for systems with closely spaced uncoupled frequencies, as exhibited 12c.

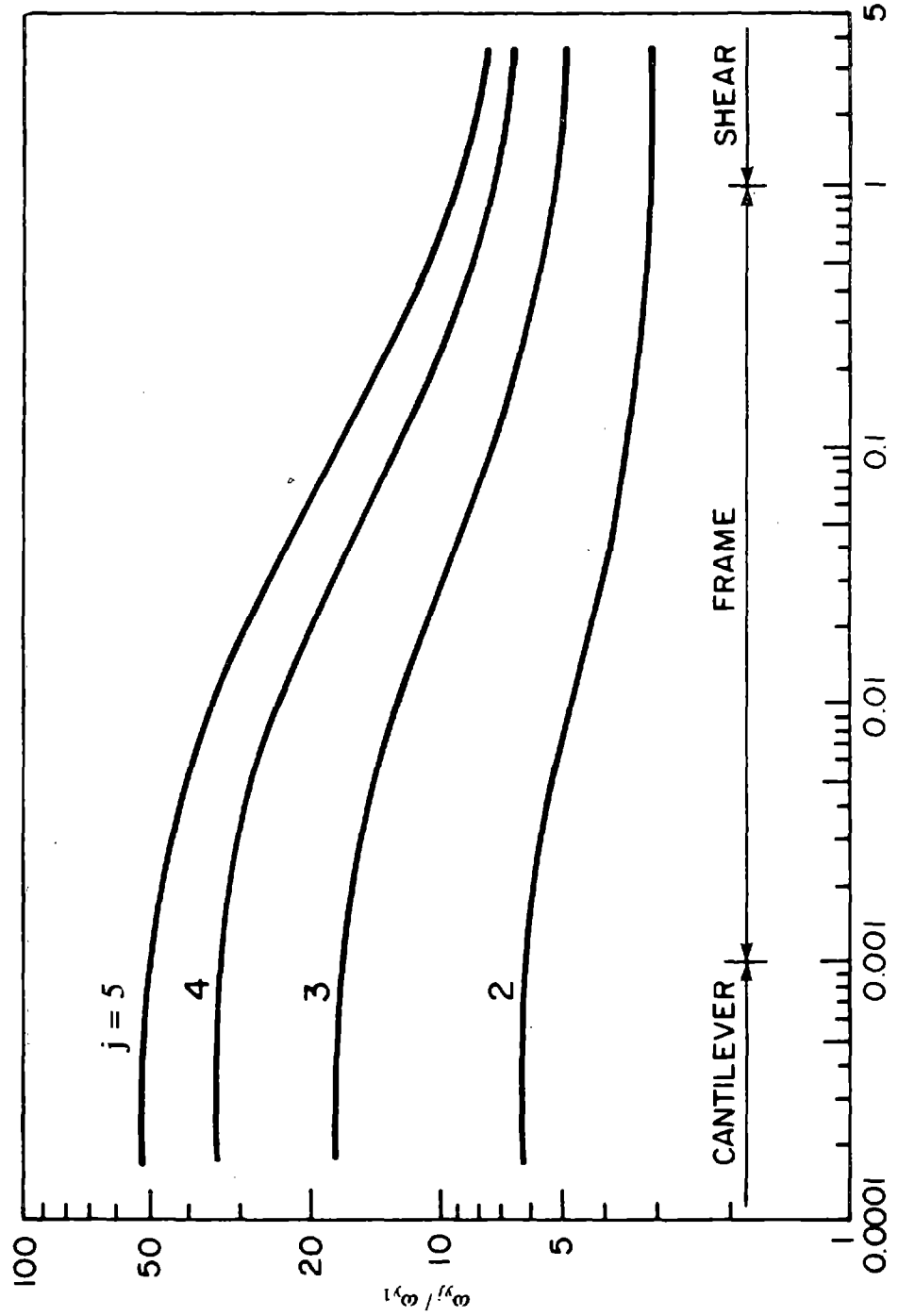

FIGURE 8 Natural Frequency Ratios for Corresponding Torsionally-uncoupled Multi-story System. (Adapted from [12]).

system behaves as a cantilever beam for small values of ρ and as a shear beam for large values of ρ. For intermediate values of ρ the corresponding torsionally-uncoupled, multi-story system behaves as a frame. The ratios ω_{nj}/ω_{y1} are shown in Figure 9 against Ω for e/r equal 0.4 and for three values of ρ equal to 0, 0.125 and ∞, representing the three different ranges of ρ. Based on the preceding observations the fundamental normalized frequency pair, consisting of ω_{11}/ω_{y1} and ω_{21}/ω_{y1}, which are equal to $\bar{\omega}_1$ and $\bar{\omega}_2$, respectively, are independent of ρ. However, higher vibration frequency pairs vary with ρ due to the dependence of ω_{yj}/ω_{y1} on ρ (Figure 8).

The coupled mode shapes are directly related by equation (4.11) to the mode shapes of the corresponding torsionally-uncoupled, multi-story system, shown in Figure 10. Both lateral and torsional components, ϕ_{ynj} and $\phi_{\theta nj}$, of the coupled mode shape $\boldsymbol{\phi}_{nj}$ are proportional to the jth mode shape of the corresponding torsionally-uncoupled system (Section 4.2) $\boldsymbol{\psi}_j$, with proportionality constants α_{yn} and $\alpha_{\theta n}$, shown in Figure 11, equal to the lateral and torsional components of the nth mode of vibration of the associated torsionally-coupled, one-story system (Section 4.3). As a result of the orthogonality property of the one-story mode shapes, $\boldsymbol{\alpha}_1^T \boldsymbol{\alpha}_2 = 0$, it can be shown that $\alpha_{y1}=\alpha_{\theta 2}$ and $\alpha_{y2}=-\alpha_{\theta 1}$. Thus, the lateral component of a coupled mode of pair 'j' equals the torsional component of the second mode of pair 'j', i.e. $\phi_{y1j}=\phi_{\theta 2j}$ and $\phi_{y2j}=-\phi_{\theta 1j}$.

It is apparent from Figure 11 that as Ω increases α_{y1} (or $\alpha_{\theta 2}$) increases while α_{y2} (or $\alpha_{\theta 1}$) decreases. For torsionally-stiff (Ω>1) systems α_{y1} approaches unity and α_{y2} approaches zero as Ω increases. Thus, in this case, the coupled modes $\boldsymbol{\phi}_{1j}$ contain predominantly lateral motions and $\boldsymbol{\phi}_{2j}$ predominantly torsional motions, as demonstrated by Figure 12a. Torsionally-flexible (Ω<1) systems with smaller e/r ratios have smaller α_{y1} values than α_{y2}, but the modes are not predominantly lateral or torsional, as is clear from Figure 12b. For systems with closely spaced uncoupled frequencies (Ω close to 1), α_{y1} and $\alpha_{\theta 1}$ are of comparable magnitudes especially for systems with small e/r. Therefore, the lateral and torsional components of a coupled mode shape are of the same order of magnitude for systems with closely spaced uncoupled frequencies, as exhibited by Figure 12c.

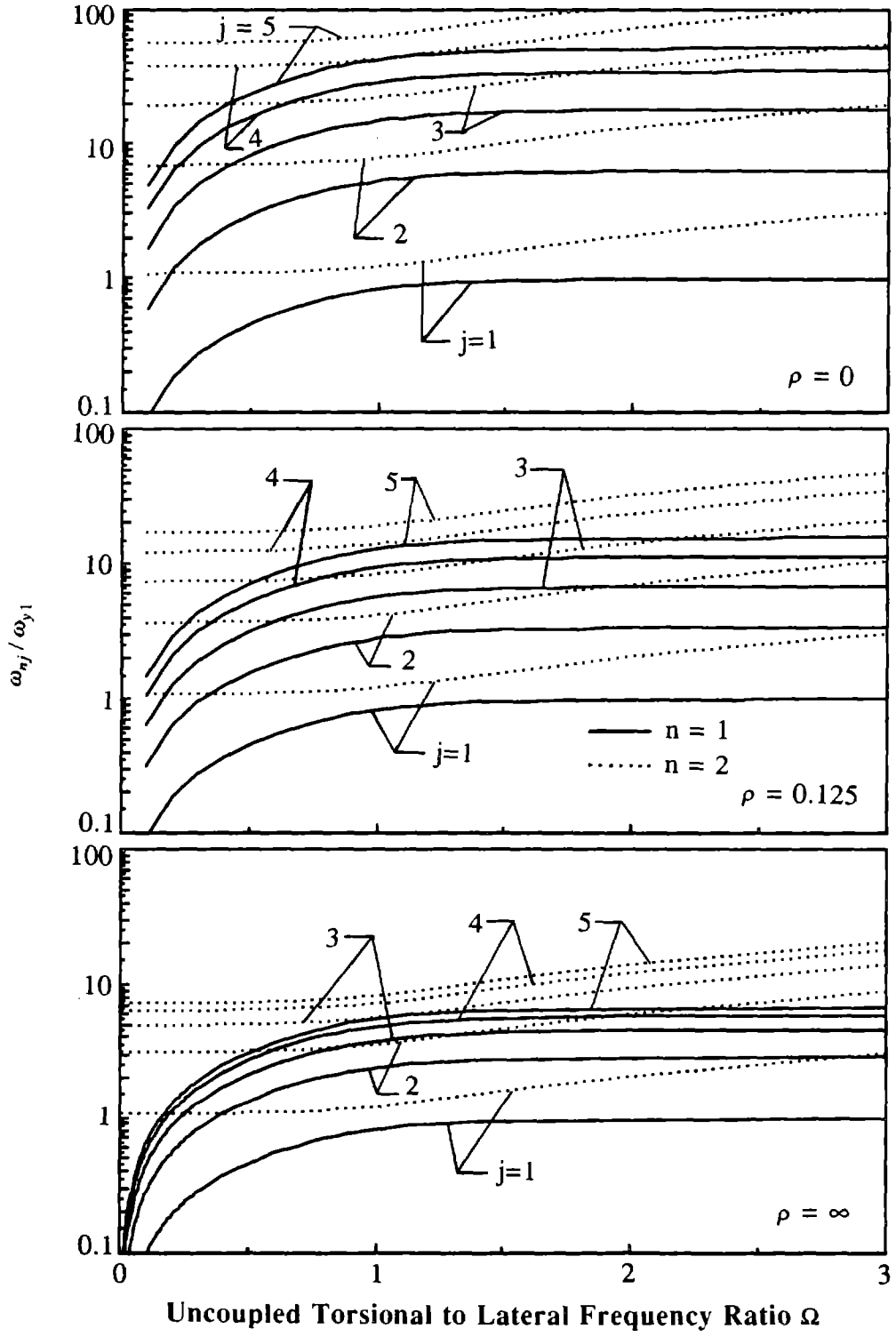

FIGURE 9 Vibration Frequency Ratios $\omega_{nj} / \omega_{y1}$. $(e/r = 0.4)$

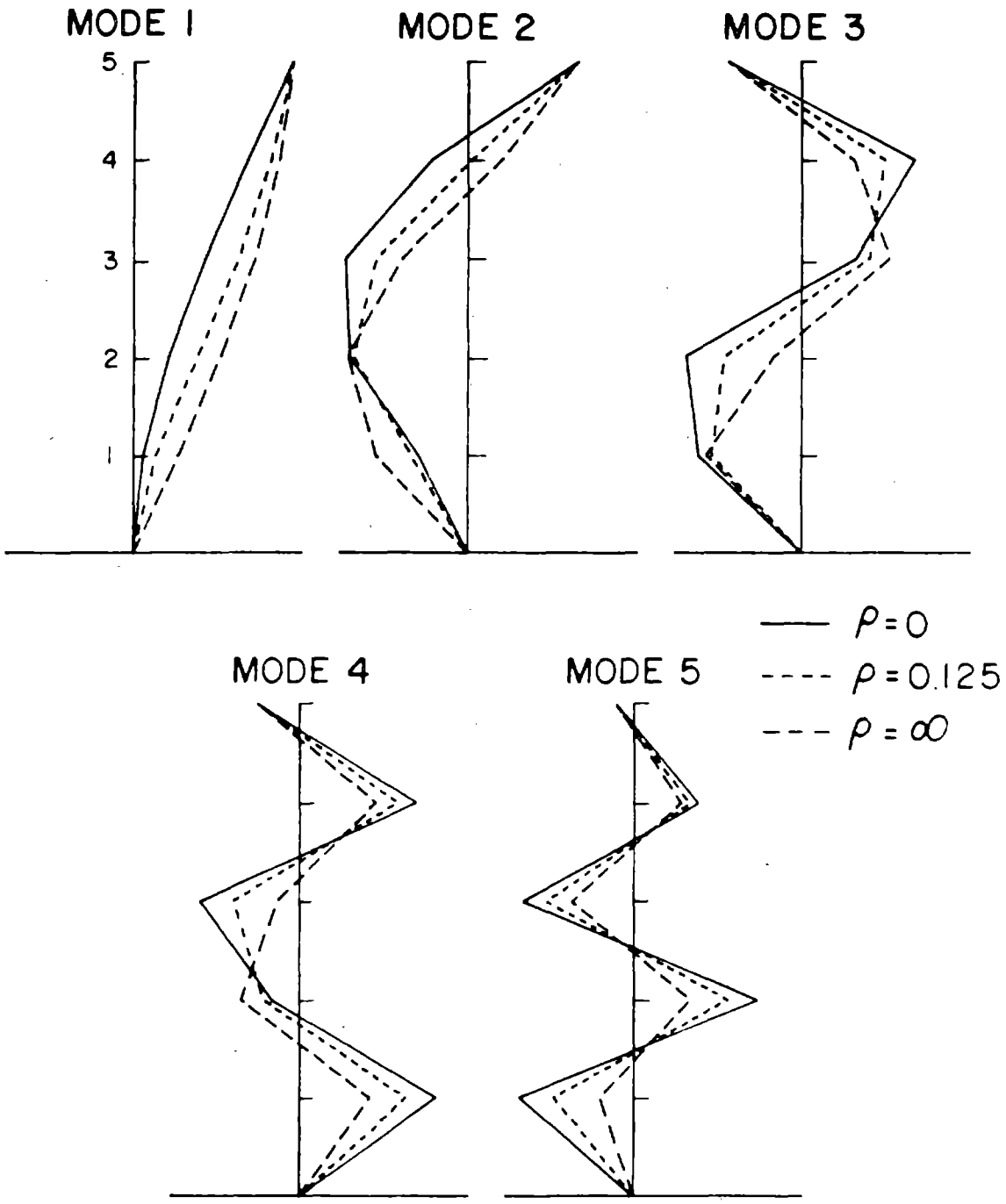

FIGURE 10 Natural Vibration Mode Shapes of the Corresponding Torsionally-uncoupled five-story System. (Adapted from [12]).

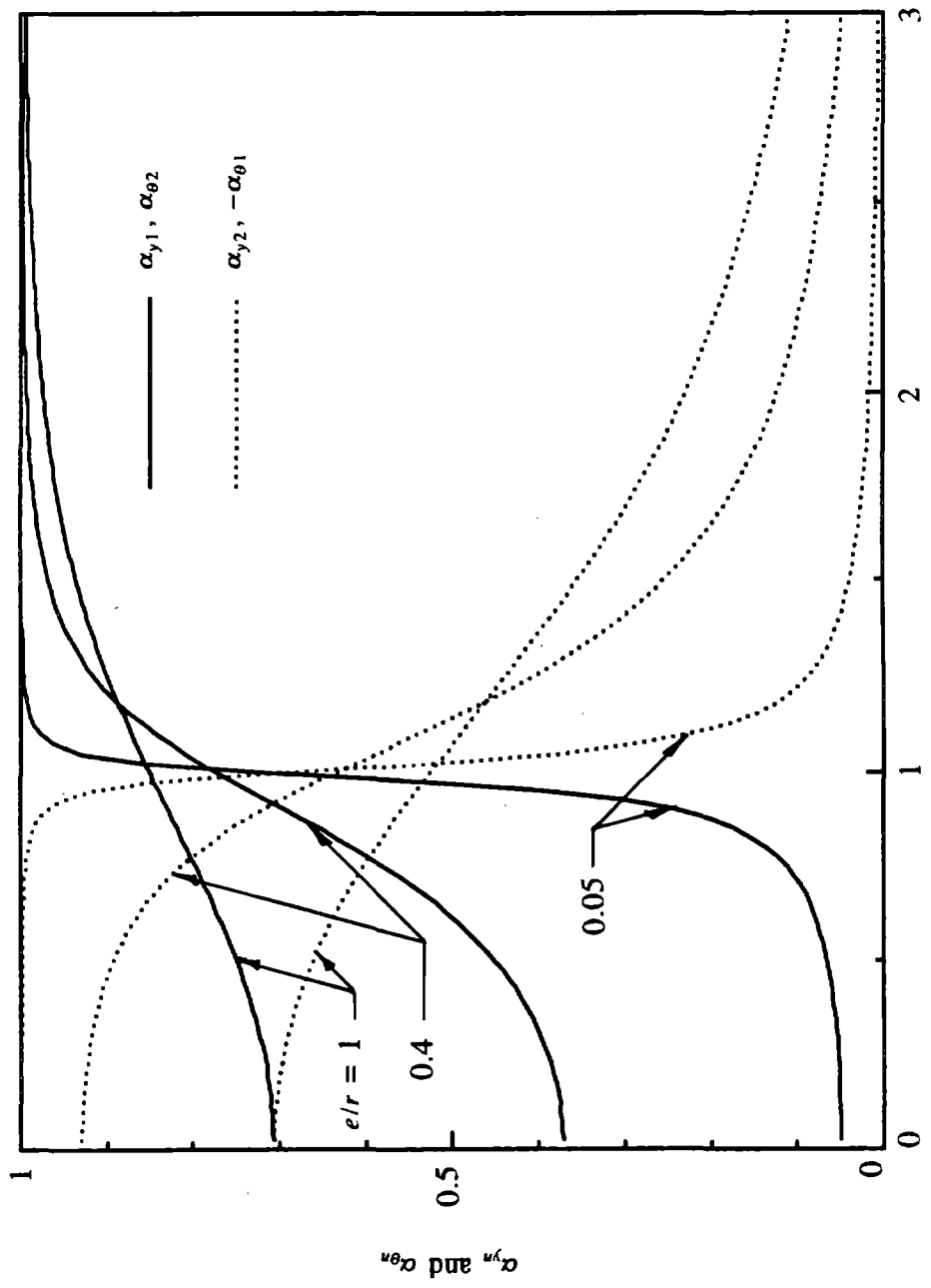

FIGURE 11 Lateral and Torsional Components, α_{yn} & $\alpha_{\theta n}$, of Vibration Mode Shapes (n=1, 2) for Associated One-story System

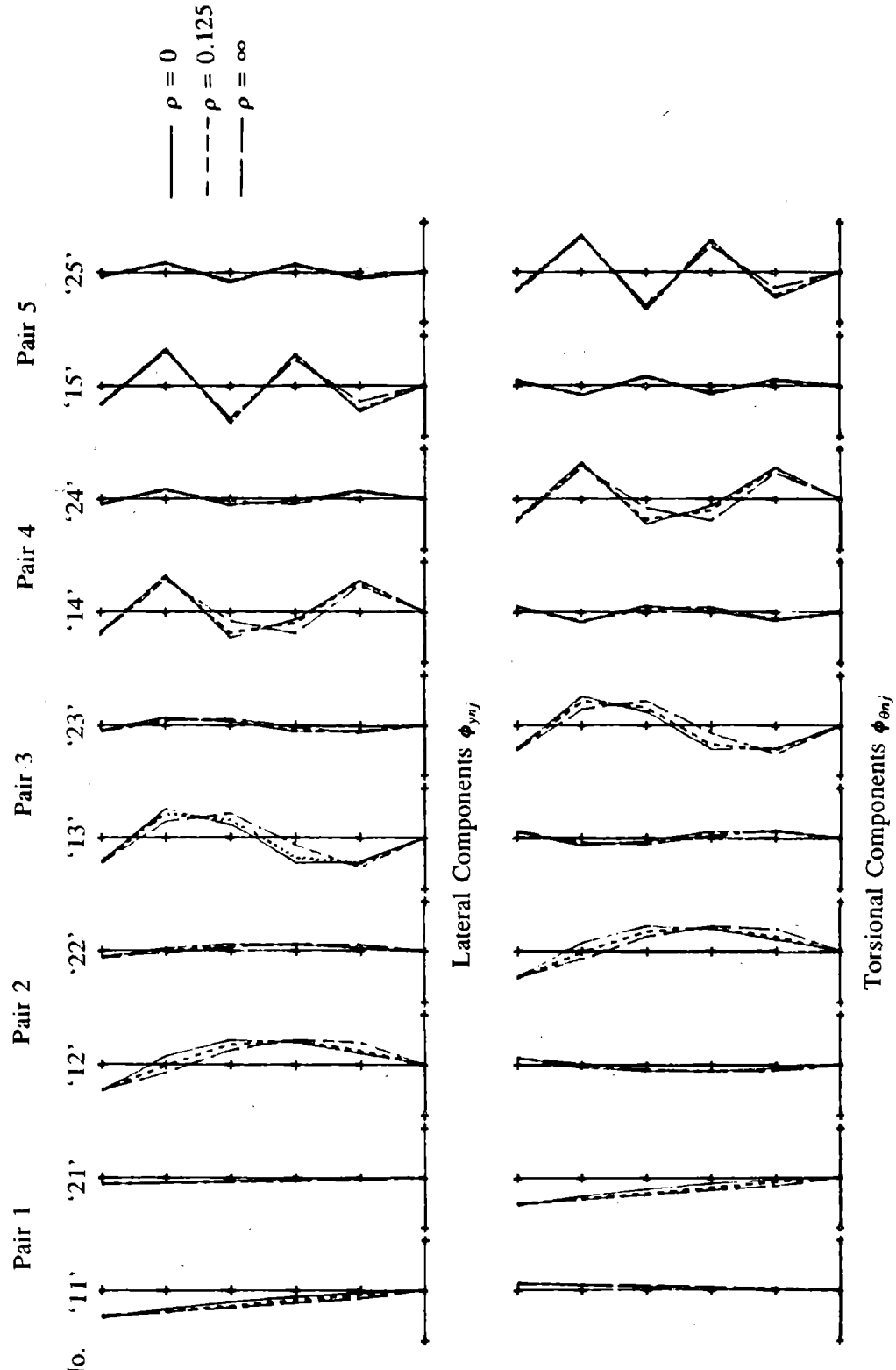

FIGURE 12a Lateral and Torsional Components of Natural Vibration Mode Shapes of Buildings with $e/r = 0.4$, $\Omega = 1.5$ and Three Values of $\rho = 0$, 0.125 and ∞.

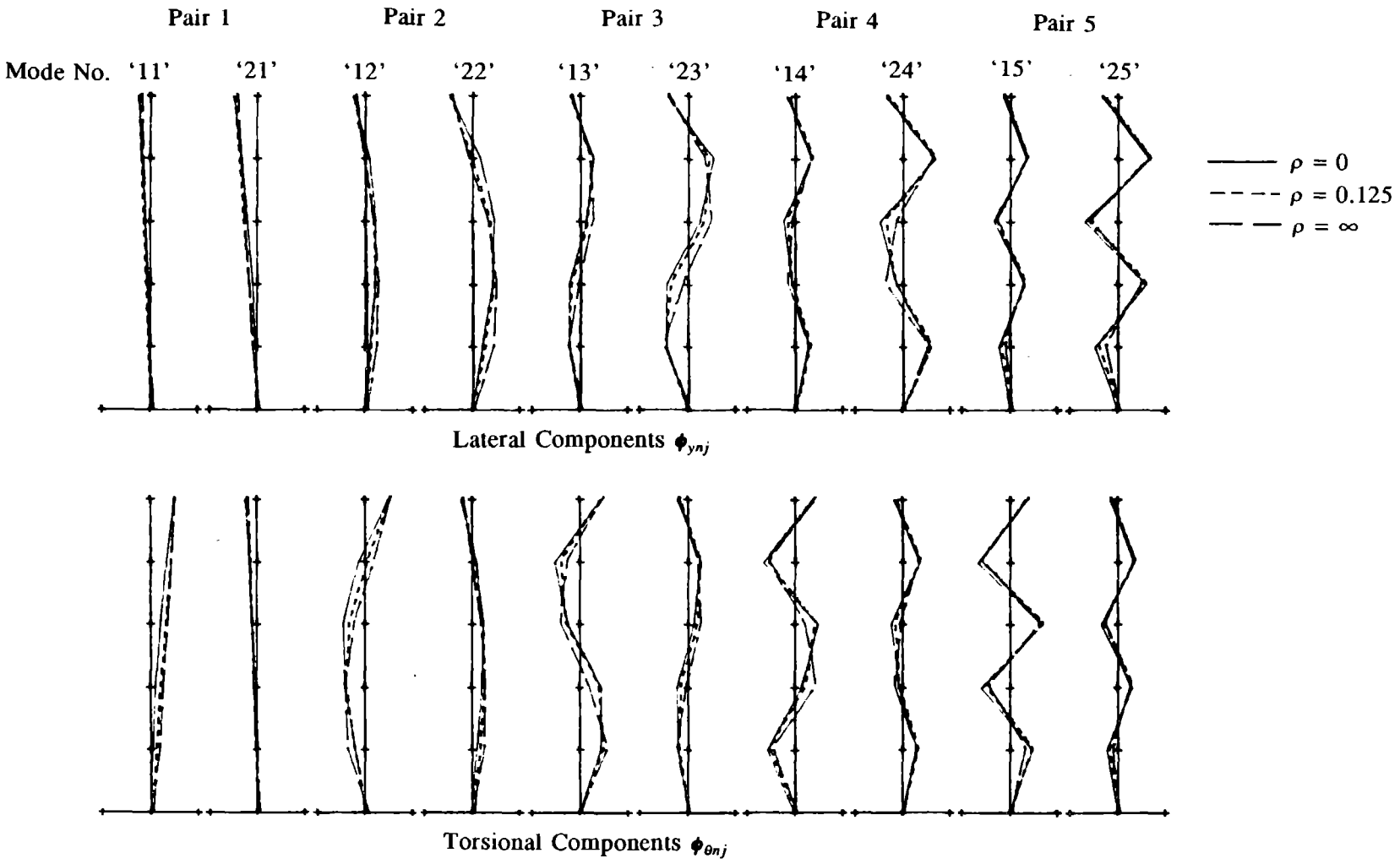

FIGURE 12b Lateral and Torsional Components of Natural Vibration Mode Shapes of Buildings with $e/r = 0.4$, $\Omega = 0.5$ and Three Values of $\rho = 0$, 0.125 and ∞.

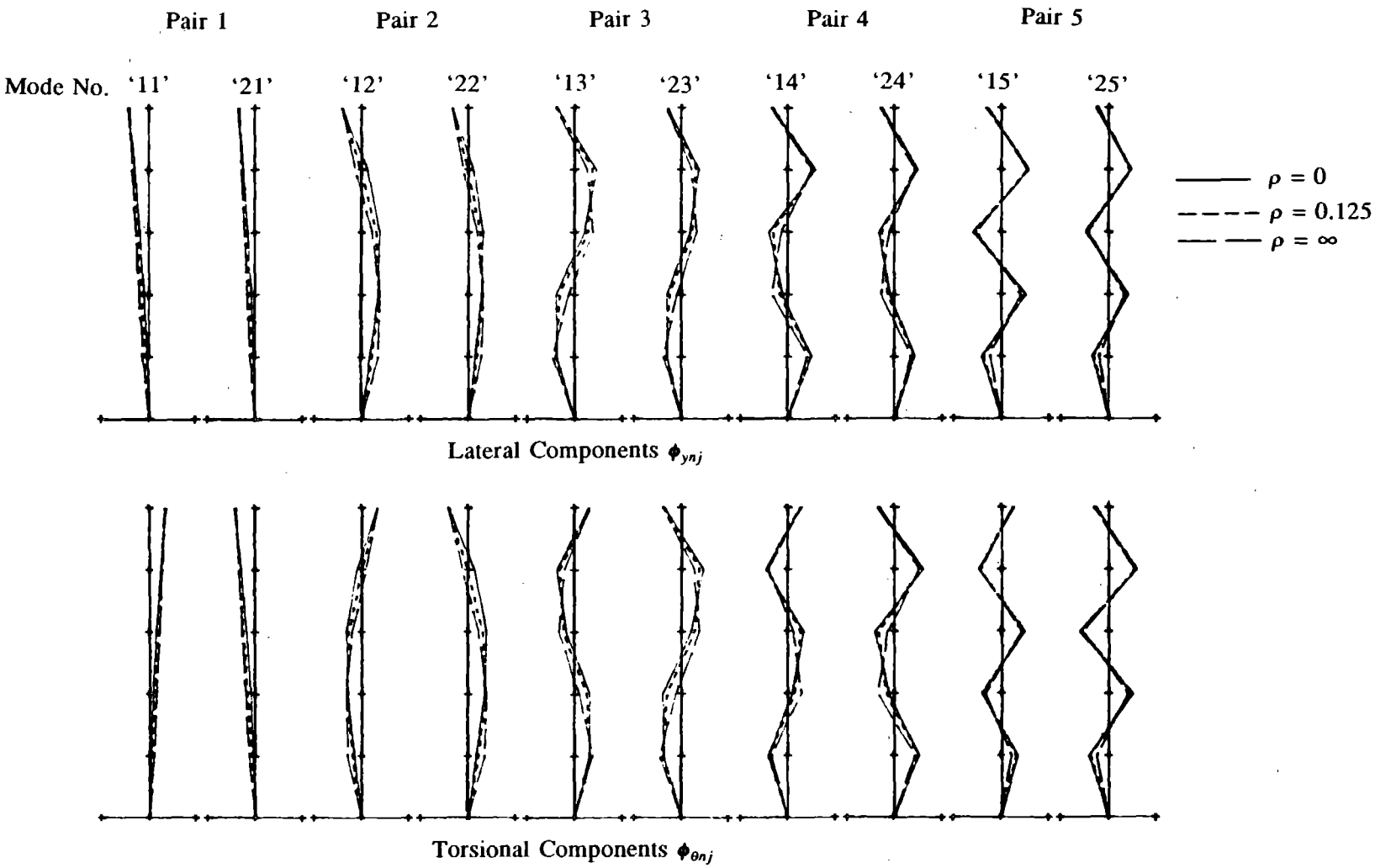

FIGURE 12c Lateral and Torsional Components of Natural Vibration Mode Shapes of Buildings with $e/r = 0.4$, $\Omega = 1$ and Three Values of $\rho = 0$, 0.125 and ∞.

The variation of the vibrational mode shapes of the torsionally-coupled building with ρ is controlled by the dependence of the uncoupled lateral mode shapes ψ_j on ρ (Figure 10). The lateral and torsional components of two modes '1j' and '2j', belonging to the same pair 'j', are proportional to ψ_j (equation (4.11)). Thus, the shapes of the components of the first pair of modes '11' and '21' is the same as ψ_1, of the second pair '12' and '22' is the same as ψ_2, ..., etc. . Since ψ_j vary significantly with ρ, as is portrayed by Figure 10, the components of each coupled mode also vary significantly with ρ, as displayed by Figures 12. It should be clear, however, that ρ plays no role in the amount of coupling that exists between the lateral and torsional components of a mode shape, since α_{yn} and $\alpha_{\theta n}$ do not depend on ρ.

Finally, the variations of the cross-correlation modal factors, $\gamma_{nj,mk}$, with system parameters are considered. These factors are computed from equation (4.36) for frequency ratios, $q_{nj,mk}$, computed by equation (4.68), and therefore directly related to the closeness of frequencies ω_{nj} and ω_{mk}. Thus, the factors are dependent on e/r , Ω and ρ. It is clear from Figure 9 that frequencies ω_{1j} and ω_{2k}, ω_{1j} and ω_{1k}, and ω_{2j} and ω_{2k}, with j=1 to 4 and k=j+1 to 5, are well separated. It follows that $\gamma_{1j,2k}$, $\gamma_{1j,1k}$ and $\gamma_{2j,2k}$ for j=1 to 4 and k=j+1 to 5, are very close to zero. Hence, cross-correlation between such modes is relatively small, justifying equation (4.70).

Cross-correlation factors $\gamma_{1j,2j}$ are independent of ρ or 'j' since $q_{1j,2j}$ equals $\bar{\omega}_1/\bar{\omega}_2$. The factors $\gamma_{1j,2j}$ are, therefore, equal to γ_{12} obtained in the case of the associated torsionally-coupled, one-story system (equation (4.38)). These are plotted in Figure 13 against Ω for various e/r values and for 5% damping. The variation of $\gamma_{1j,2j}$ or γ_{12} is closely related to the spacing of $\bar{\omega}_1$ and $\bar{\omega}_2$. Since the two coupled frequencies are closest for systems with Ω = 1 and small e/r ratios (Figure 7), $\gamma_{1j,2j}$ is largest at Ω = 1. For larger e/r values, $\bar{\omega}_1$ and $\bar{\omega}_2$ are widely spaced for any value of Ω (Figure 7) resulting in small $\gamma_{1j,2j}$. The cross-correlation terms of equation (4.70), given by its second summation, are, therefore, expected to be significant for systems with small e/r ratios and Ω = 1, i.e. closely spaced uncoupled frequencies.

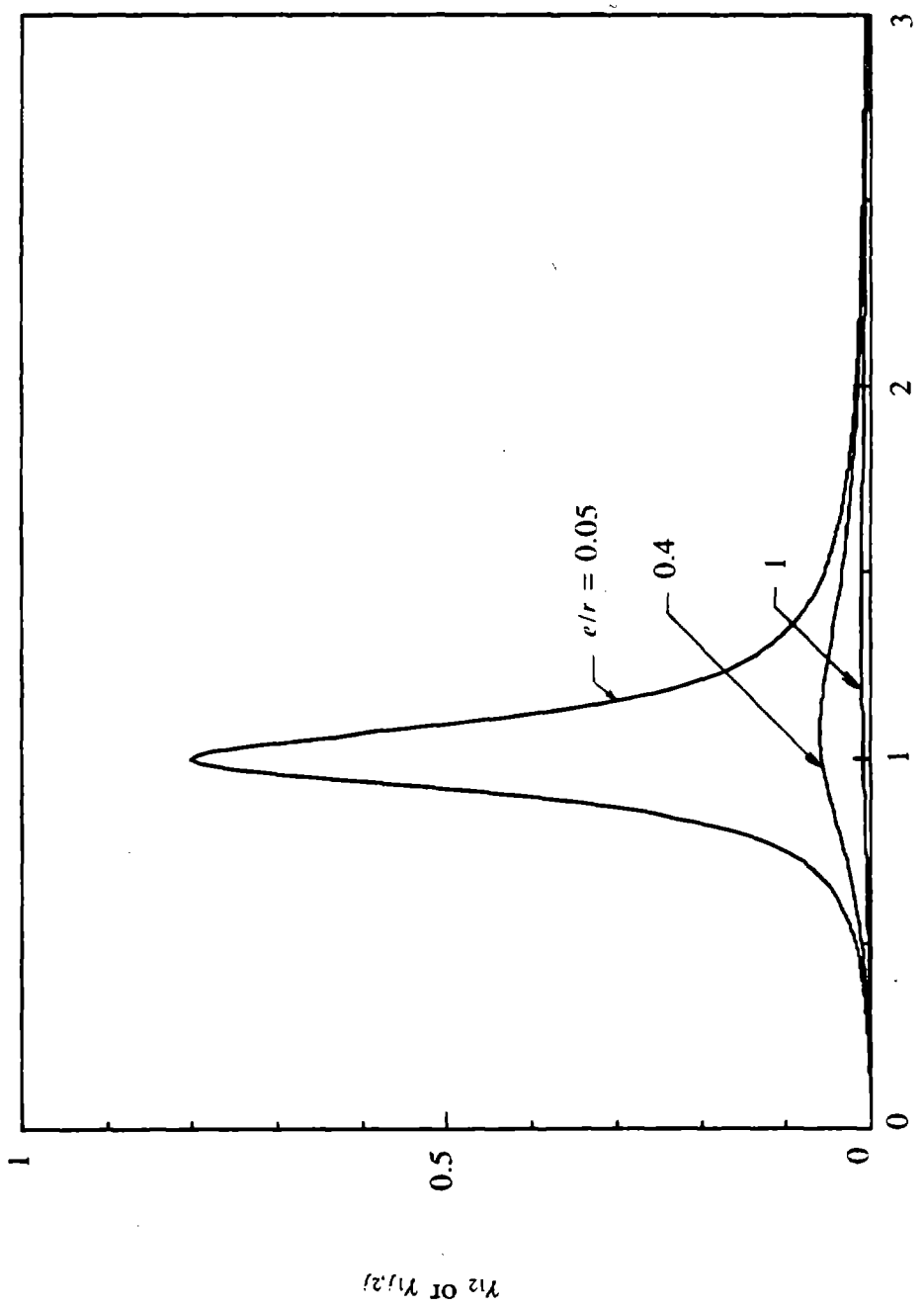

FIGURE 13 Cross-correlation Factor γ_{12} or $\gamma_{1j.2j}$ for 5 % Damping Ratio

Cross-correlation factors $\gamma_{2j,1k}$ (for j=1 to 4 and k=j+1 to 5) depend on the relative spacing of ω_{2j} and ω_{1k}. Referring to Figure 9, it is clear that these frequencies are equal at two values of Ω that depend on e/r, ρ, j and k. It follows that $\gamma_{2j,1k}$ has two maxima equal to one corresponding to these two values of Ω. Figure 14 shows $\gamma_{21,12}$ and $\gamma_{21,13}$ against Ω for e/r equal to 0.4 and values of ρ equal to 0, 0.125 and ∞. These factors are chosen without inference that their corresponding terms of equation (4.70) are the most important, but rather as representatives of $\gamma_{2j,1k}$. As e/r increases or as ρ increases the two peaks of $\gamma_{2j,1k}$ approach each other, widening the range of Ω where $\gamma_{2j,1k}$ is large. As k increases with the same j the two maxima of $\gamma_{2j,1k}$ are drawn farther apart, narrowing the range of Ω where $\gamma_{2j,1k}$ is significant. On the other hand, as j increases for the same k, (example $\gamma_{21,13}$ and $\gamma_{22,13}$), the two maxima of $\gamma_{2j,1k}$ approach each other widening the range of Ω with large $\gamma_{2j,1k}$.

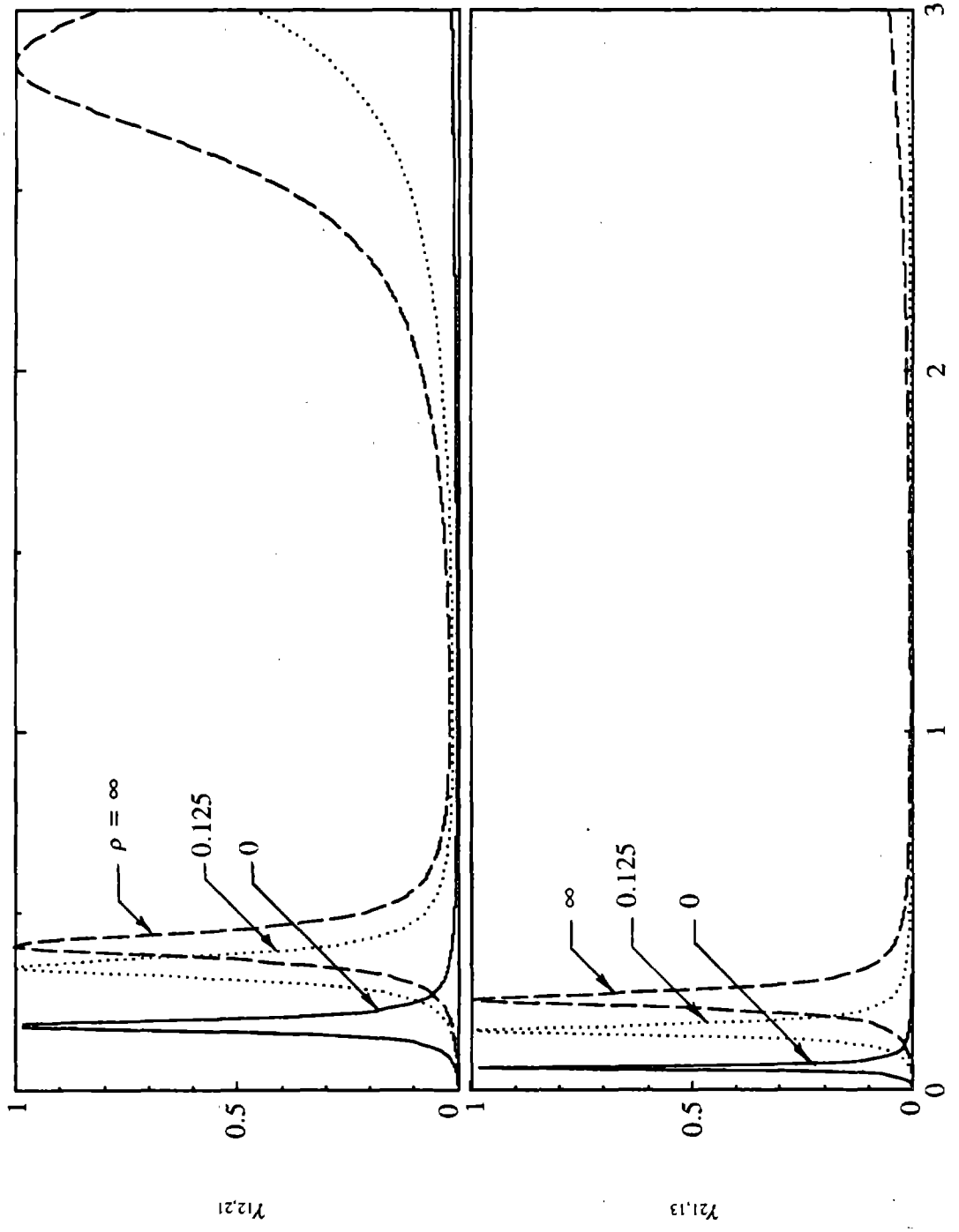

FIGURE 14 Cross-correlation Factors $\gamma_{12,21}$ and $\gamma_{21,13}$ (e/r = 0.4 and ξ = 5 %)

6. EFFECT OF FRAME ACTION

The effect of frame action on the maximum response of the torsionally-coupled, multi-story building, computed by the RSA procedure described in Section 4, is investigated next. The maximum response is plotted against T_{y1}, the fundamental lateral vibration period of the corresponding torsionally-uncoupled, multi-story system in the form of response spectra. Such plots are presented in Figures 15 and 16 for values of the beam-to-column stiffness ratio ρ equal to 0, 0.125 and ∞ and seven response quantities: base shear V_B, base torque at the center of rigidity T_{BR}, base overturning moment M_B, top floor lateral displacement at center of rigidity v_5, beam moment M_{bB} in the first story of frame (1), column moment M_{cB} in the first story of frame (1), and the column axial force P_{cB} in the first story of frame (1). The response quantities V_B , T_{BR} , M_B and v_5 (Figure 15) are selected as representatives of overall behavior of the torsionally-coupled system, and M_{bB} , M_{cB} and P_{cB} (Figure 16) as indicative of its local behavior. The response spectra are presented for systems with eccentricity ratio e/r equal 0.4 and uncoupled torsional to lateral frequency ratio Ω equal to one. The range of T_{y1} values included in the response spectra is much wider than reasonable for a five-story building. However, the dynamic response behavior of taller buildings is generally similar to that of a five-story building with the same T_{y1}. Thus the presented results are indicative of the earthquake response of buildings of varying number of stories.

The response quantities are presented in dimensionless form as defined in Figures 15 and 16 and with the normalizing factors given in Table 10, where $\bar{u}_g$ and $\bar{a}_g$ are the maximum ground displacement and ground acceleration, respectively; W_1^* and h_1^*, given by equations (4.20), are the effective weight and height for the fundamental vibration mode of the corresponding torsionally-uncoupled, multi-story system; e_1^* is the effective eccentricity of the associated torsionally-coupled, one-story system in its first vibration mode, given by equation (4.34); and $\bar{W}_1^*$ is the effective weight in the fundamental vibration mode of the associated torsionally-coupled, one-story system normalized by its weight, given by equation (4.44). The normalization factors for base shear and base overturning moment are the maximum base shear and overturning moment for a rigid (i.e. zero

Table 10 Normalization Factors

Response Quantity	Normalization Factor
Story Shears	$W_1^* \bar{a}_g / g$
Story Torques at Centers of Rigidity	$(e_1^* \overline{W}_1^*) W_1^* \bar{a}_g / g$
Story Overturning Moments	$W_1^* h_1^* \bar{a}_g / g$
Lateral Displacements at Centers of Rigidity	$\bar{u}_g$
Frame (1) Column Moments	$(EI_1/h^2)\ \bar{u}_g$
Frame (1) Beam Moments	$(EI_1/h^2)\ \bar{u}_g$
Frame (1) Column Axial Forces	$(EI_1/h^3)\ \bar{u}_g$

Table 11 Effective Weight and Height in the Fundamental Mode of the Corresponding Torsionally-uncoupled System

ρ	$\frac{W_1^*}{\text{Total Weight}}$	$\frac{h_1^*}{\text{Total Height}}$
0.	0.6787	0.7963
0.125	0.7963	0.7420
∞	0.8795	0.7027

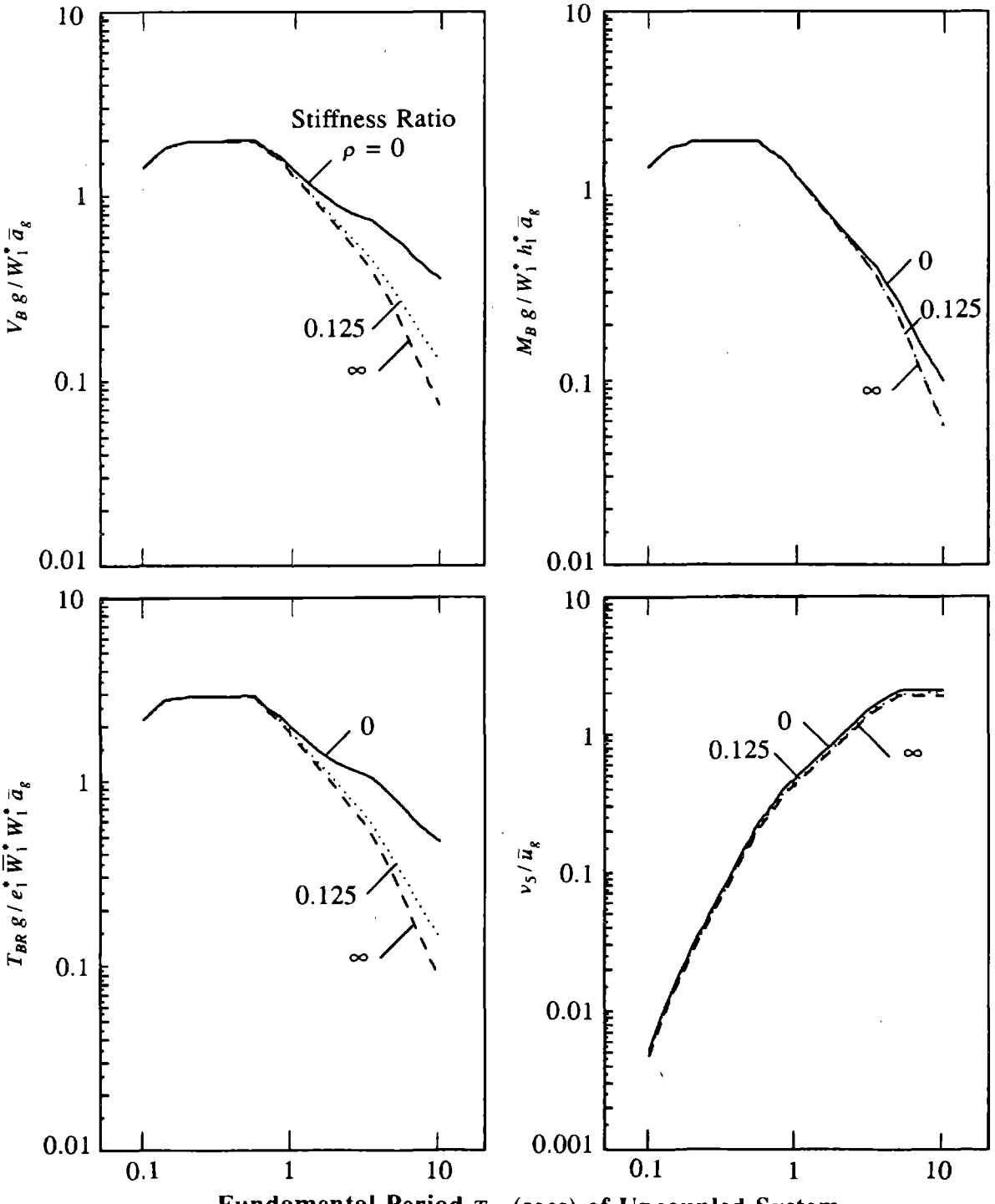

FIGURE 15 Effect of ρ on Base Shear V_B, Base Overturning Moment M_B, Base Torque at Center of Rigidity T_{BR} and Top Floor Lateral Displacement at Center of Rigidity v_5 (e/r = 0.4 and ξ = 5 %)

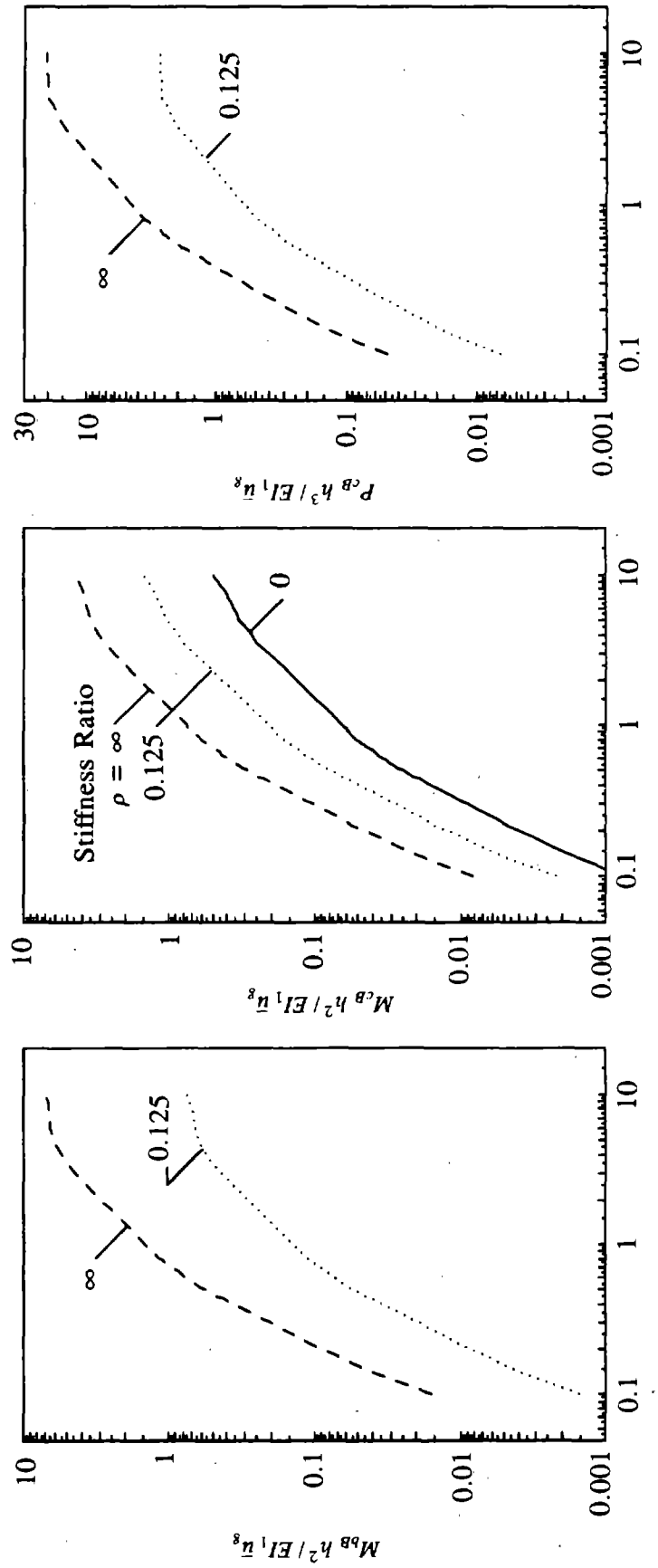

FIGURE 16 Effect of ρ on Beam Moment M_{bB}, Column Moment M_{cB} and Column Axial Force P_{cB} in Base-story of frame (1) ($e/r = 0.4$, $\Omega = 1$ and $\xi = 5$ %)

vibration period) single-degree-of-freedom system with height h_1^* and lumped weight W_1^*. Referring to equation (4.64), the normalization factor for the base torque is the torque obtained if the base shear $W_1^*\bar{a}_g/g$ of the rigid single-degree-of-freedom system is applied at a distance $e_1^*\overline{W}_1^*$ from the CR of the system. The effective weight and height, W_1^* and h_1^*, depend on ρ, (Table 11), while e_1^* and $\overline{W}_1^*$ depend on e/r and Ω (equations (4.34) and (4.44)). Similarly the normalized response quantities depend on ρ, e/r and Ω and on the variation of the earthquake response spectrum with vibration period but not on its intensity.

It is apparent from Figure 15 that the base shear, V_B, overturning moment, M_B, and torque T_{BR} vary significantly with ρ in the velocity- and displacement-controlled regions of the design spectrum, with the variation of M_B not as great as V_B or T_{BR}. In the acceleration-controlled region of the spectrum the normalized responses do not vary appreciably with ρ, but the actual response values depend on ρ because this parameter influences W_1^* and h_1^* (Table 11). The top floor displacement v_5 of frame (1) is essentially independent of ρ over a wide range of vibration periods T_{y1}.

The general trends in the variation of the three local response quantities-- beam moment, column moment and column axial force-- with ρ are the same (Figure 16). As ρ decreases, the normalized forms of both M_{bB} and P_{cB} tend to zero, while the normalized form of M_{cB} decreases to the moment in a cantilever bending beam. For a fixed T_{y1}, the column stiffness may increase as ρ decreases, and therefore M_{cB} may increase even though its normalized value decreases.

The effects of frame action, characterized by the beam-to-column stiffness ratio ρ, identified in the preceding paragraphs for torsionally-coupled buildings are similar to those observed in lateral response of torsionally-uncoupled systems [12]. The variation in response of torsionally-uncoupled systems with ρ was shown [12] to be related to the significance of higher mode contributions in response, which generally increase with decreasing ρ and with increasing T_{y1} and also depend on the response quantity considered. Similarly, the variation of the response of torsionally-coupled

buildings with ρ will be shown in Section 7 to be closely related to the significance of the higher modal-pair contributions in response.

In Figure 16 M_{bB} is the moment in the first-story beam of frame (1), and M_{cB} and P_{cB} the moment and axial force in the first-story column. In order to examine the locations of largest member forces, response spectra for the forces in the beams and columns of each story of the frame are presented in Figures 17 to 19. These results demonstrate that for the range of parameters considered, the maximum forces occur in the base story of the frame. The magnitudes of these forces decrease at higher stories with the rate of reduction tending to be greater for the larger values of ρ.

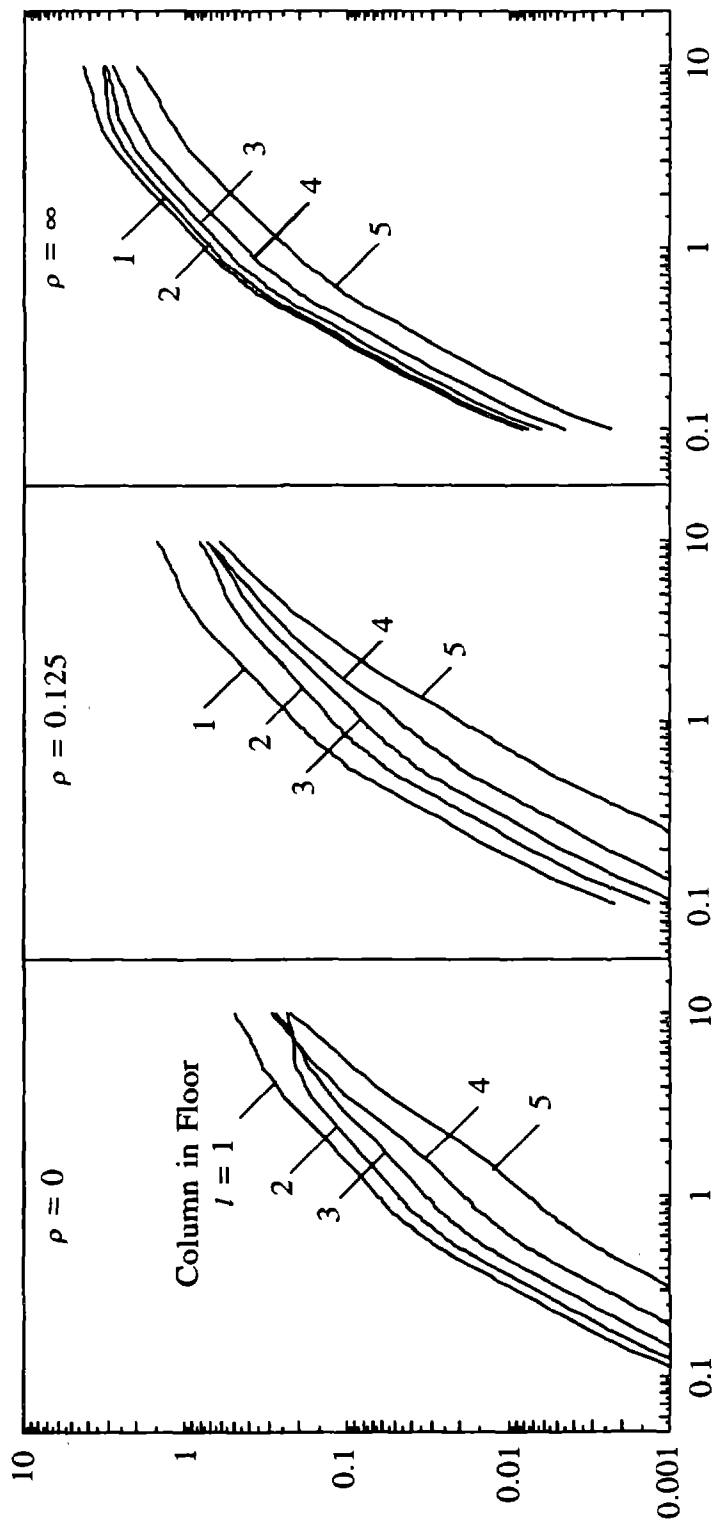

FIGURE 17 Maximum Bending Moment in Individual Columns of Frame (1) ($e/r = 0.4$, $\Omega = 1$ and $\xi = 5$ %)

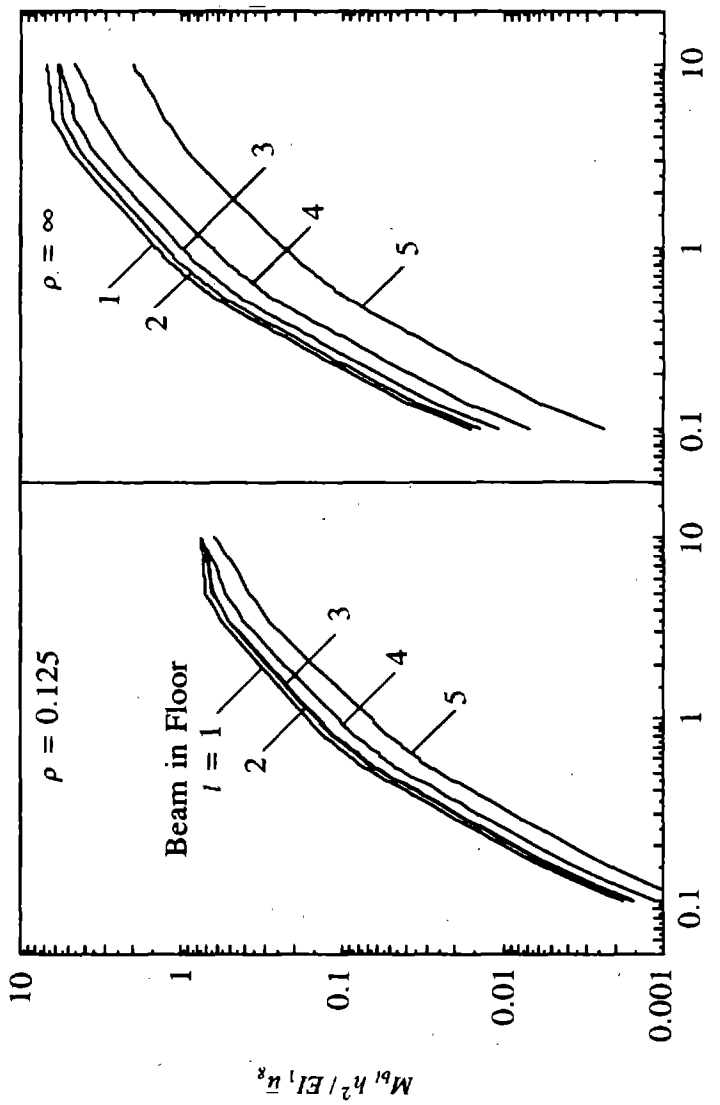

FIGURE 18 Maximum Bending Moment in Individual Beams of Frame (1) (e/r = 0.4, Ω = 1 and ξ = 5 %)

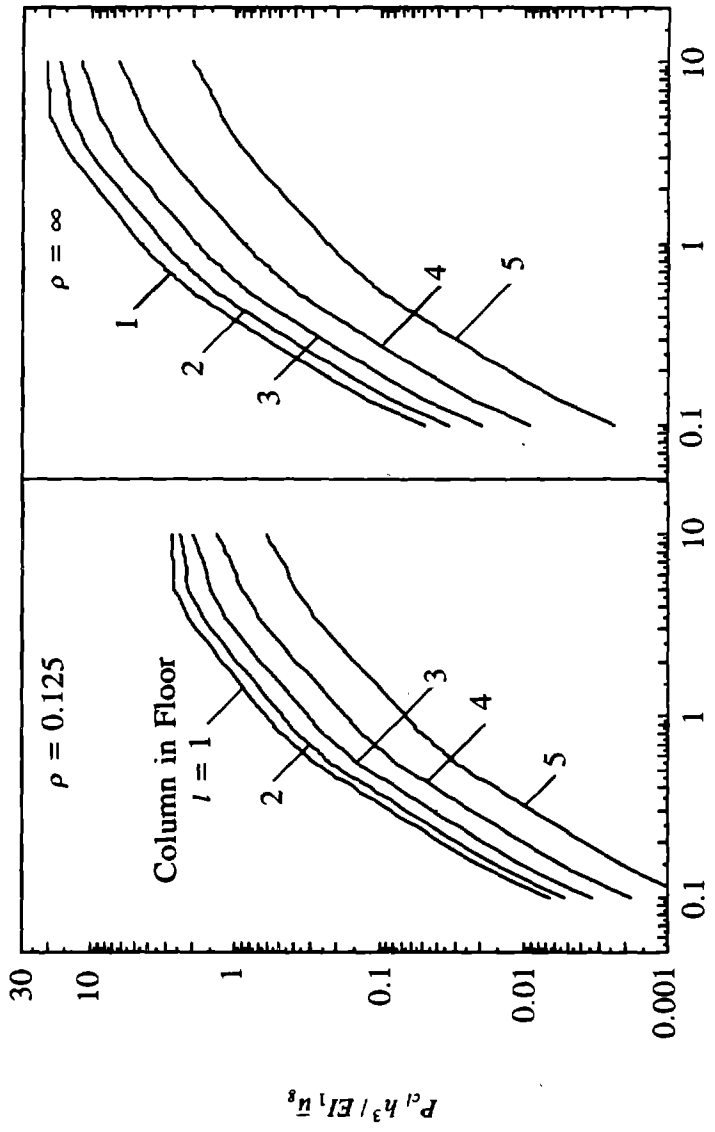

FIGURE 19 Maximum Axial Force in Individual Columns of Frame (1) (e/r = 0.4, Ω = 1 and ξ = 5 %)

7. MODAL-PAIR CONTRIBUTIONS

The maximum responses of the torsionally-coupled, multi-story building computed by the RSA procedure presented in Section 4.4 are plotted against T_{y1}, the fundamental vibration period of the corresponding torsionally-uncoupled system, in the form of response spectra. Obtained by considering varying numbers of vibration modal-pairs in RSA, such plots are presented in Figures 20 to 26 for three values of ρ = 0, 0.125 and ∞, e/r = 0.4, Ω = 1, and the seven normalized response quantities defined in Section 6.

For the subsequent interpretation of the response results, it is useful to introduce the concept of unit modal-pair response. This quantity defined for the j^{th} modal-pair is the CQC combination of the unit modal response of the structure in the two vibration modes '1j' and '2j', where the unit modal response of the building in the nj^{th} vibration mode are given by equations (4.48) to (4.66) with unit pseudo-acceleration. It is apparent from equation (4.66) that the unit response of the building in the nj^{th} vibration mode is the product of the unit modal response r_j in the j^{th} vibration mode of the corresponding torsionally-uncoupled, multi-story system (equations (4.12) to (4.19) with S_{aj} = 1), and the normalized response $\overline{r}_{nj}$ in the n^{th} vibration mode of the associated torsionally-coupled, one-story system with $S_{anj}/S_{aj} = 1$ [equations (4.42) to (4.46)]. Combination of the unit responses in vibration modes '1j' and '2j' by equation (4.35) gives the unit responses in the j^{th} modal-pair to be equal to the product of the unit modal response in the j^{th} uncoupled mode and the normalized unit modal response of the associated torsionally-coupled, one-story system, determined by equation (4.47). In discussing the contributions of various vibration modal-pairs (j=1, 2, ..., N) to the response, it is useful to normalize the unit modal-pair response as a fraction of the corresponding value for the first modal-pair. Since the normalized unit modal response of the associated torsionally-coupled, one-story system [equation (4.47)] is independent of 'j', i.e. it is the same for any pair, the normalized unit response for the j^{th} modal-pair equals the ratio of the unit modal responses in the j^{th} and fundamental lateral vibration modes of the corresponding torsionally-uncoupled system. Normalized unit modal-pair responses such as for story shears,

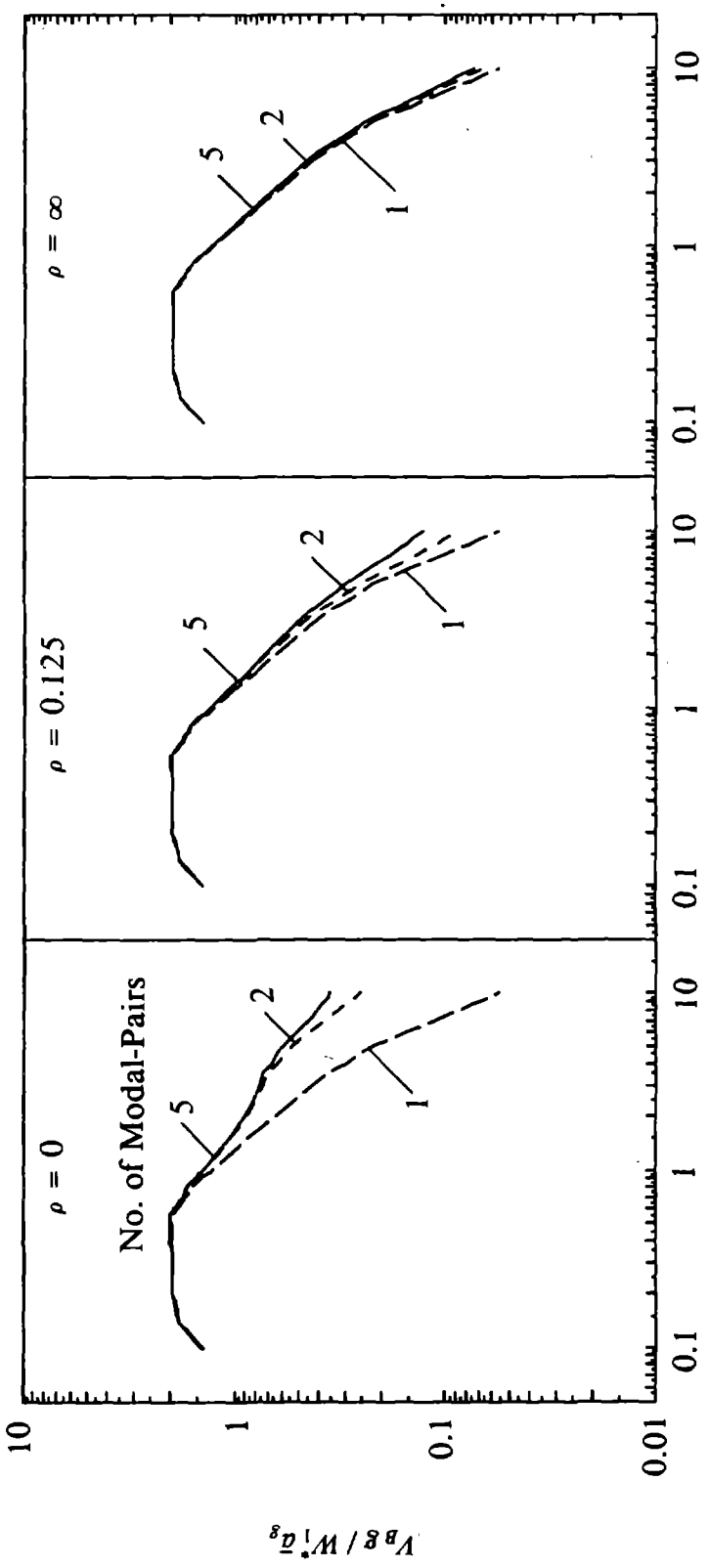

FIGURE 20 Maximum Base Shear Considering one, two and five Pairs of Vibration Modes for Three Values of ρ (e/r = 0.4, Ω = 1 and ξ = 5 %)

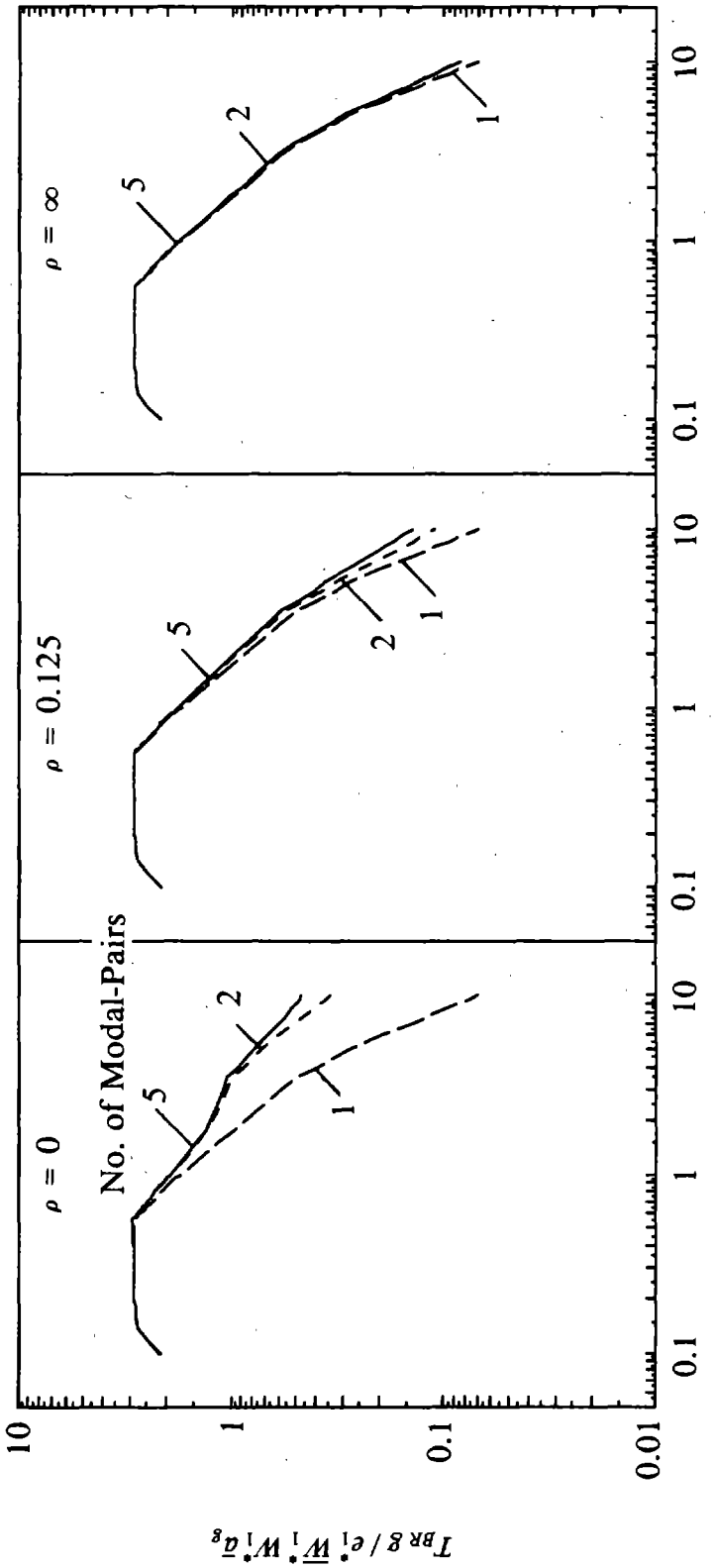

FIGURE 21 Maximum Base Torque at Center of Rigidity Considering one, two and five Pairs of Vibration Modes for Three Values of ρ (e/r = 0.4, Ω = 1 and ξ = 5 %)

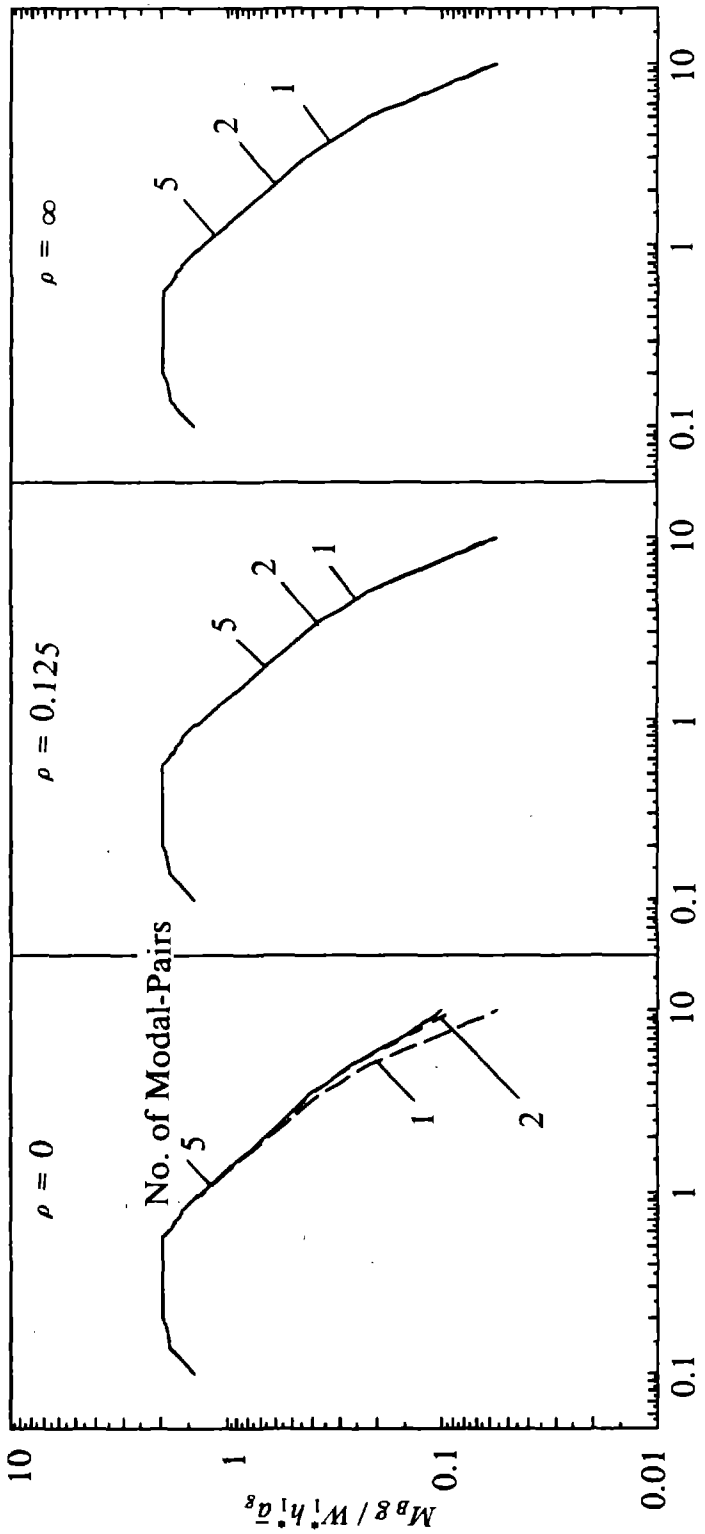

FIGURE 22 Maximum Base Overturning Moment Considering one, two and five Pairs of Vibration Modes for Three Values of ρ (e/r = 0.4, Ω = 1 and ξ = 5 %)

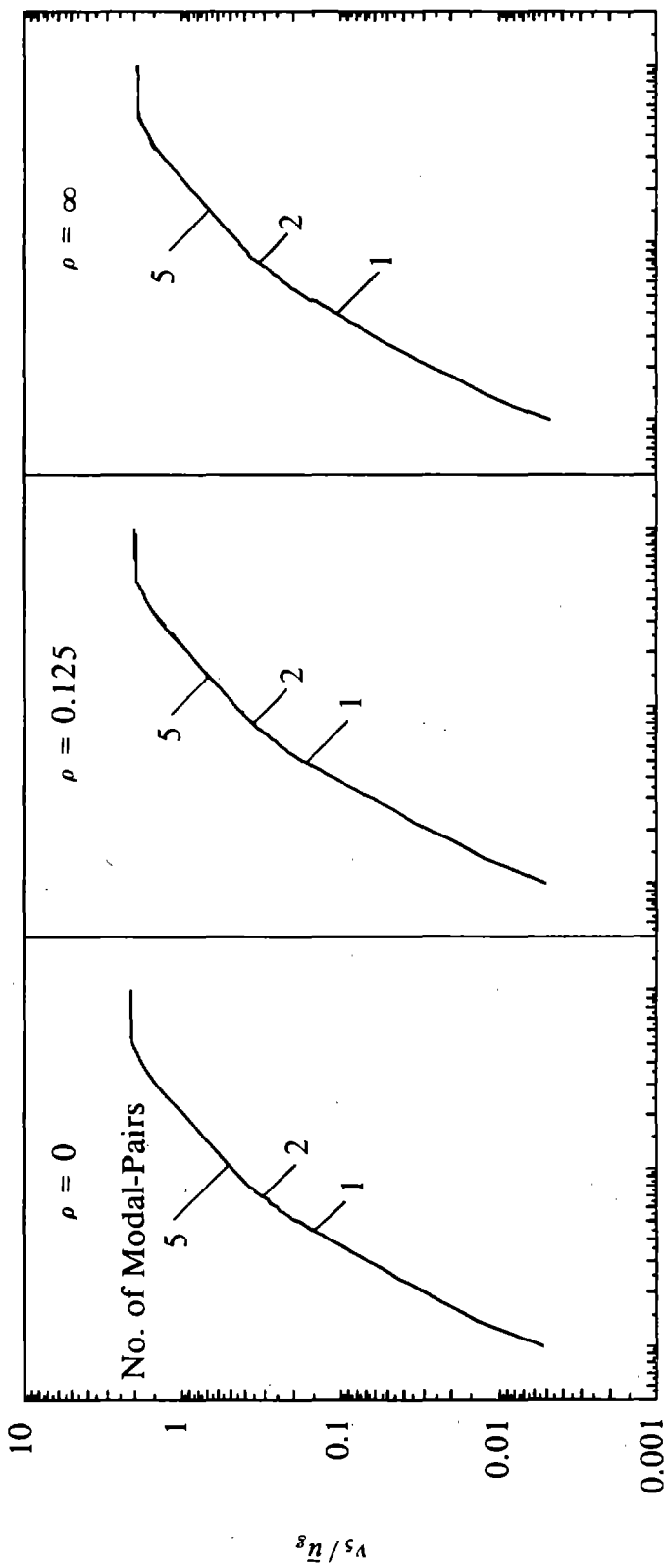

FIGURE 23 Maximum Top Floor Lateral Displacement at Center of Rigidity Considering one, two and five Pairs of Vibration Modes for Three Values of ρ (e/r = 0.4, Ω = 1 and ξ = 5 %)

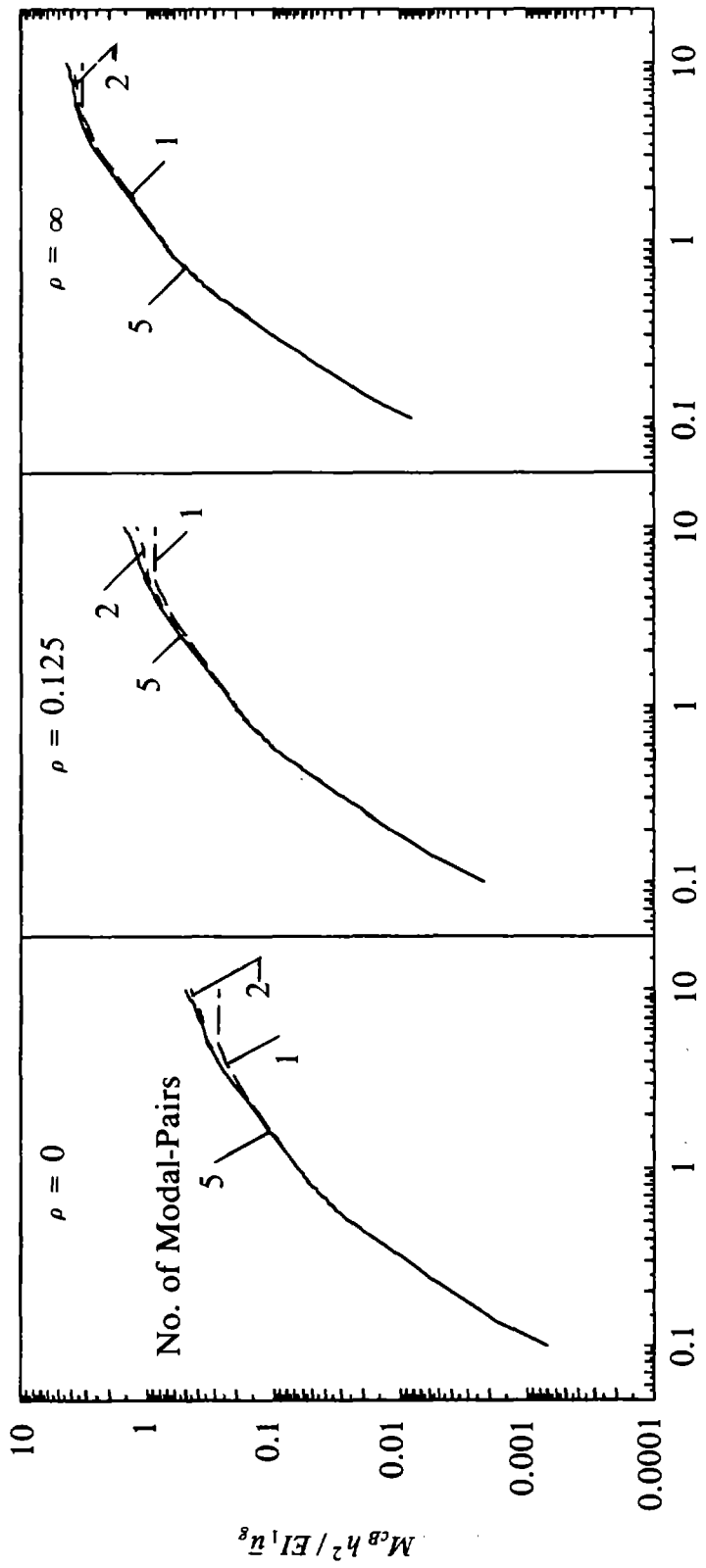

FIGURE 24 Maximum Column Moment in Base-story of Frame (1) Considering one, two and five Pairs of Vibration Modes for Three Values of ρ (e/r = 0.4, Ω = 1 and ξ = 5 %)

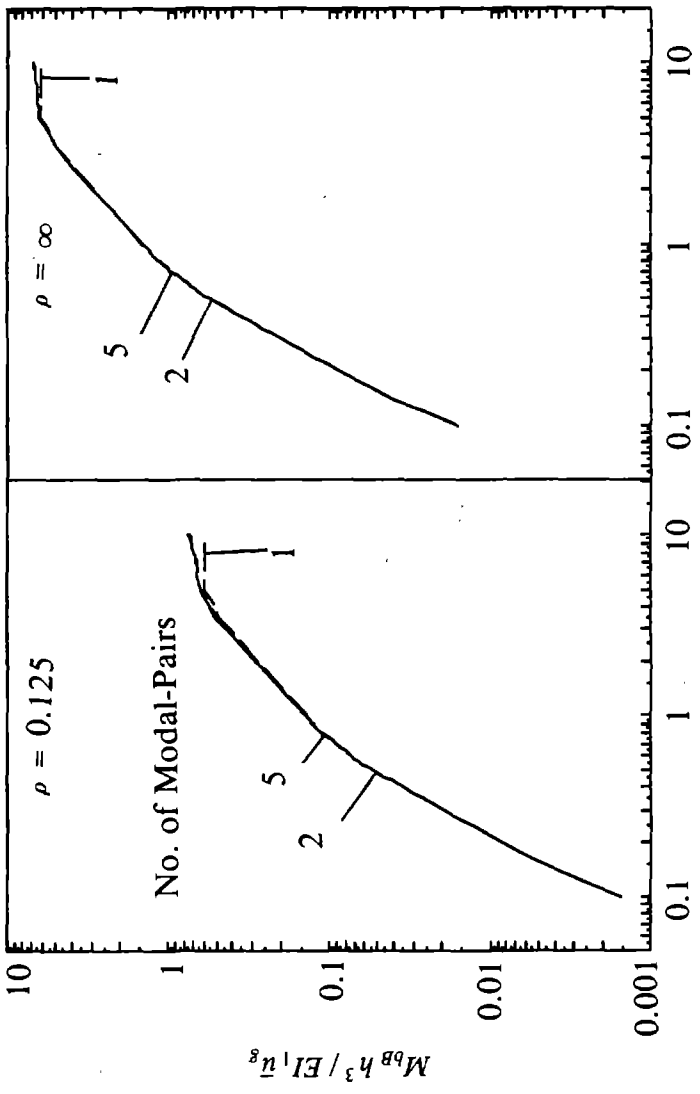

FIGURE 25 Maximum Beam Moment in Base-story of Frame (1) Considering one, two and five Pairs of Vibration Modes for Three Values of ρ (e/r = 0.4, Ω = 1 and ξ = 5 %)

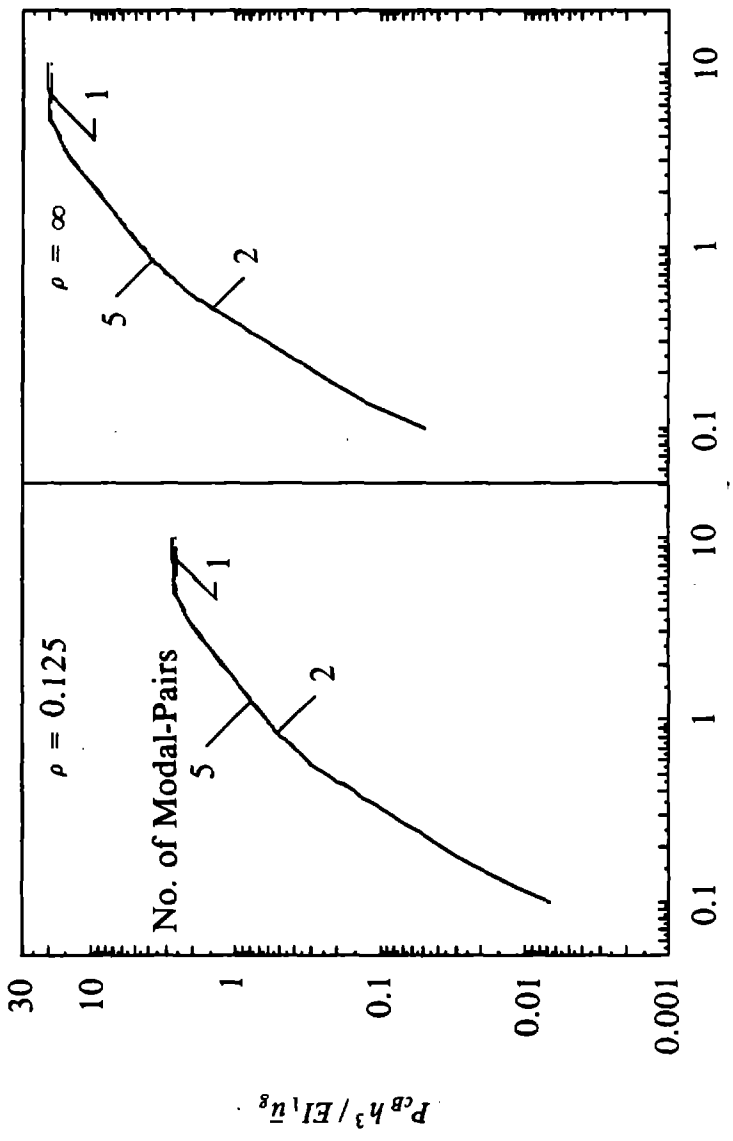

FIGURE 26 Maximum Column Axial Force in Base-story of Frame (1) Considering one, two and five Pairs of Vibration Modes for Three Values of ρ (e/r = 0.4, Ω = 1 and ξ = 5 %)

torques, overturning moments, and frame (1) lateral displacements vary with ρ but not with T_{y1}, e/r, Ω or the design spectrum. Numerical values of these unit modal-pair responses for a few of these quantities are presented in Table 12. The period dependence of the relative modal-pair contributions to a response quantity is all represented by the spectral ordinates for the various modes.

Although the contribution of a modal-pair in response is closely related to its unit modal-pair response introduced in the preceding paragraph, it is also dependent on the cross-correlation between each of the two vibration modes of the pair to modes of different pairs. These cross-correlation terms are well approximated by the terms in the third summation of equation (4.70).

The response contributions of the vibration modal-pairs higher than the fundamental modal-pair increase with increasing T_{y1} in the velocity- and displacement-controlled regions of the earthquake design spectrum. For fixed e/r, Ω and ρ values, the mode shapes, the normalized unit modal-pair responses of the building, and the ratios of vibration frequencies do not change with T_{y1}. Thus the increased contribution of the higher modal-pairs is due only to the relative values of the design spectrum ordinates, which in turn depend on the spacing of vibration periods and on the shape of the spectrum. For the selected spectrum, as T_{y1} increases within the above mentioned spectral regions, the ratio of the pseudo-acceleration spectrum ordinate for a higher vibration mode to that of the fundamental mode generally increases, resulting in increased response contributions of higher modal-pairs.

The increase in response contributions of higher modal-pairs varies with the response quantity. As suggested by the normalized unit modal-pair responses of the building (Table 12), for fixed values of e/r , Ω and ρ, Figures 20 to 23 demonstrate that the higher modal-pair contributions are much more significant for the base shear, V_B, and base torque at center of rigidity, T_{BR}, than for the base overturning moment, M_B or the top floor displacement v_5 of frame (1). Figures 24 to 26 indicate that the higher modal-pair contributions are relatively small in the local response quantities for frame (1). Among the local response quantities, these contributions are larger for the base-story column moment, M_{cB}, than for the base-story beam moment, M_{bB}, or the base-story column axial force, P_{cB}. Column moments are closely related to story shears which are affected more by higher

Table 12 Normalized Unit Modal-Pair Responses

Top Floor Displacement at Center of Rigidity			
Modal-pair	$\rho = 0$	$\rho = 0.125$	$\rho = \infty$
1	1.0	1.0	1.0
2	-0.0094	-0.0292	-0.0340
3	0.0004	0.0034	0.0060
4	0.0000	-0.0005	-0.0014
5	0.0000	0.0001	0.0003
Base Shear and Base Torque at Center of Rigidity			
Modal-pair	$\rho = 0$	$\rho = 0.125$	$\rho = \infty$
1	1.0	1.0	1.0
2	0.3040	0.1475	0.0991
3	0.1033	0.0647	0.0275
4	0.0485	0.0325	0.0085
5	0.0176	0.0111	0.0018
Base Overturning Moment			
Modal-pair	$\rho = 0$	$\rho = 0.125$	$\rho = \infty$
1	1.0	1.0	1.0
2	0.0873	-0.0030	-0.0340
3	0.0182	0.0143	0.0060
4	0.0064	0.0028	-0.0014
5	0.0020	0.0014	0.0003

modal-pair contributions whereas beam moments and column axial forces are closely related to story overturning moments which are affected less by higher modal-pair contributions.

Obviously the higher modal-pairs also affect the shear, moments and torques in all stories in addition to the base shear, base overturning moment and base torque. These effects are summarized in Figures 27 to 29 wherein the height-wise variation of story shears, story torques and story overturning moments, expressed as a ratio of the respective values at the base, are presented for buildings with selected values of T_{y1} = 0.5 and 2.5 sec, for e/r = 0.4 and Ω = 1. The height-wise variation of only the fundamental modal-pair response, which is the same regardless of T_{y1}, is also included. The presented story shears and overturning moments are also the story shears and overturning moments of frame (1), since it is the only frame in the plane of the ground motion (Figure 2a). In a lumped mass system, such as the structure considered here, the shear remains constant in each story with discontinuities at each floor. However, such a plot would not be convenient in displaying the differences among various cases and the alternative presentation with shears varying linearly over story height is used. It is apparent that the higher modal-pair contributions not only influence the magnitude of the story shears, moments and torques but also their distributions because the various vibration modal-pairs affect different portions of the building to varying degrees. The distribution, but not necessarily the actual values of forces in the upper stories, is especially affected by the higher modal-pair contributions.

It is apparent from Figures 27 and 28 that the height-wise variations of story shears and torques are similar, with differences increasing as T_{y1} increases. Since the height-wise variations of story shears and story torques are exactly the same when only the fundamental modal-pair is taken into account, and the normalized unit modal-pair responses of shears and torques are exactly the same (Table 12), the differences between the height-wise variations of story shears and story torques are only due to cross-correlation terms between vibration modes of different pairs, given by the third summation of equation (4.70).

We next examine how the higher modal-pair contributions to the response of the building are affected by the beam-to-column stiffenss ratio, ρ. As ρ decreases the normalized unit modal-pair

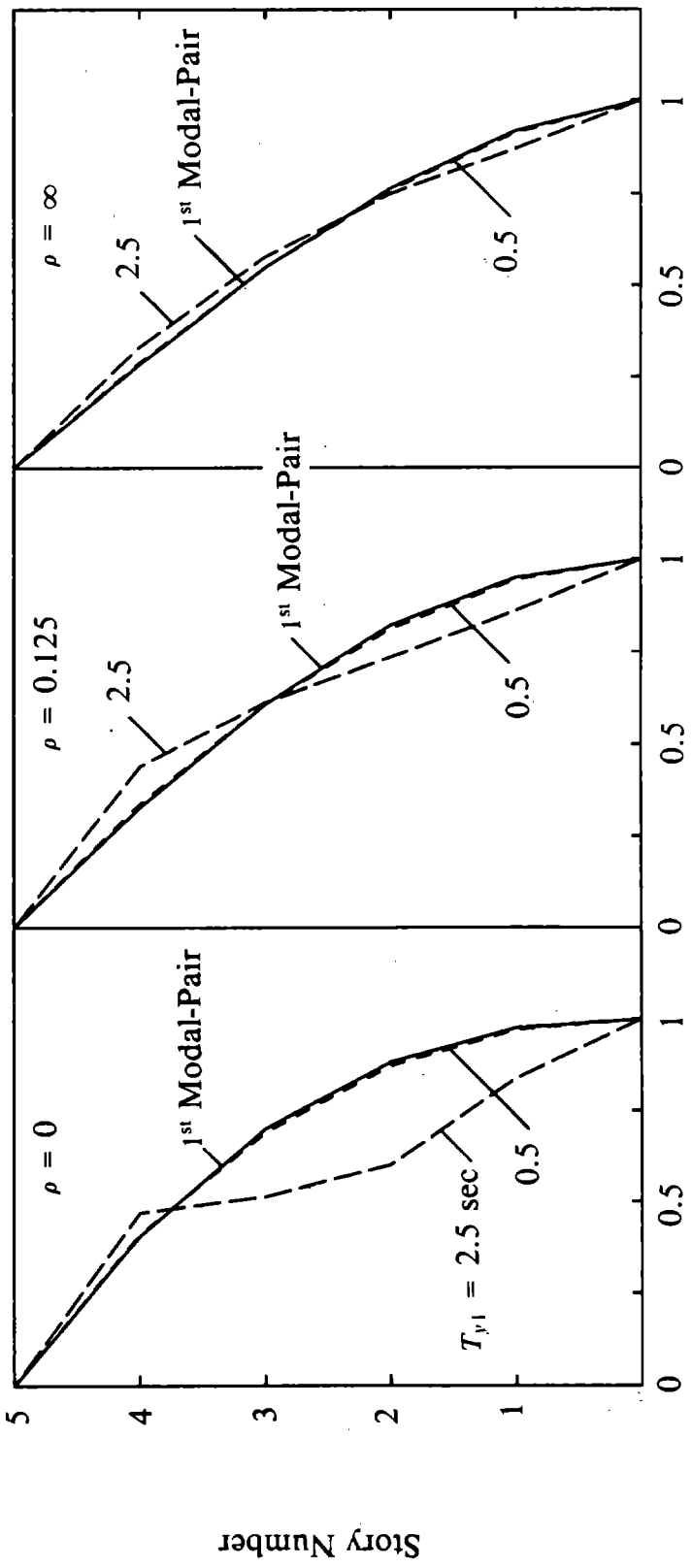

FIGURE 27 Height-wise Variation of Story Shears Including one or five Modal-pair Contributions for two Values of T_{y1} and Three Values of ρ (e/r = 0.4, Ω = 1 and ξ = 5 %).

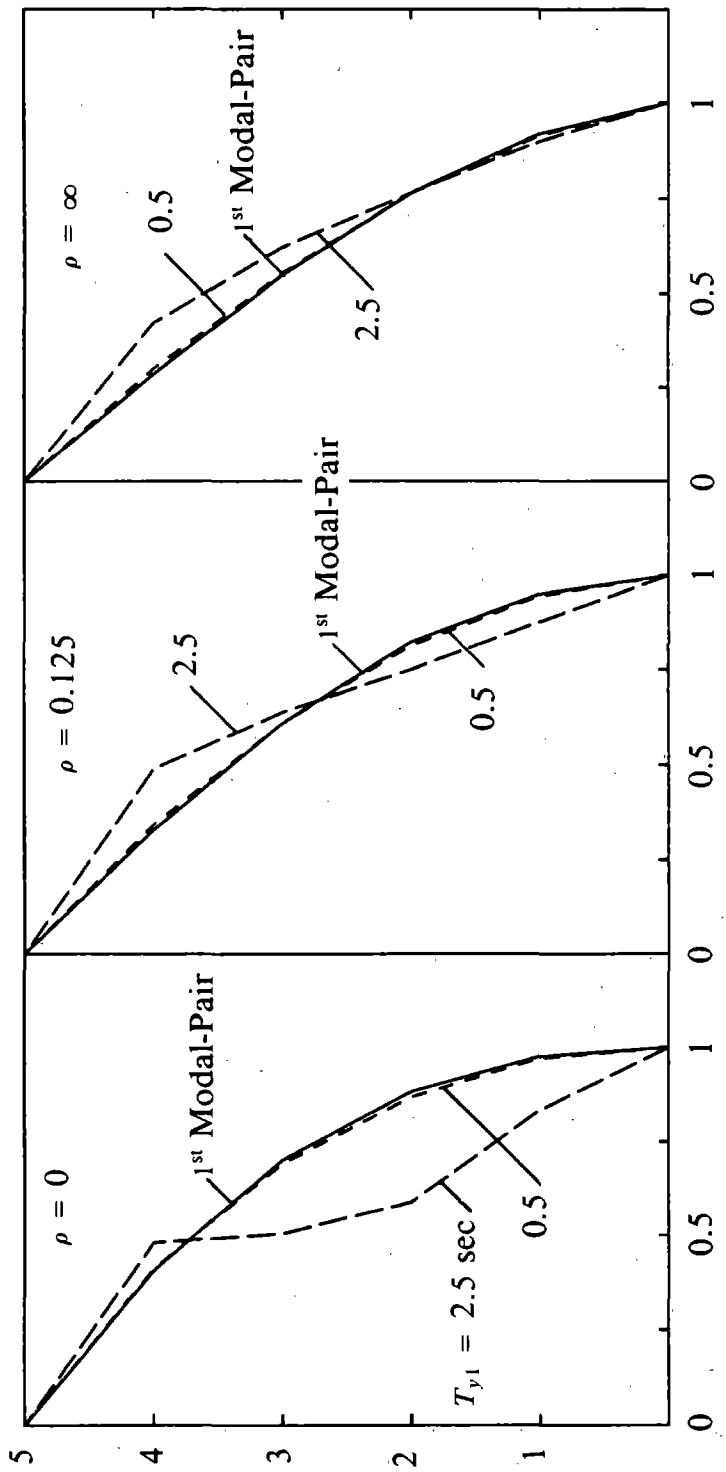

FIGURE 28 Height-wise Variation of Story Torques at Centers of Rigidity Including one or five Modal-pair Contributions for two Values of T_{y1} and Three Values of ρ (e/r = 0.4, Ω = 1 and ξ = 5 %).

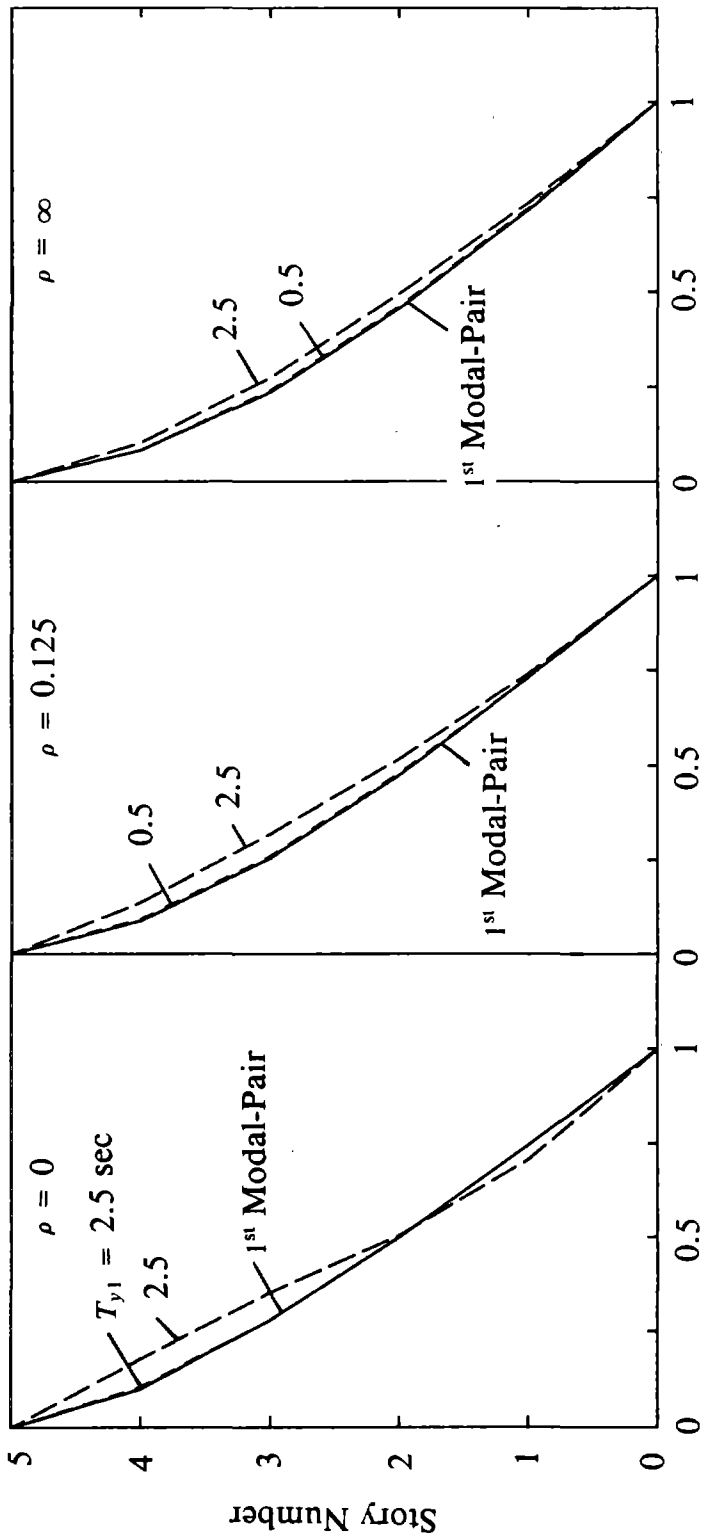

FIGURE 29 Height-wise Variation of Story Overturning Moments Including one or five Modal-pair Contributions for two Values of T_{y1} and Three Values of ρ (e/r = 0.4, Ω = 1 and ξ = 5 %).

responses of the multi-story building associated with the higher vibration modal-pairs, especially the second modal-pair, increase for the base shear, base torque and base overturning moment (Table 12). At the same time the ratios of the modal vibration frequencies with respect to the fundamental uncoupled lateral frequency increase, spreading the frequencies over a wider portion of the spectrum, thus increasing the effects of the spectrum shape, with these increases depending on the location of T_{y1}. For the selected spectrum and within the period range considered, the effects of the spectrum shape are especially significant if T_{y1} is long, with the effects decreasing as T_{y1} decreases within the velocity- and displacement-controlled regions of the spectrum (Figures 20 to 22).

The effect of ρ on the contributions of the higher modal-pairs varies with the response quantity. As suggested by the normalized unit modal-pair responses (Table 12), Figures 20 to 22 demonstrate that ρ affects the higher modal-pair contributions in the base shear and base torque at the center of rigidity more than in the base overturning moment. The top floor displacement (Figure 23) displays trends opposite to base shear, base torque and base overturning moment, in the sense that the higher modal-pair contributions decrease with decreasing ρ, but this reverse trend is supported by the normalized unit modal-pair responses of the building (Table 12). However these contributions are so small that they are of little consequence (Figure 23). The stiffness ratio ρ affects the higher modal-pair contributions in the base-story column moment in the same manner as the base shear but to a lesser degree (Figure 24). The higher modal-pair contributions in the beam moment and column axial force, which are closely related to the base story overturning moment, are smaller and are affected little by ρ (Figures 25 and 26).

Thus, higher modal-pair contributions to the response of the torsionally-coupled, multi-story building generally increase with decreasing ρ and with increasing T_{y1} and also depend on the response quantity considered. These conclusions are similar to those observed for the higher mode contributions in lateral response of torsionally-uncoupled systems [12].

Finally, the dependence of higher modal-pair response contributions on e/r and Ω is investigated. The base shear, base torque at the center of rigidity and base overturning moment are plotted against T_{y1} in the form of response spectra for systems with $\rho = 0$, considering various numbers

of vibration modal-pairs. Such plots are presented in Figures 30 to 32 for systems with e/r = 0.4 and for three values of Ω = 0.5, 1 and 1.5; and in Figures 33 to 35 for systems with Ω = 1 and for three values of e/r = 0.05, 0.4 and 1. Figures 30 to 35 indicate that, although the variations of the system response with T_{y1} depend on e/r and Ω, the higher modal-pair contributions relative to the contribution of the fundamental modal-pair are relatively insensitive to e/r or Ω. This is partly due to the fact that the normalized unit modal-pair responses are independent of e/r and Ω (Table 12); and for fixed values of ρ and T_{y1}, the uncoupled vibration periods of the building are fixed and the vibration periods of a modal-pair of the torsionally-coupled building vary with e/r and Ω (Figure 9) in such a way that the resulting variation in the spectral ordinates corresponding to these periods combine in a way that the higher modal-pair responses are relatively insensitive to e/r or Ω.

The height-wise variations of story shears and torques, expressed as a ratio of the respective values at the base, are presented in Figures 36 and 37 for systems with ρ = 0, e/r = 0.4, two values of T_{y1} = 0.5 and 2.5 sec, and three values of Ω = 0.5, 1 and 1.5; and in Figures 38 and 39 for systems with ρ = 0, Ω = 1, two values of T_{y1} = 0.5 and 2.5 sec, and three values of e/r = 0.05, 0.4 and 1. The variation of only the fundamental modal-pair response, which is the same regardless of T_{y1}, is also included in these figures. As concluded earlier, Figures 36 and 37 also indicate that for fixed e/r and ρ the height-wise variations of story shears and torques are similar, with differences more pronounced for torsionally-flexible systems (Ω<1), especially for values of T_{y1} in the velocity- or displacement-controlled regions of the spectrum. Similarly, Figures 38 and 39 indicate that for fixed Ω and ρ the differences between the height-wise variations of story shears and torques slightly increase with increase in e/r. These effects are attributed to the increase in the cross-correlation terms given by the third summation of equation (4.70), as explained earlier in this section.

Taking advantage of the fact that the earthquake response of the torsionally-coupled, multi-story buildings considered in this investigation can be estimated by considering only the first two vibration modal-pairs, and in some cases only the fundamental vibration modal-pair, it is possible to develop simplified procedures for the analysis of torsionally-coupled buildings. The natural frequency and mode shape in the nj^{th} mode of vibration of the torsionally-coupled, multi-story building

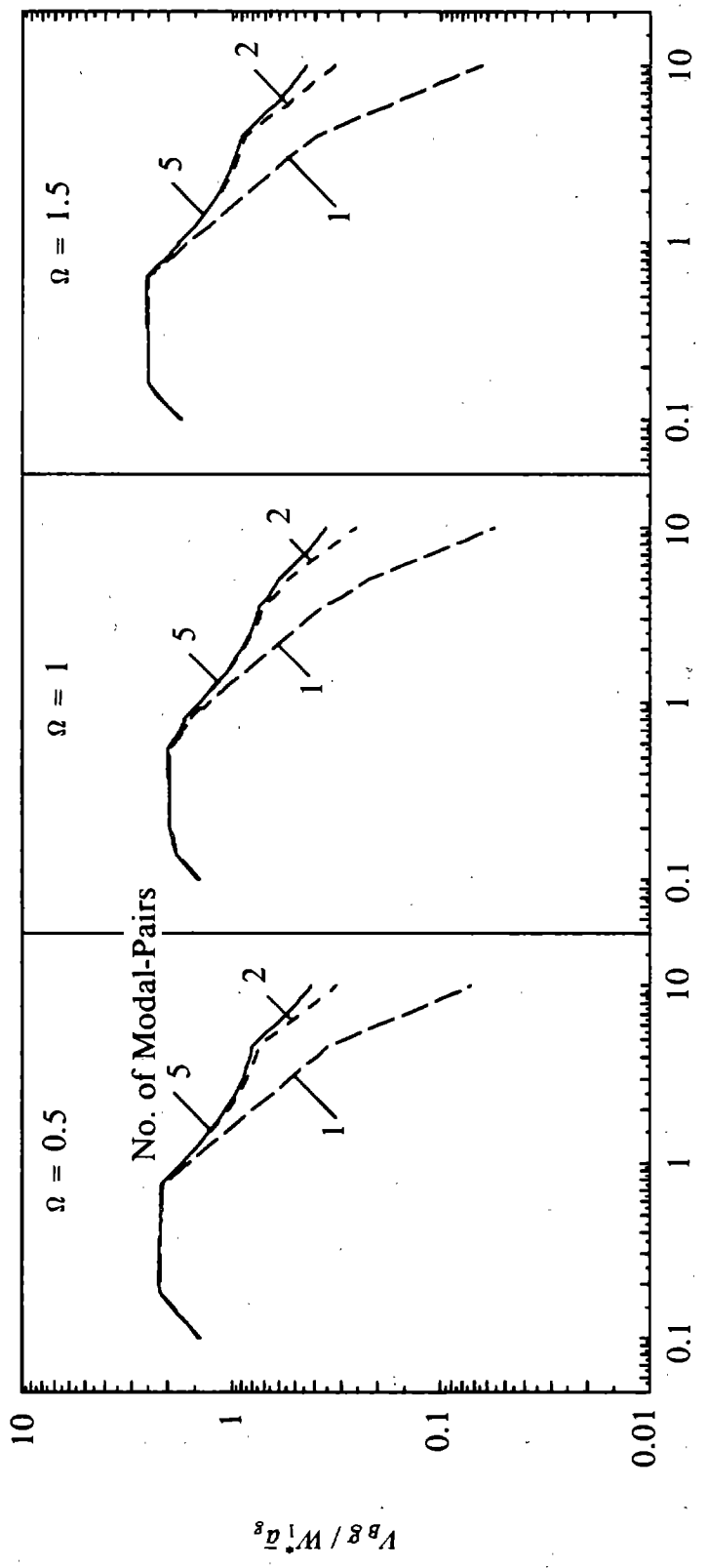

FIGURE 30 Maximum Base Shear Considering one, two and five Pairs of Vibration Modes for Three Values of Ω (e/r = 0.4, ρ = 0 and ξ = 5 %)

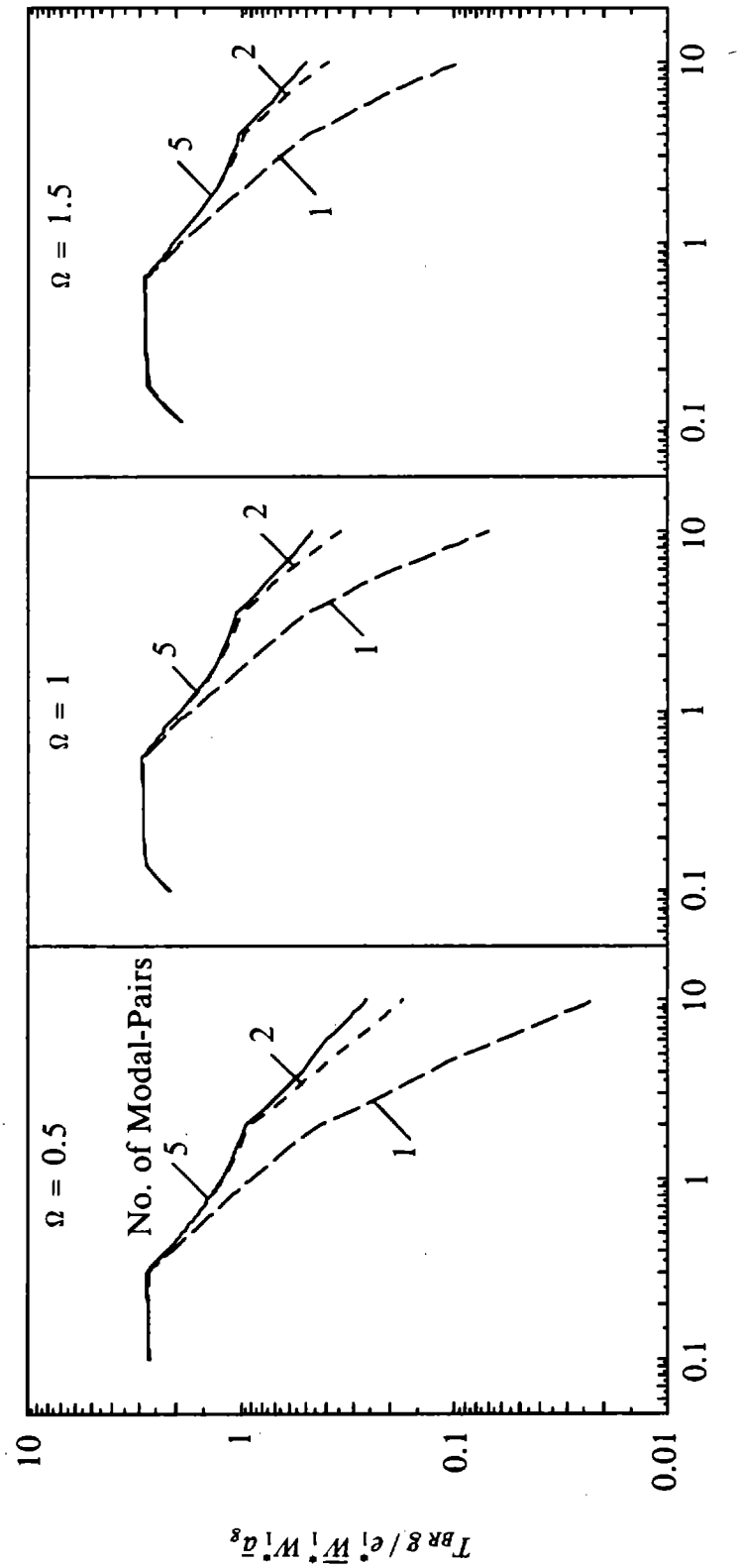

FIGURE 31 Maximum Base Torque at Center of Rigidity Considering one, two and five Pairs of Vibration Modes for Three Values of Ω (e/r = 0.4, ρ = 0 and ξ = 5 %)

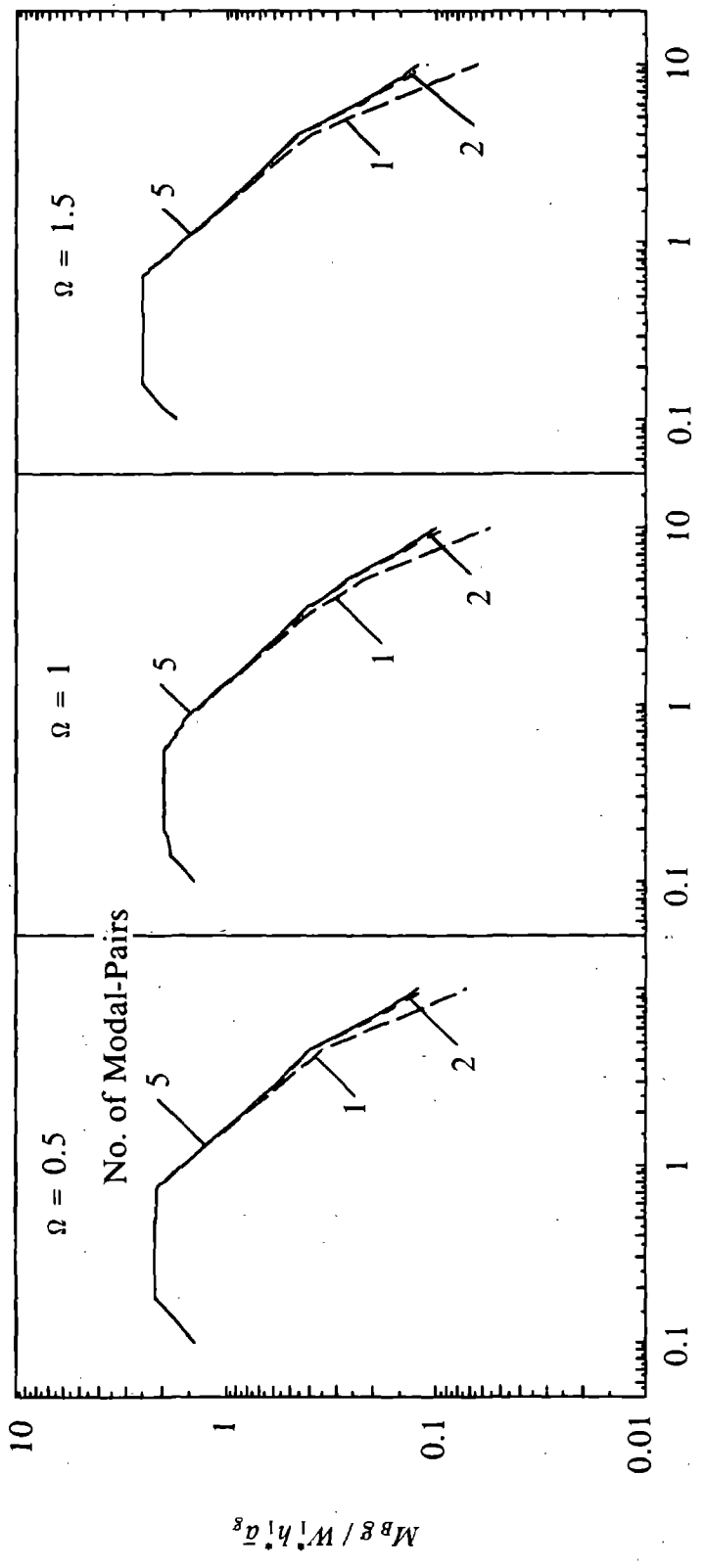

FIGURE 32 Maximum Base Overturning Moment Considering one, two and five Pairs of Vibration Modes for Three Values of Ω (e/r = 0.4, ρ = 0 and ξ = 5 %)

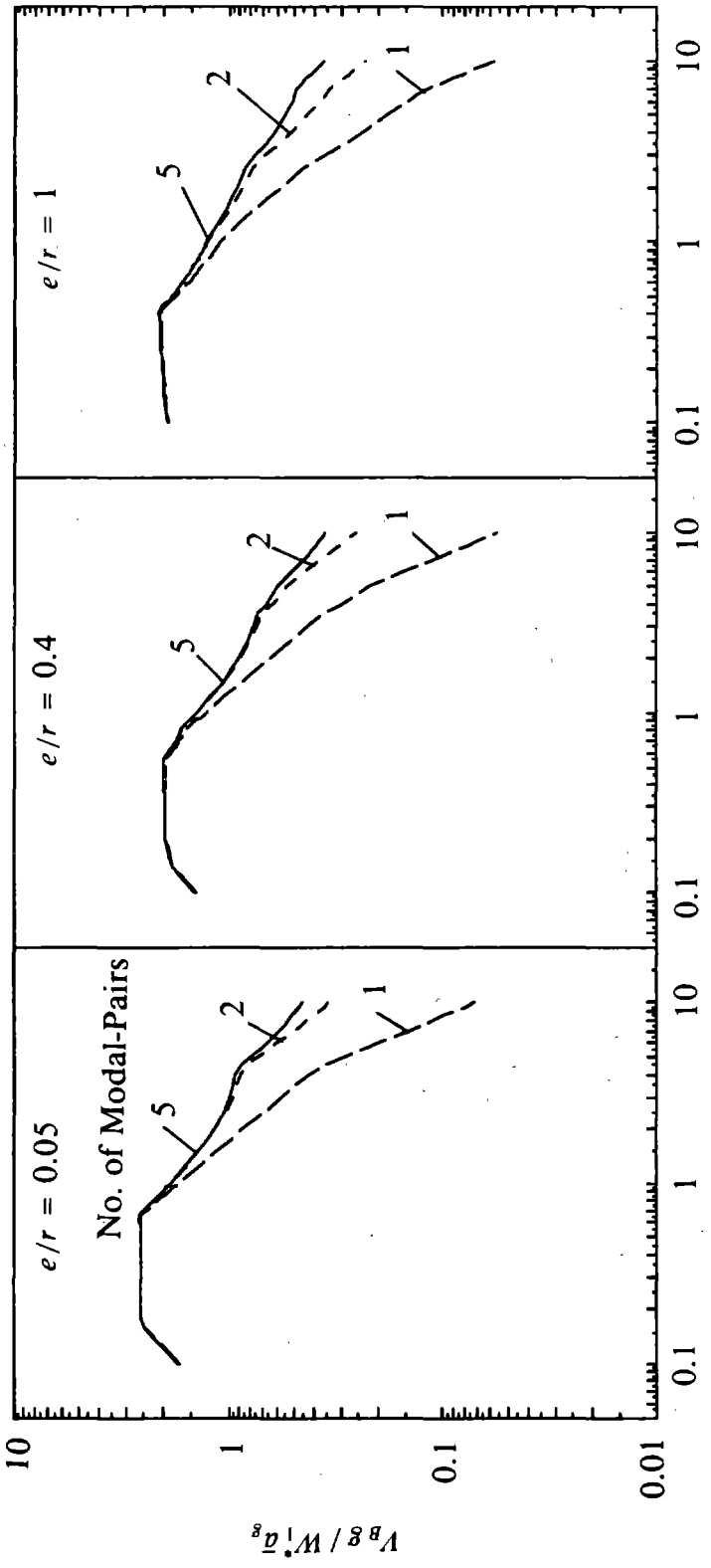

FIGURE 33 Maximum Base Shear Considering one, two and five Pairs of Vibration Modes for Three Values of e/r ($\Omega = 1$, $\rho = 0$ and $\xi = 5$ %)

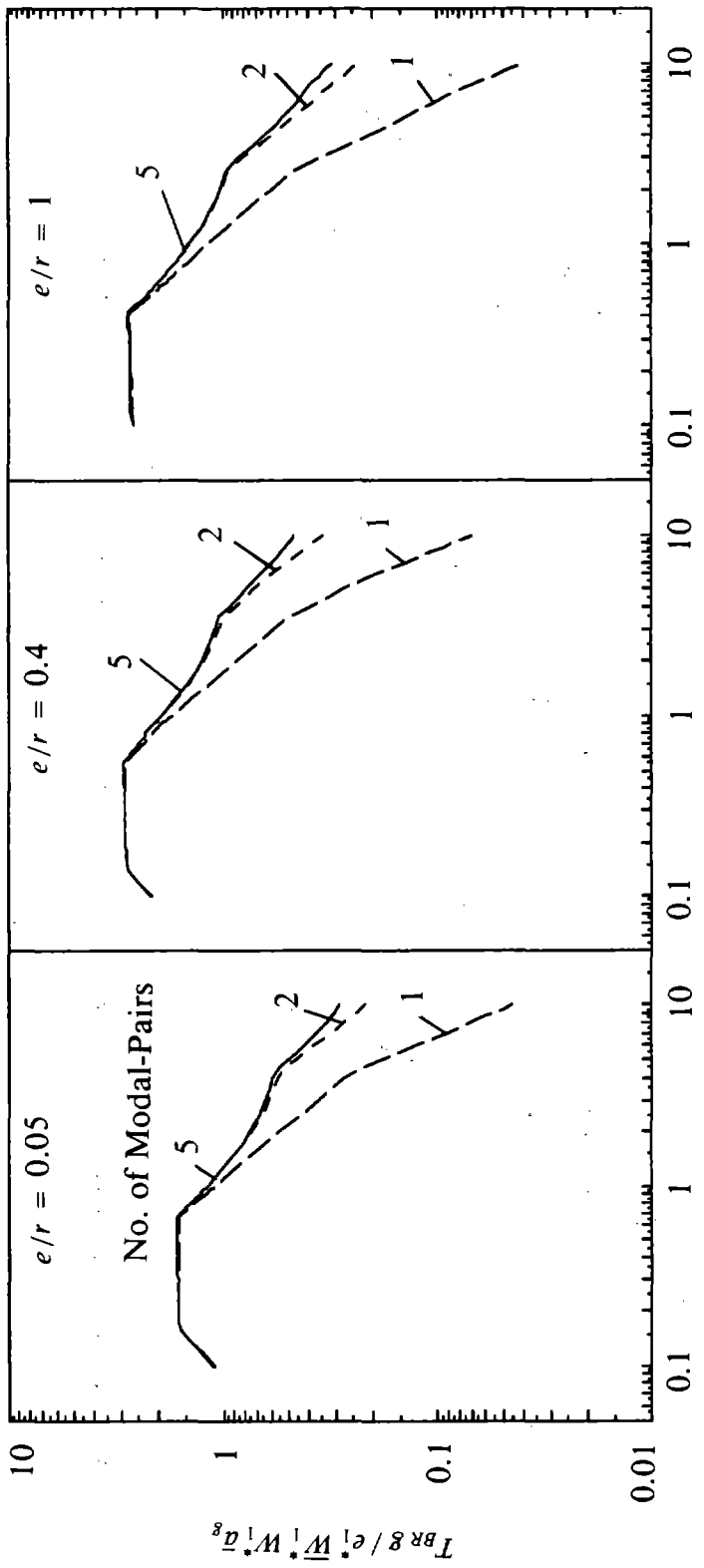

FIGURE 34 Maximum Base Torque at Center of Rigidity Considering one, two and five Pairs of Vibration Modes for Three Values of e/r ($\Omega = 1$, $\rho = 0$ and $\xi = 5$ %)

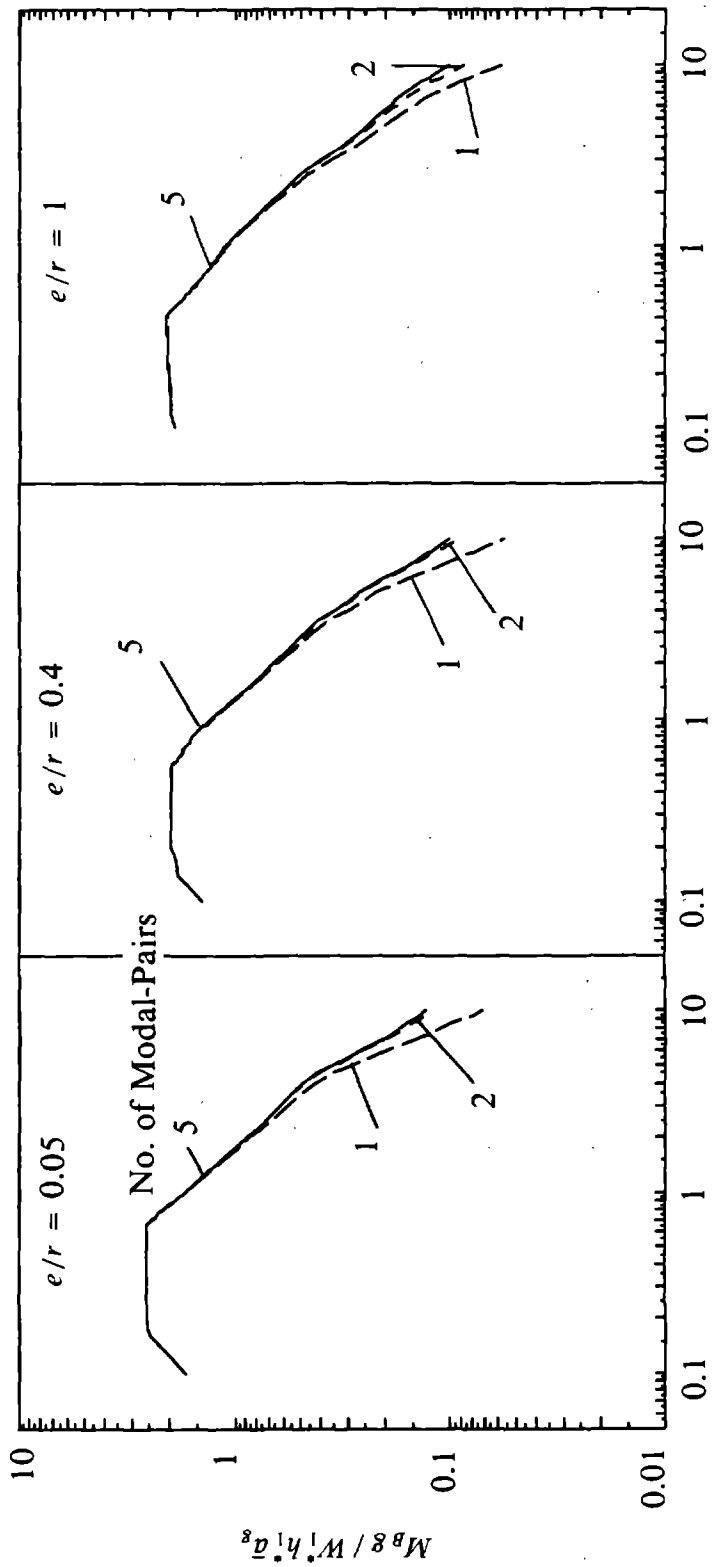

FIGURE 35 Maximum Base Overturning Moment Considering one, two and five Pairs of Vibration Modes for Three Values of e/r ($\Omega = 1$, $\rho = 0$ and $\xi = 5$ %)

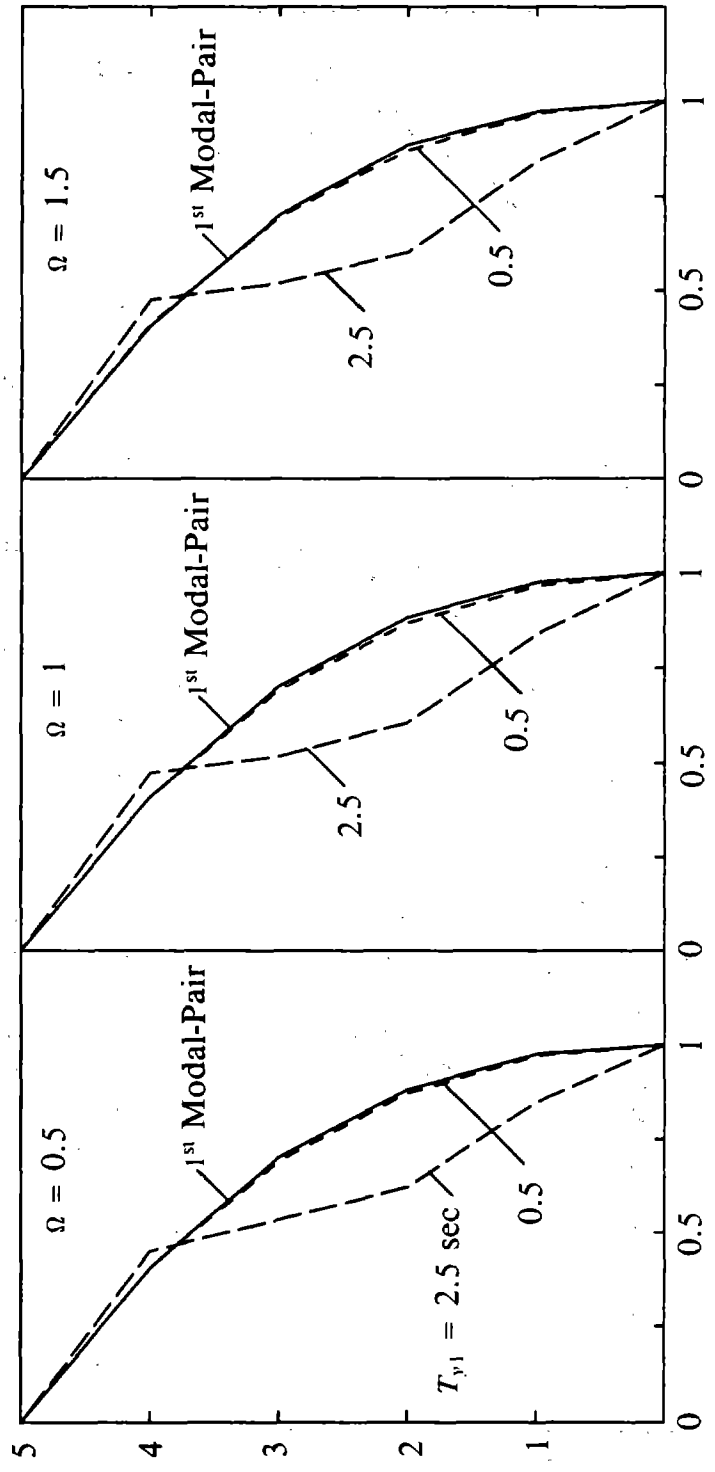

FIGURE 36 Height-wise Variation of Story Shears Including one or five Modal-pair Contributions for two Values of T_{y1} and Three Values of Ω (e/r = 0.4, ρ = 0 and ξ = 5 %).

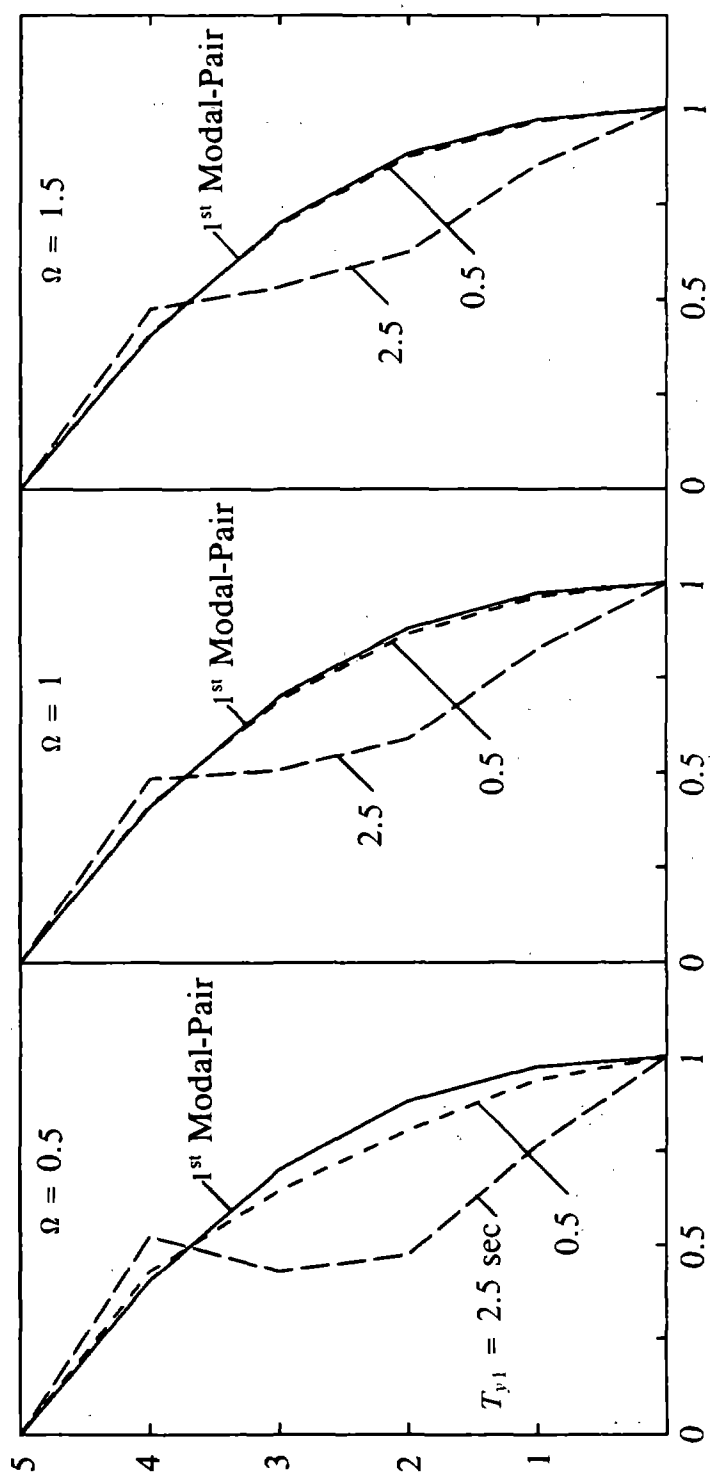

FIGURE 37 Height-wise Variation of Story Torques at Centers of Rigidity Including one or five Modal-pair Contributions for two Values of T_{y1} and Three Values of Ω (e/r = 0.4, ρ = 0 and ξ = 5 %).

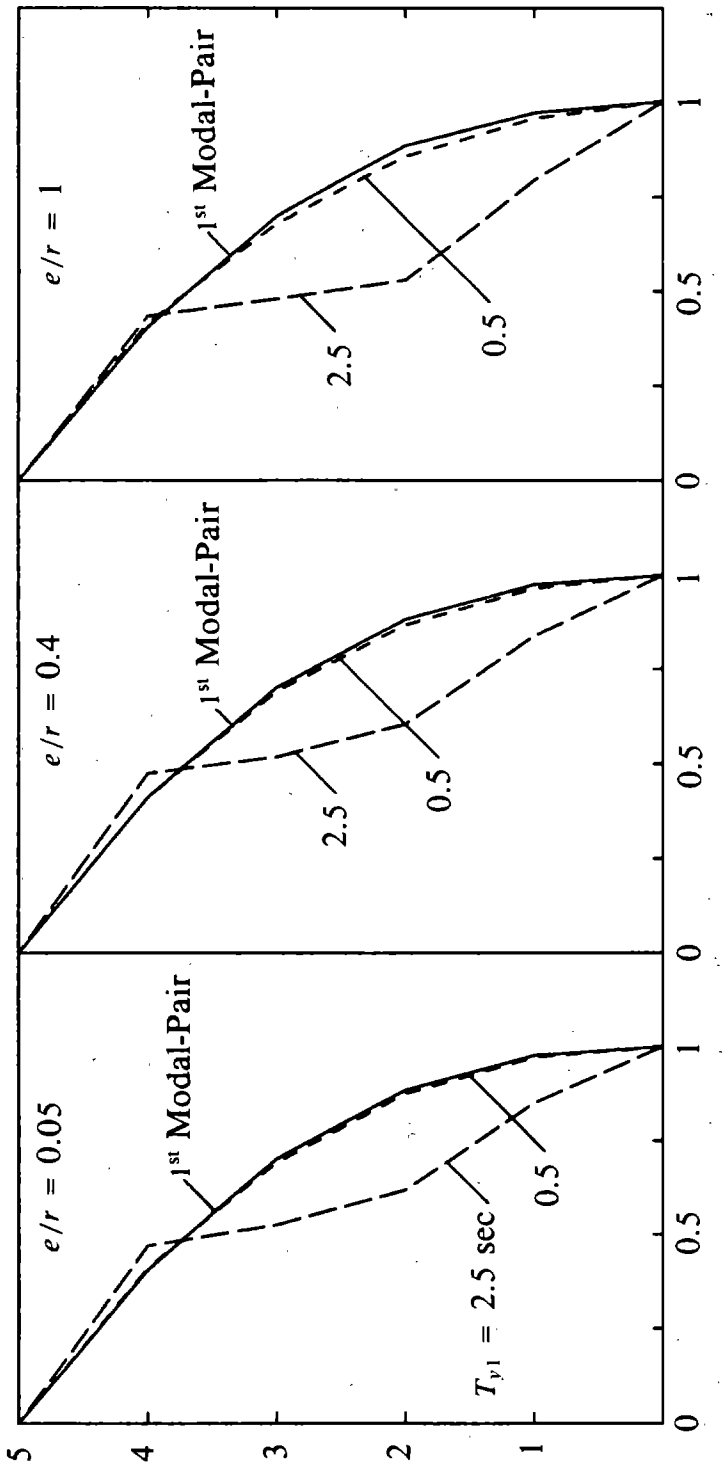

FIGURE 38 Height-wise Variation of Story Shears Including one or five Modal-pair Contributions for two Values of T_{y1} and Three Values of e/r (Ω = 1, ρ = 0 and ξ = 5 %).

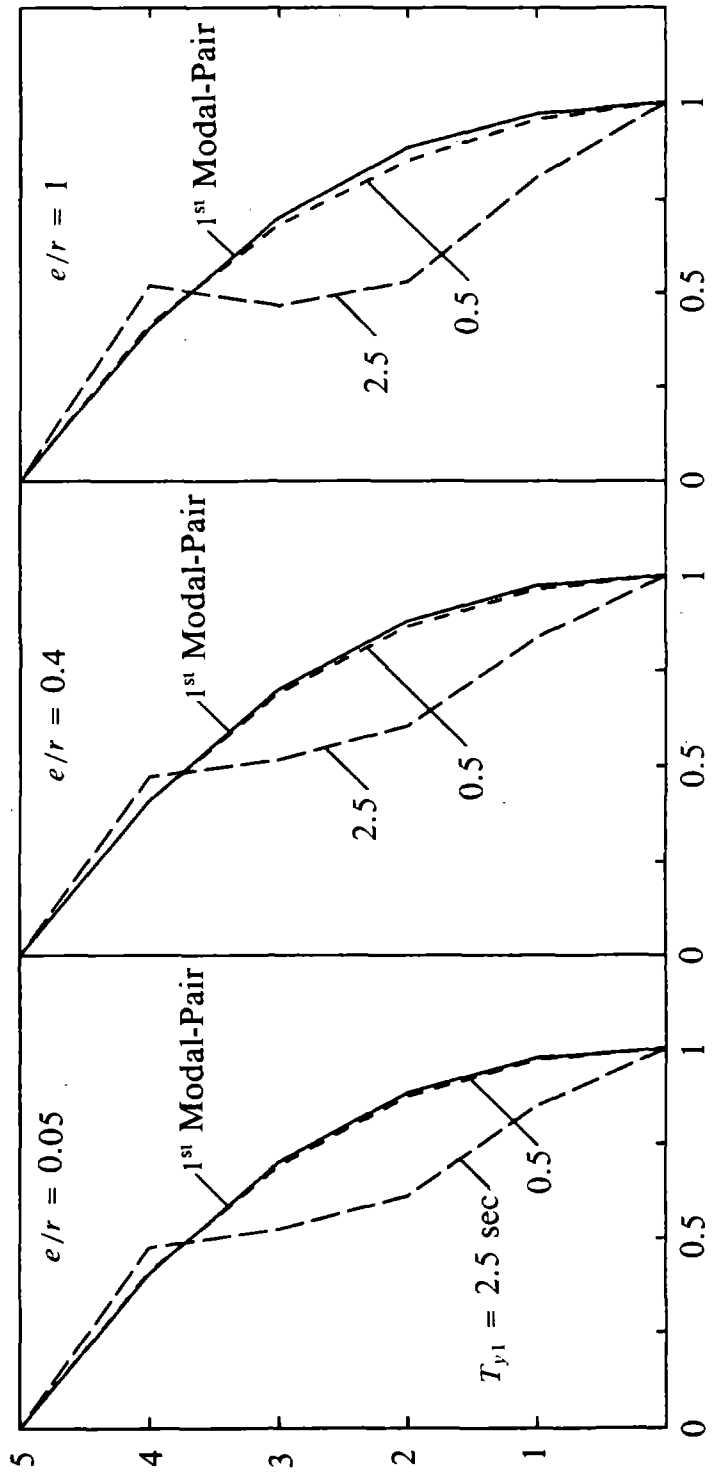

FIGURE 39 Height-wise Variation of Story Torques at Centers of Rigidity Including one or five Modal-pair Contributions for two Values of T_{y1} and Three Values of e/r (Ω = 1, ρ = 0 and ξ = 5 %).

can be computed from equations (4.10) and (4.11) knowing the j^{th} vibration frequency and mode shape of the corresponding torsionally-uncoupled, multi-story system and the n^{th} normalized frequency and mode shape of the associated torsionally-coupled, one-story system. Thus, estimates of the vibration frequencies in the first two modal-pairs of the torsionally-coupled building can be determined using estimates of the first two vibration frequencies of the corresponding torsionally-uncoupled, multi-story system determined by following the simplified procedure developed in [12]. The maximum response in the nj^{th} vibration mode of the torsionally-coupled building was also found in Section 4 to be related to the maximum response in the j^{th} vibration mode of the corresponding torsionally-uncoupled, multi-story system and the normalized maximum response in the n^{th} mode of vibration of the associated torsionally-coupled, one-story system with uncoupled lateral vibration frequency equal to ω_{yj}, the j^{th} uncoupled lateral vibration frequency. Utilizing the estimated vibration frequencies in the first two vibration modal-pairs of the torsionally-coupled, multi-story building, and the modal response maxima of the corresponding torsionally-uncoupled, multi-story system estimated by the simplified procedure developed in [12], the maximum response of the torsionally-coupled building is estimated by following the analysis procedure described in Section 4 considering only the first two vibration modal-pairs of the building. It is believed that such simplified response analyses can be applicable to more general buildings than those considered in this study.

The results obtained in this study may also be utilized in developing code-type analysis procedures by recognizing the similarity in the height-wise variations of story shears and story torques and utilizing the aforementioned fact that the response can well be approximated by the first two vibration modal-pairs.

8. EFFECTS OF LATERAL-TORSIONAL COUPLING

The lateral and torsional motions of the buildings considered were shown in Section 3 to be coupled. The effects of lateral-torsional coupling on building response are investigated by comparing the response of a torsionally-coupled, multi-story building with that of the corresponding torsionally-uncoupled, multi-story system. This comparison is presented for flat and hyperbolic pseudo-acceleration spectra, as well as the design spectrum of Figure 5. The response quantities selected to study the overall behavior of the building are: the base shear V_B, the base torque T_{BR} at the center of rigidity, the base overturning moment M_B, and the top floor lateral displacement v_5 at the center of rigidity. These quantities computed by the procedures of Section 4.4 are normalized, respectively, by V_{Bo}, $e\,V_{Bo}$, M_{Bo} and v_{5o}, where V_{Bo} and M_{Bo} are the base shear and base overturning moment of the corresponding torsionally-uncoupled system. The normalized torque $T_{BR}/e\,V_{Bo}$ can be interpreted as the ratio of the dynamic eccentricity of the system to its static eccentricity: e_d/e, where the dynamic eccentricity $e_d = T_{BR}/V_{Bo}$ is the distance from the center of rigidity at which static application of V_{Bo} results in the dynamic base torque T_{BR} at the center of rigidity. The response quantities selected as indicative of the local behavior of the building are: column moment M_{cB}, beam moment M_{bB}, and column axial force P_{cB} in the first story of frame (1). These quantities are normalized, respectively, by the responses M_{cBo}, M_{bBo}, and P_{cBo} of the corresponding torsionally-uncoupled, multi-story system.

These normalized response quantities are presented for flat and hyperbolic spectra in Figures 40 to 46, wherein they are plotted against Ω for systems with ρ = 0, 0.125 and ∞, and values of e/r = 0.05, 0.4 and 1. Also shown in these figures are the normalized responses $\bar{V}$, $\bar{M}$, or $\bar{v}$, and $\bar{T}_R$, of the associated torsionally-coupled, one-story system, defined by equations (4.39) and (4.40), which are independent of ρ. It is apparent from Figures 40 to 46 that the effects of lateral-torsional coupling on structural responses are similar for the multi-story and the associated one-story systems. For this reason, the general trends of $\bar{V}$ ($\bar{M}$, or $\bar{v}$) and $\bar{T}_R$ for the one-story system, which are independent of ρ, are described first, and then the differences that occur for the multi-story

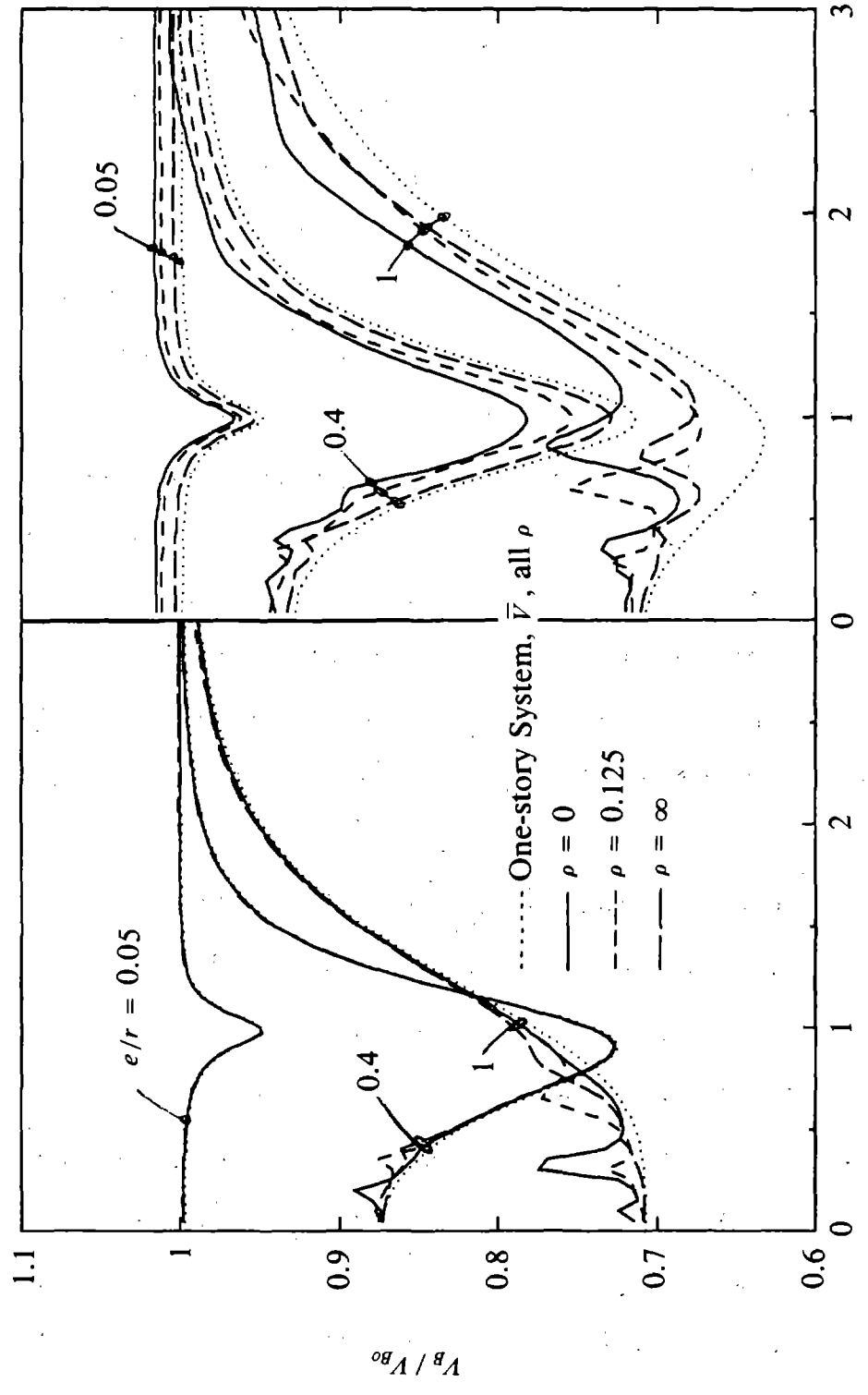

FIGURE 40 Normalized Base Shear in Multi-story Building and Associated One-story System for Flat and Hyperbolic Pseudo-acceleration Spectra (ξ = 5 %)

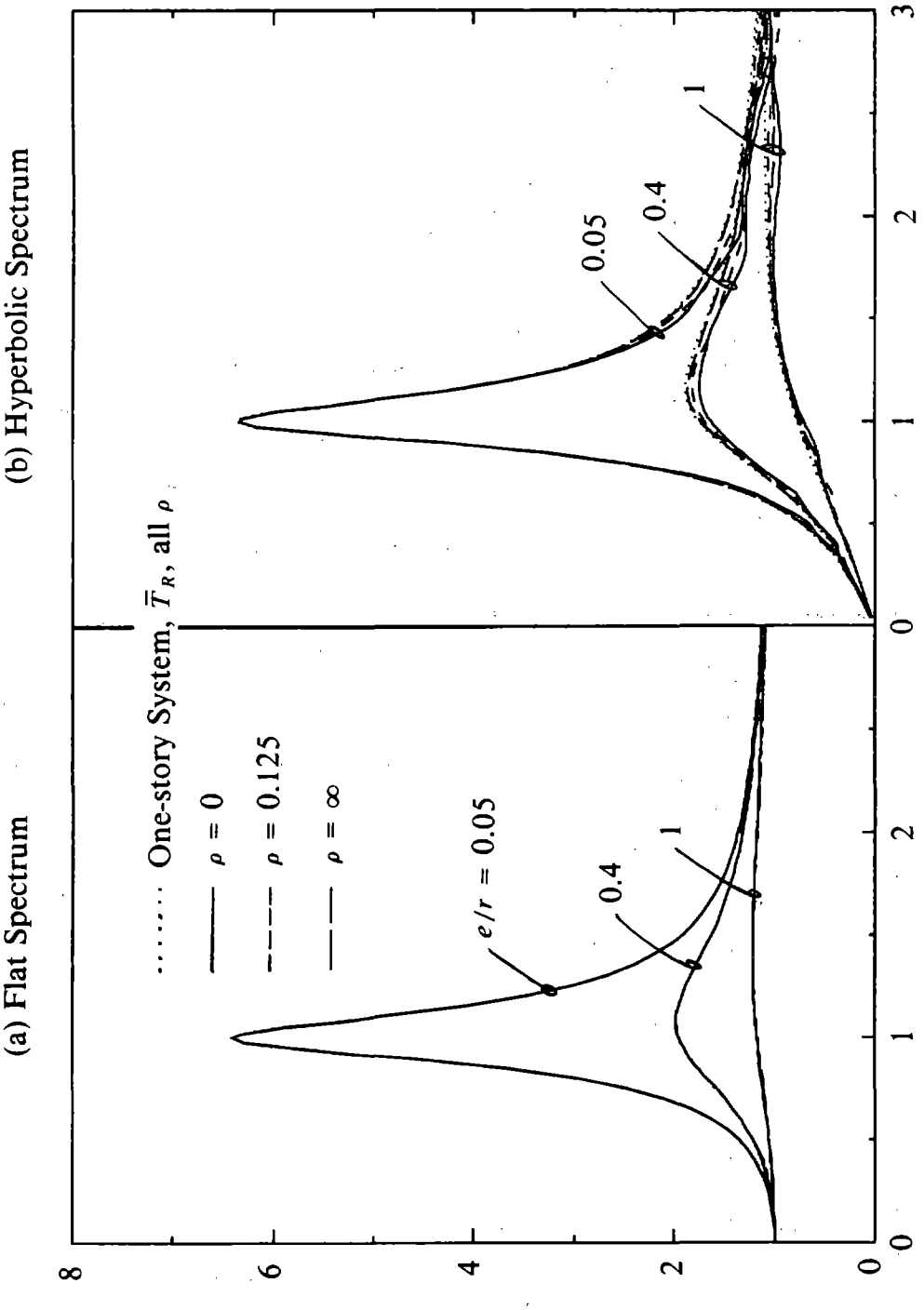

FIGURE 41 Normalized Base Torque at Center of Rigidity in Multi-story Building and Associated One-story System for Flat and Hyperbolic Pseudo-acceleration Spectra (ξ = 5 %)

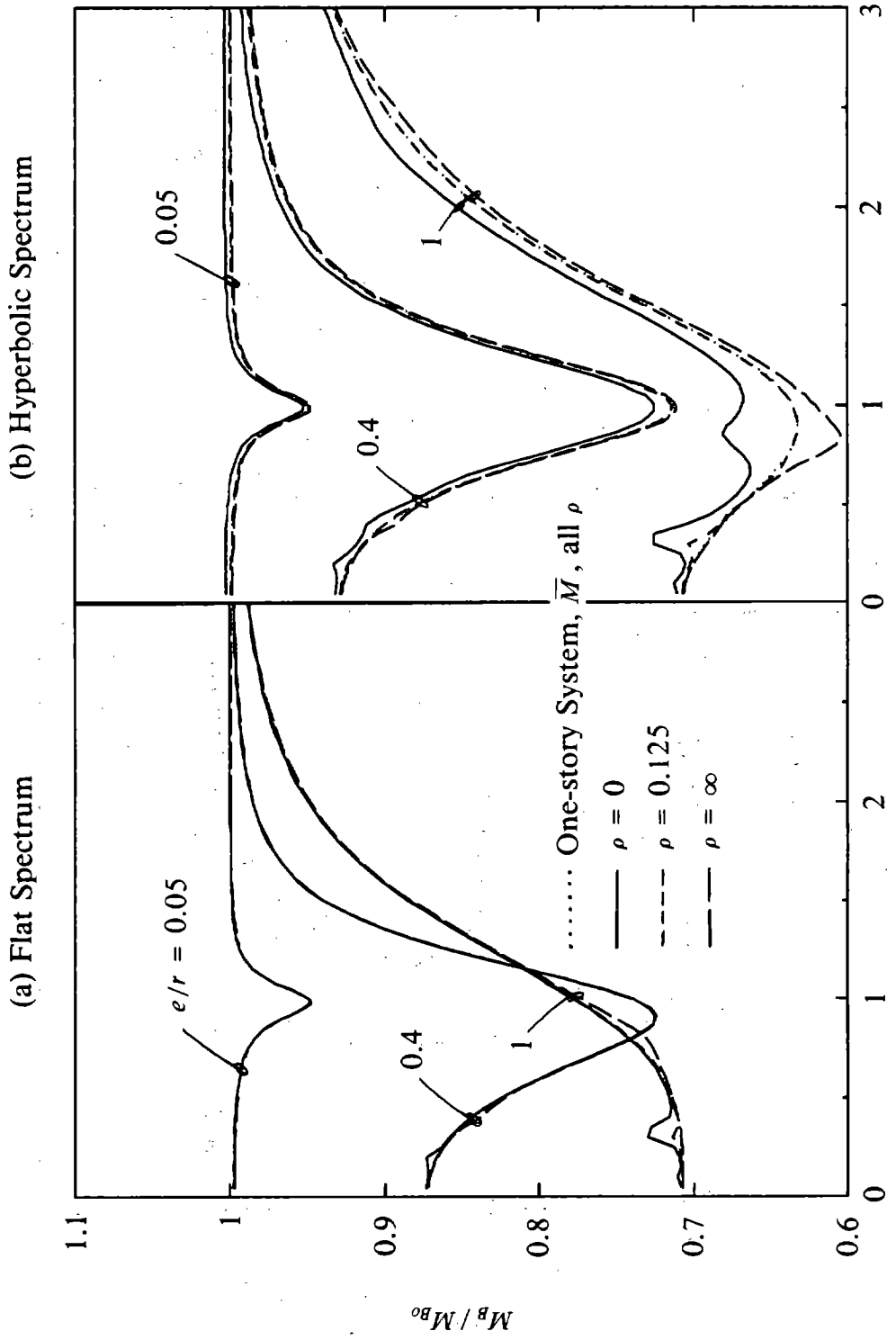

FIGURE 42 Normalized Base Overturning Moment in Multi-story Building and Associated One-story System for Flat and Hyperbolic Pseudo-acceleration Spectra (ξ = 5 %)

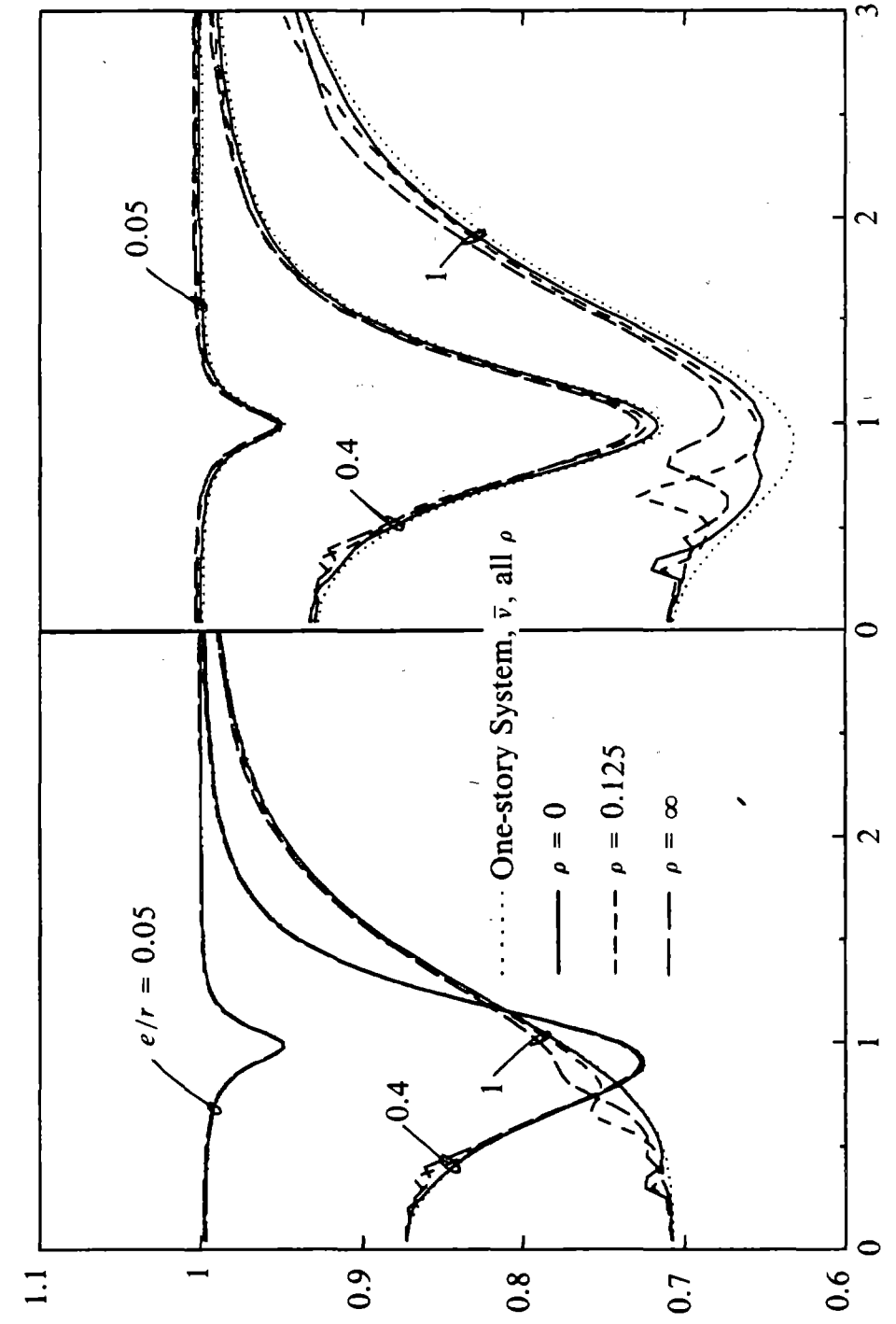

FIGURE 43 Normalized Top Floor Lateral Displacement at Center of Rigidity in Multi-story Building and Associated One-story System for Flat and Hyperbolic Pseudo-acceleration Spectra (ξ = 5 %)

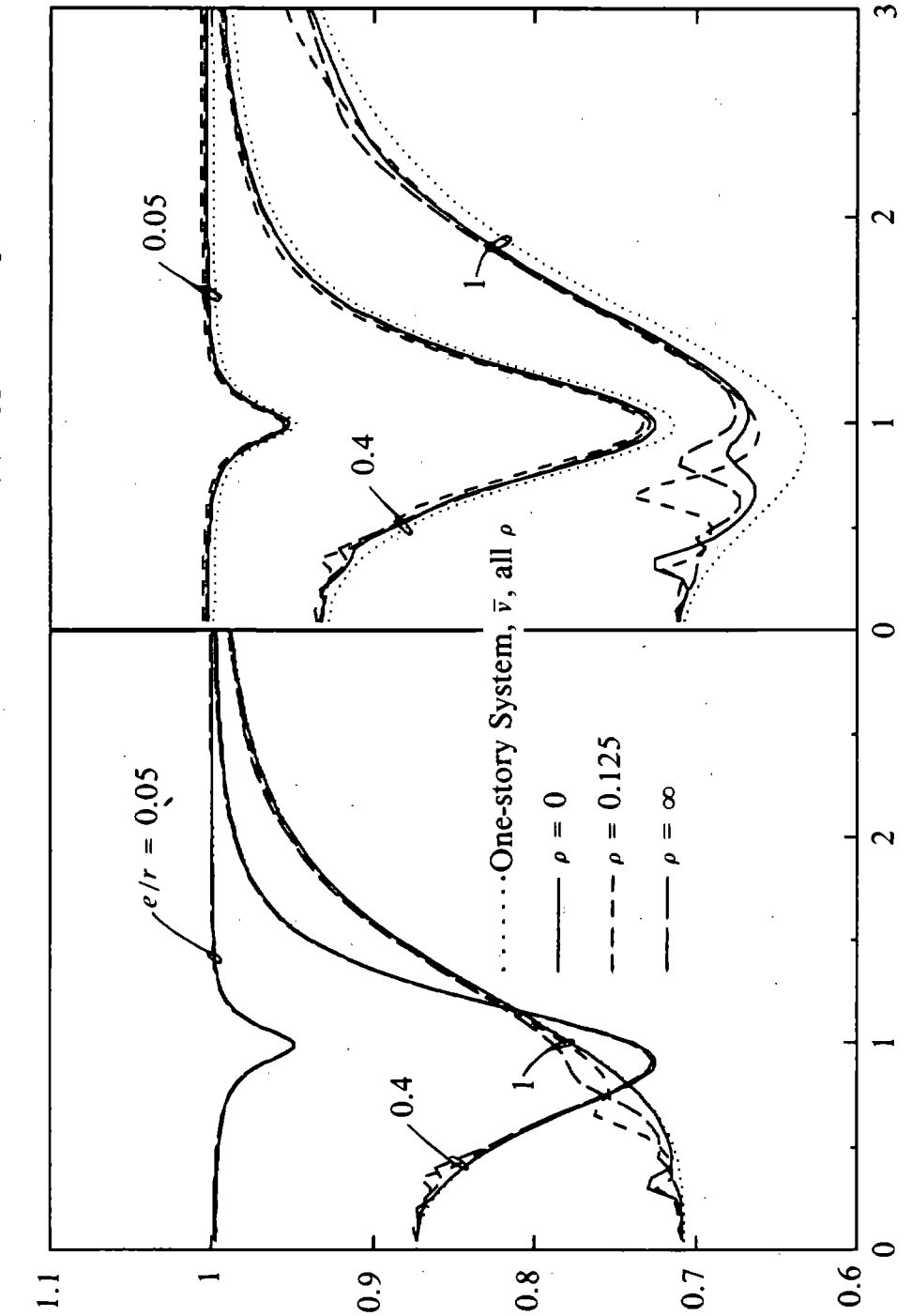

FIGURE 44 Normalized Column Moment in Base-story of Frame (1) in Multi-story Building for Flat and Hyperbolic Pseudo-acceleration Spectra (ξ = 5 %)

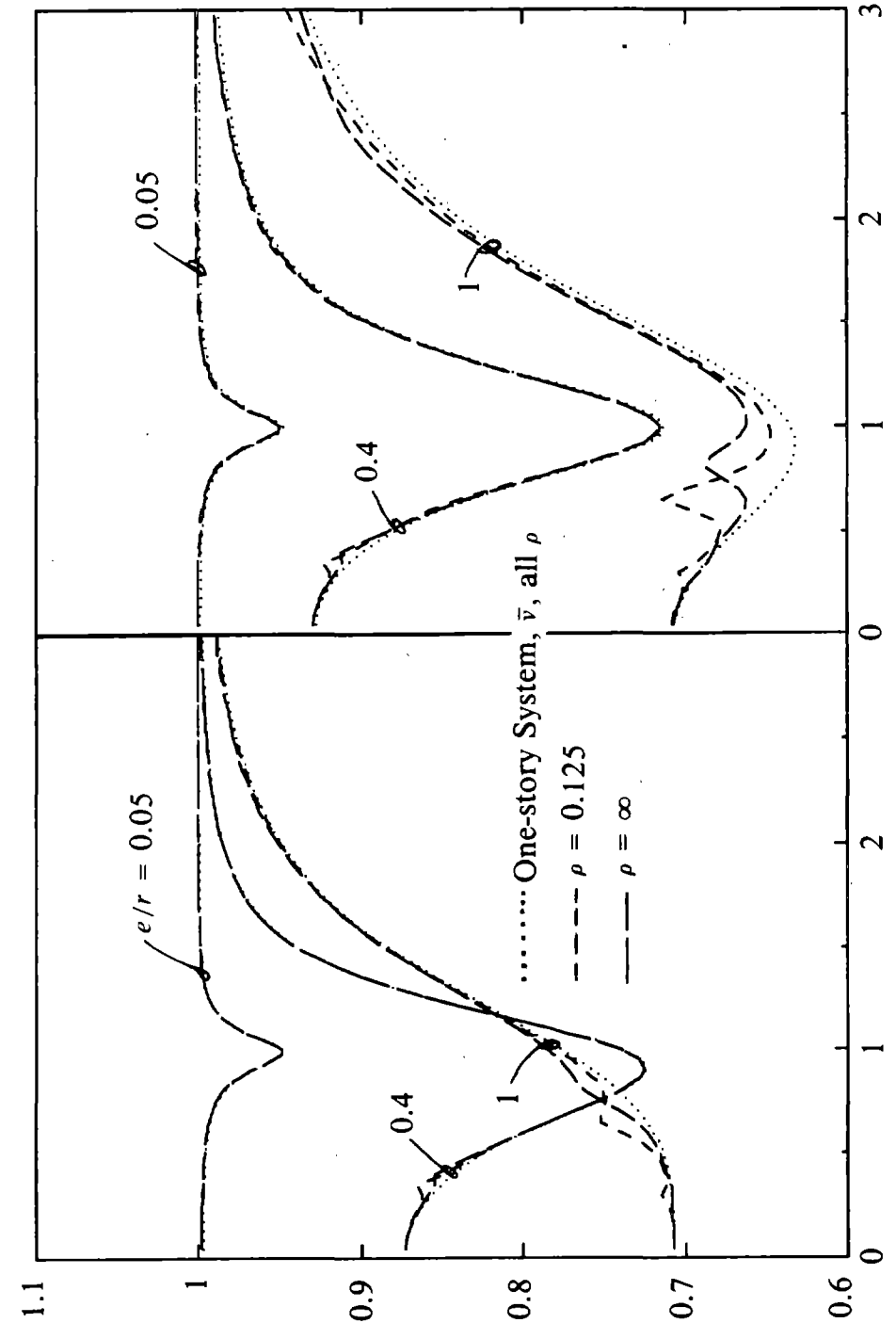

FIGURE 45 Normalized Beam Moment in Base-story of Frame (1) in Multi-story Building for Flat and Hyperbolic Pseudo-acceleration Spectra (ξ = 5 %)

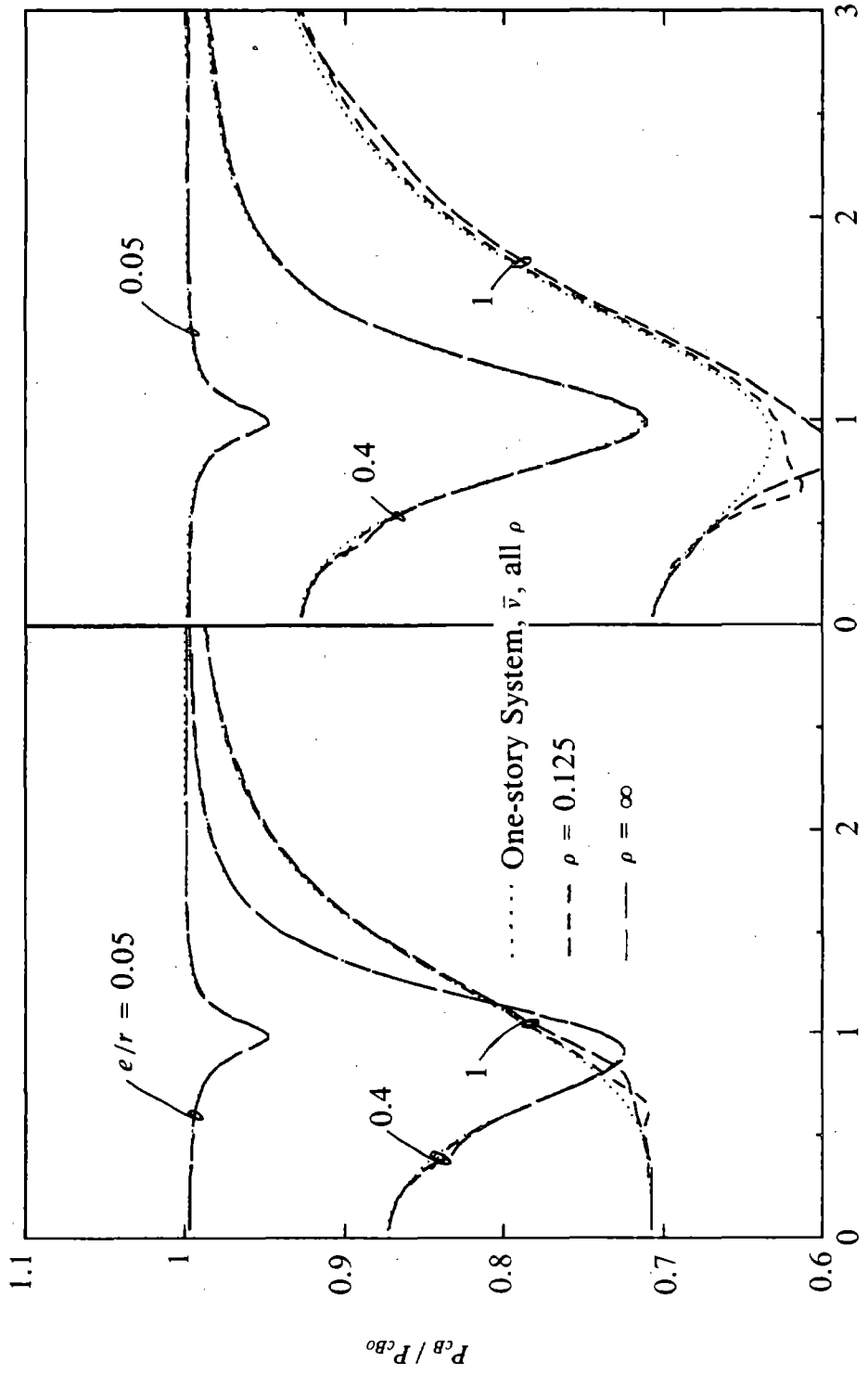

FIGURE 46 Normalized Column Axial Force in Base-story of Frame (1) in Multi-story Building for Flat and Hyperbolic Pseudo-acceleration Spectra (ξ = 5 %)

building, in which case ρ influences the response are described next. Lateral-torsional coupling has the effect of reducing $\bar{V}$ and increasing e_d/e. These effects increase as the eccentricity ratio e/r increases, and are dependent on the uncoupled torsional to lateral frequency ratio $\Omega = \omega_{\theta j}/\omega_{yj}$. For systems with smaller e/r values the effect is most pronounced, i.e. $\bar{V}$ reaches its minimum value and e_d/e its maximum value, for values of Ω around unity, i.e. when the uncoupled lateral and torsional frequencies are close to each other. As e/r increases, $\bar{V}$ reaches its minimum values at values of Ω below unity, while e_d/e reaches its maxima for values of Ω above unity. For torsionally-stiff systems (Ω>1), $\bar{V}$ approaches unity as Ω becomes large, indicating that there is essentially no reduction in the base shear, while e_d/e approaches one, implying no dynamic amplification of eccentricity. For torsionally-flexible systems (Ω<1) with smaller e/r, there is essentially no reduction in base shear. The dynamic eccentricity ratio, e_d/e, for torsionally-flexible systems approaches zero as Ω tends to zero in the case of hyperbolic spectrum, implying no torque, but approaches one in the case of flat spectrum, indicating no dynamic amplification.

These observations on how torsional coupling affects the normalized base shear and torque for the associated torsionally-coupled, one-story system generally carry over to a multi-story building. However, unlike the one-story system, the normalized quantities of the multi-story building depend on ρ. The differences between the normalized responses of the two torsionally-coupled systems--multi-story and its associated one-story-- are due to the contributions of the terms arising from cross-correlation between coupled vibration modes '2j' and '1k' (j=1 to 4; k=j+1 to 5) of the multi-story building, given by the third summation of equation (4.70) and developed further in Appendix D. These cross-correlation terms contain r_{nj}, which is defined by equation (4.66), and, for a particular response quantity, depend on e/r, Ω, ρ, and the shape of the response spectrum. The magnitude of the cross-correlation terms also depends on the higher modal-pair contributions, discussed in Section 7, to a particular response quantity. Thus, the deviations of the normalized responses of the multi-story building from those of the associated one-story system depend on e/r, Ω, ρ, the response quantity, the significance of higher modal-pair contributions, and the response

spectrum considered. Since the cross-correlation terms may assume positive or negative values (Section 4), the normalized responses of the multi-story building may be larger or smaller than the corresponding normalized responses of the associated one-story system (Figures 40 to 46). The deviations between the normalized responses of the two systems are more pronounced in the ranges of Ω where cross-correlation factors $\gamma_{21,12}$ and $\gamma_{21,13}$, shown in Figure 14, are maximum. These deviations are more significant for V_B, T_{BR} and M_{cB} than for M_B, v_5, M_{bB} or P_{cB} as demonstrated by Figures 40 to 46, since higher modal-pair contributions were observed in Section 7 to be more significant for the former response quantities compared to the latter. Also, the deviations increase with decrease in ρ in the case of V_B and T_{BR}, and to a lesser degree for M_B and M_{cB}, trends which also are related to the importance of the higher modal-pair contributions, discussed in Section 7 (see also Table 12). The deviations increase with increase in e/r and are more significant for the hyperbolic spectrum than the flat spectrum; these trends are related to magnitudes of the cross-correlation terms (Appendix D).

For a general pseudo-acceleration spectrum, the response of the torsionally-coupled multi-story building, normalized by the response of the corresponding torsionally-uncoupled, system, depends on T_{y1} in addition to the parameters: e/r, Ω, and ρ, affecting the normalized response in case of flat or hyperbolic spectra. In order to understand the role that T_{y1} plays in the effect of lateral-torsional coupling, the building response was computed for ground motions characterized by the design spectrum of Figure 5. The seven normalized quantities, V_B/V_{Bo}, $T_{BR}/r\,V_{Bo}$, M_B/M_{Bo}, v_5/v_{5o}, M_{cB}/M_{cBo}, M_{bB}/M_{bBo} and P_{cB}/P_{cBo}, are plotted in Figures 47 to 53, respectively, against Ω, for different values of e/r and ρ and two values of T_{y1} equal 0.5 and 2.5 sec. Also included in these figures are the same responses computed for the flat and hyperbolic spectra, which are independent of T_{y1} and were shown earlier in Figures 40 to 46, to provide a basis for examining the role of T_{y1}. The T_{y1} values chosen, 0.5 and 2.5 sec, are in the flat and hyperbolic branches, respectively, of the design spectrum.

The following observations are based on Figures 47 to 53. The normalized responses of systems with small e/r are relatively insensitive to the shape of the spectrum or to T_{y1}. As e/r

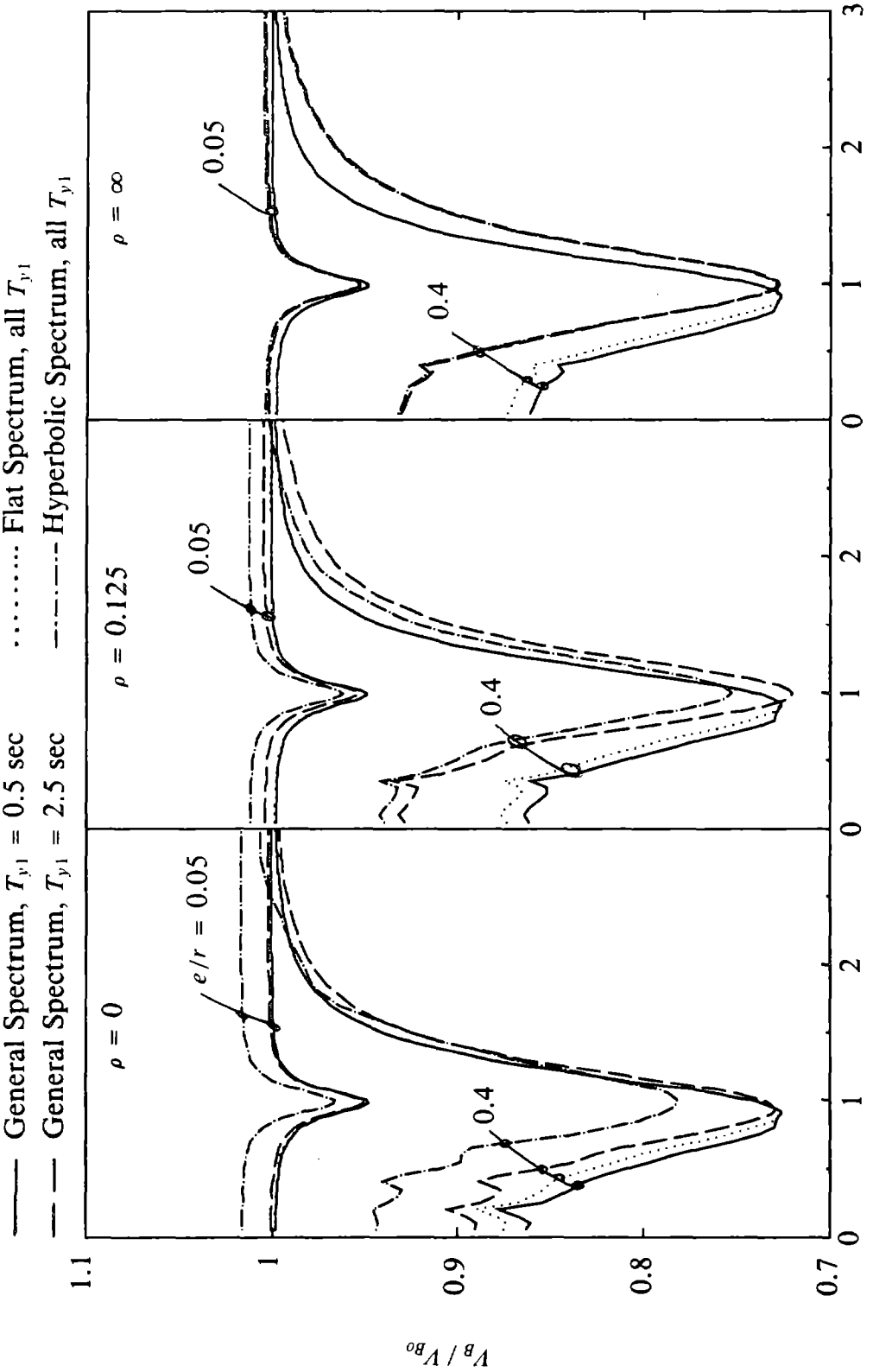

FIGURE 47 Normalized Base Shear in Systems with T_{y1} = 0.5 and 2.5 sec, and e/r = 0.05 and 0.4 for Three Response Spectra (ξ = 5 %)

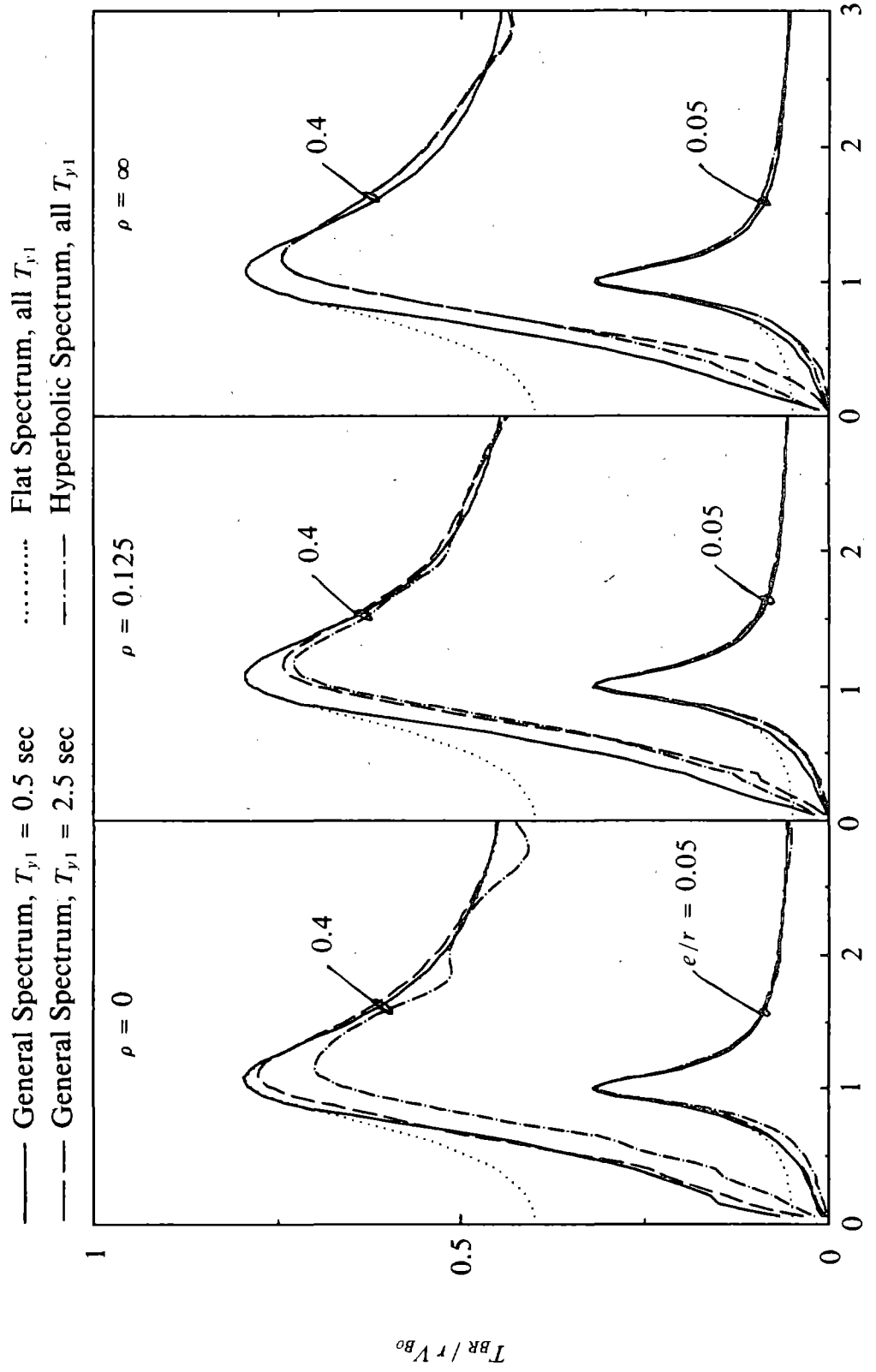

FIGURE 48 Normalized Base Torque at Center of Rigidity in Systems with T_{y1} = 0.5 and 2.5 sec, and e/r = 0.05 and 0.4 for Three Response Spectra (ξ = 5 %)

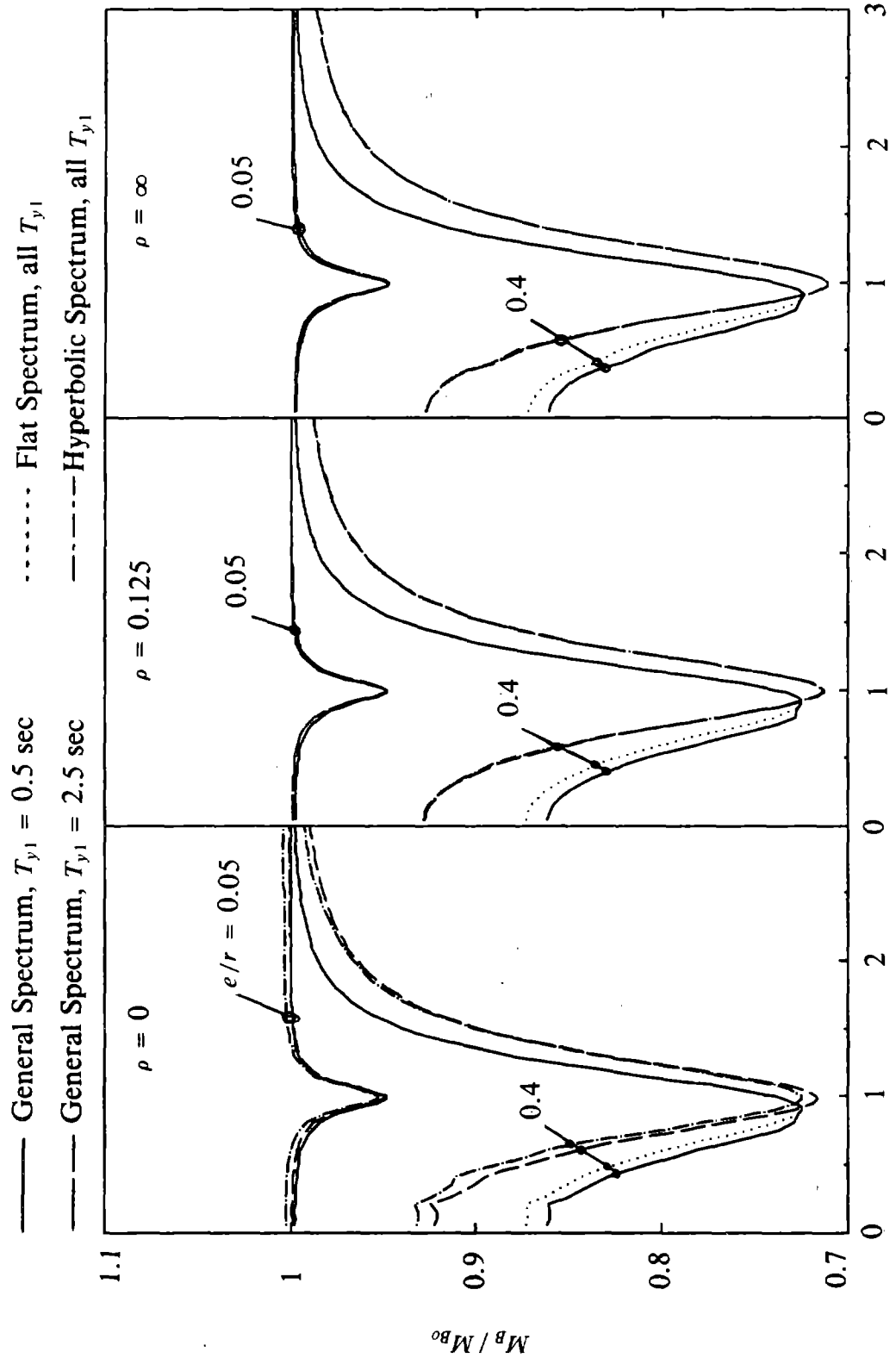

Uncoupled Torsional to Lateral Frequency Ratio $\Omega = \omega_{\theta j} / \omega_{yj}$

FIGURE 49 Normalized Base Overturning Moment in Systems with T_{y1} = 0.5 and 2.5 sec, and e/r = 0.05 and 0.4 for Three Response Spectra (ξ = 5 %)

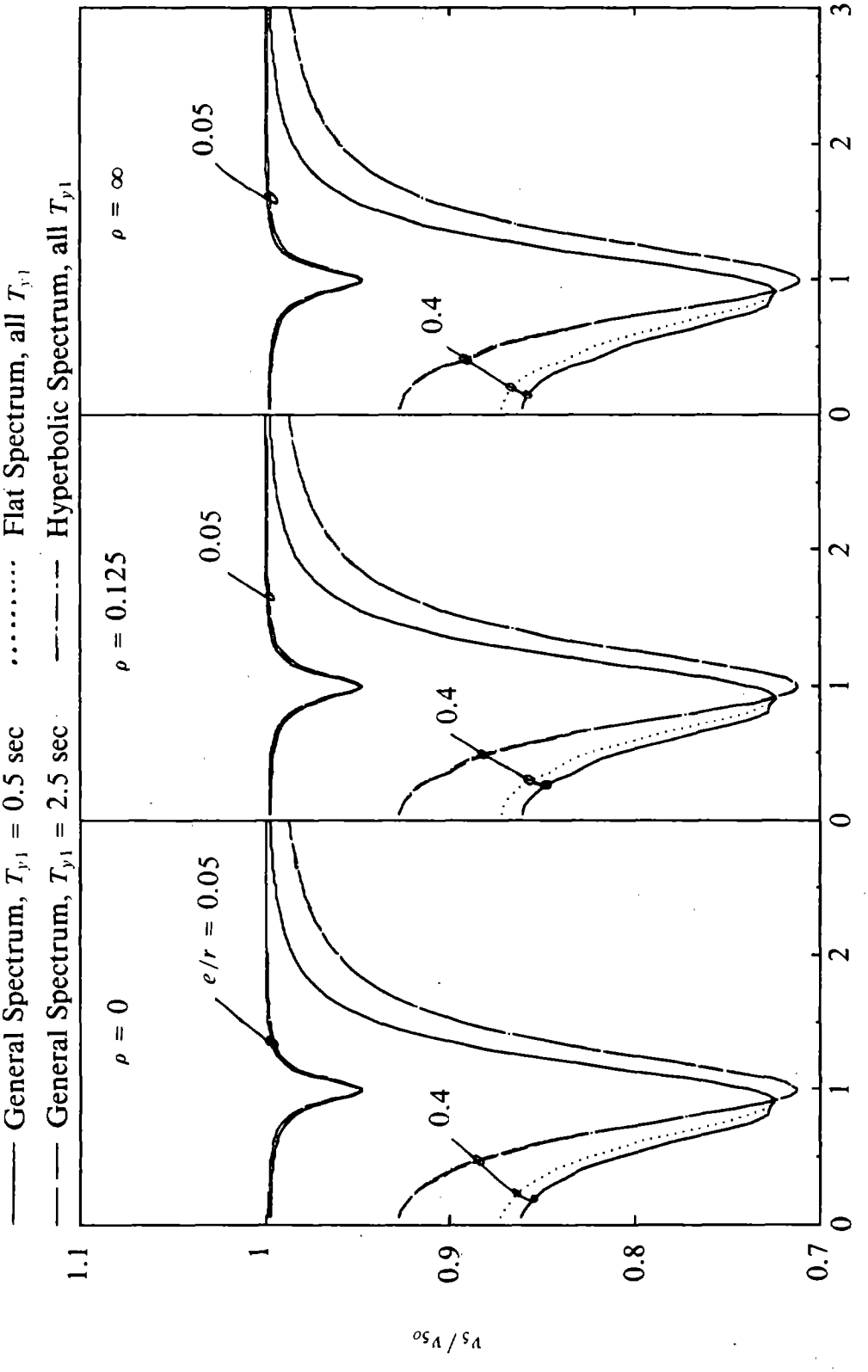

FIGURE 50 Normalized Top Floor Lateral Displacement at Center of Rigidity in Systems with T_{y1} = 0.5 and 2.5 sec, and e/r = 0.05 and 0.4 for Three Response Spectra (ξ = 5 %)

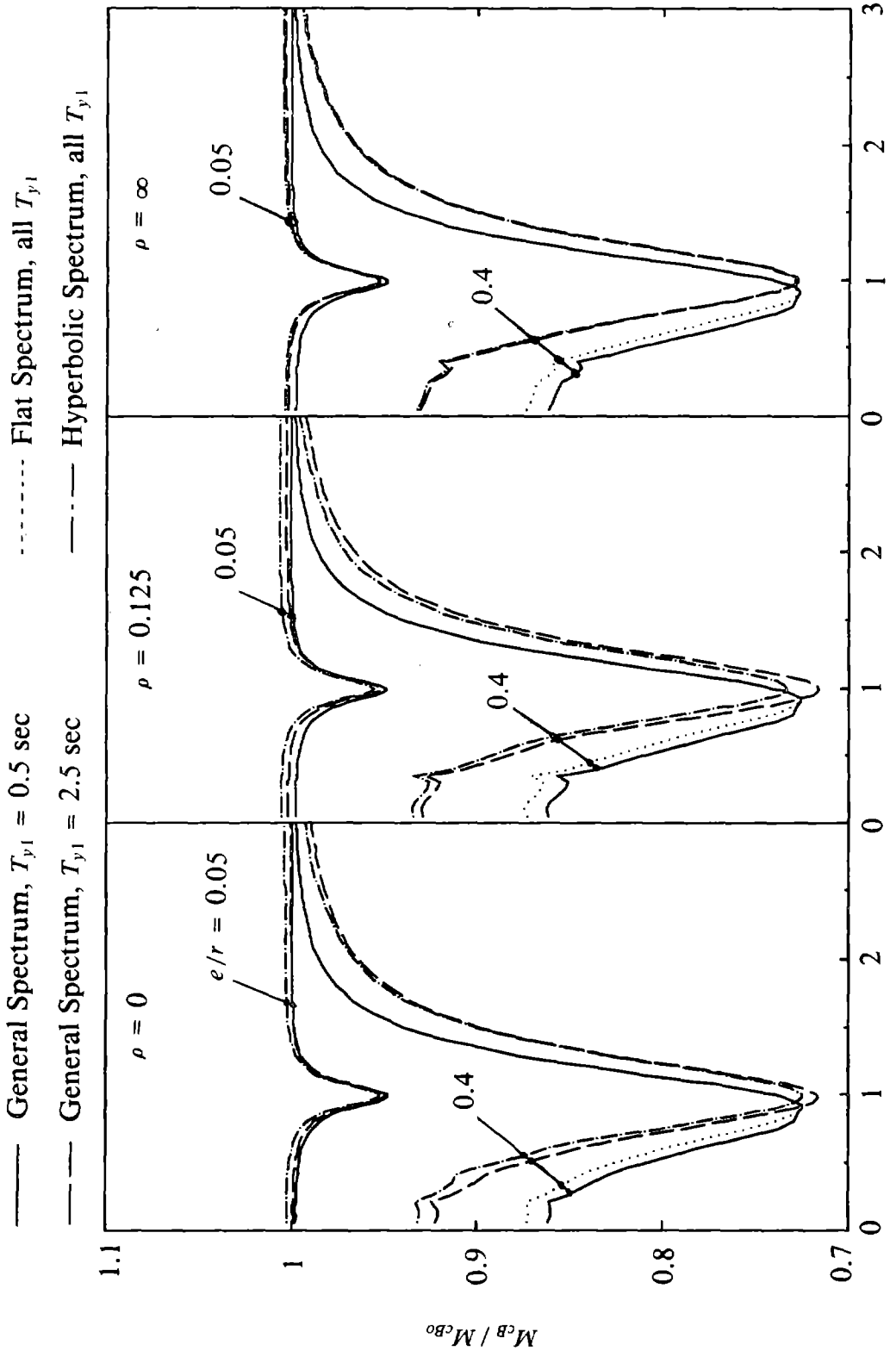

FIGURE 51 Normalized Column Moment in Base-story of Frame (1) in Systems with T_{y1} = 0.5 and 2.5 sec, and e/r = 0.05 and 0.4 for Three Response Spectra (ξ = 5 %)

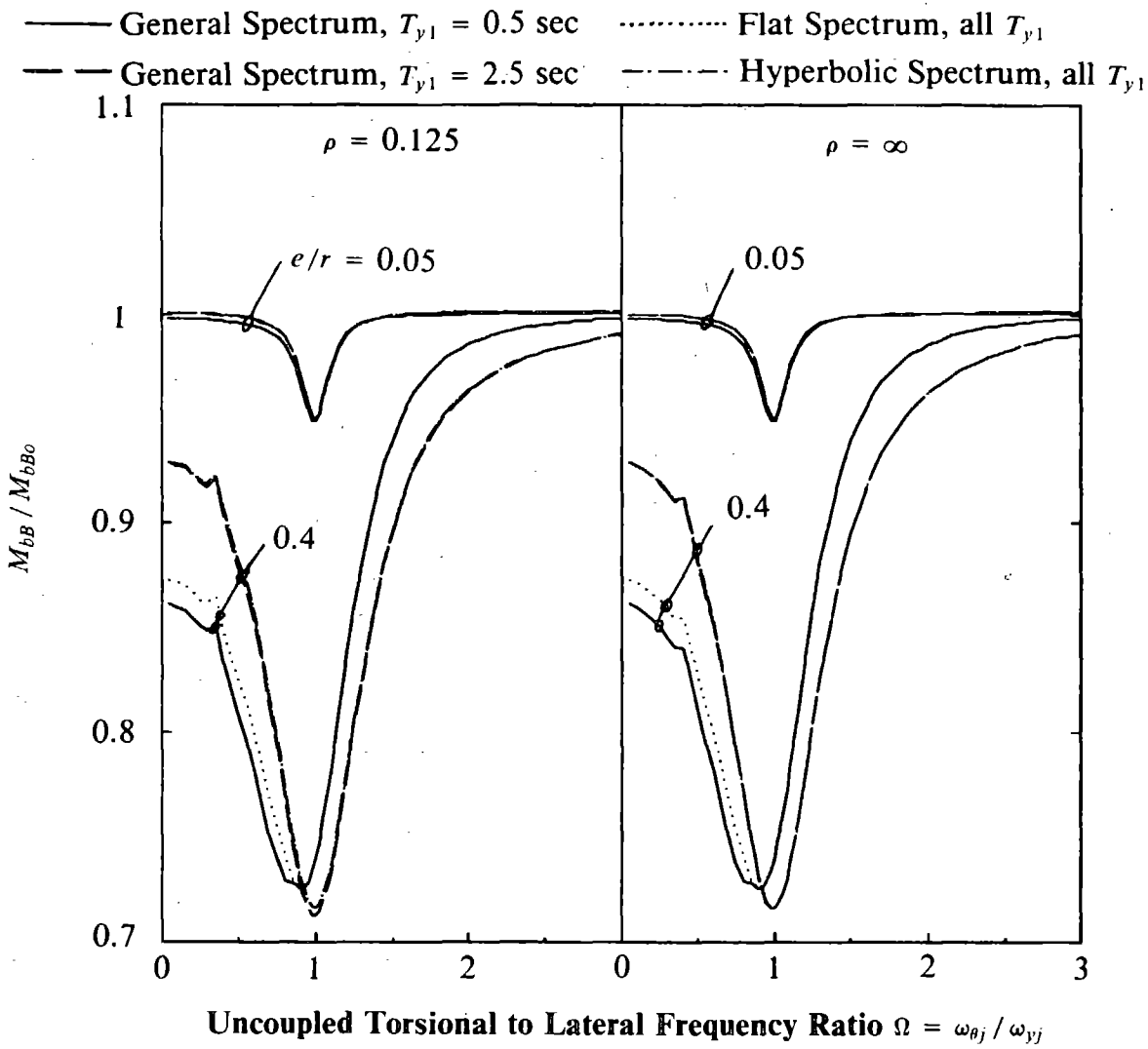

FIGURE 52 Normalized Beam Moment in Base-story of Frame (1) in Systems with T_{y1} = 0.5 and 2.5 sec, and e/r = 0.05 and 0.4 for Three Response Spectra (ξ = 5 %)

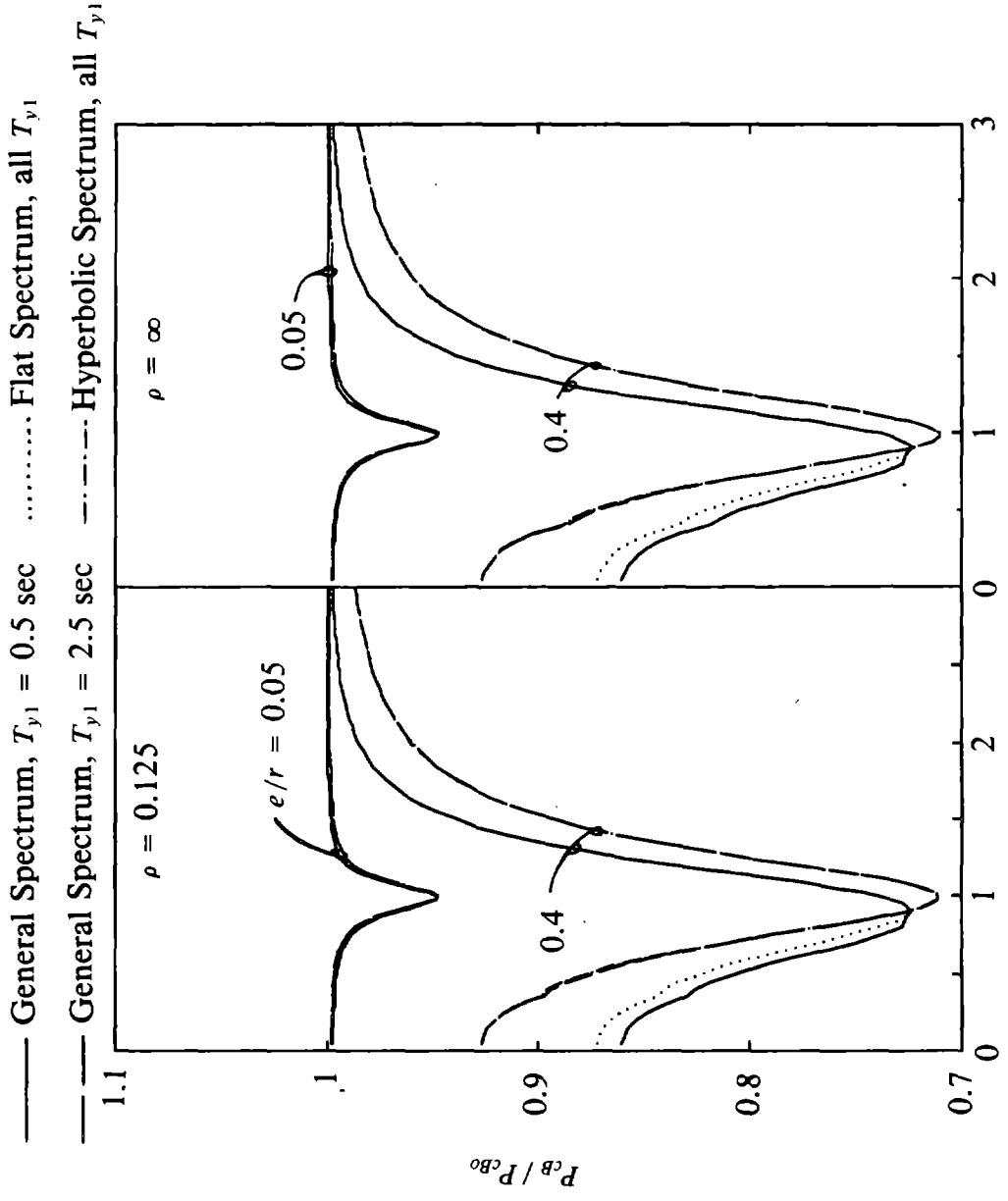

FIGURE 53 Normalized Column Axial Force in Base-story of Frame (1) in Systems with T_{y1} = 0.5 and 2.5 sec, and e/r = 0.05 and 0.4 for Three Response Spectra (ξ = 5 %)

increases, the normalized response computed for the design spectrum of Figure 5 follows that determined for the flat spectrum if T_{y1} is in the acceleration-controlled region of the spectrum, and it follows the results for the hyperbolic spectrum if T_{y1} is in the velocity-controlled region of the spectrum. As mentioned in Section 2.3, the results for the flat and hyperbolic spectra are upper bounds of the normalized quantities computed for the general spectrum.

The normalized responses for the design spectrum of Figure 5 deviate from the idealized curves for flat or hyperbolic spectra, as the case may be depending on T_{y1}, because of the vibration periods falling on different branches of the spectrum than T_{y1}, and affecting the contributions of higher modal-pairs. In other words, the deviations from the idealized curves are related closely to the contributions of modal-pairs in response. Thus, based on the earlier interpretation of higher modal-pair responses, the deviations increase with increase in e/r; they are larger for torsionally-flexible systems ($\Omega < 1$), and are dependent on the response quantity in question and on the value of ρ. The deviations for V_B, T_{BR} and M_B are larger for smaller ρ, which is supported by Table 12, and less pronounced for M_B than V_B or T_{BR}. For torsionally-flexible systems the base torque (Figure 41) is very small even for T_{y1} values in the acceleration-controlled region of the spectrum. This is because, in this case the base torque is dominated by the fundamental modal-pair (Section 7), and for torsionally-flexible systems the fundamental vibration mode is very long and falls on a different branch of the spectrum than T_{y1}, causing its contribution to the base torque to be very small.

The effect of lateral-torsional coupling on the height-wise distribution of forces is summarized in Figures 54 to 56, wherein the height-wise variations of story shears, story torques at the centers of rigidity, and story overturning moments expressed as ratios of the respective values at the base, are presented for both idealized flat and hyperbolic spectra for systems with $\rho = 0$, values of e/r equal to 0.05, 0.4 and 1, and values of Ω equal 0.5, 1 and 1.5. In order to identify the effect of lateral-torsional coupling on the height-wise variation of forces, also included in these figures are the height-wise variations of story shears and story overturning moments for the corresponding torsionally-uncoupled, multi-story system ($e/r = 0$), which depend on ρ but not on Ω. It is apparent from these figures that for a flat spectrum the height-wise variations of all forces shown are

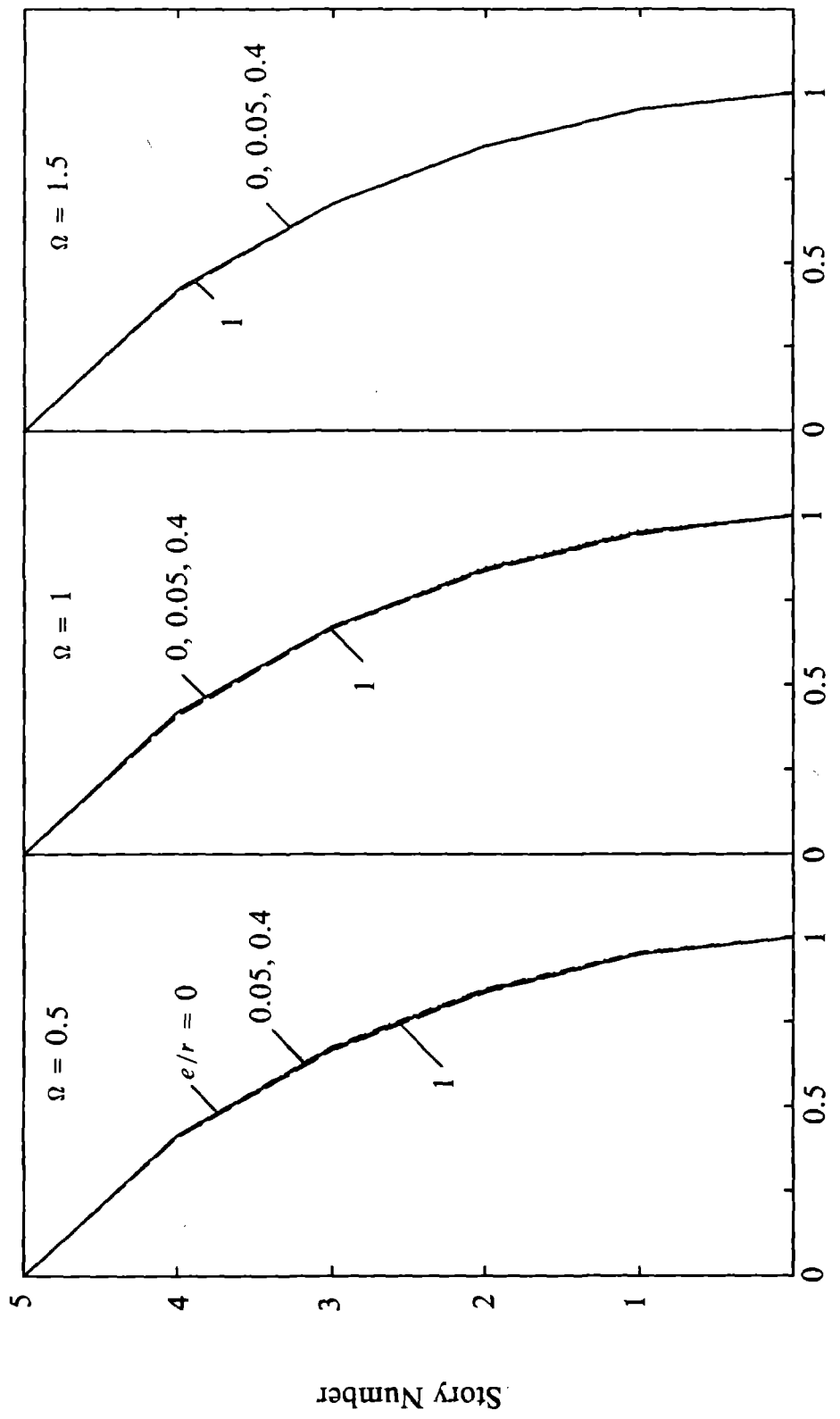

FIGURE 54a Comparison of Height-wise Variation of Story Shears in Torsionally-uncoupled (e/r = 0) and Torsionally-coupled (e/r = 0.05, 0.4 and 1) Systems for Flat Pseudo-acceleration Spectrum and Three Values of Ω (ρ = 0 and ξ = 5 %)

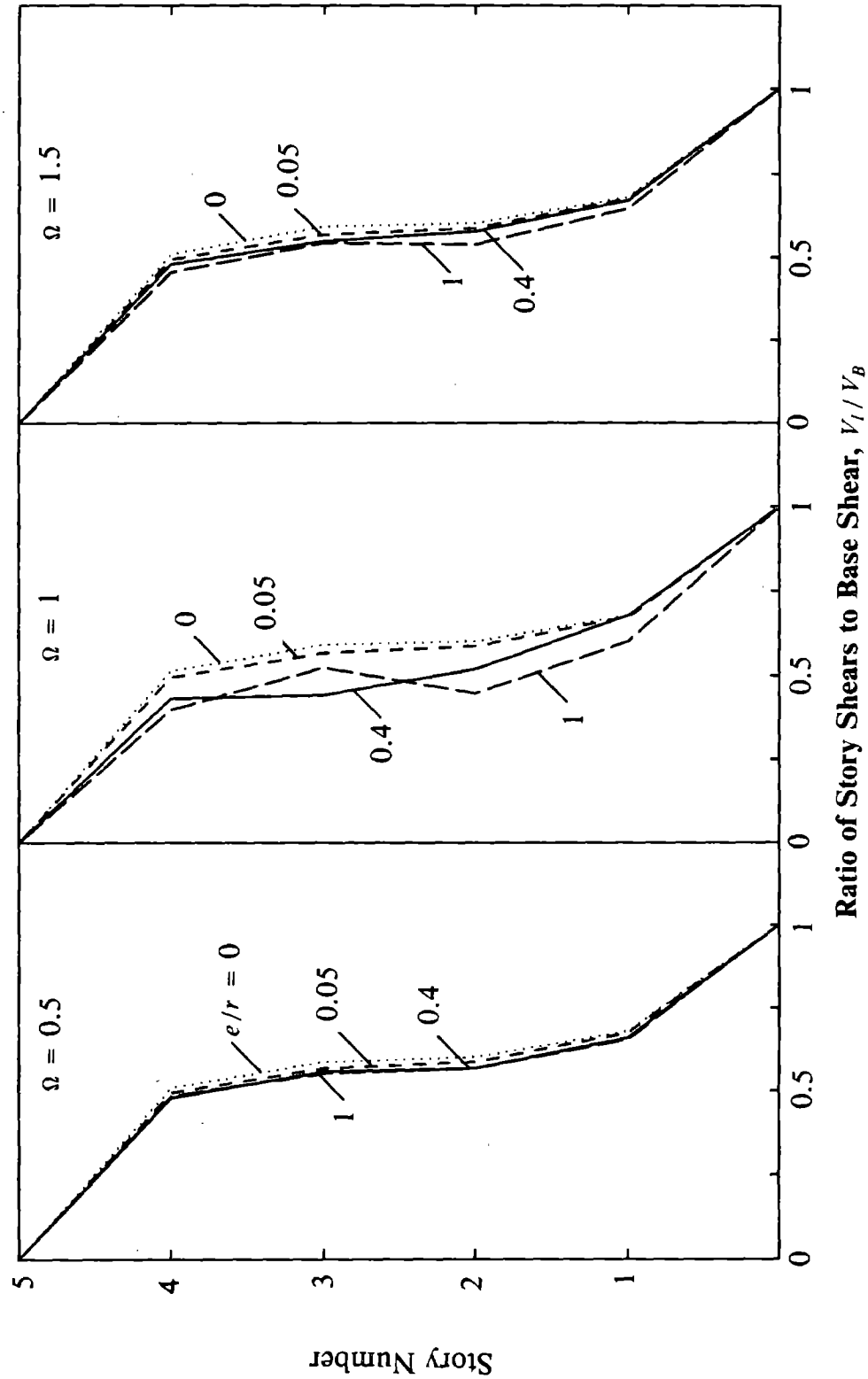

FIGURE 54b Comparison of Height-wise Variation of Story Shears in Torsionally-uncoupled (e/r = 0) and Torsionally-coupled (e/r = 0.05, 0.4 and 1) Systems for Hyperbolic Pseudo-acceleration Spectrum and Three Values of Ω (ρ = 0 and ξ = 5 %)

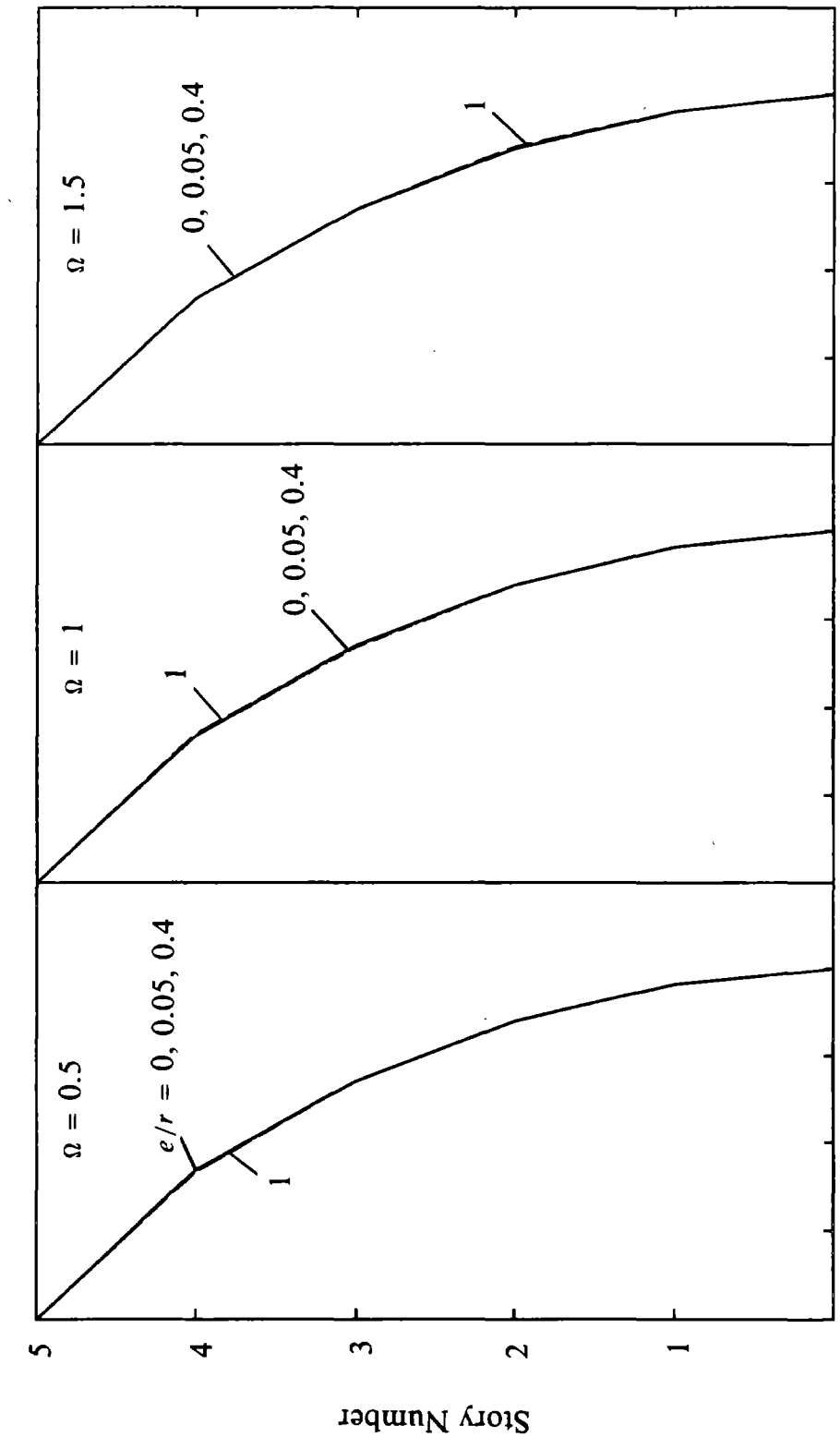

Ratio of Story Torques to Base Torque at Centers of Rigidity, T_{IR} / T_{BR}

Figure 55a Comparison of Height-wise Variation of Story Torques at Centers of Rigidity in Torsionally-coupled (e/r = 0.05, 0.4 and 1) Systems and Height-wise Variation in Story Shears in Torsionally-uncoupled (e/r = 0) Systems for Flat Pseudo-acceleration Spectrum and Three Values of Ω (ρ = 0 and ξ = 5 %)

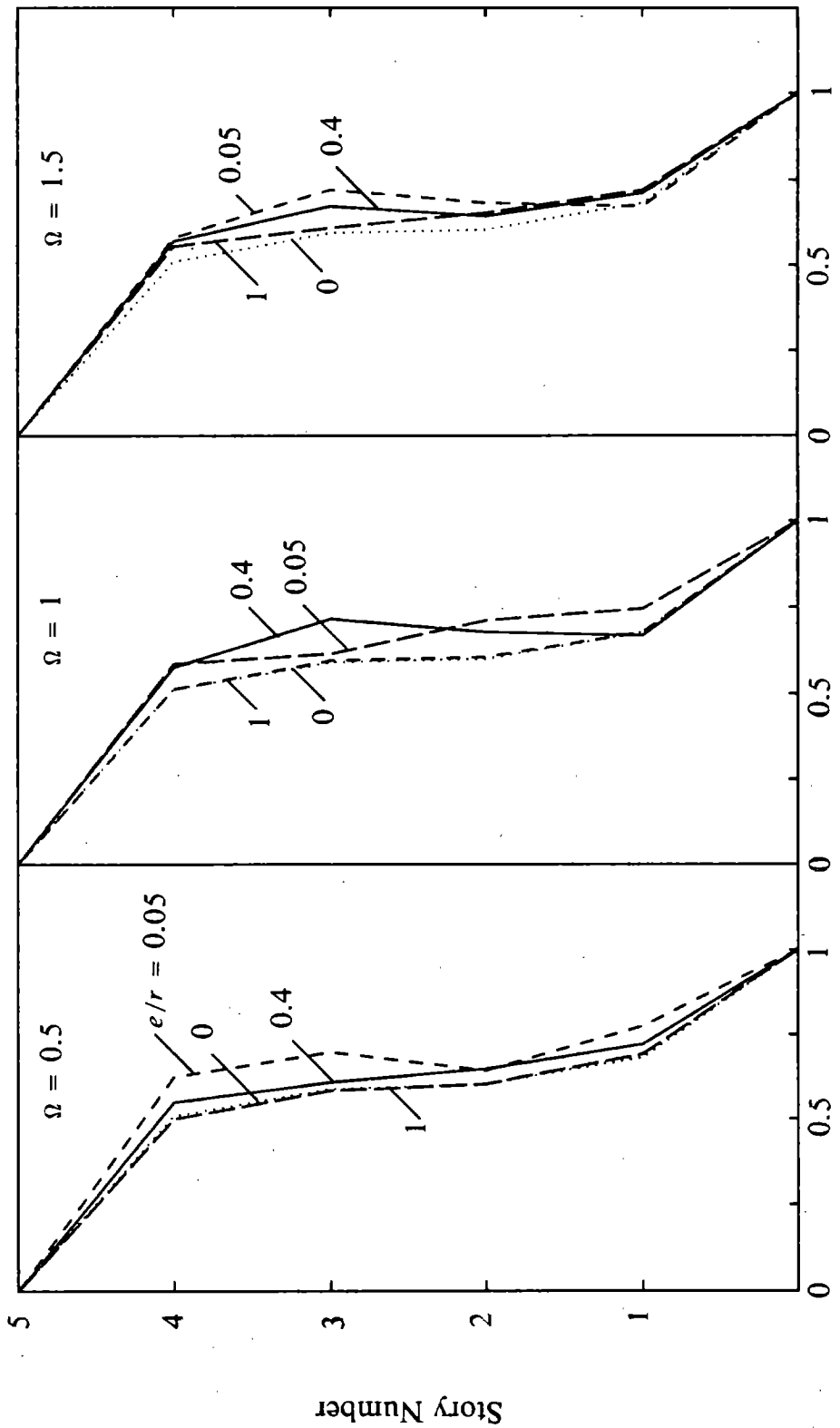

Figure 55b Comparison of Height-wise Variation of Story Torques at Centers of Rigidity in Torsionally-coupled (e/r = 0.05, 0.4 and 1) Systems and Height-wise Variation in Story Shears in Torsionally-uncoupled (e/r = 0) Systems for Hyperbolic Pseudo-acceleration Spectrum and Three Values of Ω (ρ = 0 and ξ = 5 %)

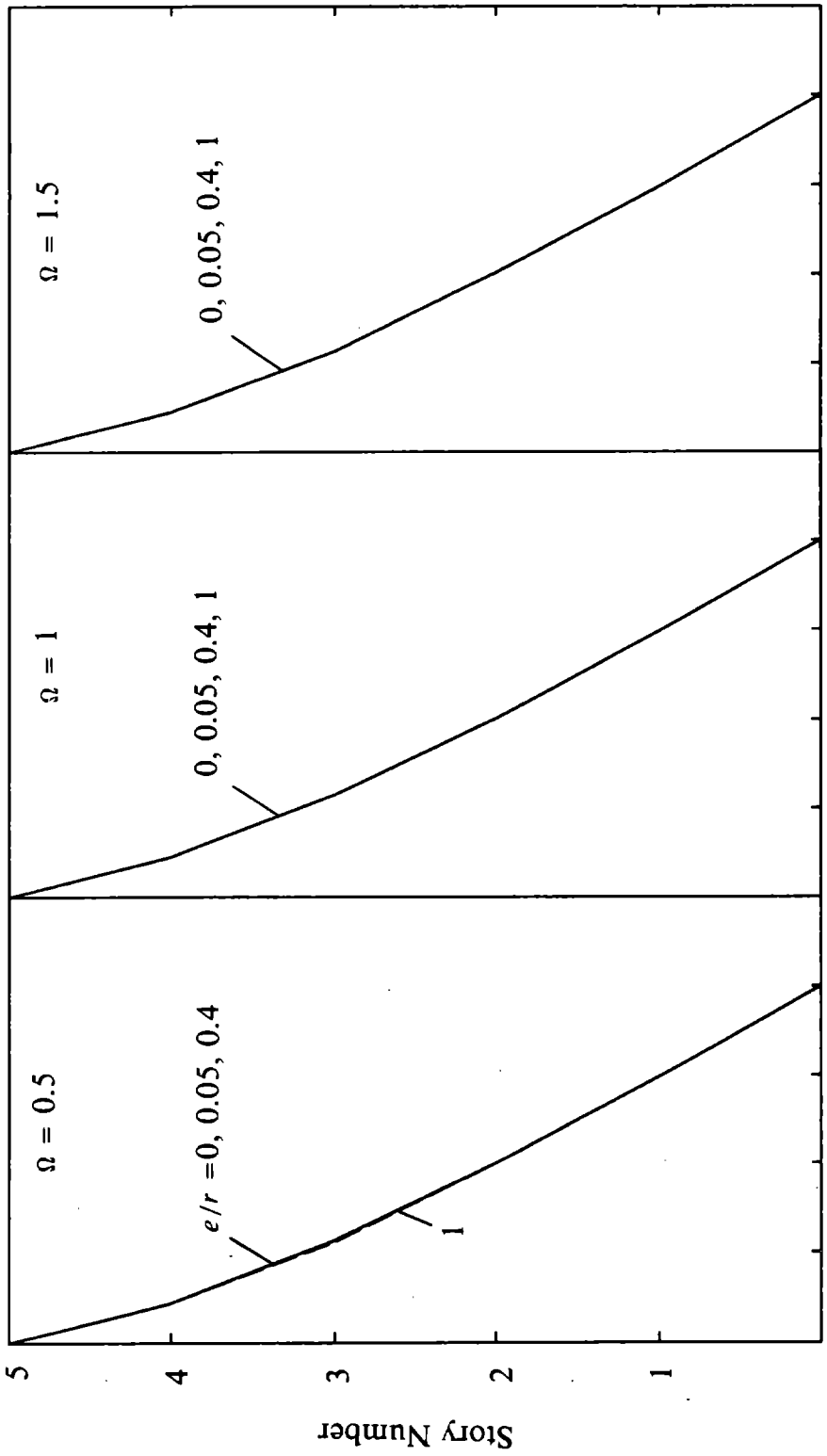

FIGURE 56a Comparison of Height-wise Variation of Story Overturning Moments in Torsionally-uncoupled (e/r = 0) and Torsionally-coupled (e/r = 0.05, 0.4 and 1) Systems for Flat Pseudo-acceleration Spectrum and Three Values of Ω (ρ = 0 and ξ = 5 %)

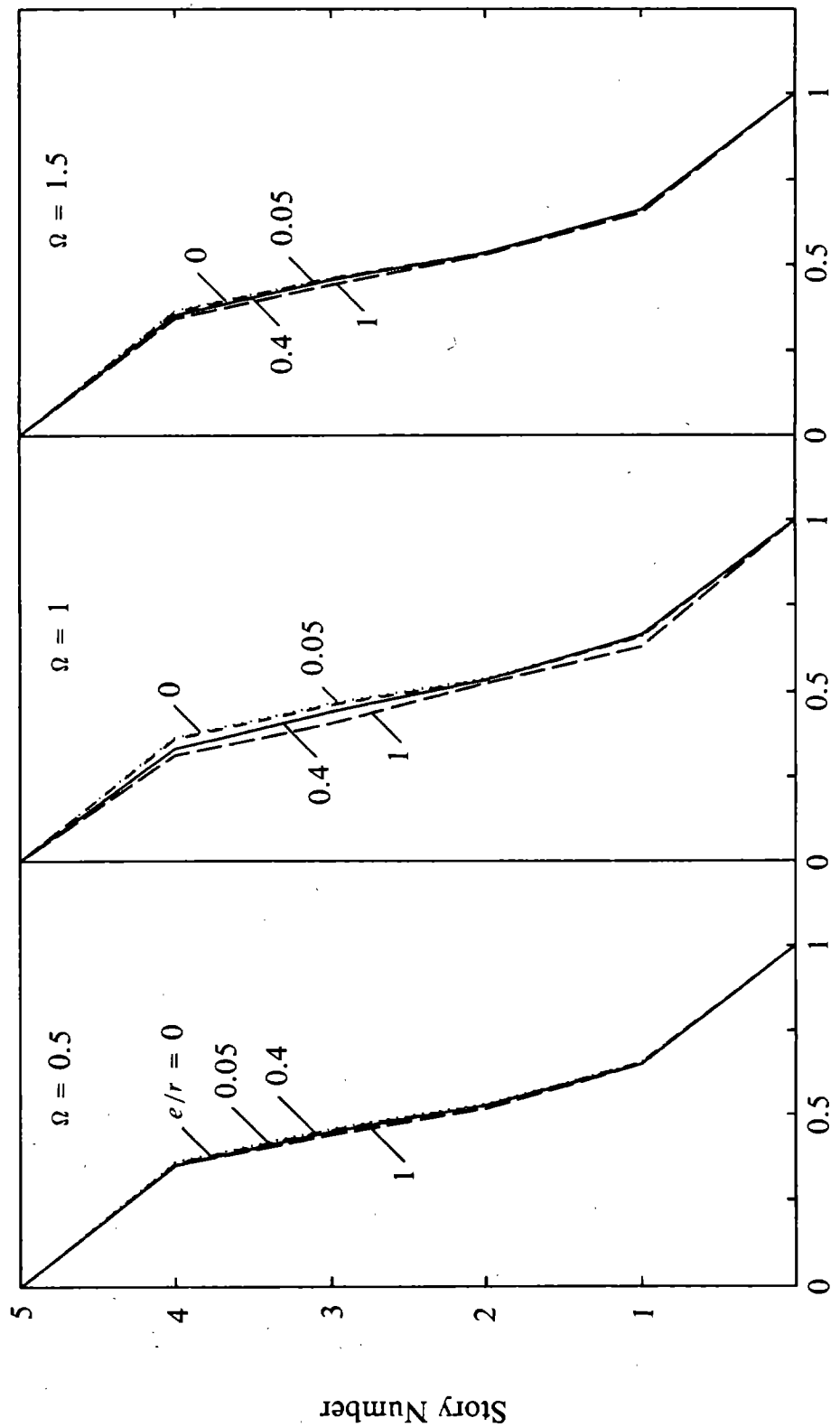

FIGURE 56b Comparison of Height-wise Variation of Story Overturning Moments in Torsionally-uncoupled (e/r = 0) and Torsionally-coupled (e/r = 0.05, 0.4 and 1) Systems for Hyperbolic Pseudo-acceleration Spectrum and Three Values of Ω (ρ = 0 and ξ = 5 %)

insensitive to the values of e/r or Ω and follow the respective variations in the corresponding uncoupled multi-story system. This can be explained by noting that the response of torsionally-coupled buildings with T_{y1} in the acceleration-controlled region, or the flat portion of the spectrum, is mainly due to the fundamental vibration modal pair-- modes '11' and '21' (Figures 20 to 23)-- and the cross-correlation terms are relatively small, thus ensuring small contributions of higher modal-pairs. As a result, the responses of the torsionally-coupled building, normalized by the responses of the corresponding torsionally-uncoupled, multi-story system, are very close to the normalized responses of the one-story system, causing the height-wise distribution of responses for the torsionally-coupled building to follow very closely those for the corresponding uncoupled system. The effect of lateral-torsional coupling on the height-wise distribution of forces is more pronounced for the hyperbolic spectrum, or the velocity-controlled region of the spectrum, with the effect increasing as e/r increases and as ρ decreases, primarily because the cross-correlation terms are more significant in this case, and increase with increase in e/r and decrease in ρ (Figures 40 to 42). For the values of Ω shown in Figures 54 to 56, the effect is generally most pronounced for systems with closely spaced uncoupled frequencies (Ω close to 1), more so for story shears and story torques than for story overturning moments, because cross-correlation terms are more significant for the former quantities than the latter (Figures 47 to 49). However, the overall effect of lateral-torsional coupling on the height-wise variations of forces is not large.

The effect of lateral-torsional coupling on the response spectra can be examined for the results presented in Figures 57 to 63. The seven response quantities of the coupled system, normalized as before, are plotted in the form of response spectra against T_{y1}, for values of e/r equal 0.05, 0.4 and 1, along with the response quantities for the corresponding uncoupled multi-story system ($e/r = 0$) to study the effect of lateral-torsional coupling.

Observations based on Figures 57 and 59 to 63 are very similar for the following response quantites: base shear V_B, base overturning moment M_B, and top floor lateral displacement v_5 at the center of rigidity; and column moment M_{cB}, beam moment M_{bB} and column axial force P_{cB} for base story of frame (1). For systems with small e/r (e.g. 0.05 or less), the response spectra are

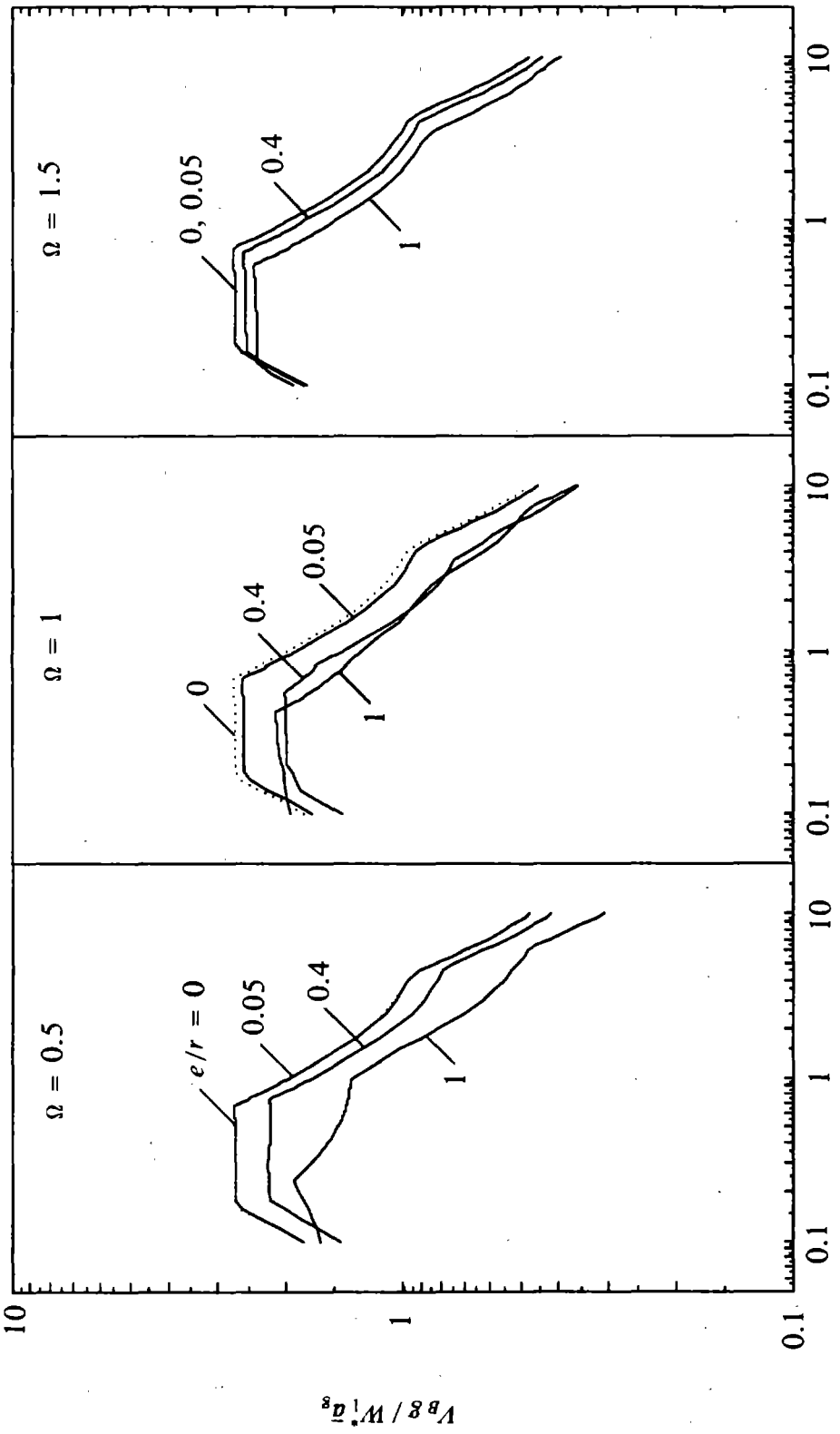

FIGURE 57 Comparison of Base Shear Response Spectra for Torsionally-uncoupled (e/r = 0) and Torsionally-coupled (e/r = 0.05, 0.4 and 1) Systems for Three Values of Ω (ρ = 0 and ξ = 5 %)

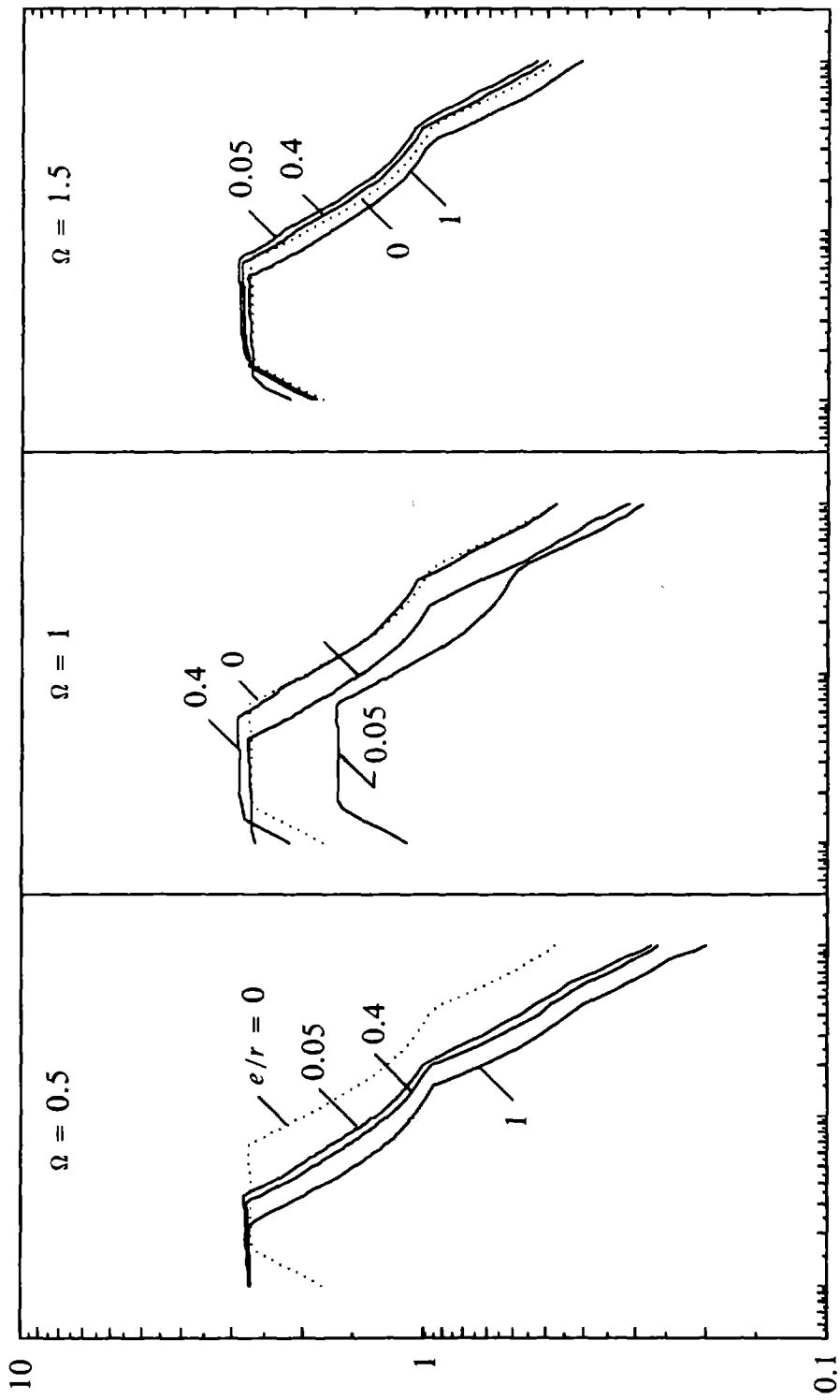

FIGURE 58 Comparison of Base Shear Response Spectra for Torsionally-uncoupled (e/r = 0) Systems and Base Torque Response Spectra at Center of Rigidity in Torsionally-coupled (e/r = 0.05, 0.4 and 1) Systems for Three Values of Ω (ρ = 0 and ξ = 5 %)

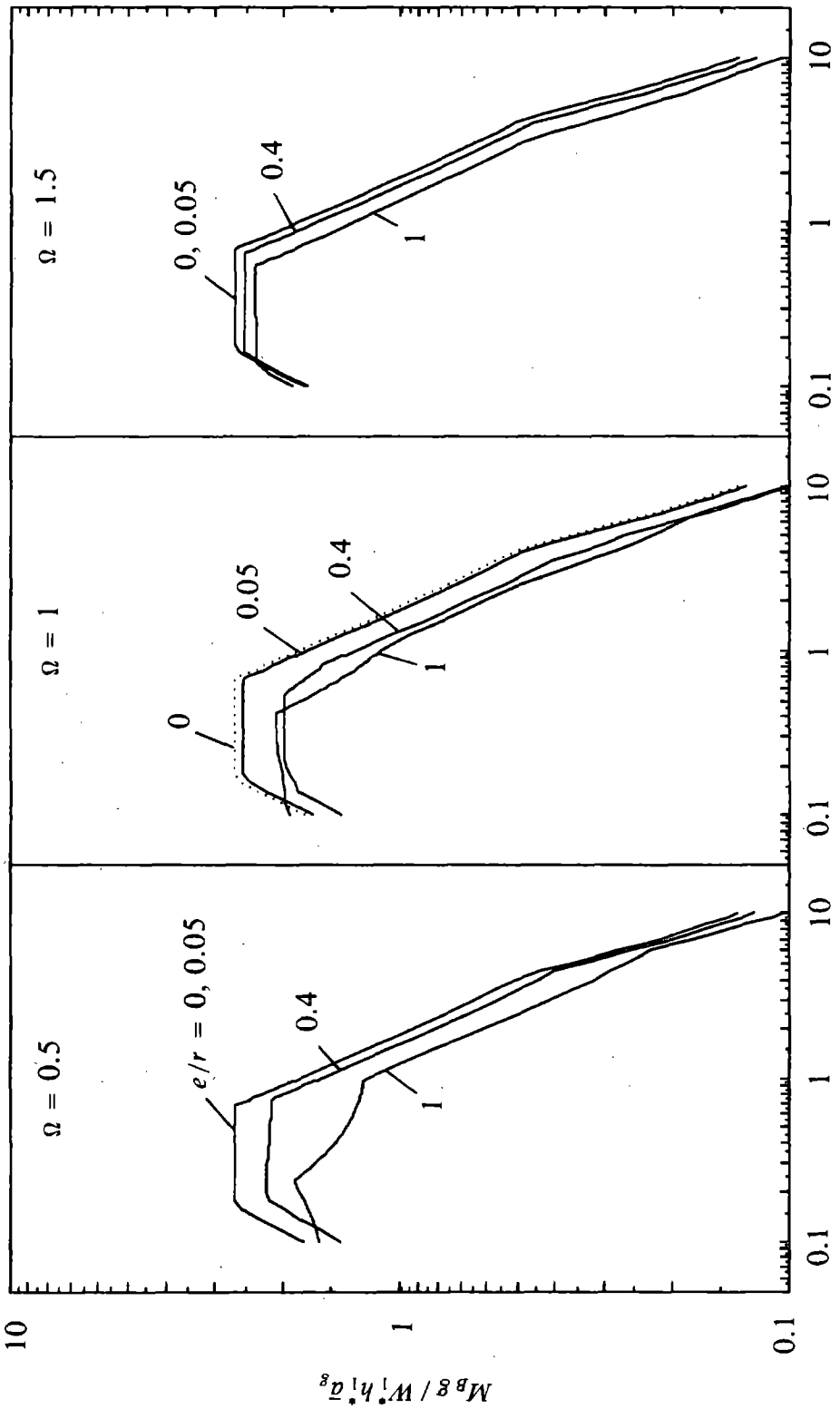

Fundamental Period T_{y1} (secs) of Uncoupled System

FIGURE 59 Comparison of Base Overturning Moment Response Spectra for Torsionally-uncoupled (e/r = 0) and Torsionally-coupled (e/r = 0.05, 0.4 and 1) Systems for Three Values of Ω (ρ = 0 and ξ = 5 %)

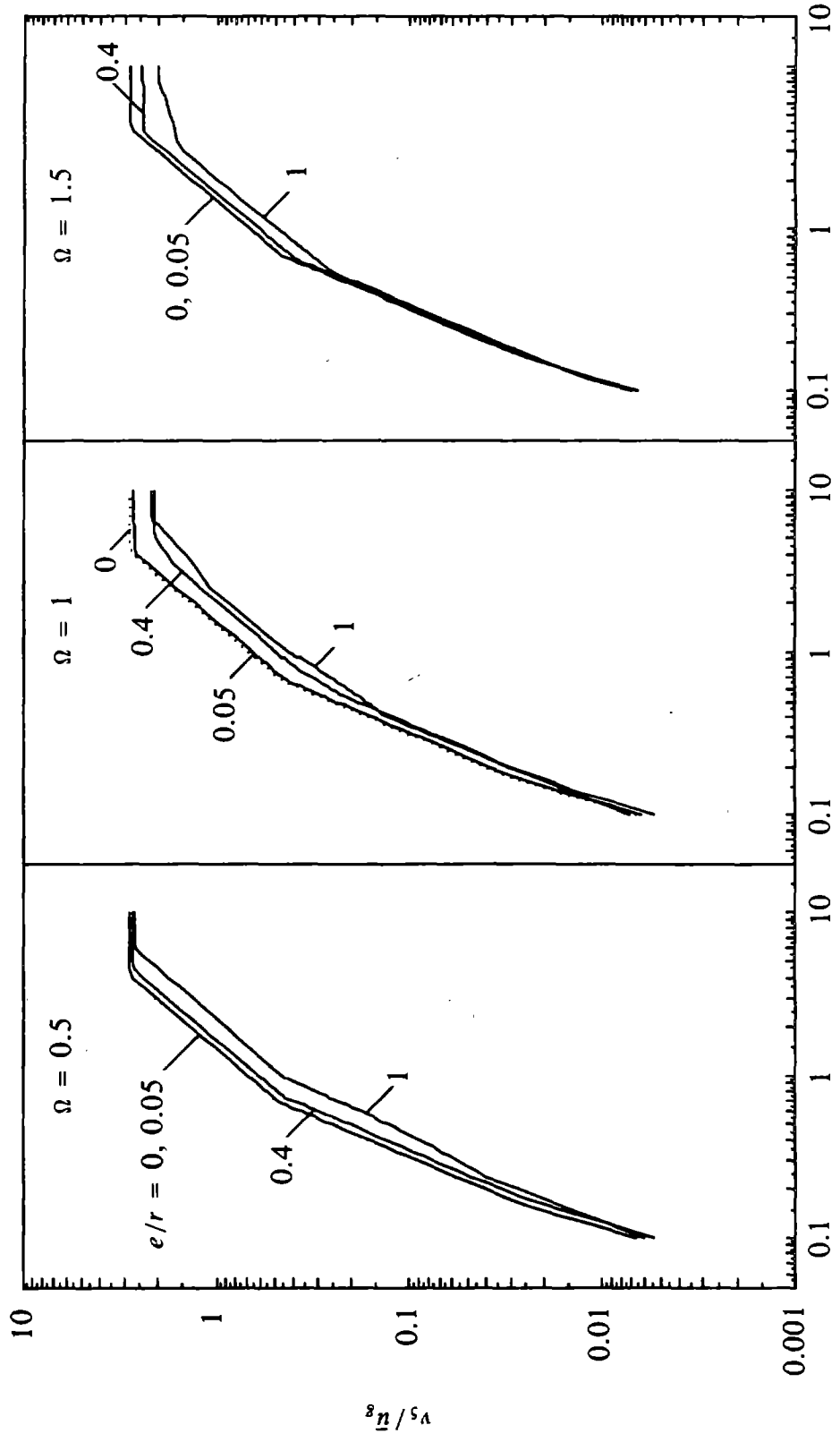

FIGURE 60 Comparison of Top Floor Lateral Displacement at Center of Rigidity Response Spectra for Torsionally-uncoupled (e/r = 0) and Torsionally-coupled (e/r = 0.05, 0.4 and 1) Systems for Three Values of Ω (ρ = 0 and ξ = 5 %)

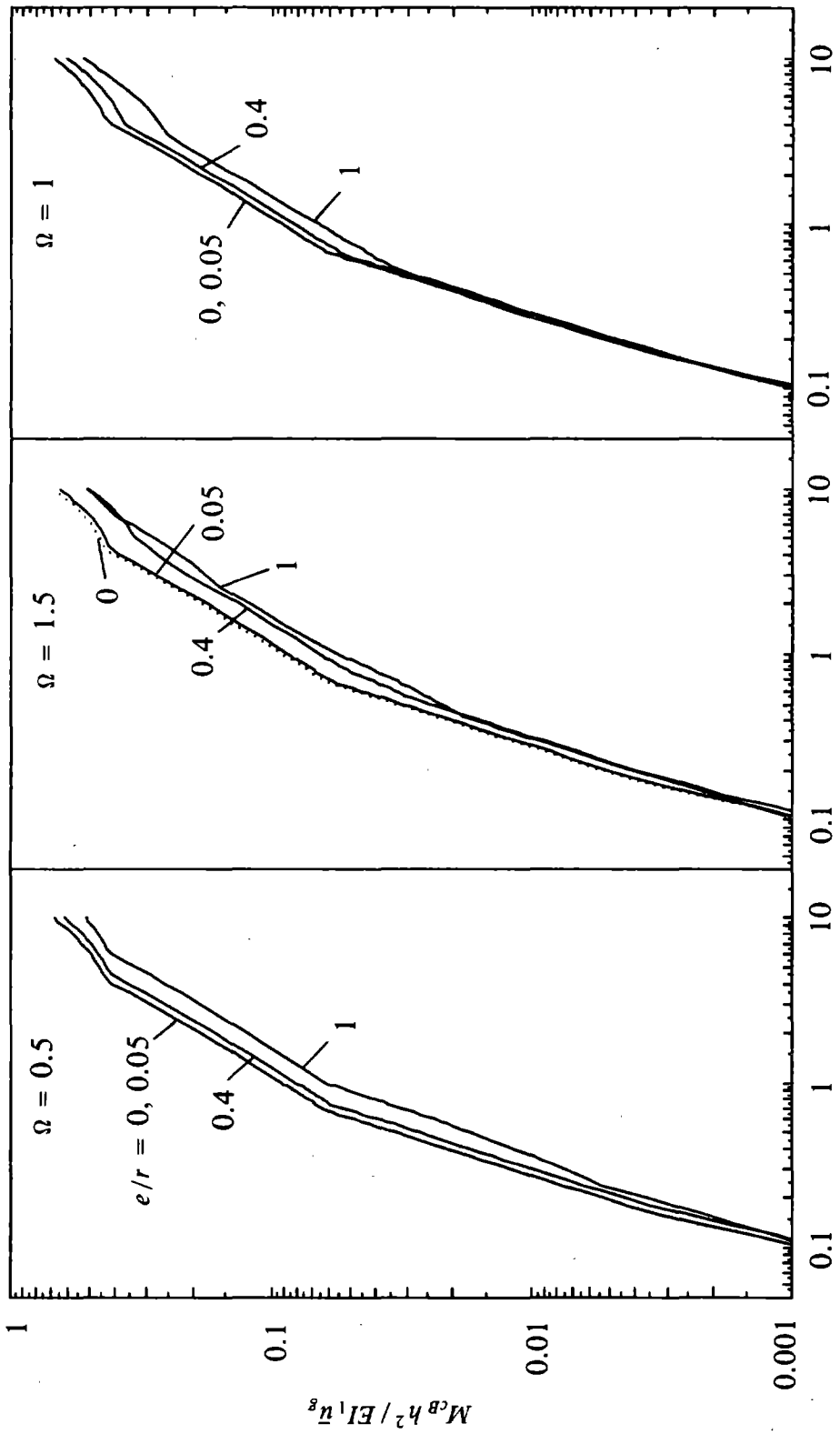

FIGURE 61 Comparison of Frame (1) Base-story Column Moment Response Spectra for Torsionally-uncoupled (e/r = 0) and Torsionally-coupled (e/r = 0.05, 0.4 and 1) Systems for Three Values of Ω (ρ = 0 and ξ = 5 %)

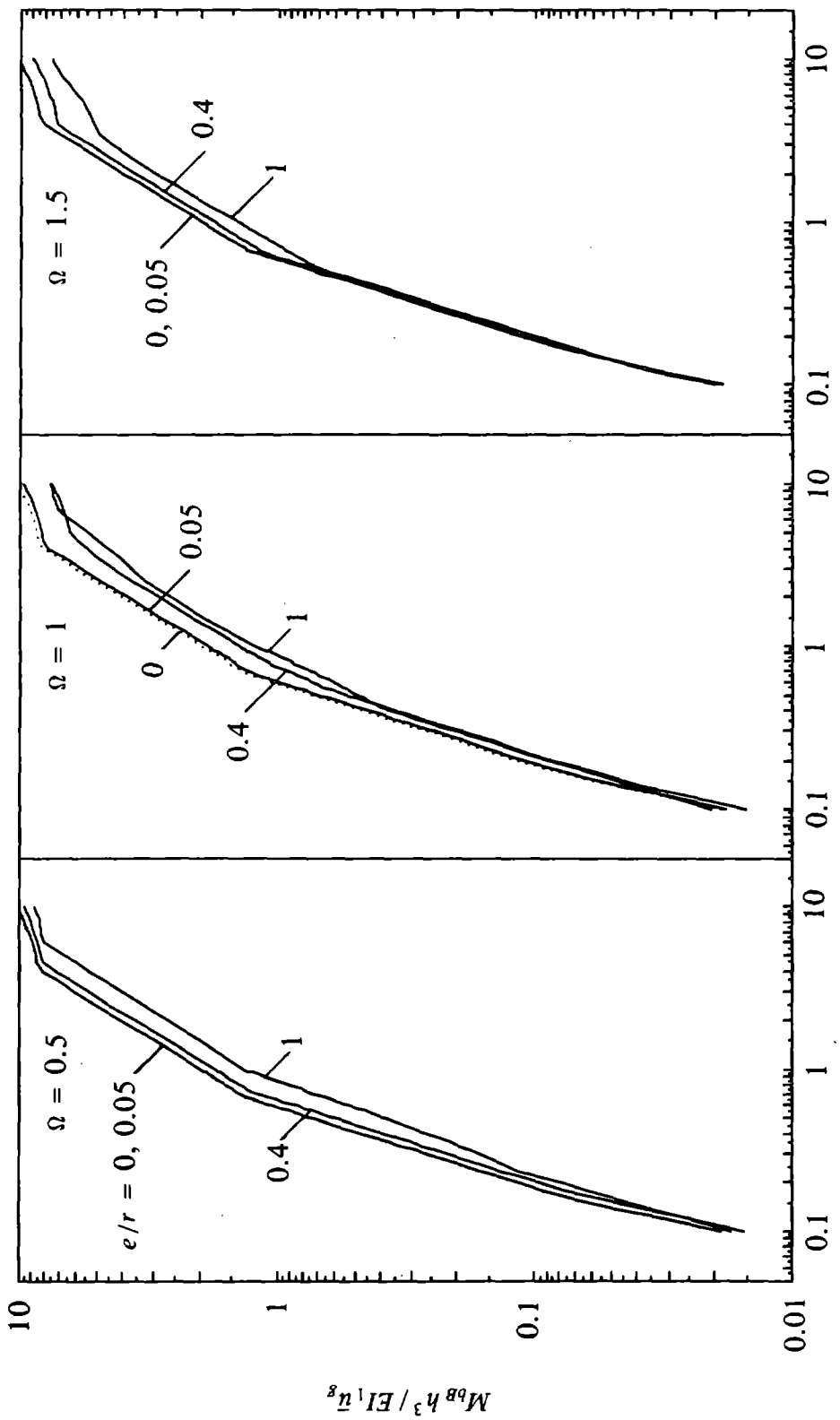

FIGURE 62 Comparison of Frame (1) Base-story Beam Moment Response Spectra for Torsionally-uncoupled (e/r = 0) and Torsionally-coupled (e/r = 0.05, 0.4 and 1) Systems for Three Values of Ω ($\rho = \infty$ and ξ = 5 %)

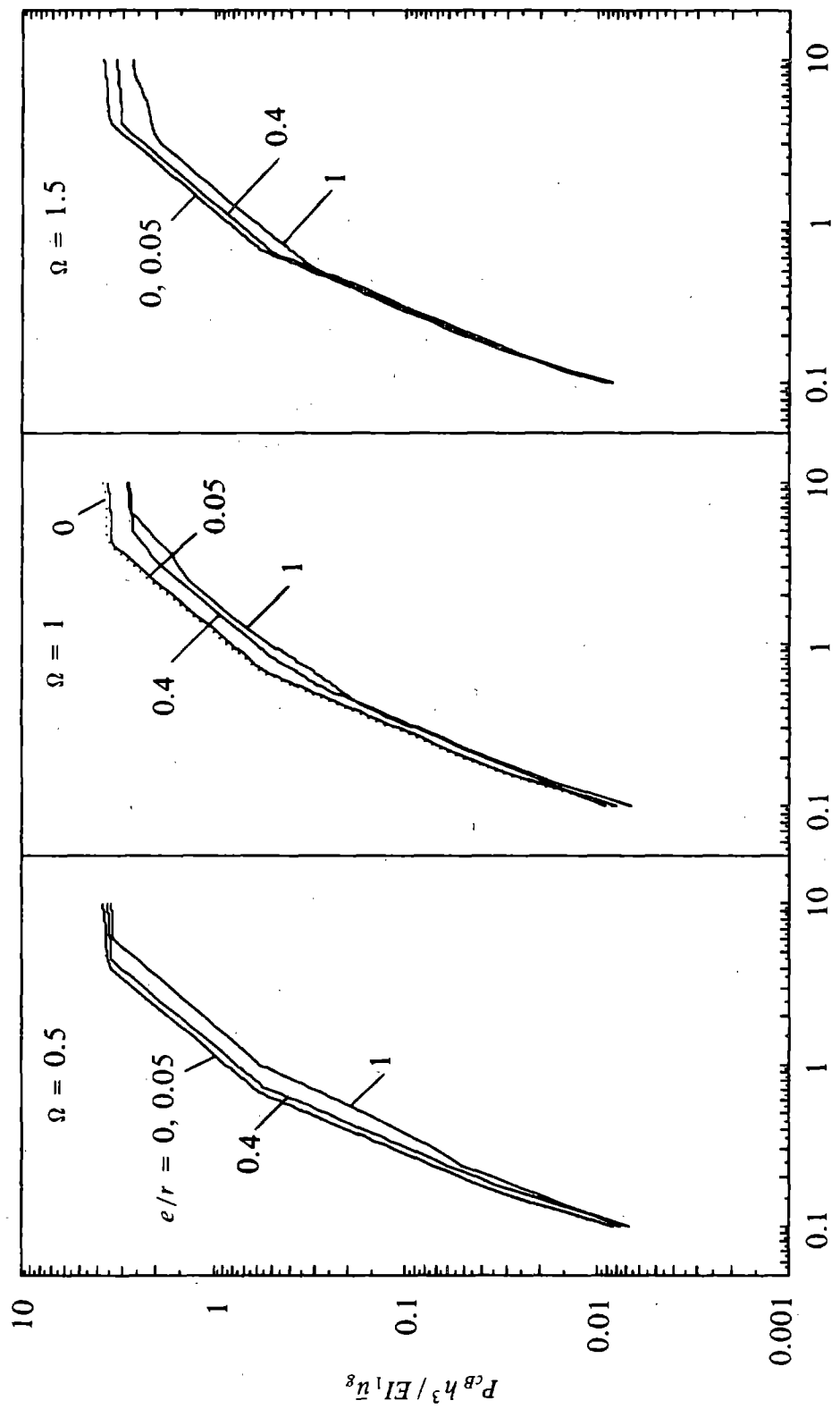

FIGURE 63 Comparison of Frame (1) Base-story Column Axial Force Response Spectra for Torsionally-uncoupled (e/r = 0) and Torsionally-coupled (e/r = 0.05, 0.4 and 1) Systems for Three Values of Ω ($\rho = \infty$ and ξ = 5 %)

essentially unaffected by lateral-torsional coupling. For torsionally-stiff systems ($\Omega > 1$), lateral-torsional coupling has relatively little effect on the response spectrum shape over a wide range of T_{y1} in the acceleration-, velocity- and displacement-controlled regions of the spectrum, even for structures with larger e/r, although there is some reduction in responses with increase in e/r, with the decrease being more pronounced for v_5, M_{cB}, M_{bB} and P_{cB} in the velocity- and displacement-controlled regions of the spectrum. For torsionally-flexible systems ($\Omega < 1$), lateral-torsional coupling also has the effect of decreasing the responses below the uncoupled values as e/r increases. This reduction occurs over a wide range of T_{y1} in the acceleration-, velocity- and displacement-controlled regions of the spectrum, but the reduction depends significantly on T_{y1} making the shape of the response spectra for the coupled systems to differ significantly from the uncoupled system, especially for larger e/r values. The reductions due to increase in e/r are more pronounced in the acceleration- and velocity-controlled regions than in the displacement-controlled region of the spectrum.

In Figure 58, the base torque at the center of rigidity normalized by $e_1^* \overline{W}_1^* W_1^* \bar{a}_g/g$, is plotted against T_{y1}. The normalization factor, as explained in Section 6, is the torque obtained if the base shear $W_1^* \bar{a}_g/g$ of a rigid single-degree-of-freedom system of lumped weight W_1^* is applied at a distance $e_1^* \overline{W}_1^*$ from the center of rigidity of the system. The torsionally-uncoupled system obviously does not experience any torque when subjected to pure translational ground motion. However, the quantity $V_{Bo} e_1^* \overline{W}_1^*$, also normalized by $e_1^* \overline{W}_1^* W_1^* \bar{a}_g/g$, i.e. $V_{Bo} g/W_1^* \bar{a}_g$ which depends only on ρ and T_{y1}, is included for comparison. For torsionally-stiff systems, or systems with closely spaced uncoupled frequencies and larger e/r values, $V_{Bo} e_1^* \overline{W}_1^*$ is a good approximation of base torque, although it may slightly underestimate it for torsionally-stiff systems with smaller e/r values. For torsionally-flexible systems $V_{Bo} e_1^* \overline{W}_1^*$ overestimates the base torque over a wide range of T_{y1} in the acceleration-, velocity- and displacement-controlled regions of the spectrum. Also, it is apparent from Figure 58 that for torsionally-flexible systems (e.g. $\Omega = 0.5$), there is a shift of the base torque response spectrum relative to that of the base shear for the corresponding torsionally-uncoupled,

multi-story system. The shift can be explained by the fact that for torsionally-flexible systems the fundamental coupled vibration period T_{11} may be much longer than T_{y1}, causing the contribution of the fundamental mode to be very small when T_{y1} is in the acceleration-controlled region of the spectrum. Since the fundamental modal-pair is the main contributor to base torque when T_{y1} is in the acceleration-controlled region (Figure C.1), it follows that the base torque is smaller in this region than $V_{Bo}e_1^*\overline{W}_1^*$. For systems with small e/r and closely spaced uncoupled frequencies, the two vibration modes within a modal pair contribute almost equally to the base torque with negative cross-correlation between the two modes of the same pair (Figure C.1). This explains the reduction of base torque relative to $V_{Bo}e_1^*\overline{W}_1^*$ for e/r equal to 0.05 and Ω equal 1 (Figure 58). It is apparent that, in general, the base torque is not satisfactorily approximated by $V_{Bo}e_1^*\overline{W}_1^*$.

9. CONCLUSIONS

A special class of buildings has been identified as buildings consisting of resisting elements (frames, shear walls, columns and shear-wall cores) arranged such that their principal axes form an orthogonal grid in plan which are connected at each floor level by a rigid diaphragm, with the following properties: (1) the centers of mass of all floors lie on a vertical line; and (2) the lateral stiffness matrices of all resisting elements along one direction are proportional (lateral stiffness matrices of the same or different elements along two orthogonal directions are not necessarily proportional). The centers of rigidity of the floors of such buildings are uniquely defined and lie on a vertical line. Thus, the static eccentricity of each floor, which is defined as the distance between the centers of mass and rigidity of the floor, is the same for all floors. This investigation has been concerned with the earthquake analysis and response of buildings belonging to this special class with the additional restriction that all frames (spanning along either of the two orthogonal directions) have proportional lateral stiffness matrices. Furthermore, the floor plans are assumed to have one axis of symmetry, although most of the development is extendable to the more general case of no axes of symmetry.

It has been shown that the natural vibration frequency ω_{nj} and shape ϕ_{nj} of the njth mode of a torsionally-coupled, N-story building are given by:

$$\omega_{nj} = \bar{\omega}_n \, \omega_{yj} \tag{4.10}$$

and,

$$\phi_{nj} = \begin{Bmatrix} \phi_{ynj} \\ \phi_{\theta nj} \end{Bmatrix} = \begin{Bmatrix} \alpha_{yn} \Psi_j \\ \alpha_{\theta n} \Psi_j \end{Bmatrix} \tag{4.11}$$

(with n = 1, 2 and j = 1, ..., N, N being the number of stories); where ω_{yj} and Ψ_j are the jth natural vibration frequency and mode shape of the corresponding torsionally-uncoupled, N-story system-- a N-DOF system with coincident centers of mass and rigidity but all other properties identical to the actual torsionally-coupled, N-story building, $\bar{\omega}_n$ is the nth vibration frequency of the associated torsionally-coupled, one-story system-- a 2-DOF system with the same eccentricity and uncoupled

torsional to lateral frequency ratio as the torsionally-coupled, multi-story building, normalized by the lateral vibration frequency of the corresponding torsionally-uncoupled, one-story system-- a system with coincident centers of mass and rigidity but all properties identical to the associated torsionally-coupled, one-story system-- and $\boldsymbol{\alpha}_n$, where $\boldsymbol{\alpha}_n^T = < \alpha_{yn} \;\; \alpha_{\theta n} >$, is the n^{th} mode shape of the associated torsionally-coupled, one-story system.

The maximum value (over time) of any response quantity r_{nj} of the torsionally-coupled, N-story building with the aforementioned properties due to its nj^{th} vibration mode is given by:

$$r_{nj} = \overline{r}_{nj}\, r_j \qquad n=1,2;\ j=1,...,N \tag{4.66}$$

where r_j is the maximum value of the same (or related-- see Table 1) response quantity of the corresponding torsionally-uncoupled, N-story system in its j^{th} lateral vibration mode; and $\overline{r}_{nj}$ is the normalized maximum value of the response quantity corresponding to r_{nj} (as given in Table 1) of the associated torsionally-coupled, one-story system with uncoupled lateral vibration frequency ω_y equal to ω_{yj}, in its n^{th} vibration mode, where the normalization is with respect to the maximum value of the corresponding response quantity in the corresponding torsionally-uncoupled, one-story system. Responses of all the systems are computed for the same earthquake design spectrum.

It has been demonstarted that the earthquake responses of two buildings with different floor plans are idenctical provided: (1) the static eccentricity ratio is the same for both buildings, (2) the two buildings have identical lateral stiffness matrices along the direction of ground motion, (3) the uncoupled torsional to lateral frequency ratio is the same in both buildings, and (4) the mass of each floor and the damping ratio are the same for both buildings.

As a result of this observation, the parametric response study is concerned with buildings having a simple floor plan, consisting of three moment resisting planar frames, only one of which is in the direction of the ground motion. This investigation has led to the following principal conclusions, which are also applicable to the special class buildings with more general plans than the simplified model:

1. The coupled lateral-torsional response of the building depends on the static eccentricity ratio e/r, the uncoupled torsional to lateral frequency ratio Ω, the joint rotation index or beam-to-column stiffness ratio of the frames ρ, T_{y1}, the fundamental lateral vibration period of the corresponding torsionally-uncoupled, multi-story system and ξ the damping ratio of the building.

2. For fixed values of e/r, Ω and ρ, the response contributions of higher vibration modal-pairs increase with increasing T_{y1} in the velocity- and displacement-controlled regions of the earthquake design spectrum.

3. For fixed values of e/r, Ω and T_{y1}, the response contributions of the higher modal-pairs increase with decreasing ρ.

4. The response contributions of higher modal-pairs vary with the response quantity in question. Among the overall response quantities, the higher modal-pair contributions are much more significant for the base shear and base torque than for the base overturning moment or the top floor lateral displacement. Among the local response quantities, the higher modal-pair contributions are more significant for the column moments than the beam moments or column axial forces.

5. The height-wise variations of story shears and story torques are similar, with differences increasing as T_{y1} increases in the velocity- and displacement-controlled regions of the spectrum.

6. The contributions of higher modal-pairs to the response of a building, expressed as fractions of the response due to the fundamental modal-pair, are relatively insensitive to e/r or Ω.

7. The effects of lateral-torsional coupling on the responses of a multi-story building and its associated one-story system are similar. Lateral-torsional coupling causes a decrease in the base shear, the base overturning moment and the top floor lateral displacement at the center of rigidity, but an increase in the base torque; these effects increase as e/r increases and are most pronounced for systems with closely-spaced uncoupled frequencies.

8. The differences between the effects of lateral-torsional coupling on the multi-story building and its associated one-story system arise due to cross-correlation terms between vibration modes belonging to different modal-pairs. These differences increase with increase in e/r, they are more pronounced for the base shear and base torque than the base overturning moment and the top floor lateral displacement; and are more pronounced for the column moment than the beam moment or column axial force in the base-story.

9. The effect of lateral-torsional coupling on the height-wise variations of forces seems not to be very significant, being more pronounced for story shears and story torques than story overturning moments. The effect increases as e/r increases and is more pronounced when T_{y1} is in the velocity-controlled region than when it is in the acceleration-controlled region of the spectrum.

10. Lateral-torsional coupling also affects the response spectra, i.e. the variations of forces with T_{y1}, to varying degrees depending on the system parameters and the response quantities. For systems with small e/r, the response spectra are essentially unaffected by lateral-torsional coupling. For torsionally-stiff systems, lateral-torsional coupling has little effect on the shape of the response spectra over a wide range of T_{y1} in the acceleration-, velocity- and displacement-controlled regions of the spectrum, although there is some reduction in responses with increase in e/r. For torsionally-flexible systems, lateral-torsional coupling also has the effect of decreasing the responses below the uncoupled values, with reduction depending greatly on T_{y1}, thus making the shape of the response spectra for the torsionally-coupled systems to differ significantly from those for torsionally-uncoupled systems.

11. For torsionally-stiff systems, or systems with closely-spaced uncoupled frequencies and larger e/r values, the base torque at the center of rigidity is approximated by the quantity $V_{Bo}e_1^*\overline{W}_1^*$, the product of the base shear V_{Bo} in the corresponding torsionally-uncoupled, multi-story system, the effective eccentricity e_1^* in the fundamental vibration mode of the associated one-story system and $\overline{W}_1^*$, the effective weight in the fundamental vibration mode of the associated

one-story system normalized by its total weight. In particular $V_{Bo}e_1^*\bar{W}_1^*$ slightly underestimates the base torque for torsionally-stiff systems with smaller e/r ratios, but overestimates it for torsionally-flexible systems over a wide range of T_{y1} in the acceleration-, velocity- and displacement-controlled regions of the spectrum, and for systems with small e/r and closely-spaced uncoupled frequencies.

Taking advantage of the fact that the earthquake response of the torsionally-coupled, multi-story buildings considered in this investigation can be estimated by considering only the first two vibration modal-pairs, and in some cases only the fundamental vibration modal-pair is sufficient, it is possible to develop simplified procedures for the analysis of torsionally-coupled buildings. The vibration frequencies and mode shapes of the first two modal-pairs of torsionally-coupled buildings can be determined utilizing estimates of the first two vibration frequencies and mode shapes of the corresponding torsionally-uncoupled, multi-story system obtained by simplified procedure presented in [12]. Similarly, utilizing the procedures developed in Section 4, modal-pairs of the torsionally-coupled system can be determined from the modal response maxima of the corresponding torsionally-uncoupled system estimated by the simplified procedure presented in [12]. It is believed that such simplified response analyses can be applicable to more general buildings than those considered in this study.

REFERENCES

1. Wilson, E.L. and Habibullah, A., "SAP80 Structural Analysis Programs for the Static and Dynamic Finite Element Analysis of Structures," 1984 Computers and Structures Inc., Berkeley, California, August 1984.

2. Wilson, E.L., Hollings, J.P. and Dovey, H.H., "Three Dimensional Analysis of Building Systems (Extended Version)," Report No. UCB/EERC 75-13, Earthquake Engineering Research Center, University of California, Berkeley, California, 1975.

3. Kan, C.L. and Chopra, A.K., "Elastic Earthquake Analysis of a Class of Torsionally Coupled Buildings," ASCE, 103, ST4, pp. 821-838, 1977.

4. Rutenberg, A., Hsu, T.I. and Tso, W.K., "Response Spectrum Techniques for Asymmetric Buildings," Earthquake Engineering and Structural Dynamics, Vol 6., pp. 427-435, 1978.

5. Tso, W.K. and Meng, V., "Torsional Provisions in Building Codes," Canadian Journal of Civil Engineering, Vol. 9, pp. 38-46, 1982.

6. Rosenblueth, E. and Elorduy, J., "Response of Linear Systems to Certain Transient Disturbance," Proceedings of the Fourth World Conference on Earthquake Engineering, Vol. 1, Santiago, Chile, pp. A1-185 to A1-196, 1969.

7. Cruz, E.F. and Chopra, A.K., "Simplified Methods of Analysis for Earthquake Resistant Design of Buildings," Report No. UCB/EERC 85-01, Earthquake Engineering Research Center, University of California at Berkeley, February, 1985.

8. Roehl, J.L., "Dynamics Response of Ground-Excited Building Frames," Ph.D. Thesis, Rice University, Houston, Texas, Oct. 1971.

9. Blume, J.A., "Dynamic Characteristics of Multi-Story Buildings," Journal of the Structural Division, ASCE, Vol. 94, NO ST2, pp. 337-402, 1968.

10. Kan, C.L. and Chopra, A.K., "Effects of Torsional Coupling on Earthquake Forces in Buildings," ASCE, 103, ST4, pp. 805-820, 1977.

11. Newmark, N.M. and Hall, W.J., "Vibrations of Structures Induced by Ground Motion," Chapter 29, Part I, in Shock and Vibration Handbook, eds. C.M. Harris and C.E. Crede, 2nd Ed., McGraw-Hill Inc., New York, 1976.

12. Chopra, A.K., "Dynamics of Structures, A Primer," Earthquake Engineering Research Institute, Berkeley, California, 1981.

13. Newmark, N.M. and Rosenblueth, E., Fundamentals of Earthquake Engineering, Prentice-Hall, Englewood Cliffs, N.J., 1971.

14. Kan, C.L. and Chopra, A.K., "Elastic Earthquake Analysis of Torsionally Coupled Multistorey Buildings," Earthquake Engineering and Structural Dynamics, 5, pp. 395-412, 1977.

15. Wilson, E.L., Der Kiureghian, A. and Bayo, E., "A Replacement for the SRSS Method in Seismic Analysis," Earthquake Engineering and Structural Dynamics, Vol. 9, pp. 187-192, 1981.

APPENDIX A: ON STATIC ECCENTRICITY

A.1 Concepts and Definitions

The **center of rigidity** of a one-story system with a rigid deck is the point in the plan of the deck through which a horizontal static force must be applied in order that it may cause the deck to translate without torsion. If the force is along either of the principal axes, which are orthogonal and pass through the center of rigidity of the system, the deck translates in the same direction as the force. If a pure torsional moment is applied at the deck, torsion of the deck takes place around the center of rigidity.

Extension of this definition to multi-story buildings is not a simple matter. As a matter of fact, it is generally not possible to determine unique centers of rigidity for multi-story buildings. It will be shown, however, that there is a special class of buildings where the centers of rigidity are uniquely determined and fall on a vertical line.

Consider a multi-story building consisting of a number of moment-resisting frames (shear walls, columns or shear-wall cores), arranged in an orthogonal grid, and joined at each story level by a rigid deck (e.g. Figure 1). The centers of mass of the building are assumed to lie on a vertical line. Without loss of generality, the resisting elements are assumed to be located symmetrically about the X-axis.

The **centers of rigidity** of the floors of the building are the points in the planes of the floors through which any set of static horizontal forces (of arbitrary magnitude and direction) must be applied in order that it may cause all decks to translate without torsion. If the forces are along either of the principal axes, which are orthogonal and pass through the centers of rigidity of the floors, the decks translate in the same direction as the forces. If a set of pure static torsional moments is applied at the decks, torsion of the decks takes place around the centers of rigidity, i.e. the centers of rigidity remain at rest.

The **static eccentricity** of a floor is simply the distance between the centers of mass and rigidity of the floor. When the static eccentricities of all floors are zero, lateral motions of the building are independent of its torsional motions, and the building is said to be uncoupled.

A.2 Locations of Centers of Rigidity

The building is subjected to a force vector $\mathbf{P}$ defined by $\mathbf{P}^T = <\mathbf{P}_y^T \ \mathbf{T}_M^T>$, where $\mathbf{P}_y$ is a vector of static horizontal forces applied at the centers of mass along the Y-axis; and $\mathbf{T}_M$ a vector of static torsional moments applied at the decks about a vertical axis. The Y-lateral displacements at the centers of mass $\mathbf{u}_y$ and deck rotations $\mathbf{u}_\theta$ about a vertical axis are determined by solving the equations of static equilibrium:

$$\mathbf{P} = \mathbf{K}\,\mathbf{u} \tag{A.1}$$

where $\mathbf{K}$ is the building stiffness matrix with respect to $\mathbf{u}$, the displacements vector given by $\mathbf{u}^T = <\mathbf{u}_y^T \ \mathbf{u}_\theta^T>$. Equations (A.1) are written explicitly as:

$$\begin{Bmatrix} \mathbf{P}_y \\ \mathbf{T}_M \end{Bmatrix} = \begin{bmatrix} \mathbf{K}_y & \mathbf{K}_{y\theta} \\ \mathbf{K}_{\theta y} & \mathbf{K}_\theta \end{bmatrix} \begin{Bmatrix} \mathbf{u}_y \\ \mathbf{u}_\theta \end{Bmatrix} \tag{A.2}$$

where $\mathbf{K}_y$, $\mathbf{K}_{y\theta}$, $\mathbf{K}_{\theta y}$ and $\mathbf{K}_\theta$ were given earlier in equations (3.5).

Alternatively, equations of static equilibrium can be written in terms of $\mathbf{u}^*$ defined by $\mathbf{u}^{*T} = <\mathbf{v}^T \ \mathbf{u}_\theta^T>$, where $\mathbf{v}$ is the Y-lateral displacements vector at the centers of rigidity:

$$\mathbf{P}^* = \mathbf{K}^*\mathbf{u}^* \tag{A.3}$$

where $\mathbf{P}^*$ is a force vector equivalent to $\mathbf{P}$ given by:

$$\mathbf{P}^* = \begin{Bmatrix} \mathbf{P}_y \\ \mathbf{T}_R \end{Bmatrix} = \begin{bmatrix} \mathbf{I} & \mathbf{0} \\ -\mathbf{e} & \mathbf{I} \end{bmatrix} \begin{Bmatrix} \mathbf{P}_y \\ \mathbf{T}_M \end{Bmatrix} = \mathbf{a}^{*T}\mathbf{P} \tag{A.4}$$

in which $\mathbf{I}$ and $\mathbf{0}$ denote identity and zero square matrices; $\mathbf{e}$ is a diagonal matrix with entries equal to the static eccentricities of the floors; and $\mathbf{a}^*$ is a simple transformation matrix, also relating $\mathbf{u}$ to $\mathbf{u}^*$ by:

$$\mathbf{u} = \begin{Bmatrix} \mathbf{u}_y \\ \mathbf{u}_\theta \end{Bmatrix} = \begin{bmatrix} \mathbf{I} & -\mathbf{e} \\ \mathbf{0} & \mathbf{I} \end{bmatrix} \begin{Bmatrix} \mathbf{v} \\ \mathbf{u}_\theta \end{Bmatrix} = \mathbf{a}^*\mathbf{u}^* \tag{A.5}$$

Substituting equations (A.1) and (A.5) into (A.4), we obtain:

$$\mathbf{P}^* = \mathbf{a}^{*T}\mathbf{P} = \mathbf{a}^{*T}\mathbf{K}\mathbf{a}^*\mathbf{u}^* \tag{A.6}$$

Comparing equations (A.3) and (A.6), it is clear that:

$$\mathbf{K}^* = \mathbf{a}^{*T}\mathbf{K}\mathbf{a}^* \tag{A.7}$$

Substituting equations (A.2) and (A.5) into (A.7), we get:

$$\mathbf{K}^* = \begin{bmatrix} \mathbf{K}_y & \mathbf{K}_{y\theta} - \mathbf{K}_y\mathbf{e} \\ \mathbf{K}_{\theta y} - \mathbf{e}\mathbf{K}_y & \mathbf{K}_{\theta R} \end{bmatrix} \tag{A.8}$$

where,

$$\mathbf{K}_{\theta R} = \mathbf{K}_\theta - \mathbf{K}_{\theta y}\mathbf{e} + \mathbf{e}(\mathbf{K}_y\mathbf{e} - \mathbf{K}_{y\theta}) \tag{A.9}$$

Utilizing equations (A.8) into (A.3), we obtain:

$$\mathbf{P}^* = \begin{Bmatrix} \mathbf{P}_y \\ \mathbf{T}_R \end{Bmatrix} = \begin{bmatrix} \mathbf{K}_y & \mathbf{K}_{y\theta} - \mathbf{K}_y\mathbf{e} \\ \mathbf{K}_{\theta y} - \mathbf{e}\mathbf{K}_y & \mathbf{K}_{\theta R} \end{bmatrix} \begin{Bmatrix} \mathbf{v} \\ \mathbf{u}_\theta \end{Bmatrix} \tag{A.10}$$

Recalling the definition of centers of rigidity given in Section A.1, it is clear that for any $\mathbf{P}_y \neq \mathbf{0}$ and $\mathbf{T}_R = \mathbf{0}$, $\mathbf{v} \neq \mathbf{0}$ but $\mathbf{u}_\theta = \mathbf{0}$. It follows that:

$$\mathbf{P}_y = \mathbf{K}_y\mathbf{v} \tag{A.11}$$

and

$$\mathbf{0} = (\mathbf{K}_{\theta y} - \mathbf{e}\mathbf{K}_y)\mathbf{v} \tag{A.12}$$

from which we can write:

$$\mathbf{e}\mathbf{P}_y = \mathbf{K}_{\theta y}\mathbf{K}_y^{-1}\mathbf{P}_y \tag{A.13}$$

Also, the definition of centers of rigidity implies that for any $\mathbf{T}_R \neq \mathbf{0}$ and $\mathbf{P}_y = \mathbf{0}$, $\mathbf{v} = \mathbf{0}$ and $\mathbf{u}_\theta \neq \mathbf{0}$, from which we obtain:

$$\mathbf{e}\mathbf{u}_\theta = \mathbf{K}_y^{-1}\mathbf{K}_{y\theta}\mathbf{u}_\theta \tag{A.14}$$

Equations (A.13) and (A.14) should be satisfied for any $\mathbf{P}_y$ or $\mathbf{T}_R$. Thus,

$$\mathbf{e} = \mathbf{K}_{\theta y}\,\mathbf{K}_{y}^{-1} = \mathbf{K}_{y}^{-1}\,\mathbf{K}_{y\theta} \tag{A.15}$$

Since $\mathbf{e}$ was defined earlier to be diagonal, it is obvious from equation (A.15) that it is generally not possible to obtain unique centers of rigidity satisfying the definition given earlier in Section A.1.

A.3 Application to the Special Class of Buildings

For the special class of buildings described in Section 2.1, the lateral stiffness matrices of all frames spanning in the same direction are proportional. This leads to equation (3.8) of Section 3:

$$\mathbf{K}_{y\theta} = \mathbf{K}_{\theta y} = \frac{C_{y\theta}}{C_y}\,\mathbf{K}_y \tag{3.8}$$

Substituting equation (3.8) into (A.15), we obtain:

$$\mathbf{e} = \frac{C_{y\theta}}{C_y}\,\mathbf{K}_y\,\mathbf{K}_y^{-1} = \frac{C_{y\theta}}{C_y}\,\mathbf{I} \tag{A.16}$$

Thus, for buildings belonging to the special class of buildings, identified in Section 2.1, the static eccentricities of all floors are the same, given by:

$$e = \frac{C_{y\theta}}{C_y} \tag{3.9}$$

Since the centers of mass lie on a vertical line, the centers of rigidity also lie on a vertical line and are uniquely defined.

APPENDIX B: FRAME LATERAL STIFFNESS MATRIX

B.1 Model Frame

The frames considered are idealized as single-bay, five-story moment resisting plane frames with constant story height = h, and bay width = $2h$ (Figure 2b). All members are prismatic with constant cross-section. Only flexural deformations are considered in the analysis of the frames. All the beams have the same flexural stiffness EI_b and the column stiffness EI_c does not vary with height.

B.2 Formulation of Lateral Stiffness Matrix

The lateral stiffness matrix of any frame can be determined by the following steps:

1. Define one rotational degree of freedom per joint and one translational degree of freedom per floor, as shown in Figure 2b.

2. Obtain the element stiffnesses:

   (a) Beams contribute to rotational degrees of freedom only. Two rotational degrees of freedom are defined per beam:

$$\begin{Bmatrix} f_{\theta p} \\ f_{\theta q} \end{Bmatrix} = \mathbf{k}_b \begin{Bmatrix} \theta_p \\ \theta_q \end{Bmatrix} \tag{B.1}$$

   where $f_{\theta p}$ and $f_{\theta q}$ are the beam end moments; θ_p and θ_q the corresponding end rotations. For the special frames considered, the joint rotation index ρ is given by:

$$\rho = \frac{1}{4}\frac{I_b}{I_c} = \frac{1}{4}\frac{I_b}{I} \tag{2.2}$$

   from which,

$$I_b = 4\rho I \tag{B.2}$$

   so that:

$$\mathbf{k}_b = 2\rho\frac{EI}{h}\begin{bmatrix} 4 & 2 \\ 2 & 4 \end{bmatrix} \tag{B.3}$$

(b) Columns contribute to four degrees of freedom: two rotational (θ_p and θ_q) and two translational (v_p and v_q):

$$\begin{Bmatrix} f_{\theta p} \\ f_{\theta q} \\ f_{vp} \\ f_{vq} \end{Bmatrix} = \mathbf{k}_c \begin{Bmatrix} \theta_p \\ \theta_q \\ v_p \\ v_q \end{Bmatrix} \tag{B.4}$$

where $f_{\theta p}$ and $f_{\theta q}$ are the column end moments; and f_{vp} and f_{vq} the lateral end forces. Column stiffness matrix $\mathbf{k}_c$ is given by:

$$\mathbf{k}_c = \frac{EI}{h} \begin{bmatrix} 4 & 2 & -\frac{6}{h} & \frac{6}{h} \\ 2 & 4 & -\frac{6}{h} & \frac{6}{h} \\ -\frac{6}{h} & -\frac{6}{h} & \frac{12}{h^2} & -\frac{12}{h^2} \\ \frac{6}{h} & \frac{6}{h} & -\frac{12}{h^2} & \frac{12}{h^2} \end{bmatrix} \tag{B.5}$$

which in partitioned form becomes:

$$\mathbf{k}_c = \frac{EI}{h} \begin{bmatrix} \mathbf{k}_{c\theta\theta} & \mathbf{k}_{c\theta v} \\ \mathbf{k}_{cv\theta} & \mathbf{k}_{cvv} \end{bmatrix} \tag{B.6}$$

3. Assemble element stiffnesses in frame global stiffness $\mathbf{k}_T$:

$$\begin{Bmatrix} \mathbf{f}_v \\ \mathbf{f}_\theta \end{Bmatrix} = \mathbf{k}_T \begin{Bmatrix} \mathbf{v} \\ \boldsymbol{\theta} \end{Bmatrix} \tag{B.7}$$

where $\mathbf{v}$ are the lateral floor displacements and $\mathbf{f}_v$ the corresponding external lateral forces; $\boldsymbol{\theta}$ are the joint rotations and $\mathbf{f}_\theta$ the corresponding external moments. One can write:

$$\mathbf{k}_T = \begin{bmatrix} \mathbf{k}_{vv} & \mathbf{k}_{v\theta} \\ \mathbf{k}_{\theta v} & \mathbf{k}_{\theta\theta} \end{bmatrix} \tag{B.8}$$

Note that beam stiffness $\mathbf{k}_b$ contribute to $\mathbf{k}_{\theta\theta}$ only, $\mathbf{k}_{c\theta\theta}$ to $\mathbf{k}_{\theta\theta}$, $\mathbf{k}_{c\theta v}$ to $\mathbf{k}_{\theta v}$, $\mathbf{k}_{cv\theta}$ to $\mathbf{k}_{v\theta}$ and $\mathbf{k}_{cvv}$ to $\mathbf{k}_{vv}$.

4. Condense out the rotational degrees of freedom to obtain the frame lateral stiffness matrix. Since the external moments corresponding to joint rotations are zero, i.e. $\mathbf{f}_\theta = \mathbf{0}$, it follows that:

$$\mathbf{0} = \mathbf{k}_{\theta v}\,\mathbf{v} + \mathbf{k}_{\theta\theta}\,\boldsymbol{\theta} \tag{B.9}$$

from which

$$\boldsymbol{\theta} = -\mathbf{k}_{\theta\theta}^{-1}\,\mathbf{k}_{\theta v}\,\mathbf{v} = \mathbf{T}\,\mathbf{v} \tag{B.10}$$

where

$$\mathbf{T} = -\mathbf{k}_{\theta\theta}^{-1}\,\mathbf{k}_{\theta v} \tag{B.11}$$

Finally:

$$\mathbf{f}_v = \mathbf{k}_{vv}\,\mathbf{v} + \mathbf{k}_{v\theta}\,\boldsymbol{\theta} = [\,\mathbf{k}_{vv} + \mathbf{k}_{v\theta}\,\mathbf{T}\,]\,\mathbf{v} \tag{B.12}$$

and,

$$\mathbf{k} = \mathbf{k}_{vv} + \mathbf{k}_{v\theta}\,\mathbf{T} \tag{B.13}$$

is the frame lateral stiffness matrix.

B.3 Dimensionless Lateral Stiffness Matrix

The beam stiffness matrix $\mathbf{k}_b$, given by equation (B.3), is rewritten as:

$$\mathbf{k}_b = 2\rho\,\frac{EI}{h}\begin{bmatrix} 4 & 2 \\ 2 & 4 \end{bmatrix} = \frac{EI}{h}\,\mathbf{k}_b^o \tag{B.14}$$

where

$$\mathbf{k}_b^o = 2\rho\begin{bmatrix} 4 & 2 \\ 2 & 4 \end{bmatrix} \tag{B.15}$$

is dimensionless and depends on ρ. Similarly, the column stiffness matrix, given by equation (B.5), is rewritten as:

$$\mathbf{k}_c = \frac{EI}{h}\begin{bmatrix} \mathbf{k}_{c\theta\theta} & \mathbf{k}_{c\theta v} \\ \mathbf{k}_{cv\theta} & \mathbf{k}_{cvv} \end{bmatrix} = \begin{bmatrix} \frac{EI}{h}\mathbf{k}^o_{c\theta\theta} & \frac{EI}{h^2}\mathbf{k}^o_{c\theta v} \\ \frac{EI}{h^2}\mathbf{k}^o_{cv\theta} & \frac{EI}{h^3}\mathbf{k}^o_{cvv} \end{bmatrix} \tag{B.16}$$

where $\mathbf{k}^o_{c\theta\theta}$, $\mathbf{k}^o_{c\theta v}$, $\mathbf{k}^o_{cv\theta}$ and $\mathbf{k}^o_{cvv}$ are dimensionless submatrices given by:

$$\mathbf{k}^o_{c\theta\theta} = \begin{bmatrix} 4 & 2 \\ 2 & 4 \end{bmatrix} \tag{B.17a}$$

$$\mathbf{k}^o_{c\theta v} = \mathbf{k}^{o^T}_{cv\theta} = \begin{bmatrix} -6 & 6 \\ -6 & 6 \end{bmatrix} \tag{B.17b}$$

$$\mathbf{k}^o_{cvv} = \begin{bmatrix} 12 & -12 \\ -12 & 12 \end{bmatrix} \tag{B.17c}$$

Since the individual stiffness submatrices contribute only to parts of the global stiffness matrix $\mathbf{k}_T$, introducing equations (B.14) and (B.16) into (B.8) leads to:

$$\mathbf{k}_T = \begin{bmatrix} \mathbf{k}_{vv} & \mathbf{k}_{v\theta} \\ \mathbf{k}_{\theta v} & \mathbf{k}_{\theta\theta} \end{bmatrix} = \begin{bmatrix} \frac{EI}{h^3}\mathbf{k}^o_{vv} & \frac{EI}{h^2}\mathbf{k}^o_{v\theta} \\ \frac{EI}{h^2}\mathbf{k}^o_{\theta v} & \frac{EI}{h}\mathbf{k}^o_{\theta\theta} \end{bmatrix} \tag{B.18}$$

where $\mathbf{k}^o_{vv}$, $\mathbf{k}^o_{\theta v}$, $\mathbf{k}^o_{v\theta}$ and $\mathbf{k}^o_{\theta\theta}$ are dimensionless submatrices, with $\mathbf{k}^o_{\theta\theta}$ the only submatrix dependent on ρ, due to dependence of $\mathbf{k}^o_b$ on ρ. Substituting equations (B.18) into (B.10) yields:

$$\boldsymbol{\theta} = -\mathbf{k}^{-1}_{\theta\theta}\mathbf{k}_{\theta v}\mathbf{v} = \mathbf{T}\mathbf{v} = \frac{-h}{EI}(\mathbf{k}^o_{\theta\theta})^{-1}\frac{EI}{h^2}\mathbf{k}^o_{\theta v}\mathbf{v}$$

$$= -\frac{1}{h}(\mathbf{k}^o_{\theta\theta})^{-1}\mathbf{k}^o_{\theta v}\mathbf{v} = \frac{1}{h}\mathbf{T}^o\mathbf{v} \tag{B.19}$$

with

$$\mathbf{T}^o = -(\mathbf{k}^o_{\theta\theta})^{-1}\mathbf{k}^o_{\theta v} \tag{B.20}$$

and

$$\mathbf{T} = \frac{1}{h}\mathbf{T}^o \tag{B.21}$$

Equations (B.12) become:

$$\mathbf{f}_v = \frac{EI}{h^3}\left[\mathbf{k}^o_{vv} + \mathbf{k}^o_{v\theta}\mathbf{T}^o\right]\mathbf{v} = \frac{EI}{h^3}\mathbf{k}^o\mathbf{v} \tag{B.22}$$

where

$$\mathbf{k}^o = \mathbf{k}^o_{vv} + \mathbf{k}^o_{v\theta}\mathbf{T}^o \tag{B.23}$$

is a dimensionless matrix that depends on ρ due to the dependence of $\mathbf{T}^o$ on ρ. Therefore, the frame lateral stiffness matrix $\mathbf{k}$ is given by:

$$\mathbf{k} = \frac{EI}{h^3}\mathbf{k}^o \tag{B.24}$$

B.4 Derivation of Equation (3.18)

Specializing equations (B.24) to frame (1) yields its lateral stiffness matrix, which also equals the building lateral stiffness matrix $\mathbf{K}_y$:

$$\mathbf{k}_{y1} = \mathbf{K}_y = \frac{EI_1}{h^3}\mathbf{k}^o_{y1} \tag{B.25}$$

where I_1 is the column moment of inertia of frame (1) and $\mathbf{k}^o_{y1}$ is a dimensionless lateral stiffness matrix which depends only on ρ_1, the joint rotation index of frame (1). Similarly, the lateral stiffness matrix of frame (2) is given by:

$$\mathbf{k}_{x2} = \frac{EI_2}{h^3}\mathbf{k}^o_{x2} \tag{B.26}$$

where I_2 is the column moment of inertia of frame (2), and $\mathbf{k}^o_{x2}$ is a dimensionless matrix which depends on ρ_2, the joint rotation index of frame (2). Clearly, when $\rho_1 = \rho_2 = \rho$ then:

$$\mathbf{k}^o_{x2} = \mathbf{k}^o_{y1} = \mathbf{k}^o \tag{B.27}$$

and,

$$\mathbf{k}_{x2} = \frac{I_2}{I_1}\mathbf{k}_{y1} = \frac{I_2}{I_1}\mathbf{K}_y \tag{3.18}$$

APPENDIX C: IMPLEMENTATION OF ANALYSIS PROCEDURE

The lateral stiffness matrices of the frames were shown in Appendix B to be proportional to a dimensionless stiffness matrix that depends only on the joint rotation index ρ. Utilizing this result and the analysis procedure described in Section 4, the response of the torsionally-coupled multi-story building of Figure 2a with $\rho_1 = \rho_2 = \rho$ is expressed in terms of dimensionless response quantities, with the purpose of improving computational efficiency.

C.1 Vibration Frequencies and Mode Shapes

C.1.1 Corresponding Torsionally-Uncoupled, Multi-story System

The lateral vibration frequencies ω_{yj} and mode shapes $\boldsymbol{\psi}_j$ are determined by solving the eigen-equations (4.2a):

$$(\mathbf{K}_y - \omega_{yj}^2 \mathbf{m})\boldsymbol{\psi}_j = \mathbf{0} \quad j=1,\ldots,N \tag{4.2a}$$

where $\mathbf{m}$ is a diagonal mass matrix of dimension N, the number of stories, of diagonal entries equal to m, the mass of each story, i.e.

$$\mathbf{m} = m\,\mathbf{m}^o = m\,\mathbf{I} \tag{C.1}$$

where $\mathbf{m}^o$ and $\mathbf{I}$ are identity matrices of dimension N. Substituting equations (B.25), (B.27) and (C.1) into (4.2a), and dividing by mh^3/EI_1, we obtain:

$$(\mathbf{k}^o - \lambda_{yj}^2 \mathbf{m}^o)\boldsymbol{\psi}_j = \mathbf{0} \tag{C.2}$$

where

$$\lambda_{yj}^2 = \frac{mh^3}{EI_1}\omega_{yj}^2 \tag{C.3}$$

from which,

$$\omega_{yj} = \sqrt{\frac{EI_1}{mh^3}}\lambda_{yj} \quad j=1,\ldots,N \tag{C.4}$$

$$\frac{\omega_{yj}}{\omega_{y1}} = \frac{\lambda_{yj}}{\lambda_{y1}} \quad \text{or} \quad \omega_{yj} = \frac{\lambda_{yj}}{\lambda_{y1}}\,\omega_{y1} \tag{C.5}$$

and,

$$\omega_{y1} = \sqrt{\frac{EI_1}{mh^3}}\,\lambda_{y1} \tag{C.6}$$

Since $\mathbf{k}^o$ depends on ρ, the dimensionless frequencies λ_{yj}, the ratios $\lambda_{yj}/\lambda_{y1}$ or ω_{yj}/ω_{y1} as well as the mode shapes $\boldsymbol{\psi}_j$ depend on ρ. Thus, the fundamental uncoupled lateral frequency ω_{y1} (or period $T_{y1} = 2\pi/\omega_{y1}$) can be varied by adequately varying the geometric constants EI_1, m and h.

C.1.2 Torsionally-coupled, Multi-story Building

The vibration frequencies ω_{nj} and mode shapes of the coupled multi-story building are determined from equations (4.10) and (4.11):

$$\omega_{nj} = \bar{\omega}_n\,\omega_{yj} \tag{4.10}$$

and,

$$\boldsymbol{\phi}_{nj} = \begin{Bmatrix} \phi_{ynj} \\ \phi_{\theta nj} \end{Bmatrix} = \begin{Bmatrix} \alpha_{yn}\,\boldsymbol{\psi}_j \\ \alpha_{\theta n}\,\boldsymbol{\psi}_j \end{Bmatrix} \tag{4.11}$$

for n=1,2 and j=1 to N, with $\bar{\omega}_n$ and $\boldsymbol{\alpha}_n$, where $\boldsymbol{\alpha}_n^T = <\alpha_{yn}\ \ \alpha_{\theta n}>$, the normalized frequencies and mode shapes of the associated one-story system. Substituting equation (C.5b) into (4.10), we get:

$$\omega_{nj} = \bar{\omega}_n \frac{\lambda_{yj}}{\lambda_{y1}}\,\omega_{y1} \tag{C.7}$$

Since $\bar{\omega}_n$ and $\boldsymbol{\alpha}_n$ depend on eccentricity ratio e/r and uncoupled torsional to lateral frequency ratio Ω, (equations (4.22) and (4.23)), and $\lambda_{yj}/\lambda_{y1}$ and $\boldsymbol{\psi}_j$ depend on ρ, it follows that the coupled frequencies ω_{nj} depend on e/r, Ω, ρ and T_{y1} (or ω_{y1}), while $\boldsymbol{\phi}_{nj}$ depend on e/r, Ω and ρ.

C.2 Modal Response Maxima

C.2.1 Corresponding Uncoupled Multi-story System

Taking advantage of the invariance of the mode shapes $\boldsymbol{\psi}_j$ and the frequency ratios ω_{yj}/ω_{y1} when T_{y1} varies, the responses of the corresponding uncoupled multi-story system in each mode are expressed in terms of dimensionless response quantities. Substituting equation (C.1) into (4.13), we obtain:

$$L_j = \boldsymbol{\psi}_j^T \mathbf{m} \mathbf{1} = m\ \boldsymbol{\psi}_j^T \mathbf{m}^o \mathbf{1} = m\ L_j^o \tag{C.8a}$$

and

$$M_j = \boldsymbol{\psi}_j^T \mathbf{m} \boldsymbol{\psi}_j = m\ \boldsymbol{\psi}_j^T \mathbf{m}^o \boldsymbol{\psi}_j = m\ M_j^o \tag{C.8b}$$

and the ratios

$$\frac{L_j}{M_j} = \frac{L_j^o}{M_j^o} \tag{C.9}$$

Using equations (C.5) and (C.9), the floor displacements vector, given by equation (4.12), becomes:

$$\mathbf{v}_j = \frac{L_j}{M_j\, \omega_{yj}^2} S_{aj}\, \boldsymbol{\psi}_j = \frac{S_{aj}}{\omega_{y1}^2} \frac{L_j^o/M_j^o}{(\lambda_{yj}/\lambda_{y1})^2} \boldsymbol{\psi}_j = \frac{S_{aj}}{\omega_{y1}^2}\, \mathbf{v}_j^o \tag{C.10}$$

where $\mathbf{v}_j^o$ is dimensionless and depends only on ρ.

The equivalent static lateral forces, given by equations (4.14), are written as:

$$\mathbf{f}_j = \omega_{yj}^2 \mathbf{m} \mathbf{v}_j = m\, S_{aj} \frac{L_j^o}{M_j^o} \mathbf{m}^o \boldsymbol{\psi}_j = m\, S_{aj}\, \mathbf{f}_j^o \tag{C.11}$$

in which equations (C.1) and (C.10) have been introduced.

Using equations (C.11) in (4.15), the vector of story shears becomes:

$$\mathbf{V}_j = \mathbf{S} \mathbf{f}_j = m\, S_{aj}\, \mathbf{S} \mathbf{f}_j^o = m\, S_{aj}\, \mathbf{V}_j^o \tag{C.12}$$

where $\mathbf{V}_j^o$ is dimensionless and depends on ρ; $\mathbf{S}$ is a summation matrix given by equation (4.17). Similarly, the vector of story overturning moments, given by equations (4.16), is written as:

$$\mathbf{M}_j = \mathbf{H}\,\mathbf{f}_j = m\,h\,S_{aj}\,\mathbf{H}^o\,\mathbf{f}_j^o = m\,h\,S_{aj}\,\mathbf{M}_j^o \tag{C.13}$$

where $\mathbf{H}$ is given by equation (4.17),

$$\mathbf{H}^o = \frac{1}{h}\,\mathbf{H} \tag{C.14}$$

and $\mathbf{M}_j^o$ is dimensionless and depends only on ρ.

Joint rotations of equations (B.19) are expressed as:

$$\boldsymbol{\theta}_j = \frac{1}{h}\,\mathbf{T}^o\,\mathbf{v}_j = \frac{1}{h}\,\frac{S_{aj}}{\omega_{y1}^2}\,\mathbf{T}^o\,\mathbf{v}_j^o = \frac{1}{h}\,\frac{S_{aj}}{\omega_{y1}^2}\,\boldsymbol{\theta}_j^o \tag{C.15}$$

where $\boldsymbol{\theta}_j^o$ are dimensionless and depend on ρ.

Beam moments are computed using equations (B.1) and (B.14) and the corresponding end joint rotations extracted from $\boldsymbol{\theta}_j$, given by equation (C.15). We can write:

$$\begin{Bmatrix} M_{bpj} \\ M_{bqj} \end{Bmatrix} = \begin{Bmatrix} f_{\theta pj} \\ f_{\theta qj} \end{Bmatrix} = \frac{EI_1}{h}\,\mathbf{k}_b^o \begin{Bmatrix} \theta_{pj} \\ \theta_{qj} \end{Bmatrix} = \frac{EI_1}{h^2}\,\frac{S_{aj}}{\omega_{y1}^2}\,\mathbf{k}_b^o \begin{Bmatrix} \theta_{pj}^o \\ \theta_{qj}^o \end{Bmatrix}$$

$$= \frac{EI_1}{h^2}\,\frac{S_{aj}}{\omega_{y1}^2} \begin{Bmatrix} M_{bpj}^o \\ M_{bqj}^o \end{Bmatrix} \tag{C.16}$$

Similarly, the column end moments are computed using equations (B.4) and (B.16) as well as the corresponding end joint rotations and end joint displacements extracted from $\boldsymbol{\theta}_j$ and $\mathbf{v}_j$, given by equations (C.15) and (C.10), respectively. We obtain:

$$\begin{Bmatrix} M_{cpj} \\ M_{cqj} \end{Bmatrix} = \begin{Bmatrix} f_{\theta pj} \\ f_{\theta qj} \end{Bmatrix} = \frac{EI_1}{h}\,\mathbf{k}_{c\theta\theta}^o \begin{Bmatrix} \theta_{pj} \\ \theta_{qj} \end{Bmatrix} + \frac{EI_1}{h^2}\,\mathbf{k}_{c\theta v}^o \begin{Bmatrix} v_{pj} \\ v_{qj} \end{Bmatrix}$$

$$= \frac{EI_1}{h^2}\,\frac{S_{aj}}{\omega_{y1}^2}\,\mathbf{k}_{c\theta\theta}^o \begin{Bmatrix} \theta_{pj}^o \\ \theta_{qj}^o \end{Bmatrix} + \frac{EI_1}{h^2}\,\frac{S_{aj}}{\omega_{y1}^2}\,\mathbf{k}_{c\theta v}^o \begin{Bmatrix} v_{pj}^o \\ v_{qj}^o \end{Bmatrix}$$

$$= \frac{EI_1}{h^2} \frac{S_{aj}}{\omega_{y1}^2} \begin{Bmatrix} M_{cpj}^o \\ M_{cqj}^o \end{Bmatrix} \tag{C.17}$$

For the first story $M_{cqj} = 0$.

Column axial forces are computed using statics. The column axial force in the l^{th} floor is obtained from:

$$P_{cj}^l = \frac{1}{2h} [M_{bpj}^l + M_{bqj}^l] + P_{cj}^{l+1} \tag{C.18}$$

with $P_{cj}^{l+1} = 0$ for $l = 5$. Thus, we can write:

$$Pclj = \frac{EI_1}{h^3} \frac{S_{aj}}{\omega_{y1}^2} [\frac{1}{2} (M_{bpj}^{lo} + M_{bqj}^{lo}) + P_{cj}^{l+1\,o}]$$

$$= \frac{EI_1}{h^3} \frac{S_{aj}}{\omega_{y1}^2} P_{cj}^{lo} \tag{C.19}$$

In summary, the modal responses of the uncoupled multi-story system can be expressed in the form:

$$r_j = r_c S_{aj} r_j^o \tag{C.20a}$$

where r_j^o, defined by equations (C.10) to (C.19), are dimensionless and depend only on ρ, while r_c are constants, also given in equations (C.10) to (C.19), that depend on m, h, EI_1 and/or ω_{y1}.

C.2.2 Torsionally-coupled, Multi-story Building

The modal responses of the torsionally-coupled multi-story building are given by equations (4.48) to (4.65), with their special form summarized in equation (4.66):

$$r_{nj} = \overline{r}_{nj} r_j \tag{4.66}$$

with $\overline{r}_{nj}$ the normalized response quantity, given by equations (4.42) to (4.46), in the associated one-story system with uncoupled lateral vibration frequency equal to ω_{yj}. These can also be written as products of dimensionless quantities that depend only on e/r and Ω, and the ratio of the pseudo-

acceleration response spectrum ordinate S_{anj}/S_{aj}:

$$\overline{r}_{nj} = \overline{r}_n^o \frac{S_{anj}}{S_{aj}} \tag{C.20b}$$

Substituting equations (C.20) into (4.66), we obtain:

$$r_{nj} = r_c S_{anj} \overline{r}_n^o r_j^o \tag{C.21}$$

Thus, the lateral displacements at the centers of mass are given by:

$$\mathbf{u}_{ynj} = \frac{S_{anj}}{\omega_{y1}^2} \bar{u}_{yn}^o \mathbf{v}_j^o \tag{C.22}$$

deck rotations:

$$\mathbf{u}_{\theta nj} = \frac{S_{anj}}{\omega_{y1}^2} \bar{u}_{\theta n}^o \mathbf{v}_j^o \tag{C.23}$$

lateral displacements at the centers of rigidity:

$$\mathbf{v}_{nj} = \frac{S_{anj}}{\omega_{y1}^2} \bar{v}_n^o \mathbf{v}_j^o \tag{C.24}$$

story shears:

$$\mathbf{V}_{nj} = m S_{anj} \bar{V}_n^o \mathbf{V}_j^o \tag{C.25}$$

story overturning moments:

$$\mathbf{M}_{nj} = m h S_{anj} \bar{M}_n^o \mathbf{M}_j^o \tag{C.26}$$

story torques at the centers of mass:

$$\mathbf{T}_{Mnj} = m r S_{anj} \bar{T}_{Mn}^o \mathbf{V}_j^o \tag{C.27}$$

story torques at the centers of rigidity:

$$\mathbf{T}_{Rnj} = m r S_{anj} \bar{T}_{Rn}^o \mathbf{V}_j^o \tag{C.28}$$

a beam moment of frame (1):

$$M_{bnj} = \frac{EI_1}{h^2} \frac{S_{anj}}{\omega_{y1}^2} \bar{v}_n^o M_{bj}^o \tag{C.29}$$

a column moment of frame (1)

$$M_{cnj} = \frac{EI_1}{h^2} \frac{S_{anj}}{\omega_{y1}^2} \bar{v}_n^o M_{cj}^o \tag{C.30}$$

and a column axial force of frame (1) by:

$$P_{cnj} = \frac{EI_1}{h^3} \frac{S_{anj}}{\omega_{y1}^2} \bar{v}_n^o P_{cj}^o \tag{C.31}$$

Equations (C.21) to (C.31) give the modal responses of the torsionally-coupled building expressed in terms of quantities r_j^o and $\bar{r}_n^o$ that are invariant as T_{y1} varies. Thus, for fixed values of ρ, e/r and Ω, r_j^o and $\bar{r}_n^o$ need to be computed once. Taking advantage of the invariances of r_j^o and $\bar{r}_n^o$ when T_{y1} changes, these were computed in advance for each e/r, Ω and ρ case, and then used for each of the different fundamental uncoupled lateral period T_{y1} considered, avoiding in this way a considerable amount of numerical computation.

C.3 Maximum Response

Maximum response of the torsionally-coupled building are computed by combining the modal maxima acording to CQC, as given by equation (4.67):

$$r = \left[\sum_{j=1}^{5} \sum_{k=1}^{5} \sum_{n=1}^{2} \sum_{m=1}^{2} \gamma_{nj,mk} \bar{r}_n \bar{r}_m r_j r_k \right]^{1/2} \tag{4.67}$$

where $\gamma_{nj,mk}$ is given by equation (4.36) for frequency ratios $q_{nj,mk}$, given by equation (4.68).

C.4 Normalization Factors

The responses are presented in dimensionless forms by normalizing each by a meaningful normalization factor, given in Table 8 for the response quantities in interest. The choices of the normalization factors for floor displacements, frame (1) beam moments, frame (1) column moments and frame (1) column axial forces are rather obvious from equations (C.24), (C.29), (C.30) and

(C.31), respectively. In these $\bar{u}_g$, the maximum ground displacement, is chosen to nondimensionalize S_{anj}/ω_{y1}^2. On the other hand, the normalization factors for story shears, story overturning moments and story torques are of special forms that require further explanation.

The normalization factors for the story shears and story overturning moments are $W_1^* \bar{a}_g/g$ and $W_1^* h_1^* \bar{a}_g/g$, where $\bar{a}_g$ is the maximum ground acceleration, W_1^* and h_1^* were defined in Section 4.2 as the effective weight and height of the uncoupled multi-story system in its fundamental vibration mode, and given by equations (4.20). These normalization factors are the base shear and base overturning moment of a rigid single-degree-of-freedom system with lumped weight W_1^* and height h_1^*. Substituting equations (C.1), (C.8) and (C.9) into (4.20), we obtain:

$$W_1^* = \frac{L_1^2}{M_1} g = m g \frac{L_1^{o^2}}{M_1^o} = m g W_1^{*o} \tag{C.32}$$

and,

$$h_1^* = \frac{h < 1 \;\; 2 \;\; 3 \;\; 4 \;\; 5 > \mathbf{m} \boldsymbol{\psi}_1}{L_1} = h \frac{< 1 \;\; 2 \;\; 3 \;\; 4 \;\; 5 > \mathbf{m}^o \boldsymbol{\psi}_1}{L_1^o}$$

$$= h \; h_1^{*o} \tag{C.33}$$

Thus, referring to equations (C.25) and (C.26) the normalization factors:

$$W_1^* \frac{\bar{a}_g}{g} = m \bar{a}_g W_1^{*o} \tag{C.34}$$

and

$$W_1^* h_1^* \frac{\bar{a}_g}{g} = m h \bar{a}_g W_1^{*o} h_1^{*o} \tag{C.35}$$

nondimensionalize $m S_{anj}$ and $m h S_{anj}$, respectively.

The normalization factor for story torques at centers of rigidity is $e_1^* \overline{W}_1^* W_1^* \bar{a}_g/g$, which as was explained in Section 6, is the torque of the rigid single-degree-of-freedom system at an eccentricity

of $e_1^* \bar{W}_1^*$, given by equation (4.46) and plotted in Figure C.1, and which equals the dynamic eccentricity of the associated one-story system in its fundamental mode, computed for unit pseudo-acceleration. The story torques given by equation (C.28) normalized by $e_1^* \bar{W}_1^* W_1^* \bar{a}_g / g$ become:

$$\frac{g}{e_1^* \bar{W}_1^* W_1^* \bar{a}_g} \mathbf{T}_{Rnj} = \frac{S_{anj}}{\bar{a}_g} \frac{\bar{T}_{Rn}^o}{\bar{T}_{R1}^o} \frac{1}{W_1^{*o}} \mathbf{V}_j^o \tag{C.36}$$

with $\bar{T}_{Rn}^o$ (n=1,2) and $\bar{T}_{R1}^o$ depending on e/r and Ω only.

With these proper normalizations, the structural characteristics (E, I_1, m, r and h) are not included in the computation of the response quantities.

C.5 Computer Program Outline

A complete, although not very detailed, flow chart of the computer program developed to carry out the computations described above is given in this section. The program is written in FORTRAN and was checked against SAP80 [1].

PROGRAM SPNRMB

Read parameters ρ, e/r and Ω

For ρ

Form the total stiffness matrix of the corresponding torsionallly-uncoupled, multi-story system $\mathbf{k}_T^o$

Compute the lateral stiffness matrix of the corresponding torsionally-uncoupled, multi-story system $\mathbf{k}^o$

Form mass matrix $\mathbf{m}^o$

Compute the uncoupled lateral frequencies λ_{yj} and mode shapes $\boldsymbol{\psi}_j$

Compute dimensionless modal responses r_j^o of the corresponding torsionally-uncoupled, multi-story system

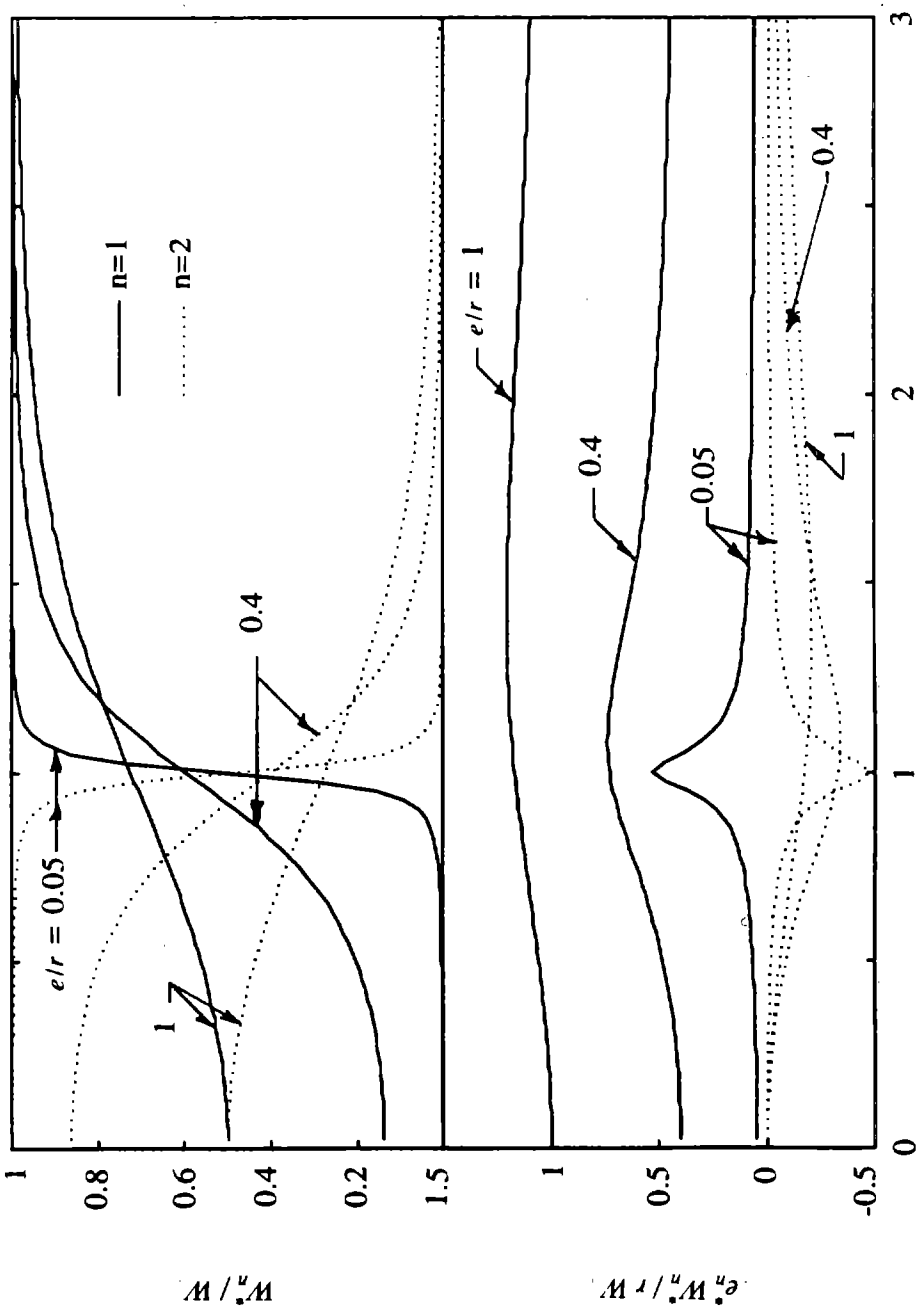

FIGURE C.1 Normalized Unit Modal Lateral and Torsional Quantities W_n^* / W and $e_n^* W_n^* / r W$ for Associated One-story Systems

For e/r and Ω

Compute normalized frequencies $\bar{\omega}_n$ and mode shapes $\boldsymbol{\alpha}_n$ of the associated torsionally-coupled, one-story system

Compute normalized dimensionless responses $\overline{r}_n^o$ of the associated torsionally-coupled, one-story system

Read number of fundamental uncoupled lateral period cases

For each fundamental uncoupled lateral period case

Read fundamental uncoupled lateral period T_{y1}

Compute frequencies $\omega_{nj} = \bar{\omega}_n (\lambda_{yj}/\lambda_{y1}) \omega_{y1}$

Read pseudo-acceleration response spectrum ordinate S_{anj}

Compute modal maxima $S_{anj}\ \overline{r}_n^o\, r_j^o$

Estimate maxima of response by CQC

Normalize responses

Print results

APPENDIX D: INFLUENCE OF MODAL CROSS-CORRELATION

D.1 Derivation of Equation (4.70)

Estimate of the maximum r of a response quantity is determined by combining its modal maxima r_{nj} according to CQC:

$$r = \left[\sum_{j=1}^{5} \sum_{k=1}^{5} \sum_{n=1}^{2} \sum_{m=1}^{2} \gamma_{nj,mk} \bar{r}_n \bar{r}_m r_j r_k \right]^{1/2} \tag{4.67}$$

where $\gamma_{nj,mk}$ is computed by equation (4.36) for frequency ratios $q_{nj,mk}$, given by equation (4.68). The cross-correlation factor $\gamma_{nj,mk}$ is negligible if $q_{nj,mk}$ is below 0.8 or above 1.25 [15].

The summation given by equation (4.67) involves $(2N)^2$ or 100 terms, which are all taken into account in this study. However, in order to interpret the results of Section 8, equation (4.67) is explicitly written as:

$$r^2 = \sum_{j=1}^{5} \sum_{n=1}^{2} r_{nj}^2 + 2 \sum_{j=1}^{5} \gamma_{1j,2j} r_{1j} r_{2j} + 2 \sum_{j=1}^{4} \sum_{k=j+1}^{5} \gamma_{2j,1k} r_{2j} r_{1k}$$

$$+ 2 \sum_{j=1}^{4} \sum_{k=j+1}^{5} \gamma_{1j,2k} r_{1j} r_{2k} + 2 \sum_{j=1}^{4} \sum_{k=j+1}^{5} \gamma_{1j,1k} r_{1j} r_{1k} + 2 \sum_{j=1}^{4} \sum_{k=j+1}^{5} \gamma_{2j,2k} r_{2j} r_{2k} \tag{4.69}$$

While the first double summation of equation (4.69) represents SRSS, the next five summations represent the cross-correlation terms between various modes of vibration: the first represents cross-correlation between modes '1j' and '2j' of the same pair 'j'; the second represents cross-correlation between modes '2j' and '1k', (j=1 to 4 and k=j+1 to 5), which are of different nature and belong to different pairs 'j' and 'k', such as modes '21' and '12', '13', '14' and '15', or '22' and '13', '14' and '15', ... etc.; the third represents cross-correlation terms between modes '1j' and '2k', (j=1 to 4 and k=j+1 to 5), which are of different nature and belong to different pairs 'j' and 'k', such as modes '11' and '22', '23', '24' and '25', or '12' and '23', '24' and '25', ... etc.; the fourth represents cross-correlation terms between modes '1j' and '1k', (j=1 to 4 and k=j+1 to 5), which are of the same nature but belong to different pairs 'j' and 'k', such as modes '11' and '12', '13', '14' and '15', or '12' and '13', '14' and '15', ... etc.; and the fifth represents cross-correlation

terms between modes '2j' and '2k', (j=1 to 4 and k=j+1 to 5), which are of the same nature but belong to different pairs 'j' and 'k', such as modes '21' and '22', '23', '24' and '25', or '22' and '23', '24' and '25', ... etc.. It is shown in Section 5 that frequencies w_{1j} and w_{2k}, w_{1j} and w_{1k}, and w_{2j} and w_{2k}, (j=1 to 4 and k=j+1 to 5), are widely spaced. It follows that $\gamma_{1j,2k}$, $\gamma_{1j,1k}$ and $\gamma_{2j,2k}$, (for j=1 to 4 and k=j+1 to 5), are negligibly small, and the last three double summations of equation (4.69) are negligible. Equation (4.69) can, therefore, be approximated by:

$$r^2 \approx \sum_{j=1}^{5} \sum_{n=1}^{2} r_{nj}^2 + 2 \sum_{j=1}^{5} \gamma_{1j,2j}\, r_{1j}\, r_{2j} + 2 \sum_{j=1}^{4} \sum_{k=j+1}^{5} \gamma_{2j,1k}\, r_{2j}\, r_{1k} \tag{4.70}$$

D.2 Normalized Coupled to Uncoupled Responses for the Idealized Spectra

The maximum response r_o of the corresponding uncoupled multi-story system is determined by combining its modal maxima r_j according to SRSS:

$$r_o^2 = \sum_{j=1}^{5} r_j^2 \tag{D.1}$$

The effect of lateral-torsional coupling is studied by comparing the coupled responses to the corresponding responses in the uncoupled system. The ratios r/r_o are given by:

$$(\frac{r}{r_o})^2 \approx \frac{\sum_{j=1}^{5} \sum_{n=1}^{2} r_{nj}^2 + 2 \sum_{j=1}^{5} \gamma_{1j,2j}\, r_{1j}\, r_{2j}}{\sum_{j=1}^{5} r_j^2} + 2\, \frac{\sum_{j=1}^{4} \sum_{k=j+1}^{5} \gamma_{2j,1k}\, r_{2j}\, r_{1k}}{\sum_{j=1}^{5} r_j^2} \tag{D.2}$$

Noting that $\gamma_{1j,2j}$ is computed for $q_{1j,2j} = \Omega_1/\Omega_2$, it is obvious that $\gamma_{1j,2j}$ equals γ_{12}, the cross-corelation factor between the two vibartion modes of the associated one-story system. Using this fact and substituting equations (C.20) and (C.21) into (D.2), we obtain:

$$(\frac{r}{r_o})^2 \approx \frac{\sum_{j=1}^{5} \sum_{n=1}^{2} (\overline{r}_n^o\, r_j^o\, S_{anj})^2 + 2\, \gamma_{12}\, \overline{r}_1^o\, \overline{r}_2^o \sum_{j=1}^{5} (r_j^o)^2\, S_{a1j}\, S_{a2j}}{\sum_{j=1}^{5} (r_j^o\, S_{aj})^2}$$

$$+ 2\,\overline{r}_1^{o}\,\overline{r}_2^{o}\,\frac{\sum_{j=1}^{4}\sum_{k=j+1}^{5}\gamma_{2j,1k}\,r_j^{o}\,r_k^{o}\,S_{a2j}\,S_{a1k}}{\sum_{j=1}^{5}(r_j^{o}\,S_{aj})^2} \tag{D.3}$$

Specializing equations (D.3) to a flat pseudo-acceleration spectrum where:

$$S_{anj} = S_{aj} = S_{a1} = S_{a2} \tag{D.4}$$

we obtain:

$$(\frac{r}{r_o})^2 \approx (\overline{r}_1^{o^2} + \overline{r}_2^{o^2} + 2\gamma_{12}\,\overline{r}_1^{o}\,\overline{r}_2^{o}) + 2\,\overline{r}_1^{o}\,\overline{r}_2^{o}\,\frac{\sum_{j=1}^{4}\sum_{k=j+1}^{5}\gamma_{2j,1k}\,r_j^{o}\,r_k^{o}}{\sum_{j=1}^{5}(r_j^{o})^2} \tag{D.5}$$

or,

$$(\frac{r}{r_o})^2 \approx \overline{r}^{\,2} + 2\,\overline{r}_1^{o}\,\overline{r}_2^{o}\,\frac{\sum_{j=1}^{4}\sum_{k=j+1}^{5}\gamma_{2j,1k}\,r_j^{o}\,r_k^{o}}{\sum_{j=1}^{5}(r_j^{o})^2} \tag{D.6}$$

in which equations (4.47) have been introduced and $\overline{r}$ is the normalized coupled to uncoupled response of the associated one-story system computed for a flat spectrum.

For a hyperbolic pseudo-acceleration spectrum we can write:

$$\frac{S_{anj}}{S_{aj}} = \frac{\omega_{nj}}{\omega_{yj}} = \Omega_n \quad \text{and} \quad \frac{S_{aj}}{S_{a1}} = \frac{\omega_{yj}}{\omega_{y1}} = \frac{\lambda_{yj}}{\lambda_{y1}} \tag{D.7}$$

Using equations (4.22), it can be shown that $\Omega_1\,\Omega_2 = \Omega$, then equations (D.3) become:

$$(\frac{r}{r_o})^2 \approx (\overline{r}_1^{o^2}\,\Omega_1^2 + \overline{r}_2^{o^2}\,\Omega_2^2 + 2\gamma_{12}\Omega\overline{r}_1^{o}\overline{r}_2^{o}) + 2\overline{r}_1^{o}\overline{r}_2^{o}\Omega\,\frac{\sum_{j=1}^{4}\sum_{k=j+1}^{5}\gamma_{2j,1k}\,r_j^{o}r_k^{o}(\lambda_{yj}/\lambda_{y1})(\lambda_{yk}/\lambda_{y1})}{\sum_{j=1}^{5}(r_j^{o}(\lambda_{yj}/\lambda_{y1}))^2} \tag{D.8}$$

or,

$$(\frac{r}{r_o})^2 \approx \overline{r}^2 + 2\,\overline{r}_1^o\,\overline{r}_2^o\,\Omega\,\frac{\sum_{j=1}^{4}\sum_{k=j+1}^{5}\gamma_{2j,1k}\,r_j^o\,r_k^o\,(\lambda_{yj}/\lambda_{y1})\,(\lambda_{yk}/\lambda_{y1})}{\sum_{j=1}^{5}(r_j^o\,(\lambda_{yj}/\lambda_{y1}))^2} \qquad \text{(D.9)}$$

where $\overline{r}$ is the normalized coupled to uncoupled response of the associated one-story system computed for a hyperbolic spectrum.

D.3 Influence of Cross-Correlation Terms

Equations (D.6) and (D.9) indicate that the normalized coupled to uncoupled responses of the multi-story building in the case of the flat or hyperbolic idealized spectra, equal the sum of the normalized coupled to uncoupled responses of the associated one-story system computed for the flat or hyperbolic spectrum, as the case may be, and terms that arise due to cross-correlation between vibration modes '2j' and '1k' (j=1 to 4 and k=j+1 to 5). In other words, the differences between the normalized responses of the two coupled systems-- multi-story and its associated one-story-- are due to the contributions of the terms arising from cross-correlation between vibration modes '2j' and '1k' for j=1 to 4 and k=j+1 to 5.

For the flat spectrum, each of the cross-correlation terms is proportional to the cross-correlation factor $\gamma_{2j,1k}$ ($\gamma_{21,12}$ and $\gamma_{21,13}$ are shown in Figure 14), the product of the normalized modal responses $\overline{r}_1^o\overline{r}_2^o$ of the associated one-story system and the product of the modal responses $r_j^o r_k^o$ of the corresponding uncoupled multi-story system. For the hyperbolic spectrum, each of the cross-correlation terms is proportional to $\gamma_{2j,1k}$, $\overline{r}_1^o\overline{r}_2^o\Omega$, $r_j^o r_k^o$ and the frequency ratios $\lambda_{yj}/\lambda_{y1}$ and $\lambda_{yk}/\lambda_{y1}$. Therefore, the values of the cross-correlation terms depend on the values of $\gamma_{2j,1k}$, $\overline{r}_1^o\overline{r}_2^o$, $r_j^o r_k^o$ and $\lambda_{yj}/\lambda_{y1}$ which in turn depend on e/r, Ω, ρ and the response quantity in question. Referring to Figure 14 it is clear that at two values of Ω (depending on e/r and ρ), the cross-correlation factors $\gamma_{2j,1k}$ are maximum. The products $2\overline{r}_1^o\overline{r}_2^o$ (for the flat spectrum) and $2\overline{r}_1^o\overline{r}_2^o\Omega$ (for the hyperbolic spectrum) are shown in Figure D.1 against Ω for values of e/r equal to 0.05, 0.4 and 1, for the base shear, i.e. $2\overline{V}_1^o\overline{V}_2^o$, (base overturning moment or lateral displacement at the center of rigidity) and

the base torque at the center of rigidity, i.e. $2\bar{T}^o_{R1}\bar{T}^o_{R2}$, of the associated one-story system. The dependence of the cross-correlation terms on r^o_j and r^o_k indicate that they are affected by the higher modal contributions to responses, given in Table 12 in normalized form. Combining observations of Figures 14 and D.1 and of Table 12, it is clear that the cross-correlation terms may have positive or negative values depending on whether r^o_j and r^o_k are of the same or opposite algebraic signs. Due to the variations of $2\bar{V}^o_1\bar{V}^o_2$ for the flat spectrum (Figure D.1), the cross-correlation terms for story shears, story overturning moments and all frame (1) member forces are significant for torsionally-flexible systems with larger e/r, especially when $\gamma_{21,12}$ is maximum. For a hyperbolic spectrum $\bar{V}^o_1\bar{V}^o_2\Omega$ of Figure D.1 is significant over a wide range of Ω, indicating that cross-correlation terms are significant for torsionally-flexible systems, torsionally-stiff systems or systems with closely-spaced uncoupled frequencies. Also it is clear from Figure D.1 that the significance of the cross-correlation terms increases with increase in e/r. Similar interpretation of $\bar{T}^o_{R1}\bar{T}^o_{R2}$ and $\bar{T}^o_{R1}\bar{T}^o_{R2}\Omega$ of Figure D.1 leads to the conclusion that cross-correlation of torsionally-stiff systems or systems with closely-spaced uncoupled frequencies are significant for both idealized spectra, less for the flat than the hyperbolic spectrum, increasing as e/r increases. The terms are more significant for base shear, base torque and frame (1) column moment in the first story than for base overturning moment, frame (1) top floor lateral displacement, frame (1) beam moment or column axial force in the first story, due to the higher modal contributions significance for the former quantities (Table 12). The cross-correlation terms are larger for smaller ρ in the case of base shear, base torque, base overturning moment, which is also supported by Table 12.

The observations made here for the cross-correlation terms explain the differences between the normalized coupled to uncoupled responses of the multi-story building and its associated one-story system discussed in Section 8.

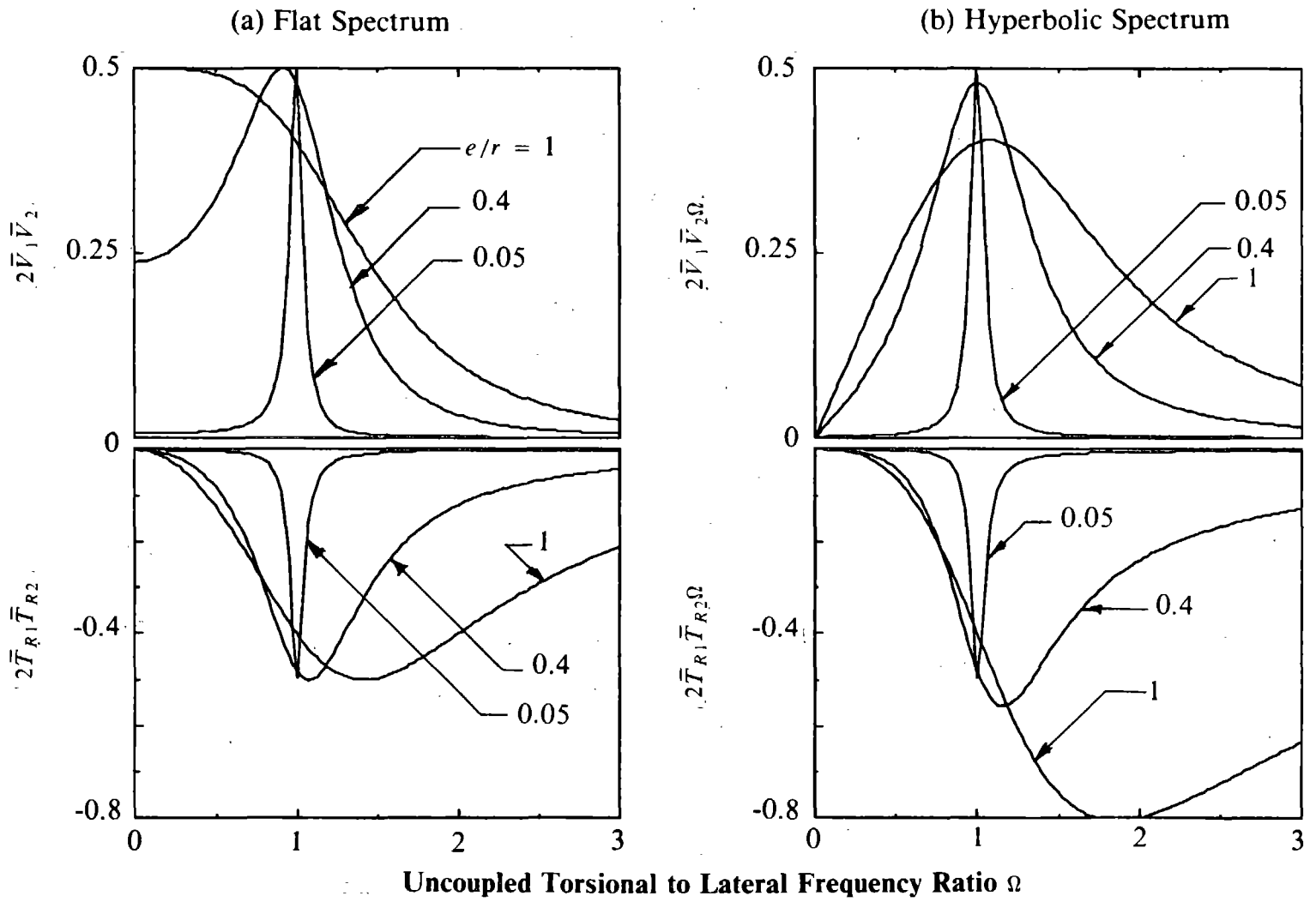

FIGURE D.1 Products $2\bar{r}_1\bar{r}_2$ (Flat Spectrum) and $2\bar{r}_1\bar{r}_2\Omega$ (Hyperbolic Spectrum)

APPENDIX E: NOTATION

$\bar{a}_g$ maximum ground acceleration

$a_{gy}(t)$ ground acceleration along the Y-axis as a function of time

$\mathbf{a}_{xi}$, $\mathbf{a}_{yi}$ transformation matrices defined by equations (3.3)

C_{xi} , C_{yi} proportionality constants for frames 'i' defined by equations (3.11) and (3.6), respectively

C_y , $C_{y\theta}$ proportionality constants defined by equations (3.7) and (3.8), respectively

C_θ , $C_{\theta R}$ proportionality constants defined by equation (3.12), and related by equation (3.13)

e static eccentricity defined as the distance between the centers of mass and rigidity of a floor

e_d dynamic eccentricity defined as the distance from the center of rigidity where the uncoupled base shear V_o should be applied to cause base torque at the center of rigidity equal to T_R

e_{dn} dynamic eccentricity in the n^{th} vibration mode of the associated one-story system; $e_{dn}/r = \bar{T}_{Rn}$

e_n^* effective eccentricity of the associated one-story system for its n^{th} vibration mode

e_1^* effective eccentricity of the associated one-story system in its fundamental vibration mode

e_{nj}^* effective eccentricity in the nj^{th} coupled vibration mode; $e_{nj}^* = e_n^*$

E modulus of elasticity

f_{yn} , $f_{\theta n}$ lateral and torsional components of $\mathbf{f}_n$

F_j force in structural member of a frame in the j^{th} vibration mode of the corresponding uncoupled multi-story system

F_{nj} force in structural member of a frame in the njth coupled vibration mode

$\mathbf{f}_n$ equivalent force vector in the nth vibration mode of the associated one-story system; $\mathbf{f}_n^T = < f_{yn}\ f_{\theta n} >$

$\mathbf{f}_j$ vector of equivalent lateral forces in the jth vibration mode of the corresponding uncoupled multi-story system

$\mathbf{f}_{nj}$ vector of equivalent forces in the njth coupled vibration mode; $\mathbf{f}_{nj}^T = < \mathbf{f}_{ynj}^T\ \mathbf{f}_{\theta nj}^T >$

$\mathbf{f}_{ynj}$, $\mathbf{f}_{\theta nj}$ lateral and torsional components of $\mathbf{f}_{nj}$

g gravitational acceleration

h story height

h_j^* effective height in the jth vibration mode of the corresponding uncoupled multi-story system

h_1^* effective height in the fundamental vibration mode of the corresponding uncoupled multi-story system

h_{nj}^* effective height in the njth coupled vibration mode; $h_{nj}^* = h_j^*$

$\mathbf{H}$ summation matrix defined by equation (4.17) for a five-story building

I , I_c moments of inertia of columns

I_b moments of inertia of beams

I_1 , I_2 moments of inertia of columns of frames (1) and (2), respectively

$\mathbf{I}$ unit matrix of dimension N

K_y lateral stiffness of the associated one-story system along the Y-axis

K_θ , $K_{\theta R}$ torsional stiffnesses of the associated one-story system defined at its centers of mass and rigidity, respectivley

$\mathbf{k}$ frames characteristic matrix

$\mathbf{k}_{xi}$, $\mathbf{k}_{yi}$ lateral stiffness matrices of frames 'i' along the X- and Y- directions, respectively

$\mathbf{k}_{y1}$, $\mathbf{k}_{x2}$ lateral stiffness matrices of frames (1) and (2), respectively

$\mathbf{K}$ building stiffness matrix defined with respect to $\mathbf{u}$

$\mathbf{K}_i$ stiffness matrix of frame 'i' computed for $\mathbf{u}$

$\mathbf{K}_y$ building lateral stiffness matrix along the Y-axis, defined by equation (3.5a)

$\mathbf{K}_{y\theta}$, $\mathbf{K}_{\theta y}$, $\mathbf{K}_{\theta}$

stiffness submatrices of $\mathbf{K}$, defined by equations (3.4) and (3.5)

L_b width of beam

L_c height of column

L_j participation factor for the j^{th} vibration mode of the corresponding uncoupled multi-story system

L_{nj} participation factor for the nj^{th} coupled vibration mode

m mass of one-story system

m_j mass at the j^{th} floor level

M , M_o base overturning moments of the associated one-story system and its corresponding uncoupled one-story system

$\bar{M}$ M/M_o

M_B , M_{Bo} base overturning moments of coupled and uncoupled multi-story buildings

M_j modal mass in the j^{th} vibration mode of the corresponding uncoupled multi-story system

M_n base overturning moment of the associated one-story system in the n^{th} vibration mode

$\bar{M}_n$ M_n/M_o

M_{bB} , M_{cB} — frame (1) base-story beam and column moments, respectively, of coupled multi-story building

M_{Bj} — base overturning moment in the j^{th} vibration mode of the corresponding uncoupled multi-story system

M_{nj} — modal mass in the nj^{th} coupled vibration mode

$\overline{M}_{nj}$ — equal $\overline{M}_n$ of the associated one-story system with uncoupled lateral vibration frequency ω_{yj}

M_{bBo} , M_{cBo} — frame (1) base-story beam and column moments, respectively, of the corresponding uncoupled multi-story system

M_{Bnj} — base overturning moment in the nj^{th} coupled vibration mode

m — mass matrix of the corresponding uncoupled multi-story system

$\mathbf{M}_j$ — vector of story overturning moments in the j^{th} vibration mode of the corresponding uncoupled multi-story system

$\mathbf{M}_{nj}$ — vector of story overturning moments in the nj^{th} coupled vibration mode

N — number of stories

P_{cB} — frame (1) base-story column axial force of coupled multi-story building

P_{cBo} — frame (1) base-story column axial force of the corresponding uncoupled multi-story system

q_{nm} — ω_n/ω_m

$q_{nj,mk}$ — ω_{nj}/ω_{mk}

r — radius of gyration of a deck about a vertical axis passing through its center of mass

r — maximum of a response quantity of coupled systems

$\overline{r}$ — r/r_o

r_j maximum of a response quantity of the corresponding uncoupled multi-story system in its j^{th} vibration mode

r_n maximum of a response quantity of the associated one-story system in its n^{th} vibration mode

r_o maximum of a response quantity of corresponding uncoupled systems (one- and multi-story)

$\overline{r}_n$ r_n/r_o

r_{nj} maximum of a response quantity in the nj^{th} coupled vibration mode

$\overline{r}_{nj}$ equal $\overline{r}_n$ of the associated one-story system with uncoupled lateral vibration frequency ω_{yj}

S_{aj} pseudo-acceleration response spectrum ordinate corresponding to T_{yj} and ξ_j

S_{an} pseudo-acceleration response spectrum ordinate corresponding to T_n and ξ

S_{ay} pseudo-acceleration response spectrum ordinate corresponding to T_y and ξ

S_{anj} pseudo-acceleration response spectrum ordinate corresponding to T_{nj} and ξ_{nj}

S summation matrix defined by equation (4.17) for a five-story building

T_n n^{th} coupled vibration period of the associated one-story system

T_y uncoupled lateral vibration period of the associated one-story system

T_M , T_R maximum base torques at centers of mass and rigidity, respectively, of the associated one-story system

T_{BR} base torque at the center of rigidity of coupled multi-story building

T_{Mn} , T_{Rn} base torques at the centers of mass and rigidity, respectively, of the associated one-story system in its n^{th} vibration mode

T_{nj} — nj^{th} coupled vibration period

T_{yj} — j^{th} uncoupled vibration period

T_{y1} — fundamental lateral uncoupled vibration period

$\bar{T}_M$ — T_M/rV_o

$\bar{T}_R$ — T_R/rV_o

$\bar{T}_{Mn}$ — T_{Mn}/rV_o

$\bar{T}_{Rn}$ — T_{Rn}/rV_o

$\bar{T}_{Mnj}$, $\bar{T}_{Rnj}$ — equal, respectively, to $\bar{T}_{Mn}$ and $\bar{T}_{Rn}$ of the associated one-story system with uncoupled lateral vibration frequency ω_{yj}

T_{BMnj} , T_{BRnj} — base torques at centers of mass and rigidity, respectively, in the nj^{th} coupled vibration mode

$\mathbf{T}_{Mnj}$, $\mathbf{T}_{Rnj}$ — vectors of story torques at centers of mass and rigidity, respectively, in the nj^{th} coupled vibration mode

$\bar{u}_g$ — maximum ground displacement

u_y — lateral displacement of the associated one-story system at its center of mass along the Y-axis

$u_y(x_i)$ — lateral displacement along the Y-axis of the associated one-story system at a distance x_i from its center of mass

u_θ — deck rotation of the associated one-story system about a vertical axis

u_{yn} — lateral displacement along the Y-axis of the associated one-story system at its center of mass in the n^{th} vibration mode

$u_{yn}(x_i)$ — lateral displacement along the Y-axis of the associated one-story system at a distance x_i from its center of mass in the n^{th} mode of vibration

$u_{\theta n}$ deck rotation of the associated one-story system in the n^{th} vibration mode

$\bar{u}_y$ u_y/v_o

$\bar{u}_y(x_i)$ $u_y(x_i)/v_o$

$\bar{u}_\theta$ ru_θ/v_o

$\bar{u}_{yn}$, $\bar{u}_{\theta n}$ u_{yn}/v_o and $ru_{\theta n}/v_o$

$\bar{u}_{yn}(x_i)$ $u_{yn}(x_i)/v_o$

$\bar{u}_{ynj}$, $\bar{u}_{ynj}(x_i)$, $\bar{u}_{\theta nj}$

equal, respectively, to $\bar{u}_{yn}$, $\bar{u}_{yn}(x_i)$ and $\bar{u}_{\theta n}$ of the associated one-story system with uncoupled lateral vibration frequency ω_{yj}

$\mathbf{u}$ displacements vector; $\mathbf{u}^T = < \mathbf{u}_y^T \; r\mathbf{u}_\theta^T >$

$\mathbf{u}_n$ displacement vector of the associated one-story system in the n^{th} vibration mode; $\mathbf{u}_n^T = < u_{yn} \; ru_{\theta n} >$

$\mathbf{u}_y$ vector of lateral displacements at the centers of mass of the multi-story building, along the Y-axis

$\mathbf{u}_\theta$ vector of deck rotations about a vertical axis

$\bar{\mathbf{u}}_n$ $\mathbf{u}_n/v_o$

$\mathbf{u}_{nj}$ displacements vector in the nj^{th} coupled vibration mode; $\mathbf{u}_{nj}^T = < \mathbf{u}_{ynj}^T \; r\mathbf{u}_{\theta nj}^T >$

$\mathbf{u}_{ynj}$ vector of lateral displacements at the centers of mass in the nj^{th} coupled vibration mode

$\mathbf{u}_{\theta nj}$ vector of deck rotations in the nj^{th} coupled vibration mode

$\mathbf{u}_{ynj}(x_i)$ vector of lateral displacements of frame 'i' spanning along the Y-axis at a distance x_i from the centers of mass of the building in the nj^{th} mode of vibration

v lateral displacement at the center of rigidity of the associated one-story system

v_n lateral displacement at the center of rigidity of the associated one-story system in the n^{th} vibration mode

v_o lateral displacement of uncoupled associated one-story system

v_5 , v_{5o} frame (1) top floor lateral displacement of coupled and uncoupled multi-story buildings

$\bar{v}$ v/v_o

$\bar{v}_g$ maximum ground velocity

$\bar{v}_n$ v_n/v_o

$\bar{v}_{nj}$ equal $\bar{v}_n$ of the associated one-story system with uncoupled lateral vibration frequency ω_{yj}

V , V_o base shears of the associated one-story system and its corresponding uncoupled one-story system

V_B , V_{Bo} base shears of the coupled and uncoupled multi-story buildings

V_n base shear of the associated one-story system in the n^{th} vibration mode

$\bar{V}$ V/V_o

$\bar{V}_n$ V_n/V_o

$\bar{V}_{nj}$ equal $\bar{V}_n$ of the associated one-story system with uncoupled lateral vibration frequency ω_{yj}

V_{Bj} base shear of the corresponding uncoupled multi-story system in the j^{th} vibration mode

V_{Bnj} base shear in the nj^{th} coupled vibration mode

$\mathbf{v}_j$ vector of lateral floor displacements of the corresponding uncoupled multi-story system in the j^{th} vibration mode

$\mathbf{v}_o$ vector of lateral floor displacements of the corresponding uncoupled multi-story system

$\mathbf{v}_{nj}$ vector of lateral floor displacements at the centers of rigidity of multi-story system in the njth coupled vibration mode

$\mathbf{V}_j$ vector of story shears of the corresponding uncoupled multi-story system in the jth vibration mode

$\mathbf{V}_{nj}$ vector of story shears in the njth coupled vibration mode

W total weight of structure

W_j^* effective weight of the corresponding uncoupled multi-story system associated with the jth vibration mode

W_n^* effective weight of the associated one-story system in its nth vibration mode

W_1^* effective weight of the corresponding uncoupled multi-story system associated with its fundamental vibration mode

$\overline{W}_n^*$ W_n^*/W

W_{nj}^* effective weight associated with the njth coupled vibration mode; $W_{nj}^* = \overline{W}_n^* W_j^*$

x_i and y_i X- and Y- distances of frames 'i' from the centers of mass

y_2 distance of frames (2) from centers of mass

α_y , α_θ lateral and torsional components of $\boldsymbol{\alpha}$

α_{yn} , $\alpha_{\theta n}$ lateral and torsional components of the nth mode shape of the associated one-story system

$\boldsymbol{\alpha}$ mode shapes of the associated one-story system; $\boldsymbol{\alpha}^T = < \alpha_y \ \alpha_\theta >$

$\boldsymbol{\alpha}_n$ nth mode shape of the associated one-story system; $\boldsymbol{\alpha}_n^T = < \alpha_{yn} \ \alpha_{\theta n} >$

γ_{nm} cross-correlation factor between coupled vibration modes 'n' and 'm' of the associated one-story system

$\gamma_{nj,mk}$ cross-correlation factor between coupled vibration modes 'nj' and 'mk' of multi-story building; n,m=1,2; j,k=1, ..., N

ω natural vibration frequencies of coupled systems

ω_n n^{th} natural vibration frequency of the associated one-story system; n=1,2

ω_y , ω_θ natural lateral and torsional vibration frequencies of the uncoupled one-story system

$\bar{\omega}$ ω/ω_y for the associated one-story system or ω/ω_{yj} for the torsionally-coupled multi-story building

$\bar{\omega}_n$ ω_n/ω_y for the associated one-story system or ω_{nj}/ω_{yj} for multi-story building and associated one-story system with uncoupled lateral vibration frequency ω_{yj}

ω_{yj} , $\omega_{\theta j}$ j^{th} uncoupled lateral and torsional natural vibration frequencies; j=1, ..., N

ω_{nj} nj^{th} natural vibration frequency of coupled multi-story building

Ω uncoupled torsional to lateral frequency ratio of multi-story building and its associated one-story system

$\boldsymbol{\phi}$ mode shapes of coupled multi-story building; $\boldsymbol{\phi}^T = < \boldsymbol{\phi}_y^T \, \boldsymbol{\phi}_\theta^T >$

$\boldsymbol{\phi}_y$, $\boldsymbol{\phi}_\theta$ lateral and torsional components of $\boldsymbol{\phi}$

$\boldsymbol{\phi}_{nj}$ nj^{th} mode shape of coupled multi-story building; $\boldsymbol{\phi}_{nj}^T = < \boldsymbol{\phi}_{ynj}^T \, \boldsymbol{\phi}_{\theta nj}^T >$

$\boldsymbol{\phi}_{ynj}$, $\boldsymbol{\phi}_{\theta nj}$ lateral and torsional components of $\boldsymbol{\phi}_{nj}$

$\boldsymbol{\psi}$ mode shapes of the corresponding uncoupled multi-story system

$\boldsymbol{\psi}_j$ j^{th} mode shape of the corresponding uncoupled multi-story system

ρ joint rotation index or beam-to-column stiffness ratio for frames

ρ_1 , ρ_2	joint rotation indices of frames (1) and (2), respectively
ξ	damping ratio
$\mathbf{0}$	zero square matrix of dimension N, or zero vector of dimension N
$\mathbf{1}$	vector of ones of dimension N

PART III

THE STATIC ECCENTRICITY CONCEPT IN BUILDING CODE ANALYSES

1. INTRODUCTION

Buildings subjected to earthquake ground motions may undergo lateral as well as torsional motions. In the case of buildings with plans having two axes of symmetry, torsional vibrations arise due to the rotational component in ground motion or due to unforseen conditions such as unsymmetric load distributions. Such torsional vibrations are usually referred to as "accidental" [1] and can not easily be taken into account in dynamic analysis. Torsional vibrations induced in a building during an earthquake can also be due to its structural asymmetry. In most building codes [e.g. 2,3,4,5], the torsional effect is treated by analyzing the building statically for the equivalent lateral forces applied eccentrically away from the centers of mass of the various floors. The eccentricity value at a floor level is computed as the sum of its so-called "accidental eccentricity" and its "structural or static eccentricity". The accidental eccentricity of a story is normally given as a fraction of the plan dimension of the story, perpendicular to the direction of lateral forces, whereas the static eccentricity at a floor level is commonly defined as the distance between its center of mass and center of rigidity, but in at least one code [4] it is defined as the distance between the center of mass and shear center of the story. In some codes, the static eccentricity is multiplied by a constant exceeding unity to account for dynamic amplification.

The determination of the locations of centers of rigidity at all floor levels is a key step in the application of building codes provisions. However, most building codes, do not provide unequivocal definitions of centers of rigidity or specify computational procedures to determine their locations. For this reason, it is still unclear what exactly is meant by centers of rigidity of multi-story buildings and whether the locations of these centers are intrinsic properties of the building, or if they are dependent on the height-wise distribution of lateral loads.

Several investigators have studied this problem over the past few years, giving different definitions of the centers. Most of the studies are restricted to buildings with resisting elements (frames and shear walls) located in an orthogonal grid in plan. The centers are referred to, in the literature, by different terms, apparently with the implication that these are different terms for the same points. Some of the terms that have been used are: centers of rigidity, centers of resistance,

centers of stiffness, shear centers, load centers, centers of twist, centers of rotation and centers of torsion. Poole [6] defines the center of rigidity of a story as the location of the resultant of the shear forces in that story of the various resisting elements when the building is subjected to a static lateral loading that causes no torsion in any of the stories. In other words, centers of rigidity are identified as the shear centers of the building. Based on this definition, a procedure to determine the centers of rigidity is given in [6]. Humar and Awad [7] define the center of resistance of a floor as a point such that when a lateral force is applied through it, the level under consideration does not undergo any rotation.

The work of Tso and Cheung [8] distinguishes between centers of rigidity, shear centers and centers of twist of a multi-story building. It is recognized that these terms as well as the term center of stiffness are interchangeable for a single-story system because in this case all the centers are coincident. Mathematical expressions are presented for the locations of centers of rigidity and centers of twist of multi-story buildings with orthogonal frame orientations in terms of the lateral forces and building stiffness submatrices. Expressions of the centers of rigidity are interpreted physically as the locations of the resultants of the elemental loads applied at each floor level, or load centers, and not as shear centers. It is also shown that the centers of twist do not generally coincide with the centers of rigidity. For a special class of buildings, with lateral stiffness matrices of all resisting frames mutually proportional, the locations of centers of twist and rigidity were shown to be coincident, independent of the lateral forces and lie on a vertical line.

Riddell and Vasquez [9] conclude that the centers of resistance exist only for a particular class of structures and that for a general multi-story building such concepts are meaningless. These particular buildings, referred to as "compensable buildings", are shown to have centers of resistance that are load independent and lie on a vertical line. The conditions satisfied by this class of buildings is in agreement with that identified in [8]. For buildings that are "nearly compensable", expressions, based on perturbation theory, are given in [9] to determine approximate locations of the centers of resistance, all lying on a vertical line.

This brief review of past studies shows clearly the inconsistencies in the definitions given for centers of rigidity. Although both studies [8] and [9] identify a class of buildings where the centers of rigidity of all floors lie on a vertical line, their authors disagree on whether the centers of rigidity exist for any multi-story building. The question of whether there is any need to distinguish between centers of rigidity, centers of twist and shear centers also remain unanswered. Consequently, it is unclear which of these centers should be chosen to define static eccentricities in the application of code provisions.

The objective of this study is to investigate further the definitions of each of the centers mentioned above. The locations of these centers are then sought for buildings with general plan layouts. The conditions to be satisfied for the centers to be coincident and uniquely defined are investigated. A number of examples is included to illustrate the findings.

2. ONE-STORY SYSTEMS

The center of rigidity, the center of twist, the shear center, the center of stiffness, and the static eccentricity are defined in this section for one-story systems. Expressions are derived for the locations of these centers as well as for the orientations of the principal axes of buildings with general plan layouts (e.g. Figure 1a). It is shown that these various centers are coincident for one-story buildings and its location depends on the stiffnesses and locations of the various resisting elements but not on the applied load. Although this study of one-story systems is straightforward, it is presented to serve as a basis for the study of the corresponding concepts in multi-story buildings.

2.1 Basic Concepts and Definitions

Consider a one-story system that consists of a rigid diaphragm or deck of an arbitrary shape (Figure 1a). The horizontal motion of the diaphragm is resisted by a number of resisting elements (frames, columns, shear walls or shear-wall cores), with arbitrary locations and with principal axes of arbitrary orientations.

The **center of rigidity** is the point on the diaghragm through which the application of a static horizontal force causes no rotation of the deck, no matter in what direction the force is applied. The **principal axes**, I and II, of the system are two orthogonal axes passing through the center of rigidity, such that if a static horizontal force is applied along one of the principal axes of the system, the diaghragm translates only in the direction of the force without any twist.

The **center of twist** is the point on the diaghragm which remains stationary when the diaghragm is subjected to a statically applied horizontal torsional moment, i.e. the diaphragm undergoes pure twist about this point.

The **shear center** is the point on the diaghragm through which the resultant of the shear forces of all resisting elements passes when the diaphragm is subjected to a system of lateral static loads whose resultant passes through the center of rigidity of the building, thus causing no rotation or twist of the diaphragm. Since the elemental shear forces in a one-story system are directly proportional to the elemental stiffnesses, the shear center is also referred to as the **center of stiffness.**

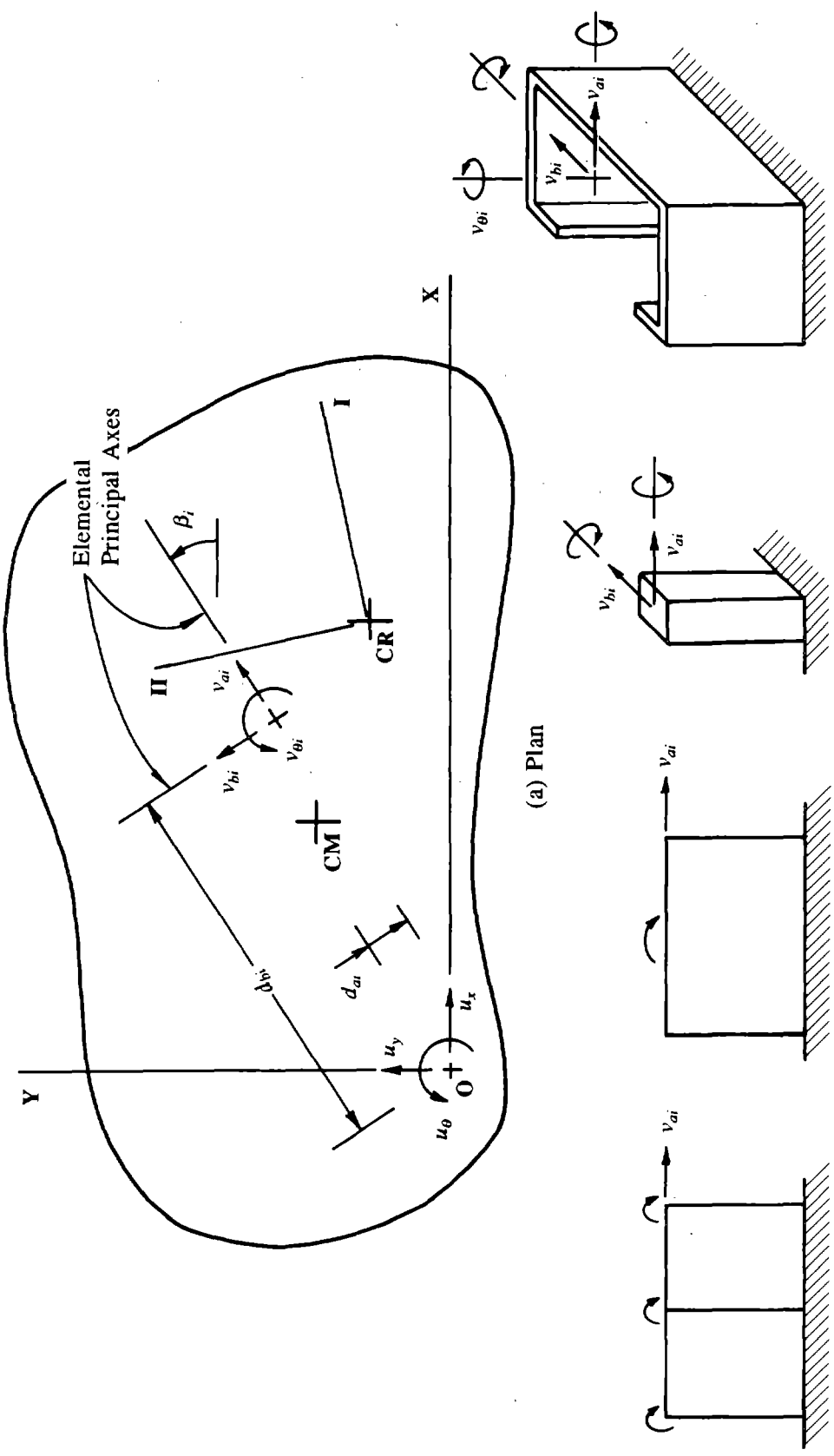

FIGURE 1 One-story System

It is shown in a subsequent section that the center of rigidity, the center of twist, and the shear center or center of stiffness of a one-story system are actually coincident.

The **center of mass** of the system is the point on the floor through which the resultant of the inertia forces of the floor passes. If the masses of individual resisting elements are negligible, the center of mass of a deck with a uniform mass distribution coincides with its geometric center.

The **static eccentricity** e of the system is defined as the distance between its centers of mass and of rigidity. In some building codes [e.g. 4], the static eccentricity is defined as the distance between the center of mass and shear center of the building. Because the shear center and center of rigidity of a one-story system are coincident, which will be proven later, the two definitions lead to the same value for the static eccentricity in this case but, as will be seen later not for multi-story buildings.

2.2 Equations of Motion

The three degrees of freedom of the system defined at an arbitrary reference point O of the deck are: two horizontal translational displacements of the deck, u_x and u_y, relative to the ground, along two orthogonal axes, X and Y, and the rotation u_θ of the deck about a vertical axis. The building stiffness matrix $\mathbf{K}$ defined at the reference point O with respect to degrees of freedom $\mathbf{u}$, where $\mathbf{u}^T = < u_x \; u_y \; u_\theta >$, is the sum of the stiffness matrices $\mathbf{K}_i$ of individual resisting elements, also computed with respect to $\mathbf{u}$:

$$\mathbf{K} = \sum_i \mathbf{K}_i \tag{2.1}$$

The stiffness matrix $\mathbf{K}_i$ of the i^{th} resisting element is derived from its lateral stiffnesses along its two principal axes-- the two orthogonal axes in a horizontal section of the element which pass through its shear center [13], such that any static lateral force passing through the shear center applied along one of the principal axes of the section causes it to translate in the same direction as the force without twist-- and its torsional stiffness about a vertical axis passing through its shear center. Lateral stiffnesses of frames and shear walls along their minor principal axes, i.e. along the

direction perpendicular to their own plane, are assumed to be negligible. Shear deformations are negligible for frame members so that only flexural deformations are considered for frames. A column contributes to system lateral stiffnesses due to its lateral stiffnesses along both of its principal axes. Because the individual torsional stiffnesses of frames, shear walls and columns are negligible, the contributions of these resisting elements to the torsional stiffness of the building are primarily due to the lateral stiffnesses of these resisting elements acting at some distance from O. On the other hand, the torsional stiffness of a shear-wall core element is significant, and its contribution to the torsional stiffness of the building is due to its torsional stiffness as well as to its lateral stiffnesses along its principal axes.

The stiffness matrix $\mathbf{K}_i$ of the i^{th} resisting element is determined by the following procedure:

1. Define the local degrees of freedom for each resisting element (Figure 1b) as follows:

   (a) For a shear wall define one translational degree of freedom at the roof level, along the plane of the shear wall, i.e. along its major principal axis, and a rotational degree of freedom about its minor principal axis, i.e. the horizontal axis perpendicular to its plane.

   (b) For a frame define one translational degree of freedom at the roof level, along the plane of the frame, i.e. along its major principal axis, and a rotational degree of freedom per joint about horizontal axes perpendicular to the plane of the frame, i.e. along the direction of its minor principal axis.

   (c) For a column define two translational degrees of freedom at the roof level along the principal axes of the column and two rotational degrees of freedom about these axes.

   (d) For a shear-wall core define five degrees of freedom: two translations along the principal axes of the core, two rotations about these axes, and one torsional rotation about a vertical axis passing through the shear center of the core.

2. Obtain a complete stiffness matrix for the resisting element for the degrees of freedom defined, taking into account flexural and shear deformations for shear walls and shear-wall cores, and only flexural deformations for frames and columns.

3. Eliminate the joint rotational degrees of freedom of the resisting elements by the static condensation process. The resulting condensed matrix $\mathbf{k}_i$ of a shear-wall core element 'i' is diagonal and of dimension equal to three, satisfying the following equation:

$$\mathbf{Q}_i = \begin{Bmatrix} Q_{ai} \\ Q_{bi} \\ Q_{\theta i} \end{Bmatrix} = \begin{bmatrix} k_{ai} & 0 & 0 \\ 0 & k_{bi} & 0 \\ 0 & 0 & k_{\theta i} \end{bmatrix} \begin{Bmatrix} v_{ai} \\ v_{bi} \\ v_{\theta i} \end{Bmatrix} = \mathbf{k}_i \ \mathbf{v}_i \tag{2.2}$$

where k_{ai} and k_{bi} are the lateral stiffnesses of the element along its two principal axes, and $k_{\theta i}$ is the torsional stiffness of the core about a vertical axis passing through its shear center. The applied static forces Q_{ai}, Q_{bi} and $Q_{\theta i}$ and resulting displacements v_{ai}, v_{bi} and $v_{\theta i}$ in these three directions are related through k_{ai}, k_{bi} and $k_{\theta i}$, respectively. Since $k_{\theta i}$ is negligible for columns, shear walls and frames, and k_{bi} is negligible for frames and shear walls, equations (2.2) are simplified for these resisting elements. For columns, we obtain:

$$\mathbf{Q}_i = \begin{Bmatrix} Q_{ai} \\ Q_{bi} \end{Bmatrix} = \begin{bmatrix} k_{ai} & 0 \\ 0 & k_{bi} \end{bmatrix} \begin{Bmatrix} v_{ai} \\ v_{bi} \end{Bmatrix} = \mathbf{k}_i \ \mathbf{v}_i \tag{2.3}$$

For shear walls and frames:

$$Q_{ai} = k_{ai} \ v_{ai} \tag{2.4}$$

4. Determine the transformation matrix $\mathbf{a}_i$, relating the resisting element displacement vector $\mathbf{v}_i$, to the system degrees of freedom $\mathbf{u}$. For a shear-wall core, $\mathbf{a}_i$ is given by:

$$\mathbf{v}_i = \begin{Bmatrix} v_{ai} \\ v_{bi} \\ v_{\theta i} \end{Bmatrix} = \begin{bmatrix} \cos\beta_i & \sin\beta_i & \pm d_{ai} \\ -\sin\beta_i & \cos\beta_i & \pm d_{bi} \\ 0 & 0 & 1 \end{bmatrix} \begin{Bmatrix} u_x \\ u_y \\ u_\theta \end{Bmatrix} = \mathbf{a}_i \ \mathbf{u} \tag{2.5}$$

and for a column, the transformation matrix $\mathbf{a}_i$ is given by:

$$\mathbf{v}_i = \begin{Bmatrix} v_{ai} \\ v_{bi} \end{Bmatrix} = \begin{bmatrix} \cos\beta_i & \sin\beta_i & \pm d_{ai} \\ -\sin\beta_i & \cos\beta_i & \pm d_{bi} \end{bmatrix} \begin{Bmatrix} u_x \\ u_y \\ u_\theta \end{Bmatrix} = \mathbf{a}_i \ \mathbf{u} \tag{2.6}$$

in which β_i is the counterclockwise angle between the X-axis and the major principal axis of

the shear-wall core or column; d_{ai} and d_{bi} are the perpendicular distances of the major and minor principal axes, respectively, from reference point O. In equations (2.5) and (2.6), the choice of a positive or a negative algebraic sign to accompany d_{ai} (or d_{bi}) depends on whether a unit u_θ rotation causes a displacement along the major (or minor) principal axis in the same or opposite direction to v_{ai} (or v_{bi}). For frames and shear walls, $\mathbf{a}_i$ is obtained from:

$$v_{ai} = < \cos\beta_i \quad \sin\beta_i \quad \pm d_{ai} > \begin{Bmatrix} u_x \\ u_y \\ u_\theta \end{Bmatrix} = \mathbf{a}_i \, \mathbf{u} \tag{2.7}$$

where β_i is the counterclockwise angle between the X-axis and the plane of the frame or shear wall, and d_{ai} is the perpendicular distance from reference point O to the plane of the frame or shear wall. Again, the choice of a positive or a negative algebraic sign to accompany d_{ai} in equation (2.7) depends on whether a unit u_θ rotation causes a displacement along the plane of the frame or shear wall in the same or opposite direction to v_{ai}.

5. The contribution of resisting element 'i' to building stiffness matrix is $\mathbf{K}_i$, and is determined by:

$$\mathbf{K}_i = \mathbf{a}_i^T \, \mathbf{k}_i \, \mathbf{a}_i = \begin{bmatrix} K_{xi} & K_{xyi} & K_{x\theta i} \\ K_{yxi} & K_{yi} & K_{y\theta i} \\ K_{\theta xi} & K_{\theta yi} & K_{\theta i} \end{bmatrix} \tag{2.8}$$

in which,

$$K_{xi} = k_{ai} \cos^2\beta_i + k_{bi} \sin^2\beta_i$$

$$K_{yi} = k_{ai} \sin^2\beta_i + k_{bi} \cos^2\beta_i$$

$$K_{\theta i} = k_{ai} \, d_{ai}^2 + k_{bi} \, d_{bi}^2 + k_{\theta i}$$

$$K_{xyi} = K_{yxi} = (k_{ai} - k_{bi}) \sin\beta_i \cos\beta_i \tag{2.9}$$

$$K_{x\theta i} = K_{\theta xi} = \pm k_{ai} \, d_{ai} \cos\beta_i - (\pm) k_{bi} \, d_{bi} \sin\beta_i$$

$$K_{y\theta i} = K_{\theta y i} = \pm k_{ai}\, d_{ai} \sin\beta_i \pm k_{bi}\, d_{bi} \cos\beta_i$$

As mentioned earlier, $k_{\theta i}$ is negligibly small for all types of resisting elements except shear-wall cores, and k_{bi} is negligible for frames and shear walls.

The building stiffness matrix **K** for degrees of freedom $\mathbf{u}^T = < u_x\ u_y\ u_\theta >$, defined at O, is given by superposition of the element stiffness matrices (equation (2.1)) resulting in:

$$\mathbf{K} = \begin{bmatrix} K_x & K_{xy} & K_{x\theta} \\ K_{yx} & K_y & K_{y\theta} \\ K_{\theta x} & K_{\theta y} & K_\theta \end{bmatrix} \tag{2.10}$$

with,

$$K_x = \sum_i K_{xi}\ ,\ K_y = \sum_i K_{yi}\ ,\ K_\theta = \sum_i K_{\theta i}$$

$$K_{x\theta} = K_{\theta x} = \sum_i K_{x\theta i}\ ,\ K_{y\theta} = K_{\theta y} = \sum_i K_{y\theta i} \tag{2.11}$$

$$K_{xy} = K_{yx} = \sum_i K_{xyi}$$

The undamped equations of motion for the one-story system, assuming linear behavior, subjected to earthquake ground motion accelerations $a_{gx}(t)$ and $a_{gy}(t)$ along the X- and Y-axes, are:

$$\begin{bmatrix} m & 0 & -my_M \\ 0 & m & mx_M \\ -my_M & mx_M & J_O \end{bmatrix} \begin{Bmatrix} \ddot{u}_x \\ \ddot{u}_y \\ \ddot{u}_\theta \end{Bmatrix} + \begin{bmatrix} K_x & K_{xy} & K_{x\theta} \\ K_{yx} & K_y & K_{y\theta} \\ K_{\theta x} & K_{\theta y} & K_\theta \end{bmatrix} \begin{Bmatrix} u_x \\ u_y \\ u_\theta \end{Bmatrix} = -m \begin{Bmatrix} a_{gx}(t) \\ a_{gy}(t) \\ -y_M a_{gx}(t) + x_M a_{gy}(t) \end{Bmatrix} \tag{2.12}$$

where m is the mass of the deck; x_M and y_M are the X and Y coordinates of the center of mass; and J_O is the polar moment of inertia of the deck about a vertical axis passing through reference point O, given by:

$$J_O = m\,(\,r^2 + x_M^2 + y_M^2\,) \tag{2.13}$$

in which r is the radius of gyration of the deck about a vertical axis passing through the center of mass of the deck. It is apparent from these equations of motion that translational ground motion along either the X- or the Y-axis will simultaneously cause both X- and Y- lateral displacements of

point O as well as torsional rotation or twist of the floor about a vertical axis.

The equations of motion written with respect to degrees of freedom defined at any point other than O can be determined by standard transformation of equation (2.12). However, the general form of the equations of motion (the mass and stiffness matrices) remains as equation (2.12) unless the degrees of freedom are defined at the center of mass or the center of rigidity, which will be shown later to coincide with the center of twist and the shear center, of the system. When the equations of motion are written with respect to degrees of freedom defined at the center of mass, the building mass matrix becomes diagonal, given by:

$$\mathbf{M}_M = \begin{bmatrix} m & 0 & 0 \\ 0 & m & 0 \\ 0 & 0 & mr^2 \end{bmatrix}$$

However, the coupling of degrees of freedom in the building stiffness matrix remains of the form given in equation (2.12). The equations of motion are then given by:

$$\begin{bmatrix} m & 0 & 0 \\ 0 & m & 0 \\ 0 & 0 & mr^2 \end{bmatrix} \begin{Bmatrix} \ddot{u}_x \\ \ddot{u}_y \\ \ddot{u}_\theta \end{Bmatrix} + \begin{bmatrix} K_x & K_{xy} & K_{x\theta} \\ K_{yx} & K_y & K_{y\theta} \\ K_{\theta x} & K_{\theta y} & K_\theta \end{bmatrix} \begin{Bmatrix} u_x \\ u_y \\ u_\theta \end{Bmatrix} = -m \begin{Bmatrix} a_{gx}(t) \\ a_{gy}(t) \\ 0 \end{Bmatrix} \tag{2.14}$$

On the other hand, if the equations of motion are written for degrees of freedom $\tilde{\mathbf{u}}$, where $\tilde{\mathbf{u}}^T = < \tilde{u}_x \;\; \tilde{u}_y \;\; u_\theta >$ with $\tilde{u}_x$ and $\tilde{u}_y$ the lateral displacements at the center of rigidity along the X- and Y-axes, the building stiffness matrix assumes the form:

$$\tilde{\mathbf{K}} = \begin{bmatrix} \tilde{K}_x & \tilde{K}_{xy} & 0 \\ \tilde{K}_{yx} & \tilde{K}_y & 0 \\ 0 & 0 & \tilde{K}_\theta \end{bmatrix} \tag{2.15}$$

since any horizontal static force applied through the center of rigidity causes only lateral displacements and no rotation of the deck (see the definition of the center of rigidity given in Section 2.1). The equations of motion written with respect to $\tilde{\mathbf{u}}$ are then given by:

$$\begin{bmatrix} m & 0 & -me_y \\ 0 & m & me_x \\ -me_y & me_x & J_R \end{bmatrix} \begin{Bmatrix} \ddot{\tilde{u}}_x \\ \ddot{\tilde{u}}_y \\ \ddot{u}_\theta \end{Bmatrix} + \begin{bmatrix} \tilde{K}_x & \tilde{K}_{xy} & 0 \\ \tilde{K}_{yx} & \tilde{K}_y & 0 \\ 0 & 0 & \tilde{K}_\theta \end{bmatrix} \begin{Bmatrix} \tilde{u}_x \\ \tilde{u}_y \\ u_\theta \end{Bmatrix} = -m \begin{Bmatrix} a_{gx}(t) \\ a_{gy}(t) \\ -e_y a_{gx}(t) + e_x a_{gy}(t) \end{Bmatrix} \tag{2.16}$$

where the X and Y components of static eccentricity e are:

$$e_x = x_M - x_R \quad \text{and} \quad e_y = y_M - y_R \tag{2.17}$$

in which x_R and y_R the X and Y coordinates of the center of rigidity; J_R is the polar moment of inertia about a vertical axis passing through the center of rigidity, given by:

$$J_R = m(e^2 + r^2) \tag{2.18}$$

The stiffness values $\tilde{K}_x$, $\tilde{K}_{xy}$, $\tilde{K}_y$ and $\tilde{K}_\theta$ with respect to $\tilde{\mathbf{u}}$, the degrees of freedom at centers of rigidity, are related to stiffness values K_x , K_{xy} , K_y and K_θ for $\mathbf{u}$, the degrees of freedom at point O, in Section 2.3. The special form of the building stiffness matrix given by equation (2.15) is the basis used in Section 2.3 to locate the centers of rigidity of the system.

A static horizontal lateral force applied through the center of rigidity along either of the system principal axes, causes the deck to displace laterally in the same direction as the force, without any twist (see Section 2.1). It follows that the building stiffness matrix defined with respect to degrees of freedom $\mathbf{u}^*$, where $\mathbf{u}^{*T} = < u_I^* \;\; u_{II}^* \;\; u_\theta >$, with u_I^* and u_{II}^* the lateral displacements at the center of rigidity along the principal axes of the system, is of the form:

$$\mathbf{K}^* = \begin{bmatrix} K_I^* & 0 & 0 \\ 0 & K_{II}^* & 0 \\ 0 & 0 & K_\theta^* \end{bmatrix} \tag{2.19}$$

with K_I^* , K_{II}^* and K_θ^* expressed in terms of K_x , K_y , K_{xy} and K_θ in Section 2.5. The special form of the building stiffness matrix given by equation (2.19) is the basis used to determine the orientations of the principal axes of the system. The building mass matrix with respect to $\mathbf{u}^*$ remains in the same form given in equation (2.12).

2.3 Location of the Center of Rigidity

From the building stiffness matrix **K** defined with respect to the degrees of freedom **u** at reference point O, where $\mathbf{u}^T = < u_x \; u_y \; u_\theta >$, the building stiffness matrix at any other point can be determined by simple transformation of **K**. In particular, the building stiffness matrix $\tilde{\mathbf{K}}$ with respect to degrees of freedom $\tilde{\mathbf{u}}$, where $\tilde{\mathbf{u}}^T = < \tilde{u}_x \; \tilde{u}_y \; u_\theta >$ is defined at the center of rigidity of the system, is related to the building stiffness matrix **K** by:

$$\tilde{\mathbf{K}} = \tilde{\mathbf{a}}^T \, \mathbf{K} \, \tilde{\mathbf{a}} \tag{2.20}$$

in which $\tilde{\mathbf{a}}$ is a transformation matrix relating **u** to $\tilde{\mathbf{u}}$:

$$\mathbf{u} = \begin{Bmatrix} u_x \\ u_y \\ u_\theta \end{Bmatrix} = \begin{bmatrix} 1 & 0 & y_R \\ 0 & 1 & -x_R \\ 0 & 0 & 1 \end{bmatrix} \begin{Bmatrix} \tilde{u}_x \\ \tilde{u}_y \\ u_\theta \end{Bmatrix} = \tilde{\mathbf{a}} \, \tilde{\mathbf{u}} \tag{2.21}$$

Substituting equations (2.21) and (2.10) into (2.20), leads to:

$$\tilde{\mathbf{K}} = \begin{bmatrix} K_x & K_{xy} & K_x y_R - K_{xy} x_R + K_{x\theta} \\ K_{yx} & K_y & K_{yx} y_R - K_y x_R + K_{y\theta} \\ K_{\theta x} + y_R K_x - x_R K_{yx} & K_{\theta y} + y_R K_{xy} - x_R K_y & \tilde{K}_\theta \end{bmatrix} \tag{2.22}$$

in which,

$$\tilde{K}_\theta = K_\theta + 2K_{\theta x} y_R - 2K_{\theta y} x_R + K_x y_R^2 - 2K_{xy} x_R y_R + K_y x_R^2$$

Comparison of equations (2.22) and (2.15) leads to the following conditions:

$$K_x y_R - K_{xy} x_R + K_{x\theta} = 0 \tag{2.23a}$$

$$K_{yx} y_R - K_y x_R + K_{y\theta} = 0 \tag{2.23b}$$

$$\tilde{K}_x = K_x \;\; , \;\; \tilde{K}_y = K_y \;\; \text{and} \;\; \tilde{K}_{xy} = \tilde{K}_{yx} = K_{xy} \tag{2.24}$$

and:

$$\tilde{K}_\theta = K_\theta - x_R^2 \, K_y - y_R^2 \, K_x + 2 \, x_R \, y_R \, K_{xy} \tag{2.25}$$

in which equations (2.23) have been utilized. Solution of equations (2.23) yields the coordinates of the center of rigidity:

$$x_R = \frac{K_x K_{y\theta} - K_{xy} K_{x\theta}}{K_x K_y - K_{xy}^2} \tag{2.26}$$

and,

$$y_R = -\frac{K_y K_{x\theta} - K_{xy} K_{y\theta}}{K_x K_y - K_{xy}^2} \tag{2.27}$$

Similar equations were also obtained by Dempsey [10].

Thus, the building stiffness matrix $\tilde{\mathbf{K}}$, defined at the center of rigidity for lateral degrees of freedom $\tilde{u}_x$ and $\tilde{u}_y$, along the X and Y directions, and deck rotation u_θ about a vertical axis, is given by:

$$\tilde{\mathbf{K}} = \begin{bmatrix} K_x & K_{xy} & 0 \\ K_{yx} & K_y & 0 \\ 0 & 0 & \tilde{K}_\theta \end{bmatrix} \tag{2.28}$$

with $\tilde{K}_\theta$ given by equation (2.25). The location of the center of rigidity is defined by its coordinates x_R and y_R, given by equations (2.26) and (2.27), relative to reference point O. It is obvious from these equations that the location of the center of rigidity of a one-story system is independent of the applied loading.

Equations (2.26) and (2.27) can be simplified further in two cases:

1. If the building has one axis of stiffness symmetry (e.g. Figure 2a), then one of the principal axes of the system coincides with its axis of symmetry, and the other is perpendicular to it. In this case, it is only natural to choose the reference X and Y axes to be in the same directions as the principal axes of the system. If the X-axis is chosen in the direction of the symmetry axis, then, referring to equations (2.9d) and (2.9e), it is apparent that the terms K_{xyi} in equation (2.11c) and $K_{x\theta i}$ in equation (2.11b) occur in pairs that are equal in absolute values but are of opposite algebraic signs. It follows that:

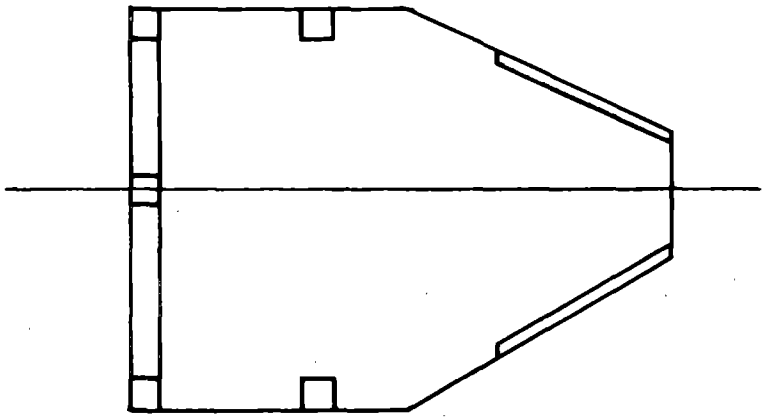

(a) One-way Symmetric Systems

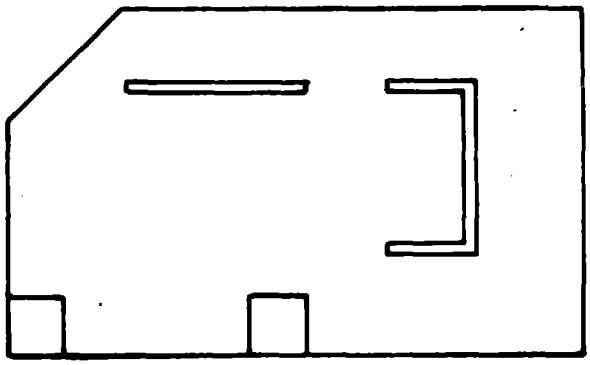

(b) Systems with Orthogonal Orientations of Elemental Principal Axes

FIGURE 2 Special Cases of Systems

$$K_{xy} = K_{yx} = 0 \quad \text{and} \quad K_{x\theta} = K_{\theta x} = 0$$

from which equations (2.26) and (2.27) are simplified to become:

$$x_R = \frac{K_{y\theta}}{K_y} \quad \text{and} \quad y_R = -\frac{K_{x\theta}}{K_x} = 0 \tag{2.29}$$

2. If the resisting elements of the building are arranged such that their principal axes form an orthogonal grid in plan (e.g. Figure 2b), then the principal axes of the system are also in the directions of the elemental principal axes. It is only natural in this case to choose the directions of the reference X and Y axes in the directions of the principal axes. It follows that β_i, the counterclockwise angle between the X-axis and the major principal axis of any resisting element is either zero or 90 degrees, and d_{ai} and d_{bi}, the perpendicular distances from reference point O to the major and minor principal axes of the element, are measured along the X- and Y-axes. Thus, equations (2.11) become:

$$K_x = \sum_i K_{xi} = \sum_i k_{xi}$$

$$K_y = \sum_i K_{yi} = \sum_i k_{yi}$$

$$K_\theta = \sum_i K_{\theta i} = \sum_i k_{\theta i} + k_{xi}\, y_i^2 + k_{yi}\, x_i^2$$

$$K_{xy} = K_{yx} = 0 \tag{2.30}$$

$$K_{x\theta} = K_{\theta x} = \sum_i K_{x\theta i} = -\sum_i k_{xi}\, y_i$$

$$K_{y\theta} = K_{\theta y} = \sum_i K_{y\theta i} = \sum_i k_{yi}\, x_i$$

where k_{xi} and k_{yi} are the lateral stiffnesses of the i^{th} resisting element along its principal axes, which are oriented along the X and Y reference axes; x_i and y_i are the X and Y distances of the principal axes of the i^{th} resisting element from the X and Y axes. Substituting equations (2.30) into (2.26) and (2.27), we obtain:

$$x_R = \frac{K_{y\theta}}{K_y} = \frac{\sum_i k_{yi}\, x_i}{\sum_i k_{yi}} \quad \text{and} \quad y_R = -\frac{K_{x\theta}}{K_x} = \frac{\sum_j k_{xi}\, y_i}{\sum_j k_{xi}} \tag{2.31}$$

Equations (2.31) are well known in the literature [e.g. 11] since most past studies have been concerned with buildings consisting of resisting elements arranged such that their principal axes form an orthogonal grid in plan.

2.4 Coincidence of Center of Twist, Shear Center and Center of rigidity

2.4.1 Center of Twist

The center of twist of the one-story system is defined in Section 2.1 as the point in the plane of the diaphragm that does not undergo any translational displacement when the diaphragm is subjected to a static horizontal torsional moment. Thus, if degrees of freedom of the diaphragm are defined at its center of twist, the building stiffness matrix obtained should be of the same form given by equation (2.15). The location of the center of twist is, therefore, determined by following the same steps as in Section 2.3 to determine the location of the center of rigidity, with x_T and y_T, the X and Y coordinates of the center of twist, substituted for x_R and y_R in equations (2.21) to (2.23). Solving the modified equations (2.23) for x_T and y_T yields the same expressions for the coordinates of the center of twist as the center of rigidity (equations (2.26) and (2.27)). Hence, the center of twist of a one-story system coincides with its center of rigidity. The same conclusion is reached in [8] using an approach based on energy principles.

2.4.2 Shear Center

The shear center of the one-story system is defined in Section 2.1 as the point in the plane of the diaphragm through which the resultant of the shear forces of the resisting elements passes when the diaphragm is subjected to a system of horizontal lateral forces causing no twist ($u_\theta = 0$) of the diaphragm. Substituting $u_\theta = 0$ in equations (2.5), the lateral displacements of the i^{th} resisting element along its principal axes are given by:

$$v_{ai} = (\cos\beta_i)\,u_x + (\sin\beta_i)\,u_y \tag{2.32a}$$

$$v_{bi} = -(\sin\beta_i)\,u_x + (\cos\beta_i)\,u_y \tag{2.32b}$$

The shearing forces Q_{ai} and Q_{bi} experienced by the ith resisting element along its principal axes are therefore given by:

$$Q_{ai} = k_{ai}\,v_{ai} = (k_{ai}\cos\beta_i)u_x + (k_{ai}\sin\beta_i)u_y \tag{2.33a}$$

$$Q_{bi} = k_{bi}\,v_{bi} = (-k_{bi}\sin\beta_i)u_x + (k_{bi}\cos\beta_i)u_y \tag{2.33b}$$

The shearing forces Q_{xi} and Q_{yi} experienced by the ith resisting element along the X and Y reference axes are the sum of the components of Q_{ai} and Q_{bi} along the X and Y axes, respectively, i.e.:

$$Q_{xi} = Q_{ai}\cos\beta_i - Q_{bi}\sin\beta_i \tag{2.34a}$$

$$Q_{yi} = Q_{ai}\sin\beta_i + Q_{bi}\cos\beta_i \tag{2.34b}$$

Substituting equations (2.33) into (2.34) and utilizing equations (2.9), results in:

$$Q_{xi} = [\,k_{ai}\cos^2\beta_i + k_{bi}\sin^2\beta_i\,]u_x + [\,(k_{ai}-k_{bi})\sin\beta_i\cos\beta_i\,]u_y = K_{xi}u_x + K_{xyi}u_y \tag{2.35a}$$

$$Q_{yi} = [\,(k_{ai}-k_{bi})\sin\beta_i\cos\beta_i\,]u_x + [\,k_{ai}\sin^2\beta_i + k_{bi}\cos^2\beta_i\,]u_y = K_{yxi}u_x + K_{yi}u_y \tag{2.35b}$$

The resultant of the shearing forces has X and Y components equal to $\sum_i Q_{xi}$ and $\sum_i Q_{yi}$, respectively, and passes through the shear center with X and Y coordinates denoted by x_S and y_S. Referring to Figure 1a, equilibrium of moments of all shearing forces acting in the plane of the diaphragm about a vertical axis passing through O, gives:

$$\sum_i \pm Q_{ai}\,d_{ai} + \sum_i \pm Q_{bi}\,d_{bi} - x_S \sum_i Q_{yi} + y_S \sum_i Q_{xi} = 0 \tag{2.36}$$

The algebraic sign accompanying Q_{ai} and Q_{bi} in equation (2.36) depends on whether the forces cause positive or negative moments about the vertical axis passing through O. Substituting equations (2.33) and (2.35) into (2.36) and utilizing equations (2.9) and (2.11), leads to:

$$(\,K_{x\theta} + K_x\,y_S - K_{xy}\,x_S\,)\,u_x + (\,K_{y\theta} + K_{xy}\,y_S - K_y\,x_S\,)\,u_y = 0 \tag{2.37}$$

Since u_x and u_y are independent, equation (2.37) results in the following two equations:

$$K_{x\theta} + K_x y_S - K_{xy} x_S = 0 \tag{2.38a}$$

$$K_{y\theta} + K_{xy} y_S - K_y x_S = 0 \tag{2.38b}$$

Equations (2.38) are equivalent to equations (2.23) which proves that the shear center is coincident with the center of rigidity.

It is apparent from the preceding results that the center of rigidity, the center of twist, and the shear center for a one-story building with rigid diaphragm are the same point. Thus, the definitions given in Section 2.1 for these three centers describe different roles of this unique point in the static response of a one-story system; i.e., there is a unique point in the plane of the diaphragm with the following properties: (1) a static horizontal force acting through the point causes no twist of the diaphragm, (2) the resultant of the shear forces experienced by the various resisting elements also passes through the point if the external applied forces cause no twist of the diaphragm; and (3) the diaphragm twists or rotates about a vertical axis passing through this point when subjected to any static torsional moment. The unique 'center' depends on the stiffness and locations of the various resisting elements but not on the applied loads.

2.5 Orientations of the Principal Axes

The orientations of the principal axes of the system are determined from the special form of the building stiffness matrix $\mathbf{K}^*$, given by equation (2.19), with respect to degrees of freedom $\mathbf{u}^*$, where $\mathbf{u}^{*T} = < u_I^* \; u_{II}^* \; u_\theta >$ with u_I^* and u_{II}^* the lateral displacements at the center of rigidity along principal axes I and II, respectively. The matrix $\mathbf{K}^*$ is related to $\tilde{\mathbf{K}}$, the building stiffness matrix defined by equation (2.28) with respect to degrees of freedom $\tilde{\mathbf{u}}$, where $\tilde{\mathbf{u}}^T = < \tilde{u}_x \; \tilde{u}_y \; u_\theta >$ with $\tilde{u}_x$ and $\tilde{u}_y$ the lateral displacements at the center of rigidity along the X and Y axes, by:

$$\mathbf{K}^* = \mathbf{a}^{*T} \tilde{\mathbf{K}} \; \mathbf{a}^* \tag{2.39}$$

The transformation matrix $\mathbf{a}^*$ relates $\tilde{\mathbf{u}}$ to $\mathbf{u}^*$:

$$\tilde{\mathbf{u}} = \begin{Bmatrix} \tilde{u}_x \\ \tilde{u}_y \\ u_\theta \end{Bmatrix} = \begin{bmatrix} \cos\eta & -\sin\eta & 0 \\ \sin\eta & \cos\eta & 0 \\ 0 & 0 & 1 \end{bmatrix} \begin{Bmatrix} u_I^* \\ u_{II}^* \\ u_\theta \end{Bmatrix} = \mathbf{a}^* \mathbf{u}^* \tag{2.40}$$

where η is the counterclockwise angle between the reference X-axis and the principal axis I of the system. Substituting equations (2.40) and (2.28) into (2.39) and comparing with equations (2.19), leads to:

$$K_I^* = K_x \cos^2\eta + K_y \sin^2\eta + 2\, K_{xy} \sin\eta \cos\eta \tag{2.41}$$

$$K_{II}^* = K_x \sin^2\eta + K_y \cos^2\eta - 2\, K_{xy} \sin\eta \cos\eta \tag{2.42}$$

$$K_\theta^* = \tilde{K}_\theta \tag{2.43}$$

and,

$$-(K_x - K_y)\sin\eta \cos\eta + K_{xy}(\cos^2\eta - \sin^2\eta) = 0 \tag{2.44}$$

which results in:

$$\tan 2\eta = \frac{2\, K_{xy}}{K_x - K_y} \tag{2.45}$$

The orientation of principal axis I is defined by the angle η, and the principal axis II is perpendicular to axis I.

Determining $\sin\eta$ and $\cos\eta$ from equation (2.45) and substituting these in equations (2.41) and (2.42) leads to:

$$K_I^*,\, K_{II}^* = \frac{K_x + K_y}{2} \pm \left[\left(\frac{K_x - K_y}{2} \right)^2 + K_{xy}^2 \right]^{1/2} \tag{2.46}$$

Thus, the building stiffness matrix $\mathbf{K}^*$ defined with respect to degrees of freedom $\mathbf{u}^*$, where $\mathbf{u}^{*T} = < u_I^*\ u_{II}^*\ u_\theta >$, is given by:

$$\mathbf{K}^* = \begin{bmatrix} K_I^* & 0 & 0 \\ 0 & K_{II}^* & 0 \\ 0 & 0 & \tilde{K}_\theta \end{bmatrix} \tag{2.47}$$

with K_I^* and K_{II}^* given by equations (2.46) and $\tilde{K}_\theta$ by equation (2.25).

For the two cases-- the case when the building has an axis of stiffness symmetry and the case when the principal axes of all resisting elements are parallel or perpendicular-- discussed in Section 2.2, equations (2.45) simplify to:

$$\tan 2\eta = \frac{2K_{xy}}{K_x - K_y} = 0 \tag{2.48}$$

since $K_{xy} = 0$. Thus the principal axes of the system are along the X- and Y- axes and equations (2.46) specialize to become:

$$K_I^* = K_x \quad \text{and} \quad K_{II}^* = K_y \tag{2.49}$$

2.6 EXAMPLE

Consider a one-story building consisting of four frames of identical lateral stiffness k, located as shown in Figure 3. Thus:

$$k_{a1} = k_{a2} = k_{a3} = k_{a4} = k$$

and,

$$k_{b1} = k_{b2} = k_{b3} = k_{b4} = 0$$

For frame (1) $d_{a1} = 0$ and $\beta_1 = 90^o$; for frame (2) $d_{a2} = a$ and $\beta_2 = 0^o$; for frame (3) $d_{a3} = 0$ and $\beta_3 = 0^o$; and for frame (4) $d_{a4} = 2a$ and $\beta_4 = 135^o$. Using equations (2.9) and (2.10), the contributions of each frame to the building stiffness matrix is given by:

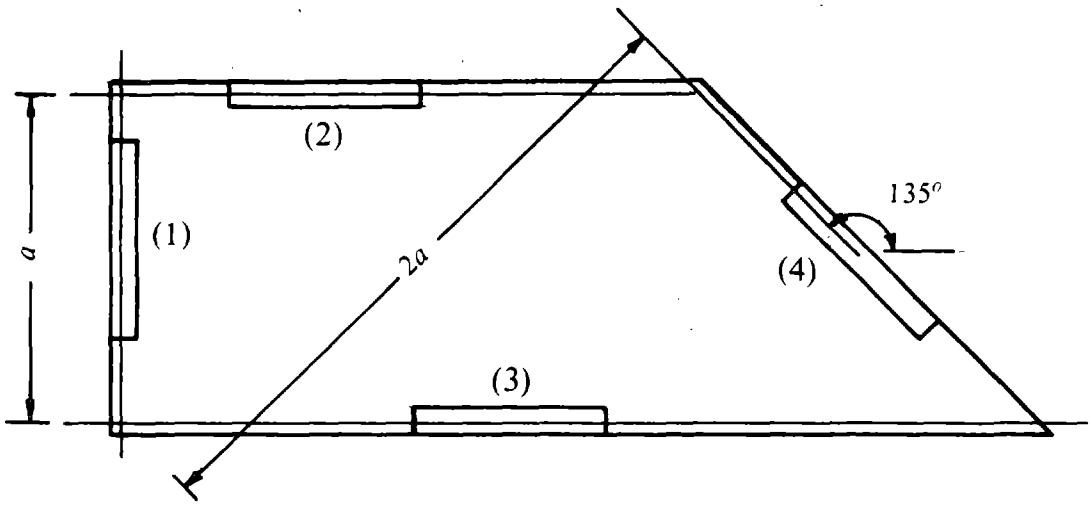

FIGURE 3 Plan of Example (Section 2.6)

$$\mathbf{K}_1 = \begin{bmatrix} 0 & 0 & 0 \\ 0 & k & 0 \\ 0 & 0 & 0 \end{bmatrix}, \mathbf{K}_2 = \begin{bmatrix} k & 0 & -ka \\ 0 & 0 & 0 \\ -ka & 0 & ka^2 \end{bmatrix},$$

$$\mathbf{K}_3 = \begin{bmatrix} k & 0 & 0 \\ 0 & 0 & 0 \\ 0 & 0 & 0 \end{bmatrix}, \text{ and } \mathbf{K}_4 = \begin{bmatrix} 0.5k & -0.5k & -1.414ka \\ -0.5k & 0.5k & 1.414ka \\ -1.414ka & 1.414ka & 4ka^2 \end{bmatrix} \tag{2.50}$$

The building stiffness matrix is given by:

$$\mathbf{K} = \begin{bmatrix} K_x & K_{xy} & K_{x\theta} \\ K_{yx} & K_y & K_{y\theta} \\ K_{\theta x} & K_{\theta y} & K_\theta \end{bmatrix} \tag{2.10}$$

with,

$$K_x = 0 + k + k + 0.5\,k = 2.5\,k$$

$$K_y = k + 0 + 0 + 0.5\,k = 1.5\,k$$

$$K_\theta = 0 + k\,a^2 + 0 + 4\,k\,a^2 = 5\,ka^2$$

$$K_{xy} = K_{yx} = 0 + 0 + 0 - 0.5\,k = -0.5\,k \tag{2.51}$$

$$K_{x\theta} = K_{\theta x} = 0 - k\,a + 0 - 1.414\,k\,a = -2.414\,ka$$

$$K_{y\theta} = K_{\theta y} = 0 + 0 + 0 + 1.414\,k\,a = 1.414\,ka$$

Substituting equations (2.51) into (2.26) and (2.27), the coordinates of the center of rigidity (center of twist or shear center) are given by:

$$x_R = \frac{(2.5)(1.414\,a) - (-0.5)(-2.414\,a)}{(2.5)(1.5) - (-0.5)^2} = 0.66\,a$$

and,

$$y_R = -\frac{(1.5)(-2.414\,a) - (-0.5)(1.414\,a)}{(2.5)(1.5) - (-0.5)^2} = 0.83\,a$$

The orientation of principal axis I is determined by substituting equations (2.51) into (2.45):

$$\tan 2\eta = \frac{2(-0.5)}{2.5 - 1.5} = -1$$

or $\eta = 135^{o}$.

3. MULTI-STORY BUILDINGS

It was demonstrated in Section 2 that the shear center, the center of rigidity, and the center of twist of a one-story system are all coincident. The location of this unique point is independent of the applied loading and can easily be determined knowing the stiffnesses and locations of the various resisting elements of the system. In this section, these concepts are extended and analyzed for multi-story buildings. It is found that the defined centers are, in general, not coincident, and their locations depend on the applied lateral or torsional loadings in addition to the stiffness properties. For a special class of multi-story buildings, identified in Section 4, the centers for each floor coincide, the centers of all floors lie on a vertical line, and are load-independent.

3.1 Basic Concepts and Definitions

Consider a multi-story building consisting of vertical resisting elements (frames, columns, shear walls or shear-wall cores), with arbitrary locations and arbitrary orientations of their principal planes, joined at each story level by rigid diaphragms or decks of arbitrary shapes (Figure 4a).

The **centers of rigidity** of the floors of the building are points on the floor diaphragms through which any set of static horizontal forces of arbitrary magnitude and direction causes no rotation or twisting of any of the floors. The **principal axes** of a floor are two orthogonal axes passing through its center of rigidity, such that any set of static horizontal forces applied simultaneously along one of the principal axes of each floor, causes each floor to displace laterally in the direction of its applied force without any twist. It is generally not possible to determine the orientations of the principal axes of the floors of a multi-story building satisfying the definition given here. Only for a special class of buildings, identified in Section 4, the principal axes of each floor can be determined, and for all floors they are found to be oriented along the same two orthogonal direction.

The **centers of twist** of the floors of the building are the points on the floor diaphragms which remain stationary when the building is subjected to any set of static horizontal torsional moments, applied at the floor levels, i.e. the floor diaphragms undergo pure twist about these points.

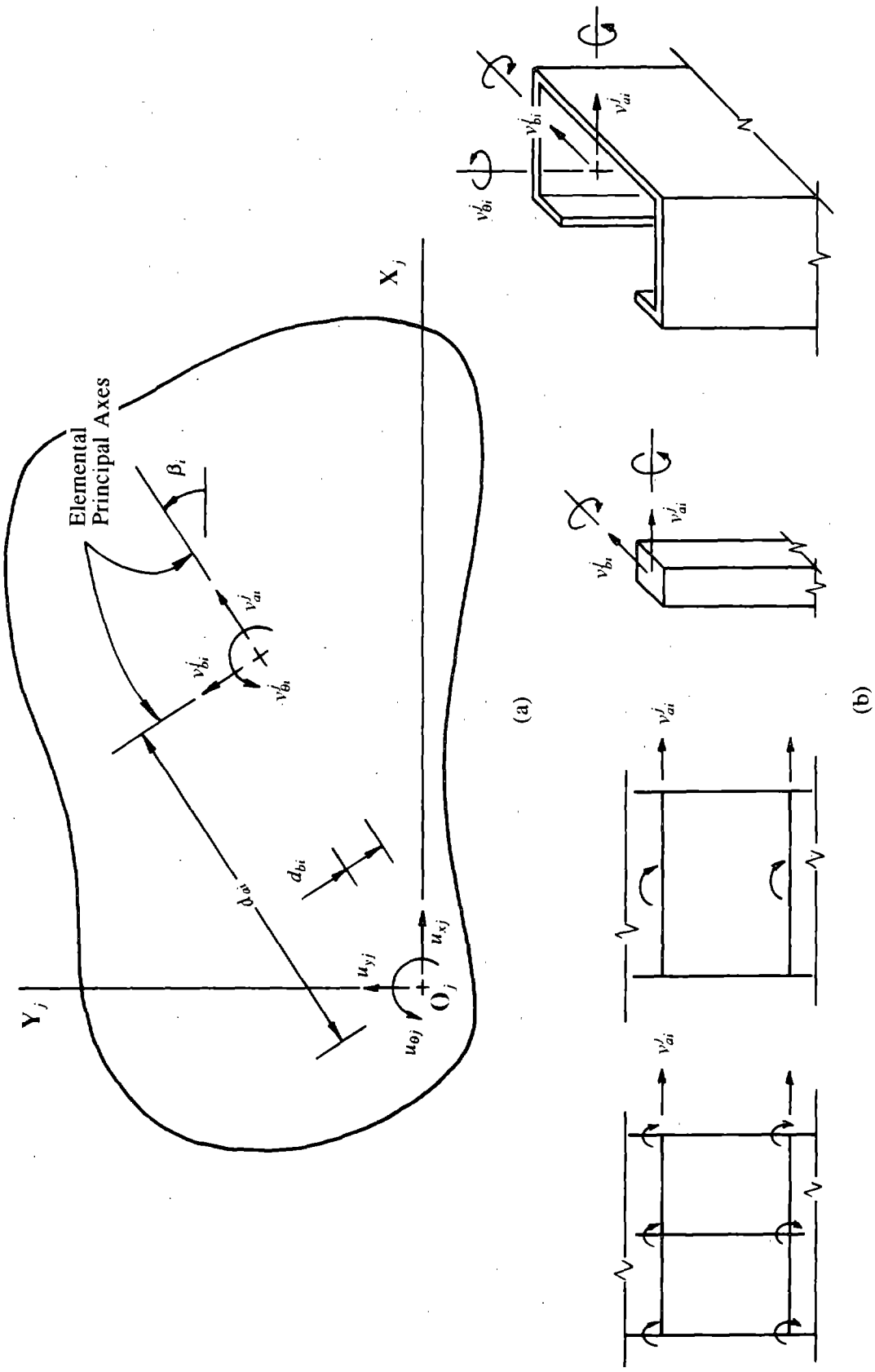

FIGURE 4 Multi-story Building

The **shear center** of a floor of the building is the point on the floor through which the resultant of the interstory shear forces at that level (due to static forces applied at the floors above and including the floor in consideration) experienced by all resisting elements passes when the floors of the building are subjected to static horizontal forces passing through the centers of rigidity of the floors, thus causing no twist in any of the floors.

The **center of mass** of a floor of the building is the point on the floor through which the resultant of the inertia forces of the floor passes. If the masses of individual resisting elements are negligible compared to the masses of the floors, the centers of mass of a building with floors having uniform mass distribution coincide with the geometric centers of the floors.

The **static eccentricity** e_j of the j^{th} floor is defined as the distance between its center of mass and its center of rigidity. In some building codes [e.g. 4], the static eccentricity of a floor is defined as the distance between its center of mass and its shear center. Since, as will be seen later, shear centers of multi-story buildings do not generally coincide with its centers of rigidity, there is more than one definition possible for static eccentricity.

3.2 Equations of Motion

A vertical axis Z, chosen as a reference axis, intersects the j^{th} floor at O_j, through which two horizontal orthogonal axes, X_j and Y_j are defined as reference axes for the j^{th} floor. The reference axes X_j (or Y_j) of all floors are chosen to be in the same direction, so that the angle between the major principal planes of the i^{th} resisting element and the plane defined by Z and X_j is the same for all floors and is denoted by β_i, measured counterclockwise from X_j, and the perpendicular distances from O_j to the major and minor principal planes of the i^{th} resisting element are the same for all floors and are denoted by d_{ai} and d_{bi}, respectively. Each floor 'j' contributes three degrees of freedom to the total number of degrees of freedom of the system: two horizontal displacements u_{xj} and u_{yj}, relative to the ground, along reference axes X_j and Y_j, and the rotation $u_{\theta j}$ of the j^{th} floor about a vertical axis. The displacements vectors $\mathbf{u}_x$, $\mathbf{u}_y$ and $\mathbf{u}_\theta$ are of dimension N, the number of stories

of the building, with entries equal to u_{xj}, u_{yj} and $u_{\theta j}$, respectively. The building stiffness matrix **K** defined with respect to the 3N degrees of freedom **u**, where $\mathbf{u}^T = <\mathbf{u}_x^T\ \mathbf{u}_y^T\ \mathbf{u}_\theta^T>$, is the sum of the stiffness matrices $\mathbf{K}_i$ of individual resisting elements, also computed with respect to **u**:

$$\mathbf{K} = \sum_i \mathbf{K}_i \tag{3.1}$$

The stiffness matrix $\mathbf{K}_i$ of the i^{th} resisting element is derived from its lateral stiffness matrices along its two principal planes-- the two mutually orthogonal vertical planes which intersect the floors of the resisting element at their principal axes, which in turn intersect at the shear centers of the element, such that any static horizontal force applied through the shear center at a floor level along either of its principal axes would cause the floor to translate in the same direction as the force without any twist [13]-- and its torsional stiffness matrix about the vertical axis of intersection of its two principal planes, i.e. about the vertical axis on which the shear centers of the resisting element lie. Lateral stiffness matrices of frames and shear walls along their minor principal planes, i.e. along the direction perpendicular to their own plane, are assumed to be negligible. Shear deformations are negligible for frame members so that only flexural deformations are considered for frames. A column contributes to system lateral stiffness matrices due to its lateral stiffnesses along both of its principal planes. Because the individual torsional stiffnesses of frames, shear walls and columns are negligible, the contributions of these resisting elements to the torsional stiffness matrix of the building are primarily due to the lateral stiffness matrices of these resisting elements acting at some distance from O_j. On the other hand, the torsional stiffness of a shear-wall core element is significant, and its contribution to the torsional stiffness matrix of the building is due to its torsional stiffness matrix as well as to its lateral stiffness matrices along its two principal planes.

The stiffness matrix $\mathbf{K}_i$ of the i^{th} resisting element is determined by the following procedure:

1. Define the local degrees of freedom for each resisting element (Figure 4b) as follows:

   (a) For a shear wall define at each floor level one translational degree of freedom along the plane of the shear wall, i.e. along its major principal plane, and one rotational degree of freedom about its minor principal plane, i.e. along a horizontal axis perpendicular to its plane.

(b) For a frame define one translational degree of freedom at each floor level, along the plane of the frame, i.e. along its major principal plane, and a rotational degree of freedom per joint about horizontal axes perpendicular to the plane of the frame, i.e. along the direction of its minor principal plane.

(c) For a column define two translational degrees of freedom at the floor level along the principal planes of the column and two rotational degrees of freedom about these planes.

(d) For a shear-wall core define five degrees of freedom at each floor level: two translations along its principal axes in the floor, two rotations about these axes, and one torsional rotation about the vertical axis of intersection of its two principal planes.

2. Obtain a complete stiffness matrix for the resisting element for the degrees of freedom defined, taking into account flexural and shear deformations for shear walls and shear-wall cores, and only flexural deformations for frames and columns.

3. Eliminate the joint rotational degrees of freedom of the resisting elements by the static condensation process. The resulting condensed matrix $\mathbf{k}_i$ of a shear-wall core element 'i' is of dimension equal to 3N, N the number of stories, satisfying the following equation:

$$\mathbf{Q}_i = \begin{Bmatrix} \mathbf{Q}_{ai} \\ \mathbf{Q}_{bi} \\ \mathbf{Q}_{\theta i} \end{Bmatrix} = \begin{bmatrix} \mathbf{k}_{ai} & \mathbf{0} & \mathbf{0} \\ \mathbf{0} & \mathbf{k}_{bi} & \mathbf{0} \\ \mathbf{0} & \mathbf{0} & \mathbf{k}_{\theta i} \end{bmatrix} \begin{Bmatrix} \mathbf{v}_{ai} \\ \mathbf{v}_{bi} \\ \mathbf{v}_{\theta i} \end{Bmatrix} = \mathbf{k}_i \, \mathbf{v}_i \tag{3.2}$$

where $\mathbf{k}_{ai}$ and $\mathbf{k}_{bi}$ are the lateral stiffness matrices of the shear-wall core along its two principal planes, and $\mathbf{k}_{\theta i}$ is its torsional stiffness matrix about the vertical axis of intersection of its two principal planes; and $\mathbf{0}$ denotes a zero square matrix of dimension N. The applied static force vectors $\mathbf{Q}_{ai}$, $\mathbf{Q}_{bi}$ and $\mathbf{Q}_{\theta i}$ and resulting displacement vectors $\mathbf{v}_{ai}$, $\mathbf{v}_{bi}$ and $\mathbf{v}_{\theta i}$ in these three directions are related through $\mathbf{k}_{ai}$, $\mathbf{k}_{bi}$ and $\mathbf{k}_{\theta i}$, respectively. Since $\mathbf{k}_{\theta i}$ is negligible for columns, shear walls and frames, and $\mathbf{k}_{bi}$ is negligible for frames and shear walls, equations (3.2) are simplified for these resisting elements. For columns, we obtain:

$$\mathbf{Q}_i = \begin{Bmatrix} \mathbf{Q}_{ai} \\ \mathbf{Q}_{bi} \end{Bmatrix} = \begin{bmatrix} \mathbf{k}_{ai} & \mathbf{0} \\ \mathbf{0} & \mathbf{k}_{bi} \end{bmatrix} \begin{Bmatrix} \mathbf{v}_{ai} \\ \mathbf{v}_{bi} \end{Bmatrix} = \mathbf{k}_i \, \mathbf{v}_i \tag{3.3}$$

For shear walls and frames:

$$\mathbf{Q}_{ai} = \mathbf{k}_{ai} \, \mathbf{v}_{ai} \tag{3.4}$$

4. Determine the transformation matrix $\mathbf{a}_i$, relating the resisting element displacement vector $\mathbf{v}_i$, to the system degrees of freedom $\mathbf{u}$. For a shear-wall core, $\mathbf{a}_i$ is given by:

$$\mathbf{v}_i = \begin{Bmatrix} \mathbf{v}_{ai} \\ \mathbf{v}_{bi} \\ \mathbf{v}_{\theta i} \end{Bmatrix} = \begin{bmatrix} \cos\beta_i \mathbf{I} & \sin\beta_i \mathbf{I} & \pm d_{ai}\mathbf{I} \\ -\sin\beta_i \mathbf{I} & \cos\beta_i \mathbf{I} & \pm d_{bi}\mathbf{I} \\ \mathbf{0} & \mathbf{0} & \mathbf{I} \end{bmatrix} \begin{Bmatrix} \mathbf{u}_x \\ \mathbf{u}_y \\ \mathbf{u}_\theta \end{Bmatrix} = \mathbf{a}_i \, \mathbf{u} \tag{3.5}$$

and for a column, the transformation matrix $\mathbf{a}_i$ is given by:

$$\mathbf{v}_i = \begin{Bmatrix} \mathbf{v}_{ai} \\ \mathbf{v}_{bi} \end{Bmatrix} = \begin{bmatrix} \cos\beta_i \mathbf{I} & \sin\beta_i \mathbf{I} & \pm d_{ai}\mathbf{I} \\ -\sin\beta_i \mathbf{I} & \cos\beta_i \mathbf{I} & \pm d_{bi}\mathbf{I} \end{bmatrix} \begin{Bmatrix} \mathbf{u}_x \\ \mathbf{u}_y \\ \mathbf{u}_\theta \end{Bmatrix} = \mathbf{a}_i \, \mathbf{u} \tag{3.6}$$

in which β_i is the counterclockwise angle between the X_j-axes and the major principal plane of the shear-wall core or column; d_{ai} and d_{bi} are the perpendicular distances from reference points O_j to the major and minor principal planes, respectively; and $\mathbf{I}$ is a diagonal unit matrix. In equations (3.5) and (3.6), the choice of a positive or a negative algebraic sign to accompany d_{ai} (or d_{bi}) depends on whether a unit $u_{\theta j}$ rotation of the j^{th} floor causes displacements along the major (or minor) principal planes in the same or opposite direction to $\mathbf{v}_{ai}$ (or $\mathbf{v}_{bi}$). For frames and shear walls, $\mathbf{a}_i$ is obtained from:

$$\mathbf{a}_i = \begin{bmatrix} \cos\beta_i \mathbf{I} & \sin\beta_i \mathbf{I} & \pm d_{ai}\mathbf{I} \end{bmatrix} \begin{Bmatrix} \mathbf{u}_x \\ \mathbf{u}_y \\ \mathbf{u}_\theta \end{Bmatrix} = \mathbf{a}_i \, \mathbf{u} \tag{3.7}$$

where β_i is the counterclockwise angle between the X_j-axes and the plane of the frame or shear wall, and d_{ai} is the perpendicular distance from reference point O_j to the plane of the frame or shear wall. Again, the choice of a positive or a negative algebraic sign to

accompany d_{ai} in equation (3.7) depends on whether a unit $u_{\theta j}$ rotation of the j^{th} floor causes a displacement along the plane of the frame or shear wall in the same or opposite direction to v_{ai}.

5. The contribution of resisting element 'i' to building stiffness matrix is $\mathbf{K}_i$, and is determined by:

$$\mathbf{K}_i = \mathbf{a}_i^T \, \mathbf{k}_i \, \mathbf{a}_i = \begin{bmatrix} \mathbf{K}_{xi} & \mathbf{K}_{xyi} & \mathbf{K}_{x\theta i} \\ \mathbf{K}_{yxi} & \mathbf{K}_{yi} & \mathbf{K}_{y\theta i} \\ \mathbf{K}_{\theta xi} & \mathbf{K}_{\theta yi} & \mathbf{K}_{\theta i} \end{bmatrix} \tag{3.8}$$

in which,

$$\begin{aligned} \mathbf{K}_{xi} &= \cos^2\beta_i \, \mathbf{k}_{ai} + \sin^2\beta_i \, \mathbf{k}_{bi} \\ \mathbf{K}_{yi} &= \sin^2\beta_i \, \mathbf{k}_{ai} + \cos^2\beta_i \, \mathbf{k}_{bi} \\ \mathbf{K}_{\theta i} &= d_{ai}^2 \, \mathbf{k}_{ai} + d_{bi}^2 \, \mathbf{k}_{bi} + \mathbf{k}_{\theta i} \\ \mathbf{K}_{xyi} &= \mathbf{K}_{yxi} = \sin\beta_i \cos\beta_i \, (\mathbf{k}_{ai} - \mathbf{k}_{bi}) \\ \mathbf{K}_{x\theta i} &= \mathbf{K}_{\theta xi} = \pm \, d_{ai} \cos\beta_i \, \mathbf{k}_{ai} - (\pm) d_{bi} \sin\beta_i \, \mathbf{k}_{bi} \\ \mathbf{K}_{y\theta i} &= \mathbf{K}_{\theta yi} = \pm \, d_{ai} \sin\beta_i \, \mathbf{k}_{ai} \pm d_{bi} \cos\beta_i \, \mathbf{k}_{bi} \end{aligned} \tag{3.9}$$

As mentioned earlier, $\mathbf{k}_{\theta i}$ is negligibly small for frames, shear walls and columns but is significant for shear-wall cores, and $\mathbf{k}_{bi}$ is negligible for frames and shear walls.

The building stiffness matrix $\mathbf{K}$ for degrees of freedom $\mathbf{u}^T = < \mathbf{u}_x \, \mathbf{u}_y \, \mathbf{u}_\theta >$, defined at reference points O_j, is given by superposition of the element stiffness matrices (equation (3.1)) resulting in:

$$\mathbf{K} = \begin{bmatrix} \mathbf{K}_x & \mathbf{K}_{xy} & \mathbf{K}_{x\theta} \\ \mathbf{K}_{yx} & \mathbf{K}_y & \mathbf{K}_{y\theta} \\ \mathbf{K}_{\theta x} & \mathbf{K}_{\theta y} & \mathbf{K}_\theta \end{bmatrix} \tag{3.10}$$

with,

$$\mathbf{K}_x = \sum_i \mathbf{K}_{xi} \ , \ \mathbf{K}_y = \sum_i \mathbf{K}_{yi} \ , \ \mathbf{K}_\theta = \sum_i \mathbf{K}_{\theta i}$$

$$\mathbf{K}_{x\theta} = \mathbf{K}_{\theta x} = \sum_i \mathbf{K}_{x\theta i} \ , \ \mathbf{K}_{y\theta} = \mathbf{K}_{\theta y} = \sum_i \mathbf{K}_{y\theta i} \tag{3.11}$$

$$\mathbf{K}_{xy} = \mathbf{K}_{yx} = \sum_i \mathbf{K}_{xyi}$$

The undamped equations of motion for the multi-story building, assuming linear behavior, subjected to earthquake ground motion accelerations $a_{gx}(t)$ and $a_{gy}(t)$ along the X_j- and Y_j-axes, are:

$$\begin{bmatrix} \mathbf{m} & \mathbf{0} & -\mathbf{m}\mathbf{y}_M \\ \mathbf{0} & \mathbf{m} & \mathbf{m}\mathbf{x}_M \\ -\mathbf{y}_M\mathbf{m} & \mathbf{x}_M\mathbf{m} & \mathbf{J}_O \end{bmatrix} \begin{Bmatrix} \ddot{\mathbf{u}}_x \\ \ddot{\mathbf{u}}_y \\ \ddot{\mathbf{u}}_\theta \end{Bmatrix} + \begin{bmatrix} \mathbf{K}_x & \mathbf{K}_{xy} & \mathbf{K}_{x\theta} \\ \mathbf{K}_{yx} & \mathbf{K}_y & \mathbf{K}_{y\theta} \\ \mathbf{K}_{\theta x} & \mathbf{K}_{\theta y} & \mathbf{K}_\theta \end{bmatrix} \begin{Bmatrix} \mathbf{u}_x \\ \mathbf{u}_y \\ \mathbf{u}_\theta \end{Bmatrix} = - \begin{Bmatrix} \mathbf{m}\mathbf{1}a_{gx}(t) \\ \mathbf{m}\mathbf{1}a_{gy}(t) \\ -\mathbf{y}_M\mathbf{m}\mathbf{1}a_{gx}(t) + \mathbf{x}_M\mathbf{m}\mathbf{1}a_{gy}(t) \end{Bmatrix} \tag{3.12}$$

where 1 denotes a vector of ones of dimension N; $\mathbf{m}$ is a diagonal mass matrix of dimension N with diagonal entry m_j equal to the mass of the jth floor; $\mathbf{x}_M$ and $\mathbf{y}_M$ are diagonal matrices of dimension N with diagonal entries equal to x_{Mj} and y_{Mj}, the coordinates of the center of mass of the jth floor relative to reference axes X_j and Y_j; $\mathbf{J}_O$ is a diagonal matrix of dimension N with diagonal entries J_{Oj}, the polar moment of inertia of the jth floor diaphragm about Z, the reference vertical axis passing through reference points O_j, given by:

$$J_{Oj} = m_j (r_j^2 + x_{Mj}^2 + y_{Mj}^2) \tag{3.13}$$

where r_j is the radius of gyration of the jth deck about a vertical axis passing through its center of mass. It is apparent from these equations of motion that translational ground motion along either the X- or the Y-axes will simultaneously cause both X- and Y- lateral displacements of points O_j as well as torsional rotations or twists of the floors about a vertical axis.

The equations of motion written with respect to degrees of freedom defined at any points other than O_j can be determined by standard transformation of equation (3.12). However, the general form of the equations of motion (the mass and stiffness matrices) remains as equation (3.12) unless the degrees of freedom are defined at the centers of rigidity provided these centers uniquely exist for the building, or at its centers of mass. When the equations of motion are written with

respect to degrees of freedom defined at the center of mass, the building mass matrix is of a special form, given by:

$$\mathbf{M}_M = \begin{bmatrix} \mathbf{m} & \mathbf{0} & \mathbf{0} \\ \mathbf{0} & \mathbf{m} & \mathbf{0} \\ \mathbf{0} & \mathbf{0} & \mathbf{J}_M \end{bmatrix}$$

where $\mathbf{J}_M$ is a diagonal matrix of dimension N with diagonal entries $J_{Mj} = m_j r_j^2$, the polar mass moment of inertia of the jth floor about a vertical axis passing through its center of mass. However, the coupling of the degrees of freedom in the building stiffness matrix remains of the form given in equation (3.12). The equations of motion are then given by:

$$\begin{bmatrix} \mathbf{m} & \mathbf{0} & \mathbf{0} \\ \mathbf{0} & \mathbf{m} & \mathbf{0} \\ \mathbf{0} & \mathbf{0} & \mathbf{J}_M \end{bmatrix} \begin{Bmatrix} \ddot{\mathbf{u}}_x \\ \ddot{\mathbf{u}}_y \\ \ddot{\mathbf{u}}_\theta \end{Bmatrix} + \begin{bmatrix} \mathbf{K}_x & \mathbf{K}_{xy} & \mathbf{K}_{x\theta} \\ \mathbf{K}_{yx} & \mathbf{K}_y & \mathbf{K}_{y\theta} \\ \mathbf{K}_{\theta x} & \mathbf{K}_{\theta y} & \mathbf{K}_\theta \end{bmatrix} \begin{Bmatrix} \mathbf{u}_x \\ \mathbf{u}_y \\ \mathbf{u}_\theta \end{Bmatrix} = - \begin{Bmatrix} \mathbf{m1}\, a_{gx}(t) \\ \mathbf{m1}\, a_{gy}(t) \\ \mathbf{0} \end{Bmatrix} \tag{3.14}$$

On the other hand, if the equations of motion are written for degrees of freedom $\tilde{\mathbf{u}}$, where $\tilde{\mathbf{u}}^T = <\tilde{\mathbf{u}}_x \ \tilde{\mathbf{u}}_y \ \mathbf{u}_\theta>$ with $\tilde{\mathbf{u}}_x$ and $\tilde{\mathbf{u}}_y$ the vectors of dimension N of jth entries $\tilde{u}_{xj}$ and $\tilde{u}_{yj}$ equal the lateral displacements at the center of rigidity of the jth floor along the X_j- and Y_j-axes, respectively, the building stiffness matrix assumes the form:

$$\tilde{\mathbf{K}} = \begin{bmatrix} \tilde{\mathbf{K}}_x & \tilde{\mathbf{K}}_{xy} & \mathbf{0} \\ \tilde{\mathbf{K}}_{yx} & \tilde{\mathbf{K}}_y & \mathbf{0} \\ \mathbf{0} & \mathbf{0} & \tilde{\mathbf{K}}_\theta \end{bmatrix} \tag{3.15}$$

since any set of horizontal static forces applied through the centers of rigidity causes only lateral displacements and no rotations of the decks (see the definition of the centers of rigidity given in Section 3.1). However, the mass matrix defined with respect to $\tilde{\mathbf{u}}$ remains in of the form given by equation (3.12), so that the equations of motion written with respect to $\tilde{\mathbf{u}}$ are given by:

$$\begin{bmatrix} \mathbf{m} & \mathbf{0} & -\mathbf{me}_y \\ \mathbf{0} & \mathbf{m} & \mathbf{me}_x \\ -\mathbf{e}_y\mathbf{m} & \mathbf{e}_x\mathbf{m} & \mathbf{J}_R \end{bmatrix} \begin{Bmatrix} \ddot{\tilde{\mathbf{u}}}_x \\ \ddot{\tilde{\mathbf{u}}}_y \\ \ddot{\mathbf{u}}_\theta \end{Bmatrix} + \begin{bmatrix} \tilde{\mathbf{K}}_x & \tilde{\mathbf{K}}_{xy} & \mathbf{0} \\ \tilde{\mathbf{K}}_{yx} & \tilde{\mathbf{K}}_y & \mathbf{0} \\ \mathbf{0} & \mathbf{0} & \tilde{\mathbf{K}}_\theta \end{bmatrix} \begin{Bmatrix} \tilde{\mathbf{u}}_x \\ \tilde{\mathbf{u}}_y \\ \mathbf{u}_\theta \end{Bmatrix} = -\begin{Bmatrix} \mathbf{m1}a_{gx}(t) \\ \mathbf{m1}a_{gy}(t) \\ -\mathbf{e}_y\mathbf{m1}a_{gx}(t)+\mathbf{e}_x\mathbf{m1}a_{gy}(t) \end{Bmatrix} \tag{3.16}$$

where $\mathbf{e}_x$ and $\mathbf{e}_y$ are diagonal matrices of dimension N with diagonal entries e_{xj} and e_{yj}, the X and Y components of the static eccentricity e_j of the jth floor, given by:

$$e_{xj} = x_{Mj} - x_{Rj} \quad \text{and} \quad e_{yj} = y_{Mj} - y_{Rj} \tag{3.17}$$

in which x_{Rj} and y_{Rj} are the X and Y coordinates of the center of rigidity of the jth floor relative to its reference axes X_j and Y_j; $\mathbf{J}_R$ is a diagonal matrix of dimension N with diagonal entries J_{Rj} equal the polar moment of inertia of the jth deck about a vertical axis passing through its center of rigidity, given by:

$$J_{Rj} = m_j (e_j^2 + r_j^2) \tag{3.18}$$

The form of $\tilde{\mathbf{K}}$ given in equation (3.15) follows from the definition given for centers of rigidity as the points on floor levels at which static horizontal forces cause no twist in any of the floors. Clearly, if the centers of rigidity are not unique, it would not be possible to determine a building stiffness matrix in the form of $\tilde{\mathbf{K}}$ given by equation (3.15). In the next section, an attempt is made to determine the conditions for existence of unique centers of rigidity utilizing the special form of $\tilde{\mathbf{K}}$ given by equation (3.15).

Horizontal torsional moments applied statically at each floor level cause no lateral displacements of the centers of twist. The form of $\tilde{\mathbf{K}}$, therefore, also satisfies the definition of centers of twist, given in Section 3.1. Again, if the centers of twist are unique, then the stiffness matrix at the centers of twist has the form given by equation (3.15). The submatrices, $\tilde{\mathbf{K}}_x$, $\tilde{\mathbf{K}}_y$, $\tilde{\mathbf{K}}_{xy}$ or $\tilde{\mathbf{K}}_{yx}$ and $\tilde{\mathbf{K}}_\theta$, are related to $\mathbf{K}_x$, $\mathbf{K}_y$, $\mathbf{K}_{xy}$ and $\mathbf{K}_\theta$, by expressions given in Section 3.3. The form of the building stiffness matrix given by equation (3.15) is the basis for locating the centers of rigidity and twist of the building if they can be uniquely defined (Sections 3.3 and 3.4).

Static horizontal lateral forces applied through the centers of rigidity along either principal axis I_j or II_j of each floor, causes each floor to displace in the direction of the force applied to it (along its I_j or II_j) without any rotation (see the definition of principal axes in Section 3.1). It follows that the building stiffness matrix defined with respect to $\mathbf{u}^*$, where $\mathbf{u}^{*T} = <\mathbf{u}_I^* \; \mathbf{u}_{II}^* \; \mathbf{u}_\theta>$ with $\mathbf{u}_I^*$ and $\mathbf{u}_{II}^*$ the vectors of lateral displacements u_{Ij}^* and u_{IIj}^* at the center of rigidity of the j^{th} floor along its principal axes I_j and II_j, is of the form:

$$\mathbf{K}^* = \begin{bmatrix} \mathbf{K}_I^* & \mathbf{0} & \mathbf{0} \\ \mathbf{0} & \mathbf{K}_{II}^* & \mathbf{0} \\ \mathbf{0} & \mathbf{0} & \mathbf{K}_\theta^* \end{bmatrix} \tag{3.19}$$

with $\mathbf{K}_I^*$, $\mathbf{K}_{II}^*$ and $\mathbf{K}_\theta^*$ expressed in terms of $\mathbf{K}_x$, $\mathbf{K}_y$, $\mathbf{K}_{xy}$ and $\mathbf{K}_\theta$ in Section 4.3. The form of building stiffness given by equation (3.19) is the basis used to determine the orientations of the principal axes of the floors of the system, again only if the centers of rigidity are uniquely defined. The building mass matrix with respect to $\mathbf{u}^*$ remains of the form given in equation (3.12).

3.3 Locations of Centers of Rigidity

3.3.1 Unique Centers of Rigidity

The building stiffness matrix $\tilde{\mathbf{K}}$ written with respect to the degrees of freedom $\tilde{\mathbf{u}}^T = <\tilde{\mathbf{u}}_x^T \; \tilde{\mathbf{u}}_y^T \; \mathbf{u}_\theta^T>$ defined at the centers of rigidity is related to the building stiffness matrix $\mathbf{K}$ written with respect to degrees of freedom $\mathbf{u}$, where $\mathbf{u}^T = <\mathbf{u}_x^T \; \mathbf{u}_y^T \; \mathbf{u}_\theta^T>$ at reference points O_j, by:

$$\tilde{\mathbf{K}} = \tilde{\mathbf{a}}^T \, \mathbf{K} \, \tilde{\mathbf{a}} \tag{3.20}$$

in which the matrix $\tilde{\mathbf{a}}$ is a transformation matrix relating $\mathbf{u}$ to $\tilde{\mathbf{u}}$:

$$\mathbf{u} = \begin{Bmatrix} \mathbf{u}_x \\ \mathbf{u}_y \\ \mathbf{u}_\theta \end{Bmatrix} = \begin{bmatrix} \mathbf{I} & \mathbf{0} & \mathbf{y}_R \\ \mathbf{0} & \mathbf{I} & -\mathbf{x}_R \\ \mathbf{0} & \mathbf{0} & \mathbf{I} \end{bmatrix} \begin{Bmatrix} \tilde{\mathbf{u}}_x \\ \tilde{\mathbf{u}}_y \\ \mathbf{u}_\theta \end{Bmatrix} = \tilde{\mathbf{a}} \, \mathbf{u} \tag{3.21}$$

where $\mathbf{x}_R$ and $\mathbf{y}_R$ are the diagonal matrices of the X and Y coordinates of the centers of rigidity of

the building. Substituting equations (3.21) and (3.10) into equation (3.20), leads to:

$$\tilde{\mathbf{K}} = \begin{bmatrix} \mathbf{K}_x & \mathbf{K}_{xy} & \mathbf{K}_x\mathbf{y}_R - \mathbf{K}_{xy}\mathbf{x}_R + \mathbf{K}_{x\theta} \\ \mathbf{K}_{yx} & \mathbf{K}_y & \mathbf{K}_{yx}\mathbf{y}_R - \mathbf{K}_y\mathbf{x}_R + \mathbf{K}_{y\theta} \\ \mathbf{y}_R\mathbf{K}_x - \mathbf{x}_R\mathbf{K}_{yx} + \mathbf{K}_{\theta x} & \mathbf{y}_R\mathbf{K}_{xy} - \mathbf{x}_R\mathbf{K}_y + \mathbf{K}_{\theta y} & \tilde{\mathbf{K}}_\theta \end{bmatrix} \tag{3.22}$$

in which,

$$\tilde{\mathbf{K}}_\theta = \mathbf{K}_\theta + \mathbf{K}_{\theta x}\mathbf{y}_R - \mathbf{K}_{\theta y}\mathbf{x}_R - \mathbf{x}_R\,(\,\mathbf{K}_{yx}\mathbf{y}_R - \mathbf{K}_y\mathbf{x}_R + \mathbf{K}_{y\theta}\,) + \mathbf{y}_R\,(\,\mathbf{K}_x\mathbf{y}_R - \mathbf{K}_{xy}\mathbf{x}_R + \mathbf{K}_{x\theta}\,)$$

Comparison of equations (3.22) and (3.15) leads to the following conditions:

$$\mathbf{K}_x\mathbf{y}_R - \mathbf{K}_{xy}\mathbf{x}_R + \mathbf{K}_{x\theta} = \mathbf{0} \tag{3.23a}$$

$$-\mathbf{K}_{yx}\mathbf{y}_R + \mathbf{K}_y\mathbf{x}_R - \mathbf{K}_{y\theta} = \mathbf{0} \tag{3.23b}$$

$$\tilde{\mathbf{K}}_x = \mathbf{K}_x \;,\; \tilde{\mathbf{K}}_y = \mathbf{K}_y \text{ and } \tilde{\mathbf{K}}_{xy} = \mathbf{K}_{xy} \tag{3.24}$$

and,

$$\tilde{\mathbf{K}}_\theta = \mathbf{K}_\theta + \mathbf{K}_{\theta x}\mathbf{y}_R - \mathbf{K}_{\theta y}\mathbf{x}_R \tag{3.25}$$

in which equations (3.23) have been utilized. Solving the simultaneous algebraic equations (3.23) yields the coordinates of the centers of rigidity:

$$\mathbf{x}_R = (\,\mathbf{K}_y - \mathbf{K}_{yx}\mathbf{K}_x^{-1}\mathbf{K}_{xy}\,)^{-1}\,(\mathbf{K}_{y\theta} - \mathbf{K}_{yx}\mathbf{K}_x^{-1}\mathbf{K}_{x\theta}\,) \tag{3.26a}$$

and,

$$\mathbf{y}_R = -\,(\,\mathbf{K}_x - \mathbf{K}_{xy}\mathbf{K}_y^{-1}\mathbf{K}_{yx}\,)^{-1}\,(\mathbf{K}_{x\theta} - \mathbf{K}_{xy}\mathbf{K}_y^{-1}\mathbf{K}_{y\theta}\,) \tag{3.26b}$$

The inverses of matrices $\mathbf{K}_x$, $\mathbf{K}_y$, $(\mathbf{K}_y - \mathbf{K}_{yx}\mathbf{K}_x^{-1}\mathbf{K}_{xy})$ and $(\mathbf{K}_x - \mathbf{K}_{xy}\mathbf{K}_y^{-1}\mathbf{K}_{yx})$ are shown in Appendix A to always exist, implying that $\mathbf{x}_R$ and $\mathbf{y}_R$ can be determined from equations (3.26). However, the matrices $\mathbf{x}_R$ and $\mathbf{y}_R$ were defined as diagonal matrices and the expressions given by (3.26) do not, in general, yield diagonal matrices (see Example 1), implying that unique centers of rigidity do not always exist. A special class of buildings with unique centers of rigidity, i.e. buildings for which equations (3.26) yield diagonal matrices, is identified in Section 4. Only for such cases is

the building stiffness matrix at the centers of rigidity of the form given by equation (3.15).

3.3.2 Load-Dependent Centers of Rigidity

However, centers of rigidity can be defined for buildings even if equations (3.26) do not yield diagonal matrices, but in such a case the locations of centers of rigidity depend on the applied set of static lateral forces. The equations of static equilibrium written with respect to $\tilde{\mathbf{u}}$ defined at the centers of rigidity are given by:

$$\tilde{\mathbf{P}} = \tilde{\mathbf{K}}\,\tilde{\mathbf{u}}$$

with $\tilde{\mathbf{K}}$ given in equation (3.22); or,

$$\begin{Bmatrix} \tilde{\mathbf{P}}_x \\ \tilde{\mathbf{P}}_y \\ \tilde{\mathbf{T}}_\theta \end{Bmatrix} = \begin{bmatrix} \mathbf{K}_x & \mathbf{K}_{xy} & \mathbf{K}_x\mathbf{y}_R - \mathbf{K}_{xy}\mathbf{x}_R + \mathbf{K}_{x\theta} \\ \mathbf{K}_{yx} & \mathbf{K}_y & \mathbf{K}_{yx}\mathbf{y}_R - \mathbf{K}_y\mathbf{x}_R + \mathbf{K}_{y\theta} \\ \mathbf{y}_R\mathbf{K}_x - \mathbf{x}_R\mathbf{K}_{yx} + \mathbf{K}_{\theta x} & \mathbf{y}_R\mathbf{K}_{xy} - \mathbf{x}_R\mathbf{K}_y + \mathbf{K}_{\theta y} & \tilde{\mathbf{K}}_\theta \end{bmatrix} \begin{Bmatrix} \tilde{\mathbf{u}}_x \\ \tilde{\mathbf{u}}_y \\ \mathbf{u}_\theta \end{Bmatrix} \qquad (3.27)$$

where $\tilde{\mathbf{P}}^T = <\tilde{\mathbf{P}}_x^T\ \tilde{\mathbf{P}}_y^T\ \tilde{\mathbf{T}}_\theta^T>$ with $\tilde{\mathbf{P}}_x$ and $\tilde{\mathbf{P}}_y$ being the vectors of static lateral forces applied at the centers of rigidity along the X_j and Y_j directions; and $\tilde{\mathbf{T}}_\theta$ the vector of applied static torsional moments about vertical axes passing through the centers of rigidity. For a particular set of forces $\tilde{\mathbf{P}}$, with $\tilde{\mathbf{P}}_x \neq \mathbf{0}$ and $\tilde{\mathbf{P}}_y \neq \mathbf{0}$ but $\tilde{\mathbf{T}}_\theta = \mathbf{0}$, it is possible to determine $\mathbf{x}_R$ and $\mathbf{y}_R$, the coordinates defining the locations of centers of rigidity where, according to the definition of Section 3.1, $\tilde{\mathbf{u}}_x \neq \mathbf{0}$ and $\tilde{\mathbf{u}}_y \neq \mathbf{0}$ but $\mathbf{u}_\theta = \mathbf{0}$. Thus, equations (3.27) specialize to:

$$\tilde{\mathbf{P}}_x = \mathbf{K}_x\tilde{\mathbf{u}}_x + \mathbf{K}_{xy}\tilde{\mathbf{u}}_y \quad \text{and} \quad \tilde{\mathbf{P}}_y = \mathbf{K}_{yx}\tilde{\mathbf{u}}_x + \mathbf{K}_y\tilde{\mathbf{u}}_y \qquad (3.28a,b)$$

and:

$$\mathbf{0} = (\ \mathbf{y}_R\mathbf{K}_x - \mathbf{x}_R\mathbf{K}_{yx} + \mathbf{K}_{\theta x}\ )\ \tilde{\mathbf{u}}_x + (\ \mathbf{y}_R\mathbf{K}_{xy} - \mathbf{x}_R\mathbf{K}_y + \mathbf{K}_{\theta y}\ )\ \tilde{\mathbf{u}}_y \qquad (3.28c)$$

Utilizing equations (3.28a) and (3.28b), equation (3.28c) can be written as:

$$\mathbf{y}_R\,\tilde{\mathbf{P}}_x - \mathbf{x}_R\,\tilde{\mathbf{P}}_y + \mathbf{K}_{\theta x}\,\tilde{\mathbf{u}}_x + \mathbf{K}_{\theta y}\,\tilde{\mathbf{u}}_y = \mathbf{0} \qquad (3.29)$$

Solving equations (3.28a) and (3.28b) for $\tilde{\mathbf{u}}_x$ and $\tilde{\mathbf{u}}_y$, leads to:

$$\tilde{\mathbf{u}}_x = (\mathbf{K}_x - \mathbf{K}_{xy}\mathbf{K}_y^{-1}\mathbf{K}_{yx})^{-1} (\tilde{\mathbf{P}}_x - \mathbf{K}_{xy}\,\mathbf{K}_y^{-1}\,\tilde{\mathbf{P}}_y) = \mathbf{A}^{-1} (\tilde{\mathbf{P}}_x - \mathbf{K}_{xy}\,\mathbf{K}_y^{-1}\,\tilde{\mathbf{P}}_y) \tag{3.30a}$$

and,

$$\tilde{\mathbf{u}}_y = (\mathbf{K}_y - \mathbf{K}_{yx}\mathbf{K}_x^{-1}\mathbf{K}_{xy})^{-1} (\tilde{\mathbf{P}}_y - \mathbf{K}_{yx}\,\mathbf{K}_x^{-1}\,\tilde{\mathbf{P}}_x) = \mathbf{B}^{-1} (\tilde{\mathbf{P}}_y - \mathbf{K}_{yx}\,\mathbf{K}_x^{-1}\,\tilde{\mathbf{P}}_x) \tag{3.30b}$$

Substituting equation (3.30) into (3.29), the latter becomes:

$$(\mathbf{y}_R + \mathbf{K}_{\theta x}\mathbf{A}^{-1} - \mathbf{K}_{\theta y}\mathbf{B}^{-1}\mathbf{K}_{yx}\mathbf{k}_x^{-1})\,\tilde{\mathbf{P}}_x - (\mathbf{x}_R - \mathbf{K}_{\theta y}\mathbf{B}^{-1} + \mathbf{K}_{\theta x}\mathbf{A}^{-1}\mathbf{K}_{xy}\mathbf{K}_y^{-1})\,\tilde{\mathbf{P}}_y = \mathbf{0} \tag{3.31}$$

Since $\tilde{\mathbf{P}}_x$ and $\tilde{\mathbf{P}}_y$ are independent, equation (3.31) leads to two conditions:

$$\mathbf{x}_R\tilde{\mathbf{P}}_y = [\tilde{\mathbf{P}}_y]\,\{\mathbf{x}_R\} = (\mathbf{K}_{\theta y}\mathbf{B}^{-1} - \mathbf{K}_{\theta x}\mathbf{A}^{-1}\mathbf{K}_{xy}\mathbf{K}_y^{-1})\,\tilde{\mathbf{P}}_y$$

and,

$$\mathbf{y}_R\tilde{\mathbf{P}}_x = [\tilde{\mathbf{P}}_x]\,\{\mathbf{y}_R\} = -\,(\mathbf{K}_{\theta x}\mathbf{A}^{-1} - \mathbf{K}_{\theta y}\mathbf{B}^{-1}\mathbf{K}_{yx}\mathbf{K}_x^{-1})\,\tilde{\mathbf{P}}_x$$

where $[\tilde{\mathbf{P}}_x]$ and $[\tilde{\mathbf{P}}_y]$ denote the diagonal matrices of vectors $\tilde{\mathbf{P}}_x$ and $\tilde{\mathbf{P}}_y$ and $\{\mathbf{x}_R\}$ and $\{\mathbf{y}_R\}$ the vector form of diagonal matrices $\mathbf{x}_R$ and $\mathbf{y}_R$. Thus,

$$\{\mathbf{x}_R\} = [\tilde{\mathbf{P}}_y]^{-1} (\mathbf{K}_{\theta y}\mathbf{B}^{-1} - \mathbf{K}_{\theta x}\mathbf{A}^{-1}\mathbf{K}_{xy}\mathbf{K}_y^{-1})\,\tilde{\mathbf{P}}_y \tag{3.32a}$$

and,

$$\{\mathbf{y}_R\} = -\,[\tilde{\mathbf{P}}_x]^{-1} (\mathbf{K}_{\theta x}\mathbf{A}^{-1} - \mathbf{K}_{\theta y}\mathbf{B}^{-1}\mathbf{K}_{yx}\mathbf{K}_x^{-1})\,\tilde{\mathbf{P}}_x \tag{3.32b}$$

Utilizing the following identities derived in Appendix A:

$$-\mathbf{K}_y^{-1}\mathbf{K}_{yx}\,\mathbf{A}^{-1} = -\mathbf{B}^{-1}\,\mathbf{K}_{yx}\,\mathbf{K}_x^{-1} \quad \text{and} \quad -\mathbf{A}^{-1}\,\mathbf{K}_{xy}\,\mathbf{K}_y^{-1} = -\mathbf{K}_x^{-1}\,\mathbf{K}_{xy}\,\mathbf{B}^{-1}$$

equations (3.32) can be simplified to become:

$$\{\mathbf{x}_R\} = [\tilde{\mathbf{P}}_y]^{-1} (\mathbf{K}_{\theta y} - \mathbf{K}_{\theta x}\mathbf{K}_x^{-1}\mathbf{K}_{xy})\,(\mathbf{K}_y - \mathbf{K}_{yx}\mathbf{K}_x^{-1}\mathbf{K}_{xy})^{-1}\,\tilde{\mathbf{P}}_y \tag{3.33a}$$

and,

$$\{\mathbf{y}_R\} = -\,[\tilde{\mathbf{P}}_x]^{-1} (\mathbf{K}_{\theta x} - \mathbf{K}_{\theta y}\mathbf{K}_y^{-1}\mathbf{K}_{yx})\,(\mathbf{K}_x - \mathbf{K}_{xy}\mathbf{K}_y^{-1}\mathbf{K}_{yx})^{-1}\,\tilde{\mathbf{P}}_x \tag{3.33b}$$

Since $[\tilde{\mathbf{P}}_y]$ and $[\tilde{\mathbf{P}}_x]$ are diagonal matrices, equations (3.33) are simplified to equations (3.26) when the product matrices $(\mathbf{K}_{\theta y} - \mathbf{K}_{\theta x}\mathbf{K}_x^{-1}\mathbf{K}_{xy})\,(\mathbf{K}_y - \mathbf{K}_{yx}\mathbf{K}_x^{-1}\mathbf{K}_{xy})^{-1}$ and $(\mathbf{K}_{\theta x} - \mathbf{K}_{\theta y}\mathbf{K}_y^{-1}\mathbf{K}_{yx})\,(\mathbf{K}_x - \mathbf{K}_{xy}\mathbf{K}_y^{-1}\mathbf{K}_{yx})^{-1}$ are diagonal, so that the locations of the centers of rigidity are unique and independent of the applied loading.

3.3.3 Example 1

Consider a five-story multi-story building consisting of four identical columns and a frame, located as shown in Figure 5. The lateral stiffness matrices of the columns along their principal planes are equal, i.e.:

$$\mathbf{k}_{a1} = \mathbf{k}_{a2} = \mathbf{k}_{a3} = \mathbf{k}_{a4} = \mathbf{k}$$

and,

$$\mathbf{k}_{b1} = \mathbf{k}_{b1} = \mathbf{k}_{b3} = \mathbf{k}_{b4} = \mathbf{k}$$

with

$$\mathbf{k} = \frac{EI}{h^3}\begin{bmatrix} 18.829 & -11.901 & 4.774 & -1.193 & 0.199 \\ -11.901 & 14.652 & -10.707 & 4.177 & -0.696 \\ 4.774 & -10.707 & 14.055 & -9.514 & 2.586 \\ -1.193 & 4.177 & -9.514 & 9.878 & -3.646 \\ 0.199 & -0.696 & 2.586 & -3.646 & 1.608 \end{bmatrix}$$

where I is the moment of inertia of the column, assumed to be the same for all floors, and h is the story height of the building. The frame is uniform with all its columns of identical moments of inertia, also equal to I; all its beams have the same moment of inertia equal to $0.8I$, and are of width $2h$. The lateral stiffness matrices of the frame along its principal planes are given by:

$$\mathbf{k}_{a5} = \mathbf{k}' \quad \text{and} \quad \mathbf{k}_{b5} = \mathbf{0}$$

with

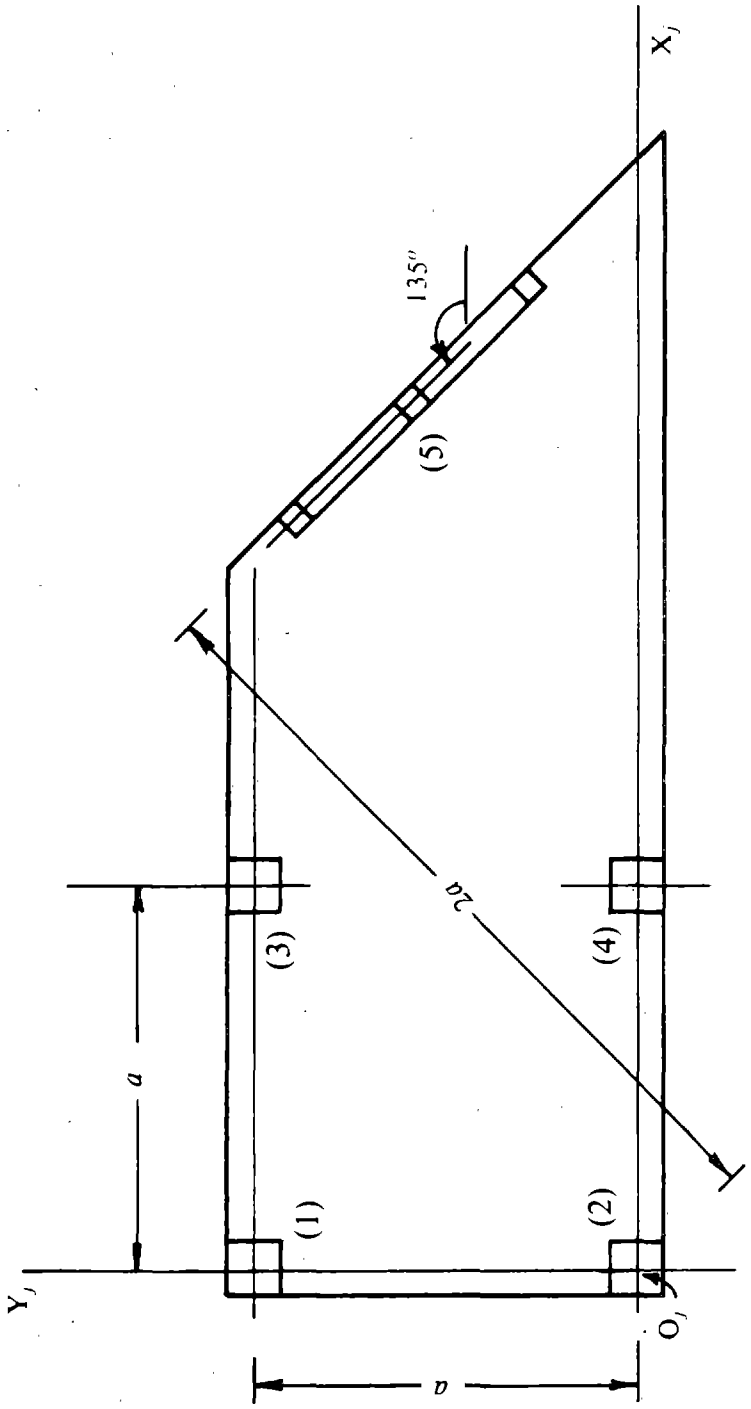

FIGURE 5 Plan of Example 1

$$\mathbf{k}' = \frac{EI}{h^3}\begin{bmatrix} 40.512 & -23.941 & 7.182 & -1.403 & 0.211 \\ -23.941 & 33.870 & -22.582 & 6.757 & -1.015 \\ 7.182 & -22.582 & 33.545 & -21.733 & 5.069 \\ -1.403 & 6.757 & -21.733 & 29.453 & -13.344 \\ 0.211 & -1.015 & 5.069 & -13.344 & 9.120 \end{bmatrix}$$

The stiffness matrix contributions of the various elements to the building stiffness matrix defined with respect to degrees of freedom at reference points O_j are:

for the columns:

$$\mathbf{K}_1 = \begin{bmatrix} \mathbf{k} & \mathbf{0} & -a\mathbf{k} \\ \mathbf{0} & \mathbf{k} & \mathbf{0} \\ -a\mathbf{k} & \mathbf{0} & a^2\mathbf{k} \end{bmatrix}, \mathbf{K}_2 = \begin{bmatrix} \mathbf{k} & \mathbf{0} & \mathbf{0} \\ \mathbf{0} & \mathbf{k} & \mathbf{0} \\ \mathbf{0} & \mathbf{0} & \mathbf{0} \end{bmatrix},$$

$$\mathbf{K}_3 = \begin{bmatrix} \mathbf{k} & \mathbf{0} & -a\mathbf{k} \\ \mathbf{0} & \mathbf{k} & a\mathbf{k} \\ -a\mathbf{k} & a\mathbf{k} & 2a^2\mathbf{k} \end{bmatrix}, \mathbf{K}_4 = \begin{bmatrix} \mathbf{k} & \mathbf{0} & \mathbf{0} \\ \mathbf{0} & \mathbf{k} & a\mathbf{k} \\ \mathbf{0} & a\mathbf{k} & a^2\mathbf{k} \end{bmatrix}$$

and for the frame:

$$\mathbf{K}_5 = \begin{bmatrix} 0.5\mathbf{k}' & -0.5\mathbf{k}' & -1.414a\mathbf{k}' \\ -0.5\mathbf{k}' & 0.5\mathbf{k}' & 1.414a\mathbf{k}' \\ -1.414a\mathbf{k}' & 1.414a\mathbf{k}' & 4a^2\mathbf{k}' \end{bmatrix}$$

Equations (3.9) and (3.10) lead to:

$$\mathbf{K}_x = \mathbf{k} + \mathbf{k} + \mathbf{k} + \mathbf{k} + 0.5\mathbf{k}' = 4\mathbf{k} + 0.5\mathbf{k}'$$

$$\mathbf{K}_y = \mathbf{k} + \mathbf{k} + \mathbf{k} + \mathbf{k} + 0.5\mathbf{k}' = 4\mathbf{k} + 0.5\mathbf{k}'$$

$$\mathbf{K}_\theta = a^2\mathbf{k} + \mathbf{0} + 2a^2\mathbf{k} + a^2\mathbf{k} + 4a^2\mathbf{k}' = 4a^2(\mathbf{k} + \mathbf{k}')$$

$$\mathbf{K}_{xy} = \mathbf{K}_{yx} = \mathbf{0} + \mathbf{0} + \mathbf{0} + \mathbf{0} - 0.5\mathbf{k}' = -0.5\mathbf{k}'$$

$$\mathbf{K}_{x\theta} = \mathbf{K}_{\theta x} = -a\mathbf{k} + \mathbf{0} - a\mathbf{k} + \mathbf{0} - 1.414a\mathbf{k}' = -2a\mathbf{k} - 1.414a\mathbf{k}'$$

$$\mathbf{K}_{y\theta} = \mathbf{K}_{\theta y} = \mathbf{0} + \mathbf{0} + a\mathbf{k} + a\mathbf{k} + 1.414a\mathbf{k}' = 2a\mathbf{k} + 1.414a\mathbf{k}'$$

The building stiffness matrix at reference points O_j is therefore given by:

$$\mathbf{K} = \begin{bmatrix} 4\mathbf{k} + 0.5\mathbf{k}' & -0.5\mathbf{k}' & -2a\mathbf{k} - 1.414a\mathbf{k}' \\ -0.5\mathbf{k}' & 4\mathbf{k} + 0.5\mathbf{k}' & 2a\mathbf{k} + 1.414a\mathbf{k}' \\ -2a\mathbf{k} - 1.414a\mathbf{k}' & 2a\mathbf{k} + 1.414a\mathbf{k}' & 4a^2(\mathbf{k} + \mathbf{k}') \end{bmatrix}$$

Equations (3.26) yield:

$$\mathbf{x}_R = \mathbf{y}_R = \begin{bmatrix} 0.791 & 0.055 & 0.011 & 0.004 & 0.009 \\ -0.103 & 0.911 & 0.086 & 0.012 & 0.042 \\ -0.196 & 0.034 & 0.957 & 0.057 & 0.121 \\ -0.225 & -0.054 & 0.093 & 0.854 & 0.318 \\ -0.242 & -0.092 & 0.032 & -0.202 & 1.498 \end{bmatrix}$$

which clearly is not diagonal. Thus the building considered does not have unique centers of rigidity. However, load-dependent centers of rigidity can be determined for the building. Assuming uniform load distributions along both the X and Y directions, i.e. $\tilde{\mathbf{P}}_x = \tilde{\mathbf{P}}_y = \mathbf{1}$, equations (3.33) yield:

$$\{\mathbf{x}_R\} = \{\mathbf{y}_R\} = \begin{Bmatrix} 0.025 \\ 0.855 \\ 1.180 \\ 0.726 \\ 1.988 \end{Bmatrix}$$

For a triangular height-wise load distribution of $\tilde{\mathbf{P}}_x^T = \tilde{\mathbf{P}}_y^T = <1\ \ 2\ \ 3\ \ 4\ \ 5>$-- a distribution which is recommended in building codes such as UBC [3] for buildings with constant story height and equal lumped story weights, equations (3.33) lead to different locations of the centers of rigidity given by:

$$\{\mathbf{x}_R\} = \{\mathbf{y}_R\} = \begin{Bmatrix} -2.112 \\ 0.651 \\ 1.196 \\ 0.652 \\ 1.843 \end{Bmatrix}$$

Actually any other load distribution would lead to different locations of the centers of rigidity.

3.3.4 Special Building Plans

Equations (3.33) can be simplified further if the principal planes of all resisting elements are parallel or orthogonal. In this case, the principal axes of the building are parallel to the elemental principal planes, and it is natural to choose the X_j and Y_j reference axes of each floor to be in the direction of the principal axes of the building. It follows that β_i, the counterclockwise angle between X_j and the major principal plane of the i^{th} resisting element, is either zero or 90 degrees, and d_{ai} and d_{bi}, the perpendicular distances from reference points O_j to the major and minor principal planes of the element are measured along the X_j and Y_j reference axes. Thus equation (3.11) becomes:

$$\mathbf{K}_x = \sum_i \mathbf{K}_{xi} = \sum_i \mathbf{k}_{xi}$$

$$\mathbf{K}_y = \sum_i \mathbf{K}_{yi} = \sum_i \mathbf{k}_{yi}$$

$$\mathbf{K}_\theta = \sum_i \mathbf{K}_{\theta i} = \sum_i (\mathbf{k}_{\theta i} + y_i^2 \mathbf{k}_{xi} + x_i^2 \mathbf{k}_{yi})$$

$$\mathbf{K}_{xy} = \mathbf{K}_{yx} = \mathbf{0} \tag{3.34}$$

$$\mathbf{K}_{x\theta} = \mathbf{K}_{\theta x} = \sum_i \mathbf{K}_{x\theta i} = -\sum_i y_i \mathbf{k}_{xi}$$

$$\mathbf{K}_{y\theta} = \mathbf{K}_{\theta y} = \sum_i \mathbf{K}_{y\theta i} = \sum_i x_i \mathbf{k}_{yi}$$

where $\mathbf{k}_{xi}$ and $\mathbf{k}_{yi}$ are the lateral stiffness matrices of the i^{th} resisting element along its principal planes, which are oriented along the X_j and Y_j axes; x_i and y_i are the X and Y distances of the principal planes of the i^{th} resisting element from the X_j and Y_j axes. Substituting equation (3.34d) into equations (3.33), leads to:

$$\{\mathbf{x}_R\} = [\tilde{\mathbf{P}}_y]^{-1} \mathbf{K}_{\theta y} \mathbf{K}_y^{-1} \tilde{\mathbf{P}}_y \tag{3.35a}$$

and,

$$\{\mathbf{y}_R\} = -[\tilde{\mathbf{P}}_x]^{-1} \mathbf{K}_{\theta x} \mathbf{K}_x^{-1} \tilde{\mathbf{P}}_x \tag{3.35b}$$

These equations were also obtained in Reference [8] wherein only buildings consisting of frames

arranged in an orthogonal grid in plan were considered. In Reference [7], the center of rigidity of a floor is defined as the point in the floor through which a static horizontal force should be applied to cause the floor to translate without rotation or twist; other floors, however, may twist or rotate. In other words, Reference [7] specializes the applied loads $\tilde{\mathbf{P}}_x$ and $\tilde{\mathbf{P}}_y$ to be vectors of zeros except for the entry corresponding to the floor in consideration, which can assume any value. The resulting coordinates of the centers of rigidity are in this case given by the diagonal entries of matrices $\mathbf{K}_{\theta y}\mathbf{K}_y^{-1}$ and $\mathbf{K}_{\theta x}\mathbf{K}_x^{-1}$.

Equations (3.33) can similarly be simplified if the building has a vertical plane of stiffness symmetry, then the lines of intersection of the symmetry plane and the floor planes are the principal axes of the floors. Hence, it is natural to choose one of the reference axes X_j or Y_j in the same direction as the principal axes of the floor. If the X_j axes are chosen in the directions of the symmetry plane, then, referring to equations (3.9d) and (3.9e), it is apparent that matrices $\mathbf{K}_{xyi}$ in equations (3.11c) and $\mathbf{K}_{x\theta i}$ in equation (3.11b) occur in pairs that are equal but of oppposite algebraic signs. Thus:

$$\mathbf{K}_{xy} = \mathbf{K}_{yx} = \mathbf{0} \quad \text{and} \quad \mathbf{K}_{x\theta} = \mathbf{K}_{\theta x} = \mathbf{0}$$

from which equations (3.33) are simplified to become:

$$\{\mathbf{x}_R\} = [\tilde{\mathbf{P}}_y]^{-1}\,\mathbf{K}_{\theta y}\mathbf{K}_y^{-1}\,\tilde{\mathbf{P}}_y \quad \text{and} \quad \{\mathbf{y}_R\} = -\,[\tilde{\mathbf{P}}_x]^{-1}\,\mathbf{K}_{\theta x}\mathbf{K}_x^{-1}\,\tilde{\mathbf{P}}_x = \mathbf{0} \tag{3.36}$$

Similarly, if the Y_j reference axes are chosen in the direction of the symmetry plane, then:

$$\{\mathbf{x}_R\} = [\tilde{\mathbf{P}}_y]^{-1}\,\mathbf{K}_{\theta y}\mathbf{K}_y^{-1}\,\tilde{\mathbf{P}}_y = \mathbf{0} \quad \text{and} \quad \{\mathbf{y}_R\} = -\,[\tilde{\mathbf{P}}_x]^{-1}\,\mathbf{K}_{\theta x}\mathbf{K}_x^{-1}\,\tilde{\mathbf{P}}_x \tag{3.37}$$

3.3.5 Example 2

Consider a five-story building (Figure 6) consisiting of four identical columns and a frame, all being the same as described in Section 3.3.3 for Example 1. The elements are arranged such that their principal planes form an orthogonal grid in plan, and the building has a plane of symmetry. The building stiffness matrix defined at reference points O_j (Figure 6) is obtained from equations (3.34) as:

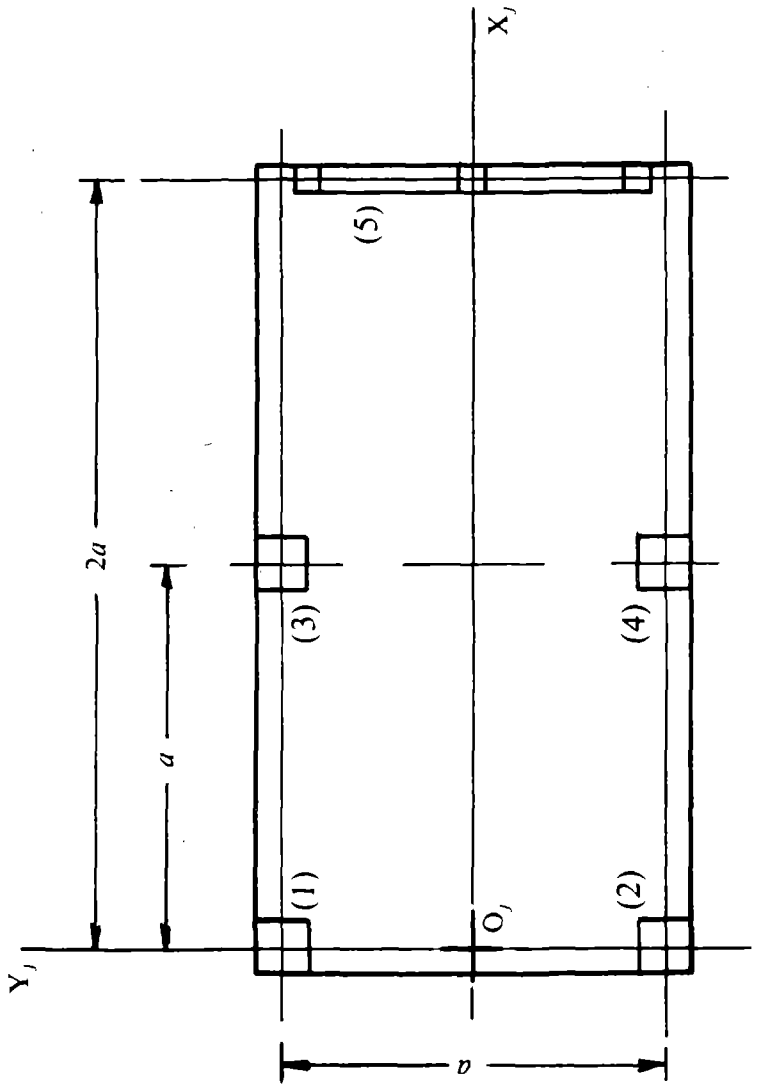

FIGURE 6 Plan of Example 2

$$\mathbf{K} = \begin{bmatrix} 4\mathbf{k} & \mathbf{0} & \mathbf{0} \\ \mathbf{0} & 4\mathbf{k} + \mathbf{k}' & 2a(\mathbf{k} + \mathbf{k}') \\ \mathbf{0} & 2a(\mathbf{k} + \mathbf{k}') & 6a^2\mathbf{k} + 4a^2\mathbf{k}' \end{bmatrix}$$

Utilizing equations (3.36) for uniform height-wise load distribution, results in:

$$\{\mathbf{x}_R\} = \begin{Bmatrix} -0.280 \\ 1.082 \\ 1.615 \\ 0.871 \\ 2.941 \end{Bmatrix} \quad \text{and} \quad \{\mathbf{y}_R\} = \mathbf{0}$$

3.3.6 Load Centers

Equations (3.35a) and (3.35b), obtained in the case of buildings consisting of frames arranged in an orthogonal grid in plan, were physically interpreted in [8] as the equations yielding the centroids of the lateral forces "applied" in the planes of the frames at each floor level when the building is subjected to a static loading that causes no twist in any of its floors (i.e. $\mathbf{u}_\theta = \mathbf{0}$). This conclusion was reached by recognizing that $\mathbf{K}_x^{-1}\tilde{\mathbf{P}}_x$ and $\mathbf{K}_y^{-1}\tilde{\mathbf{P}}_y$ are actually the vectors $\mathbf{u}_x$ and $\mathbf{u}_y$ of the X- and Y- lateral displacements experienced by each frame when the building is subjected to loads $\tilde{\mathbf{P}}_x$ and $\tilde{\mathbf{P}}_y$. Then, utilizing equations (3.34e) and (3.34f), equations (3.35a) and (3.35b) are simplified to become:

$$\{\mathbf{x}_R\} = [\tilde{\mathbf{P}}_y]^{-1}\,\mathbf{K}_{\theta y}\,\mathbf{K}_y^{-1}\,\tilde{\mathbf{P}}_y = [\tilde{\mathbf{P}}_y]^{-1}\sum_i x_i\,\mathbf{k}_{yi}\,\mathbf{u}_y = [\tilde{\mathbf{P}}_y]^{-1}\sum_i x_i\,\mathbf{Q}_{yi} \tag{3.38a}$$

and,

$$\{\mathbf{y}_R\} = -\,[\tilde{\mathbf{P}}_x]^{-1}\,\mathbf{K}_{\theta x}\,\mathbf{K}_x^{-1}\,\tilde{\mathbf{P}}_x = -\,[\tilde{\mathbf{P}}_x]^{-1}\sum_i y_i\,\mathbf{k}_{xi}\,\mathbf{u}_x = -\,[\tilde{\mathbf{P}}_x]^{-1}\sum_i y_i\,\mathbf{Q}_{xi} \tag{3.38b}$$

in which $\mathbf{Q}_{xi}$ is the vector of lateral forces "applied" along the X- direction in the plane of a frame oriented along the X- direction, and $\mathbf{Q}_{yi}$ is the vector of lateral forces "applied" along the Y- direction in the plane of a frame oriented along the Y- direction. Since $[\tilde{\mathbf{P}}_x]$ and $[\tilde{\mathbf{P}}_y]$ are diagonal matrices, x_{Rj} and y_{Rj}, the X and Y coordinates of the center of rigidity of the j^{th} floor (also the j^{th} entries of $\{\mathbf{x}_R\}$ and $\{\mathbf{y}_R\}$), are given by:

$$x_{Rj} = \frac{\sum_i x_i Q_{yij}}{\tilde{P}_{yj}} \quad \text{and} \quad y_{Rj} = \frac{\sum_i y_i Q_{xij}}{\tilde{P}_{xj}} \tag{3.39}$$

where Q_{xij}, Q_{yij}, $\tilde{P}_{xj}$ and $\tilde{P}_{yj}$ are the jth entries of vectors $\mathbf{Q}_{xi}$, $\mathbf{Q}_{yi}$, $\tilde{\mathbf{P}}_x$ and $\tilde{\mathbf{P}}_y$, respectively. It is clear from equations (3.39) that the X- and Y- coordinates of the center of rigidity of a floor can be determined by finding the location of the resultant elemental loads at that level. Thus, the centers of rigidity of such buidings are identified as the load centers [8]. A computational procedure to determine the locations of the centers of rigidity using a standard frame computer program was also presented in [8].

This physical interpretation of centers of rigidity is examined, in this section, for buildings with more general plans than those considered in [8]. Referring to equations (3.27), the application of horizontal forces $\tilde{\mathbf{P}}_y$, along the Y-axes, causing no twist in any of the floors of the building ($\mathbf{u}_\theta = \mathbf{0}$) leads to the lateral displacements $\mathbf{u}_x$ and $\mathbf{u}_y$, satisfying:

$$\mathbf{K}_x \mathbf{u}_x + \mathbf{K}_{xy} \mathbf{u}_y = \mathbf{0} \quad \text{and} \quad \mathbf{K}_{yx} \mathbf{u}_x + \mathbf{K}_y \mathbf{u}_y = \tilde{\mathbf{P}}_y \tag{3.40}$$

from which:

$$\mathbf{u}_x = -\mathbf{K}_x^{-1} \mathbf{K}_{xy} \mathbf{u}_y \quad \text{and} \quad \mathbf{u}_y = (\mathbf{K}_y - \mathbf{K}_{yx} \mathbf{K}_x^{-1} \mathbf{K}_{xy})^{-1} \tilde{\mathbf{P}}_y \tag{3.41}$$

Equation (3.33a) is simplified to become:

$$\{\mathbf{x}_R\} = [\tilde{\mathbf{P}}_y]^{-1} (\mathbf{K}_{\theta y} - \mathbf{K}_{\theta x} \mathbf{K}_x^{-1} \mathbf{K}_{xy}) \mathbf{u}_y = [\tilde{\mathbf{P}}_y]^{-1} (\mathbf{K}_{\theta y} \mathbf{u}_y + \mathbf{K}_{\theta x} \mathbf{u}_x) \tag{3.42}$$

Equations (3.9e), (3.9f) and (3.11) are substituted in equation (3.42) leading to:

$$\{\mathbf{x}_R\} = [\tilde{\mathbf{P}}_y]^{-1} \left[\sum_i (\pm d_{ai} \cos\beta_i \mathbf{k}_{ai} - (\pm) d_{bi} \sin\beta_i \mathbf{k}_{bi}) \mathbf{u}_x + \sum_i (\pm d_{ai} \sin\beta_i \mathbf{k}_{ai} \pm d_{bi} \cos\beta_i \mathbf{k}_{bi}) \mathbf{u}_y \right]$$

or,

$$\{\mathbf{x}_R\} = [\tilde{\mathbf{P}}_y]^{-1} \left[\sum_i \pm d_{ai} (\cos\beta_i \mathbf{k}_{ai} \mathbf{u}_x + \sin\beta_i \mathbf{k}_{ai} \mathbf{u}_y) + \sum_i \pm d_{bi} (-\sin\beta_i \mathbf{k}_{bi} \mathbf{u}_x + \cos\beta_i \mathbf{k}_{bi} \mathbf{u}_y) \right] \tag{3.43}$$

However, equations (3.5) and (3.2) imply that:

$$\mathbf{Q}_{ai} = \mathbf{k}_{ai}\mathbf{v}_{ai} = \cos\beta_i \mathbf{k}_{ai}\mathbf{u}_x + \sin\beta_i \mathbf{k}_{ai}\mathbf{u}_y \tag{3.44a}$$

and,

$$\mathbf{Q}_{bi} = \mathbf{k}_{bi}\mathbf{v}_{bi} = -\sin\beta_i \mathbf{k}_{bi}\mathbf{u}_x + \cos\beta_i \mathbf{k}_{bi}\mathbf{u}_y \tag{3.44b}$$

where $\mathbf{Q}_{ai}$ and $\mathbf{Q}_{bi}$ are the vectors of "applied" loads of the ith resisting element along its major and minor principal planes, due to $\tilde{\mathbf{P}}_y$. Thus, equations (3.43) can be written as:

$$\{\mathbf{x}_R\} = [\tilde{\mathbf{P}}_y]^{-1} \sum_i \pm d_{ai}\mathbf{Q}_{ai} + (\pm) d_{bi}\mathbf{Q}_{bi} \tag{3.45}$$

Since $[\tilde{\mathbf{P}}_y]$ is a diagonal matrix, the jth entry of $\{\mathbf{x}_R\}$ or the X- coordinate of the center of rigidity of the jth floor is given by:

$$x_{Rj} = \frac{\sum_i [\pm d_{ai} Q_{aij} + (\pm) d_{bi} Q_{bij}]}{\tilde{P}_{yj}} \tag{3.46}$$

where Q_{aij} and Q_{bij} are the jth entries of $\mathbf{Q}_{ai}$ and $\mathbf{Q}_{bi}$. A similar derivation would lead to the Y-coordinate of the center of rigidity of the jth floor as:

$$y_{Rj} = \frac{\sum_i [\pm d_{ai} Q_{aij} + (\pm) d_{bi} Q_{bij}]}{\tilde{P}_{xj}} \tag{3.47}$$

Although equations (3.46) and (3.47) are similar, they involve different terms Q_{aij} and Q_{bij}; those entering equation (3.47) are determined for the applied forces $\tilde{\mathbf{P}}_x$, and, those appearing in equation (3.46) are computed for $\tilde{\mathbf{P}}_y$.

Thus, the centers of rigidity (CR) of buildings with general floor plans, can also be identified as load centers. However, because the X- and Y- lateral motions of the building are no longer independent, the X- coordinates $\{\mathbf{x}_R\}$ of the CR are determined by finding the locations of the resultants of the lateral loads experienced by all the resisting elements due to lateral forces $\tilde{\mathbf{P}}_y$ applied along the Y- direction, causing no twist in any of the floors of the building; and the Y-coordinates $\{\mathbf{y}_R\}$ are determined by finding the locations of the resulatnts of the lateral loads experienced by all the resisting elements due to lateral forces $\tilde{\mathbf{P}}_x$ applied along the X- direction, causing no twist in

any of the floors of the building. This complication is not necessary if the principal planes of the resisting elements form an orthogonal grid in plan, because the X- and Y- lateral motions of such buildings are independent. Furthermore, unlike such buildings, the centers of rigidity of buildings with more general plans can not be located using a computer program for plane-frame analysis, again due to the dependence of the X- and Y- lateral motions of such buildings.

3.4 Locations of Centers of Twist

The centers of twist were defined in Section 3.1 as the points at various floor levels which remain stationary when the building is subjected to any set of static horizontal torsional moments applied at the floor levels. In accordance with this definition, the building stiffness matrix written with respect to degrees of freedom defined at the centers of twist would be of the special form of $\tilde{\mathbf{K}}$, given by equation (3.15). Hence, the locations of the centers of twist are determined by following the same steps performed above for the centers of rigidity, with $\mathbf{x}_T$ and $\mathbf{y}_T$, the diagonal matrices with entries x_{Tj} and y_{Tj}-- the X and Y coordinates of the center of twist of the j^{th} floor-- substituted for $\mathbf{x}_R$ and $\mathbf{y}_R$ in equations (3.21), (3.22), (3.23) and (3.25). Solving the modified equations (3.23) for $\mathbf{x}_T$ and $\mathbf{y}_T$ yields the same expressions for the coordinates of the centers of twist as the centers of rigidity. Hence, if expressions (3.26) yield diagonal matrices, centers of twist and centers of rigidity of the building coincide.

However, centers of twist can also be defined for buildings even if equations (3.26) do not yield diagonal matrices, but in such a case the locations of the centers of twist depend on the applied set of static torsional moments. The equations of static equilibrium, written with respect to $\tilde{\mathbf{u}}$ defined at the centers of twist, are:

$$\begin{Bmatrix} \tilde{\mathbf{P}}_x \\ \tilde{\mathbf{P}}_y \\ \tilde{\mathbf{T}}_\theta \end{Bmatrix} = \begin{bmatrix} \mathbf{K}_x & \mathbf{K}_{xy} & \mathbf{K}_x\mathbf{y}_T - \mathbf{K}_{xy}\mathbf{x}_T + \mathbf{K}_{x\theta} \\ \mathbf{K}_{yx} & \mathbf{K}_y & \mathbf{K}_{yx}\mathbf{y}_T - \mathbf{K}_y\mathbf{x}_T + \mathbf{K}_{y\theta} \\ \mathbf{y}_T\mathbf{K}_x - \mathbf{x}_T\mathbf{K}_{yx} + \mathbf{K}_{\theta x} & \mathbf{y}_T\mathbf{K}_{xy} - \mathbf{x}_T\mathbf{K}_y + \mathbf{K}_{\theta y} & \tilde{\mathbf{K}}_\theta \end{bmatrix} \begin{Bmatrix} \tilde{\mathbf{u}}_x \\ \tilde{\mathbf{u}}_y \\ \mathbf{u}_\theta \end{Bmatrix} \qquad (3.48)$$

For a particular set of forces $\tilde{\mathbf{P}}$ with $\tilde{\mathbf{P}}_x = \tilde{\mathbf{P}}_y = \mathbf{0}$ and $\tilde{\mathbf{T}}_\theta \neq \mathbf{0}$, it is possible to determine $\mathbf{x}_T$ and $\mathbf{y}_T$, the coordinates locating the centers of twist, where, according to the definition of Section 3.1,

$\tilde{\mathbf{u}}_x = \tilde{\mathbf{u}}_y = \mathbf{0}$, but $\mathbf{u}_\theta \neq \mathbf{0}$. Thus, equations (3.48) specialize to:

$$(\mathbf{K}_x \mathbf{y}_T - \mathbf{K}_{xy} \mathbf{x}_T + \mathbf{K}_{x\theta}) \mathbf{u}_\theta = \mathbf{0} \tag{3.49a}$$

and,

$$(\mathbf{K}_{yx} \mathbf{y}_T - \mathbf{K}_y \mathbf{x}_T + \mathbf{K}_{y\theta}) \mathbf{u}_\theta = \mathbf{0} \tag{3.49b}$$

Solution of equations (3.49) for $\mathbf{x}_T$ and $\mathbf{y}_T$ leads to:

$$\{\mathbf{x}_T\} = [\mathbf{u}_\theta]^{-1} (\mathbf{K}_y - \mathbf{K}_{yx}\mathbf{K}_x^{-1}\mathbf{K}_{xy})^{-1} (\mathbf{K}_{y\theta} - \mathbf{K}_{yx}\mathbf{K}_x^{-1}\mathbf{K}_{x\theta}) \mathbf{u}_\theta \tag{3.50a}$$

and,

$$\{\mathbf{y}_T\} = -[\mathbf{u}_\theta]^{-1} (\mathbf{K}_x - \mathbf{K}_{xy}\mathbf{K}_y^{-1}\mathbf{K}_{yx})^{-1} (\mathbf{K}_{x\theta} - \mathbf{K}_{xy}\mathbf{K}_y^{-1}\mathbf{K}_{y\theta}) \mathbf{u}_\theta \tag{3.50b}$$

where $[\mathbf{u}_\theta]$ represents the diagonal matrix form of vector $\mathbf{u}_\theta$ and $\{\mathbf{x}_T\}$ and $\{\mathbf{y}_T\}$ the vector forms of diagonal matrices $\mathbf{x}_T$ and $\mathbf{y}_T$. The deck rotations are determined by a static analysis of the building subjected to torsional moments $\tilde{\mathbf{T}}_\theta$ (see Example 3).

Since $[\mathbf{u}_\theta]$ is a diagonal matrix, equations (3.50) are simplified to equations (3.26) when the products of the stiffness submatrices in equations (3.50) are diagonal.

Equations (3.50) can also be simplified further in the two cases discussed in the previous section:

1. If the principal planes of all resisting elements are parallel or orthogonal, then equations (3.34) are satisfied. Substituting equations (3.34d) into equations (3.50), leads to:

$$\{\mathbf{x}_T\} = [\mathbf{u}_\theta]^{-1} \mathbf{K}_y^{-1} \mathbf{K}_{y\theta} \mathbf{u}_\theta \quad \text{and} \quad \{\mathbf{y}_T\} = -[\mathbf{u}_\theta]^{-1} \mathbf{K}_x^{-1} \mathbf{K}_{x\theta} \mathbf{u}_\theta \tag{3.51}$$

   These equations were also obtained in [14] for buildings consisting of frames arranged in an orthogonal grid in plan.

2. If the building has a vertical plane of stiffness symmetry, then choosing the X_j direction along the symmetry plane leads to:

$$\mathbf{K}_{xy} = \mathbf{K}_{yx} = \mathbf{0} \quad \text{and} \quad \mathbf{K}_{x\theta} = \mathbf{K}_{\theta x} = \mathbf{0}$$

from which equations (3.50) become:

$$\{\mathbf{x}_T\} = [\mathbf{u}_\theta]^{-1}\, \mathbf{K}_y^{-1}\, \mathbf{K}_{y\theta}\, \mathbf{u}_\theta \quad \text{and} \quad \{\mathbf{y}_T\} = -\, [\mathbf{u}_\theta]^{-1}\, \mathbf{K}_x^{-1}\, \mathbf{K}_{x\theta}\, \mathbf{u}_\theta = \mathbf{0} \tag{3.52}$$

Similarly, if Y_j are chosen in the direction of the symmetry plane, then:

$$\{\mathbf{x}_T\} = [\mathbf{u}_\theta]^{-1}\, \mathbf{K}_y^{-1}\, \mathbf{K}_{y\theta}\, \mathbf{u}_\theta = \mathbf{0} \quad \text{and} \quad \{\mathbf{y}_T\} = -\, [\mathbf{u}_\theta]^{-1}\, \mathbf{K}_x^{-1}\, \mathbf{K}_{x\theta}\, \mathbf{u}_\theta \tag{3.53}$$

Equations (3.50) to (3.53) show clearly that the locations of centers of twist depend upon the applied torsional moments (since $\mathbf{u}_\theta$ depends on $\tilde{\mathbf{T}}_\theta$). The locations are unique and independent of the applied forces only if equations (3.26) yield diagonal matrices, in which case the centers of twist and rigidity are coincident and the building stiffness matrix defined at these centers is of the form given by equation (3.15). The conditions to be satisfied for the centers of twist and rigidity to coincide, be unique and load independent are examined in Section 4.

3.4.1 Example 3

For the building of Figure 5 (Section 3.3.3), the centers of twist are determined for $\tilde{\mathbf{T}}_\theta = \mathbf{I}$, i.e. for the case when all floors are subjected to equal torsional moments. Since $\tilde{\mathbf{P}}_x = \tilde{\mathbf{P}}_y = \mathbf{0}$, the deck rotations can be determined from the solution of the static equilibrium equation written at reference points O_j, i.e.:

$$\begin{Bmatrix} \mathbf{0} \\ \mathbf{0} \\ \tilde{\mathbf{T}}_\theta \end{Bmatrix} = \begin{bmatrix} \mathbf{K}_x & \mathbf{K}_{xy} & \mathbf{K}_{x\theta} \\ \mathbf{K}_{yx} & \mathbf{K}_y & \mathbf{K}_{y\theta} \\ \mathbf{K}_{\theta x} & \mathbf{K}_{\theta y} & \mathbf{K}_\theta \end{bmatrix} \begin{Bmatrix} \mathbf{u}_x \\ \mathbf{u}_y \\ \mathbf{u}_\theta \end{Bmatrix}$$

from which we obtain:

$$\begin{Bmatrix} \mathbf{u}_x \\ \mathbf{u}_y \end{Bmatrix} = -\begin{bmatrix} \mathbf{K}_x & \mathbf{K}_{xy} \\ \mathbf{K}_{yx} & \mathbf{K}_y \end{bmatrix}^{-1} \begin{bmatrix} \mathbf{K}_{x\theta} \\ \mathbf{K}_{y\theta} \end{bmatrix} \mathbf{u}_\theta$$

Thus,

$$\tilde{\mathbf{T}}_\theta = [\, \mathbf{K}_{\theta x} \;\; \mathbf{K}_{\theta y} \,] \begin{Bmatrix} \mathbf{u}_x \\ \mathbf{u}_y \end{Bmatrix} + \mathbf{K}_\theta \, \mathbf{u}_\theta$$

or,

$$\tilde{\mathbf{T}}_\theta = \left\{ \mathbf{K}_\theta - [\, \mathbf{K}_{\theta x} \;\; \mathbf{K}_{\theta y} \,] \begin{bmatrix} \mathbf{K}_x & \mathbf{K}_{xy} \\ \mathbf{K}_{yx} & \mathbf{K}_y \end{bmatrix}^{-1} \begin{bmatrix} \mathbf{K}_{x\theta} \\ \mathbf{K}_{y\theta} \end{bmatrix} \right\} \mathbf{u}_\theta$$

Solution of these equations leads to $\mathbf{u}_\theta$. Using this procedure the coordinates of the centers of twist of the building in Example 1 is found to be:

$$\{\mathbf{x}_T\} = \{\mathbf{y}_T\} = \begin{Bmatrix} 1.208 \\ 1.251 \\ 1.282 \\ 1.305 \\ 1.323 \end{Bmatrix}$$

3.5 Locations of Shear Centers

The location of the shear center of a floor is determined by finding the centroid of the interstory shear forces experienced by individual resisting elements due to a static loading that causes no twist ($\mathbf{u}_\theta = 0$) of any of the stories (see the definition of shear centers given in Section 3.1). Substituting $\mathbf{u}_\theta = 0$ in equations (3.5), the vectors of lateral dispalcements of the i^{th} resisting element along its principal planes are given by:

$$\mathbf{v}_{ai} = \cos\beta_i \, \mathbf{u}_x + \sin\beta_i \, \mathbf{u}_y \tag{3.54a}$$

$$\mathbf{v}_{bi} = -\sin\beta_i \, \mathbf{u}_x + \cos\beta_i \, \mathbf{u}_y \tag{3.54b}$$

The vectors of applied lateral loads on the i^{th} resisting element along its principal planes are given by equations (3.2). Thus,

$$\mathbf{Q}_{ai} = \mathbf{k}_{ai} \, \mathbf{v}_{ai} = \mathbf{k}_{ai} (\cos\beta_i \, \mathbf{u}_x + \sin\beta_i \, \mathbf{u}_y) \tag{3.55a}$$

$$\mathbf{Q}_{bi} = \mathbf{k}_{bi} \, \mathbf{v}_{bi} = \mathbf{k}_{bi} (-\sin\beta_i \, \mathbf{u}_x + \cos\beta_i \, \mathbf{u}_y) \tag{3.55b}$$

The vectors of interstory shear forces $\mathbf{V}_{ai}$ and $\mathbf{V}_{bi}$ experienced by the i^{th} resisting element are related

to $\mathbf{Q}_{ai}$ and $\mathbf{Q}_{bi}$ by:

$$\mathbf{V}_{ai} = \mathbf{S}\mathbf{Q}_{ai} = \mathbf{S}\mathbf{k}_{ai}(\cos\beta_i\,\mathbf{u}_x + \sin\beta_i\,\mathbf{u}_y) \tag{3.56a}$$

$$\mathbf{V}_{bi} = \mathbf{S}\mathbf{Q}_{bi} = \mathbf{S}\mathbf{k}_{bi}(-\sin\beta_i\,\mathbf{u}_x + \cos\beta_i\,\mathbf{u}_y) \tag{3.56b}$$

where S is a summation matrix which is upper triangular, of dimension N and of the form:

$$\mathbf{S} = \begin{bmatrix} 1 & 1 & \dots & 1 & 1 \\ & 1 & \dots & 1 & 1 \\ & & \dots & & \\ & & & 1 & 1 \\ & & & & 1 \end{bmatrix} \tag{3.57}$$

The vectors of shearing forces $\mathbf{V}_{xi}$ and $\mathbf{V}_{yi}$ experienced by the i^{th} resisting element along the $\mathbf{X}_j$ and $\mathbf{Y}_j$ axes are given by:

$$\mathbf{V}_{xi} = \mathbf{V}_{ai}\cos\beta_i - \mathbf{V}_{bi}\sin\beta_i \tag{3.58a}$$

$$\mathbf{V}_{yi} = \mathbf{V}_{ai}\sin\beta_i + \mathbf{V}_{bi}\cos\beta_i \tag{3.58b}$$

Substituting equations (3.56) into (3.58) and utilizing equations (3.9), results in:

$$\mathbf{V}_{xi} = \mathbf{S}\,[(\cos^2\beta_i\,\mathbf{k}_{ai} + \sin^2\beta_i\,\mathbf{k}_{bi})\,\mathbf{u}_x + (\mathbf{k}_{ai} - \mathbf{k}_{bi})\sin\beta_i\cos\beta_i\,\mathbf{u}_y] = \mathbf{S}\,[\mathbf{K}_{xi}\,\mathbf{u}_x + \mathbf{K}_{xyi}\,\mathbf{u}_y] \tag{3.59a}$$

$$\mathbf{V}_{yi} = \mathbf{S}\,[(\mathbf{k}_{ai} - \mathbf{k}_{bi})\sin\beta_i\cos\beta_i\,\mathbf{u}_x + (\sin^2\beta_i\,\mathbf{k}_{ai} + \cos^2\beta_i\,\mathbf{k}_{bi})\,\mathbf{u}_y] = \mathbf{S}\,[\mathbf{K}_{yxi}\,\mathbf{u}_x + \mathbf{K}_{yi}\,\mathbf{u}_y] \tag{3.59b}$$

The vector of the resultants of the shearing forces has X and Y components equal to $\sum_i \mathbf{V}_{xi}$ and $\sum_i \mathbf{V}_{yi}$, respectively, with the resultant of the shearing forces acting on the j^{th} floor passing through its shear center with X and Y coordinates equal to x_{Sj} and y_{Sj}. Referring to Figure 4a, equilibrium of moments about reference axis Z of all shearing forces acting at each floor level, and presenting the results in vector form, leads to:

$$\sum_i \pm d_{ai}\mathbf{V}_{ai} + \sum_i \pm d_{bi}\mathbf{V}_{bi} - \mathbf{x}_S \sum_i \mathbf{V}_{yi} + \mathbf{y}_S \sum_i \mathbf{V}_{xi} = \mathbf{0} \tag{3.60}$$

where $\mathbf{x}_S$ and $\mathbf{y}_S$ denote the diagonal matrices of entries equal to x_{Sj} and y_{Sj}, respectively. The algebraic sign accompanying $\mathbf{V}_{ai}$ and $\mathbf{V}_{bi}$ in equation (3.60) depends on whether the forces cause

positive or negative moments about reference axis Z. Substituting equations (3.56) and (3.59) into (3.60) and then utilizing equations (3.9) and (3.28), leads to:

$$\mathbf{S}\left(\mathbf{K}_{\theta x}\tilde{\mathbf{u}}_x + \mathbf{K}_{\theta y}\tilde{\mathbf{u}}_y\right) - \mathbf{x}_S\,\mathbf{S}\,\tilde{\mathbf{P}}_y + \mathbf{y}_S\,\mathbf{S}\,\tilde{\mathbf{P}}_x = \mathbf{0} \tag{3.61}$$

Substituting equations (3.30) into (3.61), and using equations (A.7), we get:

$$\left(\mathbf{y}_S\mathbf{S} + \mathbf{S}\mathbf{K}_{\theta x}\mathbf{A}^{-1} - \mathbf{S}\mathbf{K}_{\theta y}\mathbf{K}_y^{-1}\mathbf{K}_{yx}\mathbf{A}^{-1}\right)\tilde{\mathbf{P}}_x - \left(\mathbf{x}_S\mathbf{S} - \mathbf{S}\mathbf{K}_{\theta y}\mathbf{B}^{-1} + \mathbf{S}\mathbf{K}_{\theta x}\mathbf{K}_x^{-1}\mathbf{K}_{xy}\mathbf{B}^{-1}\right)\tilde{\mathbf{P}}_y = \mathbf{0} \tag{3.62}$$

Since $\tilde{\mathbf{P}}_x$ and $\tilde{\mathbf{P}}_y$ are independent, we can write:

$$\left(\mathbf{y}_S\mathbf{S} + \mathbf{S}\mathbf{K}_{\theta x}\mathbf{A}^{-1} - \mathbf{S}\mathbf{K}_{\theta y}\mathbf{K}_y^{-1}\mathbf{K}_{yx}\mathbf{A}^{-1}\right)\tilde{\mathbf{P}}_x = \mathbf{0}$$

and,

$$\left(\mathbf{x}_S\mathbf{S} - \mathbf{S}\mathbf{K}_{\theta y}\mathbf{B}^{-1} + \mathbf{S}\mathbf{K}_{\theta x}\mathbf{K}_x^{-1}\mathbf{K}_{xy}\mathbf{B}^{-1}\right)\tilde{\mathbf{P}}_y = \mathbf{0}$$

from which we get:

$$\mathbf{x}_S\mathbf{S}\tilde{\mathbf{P}}_y = \mathbf{S}\left(\mathbf{K}_{\theta y} - \mathbf{K}_{\theta x}\mathbf{K}_x^{-1}\mathbf{K}_{xy}\right)\mathbf{B}^{-1}\tilde{\mathbf{P}}_y$$

and,

$$\mathbf{y}_S\mathbf{S}\tilde{\mathbf{P}}_x = \mathbf{S}\left(\mathbf{K}_{\theta x} - \mathbf{K}_{\theta y}\mathbf{K}_y^{-1}\mathbf{K}_{yx}\right)\mathbf{A}^{-1}\tilde{\mathbf{P}}_x$$

Let $[\mathbf{P}'_x]$ and $[\mathbf{P}'_y]$ denote the diagonal matrix forms of vectors $\mathbf{S}\tilde{\mathbf{P}}_x$ and $\mathbf{S}\tilde{\mathbf{P}}_y$, respectively, and $\{\mathbf{x}_S\}$ and $\{\mathbf{y}_S\}$ the vector forms of diagonal matrices $\mathbf{x}_S$ and $\mathbf{y}_S$, respectively. Then,

$$\{\mathbf{x}_S\} = [\mathbf{P}'_y]^{-1}\mathbf{S}\left(\mathbf{K}_{\theta y} - \mathbf{K}_{\theta x}\mathbf{K}_x^{-1}\mathbf{K}_{xy}\right)\left(\mathbf{K}_y - \mathbf{K}_{yx}\mathbf{K}_x^{-1}\mathbf{K}_{xy}\right)^{-1}\tilde{\mathbf{P}}_y \tag{3.64a}$$

and,

$$\{\mathbf{y}_S\} = -[\mathbf{P}'_x]^{-1}\mathbf{S}\left(\mathbf{K}_{\theta x} - \mathbf{K}_{\theta y}\mathbf{K}_y^{-1}\mathbf{K}_{yx}\right)\left(\mathbf{K}_x - \mathbf{K}_{xy}\mathbf{K}_y^{-1}\mathbf{K}_{yx}\right)^{-1}\tilde{\mathbf{P}}_x \tag{3.64b}$$

Although there is great similarity between equations (3.64) and (3.33), they yield different coordinates for the shear centers and centers of rigidity (see Example 4). Thus, in general, shear centers do not coincide with centers of rigidity. When the product of the stiffness submatrices of equations (3.64) leads to a diagonal matrix with equal diagonal entries, equations (3.64) simplify to

equations (3.26) and become load-independent. In this case, shear centers coincide with centers of rigidity as well as with centers of twist.

Simplification of equations (3.64) is possible in the special cases mentioned in Section 3.2, where $\mathbf{K}_{xy} = \mathbf{K}_{yx} = \mathbf{0}$, leading to:

$$\{x_S\} = [\mathbf{P}'_y]^{-1}\mathbf{S}\mathbf{K}_{\theta y}\mathbf{K}_y^{-1}\tilde{\mathbf{P}}_y \tag{3.65a}$$

and,

$$\{y_S\} = -[\mathbf{P}'_x]^{-1}\mathbf{S}\mathbf{K}_{\theta x}\mathbf{K}_x^{-1}\tilde{\mathbf{P}}_x \tag{3.65b}$$

3.5.1 Example 4

Using equations (3.64) for the building (Figure 5) desribed in Section 3.3.3, the locations of the shear centers of the building are found to be given by:

$$\{x_S\} = \{y_S\} = \begin{Bmatrix} 0.955 \\ 1.187 \\ 1.298 \\ 1.357 \\ 1.988 \end{Bmatrix}$$

4. A SPECIAL CLASS OF MULTI-STORY BUILDINGS

It is apparent from the preceding section that the centers of rigidity, the centers of twist and shear centers of multi-story buildings do not generally coincide. In order for the building to have unique, load-independent centers of rigidity that are coincident with centers of twist and shear centers, it is necessary that equations (3.26) yield diagonal matrices. The conditions to be satisfied for a building to have unique centers of rigidity are examined in this section.

4.1 Buildings with Arbitrary Orientations of Elemental Principal Planes

Consider a special class of multi-story buildings with every resisting element having lateral stiffness matrices along its principal planes of the form:

$$\mathbf{k}_{ai} = C_{ai}\,\mathbf{k} \quad \text{and} \quad \mathbf{k}_{bi} = C_{bi}\,\mathbf{k} \tag{4.1}$$

where C_{ai} and C_{bi} are constants for the i^{th} resisting element and $\mathbf{k}$ is a characteristic matrix for the building. Utilizing equations (4.1), equations (3.9) become:

$$\mathbf{K}_{xi} = (C_{ai}\cos^2\beta_i + C_{bi}\sin^2\beta_i)\,\mathbf{k} = C_{xi}\,\mathbf{k}$$

$$\mathbf{K}_{yi} = (C_{ai}\sin^2\beta_i + C_{bi}\cos^2\beta_i)\,\mathbf{k} = C_{yi}\,\mathbf{k}$$

$$\mathbf{K}_{xyi} = \mathbf{K}_{yxi} = [\,(C_{ai} - C_{bi})\sin\beta_i\cos\beta_i\,]\,\mathbf{k} = C_{xyi}\,\mathbf{k} \tag{4.2}$$

$$\mathbf{K}_{x\theta i} = \mathbf{K}_{\theta xi} = [\,\pm C_{ai}\,d_{ai}\cos\beta_i - (\pm) C_{bi}\,d_{bi}\sin\beta_i\,]\,\mathbf{k} = C_{x\theta i}\,\mathbf{k}$$

$$\mathbf{K}_{y\theta i} = \mathbf{K}_{\theta yi} = (\pm C_{ai}\,d_{ai}\sin\beta_i \pm C_{bi}\,d_{bi}\cos\beta_i)\mathbf{k} = C_{y\theta i}\,\mathbf{k}$$

Substituting equations (4.2) into (3.11), leads to:

$$\mathbf{K}_x = \sum_i \mathbf{K}_{xi} = \sum_i (C_{ai}\cos^2\beta_i + C_{bi}\sin^2\beta_i)\,\mathbf{k} = (\sum_i C_{xi})\mathbf{k} = C_x\,\mathbf{k}$$

$$\mathbf{K}_y = \sum_i \mathbf{K}_{yi} = \sum_i (C_{ai}\sin^2\beta_i + C_{bi}\cos^2\beta_i)\,\mathbf{k} = (\sum_i C_{yi})\,\mathbf{k} = C_y\,\mathbf{k}$$

$$\mathbf{K}_{xy} = \mathbf{K}_{yx} = \sum_i \mathbf{K}_{xyi} = \sum_i [\,C_{ai} - C_{bi})\sin\beta_i\cos\beta_i\,]\,\mathbf{k} = (\sum_i C_{xyi})\,\mathbf{k} = C_{xy}\,\mathbf{k} \tag{4.3}$$

$$\mathbf{K}_{x\theta} = \mathbf{K}_{\theta x} = \sum_i \mathbf{K}_{x\theta i} = \sum_i [\pm C_{ai}\, d_{ai} \cos\beta_i - (\pm)\, C_{bi}\, d_{bi} \sin\beta_i\,]\,\mathbf{k} = (\sum_i C_{x\theta i})\,\mathbf{k} = C_{x\theta}\,\mathbf{k}$$

$$\mathbf{K}_{y\theta} = \mathbf{K}_{\theta y} = \sum_i \mathbf{K}_{y\theta i} = \sum_i [\pm C_{ai}\, d_{ai} \sin\beta_i \pm C_{bi}\, d_{bi} \cos\beta_i\,]\,\mathbf{k} = (\sum_i C_{y\theta i})\,\mathbf{k} = C_{y\theta}\,\mathbf{k}$$

Substituting equations (4.3) into (3.26), leads to:

$$\mathbf{x}_R = \frac{C_x C_{y\theta} - C_{xy} C_{x\theta}}{C_x C_y - C_{xy}^2}\,\mathbf{I} \tag{4.4a}$$

and,

$$\mathbf{y}_R = -\frac{C_y C_{x\theta} - C_{xy} C_{y\theta}}{C_x C_y - C_{xy}^2}\,\mathbf{I} \tag{4.4b}$$

where **I** is a unit matrix of dimension N, the number of stories. Since **I** is diagonal, $\mathbf{x}_R$ and $\mathbf{y}_R$ obtained from equations (4.4) are also diagonal. Similarly, in order to obtain $\mathbf{x}_T$ and $\mathbf{y}_T$, the coordinates vector of the centers of twist, and $\mathbf{x}_S$ and $\mathbf{y}_S$, the coordinates vector of the shear centers, equations (4.3) are substituted into (3.50) and (3.64), respectively, resulting in:

$$\{\mathbf{x}_T\} = \{\mathbf{x}_S\} = \frac{C_x C_{y\theta} - C_{xy} C_{x\theta}}{C_x C_y - C_{xy}^2}\,\mathbf{1} \tag{4.5a}$$

and,

$$\{\mathbf{y}_T\} = \{\mathbf{y}_T\} = \; = -\frac{C_y C_{x\theta} - C_{xy} C_{y\theta}}{C_x C_y - C_{xy}^2}\,\mathbf{1} \tag{4.5b}$$

where **1** is a vector of ones.

It is apparent from equations (4.4) and (4.5) that the centers of rigidity, the centers of twist and the shear centers for the special class of buildings considered are coincident, and their locations are independent of applied forces. Since all reference points O_j are colinear and axes X_j (and Y_j) are all in the same direction, the centers of rigidity, the centers of twist and the shear centers of the building lie on a vertical line located at distances from the Z reference axis, measured along the X_j and Y_j axes, given by:

$$x_{Rj} = x_{Tj} = x_{Sj} = \frac{C_x C_{y\theta} - C_{xy} C_{x\theta}}{C_x C_y - C_{xy}^2} \tag{4.6a}$$

and,

$$y_{Rj} = y_{Tj} = y_{Sj} = -\frac{C_y C_{x\theta} - C_{xy} C_{y\theta}}{C_x C_y - C_{xy}^2} \tag{4.6b}$$

in which x_{Rj} and y_{Rj}, x_{Tj} and y_{Tj}, and x_{Sj} and y_{Sj} denote the X and Y coordinates of the centers of rigidity, the centers of twist and the shear centers of the building, respectively; these coordinates are the same for all floors. Equations (4.6) for the special class of multi-story buildings resemble equations (2.26) and (2.27) for one-story systems.

The building stiffness matrix $\tilde{\mathbf{K}}$ defined at these unique centers is given by:

$$\tilde{\mathbf{K}} = \begin{bmatrix} C_x \mathbf{k} & C_{xy} \mathbf{k} & \mathbf{0} \\ C_{xy} \mathbf{k} & C_y \mathbf{k} & \mathbf{0} \\ \mathbf{0} & \mathbf{0} & \tilde{\mathbf{K}}_\theta \end{bmatrix} \tag{4.7}$$

Figure 7 shows two simple examples of buildings with unique centers of rigidity. System 'A' of Figure 7a consists of three frames with equal lateral stiffness matrices $\mathbf{k}_A$, i.e. $C_{a1} = C_{a2} = C_{a3} = 1$. Using equations (4.3) leads to:

$$C_x^A = \cos^2 135 + \cos^2 90 + \cos^2 0 = 1.5$$

$$C_y^A = \sin^2 135 + \sin^2 90 + \sin^2 0 = 1.5$$

$$C_{xy}^A = \sin 135 \cos 135 = -0.5 \tag{4.8}$$

$$C_{x\theta}^A = a\cos 135 + a\cos 90 + a\cos 0 = 0.293\ a$$

$$C_{y\theta}^A = a\sin 135 + a\sin 90 + a\sin 0 = 1.707\ a$$

Substituting equations (4.8) into equations (4.6), leads to:

$$x_{Rj}^A = \frac{(1.5)(1.707\ a) - (-0.5)(0.293\ a)}{(1.5)(1.5) - (-0.5)^2} = 1.354\ a \tag{4.9a}$$

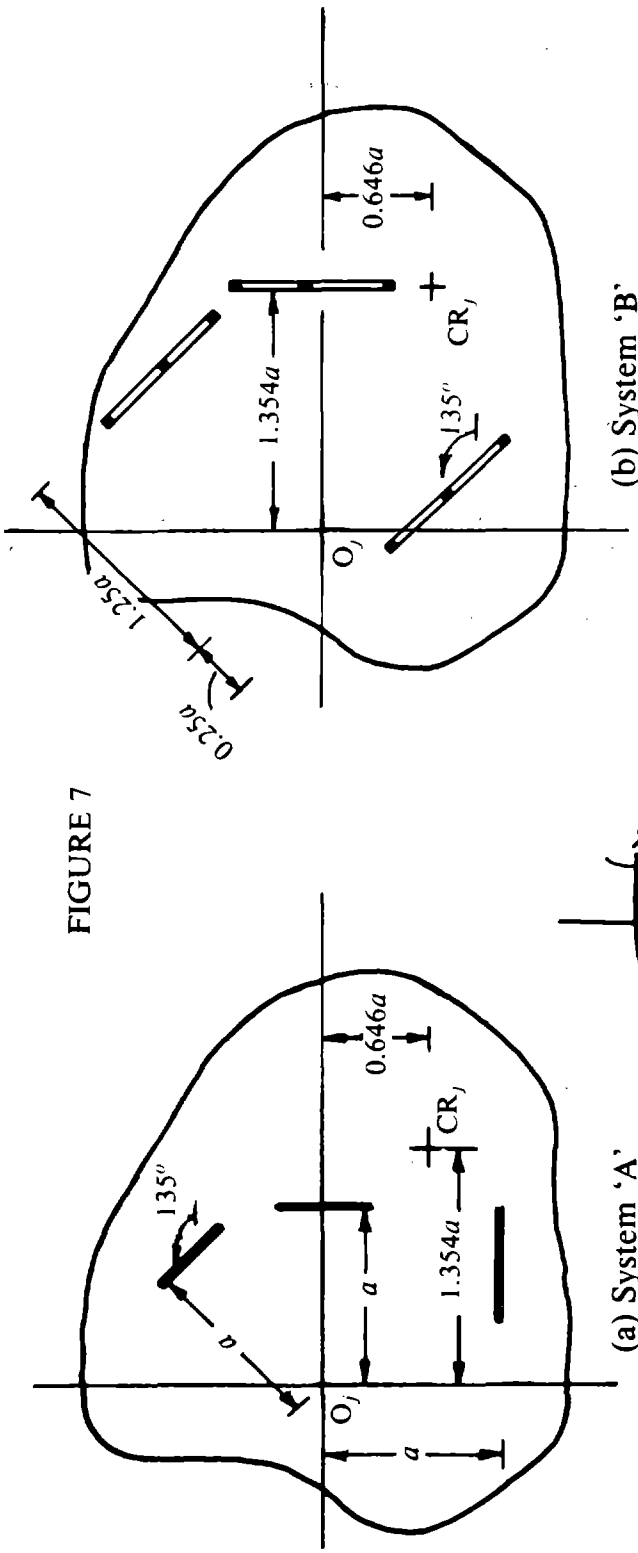

FIGURE 7

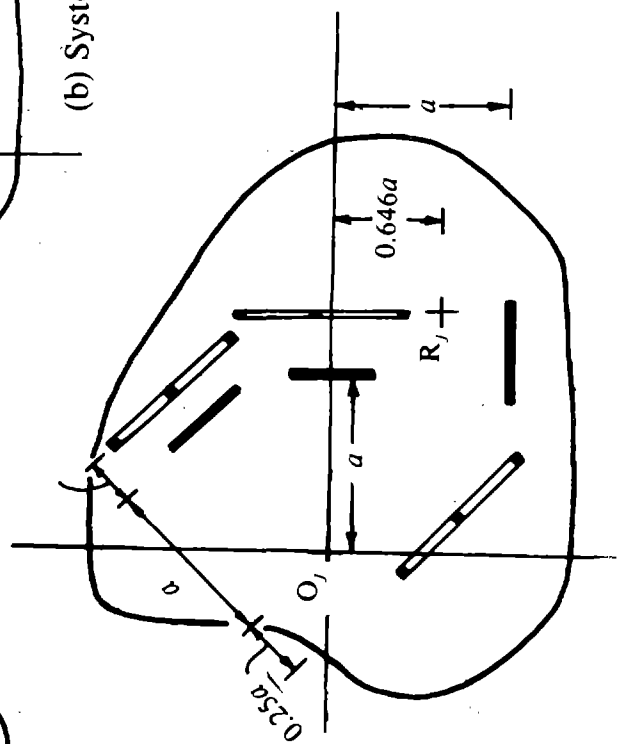

FIGURE 8 System 'C'

and,

$$y_{Rj}^{A} = -\frac{(1.5)(0.293\,a) - (-0.5)(1.707\,a)}{(1.5)(1.5) - (-0.5)^2} = -0.646\,a \tag{4.9b}$$

The other example, system 'B' of Figure 7b, has three frames of equal lateral stiffness matrix, $\mathbf{k}_B$. Using equation (4.3) leads to:

$$C_x^B = \cos^2 90 + \cos^2 135 + \cos^2 135 = 1$$

$$C_y^B = \sin^2 90 + \sin^2 135 + \sin^2 135 = 2$$

$$C_{xy}^B = 2\sin 135 \cos 135 = -1 \tag{4.10}$$

$$C_{x\theta}^B = 1.354\,a\cos 90 + 1.25\,a\cos 135 - 0.25\,a\cos 135 = -0.707\,a$$

$$C_{y\theta}^B = 1.354\,a\sin 90 + 1.25\,a\sin 135 - 0.25\,a\sin 135 = 2.061\,a$$

Substituting equations (4.11) into equations (4.6) leads to:

$$x_{Rj}^{B} = \frac{(1)(2.061\,a) - (-1)(-0.707\,a)}{(1)(2) - (-1)^2} = 1.354\,a \tag{4.11a}$$

and,

$$y_{Rj}^{B} = -\frac{(2)(-0.707\,a) - (-1)(2.061\,a)}{(1)(2) - (-1)^2} = -0.646\,a \tag{4.10b}$$

Thus, the two systems, 'A' and 'B', belonging to the special class of buildings presented above have unique centers of rigidity that are of equal coordinates x_{Rj} and y_{Rj}. Consider a multi-story sytem 'C', shown in Figure 8, that consists of the two subsystems 'A' and 'B', with the locations of the frames in 'C' relative to O_j, being the same as in 'A' and 'B'. Denote by $\mathbf{K}_A$ and $\mathbf{K}_B$ the building stiffness matrices defined at reference points O_j of systems 'A' and 'B', respectively. Then, the building stiffness matrix $\mathbf{K}_C$ at O_j of building 'C' is given by:

$$\mathbf{K}_C = \mathbf{K}_A + \mathbf{K}_B \tag{4.12}$$

Consider points R_j of system 'C' that lie on a vertical line and have coordinates equal to x_{Rj} and y_{Rj}

of systems 'A' and 'B'. The building stiffness matrix, $\mathbf{K}_{RC}$ of building 'C' at points R_j, is given by:

$$\mathbf{K}_{RC} = \tilde{\mathbf{a}}^T \mathbf{K}_C \tilde{\mathbf{a}} = \tilde{\mathbf{a}}^T \mathbf{K}_A \tilde{\mathbf{a}} + \tilde{\mathbf{a}}^T \mathbf{K}_B \tilde{\mathbf{a}} = \tilde{\mathbf{K}}_A + \tilde{\mathbf{K}}_B \tag{4.13}$$

where $\tilde{\mathbf{a}}$ is given by equation (3.21), with $\mathbf{x}_R$ and $\mathbf{y}_R$ the diagonal matrices of entries equal to x_{Rj} and y_{Rj}. Using equations (4.7) to compute $\tilde{\mathbf{K}}_A$ and $\tilde{\mathbf{K}}_B$ of systems 'A' and 'B', equations (4.12) become:

$$\mathbf{K}_{RC} = \begin{bmatrix} C_x^A \mathbf{k}_A + C_x^B \mathbf{k}_B & C_{xy}^A \mathbf{k}_A + C_{xy}^B \mathbf{k}_B & \mathbf{0} \\ C_{xy}^A \mathbf{k}_A + C_{xy}^B \mathbf{k}_B & C_y^A \mathbf{k}_A + C_y^B \mathbf{k}_B & \mathbf{0} \\ \mathbf{0} & \mathbf{0} & \tilde{\mathbf{k}}_{\theta A} + \tilde{\mathbf{k}}_{\theta B} \end{bmatrix} = \tilde{\mathbf{K}}_C \tag{4.14}$$

Due to the form of $\mathbf{K}_{RC}$, it is obvious that points R_j are the centers of rigidity of building 'C'.

Therefore, when a multi-story building consists of two or more subsystems of resisting elements, with each subsystem having unique centers of rigidity that are coincident, the system itself has unique centers of rigidity that are also coincident with those of the individual subsystems.

4.2 Buildings with Orthogonal System of Resisting Elements

Consider a building consisting of resisting elements with principal planes of each element oriented along the X- and Y- axes. Suppose that the lateral stiffness matrices $\mathbf{k}_{xi}$ and $\mathbf{k}_{yi}$ along each one of the principal planes of all resisting elements are proportional, that is:

$$\mathbf{k}_{xi} = C_{xi} \mathbf{k}_x \quad \text{and} \quad \mathbf{k}_{yi} = C_{yi} \mathbf{k}_y \tag{4.15}$$

where C_{xi} and C_{yi} are constants of the i^{th} resisting element relating its lateral stiffness matrices to $\mathbf{k}_x$ and $\mathbf{k}_y$, the characteristic matrices of the building along the X and Y principal directions. Then equations (3.34) become:

$$\mathbf{K}_x = \sum_i \mathbf{K}_{xi} = \sum_i \mathbf{k}_{xi} = (\sum_i C_{xi}) \mathbf{k}_x = C_x \mathbf{k}_x$$

$$\mathbf{K}_y = \sum_i \mathbf{K}_{yi} = \sum_i \mathbf{k}_{yi} = (\sum_i C_{yi})\,\mathbf{k}_y = C_y\,\mathbf{k}_y$$

$$\mathbf{K}_{xy} = \mathbf{K}_{yx} = \mathbf{0} \tag{4.16}$$

$$\mathbf{K}_{x\theta} = \mathbf{K}_{\theta x} = \sum_i \mathbf{K}_{x\theta i} = -\sum_i y_i\,\mathbf{k}_{xi} = -[\sum_i (C_{xi}\,y_i)]\,\mathbf{k}_x = C_{x\theta}\,\mathbf{k}_x$$

$$\mathbf{K}_{y\theta} = \mathbf{K}_{\theta y} = \sum_i \mathbf{K}_{y\theta i} = \sum_i x_i\,\mathbf{k}_{yi} = [\sum_i (C_{yi}\,x_i)]\,\mathbf{k}_y = C_{y\theta}\,\mathbf{k}_y$$

Substituting equations (4.16) into (3.35), leads to:

$$\mathbf{x}_R = \frac{C_{y\theta}}{C_y}\mathbf{I} = \frac{\sum_i C_{yi}\,x_i}{\sum_i C_{yi}}\mathbf{I} \tag{4.17a}$$

and,

$$\mathbf{y}_R = -\frac{C_{x\theta}}{C_x}\mathbf{I} = \frac{\sum_i C_{xi}\,y_i}{\sum_i C_{xi}}\mathbf{I} \tag{4.17b}$$

Since $\mathbf{I}$ is a diagonal matrix, $\mathbf{x}_R$ and $\mathbf{y}_R$ are also diagonal. These equations for the coordinates of the centers of rigidity for a multi-story building are similar to equations (2.31) obtained for one-story systems.

Therefore, buildings consisting of an orthogonal system of resisting elements with lateral stiffness matrices of all resisting elements along each principal direction proportional to each other have unique centers of rigidity, aligned on a vertical line. The same conclusion was reached in reference [8]. In this case, the building stiffness $\tilde{\mathbf{K}}$ defined at the centers of rigidity is given by:

$$\tilde{\mathbf{K}} = \begin{bmatrix} C_x\mathbf{k}_x & \mathbf{0} & \mathbf{0} \\ \mathbf{0} & C_y\mathbf{k}_y & \mathbf{0} \\ \mathbf{0} & \mathbf{0} & \tilde{\mathbf{K}}_\theta \end{bmatrix} \tag{4.18}$$

It should be apparent that the coordinates of the centers of twist and of the shear centers are also given by equations (4.17), so that all the centers are coincident, uniquely defined independent of the applied loading and lie on a vertical line.

Using the result of Section 4.1, if the building with orthogonal elemental principal planes consists of two or more subsystems, with each subsystem having unique centers of rigidity that are coincident, the building itself has unique centers of rigidity that are also coincident with those of individual subsystems.

4.3 Orientations of the Principal Axes for the Special Class of Buildings

Finally, the orientations of the principal planes of the building belonging to the special class, identified in Section 4.1, is determined in this section. The lateral displacements $\tilde{\mathbf{u}}_x$ and $\tilde{\mathbf{u}}_y$ of the centers of rigidity along X_j and Y_j directions are related to lateral displacements $\mathbf{u}_I^*$ and $\mathbf{u}_{II}^*$ of the centers of rigidity, along the principal planes of the system by the transformation matrix $\mathbf{a}^*$:

$$\tilde{\mathbf{u}} = \begin{Bmatrix} \tilde{\mathbf{u}}_x \\ \tilde{\mathbf{u}}_y \\ \mathbf{u}_\theta \end{Bmatrix} = \begin{bmatrix} \mathbf{C} & -\mathbf{S} & \mathbf{0} \\ \mathbf{S} & \mathbf{C} & \mathbf{0} \\ \mathbf{0} & \mathbf{0} & \mathbf{I} \end{bmatrix} \begin{Bmatrix} \mathbf{u}_I^* \\ \mathbf{u}_{II}^* \\ \mathbf{u}_\theta \end{Bmatrix} = \mathbf{a}^* \mathbf{u}^* \tag{4.19}$$

in which $\mathbf{C}$ and $\mathbf{S}$ are diagonal matrices with diagonal entries equal to $\cos\eta_j$ and $\sin\eta_j$, respectively, where η_j is the counterclockwise angle between the X_j reference axes and the major principal axis in the j^{th} floor. It follows that the building stiffness $\mathbf{K}^*$ defined with respect to $\mathbf{u}^*$, is given by:

$$\mathbf{K}^* = \mathbf{a}^{*T} \tilde{\mathbf{K}} \mathbf{a}^* \tag{4.20}$$

Substituting equations (4.19) and (3.15) into (4.20), and comparing with (3.19), leads to:

$$\mathbf{K}_I^* = \mathbf{C}\mathbf{K}_x\mathbf{C} + \mathbf{S}\mathbf{K}_y\mathbf{S} + \mathbf{C}\mathbf{K}_{xy}\mathbf{S} + \mathbf{S}\mathbf{K}_{yx}\mathbf{C} \tag{4.21a}$$

$$\mathbf{K}_{II}^* = \mathbf{S}\mathbf{K}_x\mathbf{S} + \mathbf{C}\mathbf{K}_y\mathbf{C} - \mathbf{C}\mathbf{K}_{yx}\mathbf{S} - \mathbf{S}\mathbf{K}_{xy}\mathbf{C} \tag{4.21b}$$

$$\mathbf{K}_\theta^* = \tilde{\mathbf{K}}_\theta \tag{4.22}$$

and,

$$\mathbf{C}\mathbf{K}_x\mathbf{S} - \mathbf{S}\mathbf{K}_y\mathbf{C} - \mathbf{C}\mathbf{K}_{xy}\mathbf{C} + \mathbf{S}\mathbf{K}_{yx}\mathbf{S} = \mathbf{0} \tag{4.23a}$$

$$-\mathbf{S}\mathbf{K}_x\mathbf{C} + \mathbf{C}\mathbf{K}_y\mathbf{S} + \mathbf{C}\mathbf{K}_{xy}\mathbf{C} - \mathbf{S}\mathbf{K}_{yx}\mathbf{S} = \mathbf{0} \tag{2.23b}$$

Addition of equations (4.23), pre-multiplying and post-multiplynig the result by $\mathbf{C}^{-1}$, yields:

$$(\mathbf{K}_x + \mathbf{K}_y)\mathbf{T} = \mathbf{T}(\mathbf{K}_x + \mathbf{K}_y) \tag{4.24}$$

where $\mathbf{T}$ is a diagonal matrix with diagonal entries equal to $\tan\eta_j$.

For systems such as those described in Section 4.1 with stiffness submatrices given by equations (4.3), equations (4.24) simplify to become:

$$\mathbf{k}\mathbf{T} = \mathbf{T}\mathbf{k} \tag{4.25}$$

Pre-multiplying and post-multiplying equations (4.23a) by $\mathbf{C}^{-1}$, and substituting equations (4.3) for $\mathbf{K}_x$, $\mathbf{K}_y$ and $\mathbf{K}_{xy}$, leads to:

$$C_x\mathbf{k}\mathbf{T} - C_y\mathbf{T}\mathbf{k} - C_{xy}\mathbf{k} + C_{xy}\mathbf{T}\mathbf{k}\mathbf{T} = \mathbf{0} \tag{4.26}$$

Using equation (4.25) and pre-multiplying by $\mathbf{k}^{-1}$, results in:

$$(C_x - C_y)\mathbf{T} - C_{xy}(\mathbf{I} - \mathbf{T}^2) = \mathbf{0} \tag{4.27}$$

or,

$$(C_x - C_y)\tan\eta_j - C_{xy}(1 - \tan^2\eta_j) = 0$$

from which,

$$\tan\eta_j = \frac{2C_{xy}}{C_x - C_y} \tag{4.28}$$

Thus, all principal axes of individual floors are parallel to one another and their orientation is given by η_j.

Equations (4.21) can now be written as:

$$\mathbf{K}_I^* = \left[\frac{C_x + C_y}{2} + \left[(\frac{C_x - C_y}{2})^2 + C_{xy}^2 \right]^{1/2} \right] \mathbf{k} = C_I^* \mathbf{k} \tag{4.29a}$$

and,

$$\mathbf{K}_{II}^* = \left[\frac{C_x + C_y}{2} - \left[(\frac{C_x - C_y}{2})^2 + C_{xy}^2 \right]^{1/2} \right] \mathbf{k} = C_{II}^* \mathbf{k} \tag{4.29b}$$

The building stiffness matrix $\mathbf{K}^*$ defined with respect to $\mathbf{u}^*$ is given by:

$$\mathbf{K}^* = \begin{bmatrix} C_I^* \mathbf{k} & \mathbf{0} & \mathbf{0} \\ \mathbf{0} & C_{II}^* \mathbf{k} & \mathbf{0} \\ \mathbf{0} & \mathbf{0} & \tilde{\mathbf{K}}_\theta \end{bmatrix} \tag{4.30}$$

The similarity with the results obtained for one-story systems (Section 2.5) is apparent.

Note that for buildings with a plane of stiffness symmetry, the plane is also a principal plane of the building. Also, if the elemental principal planes are parallel or orthogonal, the principal planes of the system are in the same directions as the elemental principal planes. For buildings such as building 'C' studied in Section 4.1, it is not possible to find principal axes that satisfy the definition given earlier, unless the principal axes of the building subsystems are oriented along the same directions.

5. CONCLUSIONS

In a one-story system, it is always possible to locate in the plane of its deck a unique point which has different roles in the static response of the system. A static horizontal lateral force passing through this point, causes the floor of the system to displace laterally without any twist, with the resultant of the shear forces experienced by various resisting elements also passing through this point. If the force applied through this point is directed along one of the principal axes of the system-- two orthogonal axes passing through this point-- the floor displaces in the direction of the applied force without any twist. If the floor is subjected to a static torsional moment about a vertical axis, the point remains at rest, i.e. the floor rotates about a vertical axis passing through this point. For this reason, the terms center of rigidity, shear center and center of twist are interchangeable in one-story systems, since they refer to a unique point with different roles in the response of the system.

Unlike one-story systems, centers of rigidity, centers of twist and shear centers of the floors of a multi-story building do not generally coincide. Their locations not only depend on the geometric and stiffness characteristics of the building, but also on the applied loading. For a special class of buildings, however, the centers of rigidity, the centers of twist and shear centers of the floors of the buildings are coincident at locations that are independent of the applied loading and lie on a vertical line. Buildings belonging to this special class consist of resisting elements that have proportional lateral stiffness matrices along both their principal planes, if the planes have arbitrary orientations, or they consist of resisting elements that have proportional lateral stiffness matrices along each of their principal planes, when these form an orthogonal grid in plan. It is possible to determine, for this special class of buildings, two principal directions along which application of lateral forces causes the floors to displace laterally without any twist. There is great similarity between the expressions of the locations of the centers and the orientations of the principal axes obtained for one-story systems and buildings belonging to this special class.

Torsional provisions in most building codes are based on the evaluation of static eccentricities, usually given as distances between the centers of mass and the centers of rigidity of a

building, with little or no explanation of how these eccentricities can be determined. Although some codes [e.g. 5] recognize the complexity of determining the centers of rigidity in some buildings, they do not provide any reasonable alternatives. It is clear that torsional provisions based on static eccentricities are strictly applicable only to the special class of buildings described above, and further work is necessary to develop code provisions for buildings not belonging to this special class.

REFERENCES

1. Newmark, N.M. and Rosenblueth, E., Fundamentals of Earthquake Engineering, Prentice-Hall, Inc., Englewood Cliffs, N.J., 1971.

2. National Building Code of Canada, 1980. Associate Committee on the National Building Code, Subsection 4.1.9.1 (17). National Reseach Council of Canada, Ottawa, Ontario.

3. International Conference of Building Officials, Uniform Building Code, 1982.

4. International Association for Earthquake Engineering, Earthquake Resistant Regulations, A World List 1980, Tokyo, August 1980, pp. 503-519.

5. International Association for Earthquake Engineering, Earthquake Resistant Regulations, A World List 1980, Tokyo, August 1980, pp. 521-571.

6. Poole, R.A., "Analysis for Torsion Employing Provisions of NZRS 4203, 1974", Bulletin of New Zealand National Society for Earthquake Engineering, Vol. 10, No. 4, 1977, pp. 219-225.

7. Humar, J.L. and Awad, A.M., "Design for Seismic Torsional Forces", Proceedings, 4th Canadian Conference on Earthquake Engineering, Vancouver, Canada, 1983, pp. 251-260.

8. Cheung, V.W.-T. and Tso, W.K., "Eccentricity in Irregular Multistory Buildings", Canadian Journal of Civil Engineering, Vol. 13, 1986, pp. 46-52.

9. Riddell, R. and Vasquez, J., "Existence of centers of Resistance and Torsional Uncoupling of earthquake Response of Buildings",

10. Dempsey, K.M., "On the Earthquake Generated Response of Torsionally Unbalanced Buildings", Report No. 177, University of Auckland, Auckland, New Zealand, 1978.

11. Kan, C.L. and Chopra, A.K., "Effects of Torsional Coupling on Earthquake Forces in Buildings," ASCE, 103, ST4, pp. 805-820, 1977.

12. Strang, G., Linear Algebra and its Applications, 2nd Edition, Academic Press, Inc., New York, N.Y., 1980.

13. Popov, E.P., Introduction to Mechanics of Solids, Prentice-Hall, Inc., Englewood Cliffs, N.J., 1968, pp. 243.

14. Tso, W.K. and Cheung, V.W.-T, "Decoupling of Equations of Equilibrium in Lateral Load Analysis of Multistory Buildings", Computers and Structures, Vol. 23, No. 5, 1986, pp. 679-684.

APPENDIX A: USEFUL MATHMATICAL FACTS

The lateral stiffness matrices $\mathbf{k}_{ai}$ and $\mathbf{k}_{bi}$ of the i^{th} resisting element along its major and minor principal planes, respectively, are positive definite matrices, because each is symmetric and real. Since submatrices $\mathbf{K}_{xi}$ and $\mathbf{K}_{yi}$, given by equations (3.9), are sums of multiples of $\mathbf{k}_{ai}$ and $\mathbf{k}_{bi}$, it follows that $\mathbf{K}_{xi}$ and $\mathbf{K}_{yi}$ are also positive definite matrices. System submatrices $\mathbf{K}_x$ and $\mathbf{K}_y$, given by equations (3.11), are summations of $\mathbf{K}_{xi}$ and $\mathbf{K}_{yi}$, and, therefore, are also positive definite matrices. Since the inverse of a positive definite matrix always exist [12], it follows that the inverses of $\mathbf{K}_x$ and $\mathbf{K}_y$, $\mathbf{K}_x^{-1}$ and $\mathbf{K}_y^{-1}$ exist.

The building stiffness matrix $\mathbf{K}$ being a positive definite matrix, its minors are also positive definite. Consider the minor matrix:

$$\mathbf{N} = \begin{bmatrix} \mathbf{K}_x & \mathbf{K}_{xy} \\ \mathbf{K}_{yx} & \mathbf{K}_y \end{bmatrix} \tag{A.1}$$

The inverse $\mathbf{N}^{-1}$ of $\mathbf{N}$ exists because $\mathbf{N}$ is positive definite. Let $\mathbf{N}^{-1}$ be given by:

$$\mathbf{N}^{-1} = \begin{bmatrix} \mathbf{N}_{11} & \mathbf{N}_{12} \\ \mathbf{N}_{21} & \mathbf{N}_{22} \end{bmatrix} \tag{A.2}$$

Since $\mathbf{N}\mathbf{N}^{-1} = \mathbf{N}^{-1}\mathbf{N} = \mathbf{I}$, we have:

$$\begin{aligned} \mathbf{K}_x\mathbf{N}_{11} + \mathbf{K}_{xy}\mathbf{N}_{21} &= \mathbf{I} \\ \mathbf{K}_{yx}\mathbf{N}_{12} + \mathbf{K}_y\mathbf{N}_{22} &= \mathbf{I} \\ \mathbf{K}_{yx}\mathbf{N}_{11} + \mathbf{K}_y\mathbf{N}_{21} &= \mathbf{0} \end{aligned} \tag{A.3}$$

and,

$$\mathbf{K}_x\mathbf{N}_{12} + \mathbf{K}_{xy}\mathbf{N}_{22} = \mathbf{0}$$

Thus,

$$\mathbf{N}_{12} = -\mathbf{K}_x^{-1}\mathbf{K}_{xy}\mathbf{N}_{22} \tag{A.4a}$$

$$\mathbf{N}_{21} = - \mathbf{K}_y^{-1} \mathbf{K}_{yx} \mathbf{N}_{11} \tag{A.4b}$$

Substituting equations (A.4) in (A.3a), we get:

$$(\mathbf{K}_x - \mathbf{K}_{xy} \mathbf{K}_y^{-1} \mathbf{K}_{yx}) \mathbf{N}_{11} = \mathbf{I} \tag{A.5a}$$

and,

$$(\mathbf{K}_y - \mathbf{K}_{yx} \mathbf{K}_x^{-1} \mathbf{K}_{xy}) \mathbf{N}_{22} = \mathbf{I} \tag{A.5b}$$

from which:

$$\mathbf{N}_{11} = (\mathbf{K}_x - \mathbf{K}_{xy} \mathbf{K}_y^{-1} \mathbf{K}_{yx})^{-1} = \mathbf{A}^{-1} \tag{A.6a}$$

and,

$$\mathbf{N}_{22} = (\mathbf{K}_y - \mathbf{K}_{yx} \mathbf{K}_x^{-1} \mathbf{K}_{xy})^{-1} = \mathbf{B}^{-1} \tag{A.6b}$$

Therefore, $(\mathbf{K}_x - \mathbf{K}_{xy} \mathbf{K}_y^{-1} \mathbf{K}_{yx})^{-1}$ and $(\mathbf{K}_y - \mathbf{K}_{yx} \mathbf{K}_x^{-1} \mathbf{K}_{xy})^{-1}$ exist.

Finally, since $\mathbf{N}$ is symmetric, $\mathbf{N}^{-1}$ is also symmetric, and:

$$\mathbf{N}_{21} = \mathbf{N}_{12}^T \quad \text{or} \quad \mathbf{N}_{21}^T = \mathbf{N}_{12}$$

Therefore,

$$- \mathbf{K}_y^{-1} \mathbf{K}_{yx} \mathbf{A}^{-1} = - \mathbf{B}^{-1} \mathbf{K}_{yx} \mathbf{K}_x^{-1} \tag{A.7a}$$

and,

$$- \mathbf{A}^{-1} \mathbf{K}_{xy} \mathbf{K}_y^{-1} = - \mathbf{K}_x^{-1} \mathbf{K}_{xy} \mathbf{B}^{-1} \tag{A.7b}$$

APPENDIX B: NOTATION

B.1 One-Story Systems

$a_{gx}(t)$ and $a_{gy}(t)$

earthquake ground motion accelerations along the X and Y axes

$\mathbf{a}_i$ transformation matrix of the i^{th} resisting element defined by equations (2.5) to (2.7)

$\tilde{\mathbf{a}}$ transformation matrix defined by equation (2.21)

$\mathbf{a}^*$ transformation matrix defined by equation (2.40)

d_{ai} and d_{bi} perpendicular distances from reference point O to the major and minor principal axes of the i^{th} resisting element

e static eccentricity of the building defined as the distance between its centers of mass and rigidity

e_x and e_y X and Y components of static eccentricity e

I and II principal axes of the system

J_O and J_R polar moments of inertia of deck about vertical axes passing through reference point O and the center of rigidity, respectively, given by equations (2.13) and (2.18)

k_{ai} and k_{bi} lateral stiffnesses of the i^{th} resisting element along its major and minor principal axes, respectively

k_{xi} and k_{yi} lateral stiffnesses of the i^{th} resisting element along its principal axes which are oriented along the X and Y axes

$k_{\theta i}$ torsional stiffness of the i^{th} shear-wall core about a vertical axis passing through its shear center

K_{xi}, K_{yi} and K_{xyi} or K_{yxi}

submatrices of $\mathbf{K}_i$ defined by equations (2.8) and (2.9)

$K_{x\theta i}$ or $K_{\theta xi}$, $K_{y\theta i}$ or $K_{\theta yi}$ and $K_{\theta i}$

submatrices of $\mathbf{K}_i$ defined by equations (2.8) and (2.9)

K_x, K_y and K_{xy} or K_{yx}

submatrices of $\mathbf{K}$ defined by equations (2.10) and (2.11)

$K_{x\theta}$ or $K_{\theta x}$, $K_{y\theta}$ or $K_{\theta y}$ and K_θ

submatrices of $\mathbf{K}$ defined by equations (2.10) and (2.11)

$\tilde{K}_x$, $\tilde{K}_y$, $\tilde{K}_{xy}$ or $\tilde{K}_{yx}$ and $\tilde{K}_\theta$

submatrices of $\tilde{\mathbf{K}}$ defined by equations (2.15), (2.24) and (2.25)

K_I^*, K_{II}^* and K_θ^*

submatrices of $\mathbf{K}^*$ defined by equation (2.19), (2.49) and (2.43)

$\mathbf{k}_i$ stiffness matrix of the i^{th} resisting element defined in equations (2.2) and (2.3)

$\mathbf{K}$ building stiffness matrix with respect to degrees of freedom $\mathbf{u}$ defined at O

$\tilde{\mathbf{K}}$ building stiffness matrix with respect to degrees of freedom $\tilde{\mathbf{u}}$ defined at the center of rigidity

$\mathbf{K}^*$ building stiffness matrix with respect to degrees of freedom $\mathbf{u}^*$ defined at the center of rigidity

$\mathbf{K}_i$ contribution of the i^{th} resisting element to $\mathbf{K}$

m mass of deck

$\mathbf{M}_M$ building mass matrix defined at its center of mass

Q_{ai} and Q_{bi} lateral forces applied at the floor level of the i^{th} resisting element along its major and minor principal axes, respectively

Q_{xi} and Q_{yi} X and Y components of the shearing force experienced by the i^{th} resisting element

$Q_{\theta i}$ torsional moment applied at the floor level of the i^{th} shear-wall core

$\mathbf{Q}_i$ vector of forces applied to the i^{th} resisting element (equations (2.2) and (2.3))

r radius of gyration of the deck about a vertical axis passing through its center of mass

u_x and u_y lateral displacements at reference point O, along the X and Y axes, respectively

u_θ deck rotation about a vertical axis

$\tilde{u}_x$ and $\tilde{u}_y$ lateral displacements at the center of rigidity, along the X and Y axes

u_I^* and u_{II}^* lateral displacements at the center of rigidity, along principal directions I and II of the building

$\mathbf{u}$ degrees of freedom defined at O; $\mathbf{u}^T = < u_x \; u_y \; u_\theta >$

$\tilde{\mathbf{u}}$ degrees of freedom defined at the center of rigidity; $\tilde{\mathbf{u}}^T = < \tilde{u}_x \; \tilde{u}_y \; u_\theta >$

$\mathbf{u}^*$ degrees of freedom defined at the center of rigidity; $\mathbf{u}^{*T} = < u_I^* \; u_{II}^* \; u_\theta >$

v_{ai} and v_{bi} lateral displacements of the floor of the i^{th} resisting element along its major and minor principal axes, respectively

$\mathbf{v}_i$ vector of displacements of the i^{th} resisting element (equations (2.2) and (2.3))

x_i and y_i X and Y distances from O to the principal axes of the i^{th} resisting element when they are oriented along the X and Y axes

x_M and y_M X and Y coordinates of the center of mass

x_R and y_R X and Y coordinates of the center of rigidity

x_S and y_S X and Y coordinates of the shear center

x_T and y_T X and Y coordinates of the center of twist

β_i counterclockwise angle between the X axis and the major principal axis of the i^{th} resisting element

η counter-clockwise angle between the X axis and principal axis I of the system

B.2 Multi-Story Buildings

$\mathbf{a}_i$ transformation matrix of the i^{th} resisting element defined by equations (3.5) to (3.7)

$\tilde{\mathbf{a}}$ transformation matrix defined by equation (3.21)

$\mathbf{a}^*$ transformation matrix defined by equation (4.19)

$\mathbf{A}$ matrix equal to $\mathbf{K}_x - \mathbf{K}_{xy}\mathbf{K}_y^{-1}\mathbf{K}_{yx}$

$\mathbf{B}$ matrix equal to $\mathbf{K}_y - \mathbf{K}_{yx}\mathbf{K}_x^{-1}\mathbf{K}_{xy}$

C_{ai} and C_{bi} proportionality constants for the i^{th} resisting element defined by equation (4.1)

C_{xi} and C_{yi} proportionality constants defined for the i^{th} resisting element defined by equations (4.15) in case all the elemental principal planes are oriented along the X and Y axes,

C_x, C_y, C_{xy}, $C_{x\theta}$ and $C_{y\theta}$

proportionality constants defined by equations (4.3) for buildings with any orientations of elemental principal axes, and by equations (4.16) for buildings with orthogonal orientations of the elemental principal planes

C_I^* and C_{II}^* proportionality constants defined by equations (4.29a,b)

$\mathbf{C}$ diagonal matrix of dimension N with j^{th} diagonal entry equal to $\cos\eta_j$

d_{ai} and d_{bi} perpendicular distances from reference points O_j to the major and minor principal planes of the i^{th} resisting element, same for all floors

e_j static eccentricity of j^{th} floor defined as the distance between its centers of mass and rigidity

e_{xj} and e_{yj} X_j and Y_j components of static eccentricity e_j

$\mathbf{e}_x$ and $\mathbf{e}_y$ diagonal matrices of diagonal entries equal to e_{xj} and e_{yj}, respectively

$\mathbf{I}$ unit matrix

I_j and II_j major and minor principal axes of the j^{th} floor

J_{Mj}, J_{Oj} and J_{Rj}

polar moments of inertia of the j^{th} floor about vertical axes passing through its center of mass, reference point O_j, and center of rigidity, respectively

$\mathbf{J}_M$, $\mathbf{J}_O$ and $\mathbf{J}_R$ diagonal matrices of diagonal entries equal to J_{Mj}, J_{Oj}, and J_{Rj}, respectively

$\mathbf{k}_{ai}$ and $\mathbf{k}_{bi}$ lateral stiffness matrices of the i^{th} resisting element along its major and minor principal planes

$\mathbf{k}_{xi}$ and $\mathbf{k}_{yi}$ lateral stiffness matrices of the i^{th} resisting element along the X and Y directions, which are also along its principal planes

$\mathbf{k}$ characteristic matrix defined for special class buildings with any orientations of elemental principal planes, given by equation (4.1)

$\mathbf{k}_x$ and $\mathbf{k}_y$ characteristic matrices defined for a special of buildings with orthogonal orientations of elemental principal planes, given by equations (4.15)

$\mathbf{K}$ building stiffness matrix with respect to degrees of freedom $\mathbf{u}$ defined at refernce points O_j

$\tilde{\mathbf{K}}$ building stiffness matrix with respect to degrees of freedom $\tilde{\mathbf{u}}$ defined at the centers of rigidity of the building

$\mathbf{K}^*$ building stiffness matrix with respect to degrees of freedom $\mathbf{u}^*$ defined at the centers of rigidity of the building

$\mathbf{K}_i$ matrix contribution of the i^{th} resisting element $\mathbf{K}$

$\mathbf{K}_{xi}$, $\mathbf{K}_{yi}$ and $\mathbf{K}_{cyi}$ or $\mathbf{K}_{yxi}$

submatrices of $\mathbf{K}_i$ given by equations (3.8) and (3.9)

$\mathbf{K}_{x\theta i}$ or $\mathbf{K}_{\theta xi}$, $\mathbf{K}_{y\theta i}$ or $\mathbf{K}_{\theta yi}$ and $\mathbf{K}_{\theta i}$

submatrices of $\mathbf{K}_i$ given by equations (3.8) and (3.9)

$\mathbf{K}_x, \mathbf{K}_y$ and $\mathbf{K}_{xy}$ or $\mathbf{K}_{yx}$

submatrices of $\mathbf{K}$ defined by equations (3.10) and (3.11)

$\mathbf{K}_{x\theta}$ or $\mathbf{K}_{\theta x}, \mathbf{K}_{y\theta}$ or $\mathbf{K}_{\theta y}$ and $\mathbf{K}_\theta$

submatrices of $\mathbf{K}$ defined by equations (3.10) and (3.11)

$\tilde{\mathbf{K}}_x, \tilde{\mathbf{K}}_y, \tilde{\mathbf{K}}_{xy}$ or $\tilde{\mathbf{K}}_{yx}$ and $\tilde{\mathbf{K}}_\theta$

submatrices of $\tilde{\mathbf{K}}$ defined by equations (3.15), (3.24) and (3.25)

$\mathbf{K}_I^*, \mathbf{K}_{II}^*$ and $\mathbf{K}_\theta^*$

submatrices of $\mathbf{K}^*$ defined by equations (3.19), (4.29) and (4.22)

m_j mass of the j^{th} story

$\mathbf{m}$ diagonal matrix with diagonal entries equal to m_j, given by equation (3.14)

$\mathbf{M}_M$ building mass matrix defined at story centers of mass

O_j reference point of the j^{th} floor lying on vertical axis Z

N number of stories

$\tilde{\mathbf{P}}$ load vector; $\tilde{\mathbf{P}}^T = < \tilde{\mathbf{P}}_x^T \ \tilde{\mathbf{P}}_y^T \ \tilde{\mathbf{T}}_\theta^T >$

$\mathbf{P}_x'$ and $\mathbf{P}_y'$ equal to $\mathbf{S}\tilde{\mathbf{P}}_x$ and $\mathbf{S}\tilde{\mathbf{P}}_y$, respectively

$\tilde{\mathbf{P}}_x$ and $\tilde{\mathbf{P}}_y$ load vectors applied at the centers of rigidity, along X_j and Y_j reference directions, respectively

$[\tilde{\mathbf{P}}_x], [\tilde{\mathbf{P}}_y], [\mathbf{P}_x']$ and $[\mathbf{P}_y']$

diagonal matrix forms of vectors $\tilde{\mathbf{P}}_x, \tilde{\mathbf{P}}_y, \mathbf{P}_x'$ and $\mathbf{P}_y'$, respectively

$\mathbf{Q}_i$ vector of forces applied at floors of the i^{th} resisting element, given by equations (3.2) and (3.3)

$\mathbf{Q}_{ai}$ and $\mathbf{Q}_{bi}$ vectors of static lateral forces applied at the floors of the i^{th} resisting element along its major and minor principal planes, respectively

$\mathbf{Q}_{\theta i}$ vector of static torsional moments applied at the floors of the i[th] resisting element about the vertical axis of intersection of its principal planes

$\mathbf{S}$ summation matrix given by equation (3.47)

$\mathbf{S}$ diagonal matrix with diagonal entries equal to $\sin\eta_j$

$\mathbf{T}$ diagonal matrix with diagonal entries equal to $\tan\eta_j$

$\tilde{\mathbf{T}}_\theta$ vector of torsional moments applied at the centers of rigidity of the building

u_{xj} and u_{yj} lateral displacements at reference points O_j of the j[th] floor, along X_j and Y_j, respectively

$\tilde{u}_{xj}$ and $\tilde{u}_{yj}$ lateral displacements at the center of rigidity of the j[th] floor, along X_j and Y_j, respectively

u^*_{Ij} and u^*_{IIj} lateral displacements at the centers of rigidity of the j[th] floor, along its principal axes, I_j and II_j, respectively

$u_{\theta j}$ rotation of the j[th] floor about a vertical axis

$\mathbf{u}$ degrees of freedom defined at O_j; $\mathbf{u}^T = < \mathbf{u}_x^T \ \mathbf{u}_y^T \ \mathbf{u}_\theta^T >$

$\tilde{\mathbf{u}}$ degrees of freedom defined at centers of rigidity; $\tilde{\mathbf{u}}^T = < \tilde{\mathbf{u}}_x^T \ \tilde{\mathbf{u}}_y^T \ \mathbf{u}_\theta^T >$

$\mathbf{u}^*$ degrees of freedom defined at centers of rigidity; $\mathbf{u}^{*T} = < \mathbf{u}_I^{*T} \ \mathbf{u}_{II}^{*T} \ \mathbf{u}_\theta^T >$

$\mathbf{u}_x$ and $\mathbf{u}_y$ vectors of displacements u_{xj} and u_{yj}, respectively

$\tilde{\mathbf{u}}_x$ and $\tilde{\mathbf{u}}_y$ vectors of displacements $\tilde{u}_{xj}$ and $\tilde{u}_{yj}$, respectively

$\mathbf{u}^*_I$ and $\mathbf{u}^*_{II}$ vectors of displacements u^*_{Ij} and u^*_{IIj}, respectively

$\mathbf{u}_\theta$ vector of rotations $u_{\theta j}$

$[\mathbf{u}_\theta]$ diagonal matrix form of vector $\mathbf{u}_\theta$

$\mathbf{v}_i$ displacements vector of the i[th] resisting element, given by equations (3.2) and (3.3)

$\mathbf{V}_{ai}$ and $\mathbf{V}_{bi}$ interstory shear forces of the i^{th} resisting element along its major and minor principal planes, respectively

$\mathbf{V}_{xi}$ and $\mathbf{V}_{yi}$ vectors of the X and Y components of interstory shear forces experienced by the i^{th} resisting element

X_j and Y_j reference axes of the j^{th} floor, same direction for all floors

x_{Mj}, x_{Rj}, x_{Sj} and x_{Tj}

X_j- coordinates of the center of mass, center of rigidity, shear center and center of twist of the j^{th} floor

y_{Mj}, y_{Rj}, y_{Sj} and y_{Tj}

Y_j- coordinates of the center of mass, center of rigidity, shear center and center of twist of the j^{th} floor

$\mathbf{x}_M, \mathbf{x}_R, \mathbf{x}_S$ and $\mathbf{x}_T$

diagonal matrices of x_{Mj}, x_{Rj}, x_{Sj} and x_{Tj}, respectively

$\mathbf{y}_M, \mathbf{y}_R, \mathbf{y}_S$ and $\mathbf{y}_T$

diagonal matrices of y_{Mj}, y_{Rj}, y_{Sj} and y_{Tj}, respectively

$\{\mathbf{x}_R\}, \{\mathbf{x}_S\}$ and $\{\mathbf{x}_T\}$

vector forms of diagonal matrices $\mathbf{x}_R$, $\mathbf{x}_S$ and $\mathbf{x}_T$, respectively

$\{\mathbf{y}_R\}, \{\mathbf{y}_S\}$ and $\{\mathbf{y}_T\}$

vector forms of diagonal matrices $\mathbf{y}_R$, $\mathbf{y}_S$ and $\mathbf{y}_T$, respectively

$\mathbf{0}$ zero matrix

β_i counterclockwise angle between X_j and the major principal plane of the i^{th} resisting element, same for all floors

η_j counterclockwise angle between X_j and I_j of the j^{th} floor

1	vector of ones of dimension N

EARTHQUAKE ENGINEERING RESEARCH CENTER REPORT SERIES

EERC reports are available from the National Information Service for Earthquake Engineering(NISEE) and from the National Technical Information Service(NTIS). Numbers in parentheses are Accession Numbers assigned by the National Technical Information Service; these are followed by a price code. Contact NTIS, 5285 Port Royal Road, Springfield Virginia, 22161 for more information. Reports without Accession Numbers were not available from NTIS at the time of printing. For a current complete list of EERC reports (from EERC 67-1) and availability information, please contact University of California, EERC, NISEE, 1301 South 46th Street, Richmond, California 94804.

UCB/EERC-80/01 "Earthquake Response of Concrete Gravity Dams Including Hydrodynamic and Foundation Interaction Effects," by Chopra, A.K., Chakrabarti, P. and Gupta, S., January 1980, (AD-A087297)A10.

UCB/EERC-80/02 "Rocking Response of Rigid Blocks to Earthquakes," by Yim, C.S., Chopra, A.K. and Penzien, J., January 1980, (PB80 166 002)A04.

UCB/EERC-80/03 "Optimum Inelastic Design of Seismic-Resistant Reinforced Concrete Frame Structures," by Zagajeski, S.W. and Bertero, V.V., January 1980, (PB80 164 635)A06.

UCB/EERC-80/04 "Effects of Amount and Arrangement of Wall-Panel Reinforcement on Hysteretic Behavior of Reinforced Concrete Walls," by Iliya, R. and Bertero, V.V., February 1980, (PB81 122 525)A09.

UCB/EERC-80/05 "Shaking Table Research on Concrete Dam Models," by Niwa, A. and Clough, R.W., September 1980, (PB81 122 368)A06.

UCB/EERC-80/06 "The Design of Steel Energy-Absorbing Restrainers and their Incorporation into Nuclear Power Plants for Enhanced Safety (Vol 1a): Piping with Energy Absorbing Restrainers: Parameter Study on Small Systems," by Powell, G.H., Oughourlian, C. and Simons, J., June 1980.

UCB/EERC-80/07 "Inelastic Torsional Response of Structures Subjected to Earthquake Ground Motions," by Yamazaki, Y., April 1980, (PB81 122 327)A08.

UCB/EERC-80/08 "Study of X-Braced Steel Frame Structures under Earthquake Simulation," by Ghanaat, Y., April 1980, (PB81 122 335)A11.

UCB/EERC-80/09 "Hybrid Modelling of Soil-Structure Interaction," by Gupta, S., Lin, T.W. and Penzien, J., May 1980, (PB81 122 319)A07.

UCB/EERC-80/10 "General Applicability of a Nonlinear Model of a One Story Steel Frame," by Sveinsson, B.I. and McNiven, H.D., May 1980, (PB81 124 877)A06.

UCB/EERC-80/11 "A Green-Function Method for Wave Interaction with a Submerged Body," by Kioka, W., April 1980, (PB81 122 269)A07.

UCB/EERC-80/12 "Hydrodynamic Pressure and Added Mass for Axisymmetric Bodies," by Nilrat, F., May 1980, (PB81 122 343)A08.

UCB/EERC-80/13 "Treatment of Non-Linear Drag Forces Acting on Offshore Platforms," by Dao, B.V. and Penzien, J., May 1980, (PB81 153 413)A07.

UCB/EERC-80/14 "2D Plane/Axisymmetric Solid Element (Type 3-Elastic or Elastic-Perfectly Plastic)for the ANSR-II Program," by Mondkar, D.P. and Powell, G.H., July 1980, (PB81 122 350)A03.

UCB/EERC-80/15 "A Response Spectrum Method for Random Vibrations," by Der Kiureghian, A., June 1981, (PB81 122 301)A03.

UCB/EERC-80/16 "Cyclic Inelastic Buckling of Tubular Steel Braces," by Zayas, V.A., Popov, E.P. and Martin, S.A., June 1981, (PB81 124 885)A10.

UCB/EERC-80/17 "Dynamic Response of Simple Arch Dams Including Hydrodynamic Interaction," by Porter, C.S. and Chopra, A.K., July 1981, (PB81 124 000)A13.

UCB/EERC-80/18 "Experimental Testing of a Friction Damped Aseismic Base Isolation System with Fail-Safe Characteristics," by Kelly, J.M., Beucke, K.E. and Skinner, M.S., July 1980, (PB81 148 595)A04.

UCB/EERC-80/19 "The Design of Steel Energy-Absorbing Restrainers and their Incorporation into Nuclear Power Plants for Enhanced Safety (Vol.1B): Stochastic Seismic Analyses of Nuclear Power Plant Structures and Piping Systems Subjected to Multiple Supported Excitations," by Lee, M.C. and Penzien, J., June 1980, (PB82 201 872)A08.

UCB/EERC-80/20 "The Design of Steel Energy-Absorbing Restrainers and their Incorporation into Nuclear Power Plants for Enhanced Safety (Vol 1C): Numerical Method for Dynamic Substructure Analysis," by Dickens, J.M. and Wilson, E.L., June 1980.

UCB/EERC-80/21 "The Design of Steel Energy-Absorbing Restrainers and their Incorporation into Nuclear Power Plants for Enhanced Safety (Vol 2): Development and Testing of Restraints for Nuclear Piping Systems," by Kelly, J.M. and Skinner, M.S., June 1980.

UCB/EERC-80/22 "3D Solid Element (Type 4-Elastic or Elastic-Perfectly-Plastic) for the ANSR-II Program," by Mondkar, D.P. and Powell, G.H., July 1980, (PB81 123 242)A03.

UCB/EERC-80/23 "Gap-Friction Element (Type 5) for the Ansr-II Program," by Mondkar, D.P. and Powell, G.H., July 1980, (PB81 122 285)A03.

UCB/EERC-80/24 "U-Bar Restraint Element (Type 11) for the ANSR-II Program," by Oughourlian, C. and Powell, G.H., July 1980, (PB81 122 293)A03.

UCB/EERC-80/25 "Testing of a Natural Rubber Base Isolation System by an Explosively Simulated Earthquake," by Kelly, J.M., August 1980, (PB81 201 360)A04.

UCB/EERC-80/26 "Input Identification from Structural Vibrational Response," by Hu, Y., August 1980, (PB81 152 308)A05.

UCB/EERC-80/27 "Cyclic Inelastic Behavior of Steel Offshore Structures," by Zayas, V.A., Mahin, S.A. and Popov, E.P., August 1980, (PB81 196 180)A15.

UCB/EERC-80/28 "Shaking Table Testing of a Reinforced Concrete Frame with Biaxial Response," by Oliva, M.G., October 1980, (PB81 154 304)A10.

UCB/EERC-80/29 "Dynamic Properties of a Twelve-Story Prefabricated Panel Building," by Bouwkamp, J.G., Kollegger, J.P. and Stephen, R.M., October 1980, (PB82 138 777)A07.

UCB/EERC-80/30 "Dynamic Properties of an Eight-Story Prefabricated Panel Building," by Bouwkamp, J.G., Kollegger, J.P. and Stephen, R.M., October 1980, (PB81 200 313)A05.

UCB/EERC-80/31 "Predictive Dynamic Response of Panel Type Structures under Earthquakes," by Kollegger, J.P. and Bouwkamp, J.G., October 1980, (PB81 152 316)A04.

UCB/EERC-80/32 "The Design of Steel Energy-Absorbing Restrainers and their Incorporation into Nuclear Power Plants for Enhanced Safety (Vol 3): Testing of Commercial Steels in Low-Cycle Torsional Fatigue," by Spanner, P., Parker, E.R., Jongewaard, E. and Dory, M., 1980.

UCB/EERC-80/33 "The Design of Steel Energy-Absorbing Restrainers and their Incorporation into Nuclear Power Plants for Enhanced Safety (Vol 4): Shaking Table Tests of Piping Systems with Energy-Absorbing Restrainers." by Stiemer, S.F. and Godden, W.G., September 1980. (PB82 201 880)A05.

UCB/EERC-80/34 "The Design of Steel Energy-Absorbing Restrainers and their Incorporation into Nuclear Power Plants for Enhanced Safety (Vol 5): Summary Report." by Spencer, P., 1980.

UCB/EERC-80/35 "Experimental Testing of an Energy-Absorbing Base Isolation System." by Kelly, J.M., Skinner, M.S. and Beucke, K.E., October 1980. (PB81 154 072)A04.

UCB/EERC-80/36 "Simulating and Analyzing Artificial Non-Stationary Earth Ground Motions." by Nau, R.F., Oliver, R.M. and Pister, K.S., October 1980. (PB81 153 397)A04.

UCB/EERC-80/37 "Earthquake Engineering at Berkeley - 1980." by , September 1980. (PB81 205 674)A09.

UCB/EERC-80/38 "Inelastic Seismic Analysis of Large Panel Buildings." by Schricker, V. and Powell, G.H., September 1980. (PB81 154 338)A13.

UCB/EERC-80/39 "Dynamic Response of Embankment, Concrete-Gavity and Arch Dams Including Hydrodynamic Interation." by Hall, J.F. and Chopra, A.K., October 1980. (PB81 152 324)A11.

UCB/EERC-80/40 "Inelastic Buckling of Steel Struts under Cyclic Load Reversal." by Black, R.G., Wenger, W.A. and Popov, E.P., October 1980. (PB81 154 312)A08.

UCB/EERC-80/41 "Influence of Site Characteristics on Buildings Damage during the October 3,1974 Lima Earthquake." by Repetto, P., Arango, I. and Seed, H.B., September 1980. (PB81 161 739)A05.

UCB/EERC-80/42 "Evaluation of a Shaking Table Test Program on Response Behavior of a Two Story Reinforced Concrete Frame." by Blondet, J.M., Clough, R.W. and Mahin, S.A., December 1980. (PB82 196 544)A11.

UCB/EERC-80/43 "Modelling of Soil-Structure Interaction by Finite and Infinite Elements." by Medina, F., December 1980. (PB81 229 270)A04.

UCB/EERC-81/01 "Control of Seismic Response of Piping Systems and Other Structures by Base Isolation." by Kelly, J.M., January 1981. (PB81 200 735)A05.

UCB/EERC-81/02 "OPTNSR- An Interactive Software System for Optimal Design of Statically and Dynamically Loaded Structures with Nonlinear Response." by Bhatti, M.A., Ciampi, V. and Pister, K.S., January 1981. (PB81 218 851)A09.

UCB/EERC-81/03 "Analysis of Local Variations in Free Field Seismic Ground Motions." by Chen, J.-C., Lysmer, J. and Seed, H.B., January 1981. (AD-A099508)A13.

UCB/EERC-81/04 "Inelastic Structural Modeling of Braced Offshore Platforms for Seismic Loading." by Zayas, V.A., Shing, P.-S.B., Mahin, S.A. and Popov, E.P., January 1981. (PB82 138 777)A07.

UCB/EERC-81/05 "Dynamic Response of Light Equipment in Structures." by Der Kiureghian, A., Sackman, J.L. and Nour-Omid, B., April 1981. (PB81 218 497)A04.

UCB/EERC-81/06 "Preliminary Experimental Investigation of a Broad Base Liquid Storage Tank." by Bouwkamp, J.G., Kollegger, J.P. and Stephen, R.M., May 1981. (PB82 140 385)A03.

UCB/EERC-81/07 "The Seismic Resistant Design of Reinforced Concrete Coupled Structural Walls." by Aktan, A.E. and Bertero, V.V., June 1981. (PB82 113 358)A11.

UCB/EERC-81/08 "Unassigned." by Unassigned, 1981.

UCB/EERC-81/09 "Experimental Behavior of a Spatial Piping System with Steel Energy Absorbers Subjected to a Simulated Differential Seismic Input." by Stiemer, S.F., Godden, W.G. and Kelly, J.M., July 1981. (PB82 201 898)A04.

UCB/EERC-81/10 "Evaluation of Seismic Design Provisions for Masonry in the United States." by Sveinsson, B.I., Mayes, R.L. and McNiven, H.D., August 1981. (PB82 166 075)A08.

UCB/EERC-81/11 "Two-Dimensional Hybrid Modelling of Soil-Structure Interaction." by Tzong, T.-J., Gupta, S. and Penzien, J., August 1981. (PB82 142 118)A04.

UCB/EERC-81/12 "Studies on Effects of Infills in Seismic Resistant R/C Construction." by Brokken, S. and Bertero, V.V., October 1981. (PB82 166 190)A09.

UCB/EERC-81/13 "Linear Models to Predict the Nonlinear Seismic Behavior of a One-Story Steel Frame." by Valdimarsson, H., Shah, A.H. and McNiven, H.D., September 1981. (PB82 138 793)A07.

UCB/EERC-81/14 "TLUSH: A Computer Program for the Three-Dimensional Dynamic Analysis of Earth Dams." by Kagawa, T., Mejia, L.H., Seed, H.B. and Lysmer, J., September 1981. (PB82 139 940)A06.

UCB/EERC-81/15 "Three Dimensional Dynamic Response Analysis of Earth Dams." by Mejia, L.H. and Seed, H.B., September 1981. (PB82 137 274)A12.

UCB/EERC-81/16 "Experimental Study of Lead and Elastomeric Dampers for Base Isolation Systems." by Kelly, J.M. and Hodder, S.B., October 1981. (PB82 166 182)A05.

UCB/EERC-81/17 "The Influence of Base Isolation on the Seismic Response of Light Secondary Equipment." by Kelly, J.M., April 1981. (PB82 255 266)A04.

UCB/EERC-81/18 "Studies on Evaluation of Shaking Table Response Analysis Procedures." by Blondet, J. M., November 1981. (PB82 197 278)A10.

UCB/EERC-81/19 "DELIGHT.STRUCT: A Computer-Aided Design Environment for Structural Engineering." by Balling, R.J., Pister, K.S. and Polak, E., December 1981. (PB82 218 496)A07.

UCB/EERC-81/20 "Optimal Design of Seismic-Resistant Planar Steel Frames." by Balling, R.J., Ciampi, V. and Pister, K.S., December 1981. (PB82 220 179)A07.

UCB/EERC-82/01 "Dynamic Behavior of Ground for Seismic Analysis of Lifeline Systems." by Sato, T. and Der Kiureghian, A., January 1982. (PB82 218 926)A05.

UCB/EERC-82/02 "Shaking Table Tests of a Tubular Steel Frame Model." by Ghanaat, Y. and Clough, R.W., January 1982. (PB82 220 161)A07.

UCB/EERC-82/03 "Behavior of a Piping System under Seismic Excitation: Experimental Investigations of a Spatial Piping System supported by Mechanical Shock Arrestors," by Schneider, S., Lee, H.-M. and Godden, W. G., May 1982, (PB83 172 544)A09.

UCB/EERC-82/04 "New Approaches for the Dynamic Analysis of Large Structural Systems," by Wilson, E.L., June 1982, (PB83 148 080)A05.

UCB/EERC-82/05 "Model Study of Effects of Damage on the Vibration Properties of Steel Offshore Platforms," by Shahrivar, F. and Bouwkamp, J.G., June 1982, (PB83 148 742)A10.

UCB/EERC-82/06 "States of the Art and Pratice in the Optimum Seismic Design and Analytical Response Prediction of R/C Frame Wall Structures," by Aktan, A.E. and Bertero, V.V., July 1982, (PB83 147 736)A05.

UCB/EERC-82/07 "Further Study of the Earthquake Response of a Broad Cylindrical Liquid-Storage Tank Model," by Manos, G.C. and Clough, R.W., July 1982, (PB83 147 744)A11.

UCB/EERC-82/08 "An Evaluation of the Design and Analytical Seismic Response of a Seven Story Reinforced Concrete Frame," by Charney, F.A. and Bertero, V.V., July 1982, (PB83 157 628)A09.

UCB/EERC-82/09 "Fluid-Structure Interactions: Added Mass Computations for Incompressible Fluid," by Kuo, J.S.-H., August 1982, (PB83 156 281)A07.

UCB/EERC-82/10 "Joint-Opening Nonlinear Mechanism: Interface Smeared Crack Model," by Kuo, J.S.-H., August 1982, (PB83 149 195)A05.

UCB/EERC-82/11 "Dynamic Response Analysis of Techi Dam," by Clough, R.W., Stephen, R.M. and Kuo, J.S.-H., August 1982, (PB83 147 496)A06.

UCB/EERC-82/12 "Prediction of the Seismic Response of R/C Frame-Coupled Wall Structures," by Aktan, A.E., Bertero, V.V. and Piazzo, M., August 1982, (PB83 149 203)A09.

UCB/EERC-82/13 "Preliminary Report on the Smart 1 Strong Motion Array in Taiwan," by Bolt, B.A., Loh, C.H., Penzien, J. and Tsai, Y.B., August 1982, (PB83 159 400)A10.

UCB/EERC-82/14 "Shaking-Table Studies of an Eccentrically X-Braced Steel Structure," by Yang, M.S., September 1982, (PB83 260 778)A12.

UCB/EERC-82/15 "The Performance of Stairways in Earthquakes," by Roha, C., Axley, J.W. and Bertero, V.V., September 1982, (PB83 157 693)A07.

UCB/EERC-82/16 "The Behavior of Submerged Multiple Bodies in Earthquakes," by Liao, W.-G., September 1982, (PB83 158 709)A07.

UCB/EERC-82/17 "Effects of Concrete Types and Loading Conditions on Local Bond-Slip Relationships," by Cowell, A.D., Popov, E.P. and Bertero, V.V., September 1982, (PB83 153 577)A04.

UCB/EERC-82/18 "Mechanical Behavior of Shear Wall Vertical Boundary Members: An Experimental Investigation," by Wagner, M.T. and Bertero, V.V., October 1982, (PB83 159 764)A05.

UCB/EERC-82/19 "Experimental Studies of Multi-support Seismic Loading on Piping Systems," by Kelly, J.M. and Cowell, A.D., November 1982.

UCB/EERC-82/20 "Generalized Plastic Hinge Concepts for 3D Beam-Column Elements," by Chen, P. F.-S. and Powell, G.H., November 1982, (PB83 247 981)A13.

UCB/EERC-82/21 "ANSR-II: General Computer Program for Nonlinear Structural Analysis," by Oughourlian, C.V. and Powell, G.H., November 1982, (PB83 251 330)A12.

UCB/EERC-82/22 "Solution Strategies for Statically Loaded Nonlinear Structures," by Simons, J.W. and Powell, G.H., November 1982, (PB83 197 970)A06.

UCB/EERC-82/23 "Analytical Model of Deformed Bar Anchorages under Generalized Excitations," by Ciampi, V., Eligehausen, R., Bertero, V.V. and Popov, E.P., November 1982, (PB83 169 532)A06.

UCB/EERC-82/24 "A Mathematical Model for the Response of Masonry Walls to Dynamic Excitations," by Sucuoglu, H., Mengi, Y. and McNiven, H.D., November 1982, (PB83 169 011)A07.

UCB/EERC-82/25 "Earthquake Response Considerations of Broad Liquid Storage Tanks," by Cambra, F.J., November 1982, (PB83 251 215)A09.

UCB/EERC-82/26 "Computational Models for Cyclic Plasticity, Rate Dependence and Creep," by Mosaddad, B. and Powell, G.H., November 1982, (PB83 245 829)A08.

UCB/EERC-82/27 "Inelastic Analysis of Piping and Tubular Structures," by Mahasuverachai, M. and Powell, G.H., November 1982, (PB83 249 987)A07.

UCB/EERC-83/01 "The Economic Feasibility of Seismic Rehabilitation of Buildings by Base Isolation," by Kelly, J.M., January 1983, (PB83 197 988)A05.

UCB/EERC-83/02 "Seismic Moment Connections for Moment-Resisting Steel Frames," by Popov, E.P., January 1983, (PB83 195 412)A04.

UCB/EERC-83/03 "Design of Links and Beam-to-Column Connections for Eccentrically Braced Steel Frames," by Popov, E.P. and Malley, J.O., January 1983, (PB83 194 811)A04.

UCB/EERC-83/04 "Numerical Techniques for the Evaluation of Soil-Structure Interaction Effects in the Time Domain," by Bayo, E. and Wilson, E.L., February 1983, (PB83 245 605)A09.

UCB/EERC-83/05 "A Transducer for Measuring the Internal Forces in the Columns of a Frame-Wall Reinforced Concrete Structure," by Sause, R. and Bertero, V.V., May 1983, (PB84 119 494)A06.

UCB/EERC-83/06 "Dynamic Interactions Between Floating Ice and Offshore Structures," by Croteau, P., May 1983, (PB84 119 486)A16.

UCB/EERC-83/07 "Dynamic Analysis of Multiply Tuned and Arbitrarily Supported Secondary Systems," by Igusa, T. and Der Kiureghian, A., July 1983, (PB84 118 272)A11.

UCB/EERC-83/08 "A Laboratory Study of Submerged Multi-body Systems in Earthquakes," by Ansari, G.R., June 1983, (PB83 261 842)A17.

UCB/EERC-83/09 "Effects of Transient Foundation Uplift on Earthquake Response of Structures," by Yim, C.-S. and Chopra, A.K., June 1983, (PB83 261 396)A07.

UCB/EERC-83/10 "Optimal Design of Friction-Braced Frames under Seismic Loading," by Austin, M.A. and Pister, K.S., June 1983, (PB84 119 288)A06.

UCB/EERC-83/11 "Shaking Table Study of Single-Story Masonry Houses: Dynamic Performance under Three Component Seismic Input and Recommendations," by Manos, G.C., Clough, R.W. and Mayes, R.L., July 1983, (UCB/EERC-83/11)A08.

UCB/EERC-83/12 "Experimental Error Propagation in Pseudodynamic Testing," by Shiing, P.B. and Mahin, S.A., June 1983, (PB84 119 270)A09.

UCB/EERC-83/13 "Experimental and Analytical Predictions of the Mechanical Characteristics of a 1/5-scale Model of a 7-story R/C Frame-Wall Building Structure," by Aktan, A.E., Bertero, V.V., Chowdhury, A.A. and Nagashima, T., June 1983, (PB84 119 213)A07.

UCB/EERC-83/14 "Shaking Table Tests of Large-Panel Precast Concrete Building System Assemblages," by Oliva, M.G. and Clough, R.W., June 1983, (PB86 110 210/AS)A11.

UCB/EERC-83/15 "Seismic Behavior of Active Beam Links in Eccentrically Braced Frames," by Hjelmstad, K.D. and Popov, E.P., July 1983, (PB84 119 676)A09.

UCB/EERC-83/16 "System Identification of Structures with Joint Rotation," by Dimsdale, J.S., July 1983, (PB84 192 210)A06.

UCB/EERC-83/17 "Construction of Inelastic Response Spectra for Single-Degree-of-Freedom Systems," by Mahin, S. and Lin, J., June 1983, (PB84 208 834)A05.

UCB/EERC-83/18 "Interactive Computer Analysis Methods for Predicting the Inelastic Cyclic Behaviour of Structural Sections," by Kaba, S. and Mahin, S., July 1983, (PB84 192 012)A06.

UCB/EERC-83/19 "Effects of Bond Deterioration on Hysteretic Behavior of Reinforced Concrete Joints," by Filippou, F.C., Popov, E.P. and Bertero, V.V., August 1983, (PB84 192 020)A10.

UCB/EERC-83/20 "Analytical and Experimental Correlation of Large-Panel Precast Building System Performance," by Oliva, M.G., Clough, R.W., Velkov, M. and Gavrilovic, P., November 1983.

UCB/EERC-83/21 "Mechanical Characteristics of Materials Used in a 1/5 Scale Model of a 7-Story Reinforced Concrete Test Structure," by Bertero, V.V., Aktan, A.E., Harris, H.G. and Chowdhury, A.A., October 1983, (PB84 193 697)A05.

UCB/EERC-83/22 "Hybrid Modelling of Soil-Structure Interaction in Layered Media," by Tzong, T.-J. and Penzien, J., October 1983, (PB84 192 178)A08.

UCB/EERC-83/23 "Local Bond Stress-Slip Relationships of Deformed Bars under Generalized Excitations," by Eligehausen, R., Popov, E.P. and Bertero, V.V., October 1983, (PB84 192 848)A09.

UCB/EERC-83/24 "Design Considerations for Shear Links in Eccentrically Braced Frames," by Malley, J.O. and Popov, E.P., November 1983, (PB84 192 186)A07.

UCB/EERC-84/01 "Pseudodynamic Test Method for Seismic Performance Evaluation: Theory and Implementation," by Shing, P.-S.B. and Mahin, S.A., January 1984, (PB84 190 644)A08.

UCB/EERC-84/02 "Dynamic Response Behavior of Kiang Hong Dian Dam," by Clough, R.W., Chang, K.-T., Chen, H.-Q. and Stephen, R.M., April 1984, (PB84 209 402)A08.

UCB/EERC-84/03 "Refined Modelling of Reinforced Concrete Columns for Seismic Analysis," by Kaba, S.A. and Mahin, S.A., April 1984, (PB84 234 384)A06.

UCB/EERC-84/04 "A New Floor Response Spectrum Method for Seismic Analysis of Multiply Supported Secondary Systems," by Asfura, A. and Der Kiureghian, A., June 1984, (PB84 239 417)A06.

UCB/EERC-84/05 "Earthquake Simulation Tests and Associated Studies of a 1/5th-scale Model of a 7-Story R/C Frame-Wall Test Structure," by Bertero, V.V., Aktan, A.E., Charney, F.A. and Sause, R., June 1984, (PB84 239 409)A09.

UCB/EERC-84/06 "R/C Structural Walls: Seismic Design for Shear," by Aktan, A.E. and Bertero, V.V., 1984.

UCB/EERC-84/07 "Behavior of Interior and Exterior Flat-Plate Connections subjected to Inelastic Load Reversals," by Zee, H.L. and Moehle, J.P., August 1984, (PB86 117 629/AS)A07.

UCB/EERC-84/08 "Experimental Study of the Seismic Behavior of a Two-Story Flat-Plate Structure," by Moehle, J.P. and Diebold, J.W., August 1984, (PB86 122 553/AS)A12.

UCB/EERC-84/09 "Phenomenological Modeling of Steel Braces under Cyclic Loading," by Ikeda, K., Mahin, S.A. and Dermitzakis, S.N., May 1984, (PB86 132 198/AS)A08.

UCB/EERC-84/10 "Earthquake Analysis and Response of Concrete Gravity Dams," by Fenves, G. and Chopra, A.K., August 1984, (PB85 193 902/AS)A11.

UCB/EERC-84/11 "EAGD-84: A Computer Program for Earthquake Analysis of Concrete Gravity Dams," by Fenves, G. and Chopra, A.K., August 1984, (PB85 193 613/AS)A05.

UCB/EERC-84/12 "A Refined Physical Theory Model for Predicting the Seismic Behavior of Braced Steel Frames," by Ikeda, K. and Mahin, S.A., July 1984, (PB85 191 450/AS)A09.

UCB/EERC-84/13 "Earthquake Engineering Research at Berkeley - 1984," by , August 1984, (PB85 197 341/AS)A10.

UCB/EERC-84/14 "Moduli and Damping Factors for Dynamic Analyses of Cohesionless Soils," by Seed, H.B., Wong, R.T., Idriss, I.M. and Tokimatsu, K., September 1984, (PB85 191 468/AS)A04.

UCB/EERC-84/15 "The Influence of SPT Procedures in Soil Liquefaction Resistance Evaluations," by Seed, H.B., Tokimatsu, K., Harder, L.F. and Chung, R.M., October 1984, (PB85 191 732/AS)A04.

UCB/EERC-84/16 "Simplified Procedures for the Evaluation of Settlements in Sands Due to Earthquake Shaking," by Tokimatsu, K. and Seed, H.B., October 1984, (PB85 197 887/AS)A03.

UCB/EERC-84/17 "Evaluation of Energy Absorption Characteristics of Bridges under Seismic Conditions," by Imbsen, R.A. and Penzien, J., November 1984.

UCB/EERC-84/18 "Structure-Foundation Interactions under Dynamic Loads," by Liu, W.D. and Penzien, J., November 1984, (PB87 124 889/AS)A11.

UCB/EERC-84/19 "Seismic Modelling of Deep Foundations," by Chen, C.-H. and Penzien, J., November 1984, (PB87 124 798/AS)A07.

UCB/EERC-84/20 "Dynamic Response Behavior of Quan Shui Dam," by Clough, R.W., Chang, K.-T., Chen, H.-Q., Stephen, R.M., Ghanaat, Y. and Qi, J.-H., November 1984, (PB86 115177/AS)A07.

UCB/EERC-85/01 "Simplified Methods of Analysis for Earthquake Resistant Design of Buildings," by Cruz, E.F. and Chopra, A.K., February 1985, (PB86 112299/AS)A12.

UCB/EERC-85/02 "Estimation of Seismic Wave Coherency and Rupture Velocity using the SMART 1 Strong-Motion Array Recordings," by Abrahamson, N.A., March 1985, (PB86 214 343)A07.

UCB/EERC-85/03 "Dynamic Properties of a Thirty Story Condominium Tower Building," by Stephen, R.M., Wilson, E.L. and Stander, N., April 1985, (PB86 118965/AS)A06.

UCB/EERC-85/04 "Development of Substructuring Techniques for On-Line Computer Controlled Seismic Performance Testing," by Dermitzakis, S. and Mahin, S., February 1985, (PB86 132941/AS)A08.

UCB/EERC-85/05 "A Simple Model for Reinforcing Bar Anchorages under Cyclic Excitations," by Filippou, F.C., March 1985, (PB86 112 919/AS)A05.

UCB/EERC-85/06 "Racking Behavior of Wood-framed Gypsum Panels under Dynamic Load," by Oliva, M.G., June 1985.

UCB/EERC-85/07 "Earthquake Analysis and Response of Concrete Arch Dams," by Fok, K.-L. and Chopra, A.K., June 1985, (PB86 139672/AS)A10.

UCB/EERC-85/08 "Effect of Inelastic Behavior on the Analysis and Design of Earthquake Resistant Structures," by Lin, J.P. and Mahin, S.A., June 1985, (PB86 135340/AS)A08.

UCB/EERC-85/09 "Earthquake Simulator Testing of a Base-Isolated Bridge Deck," by Kelly, J.M., Buckle, I.G. and Tsai, H.-C., January 1986, (PB87 124 152/AS)A06.

UCB/EERC-85/10 "Simplified Analysis for Earthquake Resistant Design of Concrete Gravity Dams," by Fenves, G. and Chopra, A.K., June 1986, (PB87 124 160/AS)A08.

UCB/EERC-85/11 "Dynamic Interaction Effects in Arch Dams," by Clough, R.W., Chang, K.-T., Chen, H.-Q. and Ghanaat, Y., October 1985, (PB86 135027/AS)A05.

UCB/EERC-85/12 "Dynamic Response of Long Valley Dam in the Mammoth Lake Earthquake Series of May 25-27, 1980," by Lai, S. and Seed, H.B., November 1985, (PB86 142304/AS)A05.

UCB/EERC-85/13 "A Methodology for Computer-Aided Design of Earthquake-Resistant Steel Structures," by Austin, M.A., Pister, K.S. and Mahin, S.A., December 1985, (PB86 159480/AS)A10.

UCB/EERC-85/14 "Response of Tension-Leg Platforms to Vertical Seismic Excitations," by Liou, G.-S., Penzien, J. and Yeung, R.W., December 1985, (PB87 124 871/AS)A08.

UCB/EERC-85/15 "Cyclic Loading Tests of Masonry Single Piers: Volume 4 - Additional Tests with Height to Width Ratio of 1," by Sveinsson, B., McNiven, H.D. and Sucuoglu, H., December 1985.

UCB/EERC-85/16 "An Experimental Program for Studying the Dynamic Response of a Steel Frame with a Variety of Infill Partitions," by Yanev, B. and McNiven, H.D., December 1985.

UCB/EERC-86/01 "A Study of Seismically Resistant Eccentrically Braced Steel Frame Systems," by Kasai, K. and Popov, E.P., January 1986, (PB87 124 178/AS)A14.

UCB/EERC-86/02 "Design Problems in Soil Liquefaction," by Seed, H.B., February 1986, (PB87 124 186/AS)A03.

UCB/EERC-86/03 "Implications of Recent Earthquakes and Research on Earthquake-Resistant Design and Construction of Buildings," by Bertero, V.V., March 1986, (PB87 124 194/AS)A05.

UCB/EERC-86/04 "The Use of Load Dependent Vectors for Dynamic and Earthquake Analyses," by Leger, P., Wilson, E.L. and Clough, R.W., March 1986, (PB87 124 202/AS)A12.

UCB/EERC-86/05 "Two Beam-To-Column Web Connections," by Tsai, K.-C. and Popov, E.P., April 1986, (PB87 124 301/AS)A04.

UCB/EERC-86/06 "Determination of Penetration Resistance for Coarse-Grained Soils using the Becker Hammer Drill," by Harder, L.F. and Seed, H.B., May 1986, (PB87 124 210/AS)A07.

UCB/EERC-86/07 "A Mathematical Model for Predicting the Nonlinear Response of Unreinforced Masonry Walls to In-Plane Earthquake Excitations," by Mengi, Y. and McNiven, H.D., May 1986, (PB87 124 780/AS)A06.

UCB/EERC-86/08 "The 19 September 1985 Mexico Earthquake: Building Behavior," by Bertero, V.V., July 1986.

UCB/EERC-86/09 "EACD-3D: A Computer Program for Three-Dimensional Earthquake Analysis of Concrete Dams," by Fok, K.-L., Hall, J.F. and Chopra, A.K., July 1986, (PB87 124 228/AS)A08.

UCB/EERC-86/10 "Earthquake Simulation Tests and Associated Studies of a 0.3-Scale Model of a Six-Story Concentrically Braced Steel Structure," by Uang, C.-M. and Bertero, V.V., December 1986, (PB87 163 564/AS)A17.

UCB/EERC-86/11 "Mechanical Characteristics of Base Isolation Bearings for a Bridge Deck Model Test," by Kelly, J.M., Buckle, I.G. and Koh, C.-G., 1987.

UCB/EERC-86/12 "Effects of Axial Load on Elastomeric Isolation Bearings," by Koh, C.-G. and Kelly, J.M., 1987.

UCB/EERC-87/01 "The FPS Earthquake Resisting System: Experimental Report," by Zayas, V.A., Low, S.S. and Mahin, S.A., June 1987.

UCB/EERC-87/02 "Earthquake Simulator Tests and Associated Studies of a 0.3-Scale Model of a Six-Story Eccentrically Braced Steel Structure," by Whittaker, A., Uang, C.-M. and Bertero, V.V., July 1987.

UCB/EERC-87/03 "A Displacement Control and Uplift Restraint Device for Base-Isolated Structures," by Kelly, J.M., Griffith, M.C. and Aiken, I.G., April 1987.

UCB/EERC-87/04 "Earthquake Simulator Testing of a Combined Sliding Bearing and Rubber Bearing Isolation System," by Kelly, J.M. and Chalhoub, M.S., 1987.

UCB/EERC-87/05 "Three-Dimensional Inelastic Analysis of Reinforced Concrete Frame-Wall Structures," by Moazzami, S. and Bertero, V.V., May 1987.

UCB/EERC-87/06 "Experiments on Eccentrically Braced Frames with Composite Floors," by Ricles, J. and Popov, E., June 1987.

UCB/EERC-87/07 "Dynamic Analysis of Seismically Resistant Eccentrically Braced Frames," by Ricles, J. and Popov, E., June 1987.

UCB/EERC-87/08 "Undrained Cyclic Triaxial Testing of Gravels-The Effect of Membrane Compliance," by Evans, M.D. and Seed, H.B., July 1987.

UCB/EERC-87/09 "Hybrid Solution Techniques for Generalized Pseudo-Dynamic Testing," by Thewalt, C. and Mahin, S.A., July 1987.

UCB/EERC-87/10 "Investigation of Ultimate Behavior of AISC Group 4 and 5 Heavy Steel Rolled-Section Splices with Full and Partial Penetration Butt Welds," by Bruneau, M. and Mahin, S.A., July 1987.

UCB/EERC-87/11 "Residual Strength of Sand from Dam Failures in the Chilean Earthquake of March 3, 1985," by De Alba, P., Seed, H.B., Retamal, E. and Seed, R.B., September 1987.

UCB/EERC-87/12 "Inelastic Seismic Response of Structures with Mass or Stiffness Eccentricities in Plan," by Bruneau, M. and Mahin, S.A., September 1987.

UCB/EERC-87/13 "CSTRUCT: An Interactive Computer Environment for the Design and Analysis of Earthquake Resistant Steel Structures," by Austin, M.A., Mahin, S.A. and Pister, K.S., September 1987.

UCB/EERC-87/14 "Experimental Study of Reinforced Concrete Columns Subjected to Multi-Axial Loading," by Low, S.S. and Moehle, J.P., September 1987.

UCB/EERC-87/15 "Relationships between Soil Conditions and Earthquake Ground Motions in Mexico City in the Earthquake of Sept. 19, 1985," by Seed, H.B., Romo, M.P., Sun, J., Jaime, A. and Lysmer, J., October 1987.

UCB/EERC-87/16 "Experimental Study of Seismic Response of R. C. Setback Buildings," by Shahrooz, B.M. and Moehle, J.P., October 1987.

UCB/EERC-87/17 "Three Dimensional Aspects of the Behavior of R. C. Structures Subjected to Earthquakes," by Pantazopoulou, S.J. and Moehle, J.P., October 1987.

UCB/EERC-87/18 "Design Procedures for R-FBI Bearings," by Mostaghel, N. and Kelly, J.M., November 1987.

UCB/EERC-87/19 "Analytical Models for Predicting the Lateral Response of R C Shear Walls: Evaluation of their Reliability," by Vulcano, A. and Bertero, V.V., November 1987.

UCB/EERC-87/20 "Earthquake Response of Torsionally-Coupled Buildings," by Hejal, R. and Chopra, A.K., December 1987.